Book of Abstracts

EGAS52 Virtual Conference
organized by the EGAS Board and the Institute of Physics in Zagreb, Croatia

July 06-08, 2021

Editor: Danijel Buhin

Conference Program

VI - EGAS52 July 06-08, 2021

	Tuesday, 6 July	Wednesday, 7 July
08:45 - 09:00	Opening	
09:00- 09:40	Jean Dalibard	Ruth Signorell
09:40 - 10:05	Dmitry S. Petrov	Elena Gryzlova
10:05 - 10:30	Henning Moritz	Giuseppe Sansone
10:30 - 10:45	**COFFEE**	**COFFEE**
10:45 - 11:25	Frédéric Merkt	Fedor Jelezko
11:25 - 11:50	Roland Wester	Christiane Morais Smith
11:50 - 12:15	Gleb Gribakin	Morgan W. Mitchell
12:15- 12:40	Marcel Mudrich	Sponsors presentation II
12:40 - 14:30	**LUNCH**	**LUNCH**
14:30- 15:10	Bernd von Issendorff	EGAS General Assembly Career Development Talks
15:10 - 15:35	Lars von der Wense	
15:35 -15:45	**COFFEE**	**COFFEE**
15:45 - 16:45	Sponsor presentations I	Marin Soljačić General public lecture
16:45 - 17:00	**COFFEE**	**COFFEE**
17:00 - 19:30	Poster session I	Poster session II

	Thursday, 8 July - CALT DAY
08:45- 09:00	
09:00- 09:15	CALT - Damir Aumiler
09:15 - 09:55	Dragan Mihailović
09:55 - 10:35	Gerry O'Sullivan
10:35 - 10:45	**COFFEE**
10:45 - 12:45	Poster session III
12:40 - 14:30	**LUNCH**
14:30- 15:10	Francesca Ferlaino
15:10 - 15:50	Rudolf Grimm
15:50 -16:30	Jun Ye
16:30 - 16:45	**CLOSING**

Tuesday, 6. July

Chair: **Alice Sinatra**, LKB, Paris, France

9:00 - 9:40 **Jean Dalibard**
Laboratoire Kastler Brossel, Collège de France, Paris, France
Investigating two-body physics in a Bose gas: the spectroscopic way

9:40 - 10:05 **Dmitry S. Petrov**
Université Paris-Saclay, CNRS, LPTMS, Orsay, France
Higher-order effective interactions for bosons near a two-body zero crossing

10:05 - 10:30 **Henning Moritz**
Institut für Laserphysik and The Hamburg Centre for Ultrafast Imaging, Universität Hamburg, Hamburg, Germany
Superfluidity in strongly correlated 2D Fermi gases crossing

Chair: **Francesco Saverio Cataliotti**, Università degli Studi di Firenze, Firenze, Italy

10:45 - 11:25 **Frédéric Merkt**
Physical Chemistry Laboratory, ETH Zurich, Zurich, Switzerland
Cold ion chemistry within the orbit of a highly excited Rydberg electron

11:25 - 11:50 **Roland Wester**
Institut für Ionenphysik und Angewandte Physik, Universität Innsbruck, Innsbruck, Austria
Controlled interactions of cold trapped negative ions

11:50 - 12:15 **Gleb F. Gribakin**
School of Mathematics and Physics, Queen's University of Belfast, Belfast, Northern Ireland, UK
Positron binding to molecules: effects of chemical composition and shape

12:15 - 12:40 **Marcel Mudrich**
Department of Physics and Astronomy, Aarhus University, Aarhus, Denmark
Dynamics of excited helium nanodropets: Ultrafast relaxation, ICD, ATI

Chair: **Thomas Udem**, Max-Planck-Institut für Quantenoptik, Garching, Germany

14:30 - 15:10 **Bernd von Issendorff**
Physics Institute, University of Freiburg, Freiburg, Germany
Matter at the nanoscale: study of the structure and dynamics of clusters

15:10 - 15:35 **Lars von der Wense**
JILA, National Institute of Standards and Technology and University of Colorado, Boulder, CO, USA
Prospects for constraining temporal variations of fundamental constants with a ^{229}Th-based nuclear frequency standard

Sponsor presentations I

Chair: **Neven Šantić**, Institute of Physics, Zagreb, Croatia

15:45 - 15:55 **Guillaume Szymczak**
Amplitude
15:55 - 16:05 **Axel Wehling**

Coherent / ICS Solutions d.o.o.
16:05 - 16:15 **Benjamin Sprenger**
Menlo Systems
16:15 - 16:25 **Reinhard Ebel**
LRM d.o.o.
16:25 - 16:35 **Gabriel Tempea**
few cycle
16:35 - 16:45 **Bojan Resan**
TLD Photonics

Poster session I

Room 1: Quantum optics, quantum information and quantum simulation & Cold gases and quantum fluids
Chair: **Hrvoje Buljan**, Faculty of Science, University of Zagreb, Zagreb, Croatia

17:00 **A. D. Manukhova** (101)
Hong-Ou-Mandel Interference via quantum non-demolition gate between atoms and mechanics
17:10 **D. Holzmann** (102)
A versatile quantum simulator for coupled oscillators using a 1D chain of atoms trapped near an optical nanofiber
17:20 **A. Biella** (106)
Measurement-Induced Entanglement Transitions and the Quantum Zeno effect: non-Hermitian physics at play
17:30 **R. Veilande** (119)
The new mathematical model of photons
17:40 **H. Tonchev** (133)
Optimization of the quantum random walk search algorithm
17:50 **H. J. Williams** (135)
Implementing Hamiltonians on a Rydberg Quantum Simulator
18:00 **S. Shevate** (140)
Construction of strontium quantum gas microscope to study relaxation dynamics in 2D lattice gases
18:10 **S. Varbev** (144)
Qubit controlled by the magnetic dark soliton
18:20 **M. Suchorowski** (146)
Interactions and dynamic of two ultracold highly-magnetic atoms in a harmonic trap
18:30 **A. Ritboon** (155)
Sequential phonon measurements of atomic motion
18:40 **L. Vranješ Markić** (281)
Quantum Monte Carlo study of trapped Bose-Bose mixtures at zero and finite temperature
18:50 **T. Mežnaršič** (285)
Phase diagram of matter-wave jets
19:00 **H. Eneriz** (296)
Loading and cooling in an optical trap via hyperfine dark states
19:10 **J. Wang** (246)
An atomic compass based on vector vortex beams

Room 2: Cold gases and quantum fluids
Chair: **Simon L. Cornish**, Durham University

17:00 **A. Pandey** (262)
Homonuclear ion-atom collisions: application to Li^+s-Li

17:10 **A. Perrin** (120)
Toward unidimensional Bose gases with tunable interactions
17:20 **T. Kirova** (121)
Ultraprecise Rydberg atomic localization by standing waves and optical vortices
17:30 **C. Oliver** (129)
Bloch oscillations in a synthetic dimension of harmonic trap states
17:40 **G. De Rosi** (131)
Dark-soliton-induced anomaly in the thermodynamic behavior of a one-dimensional Bose gas
17:50 **L. Longchambon** (136)
A versatile ring trap for quantum gases
18:00 **G.S. Sangami** (138)
Ultracold AlF molecules: theoretical insights for buffer-gas and evaporative cooling
18:10 **M. Robert-de-Saint-Vincent** (139)
Adiabatic spin-dependent momentum transfer in an SU(N) degenerate Fermi gas
18:20 **A. Wojciechowska** (141)
Large spin-orbit coupling as a source of Feshbach resonances in ultracold ion-atom mixtures
18:30 **T. Badr** (151)
Supersonic Rotation of a Superfluid: A Long-Lived Dynamical Ring
18:40 **V. Vulić** (193)
Laser Cooling of Atoms using an Optical Frequency Comb
18:50 **F. Revuelta** (163)
Dynamical localization in non-ideal kicked rotors driven by two modulations
19:00 **D. Mellado-Alcedo** (164)
Two interacting polar linear molecules in an electric field
19:10 **D. Rey** (168)
An annular quantum gas induced by dimensional reduction

Room 3: Frequency and time domain spectroscopy and metrology
Chair: **Hendrick Bethlem**, Vrije Universiteit Amsterdam, Amsterdam, The Netherlands

17:00 **P. Kowalczyk** (108)
Spectroscopic study of the $3^1\Pi_u$ state in Cs_2 molecule by polarisation labelling laser technique
17:10 **F. Schmid** (115)
Towards High-Precision Spectroscopy of the 1S–2S Transition in He^+
17:20 **R. Ferber** (122)
Extended Spectroscopic Studies and Interatomic Potential Refinement of the $c^3\Sigma^+$ (Ω=1) State in KCs
17:30 **O. Bezrodnova** (263)
Towards a high-precision measurement of the ^{3}He and T nuclei atomic mass difference at LIONTRAP
17:40 **K. Mičulis** (182)
Selective Two–Photon Excitation of Rydberg Atomic State Hyperfine Components
17:50 **G. Le Gal** (125)
Zero-field magnetometer based on the combination of atomic orientation and alignment
18:00 **I. Puljić** (137)
Towards the first strontium optical atomic clock in Croatia
18:10 **A. Sopena** (160)
Asymmetric electron angular distributions in stimulated Compton scattering from H_2 irradiated with soft-X ray laser pulses
18:20 **Katja Gosar** (166)
Single-shot Stern-Gerlach magnetic gradiometer with an expanding cloud of cold cesium atoms
18:30 **L. Busaite** (170)
Development of a 3D single-port magnetometer based on magneto-optical resonances in an alkali vapor

18:40 **A. Martínez de Velasco** (172)
Towards Ramsey-comb spectroscopy of the 1S-2S transition in singly-ionized helium
18:50 **R. Lazda** (173)
Vector magnetometry using NV centers in diamond
19:00 **J. Delgado** (179)
Attosecond Spectroscopy of Small Organic Molecules: XUV pump-XUV probe Scheme in Glycine
19:10 **F. L. Constantin** (280)
Selective Two–Photon Excitation of Rydberg Atomic State Hyperfine Components
19:20 **D. V. Brazhnikov** (297)
High-Quality Level-Crossing Resonances in a Cesium Vapor Cell for Applications in Atomic Magnetometry

Room 4: Applications to astrophysics, plasma physics, biophysics, clusters & Atom-like systems
Chair: **Sophie Kazamias**, Université Paris Saclay, Paris, France

17:00 **S. Gamrath** (103)
Calculated Oscillator Strengths for Radiative Transitions of Cosmochronological Interest in Singly Ionized Thorium (Th II)
17:10 **J. Tamuliene** (107)
Similarities of fragmentation of some amino acids under low-energy electron impact
17:20 **H. Carvajal Gallego** (111)
Large-scale atomic data calculations in Ce V–X ions for application to early kilonova emission from neutron star mergers
17:30 **J. Baier** (153)
KWISP - Latest results on the chameleon hunt at the CAST experiment at CERN
17:40 **H. Skenderović** (261)
Biological samples used for imaging
17:50 **D. Schury** (113)
Planned Laboratory Studies of N_2 reacting with H^+_3 Isotopologues
18:00 **P. Palmeri** (117)
Plasma environment effects on K lines of astrophysical interest: universal formulae for ionization potential and K-threshold shifts
18:10 **Z. Bouza** (127)
Spectral investigation of tin ions in an electron beam ion trap and laser-produced plasmas in the EUV region
18:20 **J. Sheil** (130)
Multiply-excited states and their contribution to opacity in laser-driven tin plasmas
18:30 **D. Maletić** (221)
LIBS vs ICCD imaging for atmospheric plasma jet diagnostics
18:40 **S. Gamrath** (105)
Oscillator strengths in doubly- and trebly-ionized gold deduced from core-polarization-corrected pseudo-relativistic Hartree-Fock calculations
18:50 **B. Margulis** (109)
Direct Observation of a Feshbach-resonance by Coincidence-detection of Ions and Electrons in Penning Ionization Collisions
19:00 **N. Domenikou** (142)
Shortcut to adiabaticity for a three-level quantum system near a metallic nanoparticle
19:10 **M. Mirahmadi** (145)
On the formation of van der Waals molecules through direct three-body recombination

Room 5: Atom-like systems & Fundamental physics

Chair: **Klavs Hansen**, Tianjin University, China

17:00 **N. Ladda** (229)
Photoelectron circular dichroism of fenchone using deep ultraviolet femtosecond laser pulses
17:10 **J. J. Omiste** (234)
Ultrafast photoionization of aligned excited states of neon
17:20 **F. Grilo** (236)
Comprehensive laboratory measurements resolving the LMM dieletronic recombination satellite lines in Ne-like Fe XVII ions
17:30 **F. Grilo** (237)
Observation of metastable $1s2s\ ^3S_1$ He-like oxygen decay in an electron beam ion trap
17:40 **A. Aleksanyan** (114)
Alkali atom transition cancellations within magnetic field
17:50 **H. R. Hamedi** (116)
Off-axis optical vortices using double-Raman singlet light-matter scheme
18:00 **A. Androutsopoulos** (118)
Accurate theoretical study of the spectroscopic properties of diatomic molecules including 2nd row transition metals
18:10 **P. Danev** (132)
Prospects for refining fundamental constants by spectroscopy of deuterium molecular ion
18:20 **V. A. Terashkevich** (147)
The simultaneous coupled-channel deperturbation treatment of the $X^2\Sigma^+$, $A^2\Pi$ and $B^2\Sigma^+$ states in the CN radical: the first attempt
18:30 **M. C. Mooij** (149)
A buffer gas cooled BaF beam for the NL-eEDM experiment
18:40 **E. A. Koval** (150)
Resonances in arbitrarily oriented dipoles scattering in plane
18:50 **P. Paliwal** (154)
Fano interference in quantum resonances from angle-resolved elastic scattering
19:00 **C. M. König** (157)
High-Precision Spectroscopy of Single Molecular Hydrogen Ions in a Penning Trap at Alphatrap
19:10 **O. Rousselle** (169)
How does antimatter fall?: simulation of the GBAR experiment at CERN

Wednesday, 7. July

Chair: **Alexei Grum-Grzhimailo**, Lomonosov Moscow State University, Moscow, Russia

9:00 - 9:40 **Ruth Signorell**
Department of Chemistry and Applied Biosciences, ETH Zurich, Zurich, Switzerland
Genuine properties and relaxation dynamics of solvated electrons in neutral water clusters

9:40 - 10:05 **Elena Gryzlova**
Skobeltsyn Institute of Nuclear Physics, Lomonosov Moscow State University, Moscow, Russia
Achievements of Polarization Atomic Spectroscopy with FELs

10:05 - 10:30 **Guiseppe Sansone**
Albert-Ludwigs-Universität, Freiburg, Germany
Shaping attosecond waveforms at free-electron lasers

Chair: **Szymon Pustelny**, Jagiellonian University, Krakow, Poland

10:45 - 11:25 **Fedor Jelezko**
Ulm University, Ulm, Germany
Diamond light matter quantum interface

11:25 - 11:50 **Christiane Morais Smith**
Institute for Theoretical Physics, University of Utrecht, Netherlands
TBA

11:50 - 12:15 **Morgan W. Mitchell**
The Institute of Photonic Sciences (ICFO), Barcelona, Spain
Measurement-induced, spatially-extended entanglement in a hot, strongly-interacting atomic vapor

Sponsor presentations II

Chair: **Silvije Vdović**, Institute of Physics, Zagreb, Croatia

12:25 - 12:35 **Robert Scholten**
MOGLabs
12:35 - 12:45 **Valdas Maslinskas**
Light Conversion
12:45 - 12:55 **Dario Nicolosi**
SAES

14:35 - 15:35 **Career Development Talks**
Chair: **Rosario González-Férez**, Universidad de Granada, Granada, Spain

Astrid Elbe - Aviat Networks, Munich, Germany
Leticia Tarruell - ICFO, Barcelona, Spain
Oscar Viyuela - McKinsey & Company, Boston, USA

Chair: **Hrvoje Buljan**, Faculty of Science, University of Zagreb, Zagreb, Croatia

15:45 - 16:45 **Marin Soljačić**
Research Laboratory of Electronics, Massachusetts Institute of Technology, Cambridge, MA, USA

Enabling novel light phenomena at the subwavelength scale

Poster session II

Room 1: Quantum optics, quantum information and quantum simulation & Fundamental physics
Chair: **Damir Aumiler**, Institute of Physics, Zagreb, Croatia

17:00 **S. Filatov** (177)
On Interchangeability of Probe-Object Roles in Quantum-Quantum Interaction-Free Measurement
17:10 **F. Lunić** (178)
Exact solutions of a model for synthetic anyons in a noninteracting system
17:20 **L. Ostermann** (197)
A Nanoscale Coherent Light Source
17:30 **I. Mastroserio** (201)
Complementary Experimental Quantum Embedding for Machine Learning
17:40 **S. Hernández-Gómez** (206)
Energy fluctuations of an NV spin qutrit under feedback-controlled dissipative dynamics
17:50 **J. M. Mortlock** (211)
Towards Quantum Gas Microscopy of Polar Molecules
18:00 **V. A. Knyazeva** (219)
Photon polarizations in two-photon $2s \rightarrow 1s$ decay
18:10 **V. Vujnović** (222)
Single photons behaviour in optical resonators and its applications
18:20 **C. Hölzl** (240)
Circular Rydberg states for quantum many-body physics
18:30 **G. Ferioli** (242)
Storage and release of subradiant excitations in a dense atomic cloud
18:40 **S. Rau** (264)
Precision Mass Measurement of the Deuteron's Atomic Mass
18:50 **D. Šimsa** (278)
Quantum mechanical description of hydrogen dimers

Room 2: Cold gases and quantum fluids
Chair: **Rosario González-Férez**, Universidad de Granada, Granada, Spain

17:00 **M. Kruljac** (158)
Collective light-atom interaction in free space and in an optical cavity
17:10 **A. Dombi** (165)
Collective self-trapping of atoms in a cavity
17:20 **R. Jannin** (174)
Constraining ab-initio molecular potential calculations through measurements of the spin relaxation rate in a Fermi gas of 3He
17:30 **F. B. V. Martins** (175)
Reaction between a molecule and a Rydberg atom: studying n-changing processes in He(n) + CO $\rightarrow$ C(n') + O + He
17:40 **Y. van der Werf** (176)
Narrowing of Spectroscopic Linewidths through Pauli Blockade of Stimulated Emission
17:50 **M. Uminski** (180)
Tuning ultracold collisions oh He*-Li with external magnetic field
18:00 **K. Miculis** (183)
Penning Ionization Processes Involving Cold Rydberg Alkali–Metal Atoms
18:10 **T.W. Clark** (186)

Transmission-blockade breakdown phase transition of atoms in a cavity
18:20 **G. Ness** (187)
Observing quantum-speed-limit crossover with matter wave interferometry
18:30 **E. Abdiha** (189)
Avoiding dark states in the laser cooling of TlF using additional external fields
18:40 **K. P. Horn** (190)
Feshbach resonances in half-collisions between para/ortho H_2^+ and He
18:50 **D. Buhin** (156)
Doppler cooling of atoms with a frequency comb: Rb theoretical case study
19:00 **A. Litvinov** (195)
Measuring densities of cold atomic clouds smaller than the resolution limit
19:10 **C. C. Kwong** (198)
Coherent flash effect beyond the low saturation two-level case

Room 3: Frequency and time domain spectroscopy and metrology
Chair: **Helen H. Fielding**, University College London, UK

17:00 **F. Fernández Villoria** (184)
Time-Resolved Images of Intramolecular Charge Transfer in Organic Molecules
17:10 **K. Kanika** (188)
Measurement of Magnetic Moments in Heavy, Highly Charged Ions Using Laser-Microwave Double-Resonance Spectroscopy
17:20 **S. Gravina** (194)
Development of a high-resolution mercury spectrometer at 253.7 nm for temperature metrology
17:30 **D. Kovačić** (205)
Towards blue-detuned lattice optical atomic clock
17:40 **V. Wirthl** (207)
Towards precision spectroscopy of the 2S-6P transition in atomic deuterium
17:50 **M. Forjan** (208)
Ultrafast Photogeneration of Quinone Methides from Naphthol Derivatives
18:00 **L. J. Spieß** (210)
Developments on King Plot Analysis using Highly Charged Ions
18:10 **W. van der Meer** (215)
Performing Spectroscopy in the 1.5 mm-regime on slow Ammonia in a Molecular Fountain
18:20 **S. Gerlich** (220)
Matter-Wave Interferometry as a tool for Quantum-Enhanced Metrology
18:30 **L. S. Dreissen** (239)
Precision metrology with multi-ion Coulomb crystals
18:40 **N.-H. Rehbehn** (249)
Sensitivity to new physics of isotope-shift studies using forbidden optical transitions of highly charged Ca ions
18:50 **S. V. Popruzhenko** (251)
Attosecond Time Shifts in Strong-Field Tunneling Ionization of Atoms by Tailored Laser Pulses
19:00 **M. Steinel** (260)
Sympathetic sideband cooling of $^{171}Yb^+$ by $^{88}Sr^+$ for an optical atomic clock
19:10 **R. Ferber** (123)
The Spectroscopic Observation and Analysis of Bound-Free Transitions to $a^3\Sigma^+$ and $X^1\Sigma^+$ States of KCs

Room 4: Applications to astrophysics, plasma physics, biophysics, clusters & Atom-like systems
Chair: **Robert Moshammer**, MPI für Kernphysik, Heidelberg, Germany

17:00 **H. Carvajal Gallego** (112)
Multiconfiguration Dirac–Hartree–Fock radiative data for emission lines in Ce II–IV ions and cerium opacity calculations for kilonovae
17:10 **D. Popović** (203)
Detection of low electron densities in atmospheric pressure plasma jet by laser induced avalanche ionisation
17:20 **V. Zhelyazkova** (159)
Ion-dipole and ion-quadrupole interaction effects in ion-molecule reactions at collisional energies E_{coll}/k_B between 0 and 40 K
17:30 **J. Petrović** (161)
An alternative method for determination of hardness based on LIBS
17:40 **T. Depastas** (167)
A Constrained Fermionic Dynamics study of near Ground state properties and Isospin Symmetry of the Nuclear Systems
17:50 **B. Bastian** (185)
A new end-station for synchrotron spectroscopy of helium droplets reveals interatomic Coulombic decay on a Fano resonance
18:00 **E. Sanchez** (226)
Rotational energy relaxation of diatomic molecules in superfluid helium nanodroplets. The case of the HCl, DCl and TCl molecules
18:10 **M. González** (274)
Photodissociation of Br_2 in Superfluid Helium Nanodroplets. Importance of the Recombination Process
18:20 **L. Behnke** (128)
Characterization of tin plasma driven by high-energy, 2-μm-wavelength light
18:30 **R. Radičić** (192)
Photocatalytic properties of zinc oxide prepared by thermal degradation of the cellulose template
18:40 **D. Blažeka** (196)
TiO2 nanoparticles synthesized by pulsed laser ablation in water as catalyst in photodegradation of organic pollutants under UV and visible vlight irradiation
18:50 **A. Senkić** (214)
Sulphur concentration influence on morphology and optical properties of MoS_2 monolayers
19:00 **M. Trassinelli** (134)
New stringent test of bound-state QED: high-resolution measurement of an intra-shell transition in He-like uranium
19:10 **M. D. Kiselev** (148)
Kr 3d shake-up photoelectron spectra and angular distributions

Room 5: Atom-like systems & Fundamental physics
Chair: **Goran Pichler**, Institute of Physics, Zagreb, Croatia

17:00 **H. Lee** (244)
Photoelectron circular dichroism via multiphoton ionization with varying pulse duration
17:10 **K. Hansen** (248)
From exponentials to power laws and back again
17:20 **L. Ábrók** (252)
Nondipole and channel-interference effects in the case of Kr 4p direct photoionization and 3p/3d Auger decay
17:30 **O. Borovik** (256)
Excitation of the $4p^5 5s^2 2\ ^2P_{1/2,3/2}$ states in strontium by electron impact
17:40 **J. V. Barnes** (152)
Magnetic deflection of neutral sodium-doped ammonia clusters

17:50 **L. Busaite** (171)
Dynamic nuclear spin polarization in Nitrogen–Vacancy centers in diamond
18:00 **H. Liu** (200)
Theoretical study of vibrational (de-)excitation of NO_2 and N_2O by low-energy electron impact
18:10 **O. S. Alekseeva** (202)
The VUV absorption spectra arising from collisions of Kr and Xe atoms with H_2 molecules in the short-wave region near the resonance lines $^{1,3}P_1$–$^1S_0$
18:20 **M. Eraković** (204)
Combined VCI and instanton approach for computation of vibrational spectrum in asymmetric well systems
18:30 **D. Osite** (213)
Transverse alignment-to-orientation conversion in the ground state of alkali atoms with linearly polarized laser excitation
18:40 **Z. Yibin** (225)
The simulation of unimolecular reaction rates of Lennard-Jones clusters
18:50 **P. Laha** (228)
Thermally-induced entanglement of atomic oscillators
19:00 **C. M. Rawlins** (233)
Many-body theory calculations of positron scattering and annihilation in H_2, N_2, CH_4 and CF_4

Thursday, 8. July - CALT Day

Chair: **Nataša Vujičić**, Institute of Physics, Zagreb, Croatia

9:00 - 9:15 **Damir Aumiler**
Institute of physics, Zagreb, Croatia
Centre for Advanced Laser Techniques (CALT)

9:15 - 9:55 **Dragan Mihailović**
Jožef Stefan Institute, Ljubljana, Slovenia
Non-equilibrium condensed matter: an open door to new phenomena

9:55 - 10:35 **Gerry O'Sullivan**
JUniversity College Dublin, Ireland
Spectroscopy of Laser Produced Plasmas of Highly Charged Ions to Support Short Wavelength Light Source Development

Chair **Ticijana Ban**, Institute of Physics, Zagreb, Croatia

14:30 - 15:10 **Francesca Ferlaino**
Institute of Experimental Physics, Univ. of Innsbruck, Austria
Institute for Quantum Optics and Quantum Information (IQOQI), Austrian Academy of Sciences, Innsbruck, Austria
Supersolidity in the ultracold: when atoms behave as crystal and superfluid at the same time

15:10 - 15:50 **Rudolf Grimm**
Institute for Quantum Optics and Quantum Information Austrian Academy of Sciences / Institute of Experimental Physics, Univ. of Innsbruck, Austria
Ultracold Fermion Mixtures with Strong Interactions

15:50 - 16:30 **Jun Ye**
JILA, National Institute of Standards and Technology and university of Colorado, Boulder, Colorado, USA
A molecular quantum gas with tunable interactions

Poster session III

Room 1: Quantum optics, quantum information and quantum simulation & Fundamental physics
Chair: **Ivor Krešić**, Institute of Physics, Zagreb, Croatia

10:45 **D. M. Walker** (253)
A coherent interface between helium Rydberg atoms and chip-based superconducting microwave resonators
10:55 **D. Abramović** (255)
Application of Single Photons in Holography
11:05 **C. Warnecke** (267)
A superconducting radio-frequency quadrupole resonator for metrology experiments with highly charged ions
11:15 **J. D. R. Tommey** (277)
Transverse matter-wave interferometry with Rydberg helium atoms
11:25 **L. M. Fernley** (287)
Storage Qubits and Synthetic Dimensions with Ultracold Polar Molecules
11:35 **G. Kowzan** (290)
Polarization control of rotationally-resolved third-order molecular response
11:45 **A. Serafin** (292)

Nuclear spin squeezing by continuous quantum non-demolition measurement: a theoretical study
11:55 **K. Gaul** (235)
Complementary atoms and molecules for rigorous bounds on P,T-violation
12:05 **S. Petrosyan** (241)
Amplification of Light Signal on V-type Atomic System
12:15 **M. Door** (282)
Latest Results of the High-Precision Penning Trap Mass Spectrometer PENTATRAP

Room 2: Cold gases and quantum fluids
Chair: **Neven Šantić**, Institute of Physics, Zagreb, Croatia

10:45 **T. Sánchez-Pastor** (199)
On the limits of the theoretical calculation of inelastic confinement-induced resonances
10:55 **T. Petrucciani** (212)
Spatial Bloch oscillations of a quantum gas in a "beat-note" superlattice
11:05 **J.-N. Schmidt** (217)
Angular and Radial Roton Excitations in an Oblate Dipolar Quantum Gas
11:15 **K. Dželalija** (218)
Quantum Monte Carlo study of strongly interacting bosonic one-dimensional systems in periodic potentials
11:25 **A. J. Park** (289)
Large, deep, and homogeneous optical lattices created in monolithic crossed cavities
11:35 **X. Xing** (230)
Ion loss events in a Rb-Ca^+ cold hybrid trap: photodissociation, black-body radiation and non-radiative charge exchange
11:45 **K. Pleskacz** (231)
Mapping of ion motion spectra in a linear Paul trap
11:55 **T. Cantat-Moltrecht** (232)
A Cavity-Enhanced Microscope for Cold Atoms
12:05 **L. Mazza** (110)
One dimensional Yb gases with two-body losses: strong quantum correlations in the Zeno regime
12:15 **R. Veyron** (269)
Fast in-situ absorption imaging of the local density of ultra-cold atoms in an optical lattice using an imaging lattice
12:25 **R. Muñoz-Rodriguez** (273)
Photoassociation of Rb and Hg atoms near the ^{87}Rb D_1 line at 795 nm
12:35 **A. S. Popova** (293)
Quantum Monte Carlo Simulation of Polaron Tunneling

Room 3: Frequency and time domain spectroscopy and metrology
Chair: **Silvije Vdović**, Institute of Physics, Zagreb, Croatia

10:45 **R. Steinbrügge** (265)
High Precision Calibration of Molecular Oxygen Absorption Lines Using Transitions in Highly Charged Ions
10:55 **E. A. Dijck** (268)
Characterizing a Nb superconducting radio-frequency resonator for trapping highly charged ions
11:05 **Y.-C. Cheng** (270)
Controlling phototionization with attosecond time-slit experiment
11:15 **B. Özdalgic** (271)
Hyperfine Structure Analysis of Atomic Holmium in the Visible Range

11:25 **J. Keller** (276)
Precision spectroscopy with In^+ / Yb^+ Coulomb crystals
11:35 **D. Charczun** (291)
Dual-comb spectroscopy based on measurements of cavity resonances
11:45 **M. Tamanis** (124)
Extended Spectroscopic Data and Deperturbative Analysis of $A^1\Sigma_u^+$ and $b^3\Pi_u$ States in K_2
11:55 **T.-L. Chen** (284)
Mid-Infrared Mode-Resolved Cavity Ring-Down Vernier Spectrometer using an Interband Cascade Laser Based Chip-Scale Optical Frequency Comb
12:05 **S. Dickopf** (288)
Determination of the hyperfine structure constant and the g-factors of $^3He^+$
12:15 **F. L. Constantin** (279)
Terahertz Electrometry using Precision Spectroscopy of the Hydrogen Deuteride Molecular Ions

Room 4: Applications to astrophysics, plasma physics, biophysics, clusters & Atom-like systems
Chair: **Nikša Krstulović**, Institute of Physics, Zagreb, Croatia

10:45 **N. Vujičić** (227)
Excitonic effects in CVD grown mono- and bilayer MoS_2 in the low-temeprature limit
10:55 **S. Gamrath** (104)
A new set of oscillator strengths in moderately charged indium ions for the spectral analysis of hot white dwarfs
11:05 **J. Car** (238)
A model for determination of diameter and concentration of metal nanoparticles synthesized by laser ablation in water
11:15 **H. Wei** (250)
Radiative cooling of cationic carbon clusters, C_N^+
11:25 **M. A. Mermigki** (181)
Electronic structure and Bonding Properties of Diatomic Molecule FeS
11:35 **S. Kühn** (266)
High-precision laser spectroscopy measurements of the prominent 3C/3D oscillator-strength ratio in Fe XVII
11:45 **V. Jadriško** (272)
Novel method for preparing nanoscale atomically thin heterostructure devices
11:55 **N. Selaković** (275)
Mass spectrometry and ICCD imaging of atmospheric pressure plasma jet with spiral electrodes
12:05 **A. Blech** (191)
Photoelectron circular dichroism in racemic mixtures
12:15 **C. Blondel** (216)
Old recipes to the rescue of modern data on the hyperfine structure of Xe I
12:25 **A. S. Petrovskaya** (223)
Numerical Simulation of Argon Microdischarge for Plasma Deactivation Technology
12:35 **S. Vasudevan** (224)
Photoelectron circular dichroism of heavier chalcogenofenchones using near ultra-violet femtosecond laser pulses

Room 5: Atom-like systems & Fundamental physics
Chair: **Slobodan Milošević**, Institute of Physics, Zagreb, Croatia

10:45 **J. Gębala** (162)
Cold interactions and collisions between helium ions (He^+) and metastable helium atoms (He^*)

10:55 **S. Das** (257)
Chirp and intensity dependence of the circular dichroism in ion yield of 3-methylcyclopentanone measured with femtosecond laser pulses
11:05 **A. V. Maiorova** (259)
Radiative recombination of twisted electrons with highly charge ions
11:15 **S. Bernitt** (283)
Strong Two-Electron-One-Photon Transitions in Li-like Ions
11:25 **J. Forer** (286)
Low-Energy Dissociative Recombination of CH^+
11:35 **P. Jasik** (294)
Spontaneous Electron Emission Versus Dissociation in Internally Hot Silver Dimer Anions
11:45 **S. Krishnan** (295)
Penning ionization of Camphor molecules in He nanodroplets by EUV photoexcitation: electron-ion coincidence spectroscopy
11:55 **J. Hofierka** (243)
Many-body theory of positron binding in polyatomic molecules
12:05 **B. Dutta** (245)
Probing Casimir-Polder interactions of Rydberg atoms in vapour cells
12:15 **A. R. Swann** (247)
Positron cooling in N_2 and CF_4 gases
12:25 **P. Stipanović** (254)
Four-body universality which extends from classical to quantum systems
12:35 **A. Daffurn** (258)
Gouy phase-matched angular and radial mode conversion in four-wave mixing

Investigating two-body physics in a Bose gas: the spectroscopic way

Jean Dalibard[*1]
1. Laboratoire Kastler Brossel, Collège de France, 11 Place Marcelin Berthelot, 75005 Paris, France

The thermodynamic equilibrium of any homogeneous fluid is characterized by its equation of state. This equation gives the variations of a thermodynamic potential, *e.g.* the internal energy E, with respect to a set of variables such as the number of particles, their temperature and their interaction strength. Regarding this latter variable, the relevant thermodynamic quantity for an ultra-cold gas is the so-called Tan's contact [1], which unifies many different properties from the momentum distribution to the spatial two-body correlation function.

In this talk, I will explain how one can use a Ramsey interferometric scheme between the two hyperfine clock states of rubidium atoms to map out the variations of Tan's contact in a two-dimensional Bose gas, from the strongly degenerate superfluid case to the non-degenerate case [2]. I will also show a somewhat surprising result, revealed by this precise microwave spectroscopy in a two-dimensional fluid: in spite of the fact that each clock state is non-magnetic, a mixture of the two states still displays a magnetic dipole-dipole interaction comparable to the one expected for the other (magnetic) Zeeman states [3].

References

[1] S . Tan, Annals of Physics **323**, 2971 (2008).
[2] Y.-Q. Zou, B. Bakkali-Hassani, C. Maury, É. Le Cerf, S. Nascimbene, J. Dalibard, J. Beugnon, Nature Communications **12**, 760 (2021).
[3] Y.-Q. Zou, B. Bakkali-Hassani, C. Maury, É. Le Cerf, S. Nascimbene, J. Dalibard, J. Beugnon, Phys. Rev. Lett. **125**, 233604 (2020).

[*]Corresponding author: jean.dalibard@college-de-france.fr

Higher-order effective interactions for bosons near a two-body zero crossing

A. Pricoupenko[1], **D.S. Petrov**[*1]
1. Université Paris-Saclay, CNRS, LPTMS, 91405 Orsay, France

Systems with partially attractive and partially repulsive forces, fine-tuned to an approximate overall cancellation of the mean-field term, provide an interesting platform for studying various beyond-mean-field (BMF) phenomena, remarkable recent examples being quantum droplets and dipolar supersolids (see Ref. [1] for review). In contrast to the mean-field energy, which is essentially the first-order Born integral of the interaction potential multiplied by the number of interacting pairs, the BMF term is sensitive to many-body effects reflecting the structure of the Bogoliubov vacuum, i.e., the spectrum of Bogoliubov quasiparticles and their density of states. This can lead to a rather exotic and nonanalytic dependence of the BMF energy density on the particle density ($n^{5/2}$ in $D=3$ dimensions, $n^2\ln(n)$ for $D=2$, and $n^{3/2}$ for $D=1$). On the other hand, in quasi-low-dimensional regimes one can also recover the integer-power behavior with the leading terms in the energy density proportional to n^2 and n^3, which can be interpreted, respectively, as a renormalized two-body interaction and an emergent effective three-body force [2-3].

In this work [4] we consider bosons interacting by a two-body potential V of zero mean and perturbatively calculate the ground-state energy up to terms $\propto V^3$. We find that up to this order the result is an analytic function of the density n and contains two-body corrections $\propto V^2n^2$ and $\propto V^3n^2$ as well as an effective three-body term $\propto V^3n^3$. We show that these results can be obtained from the first-quantized few-body approach and from the Bogoliubov perturbation theory. We apply our theory to a few two-body interaction potentials and, in particular, calculate the leading two-body and three-body interaction corrections for quasi-low-dimensional dipoles as a function of their tilt angle θ with respect to the confinement cylindrical symmetry axis. We find that the three-body force for quasi-two-dimensional dipoles changes from attraction to repulsion with increasing θ (see Fig. 1). For one-dimensional dipoles the dominant three-body force is attractive and second order in V except when they are aligned parallel to the axis ($\theta=0$).

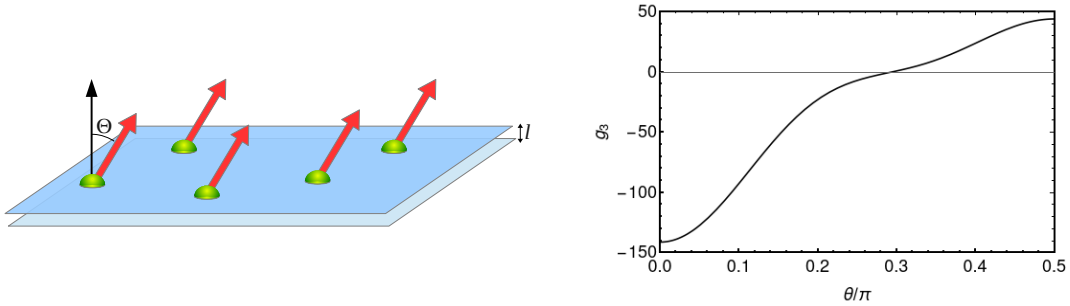

Fig. 1: Left panel: Quasi-two-dimensional dipoles, θ is the tilt angle, l is the confinement oscillator length. Right panel: the three-body coupling constant g_3 in units of $\hbar^2 r_*^3/ml$ for this geometry, m is the mass of the particles and r^* is the characteristic dipolar length. For any given θ the short-range part of the interation is assumed to be fine-tuned such that the two-body interaction is brought to a zero crossing. The effective three-body interaction monotonically changes from attractive when dipoles are perpendicular to the plane ($\theta=0$) to repulsive when they are in the plane ($\theta=\pi/2$).

Our results suggest a way to engineer systems with dominant elastic attractive and repulsive three-body forces, and can be used as a low-density reference point for the Hugenholtz-Pines method of calculating the BMF correction.

References

[1] F. Böttcher, J.-N. Schmidt, J. Hertkorn, K. S. H. Ng, S. D. Graham, M. Guo, T. Langen, T. Pfau, Rep. Prog. Phys. **84**, 012403 (2021).
[2] D. Edler, C. Mishra, F. Wächtler, R. Nath, S. Sinha, and L. Santos, Phys. Rev. Lett. **119**, 050403 (2017).
[3] P. Zin, M. Pylak, T. Wasak, K. Jachymski, Z. Idziaszek, arXiv:1911.02384.
[4] A. Pricoupenko and D. S. Petrov, Phys. Rev. A **103**, 033326 (2021).

*Corresponding author: dmitry.petrov@universite-paris-saclay.fr

Superfluidity in strongly correlated 2D Fermi gases

L. Sobirey[1], N. Luick[1], H. Biss[1], M. Bohlen[1], V. Singh[1], L. Mathey[1], T. Lompe[1], H. Moritz[*1]
1. Institut für Laserphysik and The Hamburg Centre for Ultrafast Imaging, Universität Hamburg, Luruper Chaussee 149, 22761 Hamburg

In this talk, I will review our recent work on superfluidity in homogeneous ultracold 2D Fermi gases. In the first part I will report on the observation of Josephson oscillations between two such gases [1], demonstrating phase coherence between them, enabling us to find excellent agreement with the sinusoidal current phase relation of an ideal Josephson junction and determine the critical current. In the second part I will present our measurements of the dynamic structure factor of 2D superfluids [2] . Using Bragg spectroscopy, we determine the critical velocity (see Fig. 1) and the superfluid gap in the BEC-BCS crossover, allowing for detailed comparisons with and benchmarks for theory. Our measurements enable us to directly study the role of reduced dimensionality on strongly correlated superfluids.

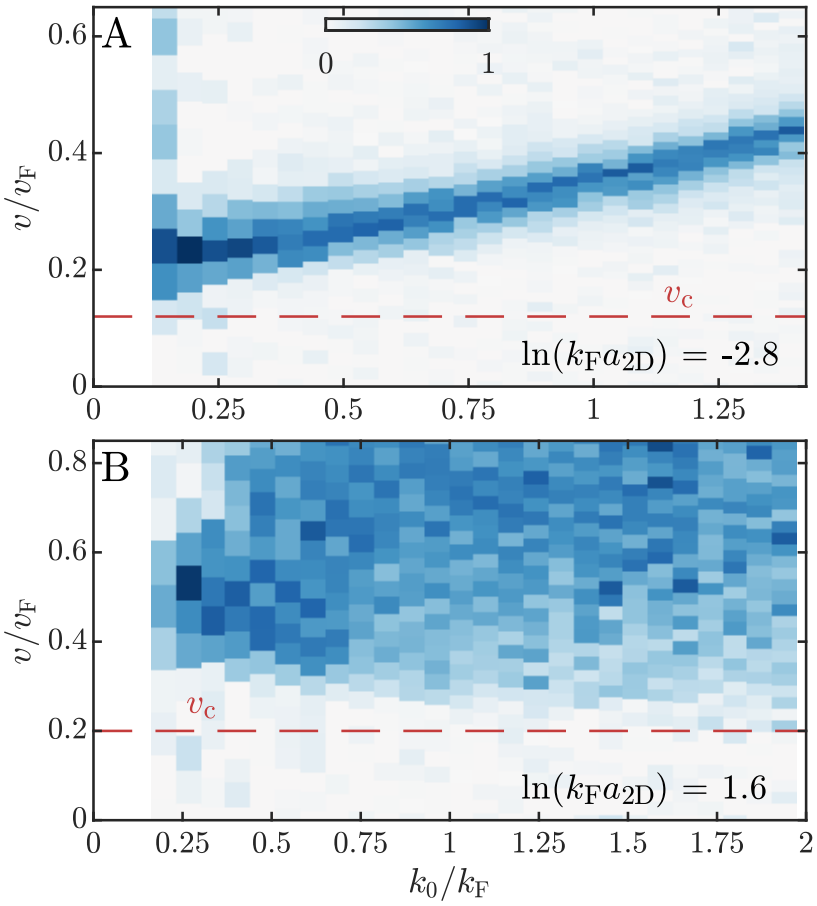

Fig. 1: Phononic and pair breaking excitations in a 2D Fermi gas. (A) Response of a gas in the BEC regime to excitations with lattice wavevector k_0 and velocity v. For small wavevectors, the moving lattice excites phononic modes at the sound velocity v_s. For larger wavevectors, the peak in the heating rate moves to higher velocities as the dispersion deviates from the linear phononic branch and single-particle excitations become dominant. (B) In the BCS regime, we observe a continuum of pair breaking excitations with a minimum of the onset velocity at $k_0 = 2k_F$. In both regimes, the heating rate is negligible for excitations that move slower than the critical velocity (red dashed lines). To enhance the visibility of weaker excitations, each column has been linearly rescaled to range from 0 to 1.

References

[1] N. Luick, L. Sobirey, M. Bohlen, V. Singh, L. Mathey, T. Lompe, and H. Moritz, Science **369**, 89 (2020).
[2] L. Sobirey, N. Luick, M. Bohlen, H. Biss, H. Moritz and T. Lompe, to appear in Science (2021).

*Corresponding author: henning.moritz@physik.uni-hamburg.de

Cold ion chemistry within the orbit of a highly excited Rydberg electron

J. Deiglmayr[1,2], K. Höveler[1], F. B. V. Martins[1], F. Merkt*[1], M. Žeško [1], V. Zhelyazkova[1]
1. Physical Chemistry Laboratory, ETH Zurich, Vladimir-Prelog-Weg 3, CH 8093 Zurich, Switzerland
2. Department of Physics, University of Leipzig, DE-04109 Leipzig, Germany

The study of ion-molecule reactions at low collision energies ($E_{\rm coll}$) below $E_{\rm coll}/k_{\rm B} = 10$ K, or low temperatures, is experimentally challenging because stray electric fields in the reaction volume heat up the ion samples. A potential difference of 1 mV across a reaction region of 1 cm accelerates the ions to 1 meV, which corresponds to heating them up to about 12 K. To overcome this problem and study ion-molecule reactions below 10 K, we have developed a new method, in which the ion molecule reaction takes place within the orbit of a Rydberg electron at high values of the principal quantum number n. In high-n Rydberg states, the Rydberg electron only very weakly interacts with the ion core, so that it does not significantly influence the ion-molecule reaction taking place within its orbit but shields the ion from heating by stray electric fields. Instead of studying exothermic and barrier-free ion-molecule reactions of the type

$$\mathrm{I}_1^+ + \mathrm{M}_1 \rightarrow \mathrm{I}_2^+ + \mathrm{M}_2, \tag{1}$$

we study the reactions

$$\mathrm{I}_1^* + \mathrm{M}_1 \rightarrow \mathrm{I}_2^* + \mathrm{M}_2, \tag{2}$$

in which I_1^* and I_2^* represent atoms or molecules in high Rydberg states with ion cores I_1^+ and I_2^+, respectively.

To reach very low collision energies, we use chip-based Rydberg-Stark decelerators and deflectors [1,2] to merge cold supersonic beams of I_1^* and M_1 and to vary their relative velocities [3]. Monitoring the product yield as a function of the relative mean velocity of the two beams, we obtain the relative reaction cross sections as a function of the collision energy. At collision energies ($E_{\rm coll}/k_{\rm B}$) below 1 K, we find that the reaction rate coefficients deviate from those estimated with Langevin-type capture models [4-6]. The deviations become particularly large when M_1 has a permanent dipole [5] or a quadrupole moment [4].

The talk will present general aspects of this new method as well as the results of studies of the reactions of H_2^+ and He^+ (I_1^+) with neutral molecules such as N_2, H_2, $\mathrm{CH}_3\mathrm{F}$, NH_3 and CH_4 (M_1) at very low collision energies and will discuss the observed low-temperature behavior in terms of the electric dipole and quadrupole moments of M_1. Our latest efforts at detecting the theoretically predicted [7-10] factor-of-two quantum enhancement of the Langevin rate coefficient at collision energies close to zero will be summarized.

References

[1] P. Allmendinger, J. Deiglmayr, J. A. Agner, H. Schmutz, and F. Merkt, Phys. Rev. A **90**, 043403 (2014).
[2] V. Zhelyazkova, M. Žeško, H. Schmutz, J.A. Agner and F. Merkt, Mol. Phys. **117**, 2980 (2019).
[3] P. Allmendinger, J. Deiglmayr, O. Schullian, K. Höveler, J. A. Agner, H. Schmutz, and F. Merkt, ChemPhysChem **17**, 3596 (2016).
[4] P. Allmendinger, J. Deiglmayr, K. Höveler, O. Schullian, and F. Merkt, J. Chem. Phys. **145**, 244316 (2016).
[5] V. Zhelyazkova, F. B. V. Martins, H. Schmutz, J. A. Agner and F. Merkt, Phys. Rev. Lett. 125, 263401 (2020).
[6] K. Höveler, J. Deiglmayr, J.A. Agner, H. Schmutz and F. Merkt, Phys. Chem. Chem. Phys. **23**, 2676 (2021).
[7] E. Vogt and G. H. Wannier, Phys. Rev. **95**, 1190 (1954).
[8] E. I. Dashevskaya, I. Litvin, E. E. Nikitin, and J. Troe, J. Chem. Phys. **122**, 184311 (2005).
[9] B. Gao, Phys. Rev. A **83**, 062712 (2011).
[10] E. I. Dashevskaya, I. Litvin, E. E. Nikitin, and J. Troe, J. Chem. Phys. **145**, 244315 (2016).

*Corresponding author: merkt@phys.chem.ethz.ch

Controlled interactions of cold trapped negative ions

Roland Wester[*1]
1. Institut für Ionenphysik und Angewandte Physik, Universität Innsbruck, Technikerstr. 25, 6020 Innsbruck, Austria

Negatively charged molecular ions have drawn a lot of attention in recent years, in particular owing to the detection of several molecular anions in cold interstellar molecular clouds. Cryogenic radiofrequency ion traps are well suited tools to study the spectroscopy as well as cold collision processes of negative ions with high resolution and high sensitivity.

Using photodetachment spectroscopy we have been able to probe rotational quantum states [1] of cold trapped anions. We have used this to study rotational state-changing collisions of the negative ions OH^- and NH_2^- with neutral helium atoms at low temperature [2,3,4] and to perform rotational terahertz spectroscopy [5,6] and infrared overtone spectroscopy [7]. We have also studied photodetachment of the interstellar anions CN^- and C_3N^- near threshold and used these data to improve the accuracies of the respective electronic affinities [8,9]. For CN^- the data are well described by the Wigner threshold law, if the permanent electric dipole moment of the neutral product is included in the analysis [8]. For C_3N^- the large permanent dipole moment of C_3N leads to a qualitatively different cross section behavior near threshold [10]. Furthermore, the rotational contour of a dipole bound state was resolved slightly below the detachment threshold [9] in agreement with calculations [11]. This state could serve as a doorway state to negative ion formation in interstellar clouds.

Recently, we have developed a two-photon scheme to probe the rotational and vibrational states of the homonuclear anion C_2^-, a candidate that has been proposed for negative ion laser cooling. Results on electronic spectroscopy and vibrational relaxation collisions of this ion will be presented [12].

References

[1] R. Otto, A. von Zastrow, T. Best, R. Wester, Phys. Chem. Chem. Phys. **15**, 612 (2013)
[2] D. Hauser, S. Lee, F. Carelli, S. Spieler, O. Lakhmanskaya, E. S. Endres, S. Kumar, F. Gianturco, R. Wester, Nat. Physics **11**, 467 (2015)
[3] F. A. Gianturco, O. Y. Lakhmanskaya, M. H. Vera, E. Yurtsever, R. Wester, Faraday Discuss. 212, 117 (2018)
[4] E. S. Endres, S. Ndengué, O. Lakhmanskaya, S. Lee, F. A. Gianturco, R. Dawes, R. Wester, Phys. Rev. A (in press)
[5] S. Lee, D. Hauser, O. Lakhmanskaya, S. Spieler, E. S. Endres, K. Geistlinger, S. S. Kumar, R. Wester, Phys. Rev. A **93**, 032513 (2016)
[6] O. Lakhmanskaya, M. Simpson, S. Murauer, M. Nötzold, E. Endres, V. Kokoouline, R Wester, Phys. Rev. Lett. **120**, 253003 (2018)
[7] O. Lakhmanskaya, M. Simpson, R. Wester, Phys. Rev. A **102**, 012809 (2020)
[8] M. Simpson, M. Nötzold, A. Schmidt-May, T. Michaelsen, B. Bastian, J. Meyer, R. Wild, F. A. Gianturco, M. Milovanovic, V. Kokoouline, R. Wester, J. Chem. Phys. 153, 184309 (2020)
[9] M. Simpson, M. Nötzold, F. A. Gianturco, T. Michaelsen, R. Wild, R. Wester, (submitted)
[10] O'Malley, Phys. Rev. **137**, A1668 (1965)
[11] S. V. Jerosimic, M. Z. Milovanovic, R. Wester, F. A. Gianturco, Adv. Quant. Chem. 80, 47 (2019)
[12] M. Nötzold *et al.* (in preparation)

*Corresponding author: roland.wester@uibk.ac.at

Positron binding to molecules: effects of chemical composition and shape

J. P. Cassidy[1], **G. F. Gribakin**[*1], **A. R. Swann**[1]
1. School of Mathematics and Physics, Queen's University of Belfast, Belfast BT7 1NN, Northern Ireland, UK

Positron annihilation in molecules is a fascinating and complex process that involves positron capture in vibrational Feshbach resonances (VFR) [1]. It is facilitated by the ability of polyatomic molecules to bind positrons, while the enhanced annihilation rates reveal the critical importance of anharmonic effects in the vibrational dynamics [2]. Observation of VFRs with a trap-based positron beam enables measurements of the positron binding energies. At present, their values are known for about 90 molecules [1,3,4]. They range from a few meV for small polyatomics (e.g, acetylene C_2H_2), to few hundred meV for large species, such as hexadecane ($C_{16}H_{34}$). By contrast, much less progress has been achieved in calculations of positron-molecule binding. *Ab initio* calculations struggle to predict binding for nonpolar species and the best agreement with experiment is at the 25% level, for acetonitrile [5].

To gain an insight into the problem of positron binding with molecules, we have developed a model-potential method that allows a systematic study for a wide range of molecular species [6,7,8]. In our method, the positron-molecule interaction is described by the potential $V(\mathbf{r}) = V_{\rm st}(\mathbf{r}) + V_{\rm cor}(\mathbf{r})$, where $V_{\rm st}$ is the electrostatic potential of the molecule, and $V_{\rm cor}$ represents positron-molecule correlation interaction. At long range, it describes polarisation of the electron cloud by the positron, $V_{\rm cor}(\mathbf{r}) \sim -\alpha/2r^4$, α being the molecular polarisability. At short range, it accounts for other types of correlations, such as virtual positronium formation. We use the following form [6]:

$$V_{\rm cor}(\mathbf{r}) = -\sum_{A=1}^{N_a} \frac{\alpha_A}{2|\mathbf{r}-\mathbf{r}_A|^4}[1-\exp(-|\mathbf{r}-\mathbf{r}_A|^6/\rho_A^6)], \tag{1}$$

where α_A are atomic hybrid polarizabilities [9], and ρ_A are cutoff radii, and the sum is over the atoms in the molecule. Values of α_A account for the chemical environment of each atom, with $\alpha = \sum_A \alpha_A$. The cutoff factor in square brackets suppresses the potential at distances close to an atomic nucleus, with ρ_A chosen by comparison with experiment or high-quality calculations.

Calculations of the binding energies ε_b for linear alkanes C_nH_{2n+2} using $\rho_{\rm C,H} = 2.25$ a.u., chosen to fit the measured ε_b for dodecane, have provided a good description of the experimental data for n =3–16, including the emergence of the second bound state for $n \geq 12$ [7]. However, the calculated ε_b demonstrated a slower growth for large n. For these molecules, the presence of conformations produced by twisting the carbon backbone turned out to be important. Our calculations show that more compact structures lead to stronger binding, and predict a temperature dependence of the measured ε_b values [8]. A study of chlorinated alkanes [4] demonstrates the critical role that the position of the Cl atoms(s) has on the binding energy for these, mostly polar, molecules, see Fig. 1. Including the nitrogen and oxygen atoms (with their own cutoff radii) allows us to achieve an excellent description of positron binding for nitriles, aldehydes and ketones. Here the difference between the calculated and measured binding energies does not exceed a few percent.

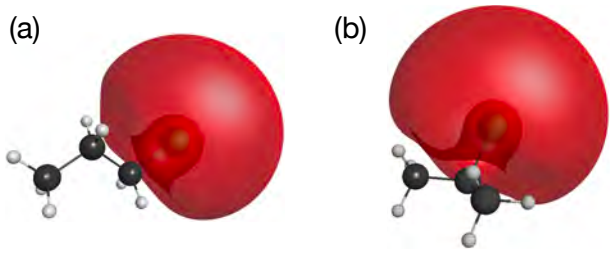

Fig. 1: Positron bound states for (a) *n*-propyl chloride ($\varepsilon_b = 95$ meV) and (b) isopropyl chloride ($\varepsilon_b = 123$ meV).

References

[1] G. F. Gribakin, J. A. Young, and C. M. Surko, Rev. Mod. Phys. **82**, 2557 (2010).
[2] G. F. Gribakin, J. F. Stanton, J. R. Danielson, M. R. Natisin, and C. M. Surko, Phys. Rev. A **96**, 062709 (2017).
[3] J. R. Danielson, A. C. L. Jones, J. J. Gosselin, M. R. Natisin, and C. M. Surko, Phys. Rev. A **85**, 022709 (2012).
[4] A. R. Swann, G. F. Gribakin, J. R. Danielson, S. Ghosh, M. R. Natisin, and C. M. Surko, arXiv:2104.05338.
[5] M. Tachikawa, Y. Kita, R. J. Buenker, Phys. Chem. Chem. Phys. **13**, 2701 (2011); M. Tachikawa, J. Phys. Conf. Ser. **488**, 012053 (2014).
[6] A. R. Swann and G. F. Gribakin, J. Chem. Phys. **149**, 244305 (2018).
[7] A. R. Swann and G. F. Gribakin, Phys. Rev. Lett. 123, 113402 (2019).
[8] A. R. Swann and G. F. Gribakin, J. Chem. Phys. **153**, 184311 (2020).
[9] K. J. Miller, J. Am. Chem. Soc. **112**, 8533 (1990).

*Corresponding author: g.gribakin@qub.ac.uk

Dynamics of excited helium nanodropets: Ultrafast relaxation, ICD, ATI

M. Mudrich*[1], A. C. Laforge[2], R. Michiels[3], Y. Ovcharenko[4], M. Abu-samha[5], L. B. Madsen[1], P. O'Keeffe[6], C. Callegari[7], A. Ciavardini[7], M. Di Fraia[7], O. Plekan[7], K. C. Prince[7], R. J. Squibb[8], R. Feifel[8], J. Eloranta[9], M. Pi[10], M. Barranco[10], T. Möller[4], F. Stienkemeier[3]

1. Department of Physics and Astronomy, Aarhus University, 8000 Aarhus C, Denmark
2. Department of Physics, University of Connecticut, Storrs, Connecticut, 06269, USA
3. Institute of Physics, University of Freiburg, 79104 Freiburg, Germany
4. Institut für Optik und Atomare Physik, Technische Universität, 10623 Berlin, Germany
5. College of Engineering and Technology, American University of the Middle East, Kuwait
6. CNR-ISM, Area della Ricerca di Roma 1, Monterotondo Scalo, Italy
7. Elettra-Sincrotrone Trieste, 34149 Basovizza, Trieste, Italy
8. Department of Physics, University of Gothenburg, Sweden
9. Department of Chemistry and Biochemistry, California State University at Northridge, USA
10. Departament FQA, Facultat de Física, Universitat de Barcelona, Spain

Wavelength-tunable extreme-ultraviolet (XUV) free-electron lasers (FEL) open up new opportunities to study ultrafast dynamics of outer and inner valence-shell excited molecules, clusters and nanoparticles. Here we discuss the dynamics initiated by resonant electronic excitation of superfluid helium nanodroplets probed by time-resolved photoelectron spectroscopy at the seeded FEL Fermi in Trieste, Italy. Three types of ultrafast relaxation are observed in different regimes of the XUV-pump and UV-probe intensity:

1) Ionization by $1+1'$-photon absorption via the resonances centered around $h\nu/e = 21.6$ and 23.8 eV is characterized by a complex relaxation dynamics of the droplets involving ultrafast localization of the excitation, electronic-state relaxation, the formation of a void bubble, and the ejection of an excited He^* atom [1], [2].

2) At pump-pulse intensities $I_{\mathrm{XUV}} \gtrsim 10^9$ Wcm^{-2}, helium nanodroplets are multiply excited. Subsequently, pairs of localized He^* excitations in one droplet autoionize by interatomic Coulombic decay (ICD) [3]. By depleting the excited-state population using a time-delayed probe pulse, we trace the ICD dynamics in time. The resulting ICD time constant, $\tau_{\mathrm{ICD}} = 0.4$-1 ps is surprisingly short and only weakly dependent on the density of He^* in the droplets. Time-dependent density functional (TDDFT) simulations show that the bubbles around each He^* merge if they are formed near each other ($\lesssim 10$ Å) thereby pushing the He^* together and accelerating the ICD reaction [4].

3) At probe-pulse intensities $I_{\mathrm{NIR,UV}} \gtrsim 10^{13}$ Wcm^{-2} and for multiply excited helium nanodroplets we observe efficient above-threshold ionization (ATI), see Fig. 1. Electron emission due to high-order ATI is enhanced by several orders of magnitude compared to gaseous He atoms. The crucial dependence of the ATI intensity on the number of excitations per droplet is interpreted as a local collective enhancement effect [5].

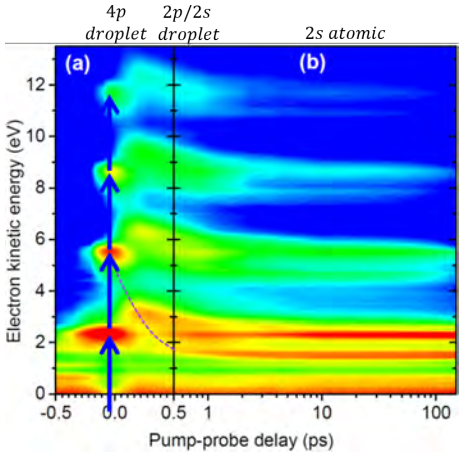

Fig. 1: Typical delay-dependent electron spectra recorded by resonant $1+n'$-photon ionization of helium nanodroplets, where $n = 1$-4. The photon energies of pump and probe pulses were $h\nu/e = 23.8$ eV and $h\nu'/e = 3.2$ eV. Adapted from [5].

References

[1] M. Mudrich *et al.*, Nat. Commun. **11**, 112 (2020).
[2] J. D. Asmussen *et al.*, submitted (arXiv:2103.05948).
[3] A. Kuleff *et al.*, Phys. Rev. Lett. **105**, 043004 (2010).
[4] A. C. Laforge *et al.*, Phys. Rev. X **11**, 021011 (2021).
[5] R. Michiels *et al.*, submitted.

*Corresponding author: mudrich@phys.au.dk

Matter at the nanoscale: study of the structure and dynamics of clusters

Bernd v. Issendorff[*1]
1. Physics Institute, University of Freiburg, 79104 Freiburg, Germany

Clusters and nanoparticles often have properties rather different to those of the corresponding bulk material, which is due to the large surface-to-volume ratio and in general to quantum size effects, the discretization of otherwise continuous densities of states. Especially the latter makes them highly interesting candidates for the study of few to many particle physics. In my talk I will first explain the intricate interplay between electronic and geometric structure in simple metal clusters, which has been clarified by a combination of photoelectron spectroscopy on free, size-selected alkali and noble metal clusters and DFT-calculations [1,2]. Then I will concentrate on two examples of recent findings. The first example is the form of the angular distributions of photoelectrons emitted from simple metal clusters [3]. These turn out to be almost classical, simply reflecting the rotational motion of the electrons within the approximately spherical clusters. It is, however, decohering many-electron dynamics which produces this behaviour via quenching of inferences, providing an interesting example of complex dynamics leading to a very simple result [4]. The second example relates to the dynamics of large silver clusters promptly heated to high temperatures by optical excitation in resonance with the plasmon resonance, as recently studied by time-resolved x-ray scattering at the free electron Laser FLASH within a larger collaboration involving the Technical University of Berlin, the MBI Berlin, the University of Rostock and the University of Freiburg. Depending on the amount of heating the clusters have been observed to melt, to enter a supercritical state where they immediately explode, or to break into larger liquid fragments. The latter could be explained by subsequent molecular dynamics simulations (Moseler group, University of Freiburg and IWM Freiburg), which found a curious soap-bubble-like expansion resulting from a simple classical cavitation effect. These examples illustrate that clusters are close to ideal model systems for the study of a broad range of phenomena.

References

[1] H.Häkkinen, M.Moseler, O.Kostko, N. Morgner, M.Astruc Hoffmann, and B.v. Issendorff, Phys. Rev. Lett. **93**, 093401 (2004).
[2] O. Kostko, B. Huber, M. Moseler, and B. v. Issendorff, Phys. Rev. Lett. **98**, 043401 (2007).
[3] C. Bartels, C. Hock, J. Huwer, R. Kuhnen, J. Schwöbel, B. von Issendorff, Science **323**, 1323 (2009).
[4] A. Piechaczek, Ch. Bartels, Ch. Hock, J.-M. Rost, and B. v. Issendorff, Phys. Rev. Lett., accepted (2021)

[*]Corresponding author: bernd.von.issendorff@uni-freiburg.de

Prospects for constraining temporal variations of fundamental constants with a ^{229}Th-based nuclear frequency standard

L. von der Wense[*1], **C. Zhang** [1], **J. Ye** [1]
1. JILA, National Institute of Standards and Technology and University of Colorado, Boulder, CO, USA

The metastable, first excited state of the ^{229}Th nucleus - usually denoted as ^{229m}Th - has long been in the scientific focus due to its extraordinary low nuclear excitation energy of about 8.1 eV [1], which offers the unique opportunity to perform laser spectroscopy of a nuclear transition thereby also enabling the development of a nuclear frequency standard [2][3]. The laser wavelength required for nuclear laser spectroscopy is about 150 nm, which is technologically challenging, yet feasible to obtain with narrow-bandwidth, as it corresponds to the 7th harmonic of an Yb-doped-fiber frequency comb [4][5].

Due to the combination of recent progress in laser technology [5], improved constraints of the nuclear excitation energy [6][7], and a novel laser excitation scheme [8], laser spectroscopy of ^{229}Th has become feasible within the past couple of years and is now in the focus of several groups worldwide. Once the direct laser excitation of ^{229m}Th is achieved, the development of a nuclear frequency standard will come into reach.

Such a nuclear frequency standard, often times also referred to as the "nuclear optical clock", is expected to have multiple fundamental physics applications [9]. The reason is a predicted extraordinary high sensitivity for variations of fundamental constants, e.g., the fine-structure constant α as well as the dimensionless quark masses [10]. This high sensitivity is caused by a large sensitivity enhancement factor, which was recently estimated to be on the order of 10^4 [11], where atomic shell transitions - used for today's most stringent constraints of temporal variations of fundamental constants [12] - exhibit typical enhancement factors between 1 and 10. A sensitivity enhancement factor of about 10^4, in combination with a small expected inaccuracy of a nuclear clock of 10^{-19} [3], offers the potential to probe temporal variations of fundamental constants at the 10^{-23} level, a five orders of magnitude improvement compared to the currently most stringent constraints [11].

In this presentation an overview of the current status of nuclear optical clock development will be provided with a special focus on the work carried out in our group at JILA.

This work is supported by AFOSR Grant No. FA9550-19-1-0148, ARO Grant No. W911NF2010182, NSF Grant No. PHY-1734006 and the National Institute of Standards and Technology. Lars v.d.Wense acknowledges support from the Alexander von Humboldt Foundation.

References

[1] L. von der Wense, B. Seiferle, *The ^{229}Th isomer: prospects for a nuclear optical clock*, Eur. Phys. J. A **56**, 277 (2020).
[2] E. Peik, C. Tamm, *Nuclear laser spectroscopy of the 3.5 eV transition in ^{229}Th*, Eur. Phys. Lett. **61**, 181 (2003).
[3] C.J. Campbell et al., *Single-Ion nuclear clock for metrology at the 19th decimal place*, Phys. Rev. Lett. **108**, 120802 (2012).
[4] A. Cingöz et al., *Direct frequency comb spectroscopy in the extreme ultraviolet*, Nature **482**, 68-71 (2012).
[5] C. Zhang et al., *Noncollinear Enhancement Cavity for Record-High Out-Coupling Efficiency of an Extreme-UV Frequency Comb*, Phys. Rev. Lett. **125**, 093902 (2020).
[6] B. Seiferle et al., *Energy of the ^{229}Th nuclear clock transition*, Nature **573**, 243-246 (2019).
[7] T. Sikorsky et al., *Measurement of the ^{229}Th isomer energy with a magnetic micro-calorimeter*, Phys. Rev. Lett. **125**, 142503 (2020).
[8] L. von der Wense, C. Zhang, *Concepts for direct frequency-comb spectroscopy of ^{229m}Th and an internal-conversion-based solid-state nuclear clock*, Eur. Phys. J. D **74**, 146 (2020).
[9] P.G. Thirolf et al., *Improving our knowledge on the ^{229m}Thorium isomer: Toward a test bench for time variations of fundamental constants*, Ann. Phys. (Berlin) 1800381 (2019).
[10] V.V. Flambaum, *Enhanced effect of temporal variation of the fine structure constant and the strong interaction in ^{229}Th*, Phys. Rev. Lett. **97**, 092502 (2006).
[11] P. Fadeev et al., *Sensitivity of ^{229}Th nuclear clock transition to variation of the fine-structure constant*, Phys. Rev. A **102**, 852833 (2020).
[12] R. Lange et al., *Improved limits for violations of local position invariance from atomic clock comparisons*, Phys. Rev. Lett. **126**, 011102 (2021).

*Corresponding author: lars.vonderwense@colorado.edu

Hong-Ou-Mandel Interference via quantum non-demolition gate between atoms and mechanics

A. D. Manukhova[*1], **A. A. Rakhubovsky**[1], **R. Filip**[1]
1. Department of Optics, Palacký University, 17. Listopadu 12, 771 46 Olomouc, Czech Republic

Quantum coupling between mechanical oscillators and atoms has been recently experimentally demonstrated using their subsequent interaction with light [1-2]. The next step is to build a hybrid atom-mechanical quantum gate showing bosonic interference effects of single quanta. We propose an experimental test of Hong-Ou-Mandel (HOM) interference between single phononic excitation and single collective excitation of atoms using the optical connection between them. A single optical pulse is sufficient to build a hybrid gate to observe the bunching of these two excitations.

The basic principle to realize the quantum non-demolition (QND) gate between a cloud of atoms and a mechanical mode of an optomechanical cavity is as follows [3]. A squeezed quantum field accompanied by strong classical fields sequentially passes through the atomic ensemble, located in the cavity, and the optomecanical cavity. We assume both intracavity interactions are QND-type characterized by controllable coupling rates. The gate with the gain G relates the quantum states of the atoms and mechanics after the interactions with their initial states and the noises and transforms the initial quadratures $\mathbf{r}^{\text{in}} = (\hat{\mathbf{X}}_a^0, \hat{\mathbf{P}}_a^0, \hat{\mathbf{X}}_m^0, \hat{\mathbf{P}}_m^0)^T$ to the final quadratures $\mathbf{r}^{\text{out}} = (x_a, p_a, x_m, p_m)^T$ as:

$$x_a = \hat{\mathbf{X}}_a^{\text{out}} = \mathfrak{T}_a \hat{\mathbf{X}}_a^0 - \mathsf{G}\,\hat{\mathbf{X}}_m^0 + \hat{\mathbf{N}}_{X_a}, \qquad x_m = \hat{\mathbf{X}}_m^{\text{out}} = \mathfrak{T}_m \hat{\mathbf{X}}_m^0 + \hat{\mathbf{N}}_{X_m}, \tag{1}$$

$$p_a = \hat{\mathbf{P}}_a^{\text{out}} = \mathfrak{T}_a \hat{\mathbf{P}}_a^0 + \hat{\mathbf{N}}_{P_a}, \qquad p_m = \hat{\mathbf{P}}_m^{\text{out}} = \mathfrak{T}_m \hat{\mathbf{P}}_m^0 + \mathsf{G}\,\hat{\mathbf{P}}_a^0 + \hat{\mathbf{N}}_{P_m}. \tag{2}$$

We demonstrate the possibility to observe an analogue of the HOM interference using the gate.

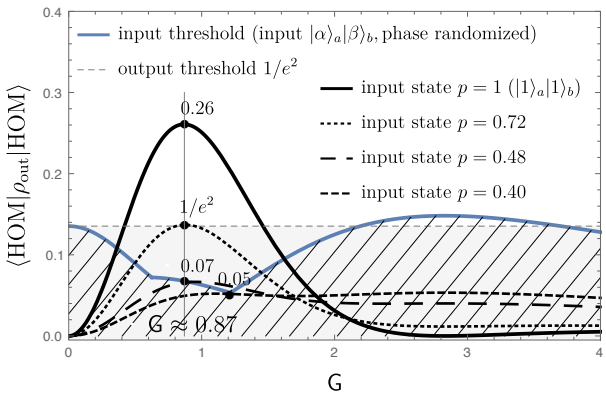

Fig. 1: $\langle \text{HOM}|\rho_{\text{out}}|\text{HOM}\rangle$ matrix element of the output state for the ideal QND gate as a function of the gain G calculated for the different cases of the input: quantum input $|1\rangle_a|1\rangle_b$ (solid black curves), mixture input $(p\,|1\rangle\langle 1| + (1-p)\,|0\rangle\langle 0|)_a \cdot (p\,|1\rangle\langle 1| + (1-p)\,|0\rangle\langle 0|)_b$ (dashed black curves, dashing scale indicates parameter p). Dashed gray line is the *output threshold*. Blue curve is the *input thresholds* (phase randomized) restricting area that covers all the possible values of the matrix elements of the output state of the gate in the case of the random coherent input with averaged phases. Here, the HOM state is defined as $|\text{HOM}\rangle = (|0\rangle_a|2\rangle_b - |2\rangle_a|0\rangle_b)/\sqrt{2}$.

We consider the HOM effect as a bunching of two excitations in one of the interacting subsystems. We demonstrate the nonclassical HOM effect, i.e. the buildup of the bunched HOM state via the second-order interference. As the input we assume incoherent mixture of vacuum and single-boson states. We investigate the dependences of the HOM matrix element of the output state on the parameters of the gate and compare it to the HOM element corresponding to the classical coherent cases using two nonclassicality thresholds (see Fig. 1).

The output atomic-mechanical state exhibits a probability of a hybrid bunching effect that proves its nonclassical aspects. This proposal opens a feasible road to broadly test such advanced quantum bunching phenomena in a hybrid system with different specific couplings.

References

[1] R . A. Thomas, M. Parniak, C. Østfeldt, C. B. Møller, C. Bærentsen, Y. Tsaturyan, A. Schliesser, J. Appel, E. Zeuthen, and E. S. Polzik, Entanglement between Distant Macroscopic Mechanical and Spin Systems, *Nature Physics* **17**, pp. 228-233 (2021).
[2] T . M. Karg, B. Gouraud, C. T. Ngai, G.-L. Schmid, K. Hammerer, and P. Treutlein, Light-Mediated Strong Coupling between a Mechanical Oscillator and Atomic Spins 1 Meter Apart, *Science* **369**, pp. 174-179 (2020).
[3] A . D. Manukhova, A. A. Rakhubovsky, and R. Filip, Pulsed atom-mechanical quantum non-demolition gate, *Nature* Quantum Information **6**(4) (2020).

*Corresponding author: alisamanukhova@gmail.com, alisadmitrievna.manukhova@upol.cz

A versatile quantum simulator for coupled oscillators using a 1D chain of atoms trapped near an optical nanofiber

Daniela Holzmann[*1], **Matthias Sonnleitner**[1], **Helmut Ritsch**[1]
1. Institute for Theoretical Physics, University of Innsbruck, Technikerstraße 25, A-6020 Innsbruck, Austria

The transversely confined propagating light modes of a nano-photonic optical waveguide or nanofiber mediate effectively infinite-range forces between quantum particles. We show that for a linear chain of particles trapped within the waveguide's evanescent field, transverse illumination with a suitable set of laser frequencies allows the implementation of a coupled-oscillator quantum simulator with time-dependent and widely controllable all-to-all interactions. At the example of the energy spectrum of oscillators with simulated Coulomb interactions we show that different effective coupling geometries can be emulated with high precision by proper choice of laser illumination conditions. Similarly, basic quantum gates can be implemented between arbitrary pairs of oscillators in the energy basis as well as in a coherent state basis. Key properties of the system dynamics and states can be monitored continuously by analysis of the out-coupled fiber fields.

[*]Corresponding author: daniela.holzmann@uibk.ac.at

Measurement-Induced Entanglement Transitions and the Quantum Zeno effect: non-Hermitian physics at play

X. Turkeshi[1,2,3], **A. Biella***[4,5], **R. Fazio**[2,6], **M. Dalmonte**[1,2], **M. Schiró** [3]

1. SISSA, via Bonomea 265, 34136 Trieste, Italy

2. ICTP, strada Costiera 11, 34151 Trieste, Italy

3. JEIP, USR 3573 CNRS, Collège de France, PSL Research University, 11 Place Marcelin Berthelot, 75321 Paris Cedex 05, France

4. Université Paris-Saclay, CNRS, LPTMS, 91405 Orsay, France

5. INO-CNR BEC Center and Dipartimento di Fisica, Università di Trento, 38123 Povo, Italy

6. Dipartimento di Fisica, Universitá di Napoli "Federico II", Monte S. Angelo, I-80126 Napoli, Italy

We investigate measurement-induced phase transitions in the paradigmatic Quantum Ising chain coupled to a monitoring environment. The dynamics alternates the unitary coherent evolution with random local measurements. This interplay allows the emergence of a sharp transition from a *critical* phase with a logarithmic scale of the entanglement entropy to an area-law phase as the measurement rate is increased [1]. We show that the non-Hermitian Hamiltonian arising from the postselected *no-click* dynamics and its associated subradiance spectral transition provide a natural framework to understand both the extended critical phase, emerging here for a model which lacks any continuous symmetry, and the entanglement transition into the area law. The non-Hermitian Hamiltonian also provide a natural framework to grasp the emergence of the Quantum Zeno effect in the rare events of the dynamics [2].

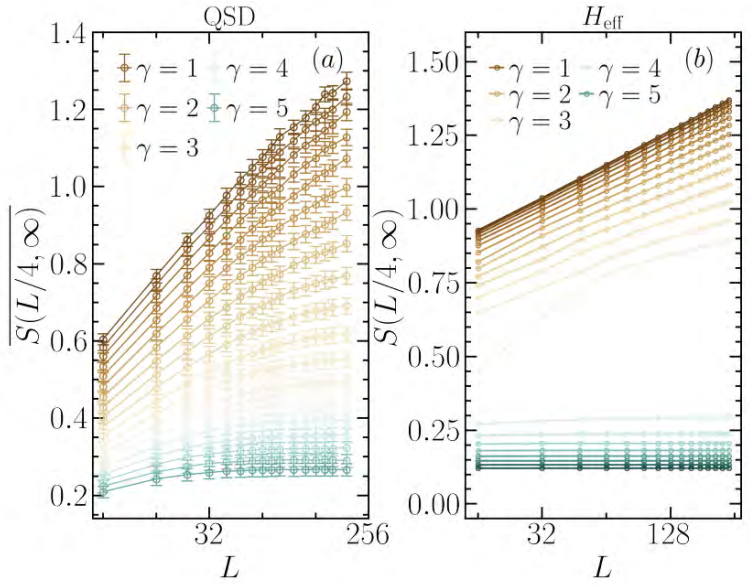

Fig. 1: Stationary-state entanglement entropy as a function of the length of the chain. (a) Average entanglement entropy for the quantum state diffusion protocol. (b) Long-time entanglement entropy for the non-Hermitian dynamics. In both cases we see a transition from a logarithmic *critical* scaling, for small measurement rate γ to an area law (constant) scaling at large γ. Different curves in the two panels correspond to increasing values of γ, from $\gamma = 0.25$ (top curve) to $\gamma = 6$ (bottom curve) with a $\Delta\gamma = 0.25$.

References

[1] X. Turkeshi, A. Biella, R. Fazio, M. Dalmonte and M. Schiro, arXiv:2103.09138 (2021).

[2] A. Biella and M. Schiró, arXiv:2011.11620 (2020).

*Corresponding author: alberto.biella@universite-paris-saclay.fr

The new mathematical model of photons

I. Bersons[1], **R. Veilande**[*1], **O.Balcers**[2]
1. Institute of Atomic Physics and Spectroscopy, University of Latvia, Riga, Latvia
2. Engineering Faculty, Vidzeme University of Applied Sciences, Valmiera, Latvia

Recently the interest for single photon technologies has rapidly increased because it is considered the main element in quantum communication technologies. But a question remains: what is a photon? In 1927 Dirac [1] proposed the quantization procedure for the Maxwell equations which was reduced to quantization of an infinite number of linear harmonic oscillators. The quantization procedure provides the correct energy and momentum of the photon and perfectly describes the creation and annihilation of photons. The quantization of the field is the cornerstone of the quantum field theory and, especially, quantum electrodynamics. Despite the great success of the quantization of light, the physics of this procedure is not so clear: what is there that oscillates and where are photons located in time and space? The definition of a photon as a first excited state of a single mode of the quantized electromagnetic field is rather abstract.

Several nonlinear equations with the electromagnetic soliton type solution were proposed [2]-[4]. A soliton is a stable formation that doesn't dissolve in space and time similar to a photon. In these models the non-linearity in the Maxwell equations is introduced by small, finite components of polarization and magnetization in a vacuum along the direction of the propagation of light.

Developing the photon models, we find the possibility to define the vector potential A_k of the field which describes the free propagation of photons [5]. The vector potential obeys two separate linear equations: one looks like the Schrödinger equation for the harmonic oscillator with the longitudinal coordinate $\eta_k = \omega t - kr$ and the second is a simple equation for polar radius ρ_k. The vector potential for one-mode $n-$photon state looks like:

$$A_{kn} = k\sqrt{\frac{\hbar c\mu}{s\sqrt{\pi}2^{n-2}n!}}H_n(s\eta_k)\exp\left(-\frac{s^2\eta_k^2}{2}-\mu\tau_k\right).$$

where $\tau_k = k^2\rho_k^2/2$ and the normalization constant is found by equating the field energy to the Plank defined energy $\hbar\omega(n+1/2)$. In the proposed model there is another vector potential, the operator, which contains the annihilation and creation operators. This vector potential describes the interaction of photons with the charged particle and looks similar as in the traditional quantization procedure.

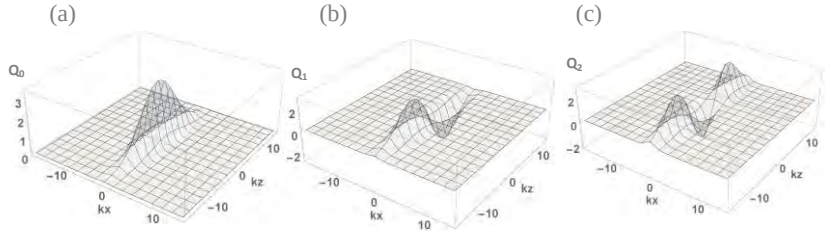

Fig. 1: The cross-section of the dimensionless functions $Q_n = A_{kn}/(k\sqrt{\hbar c})$ of the vacuum, one- and two- photons state for the parameters $s = 0.2$, $\mu = 1$ and $t = 0$ are depicted.

The obtained function contains two unknown dimensionless parameters s and μ, which determine the longitudinal and transverse size of photons. If we assume that the radius of photons is of the order of their wavelength, so the constant μ is of the order of unity, but s is small. Of course, the proposed model is only a model, and it should be tested in different processes where photons participate.

RV has been supported by ERDF project No. 1.1.1.1/18/A/155.

References

[1] P. A. M. Dirac, Proc. R. Soc. London **114**, 243 (1927).
[2] I. Bersons, Latv. J. Phys. Tech. Sci. **50**, 2, 60 (2013).
[3] I. Bersons, R. Veilande, and O. Balcers, Phys. Scr. **91**, 065201 (2016).
[4] I. Bersons, R. Veilande, and O. Balcers, Phys. Scr. **95**, 025203 (2020).
[5] I. Bersons, R. Veilande, and O. Balcers, "Mathematical models of photons" submitted to the Journal of Mathematical Physics.

*Corresponding author: rita.veilande@lu.lv

Optimization of the quantum random walk search algorithm

H. Tonchev[*1], **P. Danev**[2]
1. Institute of Solid-State Physics, Bulgarian Academy of Science, Sofia, Bulgaria
2. Institute for Nuclear Research and Nuclear Energy, Bulgarian Academy of Science, Sofia, Bulgaria

The quantum random walk search algorithm [1] is a probabilistic quantum algorithm that is quadratically faster than any classical search algorithm. This algorithm is based on the quantum analogue of classical random walk [2]. The algorithm uses an oracle, that can recognize the solution, and two coins – one to be applied to mark the searched element and one to be applied on the unmarked elements. The shift operator is used to traverse through vertex states, depending on the state of the coin. This quantum algorithm can be used to search in a database with arbitrary topology.

In our work we optimize the coins of quantum random walk search algorithm by using numerical methods, including machine learning to increase the probability to find the searched element in the quantum register. This work is a continuation of our previous study of the quantum random walk search algorithm [3].

This work was supported by the Bulgarian Science Fund under contract KP-06-M48/2 /26.11.2020.

References

[1] N. Shenvi, J. Kempe, and K. B. Whaley, "Quantum random-walk search algorithm," Phys. Rev. A, vol. 67, no. 5, p. 052307, May 2003, doi: 10.1103/PhysRevA.67.052307.
[2] J. Kempe, "Quantum Random Walks Hit Exponentially Faster," arXiv:quant-ph/0205083, May 2002, Available: http://arxiv.org/abs/quant-ph/0205083.
[3] H. Tonchev, "Alternative Coins for Quantum Random Walk Search Optimized for a Hypercube," Journal of Quantum Information Science, vol. 05, no. 01, p. 6, Mar. 2015, doi: 10.4236/jqis.2015.51002.

*Corresponding author: htonchev@issp.bas.bg

Implementing Hamiltonians on a Rydberg Quantum Simulator

H. J. Williams[*1], **P. Scholl**[1], **G. Bornet**[1], **D. Barredo**[2], **T. Lahaye**[1], **A. Browaeys**[1]
1. Université Paris-Saclay, Institut d'Optique Graduate School, CNRS, Laboratoire Charles Fabry
2. Nanomaterials and Nanotechnology Research Center, Universidad de Oviedo

Quantum simulation using synthetic systems is a promising route to solve outstanding quantum many-body problems in regimes where classical approaches fail. Here I will present recent results on the implementation of various Hamiltonians using individually trapped Rydberg atoms. With our platform we are able to create defect-free arrays of up to 200 atoms in arbitrary geometries [1]. The atoms can then be made to interact by exciting them to the Rydberg manifold. Depending on the chosen states, the atoms either interact via the van der Waals or the dipole-dipole coupling. These two types of interaction allow us to implement different Hamiltonians.

The van der Waals interaction causes the Rydberg blockade, whereby two neighbouring atoms cannot be excited into the same Rydberg state. This leads to a natural implementation of the transverse field quantum Ising model (Eq. 1) where a laser field couples the two spin states $|\uparrow\rangle$ and $|\downarrow\rangle$, with a Rabi frequency Ω and detuning δ acting as transverse and longitudinal fields, respectively. Here $U_{ij} = C_6/r_{ij}^6$ is the van der Waals interaction between atom i and j, with a separation of r_{ij}, $n_i = (1+\sigma_i^z)/2$, and σ_i are the usual Pauli matrices. I will present our results from this model on triangular and square arrays (Fig.1) which exhibit qualitatively different phases [2].

$$H_{\mathrm{TFI}} = \sum_{i<j} U_{ij} n_i n_j + \frac{\hbar\Omega}{2}\sum_i \sigma_i^x - \hbar\delta\sum_i n_i. \tag{1}$$

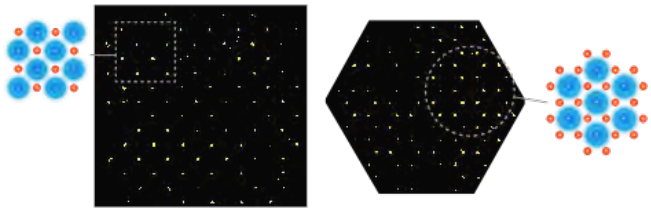

Fig. 1: Single shot fluorescence images showing the implementation of the transverse field Ising Model on a square and a triangular array, with illustrations showing the ordering via the Rydberg blockade with Rydberg atoms in blue and ground state in red.

The dipole-dipole interaction between two Rydberg states leads to a natural implementation of the XY model, with an interaction strength $J_{ij} = C_3(-\cos(\theta_{ij}))/2r_{ij}^3$, where θ_{ij} is the angle between the interatomic axis and the quantisation axis. By using this interaction in combination with external driving fields (here sequential microwave pulses around different axes), the Average Hamiltonian Theory allows us to implement XXZ Hamiltonians with controllable anisotropy (Eq. 2)[3]. The values of δ are controlled by the timings between pulses. I will present our preliminary results from this work.

$$H_{\mathrm{XYZ}} = \frac{2}{3}\sum_{i,j} J_{ij}(\delta_x\sigma_i^x\sigma_j^x + \delta_y\sigma_i^y\sigma_j^y + \delta_z\sigma_i^z\sigma_j^z). \tag{2}$$

References

[1] K.-N. Schymik, *et al.*, *Phys. Rev. A* **102**, 063107 (2020)
[2] P. Scholl, *et al.*, arXiv:2012.12268, to be published.
[3] J. Choi, *et al.*, *Phys. Rev. X* **10**, 031002 (2020)

[*]Corresponding author: hannah.williams@institutoptique.fr

Construction of strontium quantum gas microscope to study relaxation dynamics in 2D lattice gases

Sayali Shevate[*1], **Clémence Briosne-Fréjaville**[1], **Romaric Journet**[1], **Anaïs Molineri**[1], **Félix Faisant**[1], **Florence Nogrette**[1], **Marc Cheneau**[1]

1. Laboratoire Charles Fabry, Institut d'Optique Graduate School, CNRS, Université Paris-Saclay, F-91120, Palaiseau, France

Describing the relaxation dynamics of closed quantum systems far from equilibrium in greater than one dimension poses a formidable challenge to many-body physics as the existing numerical and analytical approaches have severe limitations and so far, most of the efforts have been done in one dimensional systems [1]. In this poster, we will discuss the construction of our novel experimental apparatus based on ultracold strontium-84 atoms, that aims to observe, characterize and interpret the relaxation dynamics in the quantum critical regime of the 2D Bose–Hubbard model as shown in figure 1. The observation and characterization will be performed by experimentally measuring the evolution of equal-time two-point density correlations after a quench. The experimental protocol is well established in the early experiment conducted on a 1D system [1].

This poster presents the current state of our experiment where we successfully demonstrate the generation of both kinds of magneto-optical traps of strontium - 1) along its wide transition at 461 nm and 2) along its narrow transition at 689 nm. Due to the narrow linewidth transition of 7 kHz, strontium is a promising candidate for efficient laser cooling. The next steps in our experiment will include the implementation of a quantum gas microscope which is a high resolution imaging system with single site resolution and single atom sensitivity that will enable the direct measurement of the two-point density correlations.

With the motivation to better understand the link between the elementary excitations and the relaxation dynamics, we will perform a series of experiments in which a 2D degenerate gas of strontium-84 atoms is loaded in a square optical lattice and then the lattice depth will be changed abruptly. In doing so, we are going to explore different regimes that are outside and inside the quantum critical region. Outside the quantum critical regime, the excitations have quasiparticle nature which drive the relaxation dynamics such as the ballistic spreading of correlations whereas inside the quantum critical regime, the nature of the collective excitations is more complex, less-explored and it differs strongly than the quasiparticle. Exploring these complex collective excitations is our main interest. These studies may find interesting applications in, for example, revealing the entanglement carried by quasiparticle pairs [1] and engineering of the efficient quantum channels necessary for fast quantum computations [2].

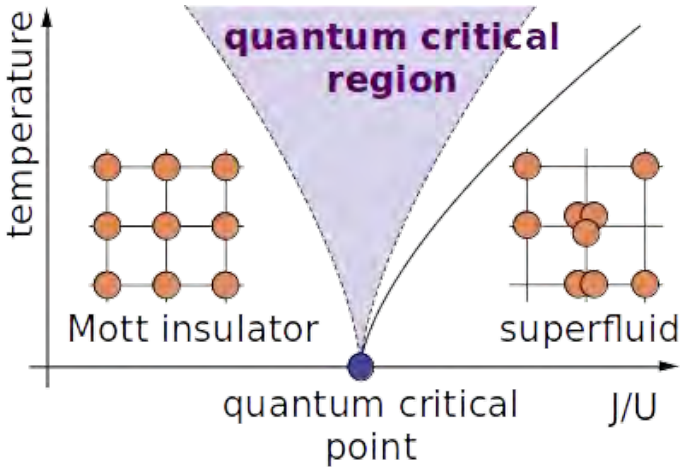

Fig. 1: The quantum critical region of the 2D Bose–Hubbard model. At a critical value of the ratio J/U between the tunnel coupling J and the on-site interaction energy U, the nature of the ground state changes from insulating to superfluid. Above this quantum critical point is the quantum critical region, where the elementary excitations can not be described as quasi-particles. The solid line to the right of the quantum critical point marks the transition from a superfluid to a normal gas. Figure adapted from [3].

References

[1] M. Cheneau, *et al.*, Light-cone-like spreading of correlations in a quantum many-body system, Nature **481**, 484 (2012).
[2] S. Bose. Quantum communication through spin chain dynamics: an introductory overview. Contemp. Phys. **48**, 13–30 (2007).
[3] Witczak-Krempa, *et al.*, The dynamics of quantum criticality via Quantum Monte Carlo and holography. Nat. Phys. **10**, 361 (2014).

*Corresponding author: sayali.shevate@institutoptique.fr

Qubit controlled by the magnetic dark soliton

S. Varbev*, **I. Boradjiev, R. Kamburova, H. Chamati**

1. Institute of Solid State Physics, Bulgarian Academy of Sciences, Tzarigradsko chaussée 72, 1784 Sofia, Bulgaria

The influence of a soliton propagating along an isotropic Heisenberg ferromagnetic spin chain on the state of a spin-$\frac{1}{2}$ localized particle embodying a qubit is studied. The Hamiltonian of the considered system reads [1, 2]

$$\hat{H} = -J\sum_n \hat{\mathbf{S}}_n \cdot \hat{\mathbf{S}}_{n+1} + \left[(\mu - \nu)H_0 - d_z\hat{S}_j^z\right]\hat{\sigma}^z - \frac{d_{xy}}{2}\left(\hat{S}_j^+\hat{\sigma}^- + \hat{S}_j^-\hat{\sigma}^+\right), \tag{1}$$

where $\hat{\mathbf{S}}_n$ are the spin vector operators, $J > 0$ is the spin-spin exchange integral, $\hat{\sigma}$ is the spin-$\frac{1}{2}$ vector operator of the qubit, H_0 is the external magnetic field in the z-direction, μ and ν are the magnetic moments per spin in the chain's sites and the qubit, respectively, d_{xy} and d_z are qubit-chain coupling parameters. In (1) the first term describes intra-spin chain interaction in the nearest neighbour approximation. The rest of the Hamiltonian corresponds to the qubit interaction with $j-$th chain spin and H_0.

In the semi–classical approximation, for large spin and wide excitations, neglecting the qubit influence on the spin chain, an isotropic Heisenberg ferromagnetic admits a dark soliton solution. Then, the qubit state dynamics is described by the two state time-dependent Schrödinger equation

$$i\frac{d}{dt}|\psi\rangle = \left[\Delta(t)\,\hat{\sigma}^z + \frac{\Omega(t)}{2}\left(\hat{\sigma}^- + \hat{\sigma}^+\right)\right]|\psi\rangle, \tag{2}$$

where the coupling $\Omega(t)$ and the detuning $\Delta(t)$ depend on the parameters of the dark soliton propagating at constant velocity and of the qubit-chain couplings d_{xy} and d_z. Analyzing Eq. (2), we established the parameter space, where we can control the state of the qubit and obtained different evolutionary patterns as switching $\frac{1}{2}$-spin as well as switching with consecutive $\frac{1}{2}$-spin return and superposition [3].

References

[1] S. Varbev, R. Kamburova, M. Primatarowa, J. Phys. Conf. Ser. **1186**, 12016 (2019).
[2] S. Varbev, I. Boradjiev, R. Kamburova, H. Chamati, J. Phys. Conf. Ser. **1762**, 1, 012018 (2021).
[3] S. Varbev, I. Boradjiev, R. Kamburova, and H. Chamati, in preparation.

*Corresponding author: stanislavvarbev@issp.bas.bg

Interactions and dynamic of two ultracold highly-magnetic atoms in a harmonic trap

M. Suchorowski[*1], **A. Dawid**[†1,2], **M. Tomza**[‡1]
1. Faculty of Physics, University of Warsaw, Warsaw, Poland
2. ICFO - Institut de Ciències Fotòniques, The Barcelona Institute of Science and Technology, Castelldefels, Spain

Since Bose-Einstein condensation had been first observed in a gas of chromium [1], dysprosium [2] and erbium [3], physicists have been extensively studying ultracold highly magnetic atoms with a large magnetic dipole moment and anisotropic long-range interactions. Quantum phase transitions of the extended Bose-Hubbard model [4], the quantum chaos [5], the existence of the roton mode [6] or the emergence of the self-bound droplets [7] were discovered in experiments with these ultracold atoms. Such exciting applications make these systems a fascinating field also for theoretical investigation.

We theoretically investigate the properties and dynamics of two ultracold highly magnetic atoms in a one-dimensional harmonic trap in the external magnetic field by means of exact diagonalization. Atoms interact via magnetic dipole-dipole interaction, which in one-dimensional limit can be approximated by effective contact spin-spin interaction [8]. We show how interactions and magnetic field impact the properties of the system and observe its dynamic after a sudden change of these parameters. We look at ground-state magnetization which can act as a guide into potential magnetic properties of a many-body system. Our research gives new insights into the possible application of highly magnetic atoms trapped in optical tweezers or optical lattice for simulations of quantum many-body systems.

References

[1] A. Griesmaier *et al.*, Phys. Rev. Lett. **94**, 160401 (2005).
[2] M. Lu *et al.*, Phys. Rev. Lett. **107**, 190401 (2011).
[3] K. Aikawa *et al.*, Phys. Rev. Lett. **108**, 210401 (2012).
[4] S. Baier *et al.*, Science **352**, 201-205 (2016).
[5] A. Frisch *et al.*, Nature **507**, 475–479 (2014).
[6] L. Chomaz *et al.*, Nature Physics **14**, 442-446 (2018).
[7] M. Schmitt *et al.*, Nature **539**, 259–262 (2016).
[8] F. Deuretzbacher *et al.*, Phys. Rev. A **81**, 063616 (2010).

[*]Corresponding author: m.suchorowsk@student.uw.edu.pl
[†]Corresponding author: anna.dawid@fuw.edu.pl
[‡]Corresponding author: michal.tomza@fuw.edu.pl

Sequential phonon measurements of atomic motion

Atirach Ritboon[*1], **Lukas Slodicka**[†1], **Radim Filip**[‡ 1]
1. Department of Optics, Palacky University, 17. listopadu 12, 771 46 Olomouc, Czech Republic

Quantum motion of trapped atoms plays a vital role in various active research fields, including quantum sensing [1], quantum simulation [2], quantum computing [3] and quantum thermodynamics [4]. Highly sensitive phonon measurements are not only much in demand and crucial, regardless of their limited dynamic ranges, but also challenging. This is similar to the case of photon counting, in which multiplexed single-photon detections gave rise to further development of powerful techniques for light detection despite their limited photon number resolution [5]. For trapped atoms, phonons are conventionally measured by coupling them with discrete internal levels, which are optically detectable [6]. The reliability and stability of the overall procedure are very essential in the same way as reliable and stable beam splitters are essential to photon counting.

As available information in a few electronic levels about the phonons is limited, the coupling needs to be sequentially repeated to further harvest the remaining information. We analyze such phonon measurements on the simplest example of the force and heating sensing using recently mastered mechanical Fock states as a probe. The protocol is summarized in the form of a quantum circuit depicted in Fig. 1. We prove that two sequential measurements are sufficient to reach sensitivity to force and heating for realistic Fock states and saturate the quantum Fisher information. It is achieved by the most reliable Jaynes-Cummings coupling. Further enhancements are expect applications of sequential

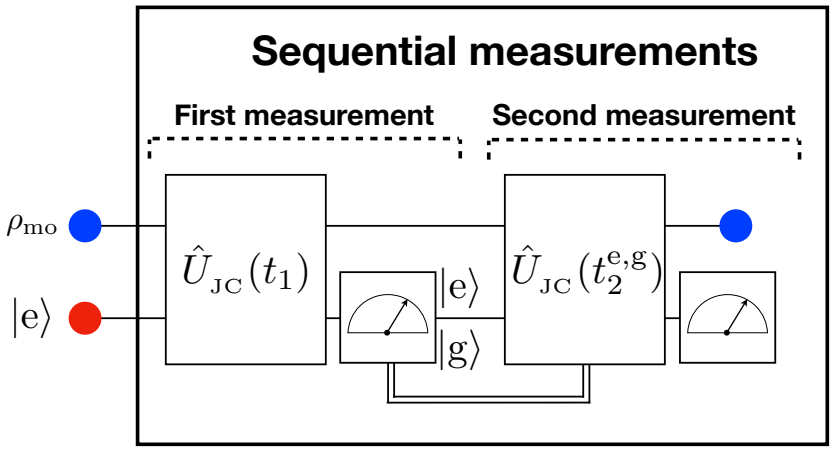

Fig. 1: The quantum circuit for two sequential measurements of the motional state $\rho_{\rm mo}$. The most basic Jaynes-Cummings interactions between the internal qubit, initially prepared in the excited state $|{\rm e}\rangle$, and the motional state of trapped ions are described by two unitary operators $\hat{U}_{\rm JC}$. The second interaction is adaptive as its interaction time $t_2^{\rm e,g}$, is chosen depending on the outcome of the first measurement.

References

[1] F. Wolf *et al.*, Nat. Commun. **10**, 1-8 (2019).
[2] R. Blatt and C. F. Roos, Nat. Phys. **8**, 277-284 (2012).
[3] H. Häffner, C. F. Roos and R. Blatt, Phys. Rep. **469**, 155-203 (2008).
[4] G. Huber *et al.*, Phys. Rev. Lett. **101**, 070403 (2008).
[5] C. Silberhorn, Contem. Phys. **48**, 143-156 (2007).
[6] D. J. Wineland, J. Res. Natl. Inst. Stand. Technol. **103**, 259 (1998).

*Corresponding author: atirach.ritboon@upol.cz
†Corresponding author: slodicka@optics.upol.cz
‡Corresponding author: filip@optics.upol.cz

Quantum Monte Carlo study of trapped Bose-Bose mixtures at zero and finite temperature

K. Dželalija[1], **V.Cikojević**[1,2], **J. Boronat**[2], **L.Vranješ Markić**[*1]

1. Faculty of Science, University of Split, R. Boškovića 33, HR-21000 Split, Croatia

2. Departament de Física, Campus Nord B4-B5, Universitat Politècnica de Catalunya, E-08034 Barcelona, Spain

We present a study of termal properties of dilute harmonically confined repulsive Bose-Bose mixture using quantum Monte Carlo methods [1]. Our results are obtained in the regime which was previously estimated as universal [2], so we do not expect them to depend on the model of the interaction potential.

We focus on temperature dependence of the superfluid density and the condensate fraction in three phases which confined Bose-Bose mixtures manifest, mixed, shell and two-blobs regime. To this end, we use the d-iffusion Monte Carlo method, in the zero-temperature limit, and the path-integral Monte Carlo method for finite temperatures. The results obtained for density profiles are compared with solutions of the coupled Gross-Pitaevskii equations for the mixture at zero temperature.

We notice the existence of an anisotropic superfluid density in the two-blobs regime. Namely, in the limit of zero temperature, the superfluid fraction is 1 when calculated with respect to the axis which passes through both components' center of mass, but below 0.5 when calculated with respect to an axis which passes through the total center of mass and is perpendicular to the previous axis. In the other two regimes the superfluidity is isotropic.

Our results also show noteworthy situations where the superfluid fraction becomes smaller than the condensate fraction when temperature increases. This effect is also observed in a single species simulation with the same interparticle interaction strength; if the strength is increased, the crossing of condensate and superfluid fraction disappears.

References

[1] K. Dželalija, V. Cikojević, J. Boronat, L. Vranješ Markić, Phys. Rev. A **102** 063304 (2020).

[2] V. Cikojević, L. Vranješ Markić, J. Boronat, New Journal of Physics, **20**, 085002 (2018).

[*]Corresponding author: leandra@pmfst.hr

Phase diagram of matter-wave jets

T. Mežnaršič[*1], **R. Žitko**[1,2], **K. Gosar** [1], **K. Arh** [1], **M. Jug** [1], **E. Zupanič** [1], **P. Jeglič**[†1]
1. Jožef Stefan Institute, Jamova 39, SI-1000 Ljubljana, Slovenia
2. University of Ljubljana, Faculty of Mathematics and Physics, Jadranska 19, Ljubljana, Slovenia

Matter-wave jets are emitted from a Bose-Einstein condensate as a consequence of periodic modulation of interatomic interaction via a Feshbach resonance [1, 2]. In quasi-1D geometry, trapped by a single dipole beam, they occupy a single angular mode, limiting the possible higher order processes [3]. Here we present the experimental observation of golden jets, named for their golden ratio momentum, along with numerical 1D Gross-Pitaevskii equation simulations, which reveal interesting behavior of jet emission depending on the frequency and amplitude of interaction modulation. Above the threshold for emission of first order jets, higher order jets gradually start appearing with increasing modulation amplitude. As we increase it even further we slowly transition into the chaotic region without discernible jets.

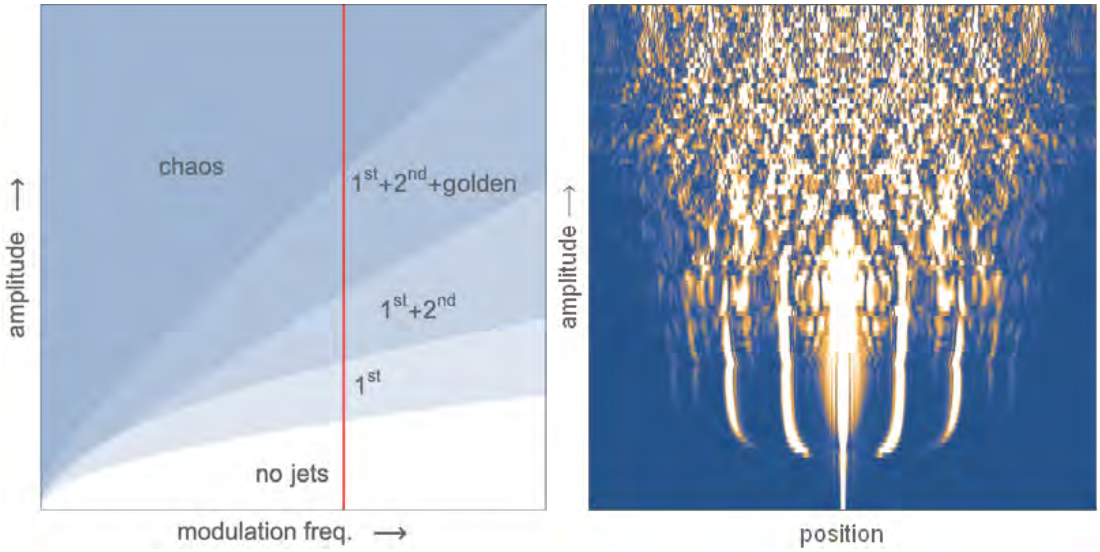

Fig. 1: Left: phase diagram of jets. Right: simulated density profile at a fixed time after interaction modulation for increasing amplitude and a selected frequency (red line in left figure).

References

[1] L. W. Clark, A. Gaj, L. Feng, and C. Chin, Nature **551**, 356 (2017).
[2] T. Mežnaršič, R. Žitko, T. Arh, K. Gosar, E. Zupanič, and P. Jeglič Phys. Rev. A **101**, 031601(R) (2020).
[3] L. Feng, J. Hu, L. W. Clark and C. Chin, Science **363**, 521 (2019).

[*]Corresponding author: tadej.meznarsic@ijs.si
[†]Corresponding author: peter.jeglic@ijs.si

Loading and cooling in an optical trap via hyperfine dark states

H. Eneriz[*1], **D. Naik**[1], **P. Bouyer**[1], **A. Bertoldi**[1]
1. LP2N, Laboratoire Photonique, Numérique et Nanosciences, Université Bordeaux-IOGS-CNRS:UMR 5298, F-33400 Talence, France

Recently self-emergence phenomena, like glassiness and crystallization, have been extensively studied using pumped condensed atomic samples, coupled to a high finesse optical resonator. So far most of these experiments have been realized in standing wave cavities, which impose the resonator geometry to the lattice being formed by the atoms and the light scattered into the cavity modes. Adopting degenerate multimode cavities opens new horizons to study order emergence effects, where compliant lattices between atoms and light can show a dynamical evolution [1].

The optical cavity we use to study self-ordering has a bow-tie geometry [2] and the intra-cavity field is in a traveling wave configuration. As a consequence, there are no constraints at the cavity mirrors on the intra-cavity light, and the phase of the expected light-atom crystals results in a free parameter. As a first step, we developed a novel protocol to load cold rubidium atoms in the telecom dipole trap enhanced by the cavity: we substituted the conventional red molasses phase with a gray molasses technique utilizing hyperfine dark and bright states arising through two-photon Raman transitions [3]. In this way we obtained a seven-fold increase in the atomic loading, and the technique was crucial to obtain an all-optical BEC in microgravity [4]. Furthermore, with the same technique we could cool the atoms directly in the dipole trap, exploiting the position dependence introduced by the differential light shift caused by the light at 1560 nm. Atoms at deeper potentials need to be addressed by a further red-detuned cooler on the D2 line, since the dipole trap creates a large differential Stark shift between ground and exited states.We could thus cool the trapped atoms by a factor of 4 (see Fig. 1) in few ms, limited by the gray molasse scheme being applied on the D2 line, and notably by the presence of the F'=3 upper level. The cooling scheme could be improved by using cooling light on the D1. In general, the cooling protocol is fast, lossless, and could be applied to other atomic species.

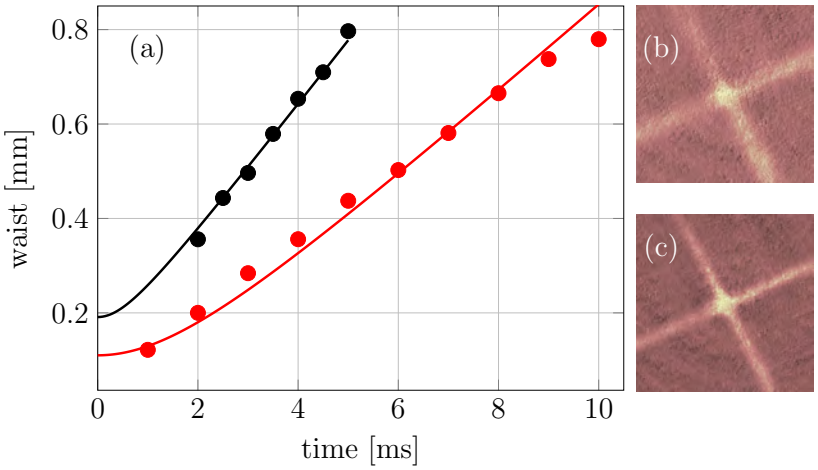

Fig. 1: (a) Ballistic expansion of the atomic cloud released from the FORT: cloud size vs time of flight. The fits (solid lines) yield a temperature of 198 μK before the cooling sweep (black points) and 48 μK after it (red points). Absorption images of the atoms before (b) and after (c) the cooling sweep, taken with a time-of-flight of 700 μs.

References

[1] Emergent crystallinity and frustration with Bose–Einstein condensates in multimode cavities. S. Gopalakrishnan, B. L. Lev, and P. M. Goldbart, Nature Physics **5**, 845 (2009).
[2] Bose–Einstein condensate array in a malleable optical trap formed in a traveling wave cavity. D. S. Naik, G. Kuyumjyan, D. Pandey, P. Bouyer, and A. Bertoldi, Quantum Sci. Technol. **3**, 045009 (2020).
[3] Loading and cooling in an optical trap via hyperfine dark states. D. S. Naik, H. Eneriz, M. Carey, T. Freegarde, F. Minardi, B. Battelier, P. Bouyer, and A. Bertoldi, Phys. Rev. Research **2**, 013212 (2020).
[4] All-Optical Bose-Einstein Condensates in Microgravity. G. Condon, M. Rabault, B. Barrett, L. Chichet, R. Arguel, H. Eneriz, D. S. Naik, A. Bertoldi, B. Battelier, A. Landragin, and P. Bouyer, Phys. Rev. Lett. **123**, 240402 (2019).

*Corresponding author: hodei.eneriz-imaz@institutoptique.fr

An atomic compass based on vector vortex beams

F. Castellucci[1], J. Wang[1,2], A. Selyem[1], T.W. Clark[3], and S. Franke-Arnold[*1]
1. School of Physics and Astronomy, University of Glasgow, G12 8QQ, United Kingdom
2. School of Physics, Xi'an Jiaotong University, Xi'an 710049, China
3. Wigner Research Centre for Physics, Hungarian Academy of Sciences, H-1525, Hungary

Light-matter interaction is of course, by its very nature, a vectorial process, with the atomic dipole Hamiltonian $H = -\mathbf{D}\cdot\mathbf{E} + g_F\mu_B\mathbf{F}\cdot\mathbf{B}$ depending on the alignment between the magnetic field $\mathbf{B}$, the optical polarization of the light $\mathbf{E}$, and the atomic spin polarization. Recent progress in generating complex vector light fields with structured transverse polarisation profiles now allows the full exploration of vectorial light matter interaction [1, 2].

In this presentation we investigate this interaction of cold rubidium atoms with vector vortex beams of the form $\mathbf{E} = E(r)[\exp(-i\ell\phi)\hat{\sigma}_+ + \exp(i\ell\phi)\hat{\sigma}_-]$, composed of light that carries opposite orbital angular momentum $\pm\ell\hbar$ in the left and right handed polarisation components $\hat{\sigma}_\pm$. The transmission of such light depends strongly on the alignment of an external magnetic field, specified by its inclination θ_B with respect to the light propagation direction and the azimuthal angle ϕ_B. We trap and cool ^{87}Rb in a standard magneto-optical trap and transfer it dynamically to a spontaneous optical force trap [3], populating the $5^2S_{1/2}F = 1$ ground state. A vector vortex beam drives the Λ transition from $m_F = \pm 1$ to the excited state $5^2P_{3/2}F' = 0, m_{F'} = 0$. The magnetic field along the beam axis leads to a small Zeeman shift, whereas its transverse component couples magnetic ground state sublevels, generating a closed loop configuration. Our experimental results can be understood conceptionally in terms of Fermi's golden rule, and agree well with simulations based on optical Bloch equations [4]. An azimuthal rotation of the magnetic field results in a $1/\ell$-fold rotation of the absorption profile (not shown), whereas an inclination results in splitting of the absorption pattern. We demonstrate that we can infer the alignment of the external magnetic field from an azimuthal Fourier analysis of the absorption profile, see Fig. 1, effectively realising an atomic compass.

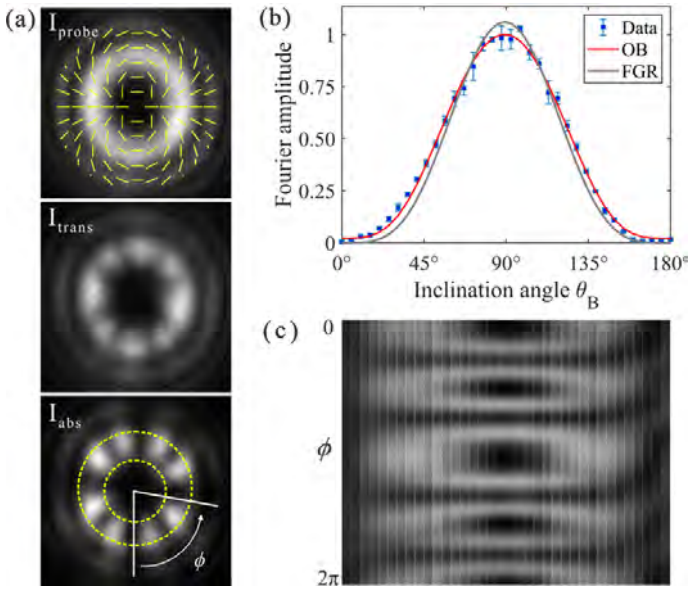

Fig. 1: (a) Intensity profile of the probe I_{probe} and overlayed polarisation structure, the transmitted intensity I_{trans} after having passed through the atomic sample, and the resulting absorption profile I_{abs}. (b) The inclination of the $\mathbf{B}$ field θ_B can be deduced from the amplitude of the $4\ell\phi$ Fourier component of I_{abs}, data (blue points), simulation based on optical Bloch equations (red line) and an analytical fit based on Fermi's golden rule (grey line). (c) Absorption as a function of the azimuthal angle Φ and the inclination angle θ_B of the magnetic field. The image is composed of polar plots of I_{abs} taken for magnetic fields with $\Delta\theta_B \simeq 5°$.

References

[1] J. Wang, F. Castellucci, and S. Franke-Arnold, AVSQuantum Science **2**, 031702 (2020).
[2] N. Radwell, T. W. Clark, B. Piccirillo, S. M. Barnett, and S. Franke-Arnold, Physical Review Letters **114**, 123603 (2015).
[3] N. Radwell, G. Walker, and S. Franke-Arnold, Physical Review A **88**, 043409 (2013).
[4] F. Castellucci, J. Wang, A. Selyem, T.W. C. Clark, and S. Franke-Arnold, in preparation.

*Corresponding author: sonja.franke-arnold@glasgow.ac.uk

Homonuclear ion-atom collisions: application to Li^+-Li

N. Joshi[*1], **M. Niranjan**[1], **A. Pandey**[†2], **O. Dulieu**[2], **R. Côté**[3,4], **S. A. Rangwala**[‡1]

1. Raman Research Institute, Light and Matter Physics, Sadashivanagar, Bangalore 560080, India
2. Université Paris-Saclay, CNRS, Laboratoire Aimé Cotton, Orsay, 91400, France
3. Physics Department, University of Massachusetts Boston, Boston, Massachusetts 02125, USA
4. Department of Physics, University of Connecticut, Storrs, CT 06269-3046, USA

The study of collisions of a trapped ion in a dilute gas of ultra-cold atomic ensemble provides knowledge of interatomic interactions in the quantum regime [1-9]. The theoretical framework of collisions for homonuclear, ground state ion-atom systems in the ultra-cold regime is presented. Total binary collision cross section (σ_{tot}) is derived, which is different from the commonly used expression, $\tilde{\sigma}_{tot}$, valid at high-energies [10]. For homonuclear case, the indistinguishability of direct elastic and resonant charge exchange (RCE) scattering channels is discussed. The standard cross-section expressions for direct elastic ($\tilde{\sigma}_{el}$) and RCE ($\tilde{\sigma}_{ce}$) channels are obtained as high energy approximations to (σ_{tot}). We show that the total cross-section is equal to the diffusion cross section, (σ_D), in the s-wave limit. The validity of the equivalence relation between the σ_D and $2 \times \tilde{\sigma}_{ce}$ is also discussed. These matters are illustrated with the aid of high quality non-relativistic potential energy curve (PEC) calculations for $^7Li^+$–^7Li [11] and $^6Li^+$–^6Li systems. The use of σ_{tot} is advocated as correct and consistent way to represent cross section. Average collision rate coefficient $\tilde{z} = < \sigma_{tot} v >_T$ is also discussed for these cases.

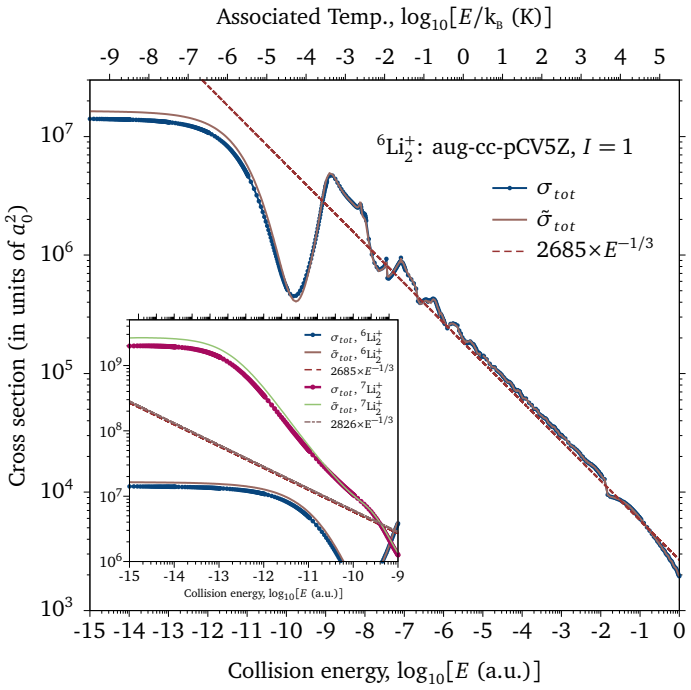

Fig. 1: σ_{tot} and $\tilde{\sigma}_{tot}$ as a function of collision energies for $^6Li^+$–^6Li system. In the inset, differences between σ_{tot} and $\tilde{\sigma}_{tot}$ in the s-wave energy regime are shown for $^6Li^+$–^6Li and $^7Li^+$–^7Li.

References

[1] L. D. Carr *et al.*, New J. Phys., vol. **11**, 055049, (2009).
[2] J. Weiner *et al.*, Rev. Mod. Phys., vol. **71**, 1, (1999).
[3] M. Tomza *et al.*, Rev. Mod. Phys., vol. **91**, 035001, (2019).
[4] R. Côté and A. Dalgarno, Phys. Rev. A **62**, 012709 (2000).
[5] R. Côté , in *Advances In Atomic, Molecular, and Optical Physics*, edited by E. Arimondo, C. C. Lin, and S. F. Yelin (Academic Press, San Diego, CA, 2016), Vol. 65, pp. 67–126.
[6] I. Sivarajah *et al.*, Phys. Rev. A **86**, 063419 (2012).
[7] S. Dutta, R. Sawant, and S. Rangwala, Phys. Rev. Lett. **118**, 113401 (2017).
[8] T. Sikorsky *et al.*, Nat. Commun. **9**, 920 (2018).
[9] K. Ravi *et al.*, Nat. Commun. **3**, 1126 (2012).
[10] H. Massey and M. RA Smith, Proc. R. Soc. Lond. A **142**, 142 (1933).
[11] A. Pandey *et al.*, Phys. Rev. A **101**, 052702 (2020).

[*]Corresponding author: njoshi@rri.res.in
[†]Corresponding author: amrendra.pandey@universite-paris-saclay.fr
[‡]Corresponding author: sarangwala@rri.res.in

Toward unidimensional Bose gases with tunable interactions

M. Ballu[1], **T. Badr**[1], **R. Dubessy**[1], **H. Perrin**[1], **A. Perrin**[*1]
1. Laboratoire de Physique des Lasers, Institut Galilée, Université Sorbonne Paris Nord, 99 av. J.-B. Clément, 93400 Villetaneuse, France

We are building an atom chip experiment, where sodium atoms are trapped magnetically, relying on the fields produced by microwires and external coils. The chip entails a coplanar waveguide especially designed for 1.6 GHz and allowing to reach large microwave amplitude in the near field, where the atoms are confined. This will allow us to investigate microwave-induced Fano-Feshbach resonance which have been theoretically predicted but never experimentally observed up to now [1]. The microwires configuration allows to reach very elongated trap geometries (aspect ratio above 100), permitting in turn the production of unidimensional Bose gases.

The atoms are first accumulated in a magneto-optical trap [2] and then transfered in a quadrupole magnetic trap. They are then transported magnetically over 60 cm to a science chamber [3], and then loaded onto a Ioffe-Pritchard trap produced by a macroscopic Z-shaped wire. After a first evaporation cooling stage, the atoms are transfered in the microtrap and cooled to degeneracy thanks to a final evaporation ramp.

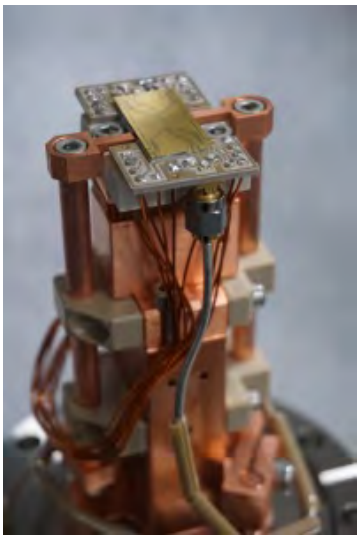

Fig. 1: View of the atom chip currently installed on the experiment.

In this poster, we will give details on our experimental procedure to obtain degenerate unidimensional Bose gases and present first results concerning the investigation of microwave-induced Feshbach resonances, as well as next experimental developments.

References

[1] D. Papoular, G. Shlyapnikov, J. Dalibard, Phys. Rev. A **81**, 041603 (2010).
[2] D. Ben Ali, T. Badr, T. Brézillon, R. Dubessy, H. Perrin and A. Perrin, J. Phys. B **50**, 055008 (2017).
[3] T. Badr, D. Ben Ali, J. Seaward, Y. Guo, F. Wiotte, R. Dubessy, H. Perrin and A. Perrin, Appl. Phys. B **125**, 102 (2019).

[*]Corresponding author: aurelien.perrin@univ-paris13.fr

Ultraprecise Rydberg atomic localization by standing waves and optical vortices

T. Kirova[*1], **N. Jia** [2], **H. R. Hamedi**[3], **S. H. Asadpour**[4], **J. Qian**[5], **G. Juzeliūnas**[3]

1. Institute of Atomic Physics and Spectroscopy, University of Latvia, Jelgavas street 3, Riga, LV-1004, Latvia
2. The Public Experimental Center, University of Shanghai for Science and Technology, Jungong Road 334, Shanghai 200093, China
3. Institute of Theoretical Physics and Astronomy, Vilnius University, Sauletėkio av. 3, Vilnius, LT-10257, Lithuania
4. Department of Physics, Iran University of Science and Technology, University St., Hengam St., Resalat Square, Tehran 13114-16846, Iran
5. State Key Laboratory of Precision Spectroscopy, Quantum Institute for Light and Atoms, Department of Physics, School of Physics and Electronic Science, East China Normal University, North Zhongshan Road 3663, Shanghai 200062, China

The spatial confinement of atoms with high precision, e.g. atom localization has been of continuous interest in quantum mechanics, while modern tools of quantum optics made the actual realization of such experiments possible. Current investigations on the topic are driven by the possibility of practical applications in nanolithography [1], laser cooling and trapping [2], and other areas of atomic physics [3].

Many problems arise when it comes to achieving localization of Rydberg atoms, due to the difficulty of confining them in a small region with high density. The strong van der Waals (vdW) interactions enhance the nonlinear properties of the Rydberg media via the dipole blockade [4] and open new opportunities for quantum optics and quantum information applications [5]. This makes the question of experimentally achievable precise localization of highly excited Rydberg atoms an important one.

We propose theoretical schemes for strongly confined atomic localization using interacting Rydberg atoms in a coherent population trapping ladder configuration, where a standing-wave or a vortex field is used as a coupling field in the second step of the ladder. Depending on the degree of compensation of the Rydberg level energy shift (induced by the vdW interaction) by the coupling field detuning, we distinguish between two antiblockade regimes, i.e., a partial antiblockade (PA) and a full antiblockade (FA).

When a standing wave is used as a coupling field, a periodic pattern of tightly localized regions can be achieved for both regimes. However, the PA allows for much faster convergence of spatial confinement, yielding a high-resolution Rydberg state-selective superlocalization for higher-lying Rydberg levels to a sub-nanometer scale. In comparison, for lower-lying Rydberg levels, the PA leads to an anomalous change of spectra linewidth, confirming the importance of using a stable uppermost state to achieve the superlocalization regime [6].

When applying a doughnut-shaped optical vortex in the second step of the ladder [7], ultraprecise two-dimensional localization solely in the zero-intensity center is achieved, within a confined excitation region down to the nanometer scale. In addition, applying an auxiliary modulation to the two-photon detuning allows for a three-dimensional confinement of the Rydberg atoms.

Our results pave one-step closer to the development of new subwavelength localization techniques via reducing the excitation volumes to nanometer level, thus representing feasible implementations for future experimental applications.

References

[1] A. N. Boto, P. Kok, D. S. Abrams, S. L. Braunstein, C. P. Williams, and J. P. Dowling, Phys. Rev. Lett. **85**, 2733 (2000).
[2] W. D. Phillips, Rev. Mod. Phys. **70**, 721 (1998).
[3] C. S. Adams, M. Sigel, and J. Mlynek, Rev. Rep. **240**, 143 (1994).
[4] M. D. Lukin, M. Fleischhauer, R. Côté, L. M. Duan, D. Jaksch, J. I. Cirac, and P. Zoller, Phys. Rev. Lett. **87**, 037901 (2001).
[5] M. Saffman, T. G. Walker, and K. Mölmer, Rev. Mod. Phys. **82**, 2313 (2010).
[6] T. Kirova, N. Jia, S. H. Asadpour, J. Qian, G. Juzeliūnas, and H. R. Hamedi, Opt. Lett. **45(19)**, 5440 (2020).
[7] N. Jia, J. Qian, T. Kirova, G. Juzeliūnas, and H. R. Hamedi, Opt. Exp. **28(24)**, 36936 (2020).

[*]Corresponding author: teo@lu.lv

Bloch oscillations in a synthetic dimension of harmonic trap states

C. Oliver[*1], **A. Smith** [1], **T. Easton** [1], **G. Salerno** [2], **N. Goldman** [3], **G. Barontini** [1], **H.M. Price** [1],
1. School of Physics and Astronomy, University of Birmingham, Edgbaston, Birmingham, UK, B15 2TT
2. Dept. Applied Physics, Aalto University, Puumiehenkuja 2 02150, Espoo, Finland
3. Université Libre de Bruxelles, CP 231, Campus Plaine, 1050 Brussels, Belgium

Since the seminal proposals of [1][2], synthetic dimensions have become a powerful method for realising theoretical models in artificial systems such as ultracold atoms and photonics [3]. In this approach, a set of states are selected and coupled together, with the coupling then being interpreted in terms of a particle hopping along a synthetic lattice formed by the states. Synthetic dimensions have proven useful as they can allow for more straightforward implementations, particularly of topological models, than is otherwise possible in experiments.

In this poster, we report on preliminary progress towards implementing a synthetic dimension based on atomic harmonic trap states [4]. In this approach, a deep harmonic trap containing cold atoms is resonantly shaken around the trapping frequency, so that the shaking potential effectively couples nearest-neighbour harmonic trap states. Within this framework, the harmonic trap states are re-interpreted as lattice sites along a synthetic dimension, where the shaking amplitude sets the effective hopping amplitude and the shaking detuning generates an effective force along the synthetic lattice. A predicted signature of the synthetic dimension is then the emergence of 1D Bloch oscillations with respect to the dimension of harmonic trap states [4]. Here, we shall discuss progress towards the practical observation of this effect based on a cold-atom set-up with a digital micro-mirror device. The experimental implementation of such a synthetic dimension will pave the way for the future investigation of 2D topological quantum Hall physics in this system, when a position-dependent shaking phase is included in the set-up.

References

[1] O. Boada *et al*, Phys. Rev. Lett. **108**, 133001 (2012).
[2] A. Celi *et al*, Phys. Rev. Lett. **112**, 043001 (2014).
[3] T. Ozawa and H.M. Price, Nature Reviews Physics **1**, 349 - 357 (2019).
[4] H.M. Price *et al*, Phys. Rev. A **95**, 023607 (2017).

[*]Corresponding author: cpo387@student.bham.ac.uk

Dark-soliton-induced anomaly in the thermodynamic behavior of a one-dimensional Bose gas

G. De Rosi[*1], **R. Rota**[†2], **G. E. Astrakharchik**[‡1], **J. Boronat**[§1]
1. Departament de Física, Universitat Politècnica de Catalunya, Campus Nord B4-B5, 08034 Barcelona, Spain
2. Institute of Physics, Ecole Polytechnique Fédérale de Lausanne (EPFL), CH-1015 Lausanne, Switzerland

In many-body systems of very different nature, the specific heat shows an anomalous temperature dependence which signals the onset of phase transitions or intrinsic features of the excitation spectrum. In a one-dimensional (1D) Bose gas, we reveal an intriguing anomaly [1], the first one in the ultracold gas field, although phase transitions cannot occur [2] and the microscopic complicated spectrum has not permitted so far a direct link with the thermodynamics. We find that the anomaly temperature is ruled by the dark soliton energy, corresponding to the maximum of the hole-excitation branch in the spectrum. We rely on Bethe Ansatz [3] to obtain the specific heat exactly and provide interpretations of the analytically tractable limits. We predict new quantum regimes. The dynamic structure factor is computed with the Path Integral Monte Carlo (PIMC) method, gaining insight into the pattern of the excitations. This allows us to formulate a microscopic interpretation of the anomaly origin when the quantum and thermal effects are comparable. The PIMC method has been applied to a 1D Bose gas for the first time in our work. Our calculations extend for a wide range of temperature compared to previous studies which were restricted only at very low temperature [4-8]. We provide indications for future observations and how the anomaly can be employed for in-situ thermometry and for identifying different collisional regimes. We introduce an innovative concept of quantum simulation [9] of thermal properties where the new dark-soliton anomaly precisely models other anomalies in condensed matter, atomic, many-body, solid-state physics and material science. The understanding of thermal properties, enhanced by the new quantum simulation, is relevant for engineering innovative materials and developing emerging quantum technologies.

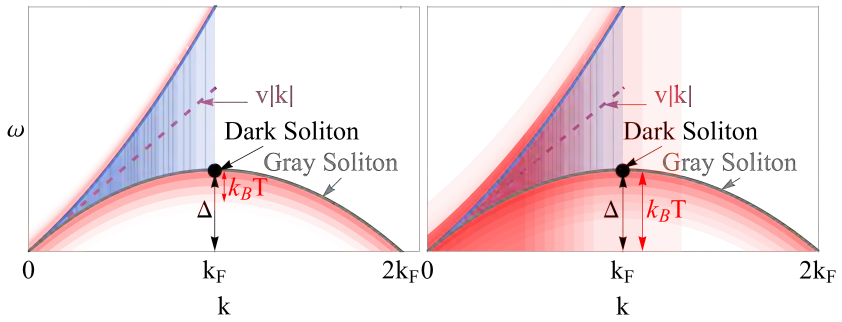

Fig. 1: Sketch of the dynamic structure factor at a temperature below (left) and around (right) the value of the Dark-Soliton Anomaly. Upper particle-like Lieb I and lower hole-like Lieb II branches are reported with solid curves. Dashed line denotes the linear phononic spectrum $\omega(k) = v|k|$ where ω is the frequency, v is the sound velocity and k is the wavenumber. The dark-soliton excitation is located at the Fermi wavenumber k_F and its energy is equal to Δ. The dynamic structure factor at zero temperature is reported with the blue shaded region with vertical lines. Its thermal contribution is instead denoted with red shading.

References

[1] G. De Rosi, R. Rota, G. E. Astrakharchik, and J. Boronat, arXiv:2104.12651 (2021).
[2] L. D. Landau and E. M. Lifshitz, *Statistical Physics: Vol. 5* (Elsevier Science, Amsterdam, 2013).
[3] C. N. Yang and C. P. Yang, Journal of Mathematical Physics **10**, 1115 (1969).
[4] A. Y. Cherny and J. Brand, Phys. Rev. A **73**, 023612 (2006).
[5] M. Panfil and J.-S. Caux, Phys. Rev. A **89**, 033605 (2014).
[6] G. Lang, F. Hekking, and A. Minguzzi, Phys. Rev. A **91**, 063619 (2015).
[7] J. De Nardis and M. Panfil, J. Stat. Mech. **2018**, 033102 (2018).
[8] E. Granet and F. H. L. Essler, SciPost Phys. **9**, 82 (2020).
[9] E. Altman, K. R. Brown, G. Carleo, L. D. Carr, E. Demler, C. Chin, B. DeMarco, S. E. Economou, M. A. Eriksson, K.-M. C. Fu, M. Greiner, K. R. Hazzard, R. G. Hulet, A. J. Kollár, B. L. Lev, M. D. Lukin, R. Ma, X. Mi, S. Misra, C. Monroe, K. Murch, Z. Nazario, K.-K. Ni, A. C. Potter, P. Roushan, M. Saffman, M. Schleier-Smith, I. Siddiqi, R. Simmonds, M. Singh, I. Spielman, K. Temme, D. S. Weiss, J. Vučković, V. Vuletić, J. Ye, and M. Zwierlein, PRX Quantum **2**, 017003 (2021).

[*]Corresponding author: giulia.de.rosi@upc.edu
[†]Corresponding author: riccardo.rota@epfl.ch
[‡]Corresponding author: grigori.astrakharchik@upc.edu
[§]Corresponding author: jordi.boronat@upc.edu

A versatile ring trap for quantum gases

Mathieu de Goër de Herve[1,2], Yanliang Guo[1,2], Camilla De Rossi[1,2], Avinash Kumar[2,1], Thomas Badr[2,1], Romain Dubessy[1,2], L. Longchambon[*1,2], Hélène Perrin[2,1]

1. Laboratoire de physique des lasers, Université Sorbonne Paris Nord F-93430, Villetaneuse, France
2. LPL CNRS UMR 7538, F-93430, Villetaneuse, France

We present here the experimental realization of an hybrid magnetic and optical ring trap [1], [2]. Fig. 1 displays its principle, relying on an optical vertical confinement and a radial confinement from an rf-dressed bubble-shaped quadrupole trap at its equator [3]. This well-controlled versatile ring trap allows a wide variety of radii (Fig. 2) and vertical and radial trapping frequencies, all independently tunable. In such a trap, we have achieved a ring-shaped Bose-Einstein condensate with no discernible thermal fraction. We discuss the feasibility for this superfluid degenerate quantum gas to enter the long-sought one-dimensional regime with periodic boundaries and find that for current experimental values and atom number around 7000 the system should reach this quasi-condensate state. We have set the atomic ring into rotation with two different excitations, one purely magnetic relying on a quadrupole deformation of the bubble profile, and the other purely optical by means of a rotating focused beam. In the latter case especially, the observation of one multiply-charged vortex at short times after the excitation and two or three vortices at longer times is a strong signal that this trap sustains multivalued quantized circulation of the superfluid. We have developed a trap decompression technique adapted to our dressed trap in order to observe a single quantum of rotation after time-of flight.

This hybrid ring is very promising for the study of 1D superfluid dynamics, for example the shock waves induced by rotation in the presence of a static barrier. Increasing again the ring confinement towards fermionization of the atoms could lead to NOON states more robust against decoherence, whereas dressing the quadrupole static magnetic field with multiple rf frequencies allows the implementation of multiple concentric rings. Tunneling between these rings is expected to build a macroscopic quantum superposition of several rotating BECs. Moreover, the recombination technique, starting from a controlled large phase winding in the ring, could ease the way to the production of quantum Hall states.

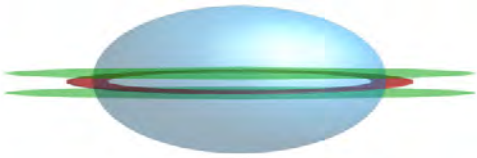

Fig. 1: Principle of the hybrid trap. The quadrupole static trap plus radiofrequency dressing provides the shell trapping surface, whereas two horizontal repulsive light sheets provide vertical confinement.

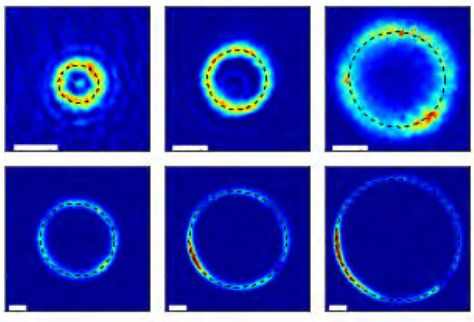

Fig. 2: Different ring diameters obtained with the hybrid trap. The white bar in all images has a length of 50 µm.

References

[1] M. de Goër de Herve, Y. Guo, C. De Rossi, A. Kumar, T. Badr, R. Dubessy, L. Longchambon, and H. Perrin, arXiv:2103.14310 [cond-mat.quant-gas], 2021, to be published.
[2] W. H. Heathcote, E. Nugent, B. T. Sheard, and C. J.Foot, New Journal of Physics, 10(4):043012, 2008
[3] O. Morizot, Y. Colombe, V. Lorent, H. Perrin, and B. M.Garraway, Phys. Rev. A,74:023617, 2006.

*Corresponding author: laurent.longchambon@univ-paris13.fr

Ultracold AlF molecules: theoretical insights for buffer-gas and evaporative cooling

Sangami.G.S[*1]

1. Faculty of Physics, University of Warsaw, Ludwika Pasteura 5, 02-093, Warsaw, Poland

Motivated by the recent experimental progress in laser cooling of AlF molecules, which have highly diagonal Franck-Condon factors, we study the electronic structure of these molecules, their interactions with He atoms, and intermolecular interactions. We employ ab initio quantum chemistry methods, such as the coupled cluster method. The potential energy surfaces for AlF - He interaction for the ground and first excited states of AlF are useful to described buffer-gas cooling, while the potential energy surfaces for AlF - AlF interaction will be used to characterize prospects for evaporative cooling. This study also enabled us to test the accuracy and feasibility of the method used and to test the energy convergence of ab initio methods.

[*]Corresponding author: sangami.gs@fuw.edu.pl

Adiabatic spin-dependent momentum transfer in an SU(N) degenerate Fermi gas

P. Bataille[1], **A. Litvinov**[1], **I. Manai**[1], **J. Huckans**[2], **F. Wiotte**[1], **A. Kaladjian**[1], **O. Gorceix**[1], **E. Maréchal**[1], **B. Laburthe-Tolra**[1], **and M. Robert-de-Saint-Vincent**[*1]

1. Laboratoire de Physique des Lasers, CNRS, UMR 7538, Université Sorbonne Paris Nord, F-93430 Villetaneuse, France

2. Department of Physics and Engineering, Bloomsburg University, Bloomsburg, Pennsylvania

For the study of strongly correlated fermionic systems, ultracold alkaline-earth atoms offer original possibilities with their large ground-state spin and spin-independent collisions (SU(N) symmetry). The nuclear nature of the spins is both a strength and a complication – for example as it prevents the simple use of magnetic forces as in a Stern-Gerlach measurement. Nevertheless, the narrow lines associated with their singlet-to-triplet transitions can be used for novel spin-sensitive manipulations schemes, e.g. effective magnetic fields as in the "Optical Stern-Gerlach" (OSG) scheme [1], and spin-orbit coupling with low levels of spontaneous emission [2].

In our experiment [3], we introduce a spin-orbit coupling scheme where a retro-reflected laser beam selectively diffracts two spin components of a degenerate Fermi gas in opposite directions. Spin sensitivity is provided by sweeping through a magnetic-field sensitive transition: the intercombination line of strontium 87. The atoms follow adiabatically dark states, which significantly suppresses spontaneous emission. The adiabaticity of the scheme makes it inherently robust. We furthermore demonstrate a generalization of the scheme, and diffract in a single shot four spin states with four different momentum transfers. The spin-orbit coupling is associated with well-defined momentum transfers, set by the two-photon recoil, such that, unlike in OSG, momentum distortion is negligible. Thus, this scheme allows simultaneous measurements of the spin and momentum distributions of a strontium degenerate Fermi gas, opening the path to momentum-resolved spin correlation measurements [4] on SU(N) quantum magnets.

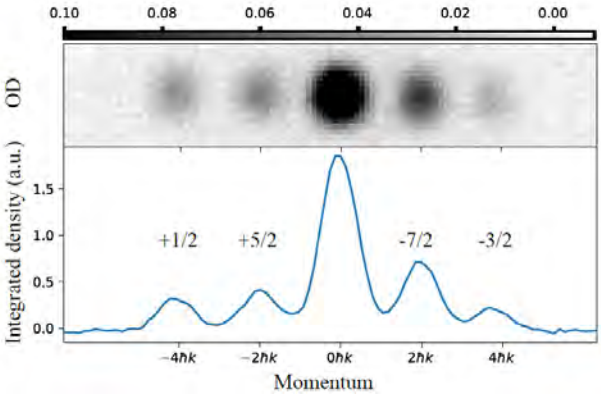

Fig. 1: Spin- and momentum resolved picture of a degenerate Fermi gas of ^{87}Sr. A quantized momentum transfer is selectively applied to four spin states in the same experimental run, here $m_F = +1/2, +5/2, -7/2, -3/2$.

References

[1] S. Taie, Y. Takasu, S. Sugawa, R. Yamazaki, T. Tsujimoto, R. Murakami, and Y. Takahashi, Phys. Rev. Lett. **105**, 190401 (2010).
[2] B. Song, C. He, S. Zhang, E. Hajiyev, W. Huang, X.-J. Liu, and G.-B. Jo, Phys. Rev. A **94**, 061604(R) (2016).
[3] P. Bataille, A. Litvinov, I. Manai, J. Huckans, F. Wiotte, A. Kaladjian, O. Gorceix, E. Maréchal, B. Laburthe-Tolra, and M. Robert-de Saint-Vincent, Phys. Rev. A **102**, 013317 (2020).
[4] G. M. Bruun, O. F. Syljuåsen, K. G. L. Pedersen, B. M. Andersen, E. Demler, and A. S. Sørensen, Phys. Rev. A **80**, 033622 (2009).

*Corresponding author: martin.rdsv@univ-paris13.fr

Large spin-orbit coupling as a source of Feshbach resonances in ultracold ion-atom mixtures

A. Wojciechowska[*1], **M. Tomza**[†1]
1. Faculty of Physics, University of Warsaw, Pasteura 5, 02-093 Warsaw, Poland

Feshbach resonances are a crucial tool, enabling to control atoms' interactions in quantum gases, which have already led to many significant breakthroughs. The following step to ultracold physics advancement is an observation of these resonances between ions and atoms. It is desirable, for instance, due to its application in quantum simulation and computing. Until recently, the ultracold regime was unattainable for ion-atom mixtures. The quantum gas consisting of lithium atoms and barium ion is the first one, where Feshbach resonances were observed, thanks to measurements by the group of Tobias Schaetz at the University of Freiburg. This confirmation of resonances itself is important progress in the fundamentals of physics, but that is not the end of the story. In the Ba^++Li mixture, we discovered that the observed Feshbach resonances originate from the second-order spin-orbit interaction, which is a unique mechanism, comparing to, for instance, neutral systems. What is more, the predicted spin-orbit coupling appears to be giant – 2 to 3 orders of magnitude larger than in neutrals. Therefore, standard approaches of solving the problem (for example perturbation theory) are likely to fail. Gaining a deep understanding of this phenomenon, allows us to probe short-range interactions in ion-atom systems. In my work, I build a theoretical model describing ion-atom interactions and collisions to confirm and characterize experimentally measured features and inspire further applications.

[*]Corresponding author: a.wojciechow37@student.uw.edu.pl
[†]Corresponding author: michal.tomza@fuw.edu.pl

Supersonic Rotation of a Superfluid: A Long-Lived Dynamical Ring

Y. Guo [*1,2], **R. Dubessy** [1,2], **M. de Goër de Herve**[1,2], **A. Kumar**[2,1], **T. Badr**[†2,1], **A. Perrin**[2,1], **L. Longchambon**[1,2], **H. Perrin**[2,1]

1. Laboratoire de physique des lasers, Université Paris 13 Sorbonne Paris Cité, 99 avenue J.-B. Clément, F-93430 Villetaneuse, France
2. LPL, CNRS UMR 7538, 99 avenue J.-B. Clément, F-93430 Villetaneuse, France

Superfluidity is a rich quantum dynamical phenomenon with striking manifestations such as the existence of a critical velocity for the creation of excitations and the appearance of quantized vortices when set into rotation. The particular case of a quantum gas rotating at an angular frequency has attracted a lot of theoretical and experimental interest, since it presents a strong analogy with a quantum system of charged particles in a uniform magnetic field, relevant for condensed matter problems.
In a superfluid quantum gas confined in a harmonic trap of radial frequency ω_r, for rotation rates $\Omega \leq \omega_r$ a dense triangular array of singly charged vortices establishes. However, reaching the situation $\Omega \geq \omega_r$ is impossible in a purely harmonic trap because the radial effective trapping in the rotating frame vanishes due to the centrifugal potential, leading to the loss of the atoms. This high rotation regime requires an anharmonic trap to counteract the centrifugal effect. In this situation a zero-density area (a hole) grows at the trap center above a critical rotation frequency Ω_h [1], leading to an annular density profile. Above a second threshold Ω_{gv}, the gas enters the so-called "giant vortex" regime, where all the vortex cores migrate close to the depleted central region. Pioneering experiments have tried to generate a ring-shaped flow in a three-dimensional condensate, either approaching Ω_h from below in an anharmonic trap such that no hole could form [2], or drilling a hole in a rotating gas confined in a harmonic trap by removing atoms with a laser pulse [3] [4], the system being strongly out of equilibrium.
Here, we present what is to our knowledge the first experimental realization of such a superfluid annular flow stabilized by its own angular momentum, as shown in Fig. 1. We demonstrate that it is a very long-lived quasi-two-dimensional (2D) stable structure that persists over more than a minute [5]. The ring atomic density distribution agrees with a zero-temperature superfluid model. We measure rotation frequencies reaching $1.06\omega_r$, corresponding to a linear supersonic velocity of Mach 18 with respect to the peak speed of sound. We also perform the spectroscopy of elementary excitations of the ring.

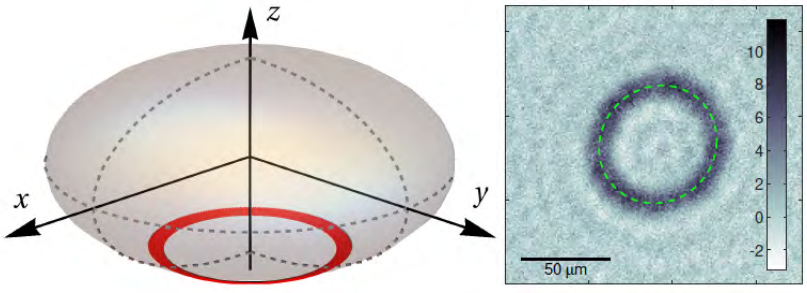

Fig. 1: Superfluid annular flow sustained by its own angular momentum. (a) Computed density contour (red annulus). (b) Experimental in situ integrated 2D density of the atomic cloud, rotating at Mach 15.

References

[1] A. Fetter *et al.*, Phys. Rev. A, **71**, 013605 (2005)
[2] V. Bretin *et al.*, Phys. Rev. Lett. **92**, 050403 (2004)
[3] P. Engels *et al.*, Phys. Rev. Lett. **90**, 170405 (2003)
[4] T. P. Simula *et al.*, Phys. Rev. Lett. **94**, 080404 (2005)
[5] Y. Guo *et al.*, Phys. Rev. Lett, **124**, 025301 (2020)

[*]Present address: Institut für Experimentalphysik, Technikerstrasse 25, 6020 Innsbruck, Austria
[†]Corresponding author: thomas.badr@univ-paris13.fr

Laser Cooling of Atoms using an Optical Frequency Comb

V. Vulić[*1], **D. Buhin**[1], **M. Kruljac**[1], **N. Šantić**[1], **F. Friebel**[2], **B. Resan**[2,3], **T. Ban**[1], **D. Aumiler**[1]

1. Institute of Physics, Bijenička c. 46, HR-10000 Zagreb, Croatia

2. School of Engineering, University of Applied Sciences and Arts Northwestern Switzerland, Klosterzelgstrasse 2, CH-5210 Windisch, Switzerland

3. Faculty of Medicine, Josip Juraj Strossmayer University, Trg Svetog Trojstva 3, HR-31000 Osijek, Croatia

1D simultaneous laser cooling of ^{87}Rb and ^{85}Rb atoms using an optical frequency comb (FC) has been demonstrated recently by our group [1]. The FC spectrum consists of a series of equally spaced narrow spectral lines, thus enabling simultaneous excitation of different atomic hyperfine transitions by different comb lines. By adjusting the pulse repetition frequency and the offset frequency, the FC spectrum was tuned to ensure that two distinct FC lines were simultaneously red-detuned from the cooling transitions, one line for each species. Starting from a pre-cooled cloud of ^{87}Rb and ^{85}Rb atoms at above-Doppler temperatures, we showed simultaneous cooling of both species down to the Doppler temperature using two counter-propagating σ^+/σ^--polarized beams from the frequency comb.

In an effort to upgrade our comb cooling experiment we are currently developing a new FC source that is based on a direct diode-pumped mode-locked Ti:sapphire picosecond laser. Direct pumping of the Ti:sapphire oscillator using low-cost blue laser diodes significantly reduces both the cost and the complexity of the laser, while using a SEmiconductor Saturable Absorber Mirror (SESAM) for modelocking ensures reliable self-starting and robust operation, with lower phase noise than by using Kerr-lens modelocking [2]. The FC will be actively stabilized by locking the pulse repetition frequency to an RF frequency standard and simultaneously locking a comb line to a continuous-wave reference laser [3, 4].

The newly developed FC source will have the advantage of higher optical power per comb line due to higher total power and a narrower optical spectrum than the FC used in [1], as well as a repetition frequency chosen so that there are comb lines simultaneously red-detuned from the cooling and near-resonant with the repumping transitions of both ^{87}Rb and ^{85}Rb atoms. These improvements should allow for simultaneous FC cooling of two atomic species directly from room temperature, thus enabling the realization of a multi-species magneto-optical trap (MOT) using only a single laser source. This will further decrease the complexity of (ultra)cold multi-atom experimental systems enabling significant advances in the fields of multispecies atom interferometry and multispecies interactions.

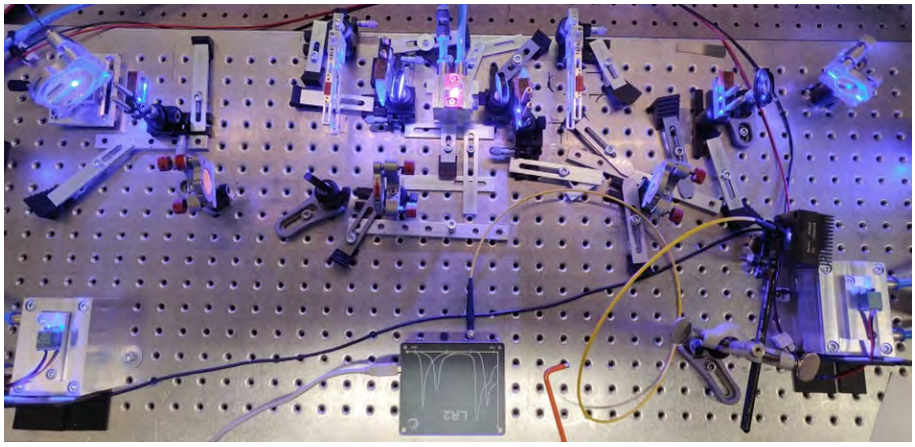

Fig. 1: Direct blue diode-pumped mode-locked Ti:sapphire picosecond laser, under development.

References

[1] D. Buhin, D. Kovačić, F. Schmid, M. Kruljac, V. Vulić, T. Ban, and D. Aumiler, Phys. Rev. A **102**, 021101(R) (2020).
[2] A. Rohrbacher, O. E. Olarte, V. Villamaina, P. Loza-Alvarez, and B. Resan, Opt. Express **25**, 10677-10684 (2017).
[3] N. Šantić, D. Buhin, D. Kovačić, I. Krešić, D. Aumiler and T. Ban, Sci. Rep. **9**, 2510 (2019).
[4] N. Šantić, *Synthetic Lorentz force for neutral cold atoms*, Ph.D Thesis (2018).

*Corresponding author: vvulic@ifs.hr

Dynamical localization in non-ideal kicked rotors driven by two modulations

F. Revuelta[*1], **R. Chacón**[2,3], **F. Borondo**[4,5]

1. Grupo de Sistemas Complejos, ETSIAAB, Alimentaria y de Biosistemas, Universidad Politécnica de Madrid, Avenida Puerta de Hierro 2-4, 28040 Madrid, Spain

2. Departamento de Física Aplicada, Escuela de Ingenierías Industriales, Universidad de Extremadura, Apartado Postal 382, 06006 Badajoz, Spain

3. Instituto de Computación Científica Avanzada (ICCAEx), Universidad de Extremadura, Apartado Postal 382, 06006 Badajoz, Spain

4. Instituto de Ciencias Matemáticas (ICMAT), Cantoblanco, 28049 Madrid, Spain

5. Departamento de Química, Universidad Autónoma de Madrid, Cantoblanco, 28049 Madrid, Spain

6. Faculty of Electrical Engineering and Computing, Unska ul. 3, 10000 Zagreb, Croatia

Dynamical localization is the quantum suppression of classical diffusion. It is a fascinating example where the quantum dynamics of a system is dramatically different from its classical counter part [1], [2], [3]. Initially, and for a short period of time, the quantum system begins to delocalize at a rate which given by the classical diffusion constant. However, after a certain time, known as localization time, the quantum motion seems to freeze, and the delocalization process thereafter disappears. This fact can be understood as the result of the balance between classical diffusion, which acts in the sense of spreading the wave-packet, and (the more subtle) quantum interference, which acts in the sense of maintaining coherence [4].

In this work [5], we study the dynamical localization taking place in an ultracold atomic gas confined in an optical lattice simultaneously shaken by two pulsatile modulations with different periods and/or waveforms. A systematic study of pulse finite-size effects and modulation waveform on this phenomenon is performed. For this purpose, we compare the classical and quantum momentum. Dynamical localization is identified when the previous difference is large. As shown in Fig. 1, the dynamical localization can survive in the presence of quasiperiodic modulations.

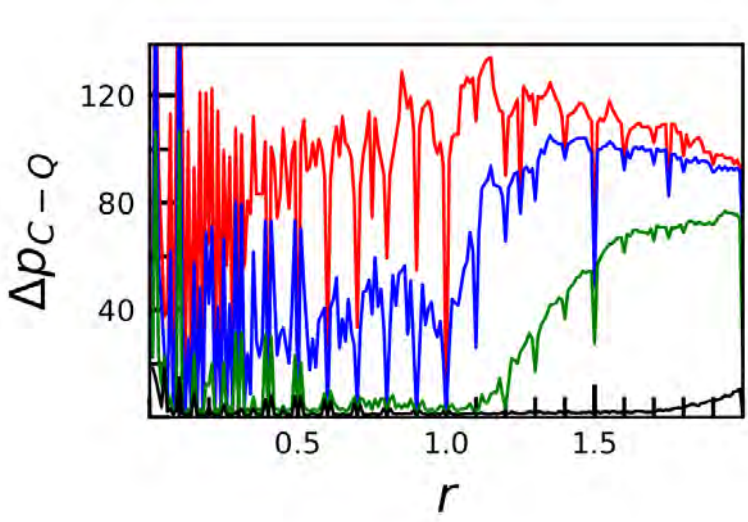

Fig. 1: Difference between the classical and quantum momentum dispersion as a function of the ratio between the modulation frequencies for three different modulation amplitudes (in different color). Dynamical localization takes place when the difference Δp_{C-Q} is large, something that The supression of dynamical localization can also occur for some quasiperiodic modulations.

References

[1] I. Guarneri, G. Casati, and V. Karle, Phys. Rev. Lett. **113**, 174101 (2014).

[2] L. E. Reichl, *The Transition to Chaos. Conservative Classical Systems and Quantum Manifestations* (Springer, New York, 1994).

[3] J. Chabé, H. Lignier, H. Cavalcante, D. Delande, P. Szriftgiser, and J. C. Garreau, Phys. Rev. Lett. **97**, 264101 (2006).

[4] G. Abal, R. Donangelo, A. Romanelli, A. C. Sicardi Schifino, and R. Siri, Phys. Rev. E **65**, 046236 (2002).

[5] F. Revuelta, R. Chacón, and F. Borondo, "Dynamical localization in non-ideal kicked rotors driven by two modulations" (in preparation).

*Corresponding author: fabio.revuelta@upm.es, https://orcid.org/0000-0002-2410-5881

Two interacting polar linear molecules in an electric field

D. Mellado-Alcedo[*1], **R. González-Férez** [1]

1. Instituto Carlos I de Física Teórica y Computacional and Departamento de Física Atómica, Molecular y Nuclear, Universidad de Granada, 18071 Granada, Spain

The long-range and anisotropic dipole-dipole interaction in cold and ultracold dipolar gases can be controlled and tuned by external fields giving rise to a rich variety of novel applications [1]. For instance, this interaction plays an important role in the control of chemical reactions in an ultracold gas of polar molecules [2]. Ultracold polar diatomic molecules coupled via the dipole-dipole interaction have been proposed for the implementation of quantum logic gates in quantum computation [3-5]. An optimal control of orientation and entanglement has been performed for two dipole-dipole coupled quantum planar rotors [6]. In this work, we investigate the entanglement and the rotational dynamics of two identical polar linear molecules in an electric field and coupled via the dipole-dipole interaction as shown in Fig. 1.

By analyzing the symmetries of the system, the time-dependent Schrödinger equation is solved describing the molecules within the rigid rotor approximation. The molecules are allowed to rotate in three dimensions and linear and sudden turning on are needed for the electric field. We explore the dependence of the rotational dynamics and entanglement on electric field parameters, dipole-dipole interaction strength and spatial configuration. If the dipole-dipole and electric field interactions are of the same order and the two molecules are in the same initial state, they reach a significant orientation but are weakly entangled. When the molecules are initially in different states, they have different mixed-field orientation and a larger entanglement is attained. In both cases, a strong dependence on the configuration angle is observed. By increasing the electric field strength, the orientation is increased and a moderate entanglement is reached.

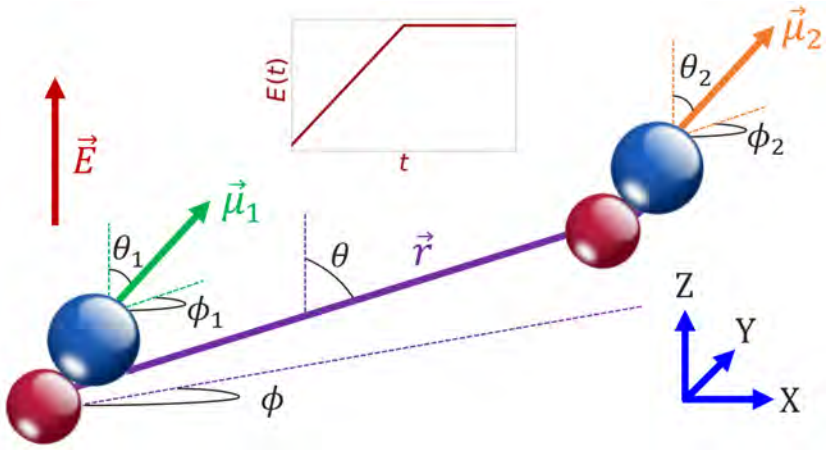

Fig. 1: Sketch (not to scale) of the two polar linear molecules in a linear switched on electric field

References

[1] T. Lahaye, C. Menotti, L. Santos, M. Lewenstein, and T. Pfau, Rep. Prog. Phys. **72**, 126401 (2009).
[2] K. K. Ni, S. Ospelkaus, D. Wang, G. Quéméner, B. Neyenhuis, M. H. G. de Miranda, J. L. Bohn, J. Ye and D. S. Jin, Nature **464**, 1324-1328 (2010).
[3] D. DeMille, Phys. Rev. Lett. **88**, 067901 (2002).
[4] A. Micheli, G. K. Brennen and P. Zoller, Nat. Phys. **2**, 341 (2006).
[5] J. Zhu, S. Kais, Q. Wei, D. Herschbach and B. Friedrich, J. Chem. Phys. **138**, 024104 (2013).
[6] H. Yu, T.S. Ho, and H. Rabitz, Phys. Chem. Chem. Phys. **20**, 13008-13029 (2018).

*Corresponding author: alcedo@ugr.es

An annular quantum gas induced by dimensional reduction

Yanliang Guo*[1], Emmanuel Mercado Gutierrez[2], David Rey†[1], Thomas Badr[1], Aurélien Perrin[1], Laurent Longchambon[1], Vanderlei S. Bagnato[2], Hélène Perrin[1], Romain Dubessy‡[1]

1. Université Sorbonne Paris Nord, Laboratoire de physique des lasers, CNRS UMR 7538, F-93430, Villetaneuse, France

2. Instituto de Física de São Carlos, Universidade de São Paulo, CP 369, São Carlos, São Paulo, 13560-970, Brazil

We report the observation of a major consequence of dimensional reduction in a system of ultracold atoms confined on an ellipsoidal surface. At LPL, we study the equilibrium and dynamical properties of Bose-Einstein condensates confined in a rf dressed quadrupole trap [1]. In this trap, atoms are confined to the —hollow— ellipsoidal isomagnetic surface of the quadrupole magnetic field selected by the frequency of an rf field. Their motion is thus essentially two-dimensional along the surface of a shell. Gravity ensures that the atoms stay at the bottom of this shell.

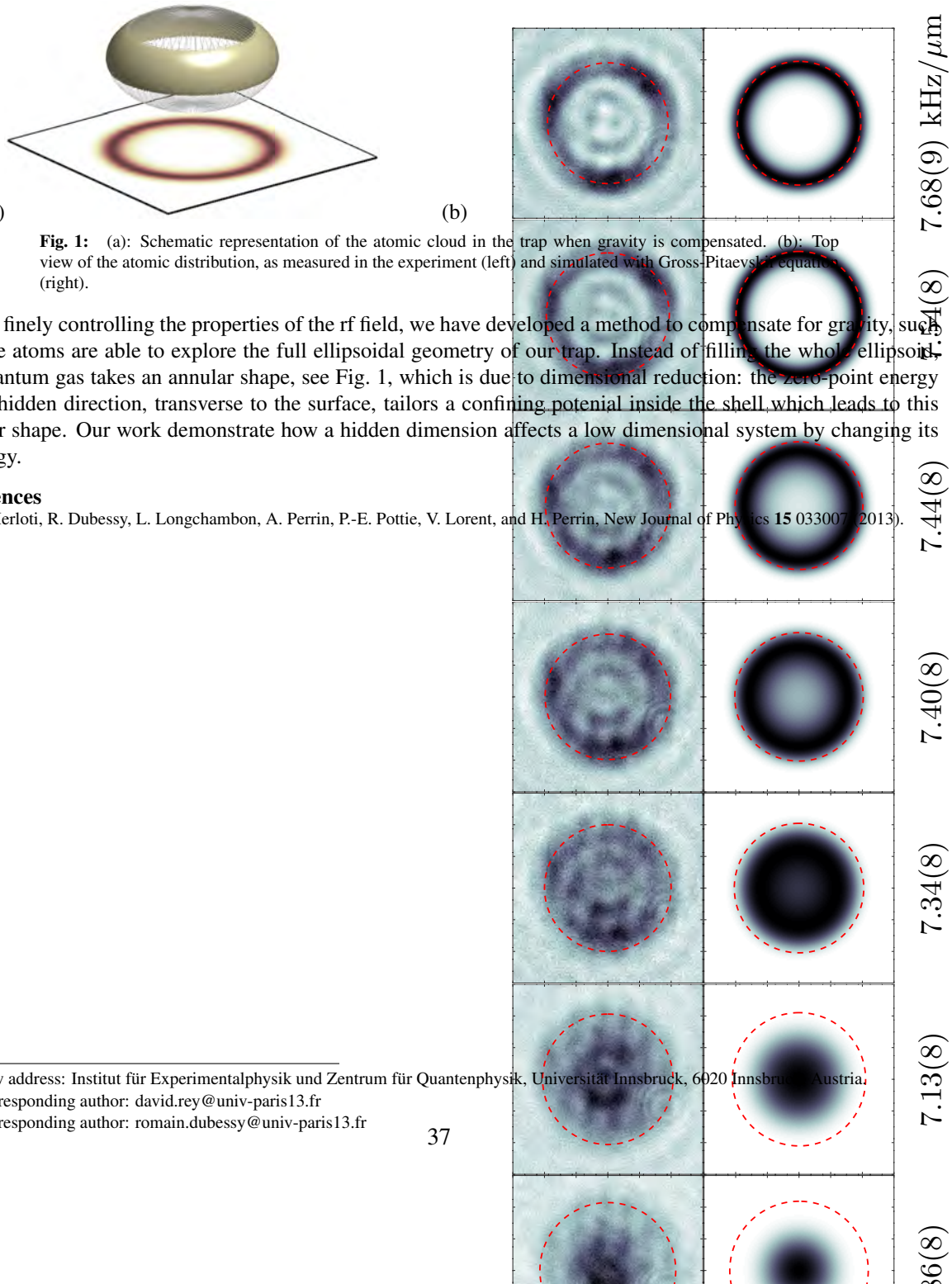

Fig. 1: (a): Schematic representation of the atomic cloud in the trap when gravity is compensated. (b): Top view of the atomic distribution, as measured in the experiment (left) and simulated with Gross-Pitaevskii equation (right).

By finely controlling the properties of the rf field, we have developed a method to compensate for gravity, such that the atoms are able to explore the full ellipsoidal geometry of our trap. Instead of filling the whole ellipsoid, the quantum gas takes an annular shape, see Fig. 1, which is due to dimensional reduction: the zero-point energy in the hidden direction, transverse to the surface, tailors a confining potenial inside the shell which leads to this annular shape. Our work demonstrate how a hidden dimension affects a low dimensional system by changing its topology.

References

[1] K. Merloti, R. Dubessy, L. Longchambon, A. Perrin, P.-E. Pottie, V. Lorent, and H. Perrin, New Journal of Physics **15** 033007 (2013).

*New address: Institut für Experimentalphysik und Zentrum für Quantenphysik, Universität Innsbruck, 6020 Innsbruck, Austria.

†Corresponding author: david.rey@univ-paris13.fr

‡Corresponding author: romain.dubessy@univ-paris13.fr

Spectroscopic study of the $3^1\Pi_u$ state in Cs_2 molecule by polarisation labelling laser technique

W. Jastrzebski[*1], **P. Kowalczyk**[†2], **J. Szczepkowski**[1], **A. Grochola**[1]

1. Institute of Physics, Polish Academy of Sciences, al. Lotników 32/46, 02-668 Warszawa, Poland

2. Institute of Experimental Physics, Faculty of Physics, University of Warsaw, ul. Pasteura 5, 02-093 Warszawa, Poland

We report an experimental study of the $3^1\Pi_u$ state in cesium dimer by the V-type optical-optical double resonance polarisation labelling spectroscopy technique [1] which allows to obtain simplified, rotationally resolved excitation spectra of Cs_2. The lowest vibrational levels $v \leq 6$ of the $3^1\Pi_u$ state were observed more than 30 years ago by Amiot [2] but, as numerous perturbations of part of these levels were not taken into account, the derived molecular constants were of limited applicability. By investigating the $3^1\Pi_u \leftarrow X^1\Sigma_g^+$ band system we extend observations of the $3^1\Pi_u$ state up to $v = 35$ with a wide coverage of J quantum numbers (see Fig.1).

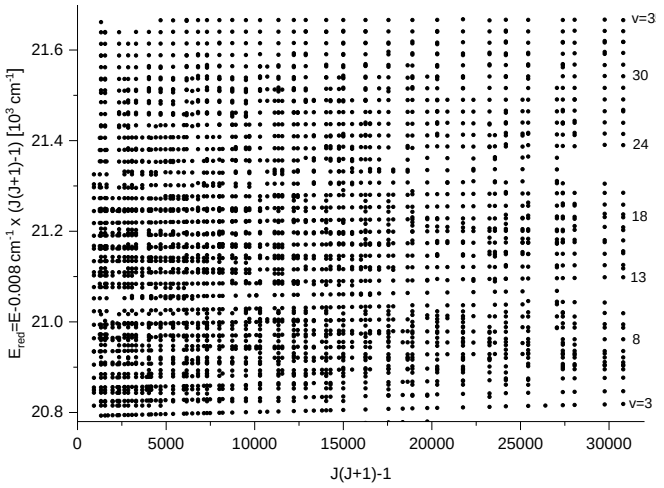

Fig. 1: Reduced term values of the observed rovibrational levels in the $3^1\Pi_u$ state plotted against $J(J+1)-1$. Two or occasionally three energies assigned to the same (v, J) quantum numbers indicate strong perturbations, presumably by the neighbouring $3^3\Pi_u$ and $4^3\Sigma_u^+$ states.

Our study reveals an intricate system of highly perturbed levels belonging to more than one electronic state. Contrary to Ref. [2] we find that only the four lowest levels of the $3^1\Pi_u$, $v = 0-3$, are free of observable perturbations and their energies can be described in a compact way by molecular constants (Table I). In the Table they are compared with predictions of the sole theoretical calculation available [3]. For the $3^1\Pi_u$ state levels with $v \geq 4$ a deperturbation analysis involving at least two other electronic states is required and the attempts of it will be discussed.

Table 1: Molecular constants (in cm^{-1}) for the $3^1\Pi_u$ state of Cs_2 representing energies of the lowest rovibrational levels ($v = 0-3$) compared with theoretical values [3]. Numbers in parentheses are uncertainties in units of the last digits.

	T_e	ω_e	B_e	$\alpha_e \times 10^4$	$D_e \times 10^8$	diss.en.
this work	20684.56(3)	30.62(1)	0.009125(30)	0.3784 (32)	0.274(9)	4911.3(9)
theory [3]	20734	29.3				

References

[1] R. Ferber, W. Jastrzebski, P. Kowalczyk, J. Quant. Spectrosc. Radiat. Transfer **58**, 53 (1997).

[2] C. Amiot, J. Chem. Phys. **89**, 3993 (1988).

[3] N. Spies, Ph. D. thesis, Universität Kaiserslautern, 1990.

[*]Corresponding author: jastr@ifpan.edu.pl

[†]Corresponding author: Pawel.Kowalczyk@fuw.edu.pl

Towards High-Precision Spectroscopy of the 1S–2S Transition in He^+

F. Schmid[*1], **A. Ozawa**[1], **J. Weitenberg**[1], **T. W. Hänsch**[1,2], **and Th. Udem**[1,2]
1. Max Planck Institute of Quantum Optics, Hans-Kopfermann-Str. 1, 85748 Garching, Germany
2. Faculty of Physics, Ludwig Maximilian University Munich, Schellingstr. 4, 80799 Munich, Germany

Precise tests of a physical theory require a system whose properties can be both measured and calculated with very high precision. One famous example is the hydrogen atom which, due to its simplicity, can be precisely described by bound-state quantum electrodynamics (QED). On the experimental side, laser spectroscopy employing frequency combs enables accurate measurements of the atomic transition frequencies. Two fundamental constants, the Rydberg constant and the nuclear charge radius, are determined by fitting the theory expression for the energy levels to the experimental data. Comparing the fundamental constants extracted from different combinations of measurements then serves as a consistency check for the theory itself.

In atomic hydrogen, the frequency of the extremely narrow 1S–2S two-photon transition was measured with a relative uncertainty below 10^{-14} [1, 2], while relative uncertainties on the 10^{-12} to 10^{-13} level have been recently achieved for broader transitions [3, 4, 5]. Trapping and cooling of atomic hydrogen under conditions suitable for high precision spectroscopy has not yet been achieved. Therefore, these experiments were performed on atomic beams where the thermal motion of the atoms ultimately limits the achievable accuracy.

We are currently setting up an experiment to perform spectroscopy on the 1S–2S transition in the simplest hydrogen-like ion, He^+. By combining the 1S–2S transition frequency with an accurate value of the helium nuclear charge radius measured by muonic helium spectroscopy [6], we will be able to make an independent determination of the Rydberg constant. This value will then be compared with the value obtained from hydrogen spectroscopy, serving as one of the most stringent tests of QED. Due to their charge, He^+ ions can be held near-motionless in the field-free environment of a Paul trap, providing ideal conditions for a high precision measurement. Furthermore, interesting higher-order QED corrections scale with large exponents of the nuclear charge, which makes this measurement much more sensitive to these corrections compared to the hydrogen case [7].

The main challenge of the experiment is that driving the 1S–2S transition in He^+ requires narrow-band radiation at 61 nm. This lies in the extreme ultraviolet (XUV) spectral range where no transparent solids and no cw laser sources exist. Our approach is to use two-photon direct frequency comb spectroscopy [5] with an XUV frequency comb. The comb is generated from an infrared high power frequency comb using intracavity high harmonic generation [8]. The spectroscopy target will be a small number of He^+ ions which are trapped in a linear Paul trap and sympathetically cooled by co-trapped Be^+ ions (see Fig. 1).

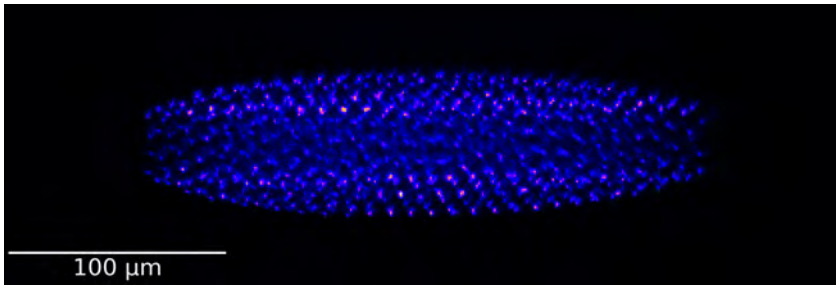

Fig. 1: Ion Coulomb crystal consisting of bright laser-cooled Be^+ ions surrounding a dark core of sympathetically cooled He^+ ions.

References

[1] C. G. Parthey *et al*., Phys. Rev. Lett. **107**, 203001 (2011).
[2] A. Matveev *et al*., Phys. Rev. Lett. **110**, 230801 (2013).
[3] A. Beyer *et al*., Science **358**, 79 (2017).
[4] H. Fleurbaey *et al*., Phys. Rev. Lett. **120**, 183001 (2018).
[5] A. Grinin *et al.*, Science **370**, 1061 (2020).
[6] J. J. Krauth *et al*., Nature **589**, 527 (2021).
[7] M. Herrmann *et al*., Phys. Rev. A **79**, 052505 (2009).
[8] I. Pupeza *et al*., Nat. Photonics **15**, 175 (2021).

*Corresponding author: fabian.schmid@mpq.mpg.de

Extended Spectroscopic Studies and Interatomic Potential Refinement of the $c^3\Sigma^+$ (Ω=1) State in KCs

R. Ferber[*1], **V. Krumins**[1], **A. Kruzins**[1], **M. Tamanis**[1], **I. Brakmane**[1], **A. Lapins**[1], **A. Oleynichenko**[2], **A. Zaitsevskii**[2], **E. Pazyuk**[2], **A. Stolyarov**[2],

1. Laser Center, Faculty of Physics, Mathematics and Optometry, University of Latvia, 19 Rainis blvd, Riga LV-1586, Latvia
2. Department of Chemistry, Moscow State University, 119991 Moscow, Leninskie gory 1/3, Russia

The present study is focused on spectroscopic investigations and electronic structure modelling of the $c^3\Sigma^+$ state of KCs; this molecule is under intensive research [1] aimed to produce it at ultracold conditions. First experiment-based results on $c^3\Sigma^+$ KCs have been obtained in recent paper [2]. In present study we applied the laser-induced fluorescence (LIF) method. The LIF spectra of the $c^3\Sigma^+ \rightarrow a^3\Sigma^+$ transition were recorded with Fourier-Transform spectrometer IFS125-HR (Bruker) using InGaAs detector. The Ti:Sapphire laser Equinox/SolsTis (MSquared) operated within 13800 - 12900 cm^{-1} range was exploited and $c \rightarrow a$ LIF signal was recorded within 9000 to 10000 cm^{-1} range. Detected LIF intensity distribution has been compared with the calculated one, which unambiguously confirms the vibrational numbering suggested in [2]. We obtained a set of about 750 new term values belonging to both e and f components, see Fig. 2, with increased accuracy of about 0.015 cm^{-1}, which are covering a more extended range of rotational and vibrational levels than in [2]. The term values were included in a direct point-wise interatomic potential reconstruction of the $c^3\Sigma^+(\Omega = 1)$ state, which explicitly takes into account the $\Lambda(\Omega)$-doubling effect. The experimental treatment of the $c^3\Sigma^+$ state was supported by the fully relativistic multi-reference coupled cluster calculation of the potential energy curves for the $c^3\Sigma^+(\Omega = 0^-, 1)$ states, as well as by the spin-forbidden $c^3\Sigma^+(\Omega = 1) - X^1\Sigma^+(\Omega = 0^+)$ and spin-allowed $c^3\Sigma^+(\Omega = 0^-, 1) - a^3\Sigma^+(\Omega = 0^-, 1)$ transition dipole moment functions.

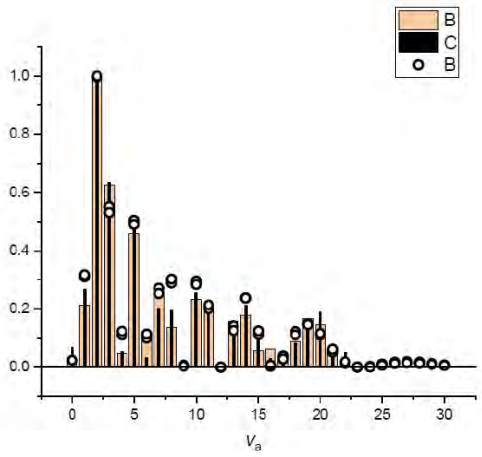

Fig.1.

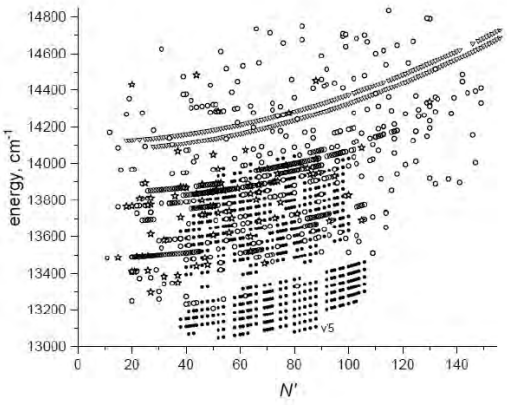

Fig.2.

Fig. 1: KCs LIF $c^3\Sigma^+ \rightarrow a^3\Sigma^+$ relative intensity distribution from the level $v' = 23$, $N' = 26$: bars – experiment, circles - calculations.
Fig. 2: KCs $c^3\Sigma^+$ state term values as dependent on rotational quantum number N' : empty circles – e levels, stars – f levels, points – data from [2], triangles – $B^1\Pi$ state data [3]

References

[1] M. Gröbner, P. Weinmann, E. Kirilov, H. C. Nägerl, Phys. Rev A **95**, 022715 (2017).
[2] J. Szczepkovski, A. Grochola, P. Kowalczyk, and W. Jastrzebski, JQSRT **204**, 133 (2018).
[3] I. Birzniece, O. Nikolayeva, M. Tamanis, and R. Ferber, J. Chem. Phys. **142**, 134309 (2015).

*Corresponding author: ruvins.ferbers@lu.lv

Towards a high-precision measurement of the ^{3}He and T nuclei atomic mass difference at LIONTRAP

Olesia Bezrodnova[*1], **Sangeetha Sasidharan**[1,2], **Sascha Rau**[1], **Wolfgang Quint**[2], **Sven Sturm**[1], **Klaus Blaum**[1]

1. Max-Planck-Institut für Kernphysik, Saupfercheckweg 1, 69117 Heidelberg, Germany
2. GSI Helmholtzzentrum für Schwerionenforschung, GmbH Planckstraße 1, 64291 Darmstadt , Germany

LIONTRAP (Light-Ion Trap) is a multi-Penning-trap mass spectrometer, optimized for measuring atomic masses of light ions with a relative precision of a few parts per trillion (ppt). The rest masses of the proton, deuteron, triton and helion (T and ^{3}He nuclei), together with the electron rest mass, serve as essential parameters for sensitive tests of fundamental physics [1]. For example, the electron-to-proton mass ratio enters the Rydberg constant, and the deuteron mass, combined with the proton mass and the neutron separation energy, allows the determination of the neutron mass and a test of special relativity. Furthermore, the helion and triton mass difference contributes to the prediction of the endpoint of the tritium β-decay energy spectrum in case the neutrino mass is zero. This value contains the information of the rest mass of the electron anti-neutrino, currently being investigated by the KATRIN collaboration [2].

In previous measurement campaigns, the masses of the proton [3], the deuteron and the HD^+ molecular ion were obtained and found to be in excellent agreement with values extracted from molecular hydrogen spectroscopy [4]. However, when combining these values with the literature value of the helion mass, an inconsistency of about five standard deviations appears, which is also known as “light ion mass puzzle”.

The present activities of the LIONTRAP group aim at the ultra-precise measurement of the helion and triton mass difference with a relative uncertainty better than 10 ppt. These measurements will provide an important input parameter for determining the electron anti-neutrino mass, and the helion mass value will further resolve the light ion mass puzzle.

In this contribution, the current status of the experiment will be presented, which includes the ^{3}He source preparation for the ongoing mass measurement campaign and the development and implementation of new techniques that will eventually enable a leap in spectroscopic resolution [5].

References

[1] E.G. Myers et al. Atoms **7(1)**, 37 (2019)
[2] M. Aker et al. Phys. Rev. Lett. **123**, 221802 (2019).
[3] F. Heiße et al. Phys. Rev. A **100**, 022518 (2019).
[4] S. Rau et al. Nature **585**, 43–47 (2020).
[5] S. Rainville et al. Nature **438**, 1096–1097 (2005).

*Corresponding author: olesia.bezrodnova@mpi-hd.mpg.de

Selective Two–Photon Excitation of Rydberg Atomic State Hyperfine Components

A. Cinins[*1], **K. Miculis**[1], **N. N. Bezuglov**[1,2], **A. Ekers**[3]

1. University of Latvia, Institute of Atomic Physics and Spectroscopy, Riga LV-1004, Latvia

2. Saint Petersburg State University, St. Petersburg 199034, Russia

3. King Abdullah University of Science and Technology (KAUST), Computer, Electrical and Mathematical Sciences and Engineering Division (CEMSE), Thuwal 23955-6900, Saudi Arabia

Upon interaction with resonant laser radiation, the stationary energy level structure of a quantum system is altered ("dressed"), forming coherent superpositions of the initial unperturbed states. Engineering the laser–dressed energy levels plays a key role in solving many problems of modern AMO physics, such as coherent population transfer using the STIRAP technique [1, 2], or storage of light pulses [3]. The task of preparing a quantum system in a specific state or superopsition of states becomes significantly more challenging if the system exhibits additional energy level structure. In fact, most realistic systems exhibit either a Zeeman sublevel structure of hyperfine (HF) structure, or both. Even relatively weak resonant laser fields can induce several HF components of a fine structure transition at once. Strong laser fields, which are commonly used in coherent control schemes, simultaneously couple multiple HF levels, forming a complicated spectrum of bright and dark dressed states [4].

We developed a general model of optically dressed states formed in a three–step ladder excitation scheme with HF splitting. Fine structure transitions $3S_{1/2} - 3P - nS_{1/2}(-nD)$ of atomic sodium were used as a model system. Dressed states formed in a strongly driven first transition are probed with a weak laser on the second transition. Each peak of the resulting Autler-Townes spectrum can be attributed to a certain pair of coupled sublevels in the first transition. We treat the absence of some bright peaks in the spectrum as a consequence of formation of multiple independent (orthogonal) ladder excitation schemes. Analysis of the independent excitation schemes reveals that in several cases, the interplay between HF interaction and Autler–Townes effect reduces the conventional electric dipole two-photon selection rule $|\Delta F| \leq 2$ to a more restrictive form of $\Delta F \equiv 0$. Further analysis indicates that in specific excitation schemes, introduction of a third, "blocking" laser enables active switching between the $|\Delta F| \leq 2$ and $\Delta F \equiv 0$ behaviours. This feature opens up a perspective to selectively address spectrally unresolved HF compenents of atomic and molecular energy levels, and therefore has various practical applications in Rydberg physics.

References

[1] N. V. Vitanov, A. A. Rangelov, B. W. Shore, and K. Bergmann, *Rev. Mod. Phys.* **89**, 015006 (2017).

[2] B. W. Shore, *Advances in Optics and Photonics* **9**, 563 (2017).

[3] O. Katz, O. Firstenberg, *Nature Communications* **9**, 2074 (2018).

[4] T. Kirova, A. Cinins, D. K. Efimov, M. Bruvelis, K. Miculis, N. N. Bezuglov, M. Auzinsh, I. I. Ryabtsev, and A. Ekers, *Phys. Rev. A* **96**, 043421 (2017).

[*]Corresponding author: arturs.cinins@lu.lv

Zero-field magnetometer based on the combination of atomic orientation and alignment

G. Le Gal[*1,2], **L.-L. Rouve**[2], **A. Palacios-Laloy**[1]
1. CEA-Leti, Université Grenoble Alpes, F-38000 Grenoble, France
2. Univ. Grenoble Alpes, CNRS, Grenoble INP, G2Elab, F-38000 Grenoble, France

Thanks to the improvement of their sensitivity, magnetometers based on optical pumping of atomic gasses -the so-called optically-pumped magnetometers (OPMs)- became serious candidates to replace superconductive-quantum interference devices for measuring ultra-low magnetic fields [1]. Our team works on OPMs based on a gas of helium-4 atoms in their 2^3S_1 metastable state. This spin-one species allows exciting both orientation ($< S_z > \neq 0$) and alignment ($< S_z^2 - S^2 > \neq 0$) polarizations in the atomic ensemble. We have recently proposed a new architecture of magnetometer pumped with elliptically polarized light which prepares both orientation and alignment for an isotropic vector measurement of the three components of a magnetic field [2]. The dynamics of atomic ensembles pumped by circularly- or linearly-polarized light and subject to magnetic fields is well known. We discuss here the more general case of a spin-one atomic state pumped with elliptically-polarized light of arbitrary ellipticity. We show how parametric resonance under several radio-frequency fields can be described analytically in this very general case using the dressed-atom formalism. As shown by Fig. 1, the theoretical expectations derived in this way are in close agreement with the experimental measurements. Additionally, we discuss some specific features of Hanle and parametric resonances of the metastable state of helium-4.

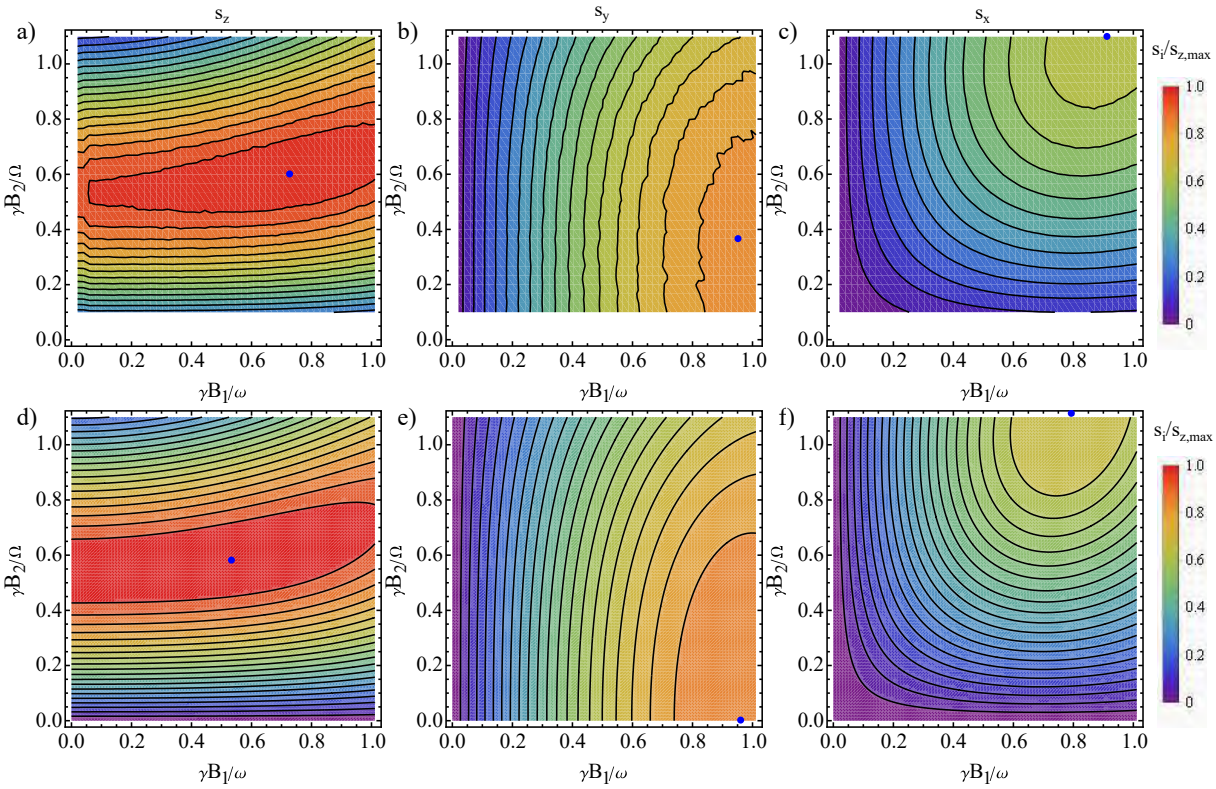

Fig. 1: Upper row: experimentally measured slopes to the B_z (s_z), B_y (s_y) and B_x (s_x) component of the magnetic field (a), b) and c) respectively) as a function of the RF fields amplitudes. Lower row: Theoretical estimations of the slopes s_z, s_y and s_x (d), e) and f) respectively) as a function of the RF fields amplitudes. The RF frequencies are $\Omega/2\pi = 15$ kHz and $\omega/2\pi = 40$ kHz. B_z is the component parallel to the atomic orientation, B_y is parallel to the atomic alignment, and B_x is orthogonal to both of them. γ is the helium-4 $2\ ^3S_1$ state gyromagnetic ratio.

References

[1] J. C. Allred, R.N. Lyman, T. W. Kornack, and M. V. Romalis, Phys. Rev. Lett. **89**, 130801 (2002).
[2] G. Le Gal *et al.*, to be published.

*Corresponding author: gwenael.legal@cea.fr

Towards the first strontium optical atomic clock in Croatia

I. Puljić[*1], **D. Aumiler**[†1], **T. Ban**[‡1], **N. Šantić**[§1]
1. Institute of Physics, Bijenička c. 46, 10000 Zagreb, Croatia

Development of atomic clocks has enabled technological and scientific advances like global navigation satellite systems, very-long-baseline interferometry, tests of general relativity and of the time-variation of fundamental physical constants, with further proposals for their use for the detection of dark mater and gravitational waves. The advent of optical frequency combs two decades ago has enabled improvements in the accuracy and precision of atomic clocks of over two orders of magnitude by enabling practical frequency measurements of optical clock transitions. Strontium is often used in such optical atomic clocks, with current state-of-the-art clocks reaching a level of stability of $10^{-17}\tau^{-1/2}$ and a level of accuracy bellow 10^{-18} [1].

In our experiment hot strontium atoms leaving the effusive oven will be first transversely cooled and then slowed down by using a Zeeman slower. Next, they enter a 2D magneto-optical trap (MOT) chamber and are pushed to a 3D-MOT chamber under a 45° angle relative to the entering direction. This way, uncooled atoms of the atomic beam do not enter the science chamber, the Zeeman slower beam is prevented from crossing the 3D-MOT and atoms in the 3D-MOT chamber are not affected by black-body radiation from the oven. In the 3D-MOT chamber, a blue and red 3D MOT will be used to cool down the atoms. Once cooled, atoms will be confined in optical tweezers or a multiplexed 1D lattice.

Stabilization of our laser systems will be based on an 1550 nm fiber laser stabilized to a high-finesse optical cavity and a low-noise frequency comb will be locked to it. The frequency comb spectrum will then be broadened with nonlinear processes to the required wavelenghts. Repumper lasers (at 679 nm and 707 nm), a red cooling laser (689 nm) and a clock laser (698 nm) will be phase locked to the frequency comb which will make the setup highly stable and simple. Also, since stabilizing both repumper lasers to the comb makes them phase coherent, it will be possible to perform Raman transitions between the long-lived states $^3P_0$ and $^3P_2$ and use them for high-resolution adressing.

References

[1] S. L. Campbell *et al.*, Science **358**, 90–94 (2017).

[*]Corresponding author: ipuljic@ifs.hr
[†]Corresponding author: aumiler@ifs.hr
[‡]Corresponding author: ticijana@ifs.hr
[§]Corresponding author: nsantic@ifs.hr

Asymmetric electron angular distributions in stimulated Compton scattering from H_2 irradiated with soft-X ray laser pulses

A. Sopena[*1,2], **A. Palacios** [1,3], **F. Catoire** [2], **H. Bachau**[2] **and F. Martín**[1,4,5]

1. Departamento de Química, Módulo 13, Universidad Autónoma de Madrid, 28049 Madrid
2. Centre des Lasers Intenses et Applications, Université de Bordeaux-CNRS-CEA, 33405 Talence Cedex, France
3. Institute for Advanced Research in Chemical Sciences, Universidad Autónoma de Madrid, 28049 Madrid, Spain
4. Instituto Madrileño de Estudios Advanzados (IMDEA) en Nanociencia, Cantoblanco, 28049 Madrid, Spain
5. Condensed Matter Physics Center (IFIMAC), Universidad Autónoma de Madrid, 28049 Madrid, Spain

The last two decades have seen the rise of X-ray free electron lasers (XFELs) throughout the world, providing ultra-short pulses with unprecedented intensities (10^{20} W/cm^2), over a large range of photon energies going from VUV to the hard X-ray domain. Besides the achievements in terms of brilliance, tremendous activity has been also devoted to the generation and control of XFEL pulses with sub-fs and even attosecond durations [1]. Extending X-ray to the attosecond domain is of crucial interest in a wide range of fundamental problems such as, for instance, resolving in time the dynamics of electronic rearrangement in atoms after core excitation or ionization [2]. New avenues are also opened to explore non-linear response in X-ray regime, like direct two-photon ionization of atoms [3] or non-linear Raman and Compton scattering processes [4].

In the present paper, we present a novel scheme of stimulated Compton scattering (SCS) on the hydrogen molecule using a highly intense ultrashort X-ray pulse with frequencies ranging from 0.5 to 1.6 keV (see Fig. 1a). We solve the time-dependent Schrödinger equation including the explicit evaluation of dipole and non-dipole terms. The short wavelength of the X-ray pulse breaks down the commonly employed dipole approximation and it is found that the coherent contributions of dipole and non-dipole effects lead to a symmetry breaking in the photoelectron emission, which strongly depends on the X-ray wavelength and the molecular orientation (see Fig. 1b). This is a pure non-linear effect captured in the low-energy lying electrons emitted after absorption and subsequent stimulated emission of photons within the energy bandwidth of the pulse.

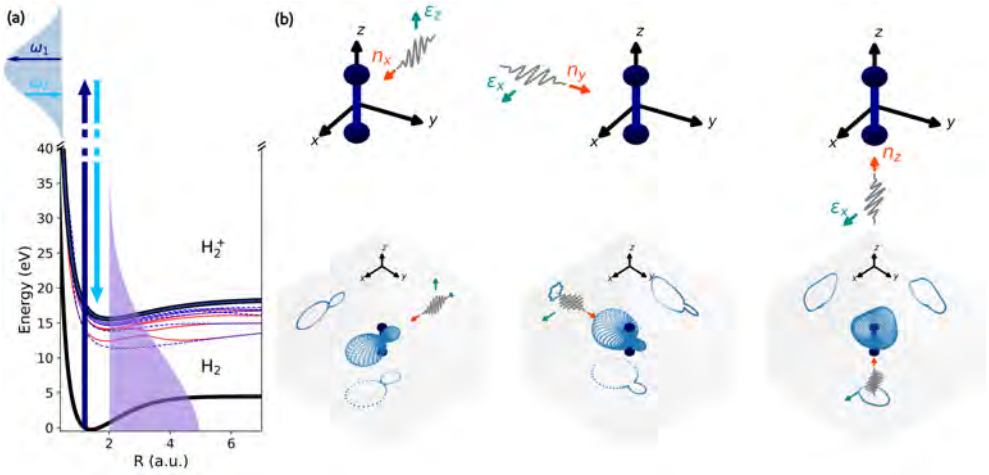

Fig. 1: (a) Schematic representation of SCS using ultrashort pulses with H_2 potential energy curves. (b) MFPADs integrated over a range of electron energies [0-2.5 a.u.] for 1.1 keV pulse with a duration of 68 as and an intensity of 10^{18} W/cm^2.

Additionally, we present results for SCS simulations using two ultrashort pulses with different photon energies and propagation directions. As seen in atoms [5], non-dipole effects depend on the relative propagation angle of the pulses presenting a maximum in the SCS ionization probability for counter-propagating pulses. In this case, the direction of the photoelectron emission asymmetry can be related to the momentum transferred to the molecule by the absorption of a photon and the subsequent emission stimulated by the second field.

References

[1] E. Hemsing *et. al.*, *Rev. Mod. Phys.* **86**, 897 (2014)
[2] S. Huang *et. al.*, *PRL* **119**, 154801 (2017)
[3] G. Doumy *et. al.*, *PRL* **106**, 083002 (2011)
[4] M. Kircher *et. al.*, *Nat. Phys.* **16**, 756 (2020)
[5] H. Bachau *et. al.*, *Phys. Rev. Lett.* **112**, 073001 (2014)

*Corresponding author: arturo.sopena@uam.es

Single-shot Stern-Gerlach magnetic gradiometer with an expanding cloud of cold cesium atoms

K. Gosar[*1,2], **T. Arh**[1,2], **T. Mežnaršič**[1,2], **I. Kvasič**[1], **D. Ponikvar**[1,2], **T. Apih**[1], **R. Kaltenbaek**[2], **E. Zupanič**[1], **S. Beguš**[3], **P. Jeglič**[1,2],

1. Jožef Stefan Institute, Jamova 39, SI-1000 Ljubljana, Slovenia
2. Faculty of Mathematics and Physics, University of Ljubljana, Jadranska 19, SI-1000 Ljubljana, Slovenia
3. Faculty of Electrical Engineering, University of Ljubljana, Tržaška cesta 25, SI-1000 Ljubljana, Slovenia

We combined the Ramsey interferometry protocol [1], the Stern-Gerlach detection scheme, and the use of elongated geometry of a cloud of fully polarized cold cesium atoms [2] to measure the selected component of the magnetic field gradient along the atomic cloud in a single shot [3]. In contrast to the standard method where the precession of two spatially separated atomic clouds is simultaneously measured to extract their phase difference [4], which is proportional to the magnetic field gradient, we demonstrated a gradiometer using a single image of an expanding atomic cloud with the phase difference imprinted along the cloud [3].

We started from a cloud of 2×10^5 cesium atoms at $T = 1.29\ \mu$K in a crossed dimple trap. We let the cold atom cloud expand along one of the dimple beams by turning off the perpendicular beam. The experiment is is schematically shown in Fig. 1a. After 20 ms the expansion becomes linear in time; at the total expansion time of 40 ms the $1/e$ width is $\sigma_x = 366$ mm. The protocol for measuring the magnetic field gradient is illustrated in Fig. 1b. It includes a Ramsey sequence composed of two $\pi/2$ RF pulses (50 kHz) that are separated by the interrogation time T_R. The absorption image of the atomic cloud is taken after the Stern-Gerlach separation of m_F-state populations in the applied magnetic field gradient $\partial B_z/\partial z$. The absorption images, from each of which the magnetic field gradient component can be extracted, are shown in Fig. 1c.

Using this single-shot Stern-Gerlach magnetic gradiometer, it is in principle possible to determine any component of the complete magnetic-field-gradient tensor $\partial B_i/\partial j$, with $i, j = x, y, z$. ∂B_i can be selected by the direction of B_0 (in Fig. 1a, this is B_x), whereas ∂j can be chosen by the orientation of the elongated cold atom cloud. The resolution of our single-shot gradiometer is not limited by thermal motion of atoms and has an estimated absolute accuracy below ± 0.2 mG/cm (± 20 nT/cm).

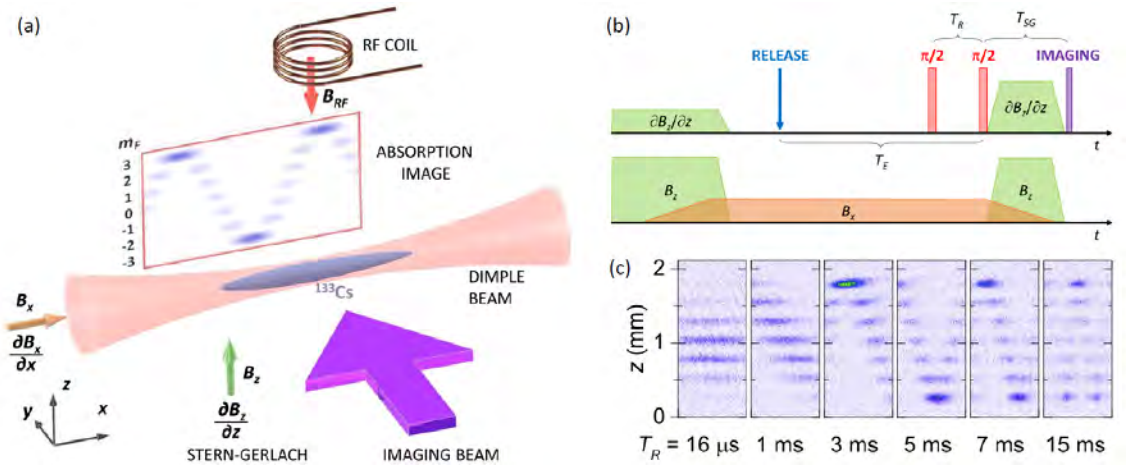

Fig. 1: (a) Schematic illustration of the magnetic gradiometer showing a cold atom cloud expanded along the dimple beam. (b) The experimental sequence for observing position-dependent Larmor precession of magnetization, caused by the $\partial B_x/\partial x$ component of the magnetic field gradient. (c) Absorption images of position dependent m_F -state populations for a range of interrogation times T_R.

References

[1] Y. Eto *et al.*, Control and Detection off the Larmor Precession of $F = 2$ ^{87}Rb Bose-Einstein Condesates by Ramsey Interferometry and Spin-Echo, Appl. Phys. Express **6**, 052801 (2013).
[2] M. Vengalattore *et al.*, Spontaneous Modulated Spin Textures in a Dipolar Spinor Bose-Einstein Condensate, Phys. Rev. Lett. **100**, 170403 (2008).
[3] K. Gosar *et al.*, Single-shot Stern-Gerlach magnetic gradiometer with an expanding cloud of cold cesium atoms, Physical Review A **103**, 022611 (2021).
[4] A. A. Wood *et al.*, Magetic tensor gradiometry using Ramsey interferometry of spinor condensates, Phys. Rev. A **92**, 053604 (2015).

*Corresponding author: katjagosar@gmail.com

Development of a 3D single-port magnetometer based on magneto-optical resonances in an alkali vapor

L. Busaite[1], **M. Auzinsh**[1], **F. Gahbauer**[1], **A. Mozers**[*1], **D. Osite**[1]
1. Laser Centre, University of Latvia, Rainis Boulevard 19, LV-1586 Riga, Latvia

Optical magnetometers based on alkali vapor cells are widely used and achieve excellent magnetic-field resolution [1]. They can be made compact and do not require cryogenics. Optical pumping magnetometers (OPM) usually create an oriented atomic state with the direction of orientation along the z-axis, which then rotates around a perpendicular magnetic field as a result of Larmor rotation. A probe beam linearly polarized along the z-axis, but propagating in a direction that is perpendicular to the magnetic field and the z-axis will have its plane of rotation shifted as it propagates through the medium of the OPM. Using a second probe beam perpendicular to the first probe beam and the z-axis, which also undergoes polarization rotation, one can measure the magnetic field in two directions. However, two or three optical ports are required. To overcome this difficulty, the OPM can be modified to work with atomic angular momentum alignment along the z-axis instead of orientation. Now a probe beam whose linear polarization vector is oriented at an angle of $\frac{\pi}{4}$ with respect to the z-axis will undergo polarization rotation, which lead to a dispersive magnetic field dependence of the absorption (see Fig. 1)[2].

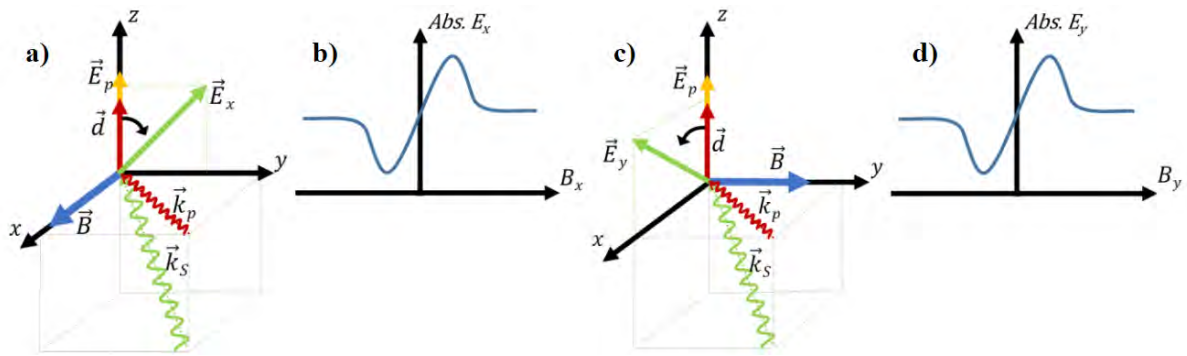

Fig. 1: Schematic representation of the dual-axis alignment OPM. Subfigure a) and c) show the polarization direction of the two probe beams, whereas b) and d) show the dispersive magnetic field dependence

This method has achieved promising results [3] in terms of resolution and does not require perpendicular optical ports. The z-component of the magnetic field can be measured using a parametric resonance magnetometer (PRM), which can be implemented using the same lasers by simply adding an appropriate RF excitation [4][5]. In this way, a 3D magnetometer can be realized.

We will model the expected signals and sensitivities of this type of magnetometer for various hyperfine transitions in alkali metal vapors, optimize the design and construct a laboratory prototype. At this conference we will present the results of our simulations.

References

[1] D. Budker, M. Romalis, Nat. Phys. **3**, 227 (2007)
[2] F. Beato, E. Belorizky, E. Labyt, M. Le Prado, and A. Palacios-Laloy, Phys. Rev. A **98**, 1 (2018)
[3] G. Le Gal, G. Lieb, F. Beato, T. Jager, H. Gilles, and A. Palacios-Laloy, Phys. Rev. Appl. **12**, 1 (2019)
[4] J. Dupont-Roc, Rev. Phys. Appliquée **5**, 853 (1970).
[5] A. Weis, G. Bison, and A. S. Pazgalev, Phys. Rev. A **74**, 33401 (2006)

*Corresponding author: arturs.mozers@lu.lv

Towards Ramsey-comb spectroscopy of the 1S-2S transition in singly-ionized helium

A. Martínez de Velasco[*1], **E. Gründeman**[1], **C. Roth**[1], **V. Barbé**[1], **M. Collombon**[1], **J.J. Krauth**[1], **K.S.E. Eikema**[1]

1. LaserLab, Vrije Universiteit Amsterdam, De Boelelaan 1105, 1081 HV Amsterdam, The Netherlands

The 1S-2S transition of hydrogenic systems is a benchmark for tests of fundamental physics [1]. The most prominent example is the 1S-2S transition in atomic hydrogen, where impressive relative accuracies have been achieved [2-3]. Nowadays, these fundamental physics tests are hampered by estimates of uncalculated higher-order QED terms and the uncertainties in the fundamental constants required for their calculation [4]. An independent, experimental approach to contribute to and further improve these fundamental physics tests is to measure the 1S-2S transition in He^+. Because He^+ has twice the nuclear charge of hydrogen, certain interesting QED contributions are strongly enhanced and can therefore be tested more precisely than in hydrogen. Furthermore, nuclear properties such as e.g. the alpha particle charge radius or nuclear polarizability contributions can be probed [4].

We aim to use the Ramsey-comb spectroscopy (RCS) method [5] in order to measure the 1S-2S transition in singly-ionized helium in the extreme ultraviolet (XUV) spectral range and contribute to fundamental tests of QED. RCS uses two amplified and up-converted pulses out of the infinite pulse train of a frequency comb laser to perform a Ramsey-like excitation. The He^+ spectroscopy scheme is based on two-photon excitation, using one XUV photon at 32 nm (generated through High-Harmonic Generation, the 25th harmonic) and one infrared photon at 790 nm from the fundamental beam. The atomic sample will consist of a He^+ ion confined in a Paul trap, sympathetically cooled by a Doppler- and Raman-cooled Be^+ ion, which has a cycling transition at 313 nm that we also use to monitor the Be^+ ion. The readout scheme for two-photon He+ excitation is based on quantum logic spectroscopy [6], which relies on detecting the recoil of He+ upon excitation, transferred to the Be^+ ion.

Recently we demonstrated that RCS can be combined with HHG [7] leading to a high precision measurement in xenon at 110 nm [8]. The many new components required for the He^+ experiment, such as a new RCS laser, the ion trap, laser cooling and imaging systems, are approaching completion and we will report on their current status. Using the RCS method we aim to do a first 1S-2S measurement of He^+ with an accuracy of 1-10 kHz, while an accuracy of better than 50 Hz should be ultimately achievable.

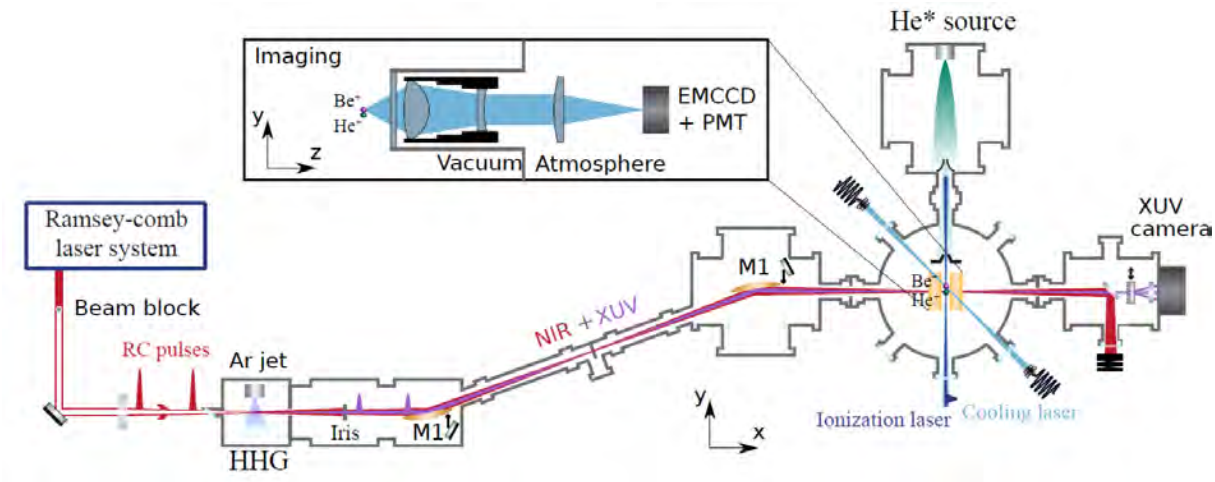

Fig. 1: Overview of our He^+ 1S-2S spectroscopy setup. Two selectively-amplified frequency comb pulses and their 25th harmonic, generated in an argon jet, are focused onto a sympathetically-cooled helium ion in a Paul trap.

References

[1] Herrmann *et al.*, Phys. Rev. A, **79**, 052505 (2009).
[2] Niering *et al.*, Phys. Rev. Lett. **84**, 5496 (2000).
[3] de Beauvoir *et al.*, Eur. Phys. J. D **12**, 61 (2000).
[4] Krauth *et al.*, PoS(FFK2019) **49**, (2019).
[5] Morgenweg *et al.*, Nature Phys. **10**, 30–33 (2014).
[6] Schmidt *et al.*, Science **309**, 749 (2005).
[7] Dreissen *et al.*, Phys. Rev. Lett. **123**, 143001 (2019).
[8] Dreissen *et al.*, Phys. Rev. A **101**, 052509 (2020).

*Corresponding author: andresmartinezdevelasco@gmail.com

Vector magnetometry using NV centers in diamond

Reinis Lazda[*1], **Laima Bušaite**[1], **Florians Gahbauers**[1], **Andris Bērziņš**[1], **Mārcis Auziņš**[1]
1. Laser Centre, University of Latvia, Jelgavas Street 3, LV-1004 Riga, Latvia

The NV center is a color defect center in diamond (see Fig. 1) whose properties make it very suitable for measuring magnetic fields (the direction and magnitude) [1]. In bulk, they give a diamond a yellowish color.

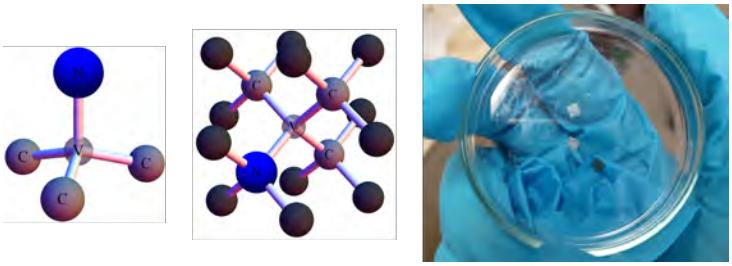

Fig. 1: Left: a single NV center, a C_{3v} symmetric structure in a diamond crystal carbon lattice consisting of a carbon atom substituting nitrogen atom and a lattice vacancy adjacent to it. Center: NV center unit cell in a diamond crystal lattice. Right: $3 \times 3 \times 0.5$ mm^3 synthetic diamonds used in the laboratory.

The sensitivity of a magnetic field measurement [2] can be estimated by the following relation:

$$\eta_{sensitivity} \approx \frac{\Delta f}{C\sqrt{N_P}}. \tag{1}$$

The main parameters are Δf - the full width at half maximum (FWHM) of the optically detected magnetic resonance (ODMR) [3], C - the ODMR contrast, N_P - the number of received photons per second (see Fig. 2).

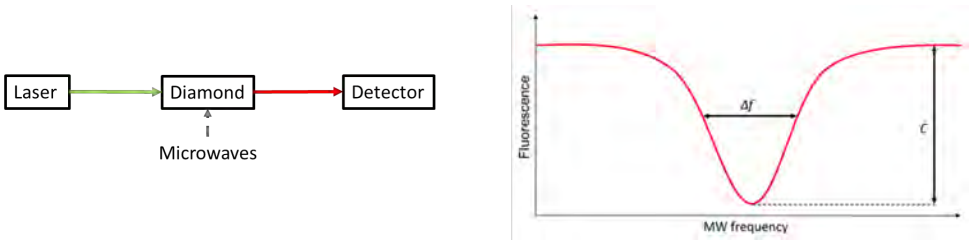

Fig. 2: Left: a simplified scheme of the ODMR experiment, when a diamond with NV centers is excited by green light, the emitted fluorescence is red. Right: a sample ODMR signal in the red fluorescence.

The properties of the diamond (lattice structure, mechanical and chemical robustness, small size) and the NV center make it suitable for making a compact magnetic field measuring platform (see Fig. 3).

Fig. 3: A handheld prototype device for measuring the direction and magnitude of a magnetic field using a diamond with NV centers.

References

[1] J ennifer M. Schloss, John F. Barry, Matthew J. Turner, and Ronald L. Walsworth, Phys. Rev. Applied **10**, 034044 (2018).
[2] J ohn F. Barry, Jennifer M. Schloss, Erik Bauch, Matthew J. Turner, Connor A. Hart, Linh M. Pham, and Ronald L. Walsworth, Rev. Mod. Phys. **92**, 015004 (2020).
[3] R einis Lazda, Laima Busaite, Andris Berzins, Janis Smits, Florian Gahbauer, Marcis Auzinsh, Dmitry Budker, and Ruvin Ferber, Phys. Rev. B **103**, 134104 (2021).

*Corresponding author: reinis.lazda@lu.lv

Attosecond Spectroscopy of Small Organic Molecules: XUV pump-XUV probe Scheme in Glycine

J. Delgado[*1], **M. Lara-Astiaso** [2] **J. González-Vázquez** [2] **P. Decleva** [3] **A. Palacios**[†2,4], **F. Martín** [1,2,5]

1. Instituto Madrileño de Estudios Avanzados en Nanociencia, 28049 Madrid, Spain
2. Departamento de Química, Módulo 13, Universidad Autónoma de Madrid, 28049 Madrid, Spain
3. Dipartamento di Scienze Chimiche e Farmaceutiche, Universitá di Trieste, 34127 Trieste, Italy
4. Institute for Advanced Research in Chemical Sciences (IAdChem), Universidad Autónoma de Madrid, 28049 Madrid, Spain
5. Condensed Matter Physics Center (IFIMAC), Universidad Autónoma de Madrid, 28049 Madrid, Spain

The availability of coherent light sources with attosecond resolution (1 as=10^{-18} s) has opened the door to resolve electron dynamics in excited and ionized complex molecules. The early electron dynamics triggered in a biomolecule is at the heart of biological processes which are essential to life. Therefore, understanding the ultrafast charge dynamics that steer these processes has become a hot topic in the field of attosecond science. Attosecond time-resolve experiments allow us to retrieve images of this charge dynamics in molecules. The first experiment retrieving a sub-femtosecond ultrafast dynamics in a biomolecule was performed by using an as UV-pump/ fs IR-probe scheme in phenylananine [1]. The sub-fs charge fluctuations where associated with electronic coherences initiated by the as pump pulse. Theorical calculations to describe this experiment were initially performed considering that the nuclei of the molecule remained fixed in space [1],[2]. How long these electronic coherences can survive when nuclear motion comes into play is a question that has yet to be solved.

In the present study, we pursue to shed some light on this matter by theoretically describing the outcome of an attosecond two-color XUV-pump/XUV- probe scheme in glycine. The broadband pump pulse ionizes the molecule, creating a coherent superposition of cationic states, which evolve in time coupled to the nuclear motion until it is probed by the second XUV pulse. An explicit evaluation of the full-electron wave function in the continuum and the inclusion of non-adiabatic effects are carried out [3]. Both aspects have been addressed in this work by combining a multi-reference static-exchange method and a surface hopping approach, respectively. We have found that, in the absence of the probe pulse, ionization can lead to fragmentation of the glycine cation through the C-C or the C-N bonds. The lower electronic states of the cation are more likely to induce elongation of the C-C bond, while the higher excited states favor elongation of the C-N bond, both of which can ultimately break. We have found that by simply varying the central frequency of the pump pulse by a few eVs, one can alter the cation dynamics favouring specific fragmentation pathways. We have also investigated the role of the probe pulse in capturing the above dynamics, first by looking at the photoelectron spectra and then at the fragmentation yields, both as a function of the pump-probe delay.

References

[1] F. Calegari, D. Ayuso, A. Trabattoni, L. Belshaw, S. De Camillis, S. Anumula, F. Frassetto, L. Poletto, A. Palacios, P. Decleva, J. B. Greenwood, F. Martín, M. Nisoli, Science **346** 336-339 (2014)
[2] Kuleff, Cederbaum, J. Phys. B: At., Mol. Opt. Phys **47** 124002 (2014)
[3] J. Delgado, M. Lara-Astiaso, J. González-Vázquez, P. Decleva, A. Palacios, F. Martín, Faraday Discuss. **Advance Article** (2021)

[*]Corresponding author: jorge.delgado@imdea.org
[†]Corresponding author: alicia.palacios@uam.es

Prospect for Probing the Time Variation of Fundamental Constants with Molecular Iodine Optical Clocks

F. L. Constantin[*1],
1. Laboratoire PhLAM, CNRS UMR 8523, University of Lille, 59655 Villeneuve d'Ascq, France

A space-time variability of fundamental constants, allowed by the dark matter couplings addressed in theories beyond the Standard Model, may be strongly constrained using optical clock comparisons or astrophysical observations [1]. The frequency measurements of molecular clocks allowed to constrain the time variation of the proton-to-electron mass ratio μ at the 10^{-14}/yr level in a few cases [2,3]. The constraint may be improved by increasing the accuracy of the clock transitions, by exploiting transitions with increased sensitivity at the variations of fundamental constants, and by performing measurements during a longer period of time. This contribution proposes to perform optical frequency measurements for Doppler-free lines of the molecular iodine in order to extract correlated temporal variations for a set of fundamental constants.
The frequencies of the transitions of the $B(0_u^+)$-$X(1\Sigma_g^+)$ electronic band of $^{127}I_2$ (Fig. 1.a) are modelled using a Dunham series expansion for the rovibronic energy levels [4]. That enables to derive the sensitivity coefficients to the variation of μ with values that are at the 10^{-2} level. The results for transitions to the levels at the limit of dissociation of the B state, that display narrow natural linewidths, are shown in Fig. 1.b. These transitions encompass the fine structure splitting of the atomic iodine and their frequencies scale approximately as α^2 in function of the fine structure constant α. On the experimental side, recent developments were directed towards space-qualified ultrastable lasers based on molecular iodine references [5-7]. A compact setup based on a frequency-tripled telecom laser locked at 514 nm allowed a frequency stability at the 10^{-14} level at 1 s [6]. The frequency uncertainty of the molecular iodine clocks were estimated at the 10^{-15} level [7]. The measurements of absolute frequencies of three optical transitions of $^{127}I_2$ pertaining to the vibronic bands indicated in Fig. 1.b have the potential to constrain conjointly the time variation of α and μ at the 10^{-14}/yr level. Using in such comparisons optical atomic clocks with improved stability and accuracy will enable access to another set of sensitivities to the variations of fundamental constants and may improve the constraints on their time variation by two orders of magnitude.

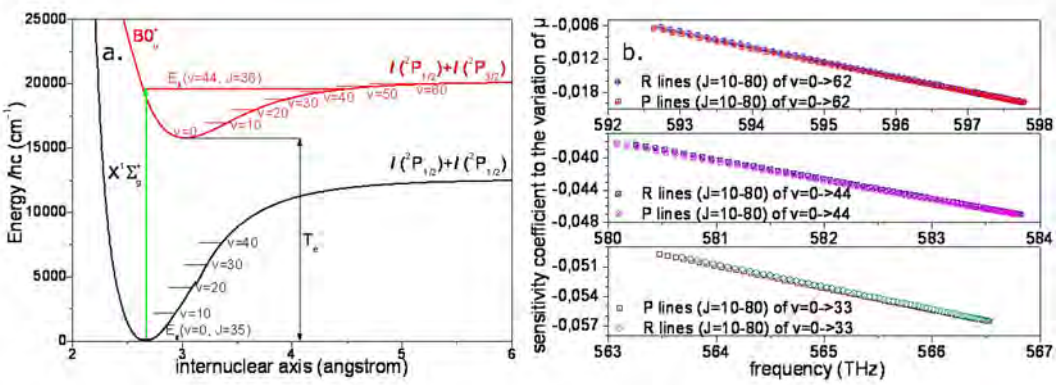

Fig. 1: a. Rovibronic energy levels adressed by the optical transitions of $^{127}I_2$. b. Dependences of the sensitivity coefficient to the variation of μ on the transition frequency in selected vibronic bands.

References

[1] M. S. Safronova *et al*, Rev. Mod. Phys. **90**, 025008 (2018).
[2] A. Shelkovnikov *et al*, Phys. Rev. Lett. **100**, 150801 (2008).
[3] J. Kobayashi, A. Ogino, and S. Inouye, Nat. Commun. **10**, 3771 (2019).
[4] S. Gerstenkom and P. Luc, J. Phys. France **46**, 867 (1985).
[5] T. Schuldt *et al*, Proc. of SPIE **10564**, 105641N (2017).
[6] J. Barbarat *et al*, Proc. of SPIE **11180**, 111800T (2018).
[7] N. Gürlebeck *et al*, Phys. Rev. D **97**, 124051 (2018).

*Corresponding author: FL.Constantin@univ-lille1.fr

High-Quality Level-Crossing Resonances in a Cesium Vapor Cell for Applications in Atomic Magnetometry

D. V. Brazhnikov[*1,2], **V. I. Vishnyakov**[1], **S. M. Ignatovich**[1], **I. S. Mesenzova**[1]
C. Andreeva [3,4], **A. N. Goncharov**[1,2,5]

1. Institute of Laser Physics SB RAS, 15B Lavrentyev Avenue, 630090 Novosibirsk, Russia
2. Novosibirsk State University, 1 Pirogov Street, 630090 Novosibirsk, Russia
3. Institute of Electronics BAS, 72 Tsarigradsko Chaussee, 1784 Sofia, Bulgaria
4. Faculty of Physics, Sofia University "St. Kliment Ohridski", 5 James Bourchier Boulevard, Sofia 1164, Bulgaria
5. Novosibirsk State Technical University, 20 Karl Marks Avenue, 630073 Novosibirsk, Russia

The nonlinear resonances induced by the zero-magnetic-field level-crossing (LC) phenomenon in an atomic ground state are known as the ground-state Hanle effect (GSHE) [1]. These resonances are nowadays applied for high-sensitivity magnetic field measurements. A single traveling light wave with linear or circular polarization is commonly utilized for GSHE-based magnetometers [2,3]. However, in recent years, several bright ideas have been introduced in the standard schemes that imply adding the second light wave (e.g., see [4-8]).

Here we propose and study a new scheme consisting of counterpropagating pump and probe beams with opposite circular polarizations. The waves excite cesium atoms in the F_g=4 ground state of the D_1 line, while a transverse magnetic field ($\mathbf{B}_x \perp \mathbf{k}$) is being scanned around zero to observe the LC resonance. An electromagnetically induced absorption (EIA) resonance can be observed (Fig. 1a). The main advantage of the proposed configuration is that an extremely high contrast of the resonance can be achieved, being accompanied by a relatively small linewidth. It is also worth noting that high-quality resonances (in terms of a contrast-to-width ratio) can be obtained at relatively small temperature and dimensions of the cell, namely the scheme provides good results in the range T=50−60 °C with a vapor cell volume of around 0.12 cm^3. We compare our scheme with a commonly used one where a single circularly polarized wave is used. As seen from Fig. 1b, the contrast can be 5 times higher in our scheme than in the ordinary single-wave configuration.

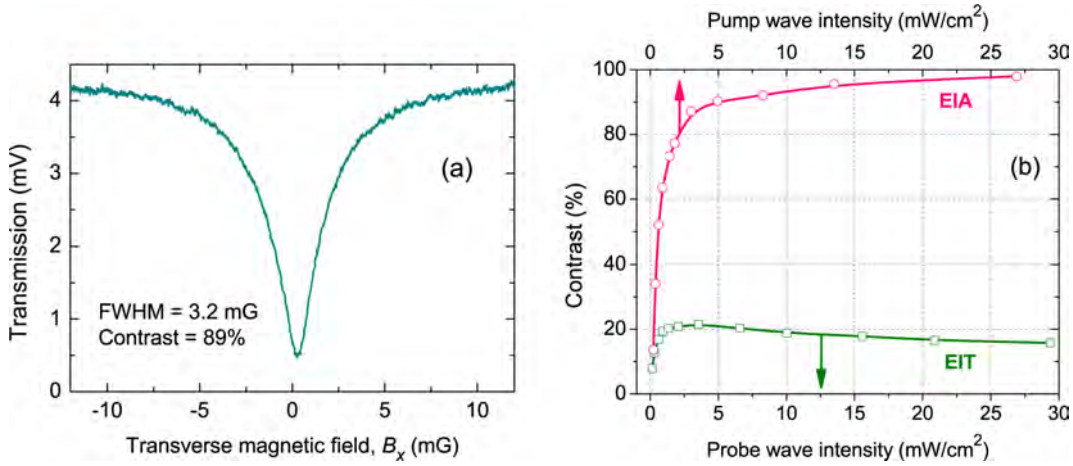

Fig. 1: (a) An example of high-contrast EIA resonance in a buffer-gas-filled (Ne, 130 Torr) Cs vapor cell. P_{probe}= 5 μW, P_{pump}=320 μW, d_{beams}=3 mm. (b) The resonance contrast under a single wave regime (EIT) and under counterpropagating waves (EIA). T=55°C.

The results open a new way for developing low-power high-sensitivity miniaturized atomic magnetometers. The work has been supported by RFBR (20-52-18004) and Bulgarian National Science Fund (KP-06-Russia/11) in the framework of a joint research project. We also thank RSF (17-72-20089). I.S. Mesenzova thanks Ministry of Science and Higher Education of the Russian Federation (Presidential Scholarship SP-269.2021.3).

References

[1] W. Gawlik, D. Gawlik, and H. Walther, in *The Hanle Effect and Level-Crossing Spectroscopy*, G. Moruzzi and F. Strumia, eds. (Springer Science+Business Media, New York, 1991).
[2] E. Alipieva, S.V. Gateva, and E. Taskova, IEEE Trans. Instrum. Meas. **54**, 738 (2005).
[3] V. Shah, S. Knappe, P. D. D. Schwindt, and J. Kitching, Nat. Photonics **1**, 649 (2007).
[4] S. Gozzini *et al.*, Opt. Lett. **42**, 2930 (2017).
[5] D. V. Brazhnikov *et al.*, Laser Phys. Lett. **15**, 025701 (2018).
[6] L. Lenci *et al.*, J. Phys. B: At. Mol. Opt. Phys. **52**, 085002 (2019).
[7] D. V. Brazhnikov, S. M. Ignatovich, A. S. Novokreshchenov, and M. N. Skvortsov, J. Phys. B: At. Mol. Opt. Phys. **52**, 215002 (2019).
[8] D. Brazhnikov *et al.*, Opt. Lett. **45**, 3309 (2020).

*Corresponding author: brazhnikov@laser.nsc.ru

Calculated Oscillator Strengths for Radiative Transitions of Cosmochronological Interest in Singly Ionized Thorium (Th II)

S. Gamrath[*1] **P. Quinet**[†1,2], **P. Palmeri**[1], **K. Wang**[3], **M.R. Godrefoid**[4]

1. Physique Atomique et Astrophysique, Université de Mons, Belgium

2. IPNAS, Université de Liège, Belgium

3. Institute Hebei Key Lab of Optic-electronic Information and Materials, The College of Physics Science and Technology, Hebei University, China

4. Chimie Quantique et Photophysique, Université Libre de Bruxelles, Belgium

Up to now, there are very few available calculations of radiative data for singly ionized thorium (Th II). This is mainly due to the complexity of its electronic configurations and to the fragmentary knowledge of its experimental spectrum.

Transition probabilities and oscillator strengths for Th II radiative transitions are important in astrophysics [1]. Indeed, Th II, as well as U II, is used as a cosmochronometer in order to determine the age of stars. More specifically, the ^{232}Th isotope, with a half-life of 14 Gyr, is used to date galactic stars [2-6]. Goriely and Clerbaux [7] pointed out that new accurate data on heavy radioactive elements could improve the accuracy of cosmochronometric analyses.

For the particular use in cosmochronology, knowing the Th II abundances in stars is of high importance. Indeed, in order to date a star, we use [8]:

$$R^{U/Th} = P^{U/Th} e^{\frac{T}{\tau_{Th}} - \frac{T}{\tau_U}} \quad (1)$$

where R is the Uranium/Thorium abundances ratio, P is the production rate, τ is the half-life and T the studied star's age. Therefore, in order to precisely determine R, a better knowledge of Th II's spectrum is necessary. We already published atomic data for the U II lines .

The accuracy of this dating technique is still hampered by the lack of available radiative parameters for Th II spectral lines. Some oscillator strengths were obtained experimentally by combining branching fraction measurements with laboratory lifetimes determined using laser spectroscopy [10-11], but these data only concern a restricted number of strong lines. In order to partly fill this gap, we carried out extensive calculations of oscillator strengths for the most intense Th II lines of potential cosmochronological interest using the pseudo-relativistic Hartree-Fock with core-polarization potential [12-13] theoretical approach. Our results will be presented at the conference.

References

[1] I.U. Roederer et al., The Astrophysical Journal 698 (2009) 1963–1980.
[2] H.R. Butcher, Nature 328 (1987), 127-131.
[3] P. François, M. Spite and F. Spite, Astron. Astrophys. 274 (1993) 821-824
[4] J.J. Cowan et al., Astrophys. J. 521 (1999) 194-205.
[5] R. Cayrel et al., ASP Conference Series 245 (2001) 244-251.
[6] C. Sneden and J.J. Cowan, RevMexAA (Serie de Conferencias) 10 (2001) 221-227.
[7] S. Goriely and B. Clerbaux, Astron. Astrophys. 346 (1999) 798-804.
[8] N. Dauphas, Lunar and Planetary Science XXXVI (2005) 1126
[9] S. Gamrath *et. al.*, MNRAS, 480, 4754-4760 (2018)
[10] H. Nilsson et al., A&A 382 (2002) 368-377.
[11] S.L. Redman et al., Astrophys. J. Suppl. Ser. 211 (2014) 4 (12pp).
[12] R.D. Cowan, The Theory of Atomic Structure and Spectra, Univ. California Press, Berkeley (1981)
[13] P.Quinet *et.al*, J. Alloys Comp., 344, 255 (2002)

[*]Corresponding author: sebastien.gamrath@umons.ac.be
[†]Corresponding author: pascal.quinet@umons.ac.be

Similarities of fragmentation of some amino acids under low-energy electron impact

J. Tamuliene[*1], **L. Romanova**[2], **V. Vukstich**[2], **A. Snegursky**[†2]

1. Vilnius University, Institute of Theoretical Physics and Astronomy, 3 Sauletekio av., 10257 Vilnius, Lithuania

2. Institute of Electron Physics, Ukr. Nat. Acad. Sci., 21 Universitetska str., 88017 Uzhgorod, Ukraine[1]

Knowledge of structure and chemical properties of amino acids is necessary to understand their reactivity and biological activity in human body, application in clinical practice for diagnosis and treatment. Recent SARS-CoV-2 outbreak stimulated coronavirus research. Coronavirus particles contain 4 major structural proteins, one of which mediates virus attachment to the body cell receptors and promotes virus entry into the affected organism cell. In light of this, destruction of these pathogenic proteins will provide an opportunity to develop methods to overcome this threat. Hence, we present the insight into the amino acid (valine, glutamine and threonine) fragmentation under the low- ($<$100 eV) energy electron impact. A mass-spectrometric technique was used to measure the mass spectra of the above acids and the appearance energies for the most prominent ionic fragments. The B3LYP/cc-pVTZ approach has accompanied these measurements to explain an experiment results. The results obtained indicate some similarities in the mass spectra of the above amino acids. They contain the NH_2-CH-COOH part that allows us to predict formation of the same fragments and, what is most important, the influence of other substitutes on the low-energy electron impact fragmentation.

The intense peaks were observed in the m/z=27–30 and 40–50 regions of the mass spectra for all molecules studied. The m/z=28 and 29 fragments are present in all mass spectra. Their chemical composition was the same in all investigated cases.

Table 1: Values of the calculated appearance energy for some main fragments produced under low-energy electron impact. The lowest appearance energies are presented.

Fragment	Appearance energy, eV		
	Valine	Glutamine	Threonine
CH_2N (m/z=28)	9.10, 9.87	12.56	10.67, 11.21
C_2H_5 (m/z=29)	10.35, 10.58	10.0	11.38, 12.05
CHO_2 (m/z=45)	11.53		12.44,12.47
C_2H_5O (m/z=45)			10.36, 9.39

The results of our theoretical analysis indicate that the m/z=28 fragment is the CH–NH^+ radical that could be formed when the CH–NH_2^+ (m/z=29) fragment loses one H atom. The values of the binding energy per atom are 2.06 eV and 2.77 eV for m/z=29 and m/z=28, respectively, indicating that the lowermass fragment has higher thermal stability. The results of comparison of the appearance energies allow us to predict that in case of valine the m/z=28 fragment could be formed directly from the parent acid molecule, while in the glutamine case this fragment formation from m/z=29 is more probable. In case of threonine both these pathways are probable due to the presence of several conformers.

Note that the most prominent peak in the glutamine mass spectrum is m/z=84. We have found that this fragment could be formed due to the loss of the $COOH^+$ (m/z=45) fragment and the H and O atoms or NH_2 and H ones. It is a reason for the absence of the m/z=45 fragment peak in the mass spectrum of glutamine. It is interesting that both ionized threonine conformers are decomposed at their equilibrium point, with fragmentation starting immediately when the molecule is on its way to lose electron. Thus, at the equilibrium point, the ionized molecule splits into the $C_2H_5NO_2$ (m/z=75) and C_2H_4O (m/z=44) or the $C_2H_4NO_2$ (m/z=74) and C_2H_5O (m/z=45) fragments. The appearance energy for $C_2H_5O^+$ is lower than that for $COOH^+$. Hence, the presence of $C_2H_5O^+$ is more probable than that of $COOH^+$. And only in case of valine the m/z=45 fragment is COOH. On the other hand, the results presented clearly indicate that the presence of the NH_2-CH-COOH fragment does not indicate formation of the $COOH^+$ fragment. Even the m/z=28 fragment could be produced in a different way. Hence, there is no doubt that the amino acid substitutes are crucial for these molecules fragmentation under low-energy electron impact.

Present study was supported in part by the Ukrainian National Research Fund (Grant No. 2020.01/0009 "Influence of ionizing radiation on the structure of amino acid molecules").

[*]Corresponding author: Jelena.Tamuliene@tfai.vu.lt

[†]Corresponding author: snegursky.alex@gmail.com

Large-scale atomic data calculations in Ce V–X ions for application to early kilonova emission from neutron star mergers

H. Carvajal Gallego[*1], **P. Palmeri**[1], **P. Quinet**[1,2]
1. Physique Atomique et Astrophysique, Université de Mons, 7000 Mons, Belgium
2. IPNAS, Université de Liège, 4000 Liège, Belgium

On August 17, 2017, the LIGO-VIRGO collaboration observed gravitational waves from a neutron star merger for the first time [1]. During this event, the ejected hot and radioactive matter gave rise to a very luminous phenomenon called kilonova, the spectral analysis of which revealed the presence of a large quantity of elements heavier than iron. Among these latter, the lanthanides (Z = 57 – 71) play a particular role because, given their rich spectra, they contribute intensely to the opacity affecting radiation emission [2]. In order to interpret the spectrum of a kilonova, it is therefore crucial to precisely know the radiative parameters characterizing these elements. While the determination of these parameters has already been the subject of various studies (see e.g. [3]), the latter only concern the first degrees of ionisation (up to 3+) and are therefore limited to the analysis of kilonovae in a temperature range below 20000 K. In order to extend the modelling of this type of celestial object to higher temperatures, corresponding to the early phases of kilonovae, it is essential to know the spectroscopic properties of lanthanide ions in higher charge stages for which practically no investigation has been published to date. Our project aims to make a significant contribution in this field as it consists of a detailed study of the radiative processes characterizing moderately charged lanthanide ions (from 4+ to 9+) and to deduce the corresponding astrophysical opacities.

As there is almost no experimental data available for these ions, our calculations are based on a multi-platform approach involving different complementary theoretical methods, namely the pseudo-relativistic Hartree-Fock (HFR) [4,5], and the fully relativistic Multiconfiguration Dirac-Hartree-Fock (MCDHF) [6-9] and Configuration Interaction Many-Body Perturbation Theory (CI+MBPT) [10,11] methods. In the absence of sufficient experimental data, this approach is the only way to estimate the accuracy of the results obtained through systematic comparisons between distinct computational procedures.

In the present contribution, we report the first results obtained as regards the atomic structures and radiative parameters in Ce V–X ions and the corresponding monochromatic opacities for application to early phases of kilonova emission spectra observed following neutron star mergers.

References

[1] B. Abbott *et al.*, Phys. Rev. Lett. **119**, 161101 (2017).
[2] D. Kasen, B. Metzger, J. Barnes, E. Quataert and E. Ramirez-Ruiz, Nature **551**, 80 (2017).
[3] P. Quinet and P. Palmeri, Atoms **8**, 18 (2020).
[4] R.D. Cowan, *The Theory of Atomic Structure and Spectra* (University of California Press, Berkeley, 1981).
[5] P. Quinet *et al.*, Mon. Not. Roy. Astron. Soc. **307**, 934 (1999).
[6] I.P. Grant, *Relativistic Quantum Theory of Atoms and Molecules* (Springer-Verlag, Berlin, 2007).
[7] P. Jönsson, G. Gaigalas, J. Biéron, C. Froese Fischer and I.P. Grant, Comput. Phys. Commun. **184**, 2197 (2013).
[8] C. Froese Fischer, M. Godefroid, T. Brage, P. Jönsson and G. Gaigalas, J. Phys. B : At. Mol. Opt. Phys. **49**, 182004 (2016).
[9] C. Froese Fischer, G. Gaigalas, P. Jönsson and J. Biéron, Comput. Phys. Commun. **237**, 184 (2019).
[10] V.A. Dzuba, V.V. Flambaum and M.G. Kozlov, Phys. Rev. A **54**, 3948 (1996).
[11] E.V. Kahl and J.C. Berengut, Comput. Phys. Commun. **238**, 232 (2019).

[*]Corresponding author: Helena.CarvajalGallego@umons.ac.be

KWISP - Latest results on the chameleon hunt at the CAST experiment at CERN

J. Baier[*1]
1. Institute of Physics, Hermann-Herder-Str. 3, 79104 Freiburg, Germany

The KWISP (Kinetic Weakly Interacting Slim Particle) detector [1],[2] is part of the CAST experiment at CERN exploring the dark sector. It utilizes an ultra-sensitive optomechanical force sensor searching for solar chameleons. Chameleons are hypothetical scalar particles postulated as dark energy candidates, which have a direct coupling to matter depending on the local matter density [3]. In the Sun chameleon particles can be produced by the conversion of photons in a strong magnetic field. Considering the density dependent characteristics a flux of solar chameleons hitting a solid surface at grazing incidence will, under certain conditions, reflect and exert the equivalent of radiation pressure on the surface. To exploit this trait the KWISP sensor consists of a thin and rigid dielectric membrane placed inside a resonant optical cavity measuring the displacement of the membrane caused by the reflection of chameleons. The detector setup and the latest results will be presented in this talk.

References

[1] M. Karuza *et al.*, *Phys. Dark Univ.* **12**, pp. 100-104 (2016), 10.1016/j.dark.2016.02.004.
[2] S. A. Cuendis *et al.*, *Phys. Dark Univ.* **26**, 100367 (2019).
[3] J. Khoury and A. Weltman, *Phys. Rev. D* **69**, 044026 (2004).

[*]Corresponding author: justin.sillvan.baier@cern.ch

Biological samples used for imaging

H. Skenderović[*1,2], **D. Abramović**[1] **N. Demoli**[2] **D. Pantelić** [3]

1. Institute of Physics, Bijenička cesta 46, 10000 Zagreb, Croatia

2. Photonics and Quantum Optics Unit Center of Excellence for Advanced Materials and Sensing Devices, Rudjer Bošković Institute, Bijenička cesta 54, HR- 10000 Zagreb, Croatia

3. Institute of Physics Belgrade, University of Belgrade, Photonics Center, Pregrevica 118, 11080 Zemun, Belgrade, Serbia

For some time, there are efforts to apply the natural biological structures as imaging detectors by using thermally-induced effects[1-3]. The read-out of those possible devices is usually all optical i.e., instead of electronic signal read from CCDs, the image information would come from light beam interaction with the sensitive area - focal point array (FPA). The foreseen advantage is multispectral sensitivity of such devices. As a most precise method for detecting sub micron changes on FPA one could use holography, as in [1]. In a possible practical implementation of this approach, artificail nanostructures will be fabricated inspired by biological samples.

In this work we present optical reading from butterfly wings by means of digital holographic microscopy in a compact Twyman - Green configuration where wings scales are used as pixels of the FPA. By shining the auxilliary laser on the wing, individual scales are excited. We show spatial and temporal sensitivity of the setup with wings. As a next step artificial nanostructures in a role of FPA will be investigated, and integrated in a compact imaging device.

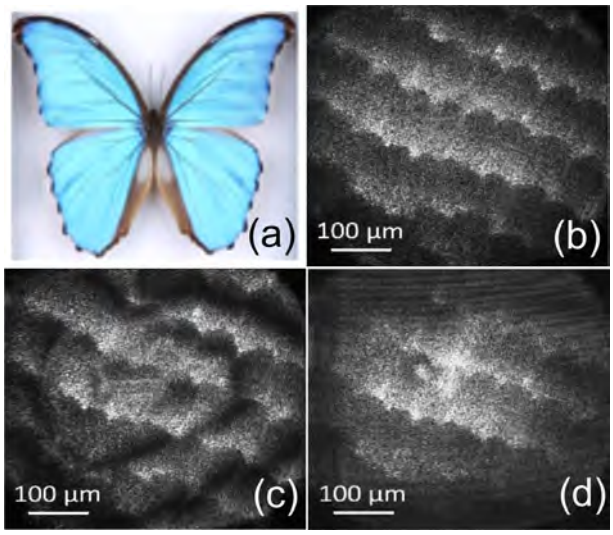

Fig. 1: Image of butterfly Morpho Peleides **(a)**. Holographic reconstruction of the wing scales **(b)**. Reconstruction of the wing excited by auxiliary laser beam **(c) and (d)**

Image of a typical butterfly is shown in Fig.1(a). The FPA in our case consists of wing scales which are imaged from the wing area sized approximately 600x600 μ^2. Individual scales can be clearly seen. Excitation of several pixels by impeding light is shown in the Fig.1.(c) and almost single pixel excitation is reconstructed in Fig.1(d). Additionally, we discuss temporal response of the wings. This research should give guidelines for nanofabrication of practical FPAs inspired by architecture designed by nature.

References

[1] D. Grujic, D. Vasiljevic, D. Pantelic, L. Tomic, Z. Stamenkovic, and B. Jelenkovic, Opt. Express **26**, 14143-14158 (2018)

[2] A. D. Pris, Y. Utturkar, C. Surman, W. G. Morris, A. Vert, S. Zalyubovskiy, T. Deng, H. T. Ghiradella, and R. A. Potyrailo, Nat.Photonics **6(3)**, 195–200 (2012)

[3] F. Zhang, Q. Shen, X. Shi, S. Li, W. Wang, Z. Luo, G. He, P. Zhang, P. Tao, C. Song, W. Zhang, D. Zhang, T. Deng, and W. Shang, Adv.Mater. **27(6)**, 1077–1082 (2015)

[*]Corresponding author: hrvoje@ifs.hr

Planned Laboratory Studies of N_2 reacting with H_3^+ Isotopologues

D. Schury[*1], **C. Bu**[1], **P.-M. Hillenbrand**[2], **X. Urbain**[3], **and D. W. Savin**[†1]
1. Columbia Astrophysics Laboratory, Columbia University, New York, NY 10027, USA
2. GSI Helmholtzzentrum, Darmstadt, 64291, Germany
3. Université catholique de Louvain, Louvain-la-Neuve, 1348, Belgium

Deuterated molecules are used to infer the temperature, chemistry, and thermal history of cosmic objects such as prestellar cores and protoplanetary disks [1]. In the very dense cold regions found in prestellar cores and the outer mid-plane of protoplanetary disks, most molecules beside hydrogen freeze onto dust grains, leaving HD as the primary deuterium reservoir in the gas phase. The HD can react with H_3^+ to form deuterated isotopologues of the ion. Subsequent ion-neutral reactions pass on the deuteration to other gas-phase species. Of particular importance is the abundance ratio for N_2D^+ and N_2H^+. Their formation occurs near the N_2 snow line of prestellar cores and protoplanetary disks and they are commonly used to trace the properties of these objects. However, to reliably interpret observations of these ions, an accurate understanding of their formation process is needed. We will use our dual-source, ion-neutral, merged-fast-beams apparatus [2][3] to measure the integral cross sections of the reaction of N_2 with H_3^+ and its isotopologues, to an accuracy of about 15%. From these results, we will derive the thermal rate coefficients used in astrochemical models. In addition, our results will help the astrophysics community to determine the validity of the commonly assumed scaling of available kinetics data for H-bearing reactions to deuterated isotopologues and also of the assumed statistical branching ratios used for the relative fractions of H-bearing and D-bearing daughter products.

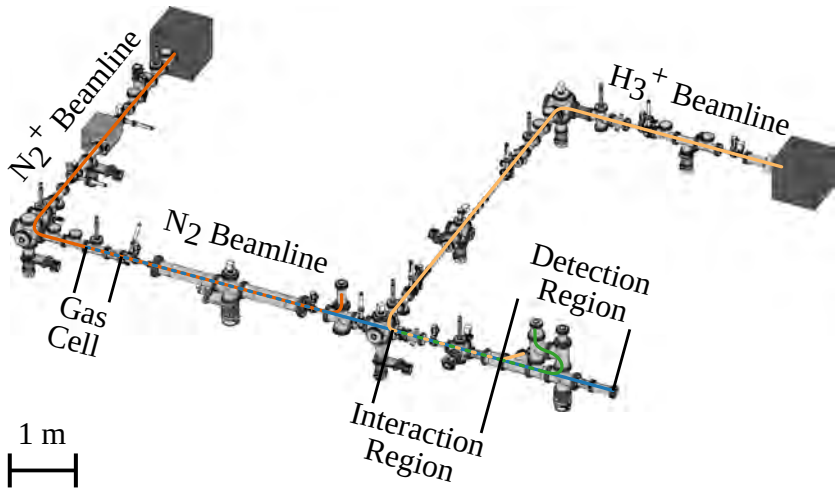

Fig. 1: Schematic of the experimental setup with particle beam trajectories indicated. The initial N_2^+ beam (dark orange) neutralizes in the gas cell and forms N_2 (blue). In the interaction region, it reacts with the superimposed H_3^+ beam (light orange) and N_2H^+ is created (green). All initial and product beams are collected in Faraday cups and particle detectors.

References

[1] Albertson T. et al., Astrophys. J. Suppl. Ser. **207**, 27 (2013), doi:10.1088/0067-0049/207/2/27
[2] O'Connor A.P. et al., Astrophys. J. Suppl. Ser. **219**, 6 (2015), doi:10.1088/0067-0049/219/1/6
[3] Bowen K.P. et al., J. Chem. Phys. **154**, 084307 (2021), doi:10.1063/5.0038434

[*]Corresponding author: daniel.schury@physik.uni-giessen.de
[†]Corresponding author: savin@astro.columbia.edu

Plasma environment effects on K lines of astrophysical interest: universal formulae for ionization potential and K-threshold shifts

J. Deprince[1,2], P. Palmeri*[1], P. Quinet[1,3], J. A. García[2,4], C. Mendoza[5], M. A. Bautista[5], T. R. Kallman[6], S. Fritzsche[7,8]

1. Physique Atomique et Astrophysique, Université de Mons - UMONS, 7000 Mons, Belgium
2. Cahill Center for Astronomy and Astrophysics, California Institute of Technology, Pasadena, CA 91125, USA
3. IPNAS, Université de Liège, 4000 Liège, Belgium
4. Dr. Karl Remeis-Observatory and Erlangen Centre for Astroparticle Physics, Sternwartstr. 7, 96049 Bamberg, Germany
5. Department of Physics, Western Michigan University Kalamazoo, MI 49008, USA
6. NASA Goddard Space Flight Center, Code 662, Greenbelt, MD 20771, USA
7. Helmholtz Institut Jena, 07743 Jena, Germany
8. Theoretisch Physikalisches Institut, Friedrich Schiller Universität Jena, 07743 Jena, Germany

Supersolar abundances have been inferred from K lines of different elements observed in X-ray spectra of X-ray binaries (XRB) and active galactic nuclei (AGN), see *e.g.* Kallman *et al.*[1], Dong *et al.*[2], Walton *et al.*[3] and Fukumura *et al.*[4]. These absorption and emission features can occur in the inner regions of the black-hole accretion disks where the plasma densities range from 10^{15} to 10^{22} cm^{-3} [5]. The emerging photons can be recorded with current space observatories such as *XMM-Newton*, *NuSTAR*, and *Chandra*, and synthetic spectra can provide measures of the composition, temperature, and degree of ionization of the plasma [6,7]. Nevertheless, the great majority of the atomic parameters used for spectral modeling that involves K-shell processes do not take density effects into account and therefore compromise their usefulness in abundance determinations beyond densities of 10^{18} cm^{-3} [8].

In a series of papers dedicated to plasma density effects on the atomic parameters used to model K lines in ions of astrophysical interest, the ionization potentials (IP), K thresholds, transition wavelengths, radiative emission rates, and Auger widths have been computed with the relativistic multiconfiguration Dirac–Fock (MCDF) method [9-11], as implemented in the GRASP92 [12] and RATIP [13] atomic structure packages. The plasma electron–nucleus and electron–electron screenings are approximated with a time-averaged Debye-Hückel (DH) potential. The datasets comprise the following ionic species: O I–O VII, by Deprince *et al.*[14]; Fe XVII–Fe XXV, by Deprince *et al.*[15]; Fe IX–Fe XVI, by Deprince *et al.*[16]; Fe II–Fe VIII, by Deprince *et al.*[17].

In the present work, the universal fitting formulae for ionization potential (IP) and K-threshold shifts proposed by Deprince *et al.*[17] are improved by further MCDF/RATIP computations of these above-mentionned parameters in other representative cosmically abundant elements, *i.e.* carbon ($Z = 6$), silicon ($Z = 14$), calcium ($Z = 20$), chromium ($Z = 24$) and nickel ($Z = 28$). These plasma effects are expected to be the main ones with potential alteration of the ionization ballance and opacities.

References

[1] T. R. Kallman *et al.*, Astrophys. J. **701**, 865 (2009).
[2] Y. Dong *et al.*, Mon. Not. Roy. Astron. Soc. **493**, 2178 (2020).
[3] D. J. Walton *et al.*, Mon. Not. Roy. Astron. Soc. **499**, 1480 (2020).
[4] K. Fukumura *et al.*, accepted to Astrophys. J. (2021), arXiv:2103.05891v1 (http://arxiv.org/abs/2103.05891v1).
[5] J. D. Schnittman *et al.*, Astrophys. J. **769**, 156 (2013).
[6] R. R. Ross & A. C. Fabian, Mon. Not. Roy. Astron. Soc. **358**, 211 (2005).
[7] J. García & T. R. Kallman, Astrophys. J. **718**, 695 (2010).
[8] R. K. Smith & N. S. Brickhouse, Adv. At. Mol. Opt. Phys. **63**, 271 (2014).
[9] I. P. Grant *et al.*, Comput. Phys. Commun. **21**, 207 (1980).
[10] B. J. McKenzie *et al.*, Comput. Phys. Commun.**21**, 233 (1980).
[11] I. P. Grant, Meth. Comput. Chem. **2**, 1 (1988).
[12] F. A. Parpia *et al.*, Comput. Phys. Commun. **94**, 249 (1996).
[13] S. Fritzsche, Comput. Phys. Commun. **183**, 1523 (2012).
[14] J. Deprince *et al.*, Astron. Astrophys. **624**, A74 (2019).
[15] J. Deprince *et al.*, Astron. Astrophys. **626**, A83 (2019).
[16] J. Deprince *et al.*, Astron. Astrophys. **635**, A70 (2020).
[17] J. Deprince *et al.*, Astron. Astrophys. **643**, A57 (2020).

*Corresponding author: Patrick.Palmeri@umons.ac.be

Spectral investigation of tin ions in an electron beam ion trap and laser-produced plasmas in the EUV region

Z. Bouza*[1], J. Scheers[1,2], A. Ryabtsev[3], R. Schupp[1], L. Behnke[1], C. Shah[4,5], J. Sheil[1], M. Bayraktar[6], J. R. Crespo López-Urrutia[4], W. Ubachs[1,2], R. Hoekstra[1,7], O. O. Versolato[1,2]

1. Advanced Research Center for Nanolithography, Science Park 106, 1098 XG Amsterdam, The Netherlands

2. Department of Physics and Astronomy, and LaserLaB, Vrije Universiteit, De Boelelaan 1081, 1081 HV Amsterdam, The Netherlands

3. Institute of Spectroscopy, Russian Academy of Sciences, Troitsk, Moscow 108840, Russia

4. Max-Planck-Institut für Kernphysik, Saupfercheckweg 1, 69117 Heidelberg, Germany

5. Current address: NASA Goddard Space Flight Center, 8800 Greenbelt Rd, Greenbelt, MD 20771, United States of America

6. Industrial Focus Group XUV Optics, MESA+ Institute for Nanotechnology, University of Twente, Drienerlolaan 5, 7522 NB Enschede, The Netherlands

7. Zernike Institute for Advanced Materials, University of Groningen, Nijenborgh 4, 9747 AG Groningen, The Netherlands

The strong extreme ultraviolet (EUV) light emission around 13.5 nm wavelength, from highly-charged tin (Sn) ions produced in an laser-produced plasma (LPP) is currently used in state-of-the-art EUV lithography [1,2]. The spectroscopic investigation of these plasmas can be quite challenging due to the complex electronic configurations of the relevant ions Sn^{5+}–Sn^{14+} [3]. The emission spectra of Sn ions generated in LPPs and in an electron beam ion trap (EBIT) are studied in EUV region to understand such plasma.

In this work, emission features of the Sn^{5+}–Sn^{10+} ions are investigated in the wavelength region between 12.6 and 20.8 nm [4]. To unravel the blended EBIT spectra of the different Sn^{q+} ions (Fig. 1), we make use of a matrix inversion method to obtain charge-state resolved EUV spectra [5]. In this method, we use the fact that each row in the 2D map of light intensities, shown in Fig. 1, represents a linear combination of unique spectra per charge state weighted by their respective fluorescence curve.

The emission features of the charge-state-resolved Sn ion spectra obtained from the EBIT are identified using the Cowan code. We then use the EBIT spectra to assign the identified features in the LPP spectra obtained from both droplet and planar solid Sn targets. In the case of the droplet target, a clear evolution of the different Sn ions are observed for different laser intensities while in the case of the solid target, plasma-self absorption effects are also observed in the form of dips in the emission spectra. Using the Cowan code we have identified spectral features corresponding to $4d-5p$, $4d-4f$, $4p-4d$ transitions as well as new identifications of $4d-5f$ and $4d-6f$ transitions in Sn^{6+} and $4p-4d$ transitions in Sn^{5+}.

We qualitatively demonstrate the potential of using emission in the studied region to individually monitor several Sn charge states that strongly contribute to the narrow EUV light emission around 13.5 nm wavelength relevant for EUV nanolithography.

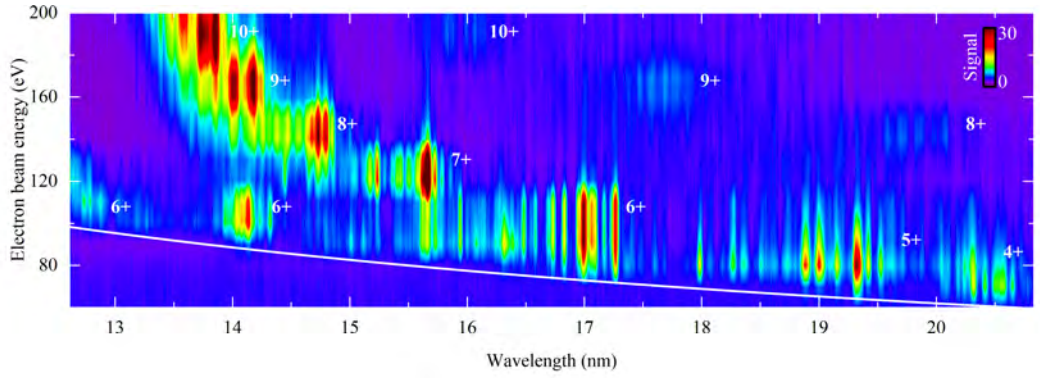

Fig. 1: 2D spectral intensity map of Sn ion emission constructed from EBIT measurements. The colour bar indicates the emission intensity and the white line represents equivalence between the electron beam energy and the photon energy.

References

[1] J. Benschop, V. Banine, S. Lok, and E. Loopstra, J. Vac. Sci. Technol. **26**, 2204 (2008).

[2] O. O. Versolato, Plasma Sources Sci. Technol. **28**, 083001 (2019).

[3] F. Torretti, J. Sheil, R. Schupp, M. M. Basko, M. Bayraktar, R. A. Meijer, S. Witte, W. Ubachs, R. Hoekstra, O. O. Versolato, A. J. Neukirch, and J. Colgan, Nat. Commun. **11**, 2334 (2020).

[4] Z. Bouza, J. Scheers, A. Ryabtsev, R. Schupp, L. Behnke, C. Shah, J. Sheil, M. Bayraktar, J. R. Crespo López-Urrutia, W. Ubachs, R. Hoekstra, and O. O. Versolato, J. Phys. B. **53**, 195001 (2020).

[5] J. Scheers, C. Shah, A. Ryabtsev, H. Bekker, F. Torretti, J. Sheil, D. A. Czapski, J. C. Berengut, W. Ubachs, J. R. Crespo López-Urrutia, R. Hoekstra, and O. O. Versolato, Phys. Rev. A. **101**, 062511 (2020).

*Corresponding author: z.bouza@arcnl.nl

Multiply-excited states and their contribution to opacity in laser-driven tin plasmas

J. Sheil[*1], **O. O. Versolato**[1,2], **A. J. Neukirch**[3], **J. Colgan**[†3]

1. Advanced Research Center for Nanolithography, Science Park 106, 1098 XG Amsterdam, The Netherlands

2. Department of Physics and Astronomy, and LaserLaB, Vrije Universiteit, De Boelelaan 1081, 1081 HV Amsterdam, The Netherlands

3. Los Alamos National Laboratory, Los Alamos, NM 87545, USA

The source of extreme ultraviolet (EUV) light in new-generation EUV lithography machines is that of a laser-driven tin plasma [1]. In these machines, plasmas are generated by irradiating disk-shaped tin ($Z = 50$) micro-droplet targets with high-intensity CO_2 (laser wavelength $\lambda = 10.6$ μm) laser pulses. Under optimum experimental conditions, the EUV spectrum of such a plasma exhibits an intense narrowband emission feature centered near a wavelength of 13.5 nm [2−4]. Importantly, this emission feature overlaps with the reflective wavelengths of molybdenum/silicon multilayer mirrors used to transport EUV photons from the light source to the wafer stage for use in the lithography process [5].

I will give an overview of our recent work on the topic of tin-ion opacities for laser-driven plasma conditions. First, I will present our calculations of tin-ion opacities for Nd:YAG laser-driven ($\lambda = 1.064$ μm) plasma conditions [6]. Detailed local thermodynamic equilibrium (LTE) opacity calculations performed with the ATOMIC code [7−8] indicate that the well-known $4p^6 4d^n - (4p^5 4d^{n+1} + 4p^6 4d^{n-1} 4f)$ transitions in $Sn^{11+} - Sn^{14+}$ ions ($n = 3-0$) only make a minor contribution to the opacity in the EUV region. Rather, it is transitions between complex, multiply excited states (doubly-, trebly- and quadruply-excited states) that dominate the opacity spectrum. Incorporating these opacities into a one-dimensional model for radiation transport in the plasma has enabled comparisons with experimentally-recorded EUV spectra. The simulated spectra are found to be in excellent agreement with experimental measurements.

Second, I will present calculations of tin-ion opacities for industrially-relevant, CO_2 laser-driven plasmas [9]. Plasmas driven by CO_2 lasers exhibit lower electron densities and temperatures than Nd:YAG-driven plasmas. As such, CO_2-driven plasmas are in truly non-LTE conditions. Unfortunately, the standard collisional-radiative approach [10] cannot be used to calculate level populations associated with multiply-excited configurations – there are simply too many levels that necessitate coupling in the rate matrix. To circumvent these difficulties, we have employed Busquet's ionization temperature method [11] to effectively "mimic" non-LTE level populations using LTE computations. We show that this approach yields excellent agreement between non-LTE and LTE-computed configuration populations. A fully level-resolved, LTE opacity calculation has then been performed for a relevant CO_2 laser-driven tin plasma condition. We have found that transitions between multiply-excited states also make a substantial contribution to opacity in CO_2 laser-driven tin plasmas.

References

[1] V. Bakshi, ed., *EUV Lithography, Second Edition* (SPIE Press, Washington, 2018).
[2] I. Fomenkov *et al.*, Adv. Opt. Techn., **6**, 173 (2017).
[3] O. O. Versolato, Plasma Sources Sci. Technol. **28**, 083001 (2019).
[4] G. O'Sullivan *et al.*, J. Phys. B: At. Mol. Opt. Phys. **48** 144035 (2015).
[5] L. Wu, Ph.D. Thesis, University of Amsterdam, 2020.
[6] F. Torretti *et al.*, Nat. Commun. **11**, 2334 (2020).
[7] N. Magee *et al.*, AIP Conf. Proc., Vol. 730 (AIP, 2004) pp. 168-179.
[8] P. Hakel *et al.* J. Quant. Spectrosc. Rad. Transf. **99**, 265 (2006).
[9] J. Sheil, O. O. Versolato, A. J. Neukirch and J. Colgan, J. Phys B: At. Mol. Opt. Phys. **54** 035002 (2021).
[10] Y. Ralchenko, ed. *Modern Methods in Collisional-Radiative Modelling of Plasmas* (Springer International Publishing, Cham, 2016).
[11] M. Busquet, Phys. Fluids B **5**, 4191 (1993).

[*]Corresponding author: j.sheil@arcnl.nl
[†]Corresponding author: jcolgan@lanl.gov

LIBS vs ICCD imaging for atmospheric plasma jet diagnostics

D. Maletić[*1,2], **D. Popović**[1], **N. Puač**[2], **Z. Lj. Petrović**[3], **S. Milošević**[1]
1. Institute of Physics, Bijenička c. 46, 10000 Zagreb, Croatia
2. Institute of Physics, University of Belgrade, Pregrevica 118, 11000 Belgrade, Serbia
3. Serbian Academy of Sciences and Arts, Knez Mihajlova 35, 11001 Belgrade, Serbia

Nowdays atmospheric pressure plasma jets (APPJs) attract a lot of attention thanks to their great application possibilities especially in biology and medicine. For each specific application it is necessary to study in detail all physical and chemical processes, both in the plasma jet and in the interaction with treated samples. To solve these complex problems many diagnostics techniques are developed such as optical emission spectroscopy (OES), mass spectrometry (MS), Schlieren imaging, laser induced fluorescence (LIF), electrical probe measurements. From the fast ICCD imaging it is found that the plasma jets are not continuous but consist of fast moving plasma packages [1]. From mass spectrometry and OES spectroscopy concentrations of the various reactive species can be determined.

In this paper we compare the fast ICCD images with the newly developed diagnostic method that utilizes the laser induced breakdown (LIB) in plasma jet for time and spatial plasma jet diagnostics proposed by D. Popović et al. [2]. Our helium plasma jet is powered with a 80 kHz high-voltage sine wave signal, the plasma is ignited in a capillary tube and propagate into the ambient air. High energy pulsed laser beam 1064nm (4ns pulse duration and 5 Hz repetition rate) was focused with the lens into the plasma jet. The laser pulse and the jet powering signal were synchronized. The laser plasma discharge is highly dependent on the concentration of seed electrons and other charged particles in the plasma jet channel. We compare the radial profiles of the plasma and the ionization wave velocities obtained with these two methods. In Fig. 1 we show the ICCD images and emission intensities of He 588 nm line for the plasma jet propagating into the open air.

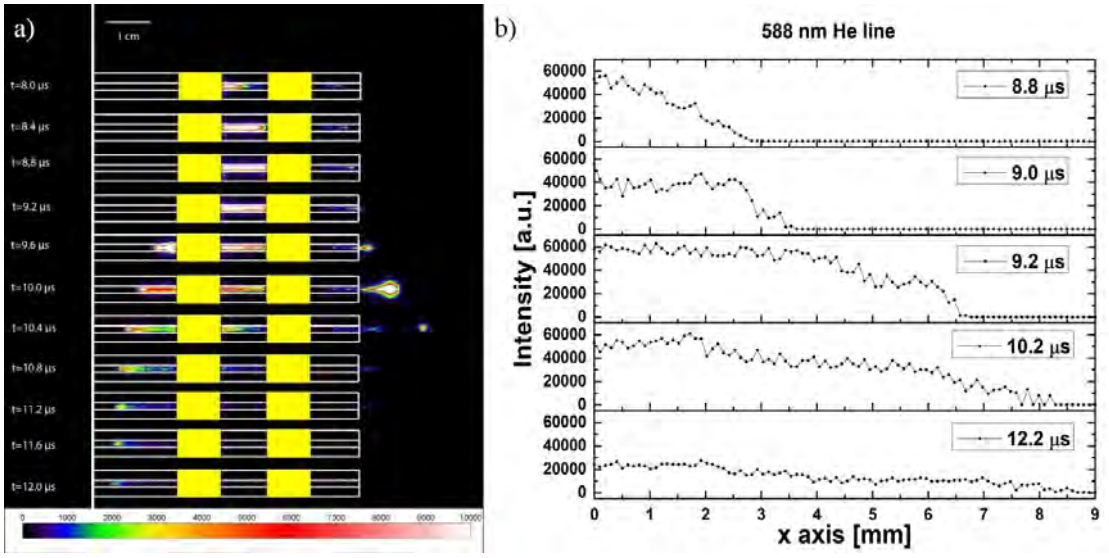

Fig. 1: a) Time resolved ICCD images of the plasma jet, from 8.0 to 12.0 μs; b) Emission profiles in the x axis direction from the plasma jet nozzle; Helium flow 2 slm and 4 W of power delivered to the plasma

We show that the laser induced breakdown spectroscopy can be used for time resolved and spatial diagnostic of the atmospheric plasma jet. This method can be used as a complementary method for the diagnostics of plasma jets together with ICCD measurements. Using the LIB we can determine the dimensions of the plasma channel and velocity of the ionization wave propagation.

References

[1] D. Maletić, N. Puač, G. Malović, A. Djordjević, Z. Lj. Petrović, J Phys. D: Appl. Phys, **5**0 (14), 145202 (2017).
[2] D. Popović, M. Bišćan and S. Milošević, Plasma Sources Sci. Technol. **2**8, 055009 (2019).

*Corresponding author: dmaletic@ifs.hr

Oscillator strengths in doubly- and trebly-ionized gold deduced from core-polarization-corrected pseudo-relativistic Hartree-Fock calculations

S. Gamrath[*1], **P. Palmeri**[1], **P. Quinet**[1,2]
1. Physique Atomique et Astrophysique, Université de Mons, 7000 Mons, Belgium
2. IPNAS, Université de Liège, 4000 Liège, Belgium

The calculation of electronic structure and radiative parameters for the lowest ionization stages of transition metal elements belonging to the sixth row of the periodic table (from Hf to Hg) is a demanding and time-consuming challenge. If neutral and singly ionized atoms of this group have been the subject of many different studies on both experimental and theoretical sides (see e.g. [1]), higher ionization stages considerably suffer from the lack of accurate atomic data. The complexity of modeling these atomic systems lies in the fact that they are characterized by low-lying configurations of the type $5d^k$, $5d^{k-1}nl$ and $5d^{k-2}nln'l'$ whose interaction gives a large number of strongly mixed valence electronic states. It is also well established that core-valence correlations play an extremely important role in heavy ions, which makes it necessary to include in purely *ab initio* calculations for sixth row elements single and double excitations from core orbitals such as 4f, 5s, 5p, and possibly 4d. This can very quickly lead to calculations including several millions or several tens of millions of configuration state functions.

Many previous works have shown that a convenient approach to obtain a large number of reliable transition rates in heavy ions is the pseudo-relativistic Hartree-Fock (HFR) method [2] in which the largest part of the intravalence correlation is represented within a configuration interaction scheme, i.e. by explicitly including a set of electronic configurations in the physical model, while core-valence correlation is approximated by a core-polarization (CPOL) model potential, giving rise to the so-called HFR+CPOL method [3,4]. This method has been succesful for predicting radiative parameters in many different situations, showing in general a very good agreement with precise experimental lifetimes measured using laser-induced fluorescence spectroscopy (see [1] and references therein). Moreover, it has been demonstrated in many different cases that the HFR+CPOL approach gives rise to similar results as those obtained with purely relativistic methods, such as the Multiconfiguration Dirac-Hartree-Fock (MCDHF) method [5,6], provided configuration interaction is considered in the calculations in a sufficiently extensive way (see e.g. [7-9]).

The present work focuses on the particular cases of doubly- and trebly-ionized gold (Au III–IV). More precisely, the relativistic Hartree-Fock approach including core-polarization effects (HFR+CPOL) has been combined to a semi-empirical adjustment of radial parameters minimizing the differences between computed energy levels and available experimental values to compute transition probabilities and oscillator strengths in these two ions. Our semi-empirical calculations took advantage of the experimental energy levels reported for the $5d^9$, $5d^86s$, $5d^87s$, $5d^86d$, $5d^76s^2$, $5d^86p$ and $5d^76s6p$ configurations in Au III [10] and the $5d^8$, $5d^76s$, $5d^66s^2$, $5d^76p$ configurations in Au IV [11]. This allowed us to produce a new set radiative decay rates for many spectral lines involving all the configurations mentioned above in these two ions of astrophysical interest, in particular for stellar nucleosynthesis studies.

References

[1] P. Quinet, Can. J. Phys. **95**, 790 (2017).
[2] R.D. Cowan, *The Theory of Atomic Structure and Spectra* (University of California Press, Berkeley, 1981).
[3] P. Quinet *et al.*, Mon. Not. Roy. Astron. Soc. **307**, 934 (1999).
[4] P. Quinet *et al.*, J. Alloys Comp. **344**, 255 (2002).
[5] I.P. Grant, *Relativistic Quantum Theory of Atoms and Molecules* (Springer-Verlag, Berlin, 2007).
[6] C. Froese Fischer, G. Gaigalas, P. Jönsson and J. Biéron, Comput. Phys. Commun. **237**, 184 (2019).
[7] E. Biémont, C. Froese Ficher, M. Godefroid, P. Palmeri and P. Quinet, Phys. Rev. A **62**, 032512 (2000).
[8] E. Biémont, V. Fivet and P. Quinet, J. Phys. B : Atom. Mol. Opt. Phys. **37**, 4193 (2004).
[9] S. Gamrath, P. Palmeri and P. Quinet, Atoms **7**, 38 (2019).
[10] A. Zainab and A. Tauheed, J. Quant. Spectrosc. Rad. Transf. **237**, 106614 (2019).
[11] J.-F. Wyart, Y.N. Joshi, A.J.J. Raassen, P.H.M. Uylings and L. Tchang-Brillet, Phys. Scr. **50**, 672 (1994).

*Corresponding author: Sebastien.Gamrath@umons.ac.be

Direct Observation of a Feshbach-resonance by Coincidence-detection of Ions and Electrons in Penning Ionization Collisions

B. Margulis[1], **J. Narevicius**[1], **E. Narevicius**[*1]

1. Department of Chemical and Biological Physics, Weizmann Institute of Science, Rehovot, Israel.

Observation of molecular dynamics with quantum state resolution is one of the major challenges in molecular physics. Complete characterization of collision dynamics leads to the microscopic understanding and unraveling of different quantum phenomena such as scattering resonances. We present a new experimental approach for observing molecular dynamics involving neutral particles and ions. Our approach utilizes Penning ionization (PI) reaction as a preparation step of the ionic system with the energy of ejected electron serving as an indicator of the formed quantum state. The coincidence detection of momenta of PI products serves as a state-to-state detection of the post-ionization ion-neutral dynamics. For $He^*(^3S,^1S)$+Ar PI reaction, we observe a Feshbach resonance arising from the coupling between an electronically excited bound $HeAr^+$ A_2 state to the scattering electronically ground He + $Ar(^3P_{1/2})$ state. Our main results are presented at Fig. 1, additionally, we found that the lifetime of the bound $HeAr^+$ A_2 state to be on the order of 1 μs.

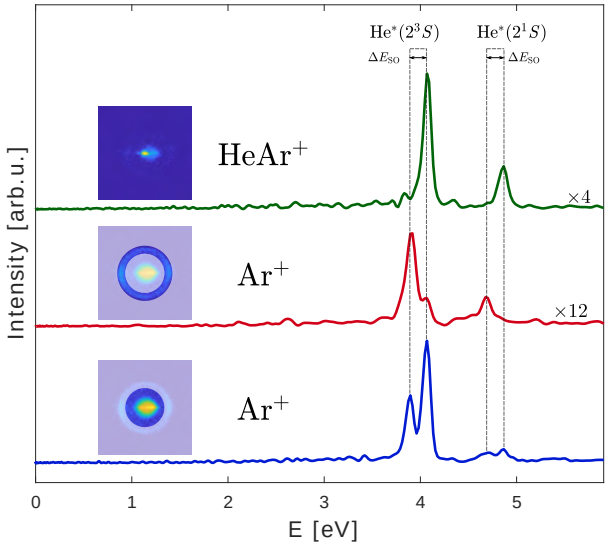

Fig. 1: Energy distribution of Penning electrons measured in coincidence to products of PI collisions. The correlation between high kinetic energy Ar^+ ions (red curve) and specific electron energy provides the observation of the scattering resonance.

References

[1] Margulis, B., Narevicius, J. & Narevicius, E. Nat Comm **11**, 3553 (2020)

*Corresponding author: edvardas.narevicius@weizmann.ac.il

Shortcut to adiabaticity for a three-level quantum system near a metallic nanoparticle

Natalia Domenikou[*1], **Dionisis Stefanatos**[1], **Vassilios Yannopapas**[2], **Ioannis Thanopulos**[1], **and Emmanuel Paspalakis**[1]

1. Materials Science Department, School of Natural Sciences, University of Patras, Patras 265 04, Greece
2. Department of Physics, National Technical University of Athens, Athens 157 80, Greece

The study of Stimulated Raman Shortcut-to-Adiabatic Passage (STIRSAP) [1-4] of three-level quantum systems, like atoms, molecules and quantum dots, has attracted significant interest in the last decade. It is a robust coherent control method for population transfer between quantum states which reduces the necessary time and improves the efficiency of quantum adiabatic evolution compared with the STIRAP method [5,6]. Studies have also shown that the presence of plasmonic nanostructures, such as a spherical metallic nanoparticle, near the quantum system may modify the population transfer process when STIRAP is used [7,8]. As coupled quantum-plasmonic nanostructures are important for quantum technology, as well as nanotechnology, applications, it is useful to study the behavior of STIRSAP for a quantum system near a metallic nanoparticle. Therefore, in this work, we present a theoretical investigation of the influence of a gold nanoparticle on the population transfer using the STIRSAP technique. We consider the density matrix approach for the system's dynamics, where we use numerical electromagnetic calculations for the electric field amplitude seen by the quantum system near the metallic nanoparticle and the modified spontaneous decay rates of the quantum system due to the Purcell effect in the presence of the metallic nanoparticle. The shortcut is such that the mixing angle is derived from Gaussian pulses [3,4]. We present numerical results for the time evolution of populations in the three different levels of the quantum system with STIRAP and STIRSAP control methods varying the distance d between the quantum system and the nanoparticle, the polarization of the pump and Stokes fields, and in the absence and presence of the metallic nanoparticle. Our results show that STIRSAP leads to efficient population transfer in the absence of the metallic nanoparticle. Also, the shortcut (STIRSAP) improves the efficiency of STIRAP method for small distances between the quantum system and the metallic nanoparticle, at shorter times compared with the simple STIRAP technique. With suitable polarization of the fields, one can obtain highly efficient and robust population transfer using STIRSAP near a metallic nanoparticle.

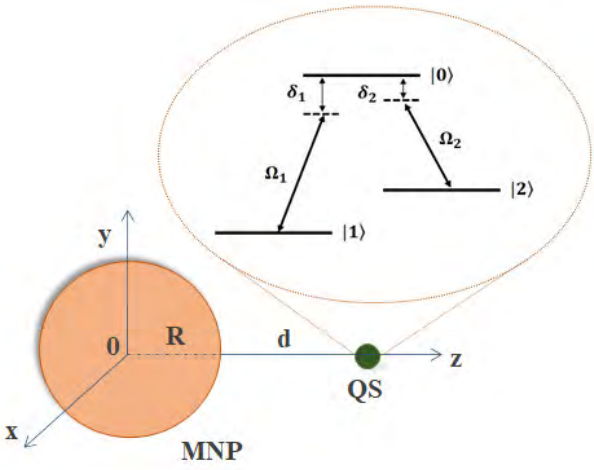

Fig. 1: The Λ-type quantum system (QS) at distance d from the surface of the spherical metallic nanoparticle (MNP) with radius R. Ω_i and δ_i, $(i = 1,2)$ are the Rabi frequencies and detunings of $|i\rangle \rightarrow |0\rangle$ field-induced transitions, respectively.

References

[1] D. Guéry-Odelin, A. Ruschhaupt, A. Kiely, E. Torrontegui, S. Martínez-Garaot, and J. G. Muga, Rev. Mod. Phys. **91**, 045001 (2019).
[2] D. Stefanatos and E. Paspalakis, EPL **132**, 60001 (2021).
[3] Y. Li and X. Chen, Phys. Rev. A **94**, 063411 (2016).
[4] D. Stefanatos, K. Blekos, and E. Paspalakis, Appl. Sci. **10**, 1580 (2020).
[5] P. Král, I. Thanopulos, and M. Shapiro, Rev. Mod. Phys. **79**, 53 (2007) .
[6] N. V. Vitanov, A. A. Rangelov, B. W. Shore, and K. Bergmann, Rev. Mod. Phys. **89**, 015006 (2017).
[7] M. Sukharev and S. Malinovskaya, Phys. Rev. A **86**, 043406 (2012).
[8] S. Dhayal and Y. V. Rostovtsev, Phys. Rev. A **93**, 043405 (2016).

*Corresponding author: domenikou.n@gmail.com

On the formation of van der Waals molecules through direct three-body recombination

M. Mirahmadi[*1], **J. Pérez-Ríos**[†1]
1. Fritz-Haber-Institut der Max-Planck-Gesellschaft, Faradayweg 4-6, D-14195 Berlin, Germany

We present a study on atom-atom-atom direct three-body recombination processes based on a classical trajectory method in hyperspherical coordinates [1]. In particular, we focus on the formation of van der Waals molecules X-RG (where RG is a rare gas atom) via X + RG + RG $\rightarrow$ X-RG + RG collisions at temperatures relevant for buffer gas cells [2]. As a result, we show that almost any X-RG molecule should appear in a buffer gas cell under appropriate conditions. It is pretty remarkable that, despite the drastic differences in the properties of the atom, X, and parameters of X-He interaction potentials, the recombination rates are of the same order of magnitude. As an example, the rates for X-He molecules are illustrated in Fig. 1.

In addition, after extending our study to ion-atom-atom systems, we have revisited the previously derived threshold law for ion-neutral-neutral three-body recombination [3]. As a result, we explain such threshold law and establish a range for its validity. Similarly, we find new and intriguing scenarios in which the branching ratio of the product states after three-body recombination deviates from the expected threshold law in the cold regime.

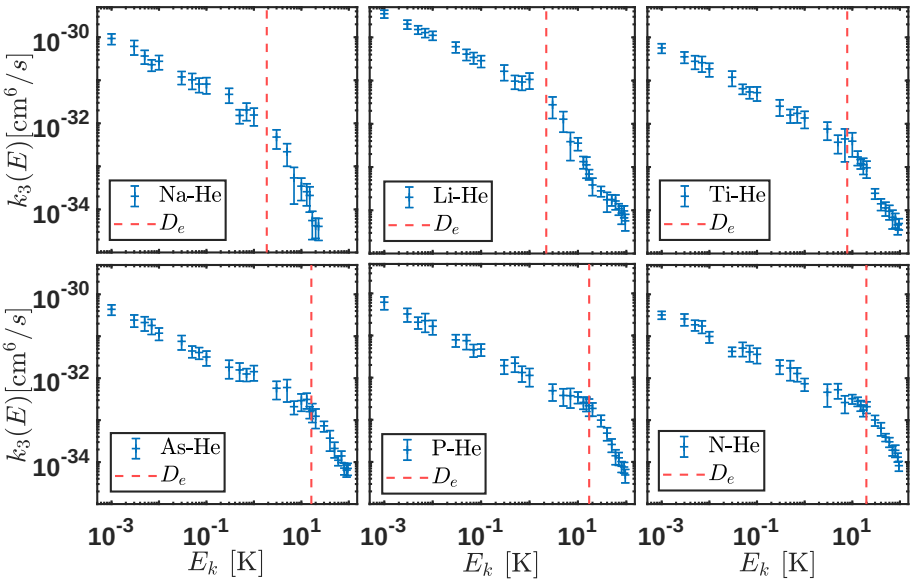

Fig. 1: Three-body recombination rate, k_3, of formation of six different X-He van der Waals molecules as a function of collision energy E_k, plotted on a log-log scale. Each red dashed line indicates the relevant dissociation energy D_e associated with the X-He molecule.

References

[1] J. Pérez-Ríos, S. Ragole, J. Wang, and C. H. Greene, J. Chem. Phys. **140**, 044307 (2014).
[2] M. Mirahmadi, and J. Pérez-Ríos, J. Chem. Phys. **154**, 034305 (2021).
[3] J. Pérez-Ríos, and C. H. Greene, J. Chem. Phys. **143**, 041105 (2015).

[*]Corresponding author: mirahmadi@fhi-berlin.mpg.de
[†]Corresponding author: jperezri@fhi-berlin.mpg.de

Photoelectron circular dichroism of fenchone using deep ultraviolet femtosecond laser pulses

N. Ladda[1], S. Vasudevan[1], S. Ranecky[1], T. Rosen[1], S. Das[1], T. Ring[1], J. Ghosh[1], H. Lee[1], H. Braun[1], A. Senftleben*[1] and T. Baumert[1]

1. Institut für Physik, Universität Kassel, Heinrich-Plett-Strasse 40, 34132 Kassel, Germany

The forward/backward asymmetry of the photoelectron angular distribution (PAD) with respect to the propagation direction of ionizing circularly polarized light of a randomly orientated chiral molecule is known as photoelectron circular dichroism (PECD) [1]. The measurement of the PAD asymmetry can be performed using velocity-map imaging (VMI) technique, where the gas phase provides a nearly collision and interaction free environment. Deep ultraviolet (DUV) femtosecond laser pulses from third harmonic (264 nm, 4.7 eV) and fourth harmonic (198 nm, 6.25 eV) generation of our Ti:Sa laser system enable a 1+1 resonance-enhanced multi-photon ionization (REMPI) process via energetically higher lying intermediate states of the chiral prototype molecule fenchone. The polarization of the harmonics was characterized and the quality of the circularly polarized light given by $|s_3/s_0|$ is above 99 %. The ionizations channels that can be identified by the different intermediate states show different amplitudes in their PECD and in the contributing Legendre coefficients.

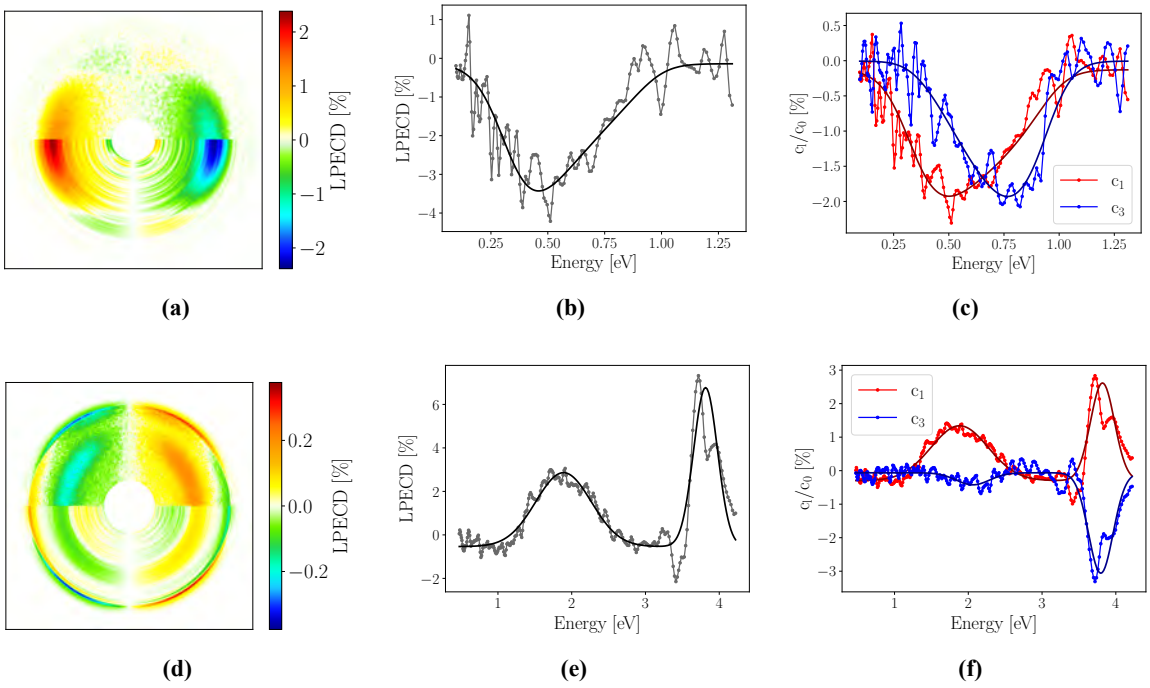

Fig. 1: Top row: measurement of (S)-$(+)$-fenchone ionized with the third harmonic of our Ti:Sa laser system in a 1+1 REMPI process. Antisymmetric PECD image, where the upper hemisphere represents the raw data and the lower hemisphere the Abel inverted data **(a)**. Corresponding LPECD plot **(b)** and contributing Legendre coefficients **(c)**. Bottom row: measurement of (R)-$(-)$-fenchone ionized with the fourth harmonic of our Ti:Sa laser system in a 1+1 REMPI process. Antisymmetric PECD image, where the upper hemisphere represents the raw data and the lower hemisphere the Abel inverted data **(d)**. Corresponding LPECD plot **(e)** and contributing Legendre coefficients **(f)**.

References

[1] B Ritchie; Phys. Rev. A 13, 1411 - 1415, 1976

*Corresponding author: Dr. Arne Senftleben; email: arne.senftleben@uni-kassel.de

Ultrafast photoionization of aligned excited states of neon

J. J. Omiste[*1], **L. B. Madsen**[2]

1. Departamento de Química, Módulo 13, Facultad de Ciencias, Universidad Autónoma de Madrid, 28049 Madrid, Spain

2. Department of Physics and Astronomy, Aarhus University, 8000 Aarhus C, Denmark

We describe numerically the ionization process induced by linearly and circularly polarized XUV attosecond laser pulses on an aligned atomic target, specifically, the excited state $\mathrm{Ne}^*(1s^2 2s^2 2p^5[^2P^o_{1/2}]3s[^1P^o])$. In order to obtain this excited atomic state we take a guess wave function within the term $[^1P^o]$ and propagate it using the time-dependent restricted-active-space self-consistent field (TD-RASSCF) method [1-2] in imaginary time to fully account for the electronic correlation. We show that correlation-assisted ionization channels can dominate over channels accessible without correlation and observe that the rotation of the photoelectron momentum distribution by circularly polarized laser pulses compared to the case of linear polarization can be explained in terms of differences in accessible ionization channels. Therefore, this investigation manifests that the electron correlation effects have to be considered to accurately describe the photoelectron emission dynamics from aligned excited states [3].

References

[1] H. Miyagi and L. B. Madsen, Phys. Rev. A **87**, 062511 (2013).
[2] H. Miyagi and L. B. Madsen, J. Chem. Phys. **140**, 164309 (2014).
[3] J. J. Omiste and L. B. Madsen, J. Phys. B At. Mol. Opt. Phys. **54**, 054001 (2021)

*Corresponding author: juan.omiste@uam.es

Comprehensive laboratory measurements resolving the LMM dieletronic recombination satellite lines in Ne-like Fe XVII ions

Filipe Grilo[1], **Chintan Shah**[*2,3], **Steffen Kühn**[3,4], **René Steinbrügge**[5], **Keisuke Fujii**[6], **José Marques**[7,1], **Ming Feng Gu**[8], **José Paulo Santos**[1], **José R. Crespo López-Urrutia**[3], **Pedro Amaro**[†1]

1. Laboratory of Instrumentation, Biomedical Engineering and Radiation Physics (LIBPhys-UNL), Department of Physics, NOVA School of Science and Technology, NOVA University Lisbon, 2829-516 Caparica, Portugal

2. NASA Goddard Space Flight Center, 8800 Greenbelt Rd, Greenbelt, MD 20771, USA

3. Max-Planck-Institut für Kernphysik, Saupfercheckweg 1, 69117 Heidelberg, Germany

4. Heidelberg Graduate School of Fundamental Physics, Ruprecht-Karls-Universität Heidelberg, Im Neuenheimer Feld 226, 69120 Heidelberg, Germany

5. Deutsches Elektronen-Sychrotron DESY, Notkestraße 85, 22607 Hamburg, Germany

6. Department of Mechanical Engineering and Science, Graduate School of Engineering, Kyoto University, Kyoto 615-8540, Japan

7. Laboratório de Instrumentação e Física Experimental de Partículas (LIP) and Faculdade de Ciências, Universidade de Lisboa, Portugal

8. Space Science Laboratory, University of California, Berkeley, CA 94720, USA

L-shell transitions of highly charged iron dominate the $15-18$Å range of the spectra emitted by astrophysical hot plasmas (MK) [1]. Due to its high ionization potential, Fe XVII is a very stable species and its emissions due to dielectronic recombination (DR) can be used as diagnostic tools to evaluate the temperature and electron density of the plasma [2].

We investigate both experimentally and theoretically the DR populating doubly excited configurations 3l3l' (LMM) in Fe XVII, one of the strongest channel for soft x-ray line formation in this ubiquitous species [3]. We used two different electron beam ion traps and two complementary measurement schemes for preparing the Fe XVII samples and evaluating their purity, observing negligible contamination effects [4]. This allowed us to diagnose the electron density in both EBITs. The measurements in one of the traps enabled the direct observation of spectral dynamics due to population time evolution, from which we achieved a good agreement with a charge-state dynamics simulation, performed for the experimental conditions. We compare experimental results from both EBITs with an independent storage ring measurement [5], as well as with configuration-interaction, multiconfiguration Dirac-Fock, and many-body perturbation theories. The latter showed outstanding predictive power in comparison with the combined independent experimental results. From these, we also inferred DR rate coefficients, which unveiled discrepancies with OPEN-ADAS [6] and AtomDB [7] databases (Fig. 1).

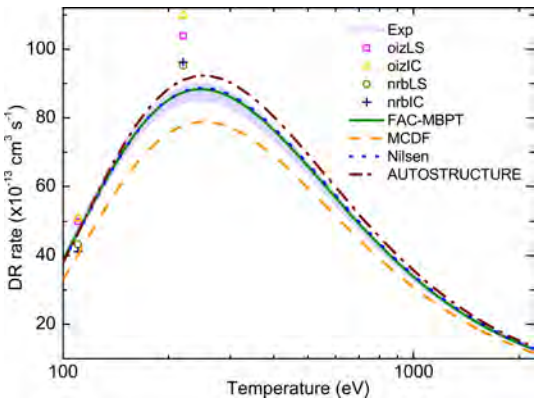

Fig. 1: Experimental and theoretical DR rate coefficients obtained with FAC-MBPT, MCDF, by Nilsen [8] and by Zatsarinny [9] (AUTOSTRUCTURE), as well as tabulated values for two temperatures from `adf09` files of OPEN-ADAS.

References

[1] Brown, G. V. 2008, Canadian Journal of Physics, 86, 199.
[2] Gu, L., Shah, C., Mao, J., et al. 2020, Astronomy&Astrophysics, 641, A93.
[3] Grilo, F., Shah, C., Kühn, S., et al. 2021, The Astrophysical Journal, in press.
[4] Shah, C., López-Urrutia, J. R. C., Gu, M. F., et al. 2019, The Astrophysical Journal, 881, 100.
[5] Schmidt, E. W., Bernhardt, D., Hoffmann, J., et al. 2009, Journal of Physics: Conference Series, 163, 12028.
[6] https://open.adas.ac.uk
[7] Foster, A. R., Ji, L., Smith, R. K., Brickhouse, N. S. 2012, The Astrophysical Journal, 756, 128.
[8] Nilsen, J. 1989, Atomic Data and Nuclear Data Tables, 41, 131.
[9] Zatsarinny, O., Gorczyca, T. W., Korista, K., Badnell, N. R., Savin, D. W. 2004, Astronomy and Astrophysics, 426, 699.

[*]Corresponding author: chintan@mpi-hd.mpg.de
[†]Corresponding author: pdamaro@fct.unl.pt

Observation of metastable $1s2s\ ^3S_1$ He-like oxygen decay in an electron beam ion trap

Filipe Grilo[*1], **Chintan Shah**[2,3], **José Marques**[4], **José Paulo Santos**[1], **José R. Crespo López-Urrutia**[3], **Pedro Amaro**[†1]

1. Laboratory of Instrumentation, Biomedical Engineering and Radiation Physics (LIBPhys-UNL), Department of Physics, NOVA School of Science and Technology, NOVA University Lisbon, 2829-516 Caparica, Portugal

2. NASA Goddard Space Flight Center, 8800 Greenbelt Rd, Greenbelt, MD 20771, USA

3. Max-Planck-Institut für Kernphysik, Saupfercheckweg 1, 69117 Heidelberg, Germany

4. Laboratório de Instrumentação e Física Experimental de Partículas (LIP) and Faculdade de Ciências, Universidade de Lisboa, Portugal

X-ray spectra from hot astrophysical plasmas contain a strong presence of spectral lines of He-like ions due to its closed shell ground state configuration [1]. Abundant light elements, like oxygen, appear in a wide range of temperatures, thus providing lines that can serve as important diagnostic probes [2]. The relative intensity ratio of their forbidden to allowed lines are key diagnostic tools of temperature and density, since the metastable state population mechanisms are highly sensitive on these physical quantities [3].

X-ray measurements of He-like oxygen excited by an electron beam in the $0.3 - 1.0$ keV energy range were made with an electron beam ion trap. The decay of the metastable $1s2s\ ^3S_1$ state population was directly observed (mean lifetime of around 956 μs in the literature [4]) using a 35 eV ms^{-1} electron beam energy sweep rate (Fig. 1).

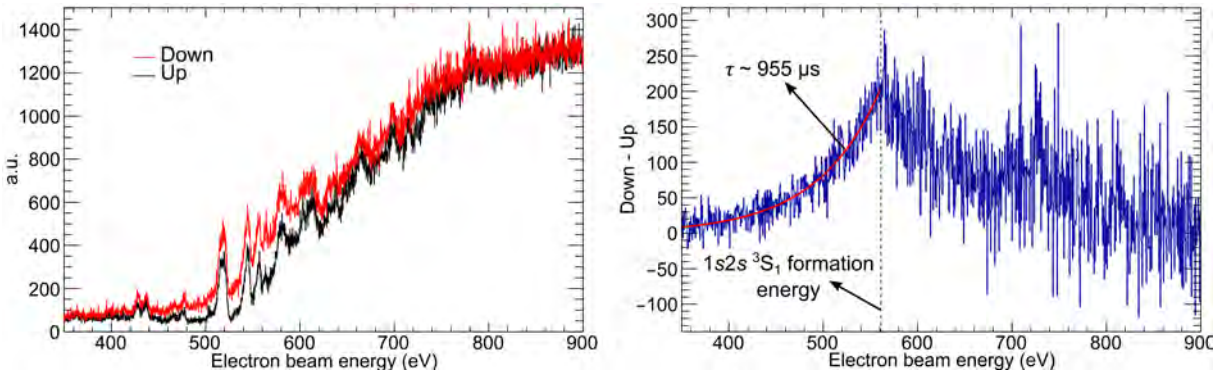

Fig. 1: Left: X-ray spectra of the downwards (red) and upwards (black) electron beam energy scan. Right: Difference between downwards and upwards spectra. The vertical dashed line indicates the $1s2s\ ^3S_1$ formation energy given by Flexible Atomic Code (FAC).

A faster scan rate of 350 eV ms^{-1} was used to obtain a stable population of a few $1s\ ^2S_{1/2}$ H-like, and mainly $1s^2\ ^1S_0$ He-like and $1s2s\ ^3S_1$ He-like oxygen ions. A good electron beam energy dispersion of 7 eV resolves the He-like dielectronic recombination (DR) structure, as well as resonant excitation (RE) superimposed to collisional excitation (CE). The ongoing data analysis indicates that DR and RE resonant structures parting from the (triplet state) $1s2s\ ^3S_1$ state have a significant role in the final spectral modeling of the astrophysical plasmas. Furthermore, the strong inner-shell CE of this state was used to estimate a relative population of 1/5 of the triplet state.

References

[1] Porquet, D., Dubau, J., Grosso, N., 2010, Space Sci Rev 157, 103–134
[2] M. Togawa, S. Kühn, C. Shah, et al. 2020, Phys. Rev. A, 102, 052831
[3] C. De Michelis and M. Mattioli, 1981 Nucl. Fusion, 21, 677.
[4] J. R. Crespo López-Urrutia, P. Beiersdorfer, D. W. Savin, K. Widmann, 1998, Phys. Rev. A, 58, 238.

[*]Corresponding author: f.grilo@campus.fct.unl.pt
[†]Corresponding author: pdamaro@fct.unl.pt

Alkali atom transition cancellations within magnetic field

A. Aleksanyan[*1,2], **R. Momier**[1,2], **E. Gazazyan**[1,3], **A. Papoyan**[1], **C. Leroy**[2]

1. Institute for Physical Research, NAS, 0203 Ashtarak, Armenia

2. Laboratoire Interdisciplinaire Carnot de Bourgogne, UMR CNRS 6303, UBFC, 21000 Dijon, France

3. Yerevan State University, 0025 Yerevan, Armenia

In this work we consider σ^+, π and σ^- optical transitions of alkali atoms within a static magnetic field. Depending on the type of transition and the involved atomic levels, the Hamiltonian matrices are of 1×1, 2×2, 3×3 or 4×4 dimension [1].

For D_1 line, which block matrices are 1×1 or 2×2 dimension, we built Hamiltonian in presence of a magnetic field in order to describe all the transitions. Eigenvalues and eigenkets describing ground and excited levels are calculated, "modified" and unperturbed transfer coefficients and expression of the transitions intensity as a function of the nuclear spin I, the magnetic quantum number m and the magnetic field magnitude B are determined. One observe that cancellations appear only for those π transitions, where the total atomic angular momenta of ground and excited states are equal to each other ($F_g = F_e$). We obtained a formula expressing the magnetic field values that cancel transitions for any alkali atom D_1 line:

$$B = -\frac{1}{\mu_B}\cdot\frac{2m}{1+2I}\cdot\frac{2\xi\varepsilon}{(g_I-g_S)\varepsilon+\dfrac{3g_I-4g_L+g_S}{3}\xi}, \tag{1}$$

where μ_B is the Bohr magneton, g_I, g_S and g_L are respectively the nuclear, electronic and angular Landé factors, ξ and ε are the energy difference of the ground and excited states, and

$$0 \le (-1)^{2I} m \le I - \frac{1}{2}. \tag{2}$$

For matrices of dimension higher than 2×2, formulas exist but are heavy, thus we have performed numerical calculations. We have analyzed $5^2S_{1/2}\rightarrow5^2P_{3/2}$ and $5^2S_{1/2}\rightarrow6^2P_{3/2}$ transition cancellations of the ^{85}Rb and ^{87}Rb alkali metal. For each considered system of ^{87}Rb we can observe 8 cancellations for σ^+ transition, 5 cancellations for π and 3 cancellations for σ^- transitions. For ^{85}Rb there are 16 cancellations for σ^+ transition, 15 for π and 11 for σ^- transitions. It is very interesting, that for some σ^- transitions, cancellation takes place more than one time.

We calculated all transition cancellations of mentioned above transitions of ^{85}Rb and ^{87}Rb alkali metal. The precision of these values is only limited by the precision of the involved physical quantities, for instance ξ and ε in (1) [2-6]. A very soon coming experiment is envisaged in order to measure precisely these B values. As a result, we expect to be able to evaluate more precisely these physical quantities. It should be noted that this modelization is an indirect way to determine precisely atomic levels of energy.

Funding. This research was sponsored in part by the NATO Science for Peace and Security Programme under grant G5794, for which A. Aleksanyan, E. Gazazyan, A. Papoyan and C. Leroy acknowledge. A. Aleksanyan also acknowledges the funding support CO.17049.PAC.AN from the Graduate School EUR EIPHI. R. Momier was supported by the French "Investissements d'Avenir" program, project ISITE-BFC (contract ANR-15-IDEX-0003).

References

[1] P. Tremblay, A. Michaud, M. Levesque, S. Thériault, M. Breton, J. Beaubien, and N. Cyr, "Absorption profiles of alkali-metal D lines in the presence of a static magnetic field", Phys. Rev. A, vol. **42**, pp. 2766–2773, Sep 1990. [Online]. Available: https://link.aps.org/doi/10.1103/PhysRevA.42.2766

[2] D. Budker, D. F. Kimball, S. M. Rochester, V. V. Yashchuk, and M. Zolotorev, "Sensitive magnetometry based on nonlinear magneto-optical rotation", Phys. Rev. A, vol. **62**, p. 043403, Sep 2000. [Online]. Available: https://link.aps.org/doi/ 10.1103/PhysRevA.62.043403

[3] E. Arimondo, M. Inguscio, and P. Violino, "Experimental determinations of the hyperfine structure in the alkali atoms", Rev. Mod. Phys., vol. **49**, pp. 31–75, Jan 1977. [Online]. Available: https://link.aps.org/doi/10.1103/RevModPhys.49.31

[4] A. Banerjee, D. Das, and V. Natarajan, "Absolute frequency measurements of the D_1 lines in ^{39}K, ^{85}Rb, and ^{87}Rb with 0.1 ppb uncertainty", EPL, vol. **65**, p. 172, 01 2004. [Online]. Available: https://doi.org/10.1209%2Fepl%2Fi2003-10069-3

[5] A. Aleksanyan, R. Momier, E. Gazazyan, A. Papoyan and C. Leroy, "Transition cancellations of ^{87}Rb and ^{85}Rb atoms in a magnetic field", J. Opt. Soc. Am. B, vol. 37, no. 11, pp. 3504-3514, Nov. 2020. [Online]. Available: https://doi.org/10.1364/JOSAB.403862

[6] R. Momier, A. Aleksanyan, E. Gazazyan, A. Papoyan and C. Leroy, "New standard magnetic field values determined by cancellations of ^{85}Rb and ^{87}Rb atomic vapors $5^2S_{1/2}\rightarrow6^2P_{1/2,3/2}$ transitions", Journal of Quantitative Spectroscopy and Radiative Transfer, vol. 257, p. 107371, Dec. 2020. [Online]. Available: https://doi.org/10.1016/j.jqsrt.2020.107371

*Corresponding author: arthuraleksan@gmail.com

Off-axis optical vortices using double-Raman singlet light-matter scheme

H. R. Hamedi[*1], **J. Ruseckas**[1], **E. Paspalakis**[2], **G. Juzeliūnas**[1]
1. Institute of Theoretical Physics and Astronomy, Vilnius University, Sauletekio 3, Vilnius LT-10257, Lithuania
2. Materials Science Department, School of Natural Sciences, University of Patras, Patras 265 04, Greece

We study the formation of off-axis optical vortices [1] propagating inside a double-Raman gain atomic medium (Fig. 1). The atoms interact with two weak probe fields as well as two strong pump beams which can carry orbital angular momentum (OAM) [2]. We consider a situation when only one of the strong pump lasers carries an OAM. A particular superposition of probe fields coupled to the matter is shown to form specific optical vortices with shifted axes. Such off-axis vortices can propagate inside the medium with sub- or superluminal group velocity depending on the value of the two-photon detuning. The superluminal optical vortices are associated with the amplification as the energy of pump fields is transferred to the probe fields. The position of the peripheral vortices can be manipulated by the OAM and intensity of the pump fields. We show that the exchange of optical vortices is possible between individual probe beams and the pump fields when the amplitude of the second probe field is zero at the beginning of the atomic cloud [3].

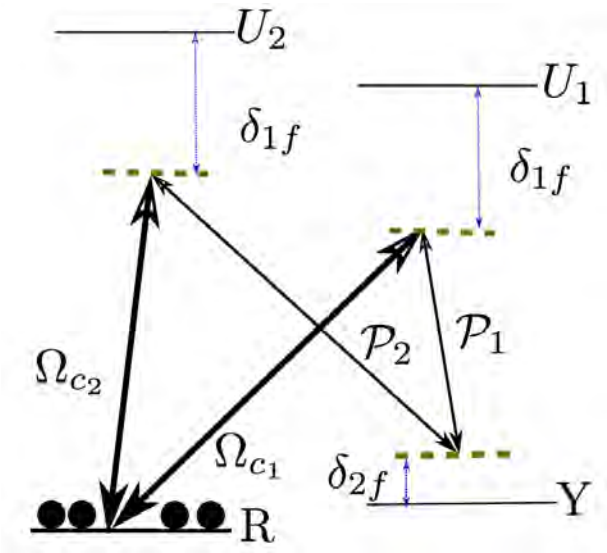

Fig. 1: Schematic diagram of the double Raman scheme.

References

[1] S. Franke-Arnold *et al.*, Optics Express, **15**, 8619-8625 (2007).
[2] L. Allen *et al.*, Prog. Opt. **39**, 291 (1999).
[3] H. R. Hamedi *et al.*, Phys. Rev. A **101**, 063828 (2020)

*Corresponding author: hamid.hamedi@tfai.vu.lt

Accurate theoretical study of the spectroscopic properties of diatomic molecules including 2nd row transition metals

Alexandros Androutsopoulos[*1], **Theodoros Depastas**[†1], **Ioannis Karapetsas**[1], **Demeter Tzeli**[1,2]

1. Laboratory of Physical Chemistry, Department of Chemistry, National and Kapodistrian University of Athens, Zografou GR-15784, Greece

2. Theoretical and Physical Chemistry Institute, National Hellenic Research Foundation, 48 Vassileos Constantinou Ave., Athens 116 35, Greece

Transition metals have very interesting properties which result from their partially occupied d orbitals with loosely bound electrons. These metals are very hard and malleable; they have high melting and boiling points, high electrical and thermal conductivity; they form colored compounds due to d-d electronic transitions. They often exhibit high catalytic activity and tend to form paramagnetic compounds. Their diatomic molecules are the simplest building blocks of solid metal compounds; therefore, an investigation of the electronic structure of the former can be proven very useful in the field of the corresponding bulk materials, crystalline or otherwise.

Here, we study the properties of seven diatomic molecules including 2nd row transition metals, i.e., MoO, MoS, Mo_2, TcN, RuC, RhB, and PdBe.[1-2] We have calculated the spectroscopic data and the potential energy curves of their low-lying states employing multi reference configuration interaction and coupled cluster methodologies in conjunction with the aug-cc-pV*n*Z(-PP) basis sets, where n = 2 - 5. We study how the gradual transition of the nuclear charge from Mo to Pd in the isoelectronic molecules (MoO, TcN, RuC, RhB, PdBe), and from O to S in (MoO, MoS) influence all calculated data and how the increase of bonding strength affects their spectroscopic data.

Moreover, specific spectroscopic data have been extrapolated in the infinite basis set size limit while the relativistic effects on molecular properties have also been included. The latter have been calculated via 9th order Douglas-Kroll-Hess approximation accomplishing a decoupling of positive- and negative-energy eigenstates of the Dirac one-electron Hamiltonian [3]. We conclude that by the employment of a relativistic approximation scheme or by the basis set limit extrapolation, the theoretical values of the spectroscopic constants approach the experimental data with significant accuracy [4].

References

[1] D. Tzeli, I. Karapetsas, *J. Phys. Chem.* **124**, 6667 (2020).
[2] A. Androutsopoulos, T. Depastas, D. Tzeli, *to be submitted*.
[3] T. Nakajima, K. Hirao, *Chem. Rev.* **112**, 1, 385 (2012).
[4] B. Simard, M.-A. Lebeault-Dorget, A. Marijnissen, and J.-J. Meulen, *J. Chem. Phys.* **108**, 9668 (1998).

*Corresponding author: alexandrosandroutsopoulos@hotmail.com
†Corresponding author: tdepastas@gmail.com

Prospects for refining fundamental constants by spectroscopy of deuterium molecular ion

P. Danev[*1], **D. Bakalov**[1], **V.I. Korobov**[2], **S. Shiller**[3]
1. Institute for Nuclear Research and Nuclear Energy, Bulgarian Academy of Science, Sofia, Bulgaria
2. Joint Institute for Nuclear Research, 141980, Dubna, Russia
3. Institut für Experimentalphysik, Heinrich-Heine-Universität, Düsseldorf, 40225 Düsseldorf, Germany

Hydrogen molecular ions, due to the possibility of precise theoretical evaluation of their spectrum, transitions, and external effect shifts, are shown to be of metrological relevance [1], [2]. The comparison of high precision experimental and theoretical results opens room for independent tests of QED and has the potential to provide accurate values of fundamental constants. One of the recent achievements in the hydrogen molecular ion spectroscopy is the determination of the proton-to-electron mass ratio with factional accuracy of $\sim 2 \times 10^{-11}$ from ro-vibrational precision laser spectroscopy of cooled and trapped HD^+ ions [3], [4]. The recent adjustments of the CODATA values of the proton charge radius and the Rydberg constant were confirmed too [3].

In homonuclear molecular ions the electric dipole transitions, between ground electronic states, are strongly suppressed and of primary laser spectroscopy interest is the electric quadrupole transition spectrum. In a continuation of our previous work on the H_2^+ ion [5], we report here the results of the calculations of the hyperfine structure of the laser-induced electric quadrupole transitions between a large set of ro-vibrational states of D_2^+ [6]. We show that the electric quadrupole moment of the deuteron can in principle be determined with low fractional uncertainty ($\simeq 1 \times 10^{-4}$) by comparing the obtained results with future data from precision spectroscopy of D_2^+.

This work was supported by the Bulgarian Science Fund under Grant No. FNI 08-17.

References

[1] S. Schiller, D. Bakalov, and V.I. Korobov, *Simplest molecules as Candidates for Precise Optical Clocks*, Phys. Rev. Lett. **113**, 023004 (2014).
[2] D . Bakalov, S. Schiller, *The electric quadrupole moment of molecular hydrogen ions and their potential for a molecular ion clock*. Appl. Phys. B (2014) **114**, pp.213-230. Erratum: Volume **116**, Issue 3, pp 777-778.
[3] S . Alighanbari, G.S. Giri, F.L. Constantin et al. *Precise test of quantum electrodynamics and determination of fundamental constants with HD+ ions*, Nature 581, 152–158 (2020)
[4] P atra *et al.*, *Proton-electron mass ratio from laser spectroscopy of HD+ at the part-per-trillion level*, Science, vol. 369 no. 6508 1238-1241 (2020)
[5] V.I. Korobov, P. Danev, D. Bakalov, and S. Schiller, *Laser-stimulated electric quadrupole transitions in the molecular hydrogen ion* H_2^+, Phys. Rev. A **97**, 032505 (2018).
[6] P. Danev, D. Bakalov, V. I. Korobov, and S. Schiller, *Hyperfine structure and electric quadrupole transitions in the deuterium molecular ion*, Phys. Rev. A 103, 012805 (2021)

[*]Corresponding author: *petar_danev@abv.bg*

The simultaneous coupled-channel deperturbation treatment of the $X^2\Sigma^+$, $A^2\Pi$ and $B^2\Sigma^+$ states in the CN radical: the first attempt

V. A. Terashkevich[*1], **E. A. Pazyuk**[†1], **A. V. Stolyarov**[1]
1. Lomonosov Moscow State University Leninskie Gory 1/3, Moscow, 119991 Russia

The CN molecule has been attracting the permanent attention of astronomical spectroscopists for more than 80 years since the first recognition of the radical in the absorption spectrum of the interstellar medium (ISM) [1]. From the point of view of theoretical molecular spectroscopy, the CN radical is of great interest due to a large number of low-lying electronic states, between which the local and regular perturbations take place (ex: [2]). Up to the date, an array of over 6000 rovibronic term values [3] belonging to the first three electronic states $X^2\Sigma^+$, $A^2\Pi$, $B^2\Sigma^+$, has been obtained by statistical artificial intelligence processing of experimental frequencies in the MW, IR and visible radiation regions. It is of fundamental interest to obtain a comprehensive set of the deperturbed molecular parameters: potential energy curves of the coupled states and relevant non-adiabatic matrix elements. This parameters would produce the still "unobserved" lines with experimental (spectroscopic) accuracy and would fulfill the existing "gaps" in the astronomical atlas. For these purposes, the reduced coupled channel approach [4] can be successfully used, which makes it possible in principle to describe overall set of experimental data in the framework of unified deperturbation model.

At the first step of this work, the systematic *ab initio* electronic structure calculation has been carried out for the lowest (1-6)$^2\Sigma^+$ and (1-5)$^2\Pi$ electronic states of the CN radical in the range of internuclear distances R = [0.75-3.0] Å. Besides the potential energy curves of electronic states, the corresponding spin-orbit and electron-rotational non-adiabatic matrix elements were evaluated along with the relevant transition dipole moment functions. To describe carbon and nitrogen atoms, the aug-cc-pCVQZ-DK full-electron basis set was used. The optimized molecular orbitals were obtained by the state-averaged self-consistent field method in an active space of 10 orbitals of $6a_1$, $2b_1$ and $2b_2$ symmetry (the point group C_{2v}). Then a dynamic correlation was taken into account using the MR-CISD method. All 13 electrons were correlated explicitly while the lowest two a_1 orbitals were kept to be doubly occupied. The impact of higher electronic excitations on the energy calculated was taken into account using the Davidson correction; the scalar-relativistic correction was estimated within the framework of the effective Douglas-Kroll Hamiltonian approach.

The *ab initio* results were then used as a trial set in the non-linear fitting procedure to the experimental term values based on iteratively solving the direct spectroscopic problem realized in the framework of the reduced coupled channel approach. In particular, the empirical potentials for the $X^2\Sigma^+$, $A^2\Pi$ and $B^2\Sigma^+$ states were defined in the analytical form - an expanded Morse oscillator (EMO). The fitted non-adiabatic matrix elements were uniformly scaled in order to ensure a maximal interlink with the corresponding initial *ab initio* functions. The current set of deperturbed parameters reproduces the most of experimental term values with uncertainty of 0.03 cm^{-1}.

References

[1] A. McKellar, The Astronomical Society of the Pacific. **307**,187, (1940).
[2] R. Ram, L. Wallace and P.F. Bernath, Journal of Molecular Spectroscopy. **263**, 82–88, (2010).
[3] A.-M. Syme, L. K. McKemmish, Monthly Notices of the Royal Astronomical Society. **499**, 25-39, (2020).
[4] S. V. Kozlov, E.A. Pazyuk, A.V. Stolyarov. Optics and Spectroscopy (English translation of Optika i Spektroskopiya). **125**, №4, 464-469, (2018).

[*]Corresponding author: terversik@yandex.ru
[†]Corresponding author: pazyuk@phys.chem.msu.ru

A buffer gas cooled BaF beam for the NL-eEDM experiment

Maarten C. Mooij[*1,2], **Wim Ubachs**[1], **H. L. Bethlem**[1,3] **and the eEDM collaboration: Parul Aggarwal**[2,3], **Alexander Boeschoten**[2,3], **Anastasia Borschevsky**[2,3], **Malika Denis**[2,3], **Kevin Esajas**[2,3], **Pi A. B. Haase**[2,3], **Steven Hoekstra**[2,3], **Klaus Jungmann**[2,3], **Virginia R. Marshall**[2,3], **Thomas B. Meijknecht**[2,3], **Rob G. E. Timmermans**[2,3], **Anno Touwen**[2,3], **Lorenz Willmann**[2,3]

1. Department of Physics and Astronomy, VU University Amsterdam, 1081 HV Amsterdam, The Netherlands
2. Nikhef, National Institute for Subatomic Physics, 1098 XG Amsterdam, The Netherlands
3. Van Swinderen Institute for Particle Physics and Gravity, University of Groningen, 9747 AG Groningen, The Netherlands

The search for the electron electric dipole moment (eEDM) is a direct method of testing fundamental theories beyond the Standard Model. We aim to improve the current best sensitivity [1] using BaF, which has a large effective internal electric field, strong laser cooling transitions, a large dipole moment and a relatively low mass [2]. A buffer gas beam source [3,4] is preferred because of the intense beam at low velocities, which leads to more efficient deceleration.

In Amsterdam we have built a cryogenic beam source. Inside a cold cell at 20 K Ba is ablated by a short laser pulse (5 ns, 532 nm, 10Hz) and reacts with SF6 to form BaF molecules. The molecules are cooled by collisions with cold Ne gas that flows continuously through the cell. Inside this Ne flow the molecules are extracted from the cell and form a beam. About 10^{10} molecules per single rotational level are produced at a velocity of 200 m/s. We are currently analyzing the source in detail. The density, velocity, positional spread and rotational temperature of the molecular beam are measured with rotationally resolved absorption and laser-induced fluorescence detection. With multi-photon ionization we can also detect the Ba atoms and Ne carrier gas.

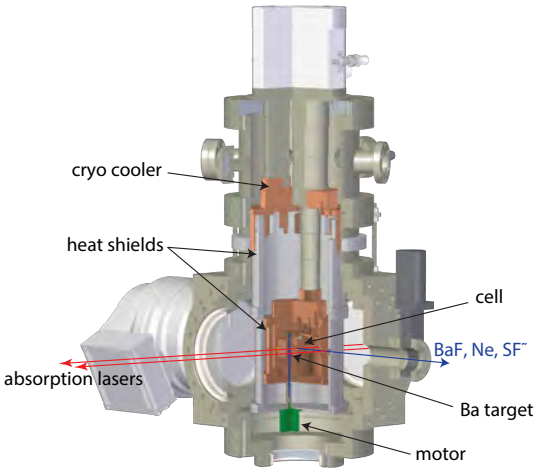

Fig. 1: Design of molecular source.

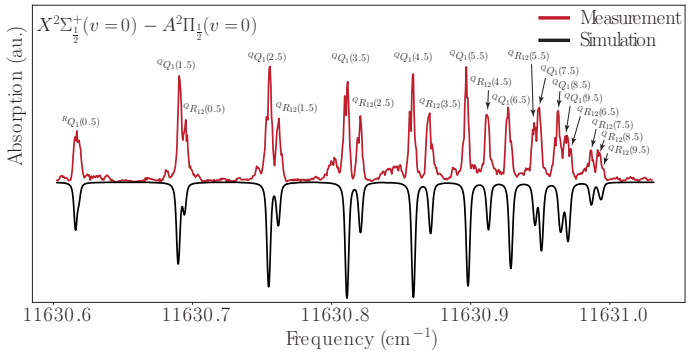

Fig. 2: Absorption spectroscopy of the $X^2\Sigma^+_{\frac{1}{2}}(v=0)$ to $A^2\Pi_{\frac{1}{2}}(v=0)$ Q-branch in BaF.

References

[1] ACME Collaboration., Andreev, V., Ang, D.G. *et al.* Nature **562**, 355–360 (2018).
[2] The NL-eEDM collaboration., Aggarwal, P., *et al.* Eur. Phys. J. D **72**, 197 (2018)
[3] Nicholas R. Hutzler, Hsin-I Lu, and John M. Doyle *Chemical Reviews* **2012** *112* (9), 4803-4827
[4] S. Truppe, *et al.*, J Mod Opt, 65:648-656, 2018.

*Corresponding author: m.c.mooij@vu.nl

Resonances in arbitrarily oriented dipoles scattering in plane

E.A.Koval[*1], **O.A.Koval**[2]

1. Bogoliubov Laboratory of Theoretical Physics, Joint Institute for Nuclear Research, Dubna, Moscow Region 141980, Russia

2. A.M. Obukhov Institute of Atmospheric Physics, Russian Academy of Sciences, Moscow 119017, Russian Federation

The impact of the short-range interaction on the resonances occurrence in the anisotropic dipolar scattering in a plane was numerically investigated *for the arbitrarily oriented dipoles* and for a wide range of collision energies.

We revealed the strong dependence of the cross section (see Fig. 2) of the dipolar scattering in plane on the radius of short-range interaction, which is modeled by a hard wall potential and by the more realistic Lennard-Jones potential, and on the mutual orientations of the dipoles.

We defined the critical (magic) tilt angle of one of the dipoles, depending on the direction of the second dipole for arbitrarily oriented dipoles. It was found that resonances arise only when this angle is exceeded.

In contrast to the 3D case, the energy dependencies of the boson (fermion) 2D scattering cross section grows (is reduced) with an energy decrease in the absence of the resonances, as shown in Fig. 1. We showed that the mutual orientation of dipoles strongly impacts the form of the energy dependencies, which begin to oscillate with the tilt angle increase, unlike the 3D dipolar scattering.

The angular distributions of the differential cross section in the 2D dipolar scattering of both bosons and fermions are highly anisotropic at non-resonant points. The results of the accurate numerical calculations of the cross section agree well with the results obtained within the Born and eikonal approximations.

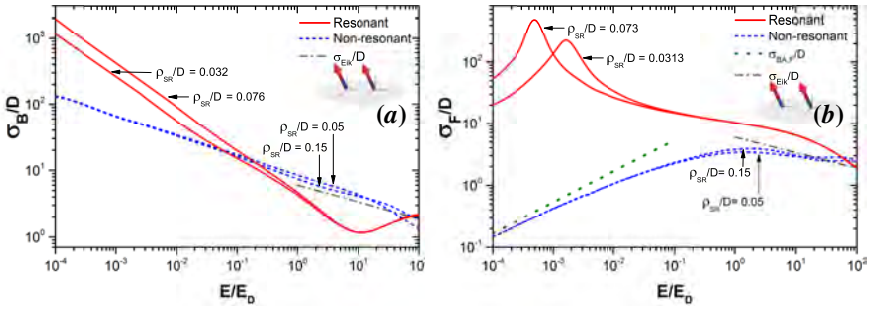

Fig. 1: The energy dependencies of the total cross section of the dipolar scattering of identical bosons $\sigma_B(E)$ ($\alpha = 45°$(a)) and identical fermions $\sigma_F(E)$ ($\alpha = 45°$(b)) for aligned dipoles configuration $\beta = 0°$ and $\gamma = \alpha$. The tilt angle exceeds the critical angle $\alpha > \alpha_c$ ($\alpha_c = 35.3°$) for such dipole mutual orientations. The curves corresponding to the resonance points in Fig. 2 are indicated by a red solid line, the non-resonant curves by a blue dashed line; the Born approximation by a green dotted line, the eikonal approximation by a gray dashed line.

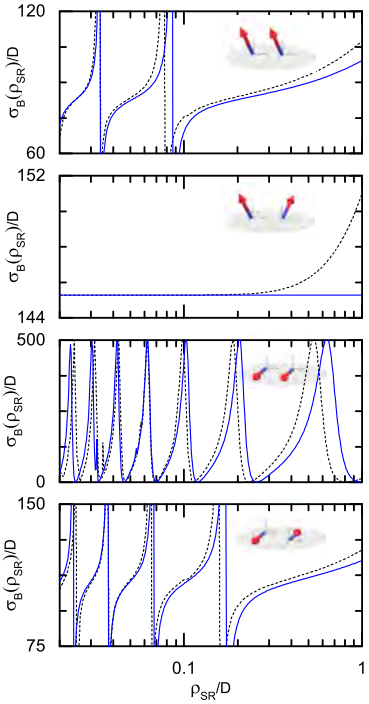

Fig. 2: The dependence of the total cross section of the dipolar low-energy scattering σ_B of *identical bosons* on the SRI radius ρ_{SR} at collisions of two aligned $\beta = 0°$ (a,c) and unaligned $\beta = 180°$ (b,d) dipoles (at $\gamma = \alpha$), tilted to the angle $\alpha = 45°$ (a,b), as well as for a limiting case of dipoles lying in the scattering plane $\alpha = 90°$ (c,d). The results obtained with the use of the hard wall potential are marked with a black dashed line, whereas those obtained by the use of the Lennard-Jones potential — by the blue solid line.

References

[1] E.A. Koval and O.A. Koval, Aspects of arbitrarily oriented dipoles scattering in a plane: Short-range interaction influence, Phys. Rev. A **102**, 042815 (2020).

[2] V. Roudnev and M. Cavagnero, Resonance phenomena in ultracold dipole–dipole scattering, J. Phys. B: At., Mol. Opt. Phys. **42**, 044017 (2009).

[3] J. Bohn, M. Cavagnero, and C. Ticknor, Quasi-universal dipolar scattering in cold and ultracold gases, New J. Phys. **11**, 055039 (2009).

*Corresponding author: e-cov@yandex.ru

Fano interference in quantum resonances from angle-resolved elastic scattering

Prerna Paliwal[1], **Alexander Blech**[2], **Christiane P. Koch**[*2], **Edvardas Narevicius**[†1]
1. Department of Chemical and Biological Physics, Weizmann Institute of Science, Rehovot, Israel
2. Dahlem Center for Complex Quantum Systems and Fachbereich Physik, Freie Universität Berlin, Berlin, Germany

Interference of a discrete quantum state with a continuum of states gives rise to asymmetric line shapes [1][2] that have been observed in measurements across nuclear, atomic, molecular as well as solid-state physics. Information about the interference is captured by some but not all measurable quantities. For example, for quantum resonances arising in single channel scattering, the signature of such interference may disappear due to the orthogonality of partial waves. We show that probing the angular dependence of the cross section allows for unveiling the coherence between the partial waves which leads to the appearance of the characteristic asymmetric Fano profiles [2]. We observe a shift of the resonance position with observation angle, in excellent agreement with theoretical predictions from full quantum scattering calculations. Using a model description for the interference between the resonant and background states, we extract the relative phase responsible for the characteristic Fano-like profile from our experimental measurements.

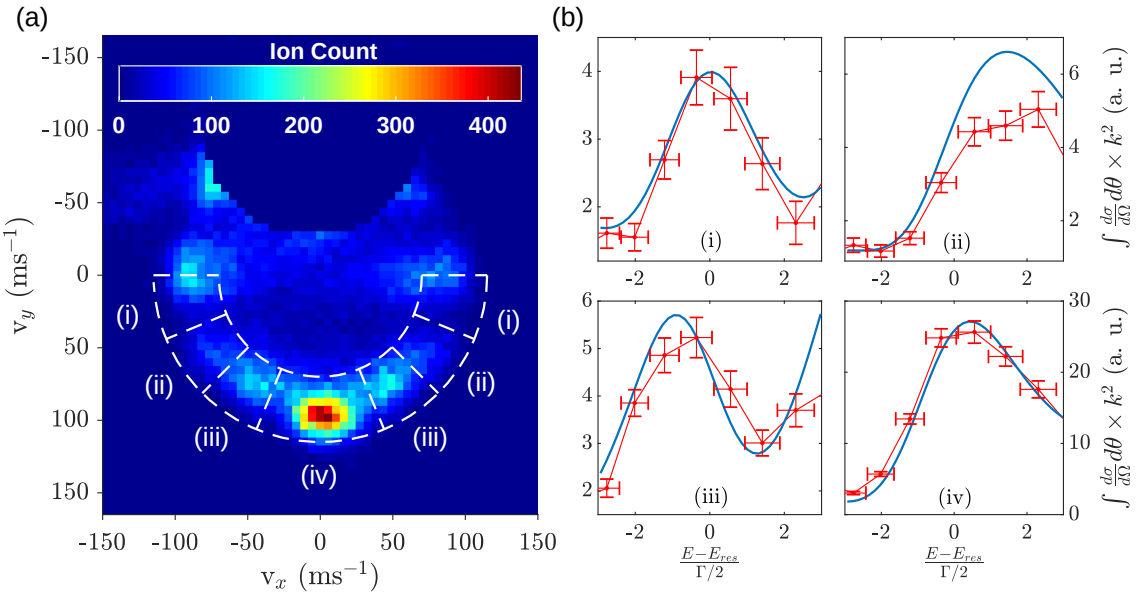

Fig. 1: Experimental and theoretical angle-resolved energy-dependent cross sections for the collision of normal deuterium molecules with metastable helium in the vicinity of the orbiting resonance at 4.8 K. (a) A typical velocity-mapped image is shown where different angular sectors are marked as regions (i) to (iv) on the annulus by white-dashed semicircles. The color bar on top represents the number of He^+ ions. The collision axis points up in this image. (b) The blue curves show the theoretical prediction for the angle-resolved energy-dependent cross section$\times k^2$ (where k is the momentum of the colliding pair) in the regions marked as (i) to (iv) in (a) and the red lines join the experimentally obtained data points. The x-axis represents $(E - E_{res})/(\Gamma/2)$ where E_{res} is the resonance energy and Γ is the resonance width. The error bars show standard deviation in experimental data points.

References

[1] U. Fano, Nuovo Cim. **12**, 154 (1935).
[2] U. Fano, Phys. Rev. **124**, 1866 (1961).

[*]Corresponding author: christiane.koch@fu-berlin.de
[†]Corresponding author: edvardas.narevicius@weizmann.ac.il

High-Precision Spectroscopy of Single Molecular Hydrogen Ions in a Penning Trap at Alphatrap

C. M. König*[1], A. Egl[1], F. Heisse[1], J. Morgner[1], T. Sailer[1], B. Tu[1], K. Blaum[1], S. Sturm[1],
1. Max-Planck-Institute for Nuclear Physics, Saupfercheckweg 1, 69117 Heidelberg, Germany

Molecular hydrogen ions are an excellent system for testing quantum electrodynamics by comparing experiments and theory. With only a single bound electron they are the simplest molecules available. We, in collaboration with the group of Stephan Schiller (University Düsseldorf), plan to perform high-precision spectroscopy on single hydrogen molecular ions in the Penning-trap setup of ALPHATRAP [1] utilizing the continuous Stern-Gerlach effect for state detection [2]. The first measurements will investigate the hyperfine structure of the HD^+ ion in the microwave regime and will thus allow extracting the coeffcients of the hyperfine hamiltonian, from which rovibrational laser spectroscopy performed on this ion species can benefit [3,4]. In the future, we aim to extend our methods to single ion rovibrational laser spectroscopy of H_2^+ at infrared wavelengths enabling the ultra precise determination of fundamental constants such as the proton-to-electron mass ratio [5]. The development of the required techniques for this measurement will be an important step towards spectroscopy of an antimatter $\overline{H}_2^-$ ion for tests of matter-antimatter symmetry which would exceed the current limits by several orders of magnitude [6]. In this contribution I will present an overview of the experimental setup and the planned measurement schemes.

References

[1] S. Sturm *et al.*, The ALPHATRAP experiment. Eur. Phys. J. Spec. Top. **227**, 1425-1491 (2019)
[2] H. Dehmelt, Proc. Natl. Acad. Sci. USA **83**, 2291 (1986)
[3] S. Alighanbari*et al.*, Nature **581**, 152-158 (2020)
[4] S. Patra *et al.*, Science 04 Sep 2020: Vol. **369**, Issue 6508, pp. 1238-1241
[5] J.-Ph. Karr, L. Hilico, J. C. J. Koelemeij, and V. I. Korobov, Phys. Rev. A **94**, 050501(R) (2016)
[6] E. Myers, Phys. Rev. A **98**, 010101(R) (2018)

*Corresponding author: ckoenig@mpi-hd.mpg.de

How does antimatter fall ?: simulation of the GBAR experiment at CERN

O. Rousselle[*1], **P. Cladé**[1], **S. Guellati**[1], **R. Guérout**[1], **S. Reynaud**[1]
1. Laboratoire Kastler Brossel, Sorbonne Université, ENS-PSL, Collège de France, CNRS, 75005 Paris, France

One of the main questions of fundamental physics is the problem of the asymmetry matter/antimatter in the universe and the action of gravity on antimatter. Tests on antimatter gravity have currently a limited precision, with the sign of gravity acceleration not yet known experimentally [1]. Ambitious projects are developed at CERN facilities to produce low energy antihydrogen with the aim of measuring the free fall of antihydrogen atoms. Among them, the GBAR experiment (*Gravitational Behaviour of Antihydrogen at Rest*) aims at measuring the gravity acceleration $\bar{g}$ of ultracold antihydrogen atoms during a free fall in Earth's gravitational field. The simulation of the free-fall chamber includes the Monte-Carlo generation of trajectories and the statistical analysis leading to the estimation of $\bar{g}$. A precision of the measurement beyond the % level is confirmed by taking into account the experimental design. Moreover, we propose to improve the accuracy of the measurement by using the idea of quantum reflection drawn from experiments performed on ultracold neutrons [2]. The quantum interference pattern obtained brings more information on the value of $\bar{g}$ than the classical method, and then improves the accuracy of the experiment by approximately 3 orders of magnitude [3].

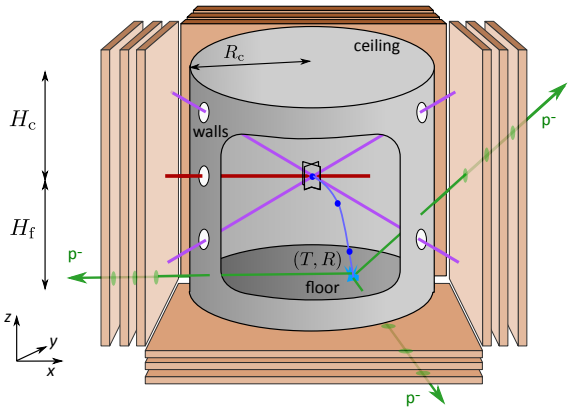

Fig. 1: Principle of the free fall measurement in the GBAR experiment. Details of the figure: cylindrical chamber (in grey); an example of antihydrogen trajectory from trap to detection surface (in blue); secondary particles produced by the annihilation (in green).

References

[1] P. Perez et al., Hyperfine Interactions **233** (2014).
[2] .V. Nesvizhevsky et al., Nature **415** (2002).
[3] .P. Crépin et al., Physical Review A **99**, 042119 (2019).

*Corresponding author: olivier.rousselle@lkb.upmc.fr

Genuine properties and relaxation dynamics of solvated electrons in neutral water clusters

R. Signorell[*1]
1. Department of Chemistry and Applied Biosciences, ETH Zurich, 8093 Zurich, Switzerland

The interest in the hydrated electron stems from its role in Chemistry and radiation damage, and from the fact that it is one of the simplest quantum solutes. We have investigated the formation and relaxation dynamics, and the genuine properties (binding energy and photoemission anisotropy) of hydrated electrons in neutral water clusters with a combination of time-resolved photoelectron velocity map imaging and electron scattering simulations [1-4].

We find hydrated electron formation and loss processes after one-photon laser excitation to be pronouncedly cluster-size dependent, indicating a minimum cluster size required to support solvated electrons. The relaxation to the ground-state hydrated electron (s-state) after one-photon laser excitation below and above band gap is completed within about 2 ps. It is suggested that this relaxation dynamics is dominated by slow and fast solvent response. The timescales are consistent with corresponding solvation timescales found in the liquid bulk and in large anion water clusters, hinting at similar mechanisms in the different systems.

The genuine properties of the ground-state hydrated electron in clusters agree well with corresponding experimental and theoretical values for the liquid, suggesting similar properties of the solvated electron in liquid water and large neutral water clusters. However, contrary to anionic water clusters neither the bulk liquid nor the neutral clusters seem to give rise to different isomers with distinct vertical binding energies.

References

[1] D. Luckhaus, Y.-I. Yamamoto, T. Suzuki and R. Signorell, Sci. Adv. **3**, e1603224 (2017).
[2] T.E. Gartmann, L. Ban, B.L. Yoder, S. Hartweg, E. Chasovskikh, and R. Signorell, J. Phys. Chem. Lett. **10**, 4777 (2019).
[3] L. Ban, C. West, E. Chasovskikh, T.E. Gartmann, B.L. Yoder and R. Signorell, J. Phys. Chem. A **124**, 7959 (2020).
[4] L. Ban, B.L. Yoder, and R. Signorell, to be published.

[*]Corresponding author: rignorell@ethz.ch

Achievements of Polarization Atomic Spectroscopy with FELs

E. Gryzlova[*1]
1. 1Skobeltsyn Institute of Nuclear Physics, Lomonosov Moscow State University, Moscow 119991, Russia

Polarization spectroscopy is a well-developed research field including a variety of phenomena, such as dichroism, electronic and ionic correlations, spin polarization etc. Nevertheless until FELs implementation such investigations in non-linear regime was available in optical domain only. With the FELs development a great number of non-linear polarization phenomena was achieved in VUV domain from *complete experiment* [1] to many-path interference in multi-photon regime [2].

One of the significant research field is determination of all (within a model) complex amplitudes describing a process using measurements of polarization parameters or vice versa characterization of unknown properties of a radiation such as degree of polarization, admixture of highest harmonics or phase offset with a help of well-known properties of some system [3]. The last is essential issue for FELs where spiky structure of the pulses prevent characterization of the pulses by conventional way.

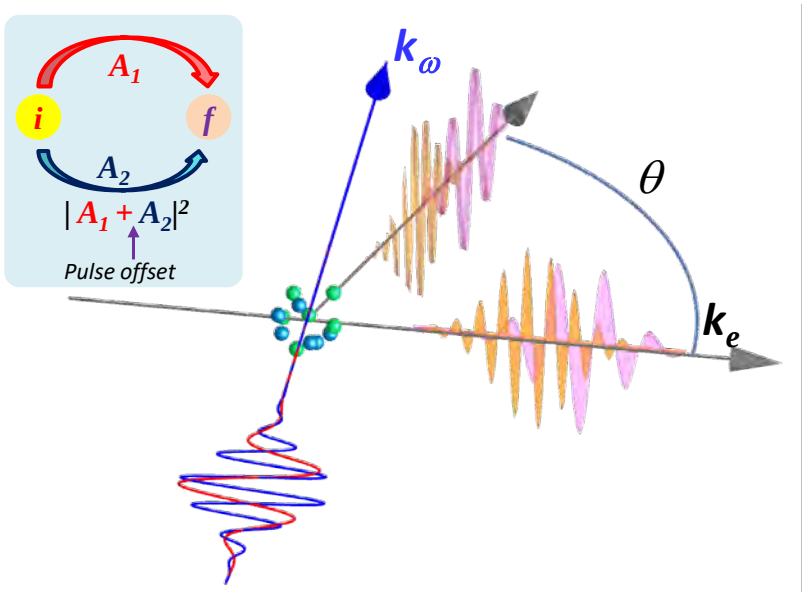

Fig. 1: The photoemission angular anisotropy as result of the interference two-photon and single-photon ionization pathways.

The radiation generated by a FEL naturally contains several harmonics, mainly mixture of fundamental and second ones. If the two colours are mutually coherent, the emitted photoelectrons may interfere. Mutual coherence means that the electromagnetic oscillations of the wavelengths have a definite phase, or temporal, relationship in a given pulse of light. If polarization of the harmonics is well defined then resulting electric strength possesses the lower symmetry than each of harmonic separately [4],[5]. This symmetry violation manifests in the observable of photoemission: photoelectron angular distribution [6], [7] and especially prominent in spin polarization [8]. The information about fields, in particularly, harmonic ratio and their phases are depicted in these values and may be extracted. At the conference new results concerning bi-chromatic ionization of an atom will be presented.

References

[1] P. A. Carpeggiani *et al.*, Nature Physics **15**, 170 (2019).
[2] P. K. Maroju *et al.*, Nature , **578**, 386 (2020).
[3] M. Di Fraia *et al.*,Phys.Rev. Lett., **123**, 213904 (2019).
[4] A. N. Grum-Grzhimailo *et al.*, Phys.Rev. A, **91**, 063418 (2015).
[5] N. Douguet *et al.*, Phys.Rev. A, **93**, 033402 (2016).
[6] E. V. Gryzlova *et al.*, Phys.Rev. A, **97**, 013420 (2018).
[7] E. V. Gryzlova *et al.*, Phys.Rev. A, **100**, 063417 (2019).
[8] E. V. Gryzlova *et al.*, Phys.Rev. A, **102**, 053116 (2020).

[*]Corresponding author: gryzlova@gmail.com

Shaping attosecond waveforms at free-electron lasers

G. Sansone[*1]
1. Albert-Ludwigs-Universität, 79104 Freiburg, Germany.

The generation of ultrashort attosecond light pulses in the extreme ultraviolet and X-ray spectral range relies on different technologies based either on intense femtosecond laser sources [1] [2] or charged particle accelerators [3][4][5]. In both cases, the emission of short wavelength radiation is due to the dynamics of free electrons, which either recombine with the parent ion after an initial tunnelling ionization process (high-order harmonic generation) or moves at relativistic velocities through a magnetic periodic structure (free-electron lasers (FELs)). The control of the motion of the electronic wavepacket (in HHG) or of the relativistic electron bunch (in FELs) offers the opportunity to manipulate the characteristics of the emitted radiation, allowing the generation of even harmonics of the fundamental radiation [6], or the sub-cycle control of the relative phase between the two-colors of an intense femtosecond XUV pulse [7].

In this presentation, I will show how the control of the electron bunch at the seeded FEL laser FERMI [8] gives the possibility to generate and shape in time an attosecond pulse train consisting of phase-locked harmonics. The experimental results demonstrate the first complete and independent amplitude and phase shaping of attosecond waveforms in the extreme ultraviolet.

For the temporal characterization a novel approach inspired by the reconstruction of reconstruction of attosecond bursts by beating of two-photon transitions [1] was developed and implemented. In this approach, the control over the delay between the attosecond waveforms and a near-infrared pulse is replaced by a correlation analysis of the single-shot photoelectron spectra generated by the combination of the two fields. This analysis gives access to the group-delay-dispersion of the harmonic spectrum, which is required for the temporal reconstruction of the waveform, together with the spectral amplitudes. Some examples of waveforms synthesized using four coherent harmonics are shown in Fig. 1.

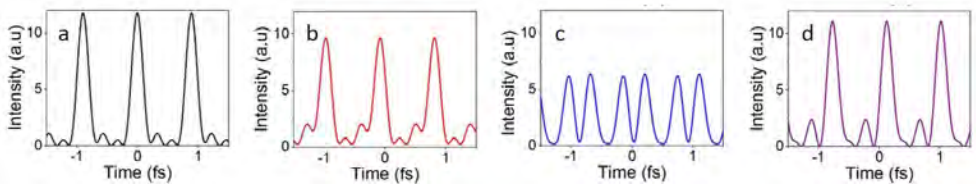

Fig. 1: Shaped attosecond waveforms using four harmonics of the seeded FEL FERMI. The differences in the intensity profiles of the electric field are induced by manipulating the group-delay dispersion of the spectrum.

References

[1] P. M. Paul *et al.*, Science **292**, 1689-1692386-391 (2001).
[2] M. Hentschel *et al.*, Nature **414**, 509–513 (2001).
[3] P. K. Maroju *et al.*, Nature **578**, 386-391 (2020).
[4] P. K. Maroju *et al.*, New J. Phys. **23**, 043046 (2021).
[5] J. Duris *et al.*. Nature Photonics **14**, 30-36 (2020).
[6] N. Dudovich *et al.*, Nature Physics **2**, 781-786 (2006).
[7] K. C. Prince *et al.*, Nature Photonics **10**, 176–179 (2016).
[8] E. Allaria *et al.*, Nature Photonics **6**, 699-704 (2012).

*Corresponding author: giuseppe.sansone@physik.uni-freiburg.de

Diamond light matter quantum interface

F. Jelezko[*1]
1. Ulm University, Germany

Applications in quantum communications require the ability to connect the state of long-living matter qubits to optical photons for generation of entanglement over long distances. Here we discuss a novel quantum interface connecting quantum states of optical photons and spins in diamond. Among many colour centres in diamond, the negatively charged silicon-vacancy (SiV) and germanium-vacancy (GeV) centre stand out due to its desirable optical properties. In particular, near transform-limited photons can be created with high efficiency due to the strong zero-phonon line emission that constitutes $\sim$70% of the total emission. SiV and GeV centers can also be created with a narrow inhomogeneous distribution that is comparable to the transform limited optical line width. These optical properties, due to the inversion symmetry of the system, which suppresses effects of spectral diffusion, recently enabled demonstration of two-photon interference from separated emitters that is a key requirement for many quantum information processing protocols. Interfacing coherent optical transitions with long-lived spin qubits will be the main topic of this talk. Prospects for realizing electrical readout of quantum registers based on optically controlled SiVV centers will be discussed.

[*]Corresponding author: fedor.jelezko@uni-ulm.de

Measurement-induced, spatially-extended entanglement in a hot, strongly-interacting atomic vapor

Jia Kong,[1,8]**, Ricardo Jiménez-Martínez**[1,3]**, Charikleia Troullinou**[1]**, Vito Giovanni Lucivero**[1]**, Géza Tóth**[4,5,6] **Morgan. W. Mitchell***[1,2]

1. ICFO-Institut de Ciències Fotòniques, The Barcelona Institute of Science and Technology, 08860 Castelldefels (Barcelona), Spain
2. ICREA – Institució Catalana de Recerca i Estudis Avançats, 08010 Barcelona, Spain
3. Kernel, Culver City, California, USA
4. Department of Theoretical Physics, University of the Basque Country UPV/EHU, Bilbao, Spain
5. IKERBASQUE, Basque Foundation for Science, E-48011 Bilbao, Spain
6. Wigner Research Centre for Physics, Hungarian Academy of Sciences, P.O. Box 49, H-1525 Budapest, Hungary
7. Donostia International Physics Center, E-20018 San Sebastián, Spain
8. Department of Physics, Hangzhou Dianzi University, 310018 Hangzhou, China

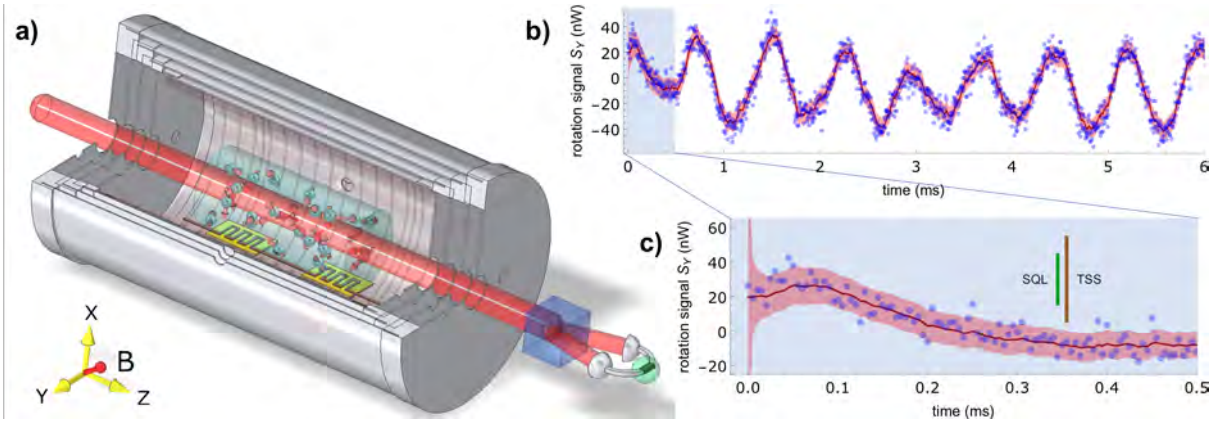

Fig. 1: Generation of a macroscopic singlet state in a SERF-regime ^{87}Rb. a) schematic of the method, b) Faraday rotation signals and Kalman filter estimation of spin dynamics, c) magnification of spin dynamics showing spin uncertainty beyond the standard quantum limit.

Quantum non-demolition (QND) measurement, in which a quantum observable is measured non-destructively, is a very useful tool in optical quantum technology. QND measurement of atoms by light has been used in quantum memory, quantum teleportation between light and atoms, sensing beyond the spin-projection noise limit, and to generate large amounts of atomic entanglement. A key figure of merit for QND measurement is the on-resonant optical depth (OD). Meanwhile many applications of QND measurement, e.g. quantum memories or quantum sensors, benefit from long T_2 spin coherence times. It is natural to ask whether hot alkali vapors in the spin-exchange-relaxation-free (SERF) regime, which show both high OD and high T_2, can be manipulated with QND measurement. This is not immediately obvious, because the SERF spin dynamics rapidly approaches a thermal spin state, whereas thermalization is, in most situations, incompatible with non-classical phenomena such as squeezing and entanglement.

Here we describe an experiment to test whether QND techniques can produce squeezing and entanglement in SERF-regime vapors [1]. We apply optical quantum non-demolition to an un-pumped SERF-regime vapor in a weak magnetic field, which rotates the spin state to make the three spin components sequentially available to QND measurement. We use Kalman filtering [2] and spin-squeezing inequalities [3] to recover the atomic spin state, including both mean and covariance matrix. We observe the generation of a "macroscopic singlet state" in which at least $1.52(4)\times10^{13}$ of the $5.32(12)\times10^{13}$ participating atoms form spin singlets, the largest entangled state ever reported. The entanglement is observed to persist for tens of spin-thermalization times, and to span thousands of times the mean inter-atomic distance. The results show that high temperatures and strong random interactions need not destroy many-body quantum coherence, that collective measurement can produce very complex entangled states, and that the hot, strongly-interacting media now in use for extreme atomic sensing are well suited for quantum technology.

References

[1] J. Kong, R. Jiménez-Martínez, C. Troullinou, V. G. Lucivero, G. Tóth, and M. W. Mitchell, Measurement-induced, spatially-extended entanglement in a hot, strongly-interacting atomic system, Nature Comms. **11**, 2415 (2020).
[2] R. Jiménez-Martínez, J. Kołodyński, C. Troullinou, V. G. Lucivero, J. Kong, and M. W. Mitchell, Signal tracking beyond the time resolution of an atomic sensor by Kalman filtering, Phys. Rev. Lett. **120**, 040503 (2018).
[3] Géza Tóth, Christian Knapp, Otfried Gühne, and Hans J. Briegel, Spin squeezing and entanglement, Phys. Rev. A **79**, 042334 (2009).

*Corresponding author: morgan.mitchell@icfo.eu

Enabling novel light phenomena at the subwavelength scale

M. Soljačić[*1]

1. Research Laboratory of Electronics, Massachusetts Institute of Technology, 02139 Cambridge, MA, USA

By nano-structuring materials at length scales smaller than the wavelength of light, one can create effective materials, exhibiting optical properties unparalleled in any naturally occurring materials. This talk will present our work in three areas of research that have recently been of particular interest to the nanophotonics community: *plasmonics*, *topology*, and *artificial intelligence*. First, via plasmonics, one can spatially confine light by orders of magnitude compared to light confinement in regular materials; conventional Maxwell's equations are no longer suitable for modelling this regime. Second, many of the exciting phenomena in topological physics can also be observed in nanophotonics, including: Chiral Edge States, Weyl points, Fermi arcs, etc. Third, numerical simulations of nanophotonics phenomena can often reproduce real experiments very closely: this makes nanophotonics a great training-ground for developing and studying new AI algorithms for science.

[*]Corresponding author: soljacic@mit.edu

Career Development Talks

Astrid Elbe

- Born and grown up in East Berlin
- Studied Mathematics and Physics, Dr. rer. nat. in Surface Physics
- Started carrier at Siemens Management Consulting in Munich
- 10 years with Infineon in Research & Development covering innovation and IP management as well as system engineering and engineering management for Security & Wirless products
- 10 years with Intel: 2011-2016 responsible for Intel's first LTE Modem System Projects for wireless handsets with customers like Samsung, LG, HTC and Apple. 2016-2021 Managing Director Intel Labs Europe responsible for leading Intel's research efforts in Europe and serving as the top Intel technical leader and spokesperson in the region, teams in Ireland and Germany
- Since beginning of 2021: Vice President Product Development at Aviat Networks, responsible to lead all product development and engineering worldwide for the company, engineering teams in Slovenia and New Zealand
- Married and 3 boys (11, 14 and 17 years old)

Leticia Tarruell

Leticia Tarruell studied physics in Madrid and Paris. She obtained her PhD in 2008, with a thesis on fermionic superfluidity at Ecole Normale Supérieure Paris. As a postdoc, she studied Fermi gases in optical lattices at ETH Zurich. After working as Chargée de Recherche CNRS at Institut d'Optique in Bordeaux, she joined ICFO as Group Leader in 2013. The Ultracold Quantum Gases group that she has established there performs quantum simulation experiments with mixtures of potassium Bose-Einstein condensates and ultracold strontium gases. She was awarded a young investigator prize of the Spanish Royal Physics Society in 2015, a Ramón y Cajal fellowship in 2016, and an ERC Consolidator Grant in 2020.

Oscar Viyuela

Oscar Viyuela García is a consultant and expert in quantum technologies at McKinsey & Company in Boston. He studied Physics at the Complutense University in Madrid, where he also did his Master and PhD thesis in quantum physics. He got the extraordinary Award to the best PhD thesis in Physics from the Complutense University and the Enrique Fuentes Quintana prize for the best doctoral thesis in Spain in Science and Engineering. During his PhD thesis, he has also worked at Scuola Normale Superiore di Pisa (Italy) and the Center for Quantum Technologies (Singapore). After his PhD thesis, he worked for 3 years as a researcher and professor at MIT and Harvard University. As a consultant, he has advised large international companies in various industries, bringing the potential of quantum computing to solve practical problems.

On Interchangeability of Probe-Object Roles in Quantum-Quantum Interaction-Free Measurement

M. Auzinsh[*1], **S. Filatov**[†1]
1. Laser Centre, University of Latvia, Rainis Boulevard 19, LV-1586 Riga, Latvia

We examine Interaction-Free Measurement [1] where both the probe and the object are quantum particles. We argue that in this case the description of the measurement procedure must by symmetrical with respect to interchange of the roles of probe and object. A thought experiment is being suggested that helps to determine what does and what doesn't happen to the state of the particles in such a setup. It seems that unlike the case of classical object, here the state of both the probe and the object must change. A possible explanation of this might be that the probe and the object form an entangled pair as a result of non-interaction.

The physical entities in our thought experiment are internal degrees of freedom (DoFs) of a two-level atom with dark and bright resonances (usually: object) and polarization degrees of freedom of a photon (usually: probe). The possible entities, however, are not limited by such selection and can be realized through spatial DoFs of an electron and a positron travelling inside intereferometer. In general, we focus on a pair of qubits which are coupled by a transforming interaction if their DoFs are aligned. But our main interest lies in understanding the result of non-interaction (such initial configurations in which the transforming interaction could happen with some probability, but didn't). In order to understand whether the state of either of the qubits changes after such non-interaction we put two conditions on the final state of the system. First, the description should be invariant with respect to exchange of the roles of "probe" and "object". Second, it should be impossible to determine the eigenbasis of preparation of individual particles in a maximally mixed ensemble [2]. Using the above conditions we examine different scenarios of non-interaction and come to the conclusion that in **any** event of non-interaction, the state of **both** qubits must change. We propose candidate mechanisms for the abovementioned dynamics, the most likely being the establishment of entanglement between the qubits.

This work is novel in two ways. First, it allows for deeper understanding of the process of quantum-quantum Interaction-Free Measurement. Second, it provides a method of testing hypotheses in realms where direct computations might not be available yet. The work can be found here [3].

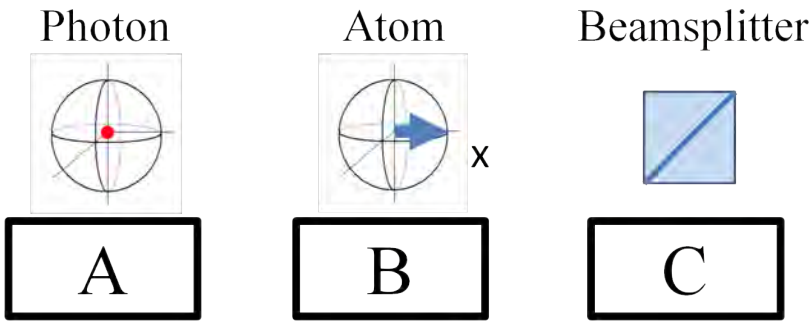

Fig. 1: Thought experimental Filter-device. Stage A produces "probes", in this case - photons. It operates in two modes, both of which correspond to Identity density matrix. Mode 1: photonic state is either (50%-50%) $|x\rangle_{ph}$ or $|y\rangle_{ph}$. Mode 2: Photonic state is either (50%-50%) $|\sigma+\rangle_{ph}$ or $|\sigma-\rangle_{ph}$. Stage B is an "object", in this case - atom. It is prepared in the state $|x\rangle_{at}$ regardless of the mode of operation of Stage A; for every photon we are using a "fresh" atom. Stage C is a beamsplitter that separates (projects) "probes" (here - photons) that haven't interacted with the "object" (here - atom) into $|x\rangle_{ph}$ and $|y\rangle_{ph}$ (basis of the "object") which later get detected by a corresponding detector. If we assume that photonic state remains unchanged after it non-interacts with the atom, two modes of operation at the Stage A will be distinguishable. Any successful description of (non-)interaction should satisfy the restrictions proposed here also if we change the basis of the "object" and measurement (stages B and C) as well as if we exchange the roles of "probe" and "object" between the photon and atom (stages A and B).

References

[1] A.C. Elitzur, L. Vaidman, Foundations of Physics **23**, 987 (1993)
[2] E. Schrödinger, Mathematical Proceedings of the Cambridge Philosophical Society, **32(3)**, 446-452 (1936)
[3] S. Filatov, M. Auzinsh, Foundations of Physics **49**, 283–297 (2019)

[*]Corresponding author: mauzins@lu.lv
[†]Corresponding author: sfilatovs@gmail.com

Exact solutions of a model for synthetic anyons in a noninteracting system

F. Lunić[*1], **M. Todorić**[1], **B. Klajn**[1], **T. Dubček**[2], **D. Jukić**[3], **H. Buljan**[†1,4]

1. Department of Physics, Faculty of Science, University of Zagreb, Bijenička c. 32, 10000 Zagreb, Croatia
2. Institute for Theoretical Physics, ETH Zürich, 8093 Zurich, Switzerland
3. Faculty of Civil Engineering, University of Zagreb, A. Kačića Miošića 26, 10000 Zagreb, Croatia
4. The MOE Key Laboratory of Weak-Light Nonlinear Photonics, TEDA Applied Physics Institute and School of Physics, Nankai University, Tianjin 300457, China

We present solutions of a theoretical model for synthetic anyons in a noninteracting quantum many-body system. Anyons [1][2] are quantum particles in 2D space with exotic exchange statistics, interpolating between bosons and fermions. They present an attractive field of research because the realization and manipulation of the so-called non-Abelian anyons could pave the way to topologically protected quantum computing [3]. They have been predicted to arise in various strongly interacting systems, most famously in fractional quantum Hall states [4]. A less explored possibility lies in weakly interacting fermions coupled to a topologically nontrivial background or external perturbations [5][6]. We consider a noninteracting system perturbed with specially tailored localized probes, giving rise to an Abelian anyonic state.

The model we study (Fig. 1(a)) is represented by the Hamiltonian for a noninteracting 2D electron gas, in a uniform magnetic field, with N external solenoids (probes) carrying a magnetic flux that is a fraction of the flux quantum. We first present the ground state of this Hamiltonian when all the states belonging to the lowest Landau-level are populated, while all other states are empty. We then show that the Berry phase accumulated as one of the probes adiabatically traverses a contour around another identical probe (Fig. 1(b)-(d)) contains a nontrivial (fractional) statistical contribution (statistical phase), indicating the anyonic nature of the ground state wave function in the coordinates of the probes. Finally, we discuss why these synthetic anyons cannot be considered emergent quasiparticles, and how this affects anyon fusion rules.

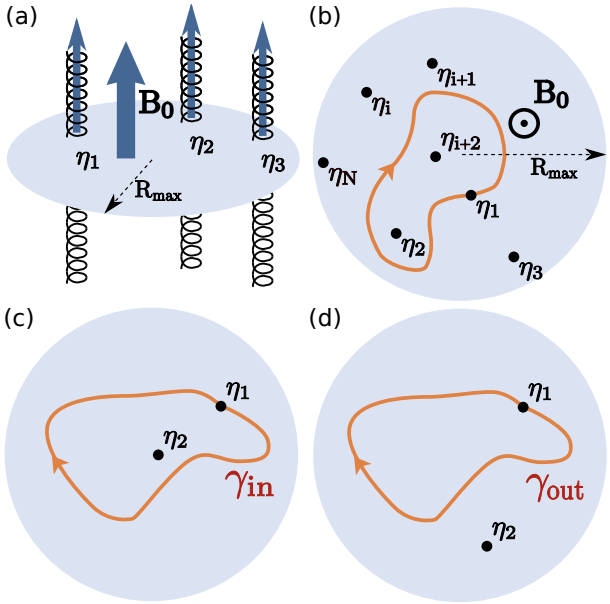

Fig. 1: (a) Sketch of the model. $\mathbf{B_0}$ is the uniform magnetic field, and η_j are the positions of the probes. (b) A possible contour of a single probe. The Berry phase depends on how many other probes are contained in the loop. (c),(d) The statistical phase is the difference between Berry phases γ_{in} and γ_{out}.

References

[1] J. Leinaas and J. Myrheim, Nuovo Cimento B **37**, 1 (1977).
[2] F. Wilczek, Phys. Rev. Lett. **49**, 957 (1982).
[3] A. Y. Kitaev, Ann. Phys. (NY) **303**, 2 (2003)
[4] D. Arovas, J. R. Schrieffer, and F. Wilczek, Phys. Rev. Lett. **53**, 722 (1984).
[5] G. Rosenberg, B. Seradjeh, C. Weeks, and M. Franz, Phys. Rev. B **79**, 205102 (2009).
[6] A. Rahmani, R. A. Muniz, I. Martin, Phys. Rev. X **3**, 031008 (2013).

[*]Corresponding author: frane@phy.hr
[†]Corresponding author: hbuljan@phy.hr

A Nanoscale Coherent Light Source

R. Holzinger [1], **D. Plankensteiner** [1], **L. Ostermann**[*1], **H. Ritsch** [1]
1. Institute for Theoretical Physics, Technikerstraße 21, A-6020 Innsbruck, Austria

A laser is composed of an optical resonator and a gain medium. When stimulated emission dominates mirror losses, the emitted light becomes coherent. We propose a new class of coherent light sources based on wavelength sized regular structures of quantum emitters whose eigenmodes form high- Q resonators. Incoherent pumping of few atoms induces light emission with spatial and temporal coherence. We show that an atomic nanoring with a single gain atom at the center behaves like a thresholdless laser, featuring a narrow linewidth. Symmetric subradiant excitations provide optimal operating conditions.

The setup under consideration is depicted in Fig. 1 (a) and (b), while Fig. 1 (c) and (d) show the emitted field from our nanoscale laser. The corresponding letter has been published in PRL in 2020. [1]

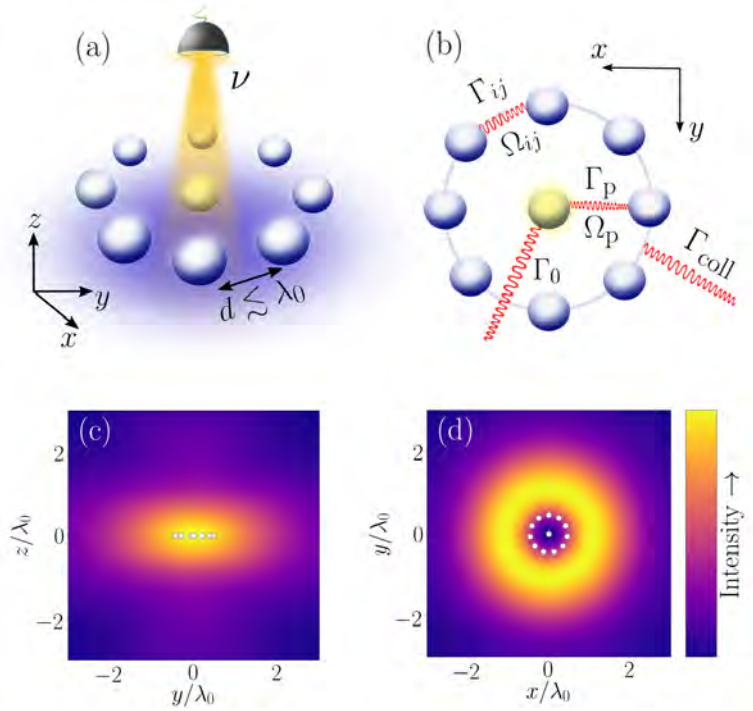

Fig. 1: *Coherent Light Emission from a Partially Pumped Atomic Array.* (a) A ring of atoms with an additional atom in its center incoherently pumped with a rate ν. (b) The atoms decay at a spontaneous decay rate Γ_0 and are collectively coupled to the center atom with dispersive coupling Ω_p and dissipative coupling Γ_p, respectively. In turn, the ring atoms have couplings Ω_{ij} and Γ_{ij} amongst each other. The symmetric excitation exhibits a collective decay rate Γ_coll. (c) The field intensity generated in the steady state for a ring of $N = 11$ atoms in the xz-plane with $y = 2.5\lambda_0$, $d = \lambda_0/5$ and $\nu = 0.1\Gamma_0$. (d) The field intensity in the xy-plane with $z = 2.5\lambda_0$.

References

[1] R. Holzinger, D. Plankensteiner, L. Ostermann, H. Ritsch: Phys. Rev. Lett. 124, 253603

*Corresponding author: laurin.ostermann@uibk.ac.at

Complementary Experimental Quantum Embedding for Machine Learning

I.Gianani[1], I. Mastroserio[*2,3,4], L. Buffoni[3], V. Cimini[1], M. Barbieri[1], L. Donati[3], N. Bruno[4], F. S. Cataliotti[3,4], and F. Caruso[3]

1. Dipartimento di Scienze, Università degli Studi Roma Tre, 00146 Rome, Italy
2. Dipartimento di Fisica Ettore Pancini, Università degli Studi di Napoli Federico II, Napoli, Italy
3. LENS & Dipartimento di Fisica e Astronomia, Università di Firenze, I-50019 Sesto Fiorentino, Italy
4. Istituto Nazionale di Ottica (CNR-INO), Largo Enrico Fermi 6, 50125 Florence, Italy

Nowadays the need of processing large amount of data is considerably increasing, and the development of supercomputers has further encouraged the advancement of Quantum Technologies and the study of algorithms in that direction. In particular, the introduction of Quantum Machine Learning algorithms has provided a remarkable speed-up over their classical counterparts [1-3]. However, the natural structure of the original data can be very complex and an intensive preprocessing is often necessary for Machine Learning algorithms to perform efficiently. In the case of binary classification problems, one would aim at achieving a geometrical representation of the data in which they are easier to be identified into distinct categories later to be analyzed.
In this context, we have developed an extensive experimental study of Quantum Embedding implementing the ideas proposed by Ref.[4] on two different experimental platforms. One is based on quantum optics and another on ultra-cold atoms. The embedding protocol concerns a novel approach to perform classification in the context of Quantum Metric Learning used in Machine Learning. We have implemented a quantum feature map that can be trained, via optimization, to separate and embed classical data points, coming from two different classes, into a much larger Hilbert space. Quantum Mechanics suggests that the natural representation of a quantum bit is the Bloch sphere, therefore the embedding we want to train will be composed of a sequence of rotations on non-commuting axes to be applied to an input qubit. The training and the parameters of the embedding are flexible and can be manipulated in order to account for the specific needs of the different experimental platforms.
We will focus on the description of the atomic platform in which we realize the embedding on a Bose-Einstein Condensate (BEC) of ^{87}Rb realized with an Atom-chip [5,6] (Fig. 1). We will illustrate how the performance of Quantum Embedding will depend on the degree of control on the actual system, thus on the level of experimental imperfections specific to the solutions adopted.
The aim of our study is to prove that this kind of approach is robust to experimental errors and that can be applied in practice, hence supporting the promising idea of hybrid quantum technologies for future Quantum Machine Learning applications.

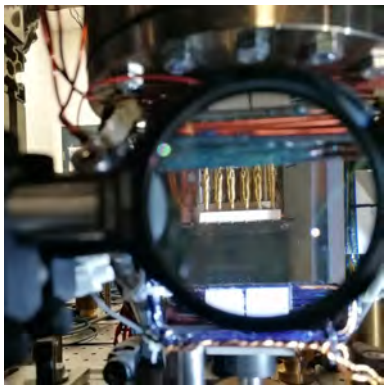

Fig. 1: The Atom Chip in the vacuum science cell to reach the BEC stadium and manipulate its internal dynamics. A micrometer Z-wire and two U-wires integrated on the chip realize the magnetic trap and the RF antennas for Rabi pulses and evaporative cooling respectively. All Zeeman states are simultaneously detected by absorption imaging.

References

[1] S. Lloyd, M. Mohseni, and P. Rebentrost, Nature Physics 10, 631 (2014).
[2] P. Rebentrost, M. Mohseni, and S. Lloyd, Physical Review Letters 113, 130503 (2014).
[3] S. Lloyd, S. Garnerone, and P. Zanardi, Nature Communications 7, 10138 (2016).
[4] S. Lloyd, M. Schud, A. Ijaz, J. Izaac, and N. Killoran, Eprint arXiv:2001.03622v2 (2020).
[5] J. Petrovic, I. Herrera, P. Lombardi, F. Schäfer, and F. S. Cataliotti, New J. Phys. 15, 043002 (2013).
[6] C. Lovecchio, F. Schäfer, S. Cherukattil, M. Ali Khan, I. Herrera, F. S. Cataliotti, T. Calarco, S. Montangero, and F. Caruso, Phys. Rev. A 93, 010304(R) (2016).

*Corresponding author: mastroserio@lens.unifi.it

Energy fluctuations of an NV spin qutrit under feedback-controlled dissipative dynamics

S. Hernández-Gómez[*1,2,3], **S. Gherardini**[1,2,4], **N. Staudenmaier**[1,2], **F. Poggiali**[1,2], **M. Campisi**[2,5,6], **A. Trombettoni**[4,7], **F. S. Cataliotti**[1,3], **P. Cappellaro**[8], **N. Fabbri**[†1,3]

1. European Laboratory for Non-linear Spectroscopy (LENS), Università di Firenze, I-50019 Sesto Fiorentino, Italy
2. Dipartimento di Fisica e Astronomia, Università di Firenze, I-50019, Sesto Fiorentino, Italy
3. Istituto Nazionale di Ottica del Consiglio Nazionale delle Ricerche (CNR-INO), I-50019 Sesto Fiorentino, Italy
4. Scuola Internazionale Superiore di Studi Avanzati (SISSA), I-34136 Trieste, Italy
5. NEST, Istituto Nanoscienze-CNR and Scuola Normale Superiore, I-56127 Pisa, Italy
6. INFN - Sezione di Pisa, I-56127 Pisa, Italy
7. Scuola Internazionale Superiore di Studi Avanzati (SISSA), I-34136 Trieste, Italy
8. Department of Nuclear Science and Engineering,Massachusetts Institute of Technology, Cambridge, MA 02139

Diamond spins disclose new possibilities for exploring how thermodynamic processes take place in open systems at the nanoscales, where fluctuations play a paramount role, and quantum features show up.

We characterize purely quantum energy fluctuations of an autonomous dissipative Maxwell demon realized by a spin qutrit formed by a Nitrogen-Vacancy (NV) center in diamond at room temperature. The autonomous Maxwell demon is implemented by applying to the spin qutrit a combination of unitary evolution drivings and series of interactions with short laser pulses. Each interaction with a short laser pulse acts as a quantum measurement, followed by an irreversible optical pumping (dissipation) that is conditioned by the quantum measurement [1,2], as schematized in Fig. 1. As a result, the autonomous dissipative Maxwell demon asymptotically brings the qutrit into a quantum (non-thermal) out-of-equilibrium steady state.

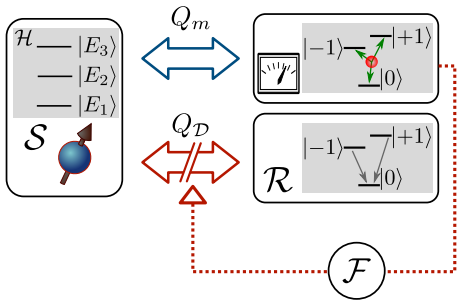

Fig. 1: A spin system S evolves under a Hamiltonian H, with eigenstates $|E_i\rangle$, $i = 1,2,3$. Upon interaction with a short laser pulse, the spin system S is subject to a quantum measurement (Q_m) of S_z, and dissipation (Q_D) towards the $m_S = 0$ spin projection. This irreversible dissipation is analogous to put the system in contact with an out-of-equilibrium reservoir R. Since the interaction betweenthe system and the reservoir is conditioned by the application of a quantum measurement, the spin qutrit dynamics is well described by an autonomous dissipative Maxwell demon.

Our work [3] generalizes the Sagawa-Ueda-Tasaki relation (originally valid for conditioned unitary evolution [4]-[6]) to conditioned dissipative dynamics, verifying it experimentally by measuring the energy change statistics of the spin qutrit. We also verify, both theoretically and experimentally, that for the specific qutrit dynamics the characteristic function of energy variation, $G(\eta) \equiv \langle e^{-\eta \Delta E} \rangle$, is time independent for a single specific value η^* of its argument. Thus, an effective Jarzynski-like fluctuation theorem holds, despite lack of unitality of the qutrit evolution. In addition, our results pave the way for the use of NV centers in diamond to further investigate open quantum system dynamics and thermodynamics, for example by exploring non-Gibbsian quantum heat engines and the role of coherence in energy exchange mechanisms.

References

[1] S. Hernández-Gómez, S. Gherardini, F. Poggiali, F. S.Cataliotti, A. Trombettoni, P. Cappellaro, and N. Fabbri, Phys. Rev. Research **2**, 023327 (2020).
[2] S. Hernández-Gómez, N. Staudenmaier, M. Campisi and N. Fabbri, New J. Phys Accepted Manuscript (2021).
[3] S. Hernández-Gómez *et al.*, in preparation.
[4] T. Sagawa and M. Ueda, Phys. Rev. Lett. **100**, 080403(2008).
[5] Y. Morikuni and H. Tasaki, Journal of Statistical Physics **143**, 1 (2011).
[6] K. Funo, Y. Watanabe, and M. Ueda, Phys. Rev. E **88**,052121 (2013).

[*]Corresponding author: hernandez@lens.unifi.it
[†]Corresponding author: fabbri@lens.unifi.it

Towards Quantum Gas Microscopy of Polar Molecules

Jonathan M. Mortlock[*1],
Jonas A. Matthies[1], **Andrew D. Innes**[1], **Mew A. Ratkata**[1], **Lewis A. McArd**[1], **Philip D. Gregory**[1],
Sarah L. Bromley[1], **Simon L. Cornish**[1]
1. Joint Quantum Centre (JQC) Durham-Newcastle, Department of Physics, Durham University, South Road, Durham, DH1 3LE

We report progress towards a Quantum Gas Microscope for polar molecules using a three species machine capable of producing Bose-condensed ^{133}Cs and ^{87}Rb, and ultracold samples of ^{41}K. The ultimate goal of our work is to use rotational excitations of polar molecules trapped in a deep optical lattice to investigate the dynamics of strongly interacting quantum systems. We intend to use a high resolution objective to achieve single-site, state resolved readout following the proposal in [1]. Such a system has been proposed to realise spin models such as the XXZ Heisenberg model with tunable anisotropic long-range couplings for studies of spin liquid and localisation phenomena [2]. Including microwave dressing between three rotational states has been suggested to realise topologically ordered matter [3].

We present three directions of progress towards preparing these molecular samples. First our work on development of an atomic microscope, including a novel scheme for optical lattice based transport of atoms. Second we report a new measurement of the ^{133}Cs 880nm tune-out wavelength which improves the value for the ratio of the $|\langle 6P_{3/2}||d||6S_{1/2}\rangle|^2$ and $|\langle 6P_{1/2}||d||6S_{1/2}\rangle|^2$ matrix elements by an order of magnitude. Finally we present work towards measurements of interspecies Feshbach resonances between ^{41}K and ^{133}Cs using ultracold mixtures in a bichromatic optical trap, a key first step towards magneto-association of these atoms.

References

[1] Jacob P. Covey New J. Phys.**20** 043031 (2018)
[2] J. L. Bohn, A. M. Rey, J. Ye Science 357, 1002–1010 (2017).
[3] Yao, N. Y. et al. Phys. Rev. Lett. 109, (2012)

*Corresponding author: jonathan.m.mortlock@durham.ac.uk

Photon polarizations in two-photon $2s \to 1s$ decay

V. A. Knyazeva[*1], **K. N. Lyashchenko**[2], **O. Yu. Andreev**[1,3]

1. St. Petersburg State University, 7/9 Universitetskaya nab., St. Petersburg, 199034, Russia

2. Institute of Modern Physics, Chinese Academy of Sciences, Lanzhou 730000, China

3. Petersburg Nuclear Physics Institute named by B.P. Konstantinov of National Research Centre "Kurchatov Institute", Gatchina, Leningrad District 188300, Russia

We investigated the differential transition probability for two-photon $2s \to 1s$ transition in H-like ions with respect to the polarization of the emitted photons. The investigation was performed for ions with atomic numbers $1 \leq Z \leq 120$.

On the basis of our relativistic calculations and works [1-2], we introduced a two-parameter approximation, which makes it possible to describe the two-photon angular-differential transition probability for the polarized emitted photons with high accuracy. The angular distribution of the emitted photons is determined by the dominant E1E1 transitions, which gives $1+\cos^2\theta$ distribution, where θ is the angle between the momenta of the emitted photons. This deviation leads to an asymmetry of the angle-differential transition probability. The reason for this deviation is the interference between E1E1 and the higher multipoles (mainly E2E2 and M1M1). The deviation from the distribution in the nonrelativistic limit was investigated in [1]. The asymmetry for unpolarized emitted photons was investigated in [3].

We found that the differential transition probability can be approximated by two parameters: the total two-photon transition probability and the asymmetry factor A. The asymmetry factors for several atomic numbers Z are given in Table 1, which also shows this factors from previous work [1]. The accuracy of this approximation is 10^{-3}% for light ions, remaining within 1% even for the superheavy ions (for the photons with equal energies). For precise experiments, it can be important that a nonzero asymmetry factor, even for light ions, could be a source of nonresonant corrections [4].

Using this approximation we investigated the emission of photons with linear and circular polarizations. The results for linear photon polarizations for several Z are presented in Fig. 1.

We also investigated the transition probabilities for the polarized initial and final electron states.

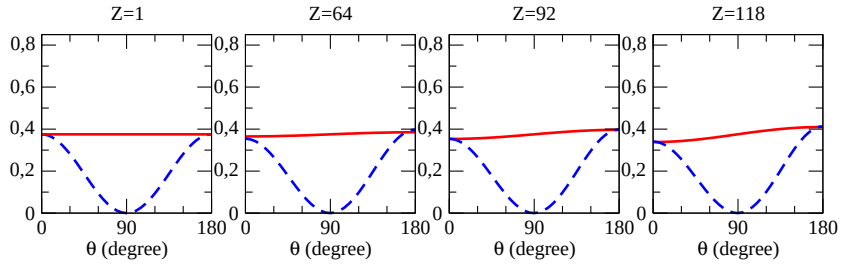

Fig. 1: The normalized differential transition probabilities as a function of the angle (θ) between the momenta of the emitted photons (k_1 and k_2, respectively) for the photons with equal energies in the case of the linear photon polarization. The red solid line represents angular dependence of the differential transition probability for the photon polarization vectors placed in the (k_1,k_2)-plane. The blue dashed line represents angular dependence of the differential transition probability for the photon polarization vectors orthogonal to the (k_1,k_2)-plane. The data are presented for atomic numbers Z = 1, 64, 92, 118.

Table 1: The transition probabilities (W , in s^{-1}) for two- photon decay of $2s$ state and the asymmetry factor (A). The digits in square brackets refer to the power of 10. The numbers in parentheses indicate the accuracy of the two- parameter approximation.

Z	W	A	A^a
1	8.22906	4.256617(3)[-6]	4.22[-6]
40	3.19889[10]	7.136(2)[-3]	7.32[-3]
64	4.97436[11]	1.940(3)[-2]	2.16[-1]
92	3.83600[12]	4.30(2)[-2]	6.06[-2]
118	1.40273[13]	6.7(1)[-2]	1.80[-1]
120	1.52661[13]	6.8(2)[-2]	2.00[-1]

^{a}[1]

References

[1] C. K. Au, *Phys. Rev. A* **14** 531 (1976).

[2] N. L. Manakov *et al. Journal of Physics B* **33** 4425 (2000).

[3] A. Surzhykov, J. P. Santos, P. Amaro, and P. Indelicato *Phys. Rev. A* **71** 022509 (2005).

[4] O. Y. Andreev, L. N. Labzowsky, G. Plunien, and D. A. Solovyev *Physics Reports* **455** 135 (2008).

*Corresponding author: viknyazeva16@gmail.com

Single photons behaviour in optical resonators and its applications

V. Vujnović[*1], **M. Pavičić**[2], **M. Stipčević** [2], **D. Jardas**[1], **M. Karuza**[1]

1. Department of Physics and Centre for Micro and Nano Sciences and Technologies, Radmile Matejčić 2, 51000 Rijeka, Croatia

2. Center of Excellence for Advanced Materials and Sensors, Institute Ruđer Boškovic, Bijenička cesta 54, 10000 Zagreb, Croatia

In our recent work we have investigated generation of additional degrees of freedom (DOF) in laser locked high Q Fabry–Pérot (FP) cavity using both single and double pass experimental setup [1]. In some quantum optics experiments [2], [3], [4] two independent light beams are required, which is usually achieved by using mutually orthogonally polarized beams of the same wavelength. In our dichroic cavity setup we showed that beside widely used polarization DOF's, it is possible to change frequency of the beam using AOM, and observe them resonate in the cavity as different TEM modes (Fig. 1). This way we obtained additional DOF in a manner of transverse electric field distribution.

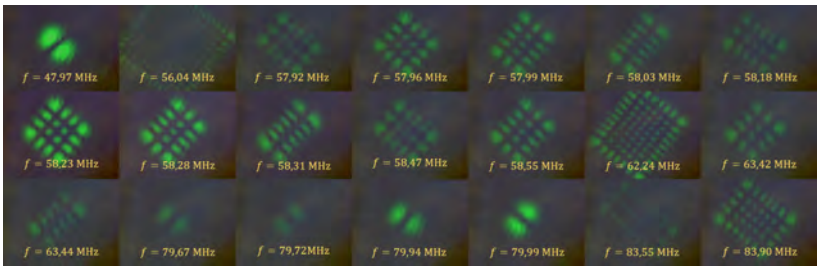

Fig. 1: Vaious TEM modes for 532 nm light while FP cavity is locked on 1064 nm TEM_{00} mode. Yellow labeled numbers correspond to the AOM frequencies used to get represented TEM mode [1]

Our goal is investigation of single photon behaviour in dichroic FP resonator as proposed in [5]. In the first experimental setup (Fig. 2) we are observing coincidences between a trigger pulse driving EOM and the pulse generated by FP cavity reflected and transmitted photons being detected on SPAD's. For that purpose we employed pseudo-single photon source [6] where faint laser pulse (FLP) is additionally switched by fast EOM, where $\approx 5\%$ of FLP's contains more than one photon. Custom made SPAD's (RBI, Photonics and Quantum Optics Laboratory) were used in combination with FPGA as photon counters.

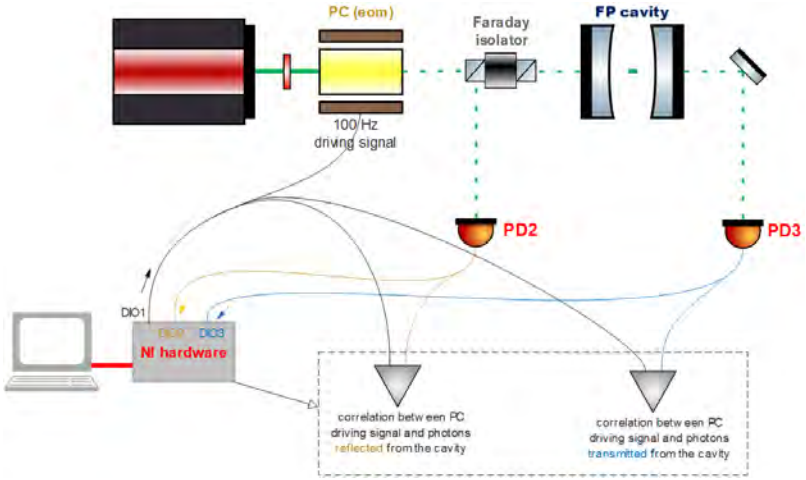

Fig. 2: A simplified scheme of the setup where the locking IR beam is not shown. The green dashed line represents FLP's which can be either transmitted or reflected by the FP cavity. The reflected (transmitted) pulses are detected by the PD2 (PD3).

In the following setup we will implement two distinguishable photonic states and test mutual coincidence while cavity is locked for one of these states. Possible applications are in fundamental research - nature of the quantum vacuum; and in quantum technology: interaction free detectors [5], quantum gates or in all-optical photonic processing.

References

[1] V. Vujnović, M. Karuza, D. Jardas, "*Dichoric Fabry-Perot cavity*", unpublished.
[2] M. Karuza et al. New J. Phys. **14**, 095015 (2012).
[3] G. Cantatore, H. Fischer, M. Karuza et al., Physics of the Dark Universe **26**, 100367, (2019).
[4] J. H. Põld, A.D. Spector, EPJ Techn. Instrum. **7**, 1 (2020).
[5] H. Paul, M. Pavičić, M., J. Opt. Soc. Am. B **14**, 1275-1279 (1997).
[6] Y. Hu, X. Peng, T. Li, H. Guo, Physics Letters A **367**, 173–176 (2007).

[*]Corresponding author: vedran.vujnovic@phy.uniri.hr

Circular Rydberg states for quantum many-body physics

C. Hölzl[*1], **A. Götzelmann**[1], **F. Meinert**[1]
1. 5. Physikalisches Institut and Center for Integrated Quantum Science and Technology, University of Stuttgart, Stuttgart, Germany

Highly excited low-l Rydberg atoms in configurable mircotrap arrays have recently proven highly versatile for studying quantum many-body spin systems with single particle control. I will report on the advances of a new project pursuing to harness high-l circular Rydberg atoms for quantum simulation. When stabilized against black body radiation (BBR) in a suitable cavity structure, circular Rydberg states promise orders of magnitude longer lifetimes compared to their low-l counterparts and thus provide an appealing potential to strongly boost coherence times in Rydberg-based interacting atom arrays. To maintain excellent high-NA optical access we exploit a novel approach using an indium tin oxide (ITO) capacitor [1], capable of surpressing the parasitic microwave BBR even in a non-cryogenic environment while beeing transparent to visible light.

References

[1] F. Meinert, C. Hölzl, M. A. Nebioglu, A. D'Arnese, P. Karl, M. Dressel and M. Scheffler (2020): Indium tin oxide films meet circular Rydberg atoms: prospects for novel quantum simulation schemes, Phys. Rev. Research **2**, 023192.

[*]Corresponding author: choelzl@pi5.physik.uni-stuttgart.de

Storage and release of subradiant excitations in a dense atomic cloud

G. Ferioli[*1], **A. Glicenstein**[1], **L. Henriet**[2], **I. Ferrier-Barbut**[1], **A. Browaeys**[1],
1. Universite Paris-Saclay, Institut d'Optique Graduate School, CNRS, Laboratoire Charles Fabry, 91127, Palaiseau, France
2. Pasqal, 2 avenue Augustin Fresnel, 91120 Palaiseau, France

Atom-light interfaces are promising for quantum information protocols or metrology. Usually, the interaction of atomic ensembles with light is treated as the sum of the independent contributions of each atom. However, when close enough, they can influence each other via their radiation, leading to a collective interaction with the light field. A dramatic manifestation is subradiance: a strongly reduced emission rate of an excitation stored in a medium. Subradiance has attracted some attention lately, as the reduced decay rate can be beneficial in some cases. For instance, it could be used to store and release light on demand. Proposals have shown that this might be done when the distance between the atoms is smaller than the wavelength of the light, and if the coupling between atoms can be controlled externally. But this regime is also very difficult to treat theoretically, making it challenging to understand subradiance beyond the regime where a single photon is stored in the ensemble.

We have for the first time observed subradiance in this regime [1]. We probe the nature of subradiant excitations when many photons are stored, and verify a conjecture about how these many-body subradiant states are constructed. Also, by applying an external control on the atoms, we perform a proof-of-principle experiment where we switch-off the interactions between atoms and release rapidly the light that was stored in subradiance. These results thus provide an important benchmark for many-body theories, and show that subradiance could provide an interesting path to tailored light-matter interfaces.

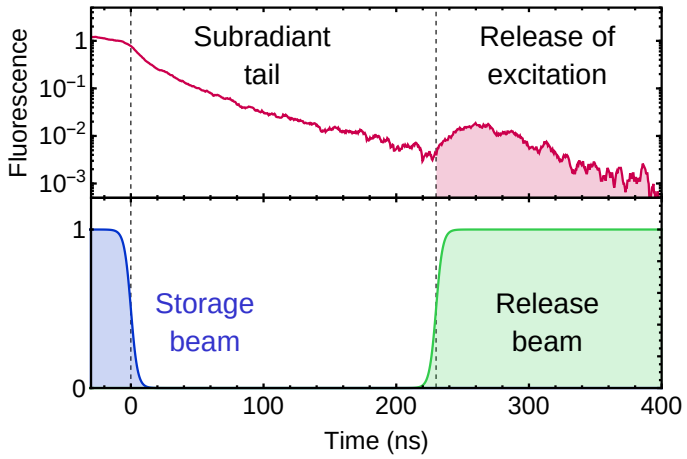

Fig. 1: Sketch of the protocol used to store and release the subradiant excitation

More recently we have also observed and characterize superradiance in this dense cloud, near Dicke's regime of an ensemble smaller than the wavelength of the optical transition. We show that contrarily to what was believed, superradiance is still present in the presence of dipole interactions. Finally, we measured the intensity correlation function and observed non-classical statistics.

References

[1] Ferioli, G., et al. "Storage and release of subradiant excitations in a dense atomic cloud." arXiv preprint arXiv:2012.10222 (2020)., PRX accepetd

*Corresponding author: giovanni.ferioli@institutoptique.fr

Precision Mass Measurement of the Deuteron's Atomic Mass

S. Rau[*1], **F. Heiße** [1], **Florian Köhler-Langes** [1], **Sangeetha Sasidharan** [1,2], **Wolfgang Quint** [2], **Sven Sturm** [1], **Klaus Blaum** [1]

1. Max-Planck-Institut für Kernphysik, Saupfercheckweg 1, 69117 Heidelberg, Germany
2. GSI Helmholtzzentrum für Schwerionenforschung GmbH, Darmstadt, Germany

The rest masses of many light nuclei, e.g. the proton, deuteron, triton and helion, are of great importance for testing our current understanding of physics as well as in metrology. One example is the mass difference of triton and helion [1], which is used for systematic studies in the determination of $m(\bar{\nu}_e)$ in the KArlsruhe TRItium Neutrino experiment KATRIN [2]. However, the relatively large ratio of the kinetic energy to the low rest mass makes measuring the masses of light ions especially challenging. Recently discussed discrepancies in light ion mass measurements, carried out at different mass spectrometers (the "light ion mass puzzle" [3]), give further motivation for independent measurements.

In this contribution, the results of LIONTRAP (Light ION TRAP) [3], an ion trap setup dedicated to high-precision mass measurements of light ions, will be presented. In a collaboration with with members from the Nuclear Chemistry Department at the University of Mainz we recently measured the deuteron's atomic mass [4] by comparing the cyclotron frequencies of a single deuteron and a bare carbon nucleus, achieving a relative mass uncertainty of 8.5×10^{-12}. Our value

$$m_d = 2.013\,553\,212\,535\,(17)\,\mathrm{u} \tag{1}$$

is a factor 2.4 more precise than the current CODATA-2018 value, which is dominated by a measurement from the University of Washington (UW) [5], but deviates by $4.8\,\sigma$. In addition to various detailed checks of our model of systematics, the good agreement with an additional mass measurement of the HD^+ molecular ion and our previously reported proton mass [3] further validates our measurement. For an overview of cyclotron frequency ratio measurements in the light sector, see Fig. 1.

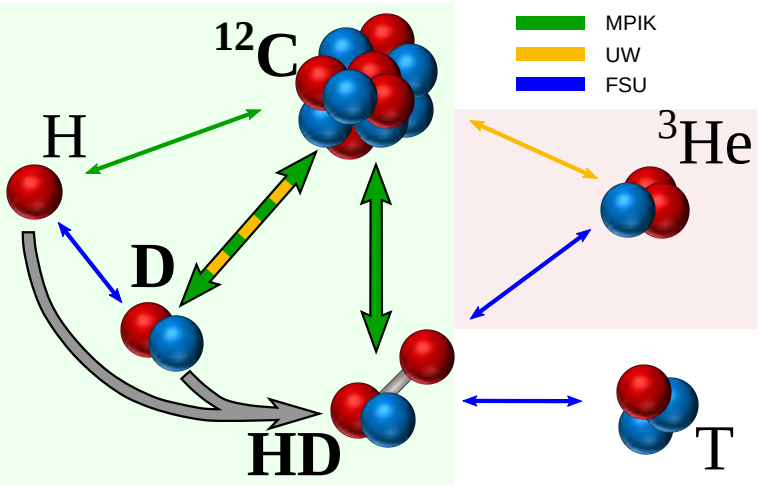

Fig. 1: Overview of cyclotron frequency ratio measurements on light ions. The measurements taken in our group (MPIK) are internally consistent and agree with the measurements taken by the FSU, but are in strong tension with the measurements by the UW.

There, a measurement of the deuteron-to-proton mass ratio by the Florida State University (FSU) [6] is shown, which agrees with the measurements taken in our group. This agreement enables a least square adjustment resulting in mass values for the proton and the deuteron with unprecedented precision. The resulting values can be used in the interpretation of high-precision measurements of ro-vibrational transitions in HD^+, enabling tests of QED and searches for fifth forces [7][8], as well as a new value for the neutron mass [4].

References

[1] E. G. Myers *et al.*, Phys. Rev. Lett. **114**, 013003 (2015)
[2] M. Aker *et al.* Phys. Rev. Lett. **123**, 221802
[3] F. Heiße *et al.* Phys. Rev. A **100**, 022518 (2019)
[4] S. Rau *et al.* Nature **585**, 43–47 (2020)
[5] S. L. Zafonte and R. S. Van Dyck, Metrologia **52**, 280 (2015)
[6] D. J. Fink and E. G. Myers, Phys. Rev. Lett. **124**, 013001 (2020)
[7] S. Patra *et al.*, Science **369**, 6508 (2020)
[8] I. V. Kortunov *et al.* Nature Physics, 1745-2481 (2021)

*Corresponding author: sascha.rau@mpi-hd.mpg.de

Quantum mechanical description of hydrogen dimers

D. Šimsa[*1,2], **M. Gustafsson**[†1]
1. Luleå university of technology, 97187 Luleå, Sweden
2. Institute of Physics of the Czech Academy of Sciences, Na Slovance 1999/2, 182 21 Prague 8

The weekly bound dimers of hydrogen and its isotopologues are extensively studied systems. Relative simplicity of the system makes it a good study tool for both experimental [1-2] and theoretical [3-5] communities. But the hydrogen dimer is not only a good system for testing, comparison and method development. Since hydrogen is the most abundant element in the Universe, the precise description is thus extremely important in astrophysics and astronomy. For example, the collision induced absorption (CIA) of $(H_2)_2$ is an important tool for studying atmospheres of giant-planets [6]. More accurate spectra will need to be analyzed after the James Webb Space Telescope (Launch date October 31, 2021) will become available.

Ab initio studies of hydrogen dimers and its isotopologues are challenging. The necessity of high accuracy with combination of mulitidimensionality of the potential energy surface (PES) makes it hard to verify the result against an experimental data.

In this work, we provide an accurate model for calculation of the dimer bound states using different PES and we suggest to use a bound-to-bound CIA spectra of $(D_2)_2$ dimer as a sensitive check of them. The results for different potentials is given in Fig. 1.

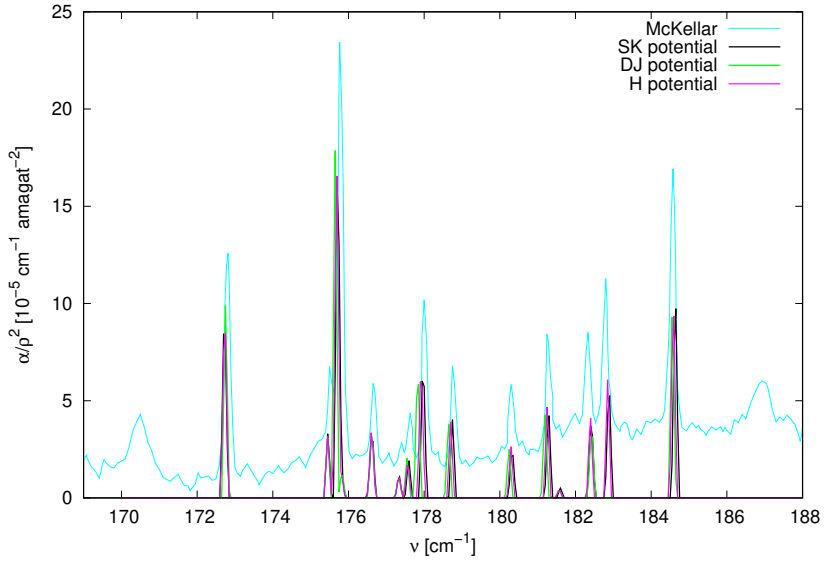

Fig. 1: CIA bound-to-bound spectra of $(D_2)_2$ for three different potentials by Schaefer and Köhler (SK) [3], Diep and Johnson (DJ) [4] and Hinde (H) [5] in comparison with the McKellar and Schaefer experimental results [7]

References

[1] A. Khan *et al.*, The Journal of Physical Chemistry Letters **11**, 2457 (2020).
[2] R. Grössle *et al.*, AIP Advances **10**, 055108 (2020).
[3] J. Schaefer and W. E. Köhler, Zeitschrift für Physik D Atoms, Molecules and Clusters **13**, 217 (1989).
[4] P. Diep and J. K. Johnson, The Journal of Chemical Physics **112**, 4465 (2000).
[5] R. J. Hinde, The Journal of Chemical Physics **128**, 154308 (2008).
[6] L. N. Fletcher, M. Gustafsson, and G. S. Orton, The Astrophysical Journal Supplement Series **235**, 24 (2018).
[7] A. R. W. McKellar and J. Schaefer, The Journal of Chemical Physics **95**, 3081 (1991).

[*]Corresponding author: simsad@fzu.cz
[†]Corresponding author: magnus.gustafsson@ltu.se

Collective light-atom interaction in free space and in an optical cavity

M. Kruljac[*1], **D. Buhin**[1], **V. Vulić**[1], **N. Šantić**[1], **I. Puljić**[1], **D. Aumiler**[1], **T. Ban**[1]
1. Institute of Physics, Bijenička c. 46, 10000 Zagreb, Croatia

Interaction of N atoms with laser radiation can differ significantly from the single atom physics. While probing a sample of high density, there is a pronounced anisotropy of the light scattering pattern, with an enhanced scattering in the forward and backward direction, compared to transverse directions. As a consequence, reduction and broadening of the laser induced force on the atomic cloud's center of mass in the forward direction can be observed. If, however, the atoms are located inside a high-finesse optical cavity, light-atom interaction can change even further compared to free space. Since all the atoms are coupled to the same cavity mode, there is a collective atom-cavity coupling proportional to the number of atoms. This collective coupling can shift the cavity resonance significantly as the atoms move through the cavity potential, resulting in a complex coupled dynamics. This coupled dynamics can even be used to cool and trap the atoms in the cavity mode, relying on the photon loss out of the cavity as a dissipation mechanism, instead of the spontaneous emission as in the standard Doppler cooling techniques. This cavity cooling technique could, in theory, be used to cool any polarizable particles, regardless of their internal energy structure [1].

In free space, we experimentally investigated the signature of collective effects in a cold cloud of ^{87}Rb atoms by probing the cloud with a femtosecond pulsed laser, whose spectrum forms a frequency comb (FC). We observed reduction and broadening of the FC-induced force on the cloud as the cloud's optical depth increases. We compared the measured results with two theoretical models, developed for cw interaction, and found good agreement [2].

With a horizontal high-finesse optical cavity mounted inside the vacuum chamber, we loaded the atoms in the center of the cavity and probed them longitudinally, pumping the cavity mirrors with a cw laser. Tuning the probing laser dozens of linewidths to the blue of an atomic transition (where heating, at most, is expected for free space scattering), we observe trapping of the atoms along the cavity axis, as well as slowing of the cloud's free fall along the vertical axis due to gravity. This shows a collective dynamic that cannot be explained by standard free space scattering of atoms. We plan to investigate this dynamics even further, pumping the atoms transversally to the cavity axis (where phenomena like spontaneous self-organization are expected) and replacing the cw laser with a frequency comb [3]. Modes of the FC can be matched with the cavity modes, coupling a large number of frequencies into the cavity which creates a more complex potential, compared to a single-frequency standing wave.

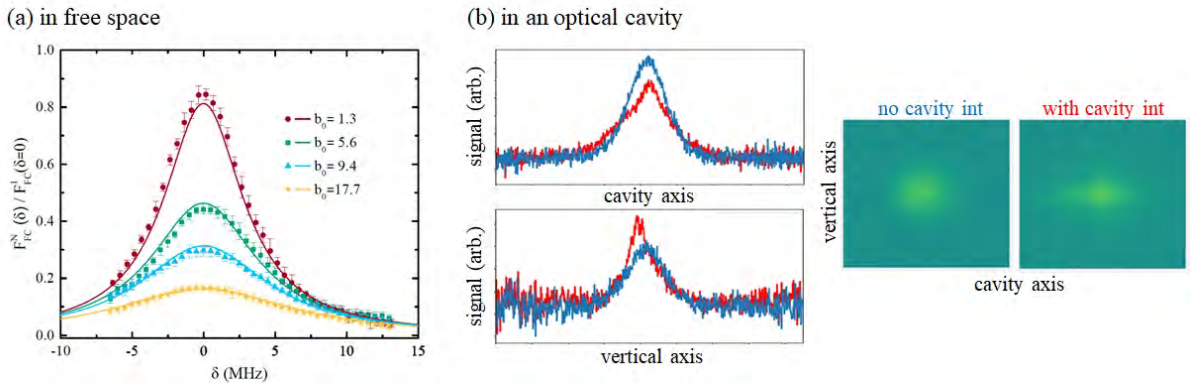

Fig. 1: a) Reduction and broadening of the free-space FC-induced force for different optical depths b_0 of the cloud. Solid lines are theoretical predictions based on a Timed-Dicke state model, and the force values are scaled to the single atom value. b) Absorption images of the MOT cloud without (blue) and with (red) the interaction with a cavity beam. On the left, data along the horizontal (cavity) axis and the vertial (direction of gravity) axis are shown. The corresponding 2D images, from which the graphs were extracted, are shown on the right.

References

[1] H. Ritsch, P. Domokos, F.Brennecke, T. Esslinger, Rev. Mod. Phys. **85**, 553-601(2012).
[2] M. Kruljac, D. Buhin, D. Kovačić, V. Vulić, D. Aumiler, T. Ban, *submitted to Phys. Rev. A* (2021).
[3] V. Torggler, I. Krešić, T. Ban and H. Ritsch, New Journal of Physics **22**, 063003 (2020).

*Corresponding author: mkruljac@ifs.hr

Collective self-trapping of atoms in a cavity

A. Dombi[*1], **T. W. Clark**[1], **F. I. B. Williams**[1], **F. Jessen**[2], **J. Fortágh**[2], **D. Nagy**[1], **A. Vukics**[1], **P. Domokos**[1]
1. Institute for Solid State Physics and Optics, Wigner Research Centre for Physics, H-1525 Budapest P.O. Box 49, Hungary
2. Physikalisches Institut, Eberhard Karls Universität Tübingen, D-72076 Tübingen, Germany

Experimental study of an ensemble of cold atoms placed in a spatially and spectrally selected, discrete, resonant mode of a high finesse optical cavity can yield precious insight into the dynamics of photon-atom interaction. The dynamics of both the atoms and the light field have to be taken into account for understanding such systems, which is the generic feature of cavity quantum electrodynamics [1]. The atoms not only move under the forces from the light field but exhibit a strong back action on the state of the field [2]. While the light field is influenced by the averaged interaction with the atoms, the "optical centre of mass" [3], individual atoms communicate between themselves through their mutual coupling to the cavity field mode [4] leading to various collective light scattering and synchronisation effects.

We experimentally demonstrate the collective self-trapping of atoms in a laser-driven optical resonator. Self-trapping has been demonstrated before based on the nonlinear interaction between ultracold atoms in a bosonic Josephson junction [5]. In our system however, the dynamically coupled cavity field is the key to the effect. The laser frequency is tuned away from the mode resonance such that the light cannot penetrate into the optical resonator. However, when atoms are present, the mode frequency is pulled closer to that of the driving laser, and light is injected into the cavity. This light is far detuned from atomic resonances, so its mechanical effect is limited to the optical dipole force. In the case of red detuning, with respect to the atomic resonances, the field creates an optical dipole trap, attracting atoms towards the field maxima, *i.e.* the antinodes along the cavity axis. In a cavity-based, dynamic, optical trap the collective effect of the atomic cloud is needed to let the necessary amount of light into the cavity. Therefore, whereas a single atom would not be trapped, a cloud with a sufficient number of atoms will be captured in the cavity mode volume under the same external conditions. Such an effect has now been observed.

In order to study the self-trapping effect quantitatively, we need to define a characteristic trapping time. We opt for the definition that the trapping time is the interval between the point of maximum transmission and the midpoint between that and minimum transmission, corresponding to the empty cavity. A typical example of the time evolution of the cavity output power, along with the representation of the trapping time is shown in Fig.1.

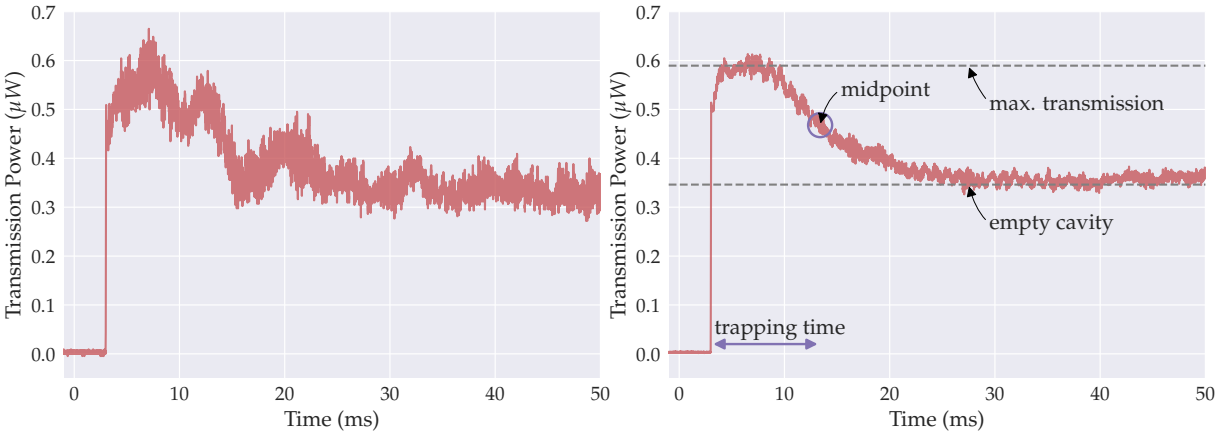

Fig. 1: Time evolution of the cavity output power with 5 μs resolution. The left panel shows a single recorded trajectory, where the non-trivial motional dynamics of the atomic cloud in the dynamically changing cavity field leads to various oscillatory features. As this depends heavily on uncontrolled initial conditions, averaging over ten such trajectories reveals a simple deterministic evolution, as shown in the right panel.

References

[1] S. Haroche and J.-M. Raimond, Exploring the Quantum (Oxford University Press, 2006)
[2] S. Gupta, K. L. Moore, K. W. Murch, and D. M. Stamper-Kurn, Phys. Rev. Lett. 99, 213601 (2007)
[3] T. P. Purdy, D. W. C. Brooks, T. Botter, N. Brahms, Z. Y. Ma, and D. M. S. Kurn, Phys. Rev. Lett. 105, 133602 (2010)
[4] V. D. Vaidya, Y. Guo, R. M. Kroeze, K. E. Ballantine, A. J. Kollár, J. Keeling, and B. L. Lev, Physical Review X 8, 011002 (2018), publisher: American Physical Society
[5] A. Reinhard, J.-F. Riou, L. A. Zundel, D. S. Weiss, S. Li, A. M. Rey, and R. Hipolito, Physical Review Letters 110, 033001 (2013), publisher: American Physical Society

*Corresponding author: dombi.andras@wigner.hu

Constraining ab-initio molecular potential calculations through measurements of the spin relaxation rate in a Fermi gas of ^{3}He*

R. Jannin[*1], **K. Steinebach**[1], **Y. van der Werf**[1], **H. L. Bethlem**[1], **K. S. E. Eikema**[1]
1. LaserLaB, Department of Physics and Astronomy, Vrije Universiteit, De Boelelaan 1085, 1081 HV Amsterdam, The Netherlands

The behaviour of ultracold trapped fermionic gasses is dictated by Fermi-Dirac statistics, and therefore very different phenomena are observed than for bosonic gasses. In particular, the Pauli exclusion principle inhibits the collision of two identical fermions in the *s*-wave channel, resulting in a suppression of collisions within spin-polarized degenerate Fermi gases of atoms cooled below the milliKelvin regime, as the *p*-wave channel processes are basically negligible at that temperature. This effect is commonly used for the realization of atomic clocks based on fermions trapped in optical lattices so that the measured transition frequency is free from collisional shifts.

However, despite their suppression in a spin polarized sample, collisions can still occur because of depolarisation induced by spin-dipole interaction in the sample. Metastable Helium (in the 2^3S_1 state) possesses a large internal energy of 19.8 eV, which is sufficient for Penning ionization to occur when a pair of atoms collide. Depolarization due to spin-dipole interaction in an optically trapped gas will thus result in losses through two processes: the first corresponds to spontaneous spin-flips with a gain of kinetic energy sufficient to escape the trapping potential (spin relaxation), and the second involves immediate ionization after a spin flip (relaxation-induced Penning ionization).

The rates of these two processes have been calculated in the case of the ^{4}He isotope in the presence of an external constant magnetic field [1][2], as shown in Fig. 1. Interestingly, the calculated value of the applied magnetic field at which the minimum spin relaxation rate is obtained is highly dependent on the molecular potential of the $^5\Sigma_g^+$ electronic state of the colliding pair, allowing to experimentally constraint ab-initio calculations of such a potential. However, the bosonic nature of metastable ^{4}He, where *s*-wave collision channels are allowed, lead to three-body recombination dominated losses, making the determination of the spin relaxation contribution difficult [3]. In contrast, an optically trapped degenerate Fermi gas of ^{3}He* is an ideal candidate for such a measurement as *s*-wave collisions are strongly suppressed.

In our experiment we prepare degenerate Fermi gases of metastable ^{3}He confined in an optical dipole trap at 1557 nm. A bias magnetic field is then turned on and the evolution of the number of atoms is measured to extract the rate of the spin relaxation process. We will present our experimental results and compare them to theoretical calculations for ^{3}He that we performed.

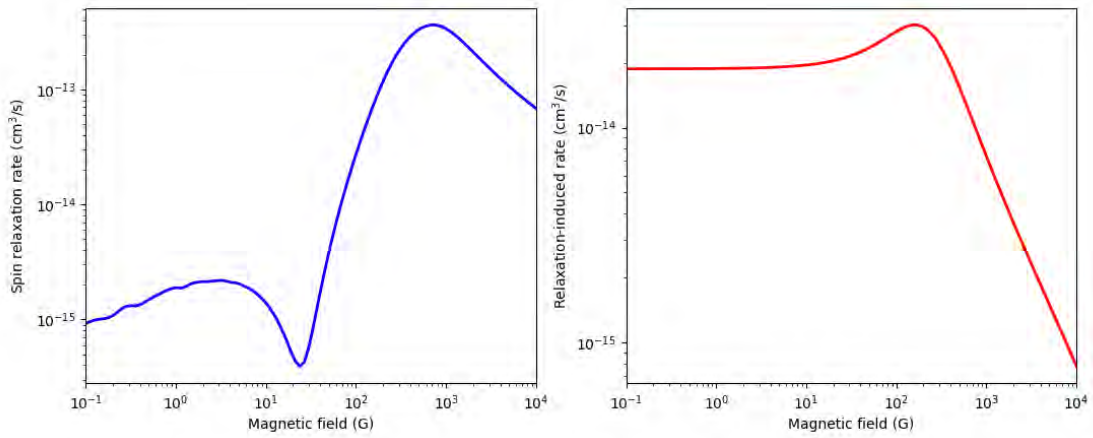

Fig. 1: Dependance of the calculated spin relaxation (left) and relaxation-induced Penning ionization (right) rates on an applied magnetic field for metastable ^{4}He.

References

[1] P. O. Fedichev, M. W. Reynolds, U. M. Rahmanov, and G. V. Shlyapnikov, Phys. Rev. A **53**, 1447 (1996).
[2] P. J. Leo, V. Venturi, I. B. Whittingham, J. F. Babb, Phys. Rev. A **64**, 042710 (2001).
[3] J. S. Borbely, R. van Rooij, S. Knoop, and W. Vassen, Phys. Rev. A **85**, 022706 (2012).

[*]Corresponding author: r.jannin@vu.nl

Reaction between a molecule and a Rydberg atom: studying n-changing processes in $\mathrm{He}(n) + \mathrm{CO} \rightarrow \mathrm{C}(n') + \mathrm{O} + \mathrm{He}$

F. B. V. Martins[1], **V. Zhelyazkova**[1], **J. A. Agner**[1], **H. Schmutz**[1], **F. Merkt**[*1]
1. Laboratory of Physical Chemistry, ETH Zurich, CH-8093 Zurich, Switzerland

Ion-molecule reactions are usually challenging to study at low temperatures. In recent years, an approach based on merged beams of molecules (A) in the ground state and a Rydberg species [B(n)] has been shown to be a successful way of studying A+B$^+$ reactions, making it possible to reach collision energies as low as $\sim k_B \cdot 100$ mK [1-3]. We present experimental studies of the reaction between CO molecules and helium atoms excited to Rydberg-Stark states [He(n)] in a merged-beam apparatus. The supersonic beams of CO and of He(n) excited to states with principal quantum number n in the range $27-45$ are merged with a surface deflector [4,5]. The product ions are collected in a time-of-flight mass spectrometer and detected with a micro-channel plate detector.

In previous studies [1-3], the reaction between a Rydberg atom and a molecule was considered to be equivalent to the corresponding ion-molecule reaction. The Rydberg electron typically acts as a spectator and its only role is to shield the ions from stray electric fields [6-8]. In reactions forming molecular Rydberg states with rovibrationally excited ion cores, autoionization promptly releases the electron. In the He(n)+CO reaction, however, long-lived atomic C(n') atoms are formed. This reaction system thus offers the possibility to study n-changing processes taking place before and during the reaction.

We study the Rydberg-Stark-state distribution of the He(n) atoms and of the C(n) products experimentally by pulsed-field ionization [see Fig. 1(a)] and theoretically. The integrated signal from pulsed-field ionized He(n) and C(n) recorded with different electric field values is compared to the predicted diabatic ionization for a distribution of Rydberg-Stark states. The He sample initially excited to a specific n state is redistributed among a number of states prior to the reaction via fluorescence and blackbody-radiation-induced transitions during the 85-μs time between excitation and detection. We calculate the rates of these radiative processes and include them in Monte Carlo simulations to model the evolution of the He(n) population and its n-distribution. The agreement between the modeled ionization and the measured ionized He(n) signal in Fig. 1(b) confirms that a range of Rydberg-Stark states of He are populated. The discrepancy between experimental and modeled ionization of C(n) can be explained by the different ionization dynamics of C(n) or changes in the Rydberg state during the reaction. This finding indicates the validity of the Rydberg-electron-spectator model.

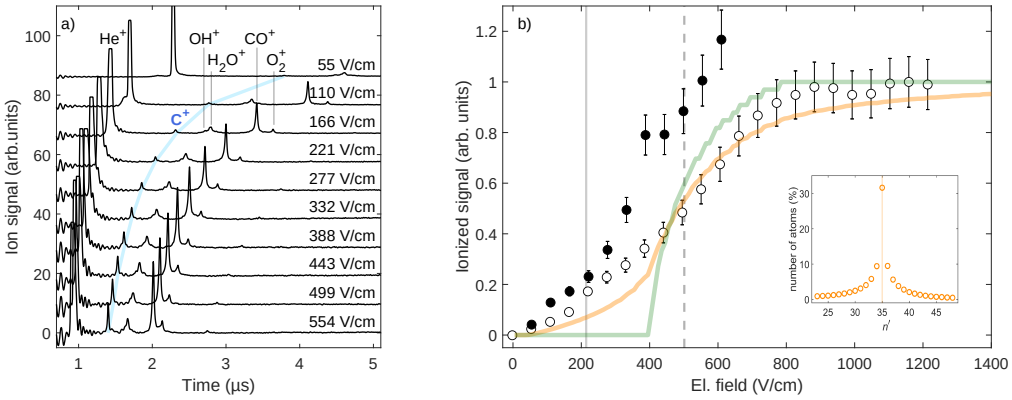

Fig. 1: (a) Time-of-flight mass spectra of the He(n)+CO reaction with He atoms initially excited to $n = 35$ Rydberg states at several electric fields. (b) Integrated pulsed-field ionization signal of He(n) (open circles), initially excited to the $n = 35$ state and C(n) (black dots). The modeled ionization signal that accounts for the distribution of n states shown in the inset (single-n state) at the time of ionization is represented by the orange (green) line. The full (dashed) vertical line in (b) corresponds to the adiabatic (diabatic) ionization threshold of atoms with $n = 35$.

References

[1] P. Allmendinger, J. Deiglmayr, O. Schullian, K. Höveler, J. A. Agner, H. Schmutz, and F. Merkt, Chem. Phys. Chem. **17**, 3596 (2016).
[2] V. Zhelyazkova, F. B. V. Martins, J. A. Agner, H. Schmutz, and F. Merkt, Phys. Rev. Lett. **125**, 263401 (2020).
[3] K. Höveler, J. Deiglmayr, J. A. Agner, H. Schmutz, and F. Merkt, Phys. Chem. Chem. Phys. **23**, 2676 (2021).
[4] P. Allmendinger, J. Deiglmayr, J. A. Agner, H. Schmutz, and F. Merkt, Phys. Rev. A **90**, 043403 (2014).
[5] V. Zhelyazkova, M. Žeško, H. Schmutz, J. A. Agner, and F. Merkt, Mol. Phys. **117**, 2980 (2019).
[6] S. T. Pratt, J. L. Dehmer, P. M. Dehmer, and W. A. Chupka, J. Chem. Phys. **101**, 882 (1994).
[7] E. Wrede, L. Schnieder, K. Seekamp-Schnieder, B. Niederjohann, and K. H. Welge, Phys. Chem. Chem. Phys. **7**, 1577 (2005).
[8] M. Matsuzawa, Phys. Rev. A **82**, 054701 (2010).

[*]Corresponding author: frederic.merkt@phys.chem.ethz.ch

Narrowing of Spectroscopic Linewidths through Pauli Blockade of Stimulated Emission

Y. van der Werf[1], **R. Jannin**[1] **K. Steinebach**[1], **H.L. Bethlem**[1], **K.S.E. Eikema**[*1]
1. LaserLaB Vrije Universiteit, De Boelelaan 1085, 1081HV, Amsterdam, The Netherlands

We demonstrate, for the first time to our knowledge, the effect of Pauli Blockade on stimulated emission, and its effect on spectral line shapes.

When fermionic atoms are cooled to quantum degeneracy, their quantum statistical behaviour starts to dominate the atom dynamics and interactions, leading to many interesting phenomena. In our experiment, we prepare degenerate Fermi gases (DFG) of ^{3}He in the metastable 2^3S_1 $(F = 3/2)$ state, which we excite to the 2^1S_0 $(F = 1/2)$ state with a frequency-comb referenced stable laser at 1557 nm. A spectrum is recorded by observing the remaining 2^3S_1 fraction after excitation. The atoms are confined in a dipole trap at the magic wavelength, where they experience no differential AC Stark shift from the trapping light, and thus the spectral lineshape (at low intensity) is purely determined by Fermi-Dirac statistics.

Here, we demonstrate that our spectroscopic linewidth is reduced compared to the expected Doppler broadened profile based on the DFG momentum distribution [1,2]. We explain this as an effect of Pauli blockade, which strongly inhibits stimulated emission from the 2^1S_0 back to the 2^3S_1 state for the densely occupied low-momentum states. This effect is seen because of the much larger finite linewidth of the laser (a few kHz) compared to the trap level spacing. The sparsely occupied high momentum states (contributing most to the Doppler broadening) are less affected by the blockade and have a higher probability to de-excite to the metastable state through stimulated emission, effectively narrowing the line.

As an experimental verification, we decrease the lifetime of the 2^1S_0 state through optical pumping to the short-lived 4^1P_1 level with 397 nm light, thus strongly decreasing the probability for stimulated emission at 1557 nm and lifting the effect of the Pauli blockade. We show that for a wide range of 397 nm laser powers, the Doppler broadened linewidth is retrieved, and we find excellent agreement between modelled line widths and experimental data over a range of thermodynamical parameters of the DFG.

This experiment explores a new facet of exotic phenomena related to Pauli blockade in degenerate Fermi gases based on suppressed stimulated emission, while several other experiments recently demonstrated its effect on inhibition of spontaneous decay [3,4,5]. Moreover, the narrowing effect is beneficial for the purpose of precision spectroscopy and could provide a new tool in developing precision measurements on trapped fermionic samples.

References

[1] R.P.M.J.W. Notermans *et al.*, Comparison of Spectral Linewidths for Quantum Degenerate Bosons and Fermions, *Phys. Rev. Lett.* **117, 213001** (2016)
[2] G. Juzeliunas and M. Masalas, Absorption by cold Fermi atoms in a harmonic trap, *Phys. Rev. A* **63, 061602** (2001)
[3] C. Sanner *et al.*, Pauli blocking of atomic spontaneous decay, **arXiv:2103.02216 (2021)**.
[4] A. B. Deb and N. Kjærgaard, Observation of pauli blocking in light scattering from quantum degenerate fermions, **arXiv:2103.02319 (2021)**.
[5] Y. Margalit *et al.*, Pauli blocking of light scattering in degenerate fermions,**arXiv:2103.06921 (2021)**.

*Corresponding author: k.s.e.eikema@vu.nl

Tuning ultracold collisions oh He*-Li with external magnetic field

M. Umiński[*1], **P. Żuchowski**[†1], **M. Borkowski**[2]

1. Institute of Physics, Faculty of Physics, Astronomy and Informatics, Nicolaus Copernicus University, Grudziadzka 5, 87-100 Torun, Poland
2. Van der Waals-Zeeman Institute, Institute of Physics, University of Amsterdam, Science Park 904, 1098 XH Amsterdam, the Netherlands

One of the main goals of studying cold matter is to broaden our knowledge of mechanisms underlying chemical reactions. Recent advances in the field of cold matter experiments ([1],[2]) bring us closer to observing how chemical reactions may be precisely controlled. Feshbach resonances, which we observe in cold regime, are a quantum phenomenon playing a crucial role in the results of atom and molecule collisions. Alkali atoms and helium are good examples to observe due to their simple structures. Here we are examining a model system in which chemical reaction controlled by external field can be studied: the cold collisions of Li atoms with metastable helium (labelled as He*) in magnetic field.

He*-Li molecules may come in one of two spin states: a stable, spin-polarized quartet state and unstable, lowspin doublet state, in which we observe the Penning ionization. The bound states are mixtures of these two states.

To describe them we use two interaction potentials: a real, published before Morse/Long- Range potential describing quartet state and a predicted, theoretical complex potential of doublet state. To characterize the lowenergy collisions we use the renormalized Numerov method and discrete variable representation.

As we are interested in dependency on external magnetic field, we also consider Zeeman effect, which allows us to carefully shift Energy levels. Using this, we may tune our system to allow Feshbach resonances to happen. In proximity of resonances, we expect to observe increased rate of inelastic reactions, and thus ion production. Depending on the composition of these two states, the Feshbach resonances, which originate from them, might have different loss rates and shapes. Taking advantage of the mentioned properties we may, for the first time, observe chemical reactions induced by magnetic field.

References

[1] K. Dulitz *et al.*, J. Chem. Phys. **150**, 34201 (2019)
[2] E. Narevicius *et al.*, Nat. Chem. **13**, 94-98 (2021)

[*]Corresponding author: marcin.uminski@doktorant.umk.pl
[†]Corresponding author: pzuch@fizyka.umk.pl

Penning Ionization Processes Involving Cold Rydberg Alkali–Metal Atoms

K. Miculis[*1], **A. Cinins**[1], **N. N. Bezuglov**[1,2]
1. University of Latvia, Institute of Atomic Physics and Spectroscopy, Riga LV-1004, Latvia
2. Saint Petersburg State University, St. Petersburg 199034, Russia

The Penning ionization (PI) processes in cold gas media of alkali atoms are investigated in this contribution. The corresponding autoionization widths show a drastic dependence (by orders of magnitude) on the orbital quantum numbers of Rydberg atoms involved in a long-range dipole-dipole interaction. Nontrivial dependence of PI efficiency on the size of colliding particles was considered, with a particular accent to the applications for the research of cold matter created in experiments with magneto-optical traps. We described analytically optimal, highly asymmetric configurations of atomic Rydberg pairs, which lead to explosive intensification (by several orders of magnitude) of free electron escaping due to PI [1]. This property may be favorable for the generation of primary (seeding) charged particles when a cold Rydberg medium evolves into a cold plasma. Under the frame of the semiclassical approach, we obtained universal analytical formulas containing two fitting parameters which allow one to evaluate PI rate constants. We have calculated both the optimal $\{n_i l_i, n_{d\_opt} l_d\}$ pairs and the corresponding reduced Penning autoionization widths $\acute{\Gamma}_{opt}(n_i l_i)$ for different configuration of alkali atoms and presented the results obtained in the tabulated form. As an example, the case of p-states ($l_i = l_d = 1$) for H and Na atoms are provided in Fig. 1.

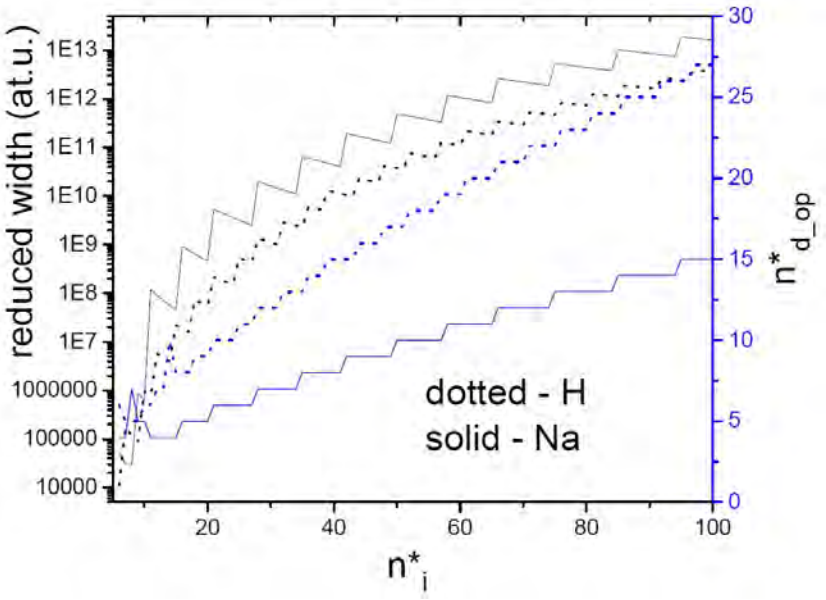

Fig. 1: The optimal $n_i - n_{d\_opt}$ pair and the corresponding reduced autoionization width $\acute{\Gamma}_{opt}(n_i l_i)$ in the cases of sodium and hydrogen atoms with $l_i = l + d = 1$.

References

[1] D. K. Efimov, K. Miculis, N. N. Bezuglov, A. Ekers, *J. Phys. B.*, **49**, 125302 (2016).

*Corresponding author: michulis@latnet.lv

Transmission-blockade breakdown phase transition of atoms in a cavity

T.W. Clark[*1], **A. Dombi**[†1], **F. I. B. Williams**[1], **Á. Curkó** [1], **J. Fortágh** [2], **D. Nagy** [1], **A. Vukics** [1], **P. Domokos** [1],

1. Institute for Solid State Physics and Optics, Wigner Research Centre for Physics, H-1525 Budapest P.O. Box 49, Hungary
2. Physikalisches Institut, Eberhard Karls Universit at Tubingen,Auf der Morgenstelle 14, D-72076 Tubingen, Germany

We demonstrate, both theoretically and in practise, a novel type of phase transition in a many-atom cavity QED system. The light transmission of a laser-driven optical resonator can have two distinct, robust states depending on the state of an ensemble of cold atoms trapped within the cavity mode. Atoms in their initially prepared pure state blockade the transmission by causing a large detuning of the cavity mode from the laser drive. The atoms can transition into an uncoupled state via a non-linear channel which is suppressed in the blockaded phase, however, opens up in a critical run-away process to guide the whole cavity system into a transparent phase. The experiment allows for a time-resolved direct observation of the transition between two phases as well as the quantification of the enhanced fluctuations in the critical region.

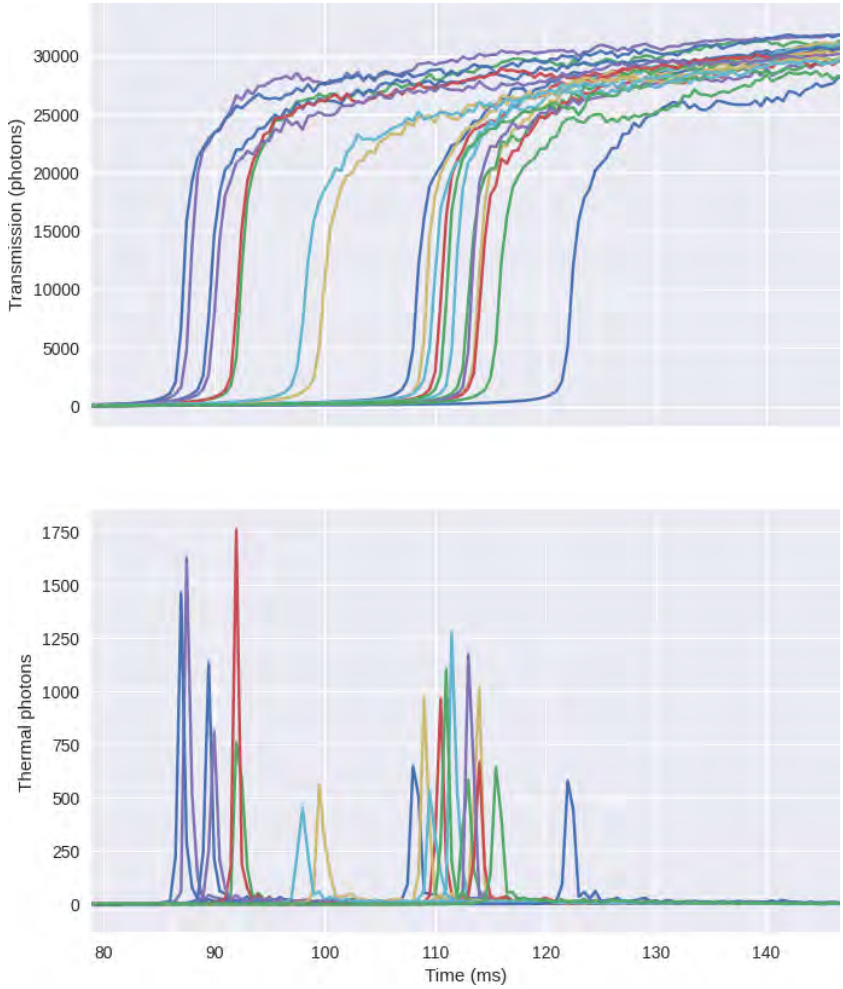

Fig. 1: Schematic summary of a new type of phase transmission, dubbed a *transmission blockade* breakdown, where different colours represent different repetitions of the same experiment. The time evolution of the transmitted intensity is plotted (above), exhibiting the switch from the blockaded phase into a transparent one. The transition is accompanied by the increase of thermal fluctuations, represented by thermal photon numbers, as extracted from the photon statistics of the transmitted light.

[*]Corresponding author: thomas.clark@wigner.hu
[†]Corresponding author: dombi.andras@wigner.hu

Observing quantum-speed-limit crossover with matter wave interferometry

Gal Ness[*1], **Manolo R. Lam**[2], **Wolfgang Alt**[2], **Dieter Meschede**[2], **Yoav Sagi**[1], **Andrea Alberti**[2]
1. Physics Department, Technion – Israel Institute of Technology, Haifa 32000, Israel
2. Institut für Angewandte Physik, Universität Bonn, D-53115 Bonn, Germany

Quantum mechanics sets fundamental limits on the speed at which quantum states can transform over time. Two well-known quantum speed limits are the Mandelstam-Tamm (MT) and the Margolus-Levitin (ML) bounds, which relate the maximum rate of evolution to the energy uncertainty and mean energy of the system, respectively. We perform fast matter wave interferometry experiments and track the motion of a single atom in a spin-dependent lattice. This setup constitutes a multi-level quantum system in which we concurrently test both speed limits. Our data reveal two different regimes: one where the MT limit constrains the evolution at all times, and a second where a crossover to the ML limit occurs at longer times. We take a geometric approach to quantify the deviation from the speed limit, measuring how far the quantum evolution of the matter wave deviates from the geodesic trajectory in the Hilbert space of the multi-level system. Our results[1], establishing the role of quantum speed limits beyond the simple two-level system, are important for understanding the ultimate performance of quantum computing devices and related advanced quantum technologies.

For time-independent Hamiltonian, the ML and MT bounds restrict the maximal state evolution rate via the two-time state overlap by means of the mean energy above ground state $E \equiv \langle \hat{H} \rangle$ and the energy uncertainty $\Delta E \equiv \langle \hat{H}^2 - E^2 \rangle^{1/2}$, respectively:

$$|\langle \psi(0) \,|\, \psi(t) \rangle| \geq \cos\left(\sqrt{\frac{\pi E t}{2\hbar}}\right), \qquad |\langle \psi(0) \,|\, \psi(t) \rangle| \geq \cos\left(\frac{\Delta E t}{\hbar}\right). \tag{1}$$

Each of these limits is valid until the corresponding orthogonalization time: $\tau_{\mathrm{ML}} \equiv \pi\hbar/(2E)$ and $\tau_{\mathrm{MT}} \equiv \pi\hbar/(2\Delta E)$. Exploiting fast Raman-Ramsey interrogation technique, we obtain the two-time state overlap $\langle \psi(0) \,|\, \psi(t) \rangle$ as a function of time t. The temporal evolution of the Ramsey fringe contrast directly translates into the modulus of the overlap, as its phase provides the overlap's argument. We also extract E, and ΔE, that enable the testing of Eq. (1) and quantify the distinction of the actual state trajectory from the limit.

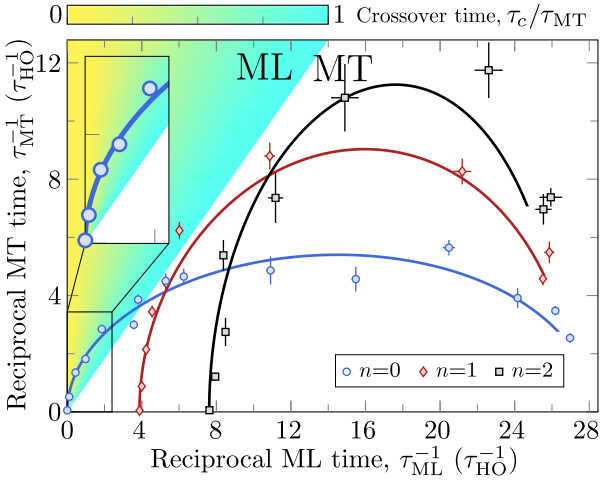

Fig. 1: Quantum-speed-limit crossover, reproduced from [1]. Measured orthogonalization times, τ_{ML} and τ_{MT}, displayed through their reciprocals, with n the quantum number characterizing the initial wave packet shape. When $\Delta E < E$ (and thus $\tau_{\mathrm{ML}} < \tau_{\mathrm{MT}}$), the dynamics are restricted by the MT bound only. However, if $\tau_{\mathrm{MT}} < \tau_{\mathrm{ML}}$, a crossover to the ML bound is manifested at longer times. Shades in color identify the ML regime, where a crossover manifests at time τ_c, as opposed to the MT regime (uncolored area), where no crossover occurs. Inset highlights data points in the ML regime. Values are expressed in units of the reciprocal of the trap oscillation period, which is around 16μs.

References

[1] Gal Ness, Manolo R. Lam, Wolfgang Alt, Dieter Meschede, Yoav Sagi, Andrea Alberti, *arXiv:*2104.05638 (2021).

*Corresponding author: gn@technion.ac.il

Avoiding dark states in the laser cooling of TlF using additional external fields

Elahe Abdiha[*1], **Christiane P. Koch**[†1]
1. Freie Universität Berlin, department of Physics, Arnimallee 14, 14195 Berlin, Germany

Ultracold heteronuclear diatomic molecules have become a platform for research in many areas such as examination of fundamental physics. Among other techniques to achieve cold samples of molecules, laser cooling is a reliable and feasible method. Laser cooling of molecules faces more obstacles compared to that of atoms due to their complex energy level structure i.e. their vibrational and rotational degrees of freedom. However, for some specific molecules, this can be overcome by carefully choosing a suitable molecular transition. Here, we study the laser cooling of Thallium Fluoride (TlF). In addition to the investigation of the violation of parity and time-reversal invariance, this molecule is attractive for measuring the Schiff moment of the Tl nucleus due to its high polarizability and high mass. In principle, optical cooling requires optical cycling between the ground state and the excited state of the molecule. Loss of even a very small fraction of the population to other energy levels, so-called dark states, prevents having as many times absorption and emission cycles as needed for cooling. We seek to identify suitable external fields to inhibit population trapping in the dark states during the laser cooling of TlF using quantum optimal control and the concept of mutually unbiased bases.

[*]Corresponding author: elahe.abdiha@fu-berlin.de
[†]Corresponding author: christiane.koch@fu-berlin.de

Feshbach resonances in half-collisions between para/ortho H_2^+ and He

Karl P. Horn[*1], **Prerna Paliwal**[2], **Daniel M. Reich**[1,3], **Arthur Christianen**[4], **Gerrit Groenenboom**[4], **Ad van der Avoird**[4], **Yuval Shagam**[2], **Nabanita Deb**[2], **Edvardas Narevicius**[2], **Christiane P. Koch**[1,3]

1. Theoretical Physics, Universität Kassel, Germany
2. Department of Chemical Physics, Weizmann Institute of Science, Rehovot, Israel
3. Theoretical Physics,Freie Universität Berlin, Germany
4. Theoretical Chemistry, IMM, Radboud University, Nijmegen, Netherlands

Novel experimental setups allow collision energies to be tuned to sufficiently cold temperatures, such that fundamental quantum phenomena such as resonances begin to emerge. In particular, $4He - H_2^+$ half-collisions can be prepared via Penning ionisation in merged supersonic beams of $4He^*$ and H_2. These collisions reveal significant differences in rotational distributions when using either para or ortho H_2^+ as a collision partner. We provide an explanation of the observed disparity in terms of the dominating influence of Feshbach resonances in the vibrationally excited states of the two spin isomers. Numerical simulation of the half-collision process, utilizing a state-of-the-art potential and full coupled channels calculations allows us to study the character of these resonances. Our calculations show that this character depends sensitively on the mass of the utilised helium isotope as would be expected for Feshbach resonances.

*Corresponding author: karlhorn@physik.uni-kassel.de

Doppler cooling of atoms with a frequency comb: Rb theoretical case study

D. Buhin* [1], **N. Šantić**[1], **M. Kruljac**[1], **V. Vulić**[1], **T. Ban**[1], **D. Aumiler**[1]
1. Institute of Physics, Bijenička c. 46, 10000 Zagreb, Croatia

Optical frequency combs (FCs) are unique sources of light, with applications ranging from high precision spectroscopy to quantum communication. In the recent literature, there were demonstrations of frequency comb cooling of atoms and ions [1-3] as well as simultaneous cooling of multiple atomic species [4]. These demonstrations are opening the way towards the cooling of atoms with strong cycling transitions in the VUV spectral range such as hydrogen, oxygen and other biologically important atoms. In order to fully understand the comb cooling experimental results and provide physical insight into the comb-atom interaction, it is crucial to develop theoretical models that describe the interaction of multi-level atoms with the frequency comb.

In this work we present the theoretical model that quantitatively describes the interaction of six-level atoms with two counter-propagating beams of a frequency comb, i.e. 1D Doppler cooling of Rb atoms with a frequency comb. The temporal evolution of the atomic system is described by the optical Bloch equations, and stationary state solutions for the excited state populations are used to calculate the radiation pressure force and diffusion exerted on atoms. The steady-state temperature of the atoms is then calculated using the Fokker-Planck equation.

We use the developed theoretical model to study the complex interplay of comb parameters and the atomic energy level structure that drives the comb cooling process. The radiation pressure force of a frequency comb, which consists of many equidistant comb modes, is much more complex than in the case of standard continuous-wave laser cooling. Consequently, even slight changes in comb parameters can lead to significant changes in the radiation pressure force and diffusion, and therefore to the final temperature of atoms. We analyze how the comb parameters affect the cooling process and provide some general guidelines regarding the effective use of frequency combs in the laser cooling of atoms.

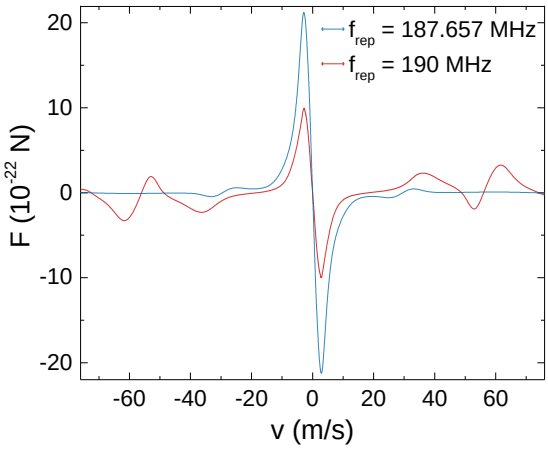

Fig. 1: Radiation pressure force in 1D frequency comb cooling of Rb atoms as a function of atomic velocity, for two nearby pulse repetition frequencies.

References

[1] A. M. Jayich, X. Long, and W. C. Campbell, Phys. Rev. X **6**, 041004 (2016)
[2] M. Ip, A. Ransford, A. M. Jayich, X. Long, C. Roman, and W. C. Campbell, Phys. Rev. Lett. **121**, 043201 (2018)
[3] N. Šantić, D. Buhin, D. Kovačić, I. Krešić, D. Aumiler, and T.Ban, Sci. Rep. **9**, 2510 (2019)
[4] D. Buhin, D. Kovačić, F. Schmid, M. Kruljac, V. Vulić, T. Ban, and D. Aumiler, Phys. Rev. A **102**, 021101(R) (2020)

*Corresponding author: dbuhin@ifs.hr

Measuring densities of cold atomic clouds smaller than the resolution limit.

A. Litvinov[*1], **P. Bataille**[1], **O. Gorceix**[1], **P. Pedri**[1], **E. Maréchal**[1], **M. Robert-de-Saint-Vincent**[1], **B. Laburthe-Tolra**[1],

1. Laboratoire de Physique des Lasers, CNRS, UMR 7538, Université Sorbonne Paris Nord, F-93430 Villetaneuse, France

The cold atoms community explores the physics of dense cloud of atoms, which reveal interesting phenomena in extremely small and local features such as vortices, density fluctuations, etc. Resolving such structures is a difficult but rewarding problem that prompted important technical developments, using for example fluorescence imaging with high-resolution objectives [1], the newly demonstrated quantum gas magnifier [2], super-resolution imaging [3],[4]. In the case of standard absorption imaging of extremely small and dense objects, the Beer-Lambert law is non linear and cannot be averaged over the imaging resolution. This excludes the imaging of small features, and can also significantly distort large features.

We experimentally demonstrate that it is still possible to accurately measure the size and local density of an object, even when this object is smaller than the imaging resolution, taking benefit of the non-linearity of the Beer-Lambert law. The number of photons absorbed by a given number of atoms depends on the size of the sample especially when it becomes optically dense. The method relies on making an ansatz on the cloud shape along the unresolved dimension(s), and providing an additional information such as the total number of atoms. We experiment our method to measure transverse sizes as small as one fifth of our imaging resolution of *in-situ* absorption images of quasi-1D ^{87}Sr Fermi gases. The measurement is in good agreement with theoretical predictions. Moreover, we show that the distorted image of density profiles along the long axis can be reconstructed in agreement with theoretical predictions of Fermi distributions.

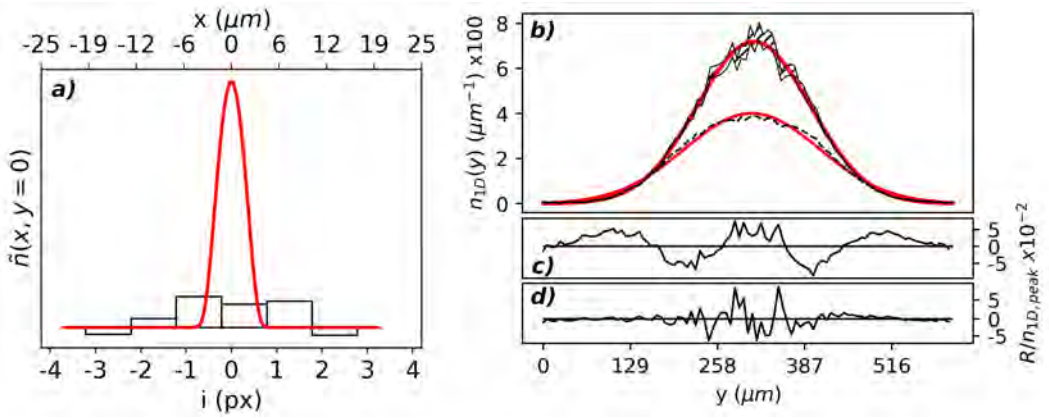

Fig. 1: Recovering density profiles from distorted absorption images of quasi-1D tightly confined gas. a) Cross section along the unresolved short axis of the column density imaged by absorbtion imaging. The raw data (black squares) shows diffraction fringes leading to negative optical depth. The red line is the result of our method using a gaussian shape ansatz along the unresolved axis. b) Density per unit length along the resolved long axis, $n_{1D}(y) = \int dx n(x,y)$ deduced either by integrating the pixelated optical depth along the short axis ("raw data", black dashes), or by our method (black hash, the area of which describing the uncertainty). The two red lines are Gaussian fits for the raw data (upper normalized residuals at c)) and for the 1D density obtained by our method (lower normalized residuals d)). c) The residuals show that the raw data differs significantly from the expected Gaussian shape of a thermal gas. d) Our method recovers this expected Gaussian shape.

References

[1] Christian Gross and Immanuel Bloch, Science, **357**, 995 (2017).
[2] Luca Asteria, Henrik P. Zahn, Marcel N. Kosch, Klaus Sengstock, Christof Weitenberg, arXiv:2104.10089 (2021).
[3] S. Subhankar, Y. Wang, T-C. Tsui, S.L. Rolston, and J.V. Porto, Phys. Rev. X **9**, 021002 (2019).
[4] Mickey McDonald, Jonathan Trisnadi, Kai-Xuan Yao, and Cheng Chin, Phys. Rev. X **9**, 021001 (2019).

[*]Corresponding author: andrea.litvinov@univ-paris13.fr

Coherent flash effect beyond the low saturation two-level case

C. C. Kwong[*1,2], **C. S. Madasu**[1,2], **T. Wellens**[3], **K. Pandey**[4], **D. Wilkowski**[1,2,5,6]

1. Nanyang Quantum Hub, SPMS, Nanyang Technological University, 21 Nanyang Link, Singapore 637371, Singapore

2. MajuLab, International Joint Research Unit UMI 3654, CNRS, Université Côte d'Azur, Sorbonne Université, National University of Singapore, Nanyang Technological University, Singapore

3. Physikalisches Institut, Albert-Ludwigs-Universität, Hermann-Herder-Strasse 3, D-79104 Freiburg, Germany

4. Department of Physics, Indian Institute of Technology Guwahati, Guwahati, Assam 781039, India

5. Centre for Quantum Technologies, National University of Singapore, 117543 Singapore, Singapore

6. Centre for Disruptive Photonic Technologies, The Photonics Institute, Nanyang Technological University, Singapore 637371, Singapore

A short coherent flash of light is emitted in the forward direction by an optically thick medium, when a quasi-resonant probe beam is switched-off abruptly [1]. The coherently transmitted field E_t can be decomposed into the incident field E_i and a two-level forward scattered field E_s, *i.e.*, $E_t = E_i + E_s$. Due to the finite response time of the atoms, we have $E_i = 0$ and $E_t = E_s$ at the moment of probe extinction, enabling a measurement of the forward scattered field from a flash measurement [1]. Furthermore, the lifetime of the flash is cooperatively shortened, and scales as $\tau_f \sim 1/b_0\Gamma$ [2], where Γ is the natural linewidth of the transition and b_0 is the resonant optical thickness at zero temperature. Here, we present two studies that go beyond the case of two-level system at low saturation.

In the first case, we study the flash effect at high saturation of a two-level transition in cold strontium atoms [3]. At high saturation, inelastic scattering of light by the atoms becomes important. Nevertheless, our experimental result is consistent with only the elastic scattering contributing to the forward scattered light. This is expected since E_s is coherent with E_i . We then derive an analytical expression, close to resonance at high saturation, to compute the total power of elastic scattering from the forward scattered power. By measuring the forward scattered power through the flash effect, we can compute the elastically scattered power in our experiment, and find a good agreement at high saturation with simulation results based on Maxwell-Bloch equations (see left panel of Fig. 1).

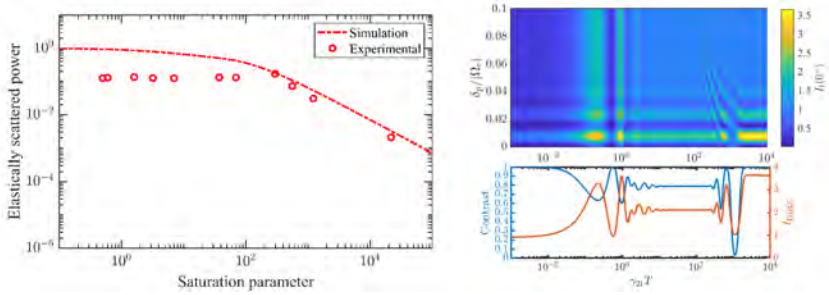

Fig. 1: (left panel) Comparison between experimental measurement of the total elastically scattered power, with the simulated values based on Maxwell Bloch equations. This probe detuning is $\delta/\Gamma = -2$. A good agreement is obtained at large saturation parameter. (right panel) The upper 2D plot presents the flash intensity during probe extinction. We assume that there is no ground state decoherence, $b_0 = 200$, and $\Omega_c = \gamma_{21}/2$ with γ_{21} is the natural linewidth of the probed transition. The inteference fringe as a function of detuning can be observed over a wide range of modulation period T. The lower plot shows the variation of inteference signal and contrast at different T.

In the second case, our theoretical study of the flash effect in an optically thick ensemble of three-level atoms in Λ-configuration, reveals a self-aligning homodyne interference that allow a precise determination of the two-photon resonance. In presence of electromagnetically induced transparency (EIT), the transmitted field decomposes into $E_t = E_i + E_s + E_{EIT}$, where E_{EIT} is the field of the EIT slow light. A flash is emitted when the weak probe beam (targeting a transition of linewidth γ_{21}) is abruptly turned off, while the control beam (Rabi frequency of Ω_c) is kept always on. Since E_{EIT} has a long delay, it is involved in a homodyne inteference with the flash field (E_s). This interference is sensitive to the phase difference between E_s and E_{EIT}. Within the narrow transparency window, the phase of E_s remains constant while E_{EIT} undergoes rapid change of its phase by π, over a small probe detuning δ_p of $\pi|\Omega_c|^2/(b_0\gamma_{21})$. The interference finge separation is narrowed due to the factor $1/b_0$, indicating a cooperative enhancement of the sensitivity in detecting the two-photon resonance. The duty cycle of this measurement can be increased with a periodic square pulse modulation of the probe beam. A strong interference signal $I_{\max}$ and good fringe contrast is still maintained at short modulation period (see right panel of Fig. 1). This technique could be a useful tool to measure the two-photon resonance for sensing applications.

References

[1] M. Chalony *et al.*, Phys. Rev. A **84**, 011401(R) (2011); C. C. Kwong *et al.*, Phys. Rev. Lett. **113**, 223601 (2014).
[2] C. C. Kwong, T. Yang, D. Delande, R. Pierrat and D. Wilkowski, Phys. Rev. Lett. **115**, 223601 (2015).
[3] C. C. Kwong, T. Wellens, K. Pandey and D. Wilkowski, Phys. Rev. A **102**, 063722 (2020).
[4] C. S. Madasu, C. C. Kwong, D. Wilkowski and K. Pandey, in preparation.

*Corresponding author: changchikwong@ntu.edu.sg

Time-Resolved Images of Intramolecular Charge Transfer in Organic Molecules

F. Fernández[*1,2], **J. González**[†1], **A. Palacios**[1], **F. Martín**[1,2]
1. Departamento de Química, Universidad Autónoma de Madrid, Madrid, 28049, Spain
2. Instituto Madrileño de Estudios Avanzados en Nanociencia (IMDEA-Nano), Madrid, 28049, Spain

Ever since the first models of organic solar cells were proposed more than 40 years ago, the search for new materials with the ability to produce a charge separation, necessary for photovoltaic applications, has kept drawing the scientific community's attention.

Organic photovoltaic devices usually achieve charge photogeneration by using charge transfer complexes, which act as an intermediate step between exciton dissociation and charge extraction.

In order to capture the real time evolution of such electronic process, which takes place in the time range between tens of attoseconds to a few femtoseconds, a sub-femtosecond time-resolution is required. Therefore, in this work we propose the use of a pump-probe scheme employing ultrafast laser sources to track the charge transfer process using as target a typical donnor-acceptor molecule in the gas phase. In particular, we investigate the ultrafast dynamics following the excitation of para-nitroaniline (PNA), which has been extensively studied in a solvent, both theoretically [1-3] and experimentally [1, 4-6], while scarcer works have been performed in gas phase to date.

We thus propose the use of a pump-probe scheme, using a few-fs UV pulse to excite the target. The ensuying electron-nuclear dynamics will be later probed by a time-delayed attosecond XUV pulse which will ionize the molecule. The time-varying ionization yields are expected to capture the complex dynamics triggered in the excited molecule.

In a first approach, using the fixed nuclei approximation, we retrieve the time evolution of the excited wave packet by analyzing the electron density variation, computed through a transition density matrix formalism. The imprint of these dynamics is later retrieved into the cation with the time-delayed absorption of the probe pulse.

We later explored how these electron dynamics evolved when coupled with the nuclear degrees of freedom, when non-adiabatic couplings come into play. The coupled electron-nuclear motion is described by means of a surface-hopping method, i.e. within a semi-classical picture. In short, the time-dependent wave function is retrieved at each time step, computing the electronic structure on-the-fly by means of a quantum mechanical description, while the nuclear dynamics follows the classical equations of motion.

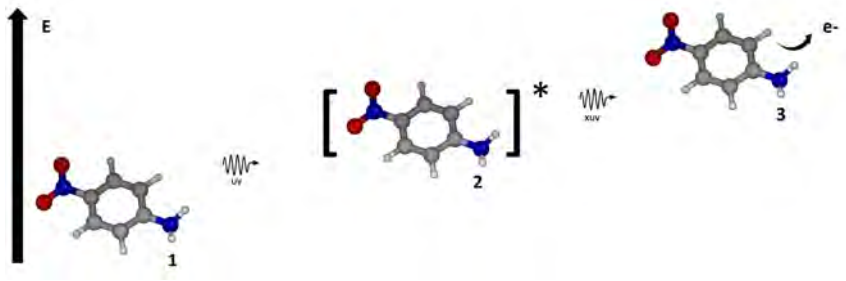

Fig. 1: Diagram of the pump probe scheme.

References

[1] Kovalenko S *et al.*, Chem. Phys. Lett. **323**, 3-4 312-322 (2000).
[2] Kosenkov D *et al.*, J. Phys. Chem. A **115**, 4 392–401 (2011).
[3] Bigelow R *et al.*, Theoret. Chim. Acta **100**, 30 12369-12373 (1983).
[4] Sinha H *et al.*, J. Am. Chem. Soc. **113**, 16 6062–6067 (1991).
[5] Schuddeboom W *et al.*, J. Phys. Chem. **100**, 30 12369-12373 (1996).
[6] Millefiori S *et al.*, Spect. Chim. Acta **33**, 1 21-27 (1977).

[*]Corresponding author: francisco.fernandez@imdea.org
[†]Corresponding author: jesus.gonzalezv@uam.es

Measurement of Magnetic Moments in Heavy, Highly Charged Ions Using Laser-Microwave Double-Resonance Spectroscoypy

Kanika[*1,2] **J. W. Klimes**[†1,2,3], **P. Baus**[4], **G. Birkl**[4], **Z. Guo**[1,2,3], **W. Quint**[1,2], **M. Vogel**[1],
1. GSI Helmholtz Center for Heavy Ion Research, Planckstr. 1, 64291 Darmstadt, Germany
2. Heidelberg Graduate School for Fundamental Physics, Im Neuenheimer Feld 226, 69120 Heidelberg, Germany
3. Max Planck Institute for Nuclear Physics, Saupfercheckweg 1 69117 Heidelberg, Germany
4. Institute for Applied Physics, TU Damrstadt, Schlossgartenstr. 7, 64289 Darmstadt, Germany

In ARTEMIS [1] [2] laser-microwave double-resonance spectroscopy [3] will be used to measure the intrinsic magnetic moments of both electrons and nuclei in heavy, highly charged ions (HCIs). This provides a probe of strong-field quantum electrodynamics. Figure 1 shows the level scheme for boron-like argon and the transitions used for the measurement. The fine structure and Zeeman transitions are shifted to the optical and microwave regimes respectively. A closed optical cycle is used as a probe of successful induction of spin flips by microwave stimulus.

The ARTEMIS Penning trap has two sections: the spectroscopy trap (ST) and creation trap (CT), and can store ion densities up to 10^6 cm^{-3} for several days or even weeks. This is possible due to the vacuum pressure $< 10^{-15}$ mbar in the trap center, which is in turn made possible by a cryogenic environment at nearly 4 K. The ST uses a half-open design for optical and ion access [3]. On the closed side spectroscopic access is provided by a transparent endcap electrode with a conductive indium-tin-oxide coating. This provides ≈ 2 sr conical access to the trap center for irradiation and detection of fluorescence light. This is more than an order of magnitude greater than conventional cylindrical designs with similar harmonicity and tunability. On the open side HCIs can be injected from the adjacent CT, where they can be created in situ via electron impact ionization or captured from an external source.

Currently, ARTEMIS is working toward a measurement of the 2p electron in a test ion, Ar^{13+}, which has a well known and accessible fine-structure transition. Also the experiment is preparing for capture of heavy, HCIs such as Pb^{81+} and Bi^{82+} from the HITRAP facility at GSI.

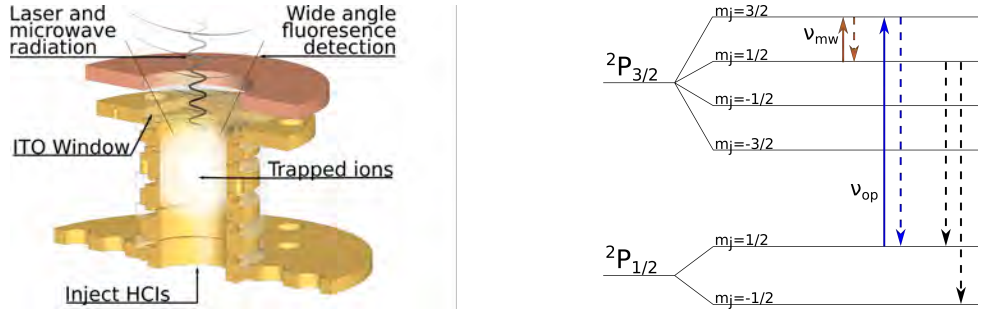

Fig. 1: (Left) Schematic of the ST showing a double-resonance measurement of trapped ions. (Right) Level scheme of Ar^{13+} with relevant spectroscopic transitions. ν_{op} denotes a closed-cycle optical transition, and dotted lines are spontaneous or stimulated decay channels. The Zeeman transition of interest, ν_{mw}, is in the microwave regime for the given charge state and magnetic field strength.

References

[1] W. Quint *et al.*, Phys. Rev. A **78**, 03251 (2008)
[2] S. Sturm, *et al.*, Atoms **5**, 4 (2017)
[3] D. V. Lindenfels *et al.*, Phys. Rev. A **87**, 023412 (2013)
[4] .S: Ebrahimi *et al.*, Phys. Rev. A **98**, 023423 (2018)

[*]Corresponding author: k.kanika@gsi.de
[†]Corresponding author: j.klimes@gsi.de

Development of a high-resolution mercury spectrometer at 253.7 nm for temperature metrology

S. Gravina[*1], **C. Clivati**[2], **G. Lopardo**[2], **F. Bertiglia**[2], **A. Castrillo**[1], **A. Sorgi**[3,4], **P. Cancio Pastor**[3,4], **F. Levi**[2] **and L. Gianfrani**[†1]

1. Department of Mathematics and Physics, Università degli Studi della Campania "Luigi Vanvitelli", viale A. Lincoln 5, 81100 Caserta, Italy
2. Istituto Nazionale di Ricerca Metrologica (INRiM), Strada delle Cacce 91, 10135 Torino, Italy
3. Istituto Nazionale di Ottica (CNR-INO), via N. Carrara 1, 50019 Sesto Fiorentino, Italy
4. European Laboratory for Nonlinear Spectroscopy (LENS), via N. Carrara 1, 50019 Sesto Fiorentino, Italy

Temperature is one of the most difficult physical quantities to measure. According to the recent revision of the International System (SI), the unit kelvin is defined in terms of a fixed value of the Boltzmann constant [1]. Such a definition encourages the development of primary thermometers operating in absolute mode [2, 3]. Here, we report on a new implementation of Doppler-broadening gas thermometry, which appears to be a very promising way for the pratical realization of the new kelvin. Our method is based on the precise observation of the shape of the $6s^2\ {}^1S_0 \rightarrow 6s6p\ {}^3P_1$ intercombination transition at 253.7 nm in mercury vapors, for a pair of bosonic isotopes, namely, ^{200}Hg and ^{202}Hg. The generation of coherent UV radiation has been performed by means of double stage Second Harmonic Generation (SHG) scheme. The pump laser is an external-cavity diode laser which emits at 1014.8 nm with a power level of about 65 mW. After a single passage through a periodically-poled lithium niobate crystal, the near-infrared radiation is converted into green light at 507.4 nm and used for injection locking of a high-power diode laser. Then, a second SHG process generates the 253.7 nm radiation through a β-barium borate crystal placed inside a resonant cavity, employing the common bow-tie design. In this scheme, the measured UV power is up to 250 μW. The realized source shows over 10 GHz mode-hop-free tunable range [4]. Laser-gas interaction takes place inside an isothermal cell filled with mercury vapors. An important requirement for the DBT experiment is the highly precise and accurate control of the laser frequency. To this purpose, the near-IR pump laser will be stabilized against an ultra-stable optical reference at 1014.8 nm. Figure 1 shows an example absorption spectrum obtained by scanning continuously the frequency of the near-infrared radiation across the ^{200}Hg and ^{202}Hg intercombination lines. The UV transmitted signal spectrum after the isothermal cell has been recorded by using a silicon carbide (SiC) photodiode whose linearity of the responsivity in the deep-ultraviolet region has been studied by using a variant of the intensity-ratio method [5]. We report on preliminary tests and measurements characterizing the present status of the spectrometer. We also present a new determination of the Einstein coefficient for the mercury intercombination line.

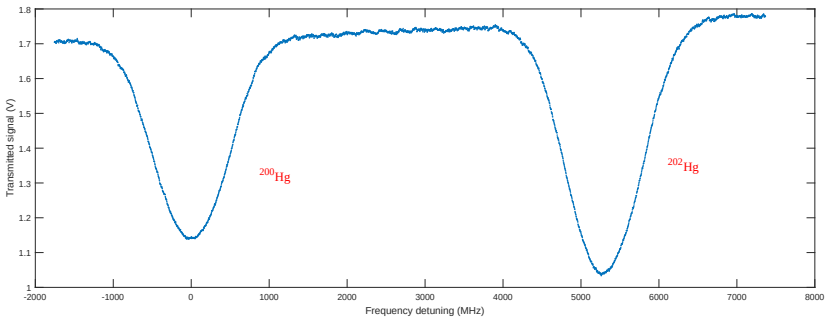

Fig. 1: Hg absorption signal in coincidence with the intercombination transition at 282.15 K.

References

[1] G. Machin, Measurement Science and Technology **29**, 022001 (2018).
[2] D. R. White, Contemporary Physics, 1-21 (2021).
[3] L. Gianfrani, Philosophical Transactions of the Royal Society A **374**, 20150047 (2016).
[4] C. Clivati, S. Gravina, A. Castrillo, G. A. Costanzo, F. Levi and L. Gianfrani, Optics Letters **45**(13), 3693-3696 (2020).
[5] H. Dinesan, S. Gravina, C. Clivati, A. Castrillo, F. Levi and L. Gianfrani, Metrologia **57**(6), 065001 (2020).

[*]Corresponding author: stefania.gravina@unicampania.it
[†]Corresponding author: livio.gianfrani@unicampania.it

Towards blue-detuned lattice optical atomic clock

D. Kovacic[*1,2], **M. Witkowski**[2], **S. Bilicki**[2], **M. Bober**[2], **V. Singh** [2], **A. Tonoyan** [2,3] **and M. Zawada**[2]

1. Institute of Physics, Bijenička c. 46, 10000 Zagreb, Croatia

2. Institute of Physics, Faculty of Physics, Astronomy and Informatics, Nicolaus Copernicus University,Grudziadzka 5, PL-87-100 Toruń, Poland

3. Institute for Physical Research, National Academy of Sciences of Armenia, Ashtarak 2, Armenia

Most strontium-based optical clocks employ a red-detuned optical lattice with wavelength of 813 nm to trap atoms. For this wavelength (one of the possible magic wavelengths) scalar polarizabilities of ground and excited states of clock transition are identical and the light shift of clock transition is largely suppressed. However, for a red-detuned lattice atoms are loaded into maxima of light intensity which leads to undesirable higher-order light shifts which can be difficult to compensate. On the other hand, atoms in a blue-detuned optical lattice (with magic wavelength of 390 nm) are loaded into light intensity minima, reducing light-induced perturbations of clock transition.

We present experimental and theoretical results related to the development of the Sr optical atomic clock based on a blue-detuned wavelength optical lattice at 390 nm. We determine photoionization losses for $^1P_1$ and $^3S_1$ states in ^{88}Sr and perform a study of feasibility of applying blue-detuned lattice in optical clocks. We measure the photoionization cross section of the $^1P_1$ state of ^{88}Sr at 390 nm by comparing the decay times of the blue MOT fluorescence at 461 nm with and without the presence of the 390 nm probe light. For the photoionization cross section for $^3S_1$ state we measure light-induced atomic losses from the optical trap at 813 nm for various trap depths during standard clock cycle with and without the presence of 390 nm beam. These photoionization cross sections are then used to calculate photoionization loss rates for $^1P_1$ and $^3S_1$ states in blue-detuned lattice for different lattice depths and compared with the natural decay rates of the two states. Finally, we consider atoms trapped in vertical optical lattice. Due to presence of gravity, energies of atoms in adjacent lattice sites are not degenerate and we therefore must calculate eigenstates of Hamiltonian (called Wannier-Stark states). These states consist of a main central peak and two smaller 'revival' peaks in side wells of the lattice. We calculate these states for a blue-detuned lattice and compare with the more commonly used red-detuned lattice, giving us valuable information on experimental requirements to ensure strong trapping of atoms in a blue-detuned lattice.

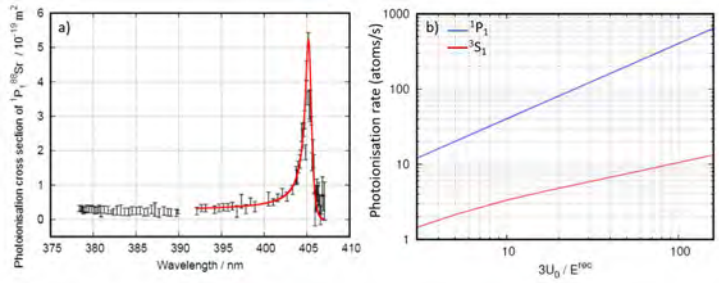

Fig. 1: The photoionisation cross section from the $^1P_1$ state as a function of the wavelength of the ionising light (Fig 1a). Photoionization rates for $^1P_1$ and $^3S_1$ states for different 3D lattice depths for 390 nm magic wavelength lattice (Fig 1b)

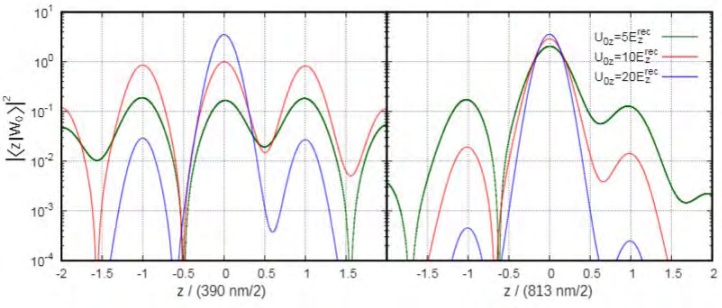

Fig. 2: Wannier-Stark states for different lattice depths for 390 nm (left) and 813 nm (right) magic wavelength lattices

*Corresponding author: dkovacic@ifs.hr

Towards precision spectroscopy of the 2S-6P transition in atomic deuterium

V. Wirthl[*1], **L. Maisenbacher**[1], **A. Grinin**[1], **D. Taray**[1], **A. Matveev**[2], **R. Pohl**[1,3], **T. W. Hänsch**[1,4], **Th. Udem**[1,4]

1. Max Planck Institute of Quantum Optics (MPQ), 85748 Garching, Germany
2. Russian Quantum Center, 121205 Moscow, Russia
3. Johannes Gutenberg University, 55128 Mainz, Germany
4. Ludwig Maximilian University (LMU), 80539 Munich, Germany

Similar to atomic hydrogen, precision laser spectroscopy of atomic deuterium can be used to determine physical constants and to test Quantum Electrodynamics. The isotope shift of the 1S-2S transition [1] links transition frequency measurements between hydrogen and deuterium through the squared deuteron-proton charge radius difference [2,3]. A combination of the 1S-2S transition frequency with additional measurements in deuterium allows a determination of the deuteron radius independent of the proton radius [4]. These determinations are however discrepant with results obtained in muonic deuterium [5], similar to the proton radius puzzle in hydrogen. Contrary to hydrogen [6,7], no recent measurements in deuterium are available (see Fig. 1).

We are working towards a measurement of the 2S-6P transition in deuterium. In contrast to hydrogen, simultaneous excitation of unresolved hyperfine components can not be avoided for the 2S-6P transition in deuterium due to the different nuclear spin and the selection rules. This complicates the situation and may lead to quantum interference between unresolved components [8]. Since these effects depend on laser polarization, we developed an improved active fiber-based retroreflector with a polarization monitor [9]. Furthermore, we find that in our case the unresolved quantum interference is expected to be strongly suppressed, making a 2S-6P deuterium measurement with similar precision as for hydrogen feasible.

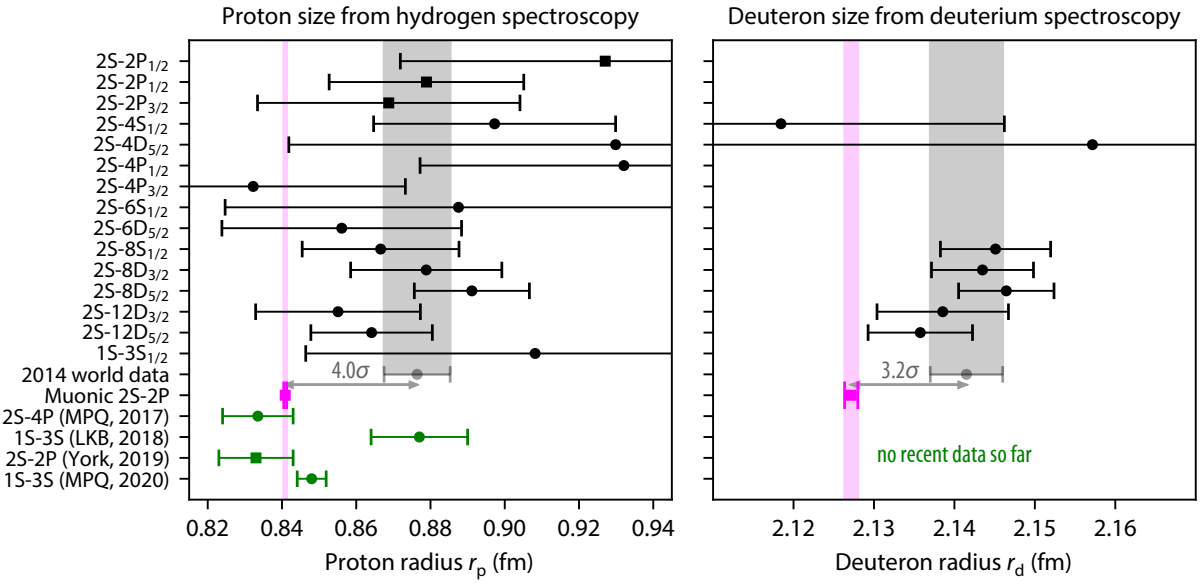

Fig. 1: Proton (left) and deuteron (right) charge radii extracted from precision spectroscopy of hydrogen and deuterium, respectively. Each point is a combination of the 1S-2S transition measurement combined with a second transition measurement shown on the left scale. Data points summarized in '2014 world data' are shown in black, the values from muonic hydrogen or deuterium in magenta, and recent spectroscopic measurements from regular hydrogen in green. In contrast to hydrogen, so far no recent data is available in deuterium.

References

[1] C. G. Parthey *et al.*, Phys. Rev. Lett. **104**, 233001 (2010).
[2] U. D. Jentschura *et al.*, Phys. Rev. A **83**, 042505 (2011).
[3] K. Pachucki *et al.*, Phys. Rev. A **97**, 062511 (2018).
[4] R. Pohl *et al.*, Metrologia **54**, L1 (2017).
[5] R. Pohl *et al.*, Science **353**, 669–673 (2016) .
[6] A. Beyer *et al.*, Science **358**, 79-85 (2017).
[7] A. Grinin *et al.*, Science **370**, 1061-1066 (2020).
[8] Th. Udem *et al.*, Ann. d. Ph. **531**, 1900044 (2019) .
[9] V. Wirthl *et al.*, Opt. Express **29**(5), 7024-7048 (2021).

*Corresponding author: vitaly.wirthl@mpq.mpg.de

Ultrafast Photogeneration of Quinone Methides from Naphthol Derivatives

M. Forjan[*1], **S. Vdović**[1], **M. Šekutor**[2], **N. Basarić**[2]
1. Institute of Physics, Bijenička c. 46, 10000 Zagreb, Croatia
2. Ruđer Bošković Institute, Bijenička c. 54, 10000 Zagreb, Croatia

Quinone methides (QMs), important intermediates in the chemistry and photochemistry of phenols, naphthols, anthrols etc., attracted attention owing to their biological activity [1][2] and increasing number of applications in organic synthesis [3][4]. However, the polar structure of QMs, which results in their high electrophilic and nucleophilic reactivity[5], makes them usually short-lived [6], so that they cannot be stored and have to be generated in situ. Among the methods for the generation of QMs, photochemical reactions are particularly appealing due to their ability to temporally and spatially control the activation event. For the applications of QMs in biological systems it is pivotal to fully unravel all details of the photochemical reaction mechanisms and characterize all intermediates that exist from the moment of photoactivation to the generation of QMs in the ground state. In fact, biological molecules may interact with these intermediates and thereby change reaction pathways and products [7].

By using ultrafast transient absorption, photochemical generation of QM from naphthol and adamantyl-naphthol in a solution at room temperature was tracked in real time with time resolution of 300fs. Pump beam wavelength of 267nm was obtained by setting up a third harmonic setup at one branch of fundamental 800nm beam. Pump energy per pulse was set up to be at around 250nJ. White light probe beam was generated in 3mm thick CaF_2 window which was constantly displaced to avoid material degradation. White light spectral range was spread out from 320nm to 700nm, hence, ultrafast dynamics in UV and visible part of the spectrum could be monitored. Time window for dynamics monitoring depended on the length of translation stage which was 20cm long, therefore dynamics in 1 ns time window could be monitored.

Surprisingly, although molecules possess the same chromophore (naphthol) the photochemical pathway of QM generation by photodehydration is different. In the case of adamantyl-naphthol, ground state QMs are produced directly via excited state QMs with no other intermediates or species participating in a reaction. In the case of naphthol, naphthol radical cation and phenoxyl radical participate in a reaction. Naphthol radical cation by deprotonation gives phenoxyl radical which decays by elimination of radical $OH^{\bullet}$ giving QM.

Therefore by using ultrafast transient absorption, photochemical reaction pathway has been completely revealed and all intermediates have been identified.

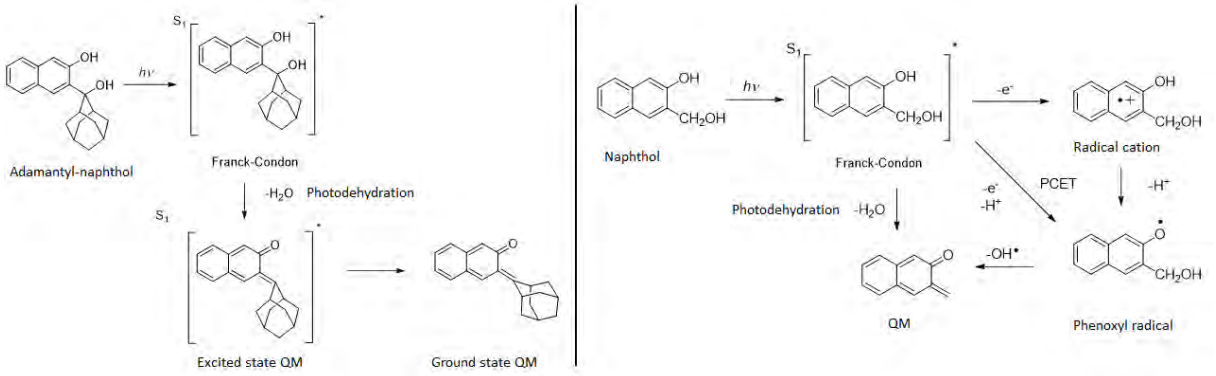

Fig. 1: Photochemical reaction pathways of QM generation from adamantyl-naphthol (left) and naphthol (right).

References

[1] Rokita, S. E., Ed. Quinone Methides; Wiley: Hoboken, 2009.
[2] Freccero, M. Quinone Methides as Alkylating and Cross-Linking Agents. Mini Rev. Org. Chem. 2004, 1, 403-415.
[3] Van De Water, R.; Pettus, T. R. R. o-Quinone Methides: Intermediates Underdeveloped and Underutilized in Organic Synthesis. Tetrahedron 2002, 58, 5367-5405.
[4] Pathak, T. P.; Sigman, M. S. Applications of ortho-Quinone Methide Intermediates in Catalysis and Asymmetric Synthesis. J. Org. Chem. 2011, 76, 9210-9215.
[5] Toteva, M. M.; Richard, J. P. The Generation and Reactions of Quinone Methides. Adv. Phys. Org. Chem. 2011, 45, 39-91.
[6] Wan, P.; Barker, B.; Diao, L.; Fischer, M.; Shi, Y.; Yang, C. Quinone Methides: Relevant Intermediates in Organic Chemistry. Can. J. Chem. 1996, 74, 465-475.
[7] Percivalle, C.; Doria, F.; Freccero, M. Quinone Methides as DNA Alkylating Agents: An Overview on Efficient Activation Protocols for Enhanced Target Selectivity Curr. Org. Chem. 2014, 18, 19-43.

[*]Corresponding author: mforjan@ifs.hr

Developments on King Plot Analysis using Highly Charged Ions

L. J. Spieß*[1], S. A. King[1], P. Micke[1,2], A. Wilzewski[1], E. Benkler[1], T. Leopold[1], M. K. Rosner[2], J. R. Crespo López-Urrutia[2], P. O. Schmidt[1,3]

1. Physikalisch-Technische Bundesanstalt, Bundesallee 100, 38116 Braunschweig, Germany
2. Max-Planck-Instituts für Kernphysik, Saupfercheckweg 1, 69117 Heidelberg, Germany
3. Institut für Quantenoptik, Leibniz Universität Hannover, Welfengarten 1, 30167 Hannover, Germany

Precision measurements of isotope shifts can provide a stringent test of fundamental physics, and potentially reveal new physics beyond the Standard Model. When measuring the isotope shift for two transitions of very different character in a given element, a so-called King plot analysis can be applied where any observed non-linearities may indicate an as-yet unknown fifth force or non-gravitational coupling to dark matter. Non-linearities in the King plot can also arise from effects within the Standard Model. Adding more transitions to the analysis can suppress these effects [1] and potentially allows the contributions from new physics. Optical clocks are the ideal instruments to achieve the required precision, reaching down to a fractional uncertainty below 10^{-18}. However, investigations to-date have focused on neutral or singly-charged atoms, which exhibit only a limited number of suitable electric-dipole-forbidden transitions. By variation of the charged state this can be expanded to highly charged ions (HCI) which would vastly increase the number of available transitions [2].

So far, the use of HCI for this purpose was prevented by the high temperature (≈MK) at which HCI are produced and typically stored and the corresponding Gigahertz resolution from Doppler-broadening. This has been overcome by extraction of HCI from a plasma in our electron beam ion trap (EBIT) [3] and transport to a linear Paul trap, where a single HCI is recaptured and sympathetically cooled using Be^+ [4][5]. Reduction to a HCI-Be^+ two-ion crystal allows for the use of quantum logic techniques for high-precision measurements, which we have successfully demonstrated with $^{40}Ar^{13+}$ [6]. Recently, we have shown the control of temperature-induced motional shifts to a fractional uncertainty below 10^{-18} using algorithmic cooling [7], competitive with state-of-the-art optical clocks. This will soon allow us to perform the first absolute frequency measurement of a transition in a HCI with an accuracy below 1 Hz, improving the value by more than six orders of magnitude.

We are planning to perform the first isotope shift measurement of a HCI with an expected relative uncertainty below 10^{-15}. As a proof-of-principle measurement we will compare our measurements in $^{40}Ar^{13+}$ against the rare isotope $^{36}Ar^{13+}$, which we have successfully extracted from our HCI source (Fig. 1) and recaptured in the Paul trap. Simultaneously we are preparing the measurement of isotope shifts in highly charged Ca. Injection of Ca from a solid-state target into the EBIT has been demonstrated. In parallel with this work, a new Paul trap for reduced systematic shifts and a new ultra-stable clock laser are being developed. This will allow spectroscopy of Ca^{14+} at even lower levels of systematic uncertainty.

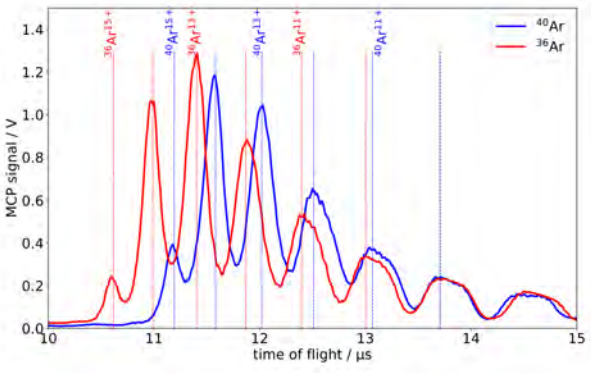

Fig. 1: Time of flight spectra of $^{40}Ar^{13+}$ and $^{36}Ar^{13+}$ after extraction from our HCI source. The different species separate based on their charge-to-mass ratio and are readily identified using a microchannel plate (MCP) detector.

References

[1] J. C. Berengut *et al.*, Phys. Rev. Research **2**, 043444, 2020.
[2] M. G. Kozlov *et al.*, Rev. Mod. Phys. **90**, 045005, 2018.
[3] P. Micke *et al.*, Rev. Sci. Instrum. **89**, 063109 2018.
[4] L. Schmöger *et al.*, Science **347**, 1233-1236, 2015.
[5] T. Leopold *et al.*, RSI **90**, 073201, 2019.
[6] P. Micke *et al.*, Nature **578**, p. 60–65, 2020.
[7] S. A. King *et al.*, arXiv:2102.12427v2, 2021.

*Corresponding author: lukas.spiess@quantummetrology.de

Performing Spectroscopy in the 1.5 μm-regime on slow Ammonia in a Molecular Fountain

W. van der Meer[*1], **H. L. Bethlem**[1]
1. LaserLaB, Department of Physics and Astronomy, Vrije Universiteit, De Boelelaan 1081, 1081 HV Amsterdam, The Netherlands

In a molecular fountain [1], molecules are released upwards, decelerated and launched upwards by electric fields, and observed as they fall back under gravity. This setup enables us to perform high-precision spectroscopy on various molecules.

Our molecular fountain decelerates vertically moving ammonia molecules down from 300 m/s to 90 m/s using a conventional Stark decelerator. These molecules are then further decelerated and launched upwards by a traveling wave decelerator [2]. They are focused in the transverse direction by a quadrupole and in the longitudinal direction by two ring electrodes. A focused UV laser then ionizes the molecules, the resulting ions are extracted and detected.

By exciting the molecules to a suitable vibrationally excited state, e.g. for ammonia the $\nu_1 + \nu_3$ overtone, their Stark effect changes. Hence, they will be focused worse by the focussing electric fields. The density of excited ammonia molecules in the detection zone will then be lower, thus providing an accurate way of finding the transition frequency. There are two areas where the molecules can be excited, namely in the first field-free region of the rising beam, or in the free-falling region of the rising and falling beams. The first option has more molecules, hence it gives a clearer signal, but it does have a Doppler shift and a maximum interaction time of 5 ms. The second option has an interaction time of up to 266 ms.

To perform the spectroscopic measurements, we lock a diode laser around 1520 nm to a frequency comb using a phase lock. The linewidth of the infrared laser is then reduced to below 100 kHz. We can use this setup to measure single photon transitions and plan to use it to measure Raman transitions and two-photon transitions as well.

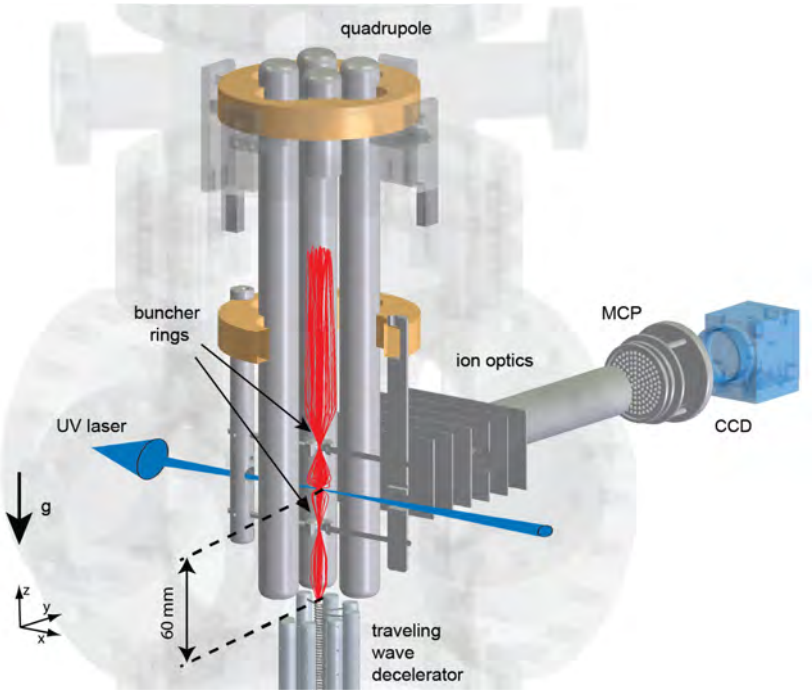

Fig. 1: Schematic view of the top part of the vertical beam machine showing the end of the traveling wave decelerator, the quadrupole lens system and simulated trajectories in red. The molecules are ionized by a UV laser and imaged on a phosphor screen located behind a multichannel plate (MCP). The image is recorded using a charge coupled device (CCD) and a photo-multiplier tube (not shown). The infrared laser (not shown) shines vertically down from the top through the buncher rings.

References

[1] C. Cheng *et al.*, Phys. Rev. Lett. **117**, 253201 (2016)
[2] P. Jansen *et al.*, Phys. Rev. A **88**, 043424 (2013)

*Corresponding author: w.vander.meer@vu.nl

Matter-Wave Interferometry as a tool for Quantum-Enhanced Metrology

S. Gerlich[*1], **Y.Y. Fein**[1], **S. Pedalino**[1] **F. Kiałka**[1], **Philipp Geyer**[1], **Markus Arndt**[1]
1. Fakultät für Physik, Universität Wien, Boltzmanngasse 5, 1090 Wien, Austria

The Viennese Long-baseline Universal Matter-wave Interferometer (LUMI) has opened new avenues for the exploration of the wave-nature of massive particles. The universality of the grating mechanisms used in LUMI makes it possible to explore, in the same instrument, the quantum behaviour of a large variety of different particles ranging from single atoms to complex molecules, consisting of more than 2000 atoms, with masses of up to 28.000 u and de Broglie wavelengths down to 40 fm [1].

LUMI is sensitive to external forces as small as 10^{-26} N. While this puts high experimental demands on the vibration insulation and, for example, even necessitates compensation of the Coriolis force [2], it also makes LUMI an ideal platform for atomic and molecular metrology applications. The versatile and modular design of the interferometer allows for the introduction of precisely controlled electric and magnetic fields and provides optical access for spectroscopy lasers. The universality of LUMI makes it possible to calibrate these fields to the well known properties of particles such as alkali atoms and to then study the electronic, optical and magnetic properties of a nearly unlimited variety of more complex particles with high precision and in free flight.

We demonstrate the capabilities of LUMI with new precision measurements of the polarizability of the fullerenes C_{60} and C_{70} calibrated to cesium atoms [3], and of dynamically induced susceptibilities of tailored tripeptides [4]. We also study the magnetic properties of aromatic and non-aromatic hydrocarbons [5]. Finally, we present the first measurement of ground-state diamagnetism of isolated neutral atoms and show the isotope dependence of the interference visibility due to the nuclear magnetic moment, thereby demonstrating a new method for isotope selection [6].

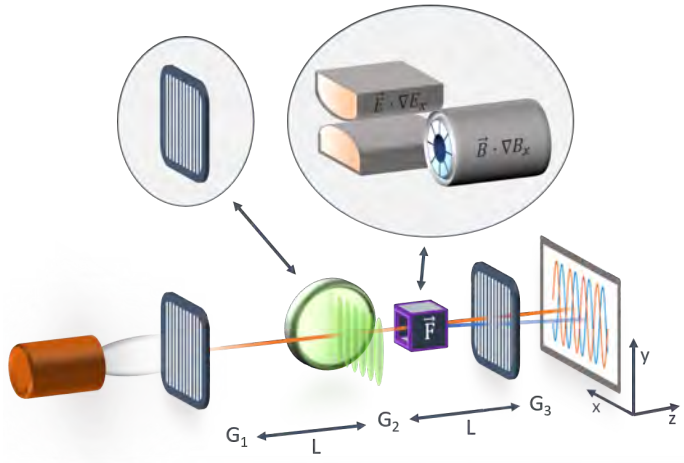

Fig. 1: LUMI is a three-grating, Talbot-Lau-type interferometer with an overall span of 2 m. The central grating G_2 can be toggled between a SiN_x mask, which is preferable for fast particles with low polarizablity such as single atoms and small molecules, and an optical phase grating, which is required for more massive and highly-polarizible particles. Precisely controlled, homogeneous electric and magnetic force-fields can be applied through specially designed electrodes and magnets. Monitoring the resulting shift of the interference pattern with nanometer resolution allows for the detection of forces as small as 10^{-26} N.

References

[1] Y. Fein, P. Geyer, P. Zwick, F. Kiałka, S. Pedalino, M. Mayor, S. Gerlich, M. Arndt, Nat. Phys. **15**, 1242 (2019).
[2] Y. Fein, F. Kiałka, P. Geyer, S. Gerlich, M. Arndt, New J. Phys. **22**, 033013 (2020).
[3] Y. Fein, P. Geyer, F. Kiałka, S. Gerlich, M. Arndt, Phys. Rev. Research **1**, 033158 (2019).
[4] J. Schätti, V. Köhler, M. Mayor, Y.Y. Fein, P. Geyer, L. Mairhofer, S. Gerlich, M. Arndt, J. Mass Spectrom. **55**, e4514 (2020).
[5] Y. Fein, A. Shayeghi, F. Kiałka, P. Geyer, S. Gerlich, M. Arndt, Phys. Chem. Chem. Phys. **22**, 14036 (2020).
[6] Y. Fein, A. Shayeghi, L. Mairhofer, F. Kiałka, P. Rieser, P. Geyer, S. Gerlich, M. Arndt, Phys. Rev. X **10**, 011014 (2020).

*Corresponding author: stefan.gerlich@univie.ac.at

Precision metrology with multi-ion Coulomb crystals

L.S. Dreissen[*1], **D. Kalincev**[1], **C-H. Yeh**[1], **H.A. Fürst**[1,2], **A.P. Kulosa**[1], **T.E. Mehlstäubler**[1,2]
1. Physikalisch-Technische Bundesanstalt, Bundesallee 100, 38116 Braunschweig, Germany
2. Institut für Quantenoptik, Leibniz Universiät Hannover, Welfengarten 1, 30167 Hannover, Germany

Optical clock experiments based on precision spectroscopy of a single trapped ion has become increasingly more accurate over the past decades and enables the search for new physics with high sensitivity [1]. The resolution of these systems is nowadays limited by the poor signal-to-noise ratio of a single ion. Therefore, scaling to 1D ion Coulomb crystals, while preserving the accuracy, is highly desirable. In the field of quantum simulation, scaling to even 2D or 3D systems is becoming more realistic and enables simulations of more complex Hamiltonians [2]. We have investigated motional effects in ion Coulomb crystals and calculated the influence of these effects on precision spectroscopy and coherent manipulation of higher dimensional systems [3]. By characterizing motional heating in linear chains of ions especially under the influence of the radio-frequency (rf) trapping field, we were able to extrapolate theoretically to 2D and 3D crystals see Fig. 1(a)), where exposure to high rf fields is inevitable. We further calculated time dilation shifts and thermal decoherence effects of each individual ion due to their thermal motion.
With the obtained knowledge on the influence of motional heating, we are performing precision experiments to test local Lorentz invariance (LLI) with trapped $^{172}Yb^{+}$ ions to search for physics beyond the Standard Model. After demonstrating coherent excitation of the highly forbidden electric octupole (E3) transition [4], we are able to exploit the high intrinsic sensitivity to Lorentz violation of the meta-stable ($\tau \approx 6$ years) $^2F_{7/2}$ state [5], where we perform rf spectroscopy of the individual Zeeman sublevels using a composite pulse scheme which suppresses magnetic field noise [6], see Fig. 1 (c). This combination allows us to profit from long interrogation times and enables scaling of the ion number. We are currently working on the first demonstration of this technique with a single Yb^{+} ion, after which we will scale it up to ≈ 10 ions to improve on the current test of LLI [7].

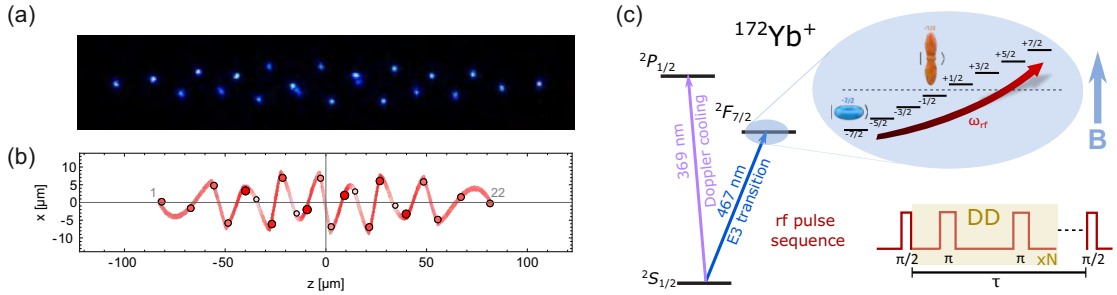

Fig. 1: (a) An image of a 3D 22-ion helix shaped crystal used as an example to calculate motional heating and spectroscopic properties. (b) The simulated ion crystal and a spline to indicate more clearly the helix structure. (c) A simplified energy structure of $^{172}Yb^{+}$ and a zoom-in of the Zeeman sub-levels of the meta-stable $^2F_{7/2}$ state. The wavefunctions of the $m_j=\pm 1/2$ state and the $m_j=\pm 7/2$ are orthogonal and, therefore, Lorentz violation may be observed by detecting the energy splitting while the earth rotates. A composite rf pulse sequence (Dynamical Decoupling) is used to suppress magnetic field noise.

References

[1] M.S. Safranova *et al.*, Rev. Mode. Phys. 90:025008 (2018).
[2] J. Zhang *et al.*, Nature 551(7682):601-604 (2017).
[3] D. Kalincev *et al.*, Accepted for publication in *Quantum Science and Technology* (2021).
[4] H.A. Fürst *et al.*, Phys. Rev. Lett. 125, 163001 (2020).
[5] V.A. Dzuba *et al.*, Nat. Physics 12, 465-468 (2016).
[6] R. Shaniv *et al.*, Phys. Rev. Lett. 120, 103202 (2018).
[7] C. Sanner *et al.*, Nature 567, 204-208 (2019).

*Corresponding author: laura.dreissen@ptb.de

Sensitivity to new physics of isotope-shift studies using forbidden optical transitions of highly charged Ca ions

N.-H. Rehbehn[*1], **M. K. Rosner**[1], **H. Bekker**[1,3], **J. C. Berengut**[1,7], **P. O. Schmidt**[2,8], **S. A. King**[2], **P. Micke**[2,1], **M. F. Gu**[6], **R. Müller**[2,4], **A. Surzhykov**[2,4,5], **J. R. Crespo López-Urrutia**[†1]

1. Max-Planck-Institut für Kernphysik, D–69117 Heidelberg, Germany
2. Physikalisch–Technische Bundesanstalt, D–38116 Braunschweig, Germany
3. Helmholtz-Institut Mainz, Johannes Gutenberg University, D–55128 Mainz, Germany
4. Technische Universität Braunschweig, D–38106 Braunschweig, Germany
5. Laboratory for Emerging Nanometrology Braunschweig, D-38106 Braunschweig, Germany
6. Space Science Laboratory, University of California, Berkeley, CA 94720, USA
7. School of Physics, University of New South Wales, Sydney, New South Wales 2052, Australia
8. Leibniz Universität Hannover, D–30167 Hannover, Germany

Promising atomic-physics based searches (for a recent review, see [1]) for phenomena beyond the current Standard Model (SM) of particle physics are feasible through isotope-shift spectroscopy, which is sensitive to a hypothetical fifth force between the neutrons of the nucleus and the electrons of the shell [2,3]. Such an interaction would be mediated by a new particle, which could in principle be associated with dark matter. In so-called King plots, the mass-scaled frequency shifts of two optical transitions are plotted against each other for a series of isotopes. Subtle deviations from the expected linearity could reveal such a fifth force. Since highly charged ions (HCI) are expected to be most suitable for this purpose [4], we study experimentally and theoretically six forbidden transitions in ions of Ca, an element with five stable isotopes of zero nuclear spin. Some of the transitions are suitable for upcoming high-precision coherent laser spectroscopy and optical clocks. Our results [5] provide a sufficient number of clock transitions which enable an application of the generalized King plot method [6], also in combination with those of singly charged Ca^+ [7,8]. This will allow future high-precision measurements to remove higher-order SM-related nonlinearities and open a new door to yet more sensitive searches for unknown forces and particles. We are currently investigating also optical transitions of Xe HCI. Since this element has an even greater number of stable isotopes with zero nuclear spin than Ca, this will extend the reach of the generalized King plot method [6].

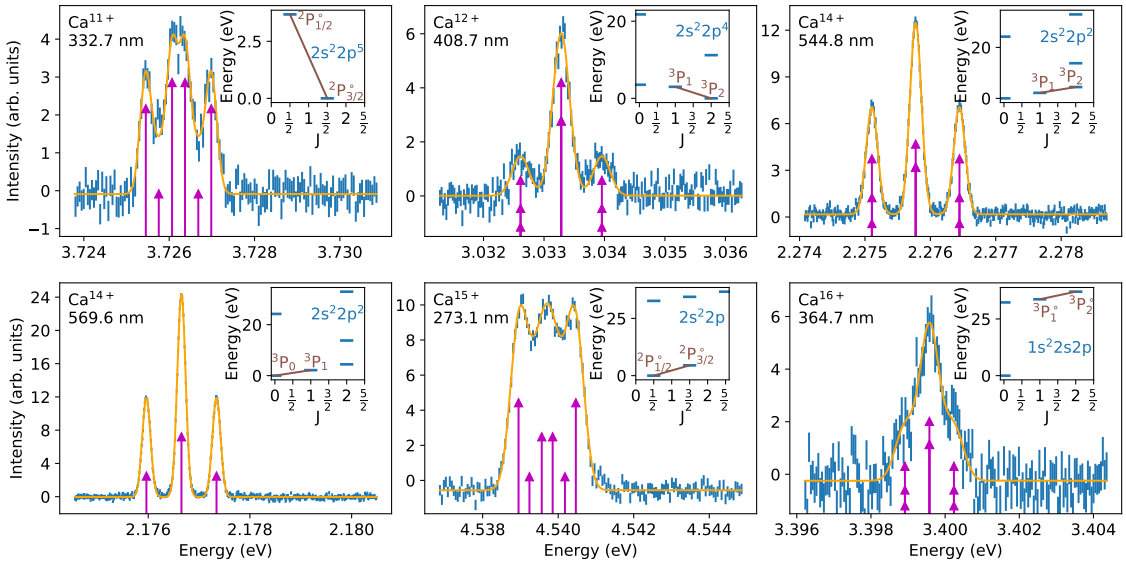

Fig. 1: Fits to the Zeeman components of the studied optical transitions. Magenta arrows mark their positions and relative intensities. The inset shows simplified level diagrams with total angular momentum J [5].

References

[1] M. S. Safronova *et al.*, Rev. Mod. Phys. **90**, 025008 (2018).
[2] C. Delaunay, R. Ozeri, G. Perez, and Y. Soreq, Phys. Rev. D **96**, 093001 (2017).
[3] J. C. Berengut *et al.*, Phys. Rev. Lett. **120**, 091801 (2018).
[4] M. G. Kozlov, M. S. Safronova, J. R. Crespo López-Urrutia, and P. O. Schmidt, Rev. Mod. Phys. **90**, 045005 (2018).
[5] N. -H. Rehbehn *et al.*, Phys. Rev. A **103**, L040801 (2021).
[6] Julian C. Berengut, Cédric Delaunay, Amy Geddes, and Yotam Soreq, Phys. Rev. Res. **2**, 043444 (2020).
[7] C. Solaro *et al.*, Phys. Rev. Lett. **125**, 123003 (2020).
[8] I. Counts *et al.*, Phys. Rev. Lett. **125**, 123002 (2020).

[*]Corresponding author: nils.rehbehn@mpi-hd.mpg.de
[†]Corresponding author: crespojr@mpi-hd.mpg.de

Attosecond Time Shifts in Strong-Field Tunneling Ionization of Atoms by Tailored Laser Pulses

S.V. Popruzhenko[*1], **D.I. Tyurin**[†2]

1. Prokhorov General Physics Institute of the Russian Academy of Sciences, Vavilov Str. 38, Moscow 119991, Russia
2. National Research Nuclear University MEPhI, Kashirskoe Ave. 31, Moscow 115409, Russia

A possibility to experimentally measure the time spent by an electron under the potential barrier during its tunnel ionization from an atom or molecule has remained the subject of active discussions during several past decades (see recent review [1] and references therein). It is now almost generally accepted the this time itself is not an observable and can only be defined within some model and then extracted from the experimentally measurable momentum distribution of photoelectrons. In other words, this value is model-dependent. Notwithstanding that, discussions of different approaches and algorithms for extraction of the tunneling time delay remain in the focus of the strong-field atomic physics, see e.g. [1-5] for an overview.

Models underlying the tunneling time concept in strong-field ionization typically involve pictures based on classical trajectories the electron moves along starting from some spatial point known as the tunnel exit. Within this framework, it is usually assumed that, if no tunnel delay takes place, the electron appears in the continuum with the highest probability at such time instant $t_0 = t_m$ that the absolute value of the electric field $\mathbf{E}(t_m)$ of the laser wave is maximal. The subsequent motion of the electron is dictated by Newton's equation whose solution establishes the mapping $t_0 \to \mathbf{p}$ with $\mathbf{p}$ being the photoelectron momentum in the detector. A high-resolution measurement of the photoelectron distribution allows determining the most probable momentum with an accuracy sufficient to localize the corresponding time t_* of the electron's "birth" within a few attoseconds. If the time instants t_* and t_m appear different, this can be interpreted as a consequence of the delayed electron escape. Within the single-active-electron picture of ionization (explicitly valid for the hydrogen atom and applicable as a good approximation for ionization of complex atoms in low-frequency laser fields) the value of this delay is identified with the time spent under the potential barrier.

In this work, we demonstrate that, regardless of the hypothetical tunneling time delay, a small time shift (of any sign) between the maximum t_m of the electric field amplitude value and the value t_* which can be extracted from position of the momentum distribution maximum, can emerge due to asymmetry of the laser pulse. Using the Strong Field Approximation [6-8] and its interpretation in terms of complex-time trajectories [9] we show that the difference between the two times is

$$\Delta t = t_m - t_* \simeq a\gamma^2/\omega \tag{1}$$

where ω is the laser field frequency, γ is the Keldysh parameter [6,9] and the dimensionless coefficient a depends on the waveform $\mathbf{E}(t)$. In the static-field limit $\gamma \to 0$, $\Delta t \to 0$, and the tunneling proceeds with the highest probability at the field maximum. For some special waveforms including symmetric pulses $\mathbf{E}(t_m + \tau) = \pm\mathbf{E}(t_m - \tau)$ the coefficient $a \equiv 0$ so that $\Delta t = 0$ too. However, in time-dependent fields of arbitrary pulse shape, the shift (1) appears nonzero and can span from a few attoseconds to hundreds of attoseconds, depending on the waveform $\mathbf{E}(t)$ and the Keldysh parameter. We demonstrate the appearance of this shift and numerically investigate its parametric dependence for ionization of hydrogen by a 5-cycle circularly polarized pulse of intensity $\approx 10^{14}$W/cm^2 and wavelength $\lambda = 800$nm and different degrees of asymmetry. For these parameters and the degree of the electric field waveform asymmetry on the level of 10%, the shift (1) appears a few attoseconds, which is comparable to the accuracy of the experimental measurements reported in [5] where no contribution of the tunneling time delay into the offset angle of the momentum distribution has been found.

Similarly to the tunneling time delay, the attosecond time shift (1) is not an observable quantity and therefore it needs a theoretical model for its determination. Obviously, the presence of such shift generates an additional uncertainty in the algorithms aimed at the extraction of the hypothetical tunneling time delay.

References

[1] U. S. Sainadh, R. T. Sang, I. V. Litvinyuk, J. Phys. Phot. **2**, 042002 (2020).
[2] A. S. Landsman and U. Keller, J. Phys. B: At. Mol. Opt. Phys. **47**, 204024 (2014).
[3] L. Torlina, F. Morales, J. Kaushal, *et al.,* Nat. Phys. **11**, 503 (2015).
[4] H. Ni, U. Saalmann, and J.-M. Rost, Phys. Rev. Lett. **117**, 023002 (2016).
[5] U. S. Sainadh, H. Xu, X. Wang, *et al.,* Nature **568**, 75 (2019).
[6] L. V. Keldysh, Zh. Eksp. Teor. Fiz. **47**, 1945 (1964) [Sov. Phys. JETP **20**, 1307 (1965)].
[7] F. H. M. Faisal, J. Phys. B **6**, L89 (1973).
[8] H. R. Reiss, Phys. Rev. A **22**, 1786 (1980).
[9] V. S. Popov Usp. Fiz. Nauk **147**, 921(2004) [Phys. Usp. **47**, 855 (2004)].

[*]Corresponding author: sergey.popruzhenko@gmail.com
[†]Corresponding author: Denisturin1999@yandex.ru

Sympathetic sideband cooling of $^{171}Yb^+$ by $^{88}Sr^+$ for an optical atomic clock

M. Steinel*[1], H. Shao[1], T. Lindvall[2], M. Filzinger[1], N. Huntemann[1], R. Lange[1], B. Lipphardt[1], T. Mehlstäubler[1], Chr. Tamm[1], E. Peik[1]

1. Physikalisch-Technische Bundesanstalt, Bundesallee 100, 38116 Braunschweig, Germany

2. VTT Technical Research Centre of Finland, National Metrology Institute VTT MIKES, P.O. Box 1000, 02044 VTT, Finland

The frequency instability of single-ion optical clocks is fundamentally limited by the spectral resolution that is achieved in the excitation of the reference transition. The achievable resolution is typically limited by the coherence time of the light-atom-interaction. Excitation of highly forbidden reference transitions by ultra-stable lasers permits coherence times in the range of several seconds, so that comparisons between single-ion clocks with statistical uncertainty at the 10^{-18} level appear possible with averaging times of a few hours.

$^{171}Yb^+$ possesses an electric octupole (E3) transition at 467 nm with an excited state lifetime of several years. For second-long laser interrogation pulses, anomalous heating can limit the coherence between the ion and the laser even if it is cooled to its motional ground state initially, and the provided laser coherence time is sufficiently high. Direct laser cooling during spectroscopy is not possible with a single ion, but a co-trapped ion from a different species makes sympathetic cooling possible. Resolved sideband cooling on the clock transition of the ancillary ion removes thermal energy gained by the two-ion crystal during spectroscopy, if all relevant normal modes of the secular motion of the two-ion crystal are addressed.

We choose $^{88}Sr^+$ as our ancillary ion for two major reasons. The $^{88}Sr^+$ clock transition used for sideband cooling is close to the *magic wavelength* where the light shift of the $^{171}Yb^+$ E3 transition is zero. Consequently, the light shift induced by resolved sideband cooling is comparatively low. Secondly, a large contribution to the total uncertainty of the $^{171}Yb^+$ E3 transition stems from black-body radiation (BBR) of the ion environment. The sensitivity of $^{88}Sr^+$ to BBR is well known [2], so it can act as an in-situ sensor for the temperature of its environment, if additional shifts are suppressed [3]. The more accurately known temperature reduces the uncertainty of the BBR shift of the $^{171}Yb^+$ E3 transition. Additionally, the sensitivity of $^{171}Yb^+$ to BBR radiation can also be measured with greater accuracy, if the relative shift for both clock transitions is measured using a strong infrared laser field.

In preparation to the BBR measurements, we performed experiments with $^{171}Yb^+$ and $^{88}Sr^+$ in a linear segmented ion trap based on a stacked design of four printed circuit boards [4]. Doppler cooling and resolved sideband cooling for both species has been observed. The interplay between the Zeeman splitting of $^{88}Sr^+$ and its secular frequencies in the harmonic potential generated by the trapping field imposes limitations on the minimum duration of the sideband cooling pulses. We discuss both pulsed sideband cooling and continous sideband cooling and compare the final temperature, cooling time and ease of use. To find a good combination of cooling pulses on the first and second-order motional sidebands, we employ a simulation of the cooling process and anomalous as well as recoil heating [5]. Finally, we measure the heating rate of the different secular modes and find a large difference between the axial and radial secular modes. We attribute this difference to uncompensated micromotion along the trap axis caused by misalignment of the trap electrodes.

This project 17FUN07 CC4C has received funding from the EMPIR programme co-financed by the Participating States and from the European Union's Horizon 2020 research and innovation programme. The work is also supported by the Deutsche Forschungsgemeinschaft (DFG, German Research Foundation) under CRC 1227 DQ-mat within project B02.

References

[1] D. Kalincev et. al. , *Motional heating of spatially extended ion crystals*, arxiv:2012.10336 [physics.atom-ph] (2020).

[2] P. Dubé et. al. , *High-Accuracy Measurement of the Differential Scalar Polarizability of a $^{88}Sr^+$ Clock Using the Time-Dilation Effect*, Phys. Rev. Lett. 112, 173002 (2014).

[3] K. J. Arnold et al., *Blackbody radiation shift assessment for a lutetium ion clock*, Nature Communications 9, 1650 (2018).

[4] K. Pyka, et. al. , *A high-precision segmented Paul trap with minimized micromotion for an optical multiple-ion clock*, Appl. Phys. B 114, 231 (2014).

[5] Chen et al., *Sympathetic Ground State Cooling and Time-Dilation Shifts in an $^{27}Al^+$ Optical Clock*, Phys. Rev. Lett. 118, 053002 (2017).

*Corresponding author: martin.steinel@ptb.de

The Spectroscopic Observation and Analysis of Bound-Free Transitions to $a^3\Sigma^+$ and $X^1\Sigma^+$ States of KCs

R. Ferber*[1], V. Krumins [1], A. Kruzins [1], M. Tamanis [1], A. Oleynichenko [2,3], A. Zaitsevskii [2,3], E. Pazyuk [2], A. Stolyarov [2],

1. Laser Center, Faculty of Physics, Mathematics and Optometry, University of Latvia, 19 Rainis blvd, Riga LV-1586, Latvia
2. Department of Chemistry, Moscow State University, 119991 Moscow, Leninskie gory 1/3, Russia
3. NRC Kurchatov Institute - PNPI, Orlova Roshcha, Gatchina 188300, Russia

Valuable information about short-range repulsive part of the ground state interatomic potential can be obtained from a scattering experiment and/or observations of bound-free radiative transitions provided the excited state potentials are known well enough. In present study we report on observation and modelling of relative intensity distributions into a continuous oscillation structure of bound-free transitions coming from the excited $(4)1\Sigma^+$ and $c^3\Sigma^+$ states of KCs to the lowest ground $X^1\Sigma^+$ and $a^3\Sigma^+$ states. The Fourier-transform spectrometer Bruker IFS-125HR was used to record the laser-induced fluorescence (LIF) spectra that included both bound-bound and bound-free continuum rovibronic transitions. Fig. 1a presents a $c^3\Sigma^+ \rightarrow a^3\Sigma^+$ LIF spectrum from the upper rovibronic level $v' = 27$, $N' = 48$ induced by a Ti:Sapphire laser Equinox/SolsTis (MSquared). The a-state potential used for spectrum simulation (red curve in Fig.1a) is presented in Fig. 1b, see dotted curve, along with previous potentials from Refs. [1,2]; information on the $c^3\Sigma^+$ potential from [3] was used.

The probe of the repulsive part of the ground singlet $X^1\Sigma^+$ state potential of KCs above the dissociation limit was based on the observation of bound-free transitions in the $(4)^1\Sigma^+ \rightarrow X^1\Sigma^+$ LIF spectra excited with a single-mode dye laser Coherent 699-21, see Fig. 1c. The $(4)^1\Sigma^+$ state has been experimentally studied in [4,5], hence, its spectroscopic properties are well known, including the adiabatic potential energy curve. According to Ref. [4] the bound-free transitions from the $(4)^1\Sigma^+$ state can be observed at excitation of high vibrational levels, $v' > 44$. To achieve a high contrast of the bound-free signal the upper rovibronic levels with low rotational quantum number J' were selected. The spin-allowed $(4)^1\Sigma^+ \rightarrow X^1\Sigma^+$, $c^3\Sigma^+ \rightarrow a^3\Sigma^+$ and spin-forbidden $(4)^1\Sigma^+ \rightarrow a^3\Sigma^+$ transition dipole moments required for the simulation of the observed spectra were obtained in the framework of fully relativistic multi-reference coupled cluster calculation [6].

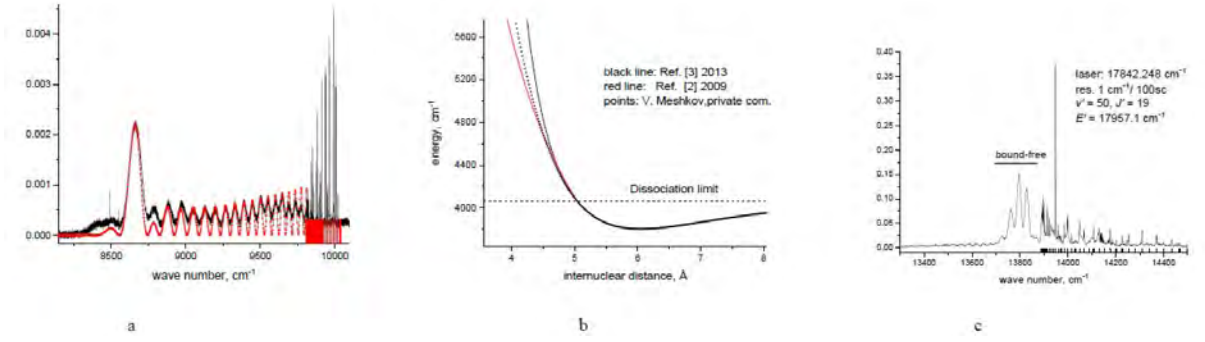

Fig. 1: a - $c^3\Sigma^+ \rightarrow a^3\Sigma^+$ spectrum, b - $a^3\Sigma^+$ state potentials, c - $(4)^1\Sigma^+ \rightarrow X^1\Sigma^+$ and $(4)^1\Sigma^+ \rightarrow a^3\Sigma^+$ spectra.

References

[1] R. Ferber *et al.*, Phys. Rev. A **80**, 062501 (2009).
[2] R. Ferber*et al.*, Phys. Rev. A **88**, 012516 (2013).
[3] J. Szczepkovski *et al.*, JQSRT **204**, 133 (2018).
[4] L. Busevica *et al.*, J. Chem. Phys. **134**, 104307 (2011).
[5] I. Klincare *et al.*, Phys. Rev. A **85**, 062520 (2012).
[6] A. Zaitsevskii *et al.*, Phys. Rev. A **96**, 022516 (2017).

*Corresponding author: ruvins.ferbers@lu.lv

Multiconfiguration Dirac–Hartree–Fock radiative data for emission lines in Ce II–IV ions and cerium opacity calculations for kilonovae

H. Carvajal Gallego[*1], **P. Palmeri**[1], **P. Quinet**[1,2]
1. Physique Atomique et Astrophysique, Université de Mons, 7000 Mons, Belgium
2. IPNAS, Université de Liège, 4000 Liège, Belgium

Large-scale calculations of atomic structures and radiative properties have been carried out for singly, doubly, and trebly ionized cerium. For this purpose, the purely relativistic multiconfiguration Dirac–Hartree–Fock (MCDHF) method [1-4] was used, taking into account the effects of valence–valence (VV) and core–valence (CV) electronic correlations in detail. The results obtained were then used to calculate the expansion opacities characterizing the kilonovae observed as a result of neutron star mergers. Comparisons with previously published experimental and theoretical studies have shown that the results presented in this work are the most complete currently available, in terms of quantity and quality, concerning the atomic data and monochromatic opacities for Ce II, Ce III, and Ce IV ions.

In order to obtain atomic parameters as reliable as possible, different physical models including VV and CV correlations were considered in a systematic and progressive manner for each ion. The quality of the results obtained could be highlighted thanks to the convergence of the parameters calculated from the different theoretical models and also thanks to the good agreement observed by comparing the theoretical energy levels with the available experimental data [5], the deviation being generally of the order of a few percent. This allowed us to determine a new set of reliable transition probabilities and oscillator strengths for a large amount of spectral lines in Ce II, Ce III, and Ce IV, that were then used to calculate astrophysical opacities in the context of kilonovae.

More precisely, the atomic parameters obtained in this work for 30194 electric dipole (E1) transitions in Ce II, 77044 E1 transitions in Ce III, and 37 E1 transitions in Ce IV, were used to compute expansion opacities required for radiative transfer simulations of kilonovae, radioactively powered by electromagnetic emission from neutron star mergers. Our results were compared with data deduced from transition rates previously published, such as those compiled in the DREAM database [6,7]. The latter being systematically based on a much smaller number of lines and on less elaborate theoretical approaches than the one adopted in our investigation, we can conclude that the present work constitutes a substantial and reliable contribution to the study of opacities affecting the emission spectra of kilonovae produced during neutron star mergers.

References

[1] I.P. Grant, *Relativistic Quantum Theory of Atoms and Molecules* (Springer-Verlag, Berlin, 2007).
[2] P. Jönsson, G. Gaigalas, J. Biéron, C. Froese Fischer and I.P. Grant, Comput. Phys. Commun. **184**, 2197 (2013).
[3] C. Froese Fischer, M. Godefroid, T. Brage, P. Jönsson and G. Gaigalas, J. Phys. B : At. Mol. Opt. Phys. **49**, 182004 (2016).
[4] C. Froese Fischer, G. Gaigalas, P. Jönsson and J. Biéron, Comput. Phys. Commun. **237**, 184 (2019).
[5] A. Kramida, Yu. Ralchenko, J. Reader and NIST ASD Team, https://physics.nist.gov/asd (accessed Januray 2020).
[6] https://hosting.umons.ac.be/html/agif/databases/dream.html (accessed January 2020).
[7] P. Quinet and P. Palmeri, Atoms **8**, 18 (2020).

[*]Corresponding author: Helena.CarvajalGallego@umons.ac.be

Detection of low electron densities in atmospheric pressure plasma jet by laser induced avalanche ionisation

D. Popović[*1,2], **D. Maletić**[1,3], **A. Opančar**[4], **S. Milošević**[1]

1. Institute of Physics, Bijenička c. 46, 10000 Zagreb, Croatia
2. Jožef Stefan Institute, Jamova c. 39, 1000 Ljubljana, Slovenia
3. Institute of Physics, University of Belgrade, Pregrevica 118, 11080 Belgrade, Serbia
4. Department of Physics, University of Zagreb, Bijenička c. 32, 39, 10000 Zagreb, Croatia

The electron density in low-temperature non-equilibrium plasmas can easily get below the detection limit of standard detection techniques such as Thomson scattering, laser interferometry, or optical emission spectroscopy (Stark width measurement). Measuring the low electron densities is especially important in case of repetitive discharges, when residual electrons from previous discharge affect the initiation of the next one.

Here we present the principles of using laser induced avalanche ionisation to measure low density of electrons in a helium atmospheric pressure plasma jet, from 10^{13} cm^{-3} down to 10^{7} cm^{-3}, using Nd:YAG laser with 4 ns pulse duration, at 1064 nm [1] and 5 Hz repetition rate. Similar technique can be used for remote detection of radioactive sources, but with mid-IR (3.9 μm) picosecond laser [2]. The few electrons present in the laser focal volume are accelerated and collide with the gas atoms leading to electron avalanche and gas breakdown. This way the initial electron density, too low to measure, increases to a value above the detection limit of standard techniques. The only problem left then is tracing back the process with a good enough model.

The plasma source used was set at the pulse repetition rate of 10 kHz, pulse width of 10 μs, and amplitude of 4 kV. We present results obtained by optical emission spectroscopy of the laser plasma. The plasma jet and the laser plasma are shown in the Fig. 1. The initial electron density is controlled by changing the time delay between the laser pulse and voltage pulse. This way we can obtain the time evolution of the electron density in the plasma jet.

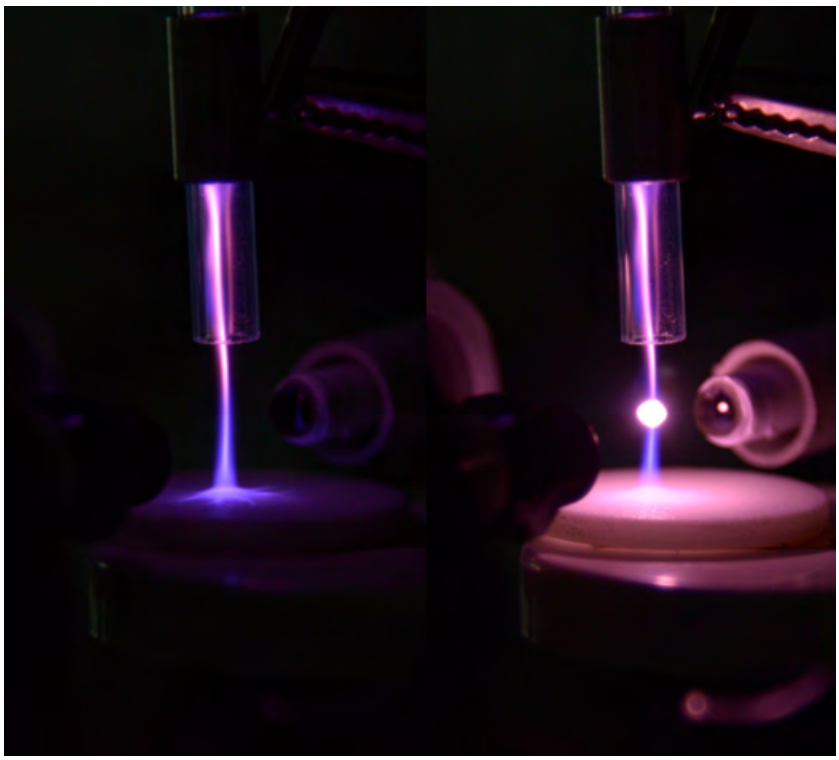

Fig. 1: A photo of an atmospheric pressure plasma jet (left) and the laser plasma (right) when a laser is focused in the plasma jet (laser in sync with the discharge).

References

[1] D. Popović, M. Bišćan and S. Milošević, Plasma Sources Sci. Technol. **28**, 055009 (2019).
[2] D. Woodbury, R. M. Schwarz and H. M. Milchberg, Optica **6**, 811-820 (2019).

*Corresponding author: dpopovic@ifs.hr

Ion-dipole and ion-quadrupole interaction effects in ion-molecule reactions at collisional energies $E_{\mathrm{coll}}/k_{\mathrm{B}}$ between 0 and 40 K.

V. Zhelyazkova[1], **F. B. V. Martins**[1], **J. A. Agner**[1], **H. Schmutz**[1], **and F. Merkt**[1]
1. Laboratory of Physical Chemistry, ETH Zürich, CH-8093, Zürich, Switzerland

Ion-molecule reactions are a class of barrierless, exothermic reactions which are important for the synthesis of molecules in the interstellar medium [1]. These reactions proceed with high rate coefficients even at low temperatures and are usually modelled by the classical Langevin model. The Langevin rate coefficient, k_{L}, is temperature-independent and given by: $k_L = \sqrt{\pi\alpha' q^2/(\varepsilon_0\mu)}$, where α' is the polarizability volume of the molecule, q is the ionic charge and μ is the ion-molecule reduced mass.

Ion-molecule reactions are challenging to study at temperatures below 10 K because of stray-electric-fields-induced heating of the ions and space-charge effects. In the recent years, a new experimental technique, based on replacing the ion with an atom or molecule in a Rydberg state, has made it possible to study the corresponding ion-molecule reactions at temperatures as low as 100 mK [2-5]. This method relies on using a surface-deflector to merge a supersonic beam of Rydberg atoms or molecules with a supersonic beam of ground state (GS) molecules. The ion-molecule reaction takes place within the orbit of the Rydberg electron, and is not affected by it. By tuning the relative velocity of the two beams, v_{rel}, one can vary the collisional energy of the reaction $E_{\mathrm{coll}} = \mu v_{\mathrm{rel}}^2/2$, in the centre-of-mass reference frame.

We present experimental and theoretical studies of reactions involving Rydberg helium [He(n)] and simple molecules. The helium atoms are excited to a low-field-seeking Rydberg-Stark state, with a principal quantum number $n = 30$, and deflected and merged with the GS supersonic beam using a curved surface-electrode Rydberg-Stark decelerator. The merged beams enter a time-of-flight mass spectrometer in which the formed product ions are extracted and detected with a microchannel plate (MCP) detector. We monitor the product-ion yield as a function of the He(n) velocity with the GS beam velocity kept constant. The results of these measurements for the $\mathrm{He}(n) + \mathrm{ND_3}$ and $\mathrm{He}(n) + \mathrm{N_2}$ reactions are displayed in Fig. 1 (a) and (b), respectively.

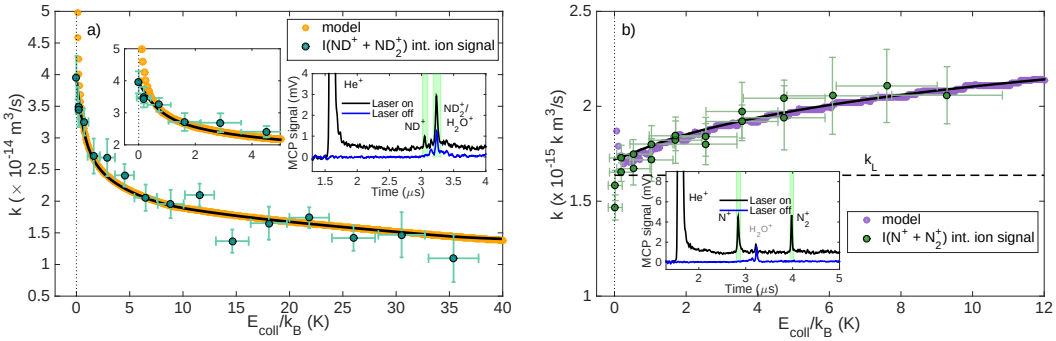

Fig. 1: Experimentally measured (green circles) and modelled (orange and purple circles and black curves) total product ion yields of the $\mathrm{He}^+ + \mathrm{ND_3}$ (a) and $\mathrm{He}^+ + \mathrm{N_2}$ (b) reactions versus collisional energy. Displayed in the insets are the mass-resolved ion-product traces recorded with the MCP at $E_{\mathrm{coll}}/k_{\mathrm{B}} \approx 1$ K.

The measured total product yields, I, display a significant dependence on the collisional energy, E_{coll}, when the molecule has a permanent dipole or quadrupole moments. With decreasing E_{coll}, we observe a significant increase of I in the case of a molecule with a permanent dipole moment μ_{el} (e.g., ammonia, $\mu_{\mathrm{el}} = 1.468$ D), and a pronounced suppression of I in the case of a molecule with a negative Q_{zz} component of the quadrupole moment (e.g., $\mathrm{N_2}$, $Q_{zz} = -1.036$ a.u.). We calculate the reaction rate coefficients using a capture model that includes the rotational-state-dependent energy shift of the molecule in the electric field of the He^+ ion and average over the rotational state population distribution in the supersonic source, including nuclear spin statistics effects. The agreement between the experimental data and the model is very good for a number of molecules: $\mathrm{CH_3F}$ [4], $\mathrm{NH_3}$, $\mathrm{ND_3}$, $\mathrm{N_2}$ and CO. The observed significant deviation from the Langevin model is attributed to the locking of the molecular angular momentum at low collisional energies [6].

References

[1] D. Smith, Chem. Rev. **92**, 1473 (1992).
[2] P. Allmendinger, J. Deiglmayr, O. Schullian, K. Höveler, J. A. Agner, H. Schmutz, and F. Merkt, Chem. Phys. Chem. **17**, 3596 (2016).
[3] P. Allmendinger, J. Deiglmayr, K. Höveler, O. Schullian, and F. Merkt, J. Chem. Phys. **145**, 244316 (2016).
[4] V. Zhelyazkova, F. B. V. Martins, J. A. Agner, H. Schmutz, and F. Merkt, Phys. Rev. Lett. **125**, 263401 (2020).
[5] K. Höveler, J. Deiglmayr, J. A. Agner, H. Schmutz, and F. Merkt, Phys. Chem. Chem. Phys. **23**, 2676 (2021).
[6] J. Troe, Chem. Phys. **87**, 2773 (1987).

An alternative method for determination of hardness based on LIBS

J. Petrovic[*1], **S. Zivkovic**[1], **M. Radenkovic**[1], **J. Ciganovic**[1], **I. Cvijovic Alagic**[1], **M. Momcilovic**[†1]
1. Vinča Institute of Nuclear Sciences – National Institute of the Republic of Serbia, University of Belgrade, P.O.B. 522, 11001, Belgrade, Serbia

In various industrial and metallurgical applications it is necessary to determine the mechanical properties of materials. One of the most important material characteristics is its hardness. An alternative Laser Induced Breakdown Spectroscopy (LIBS) setup based on the TEA CO_2 laser was used to examine different sets of samples: cast iron, aluminum alloys and lead glass.[1,2] The standard method for measuring hardness uses the Vickers test, which is defined by the ratio of the injected force applied and the surface area of the resulting impression. The instrument used for the measurement imposes specific conditions on the samples, such as the surface treatment and the dimensions of the sample, which limits the application for in situ measurement. On the other hand, the LIBS technique has the ability to measure the hardness of samples on the site as well as those that are remote, without previous complex sample preparation. Samples were analyzed to establish the correlation between surface hardness and the ratio of ionic and atomic emission lines induced by laser irradiation. The work of various researchers confirmed that the values of the intensity of emission lines can be correlated with the hardness of the samples. This connection originates from the speed of the shock wave that occurs during the interaction of laser radiation and the target. In the interaction, plasma expansion and a large number of collisions of constituents in the plasma occur, which increases the number of ionized species. This correlation depends on the role of the laser shock wave on the ionization rate of the ablated target atomic material.

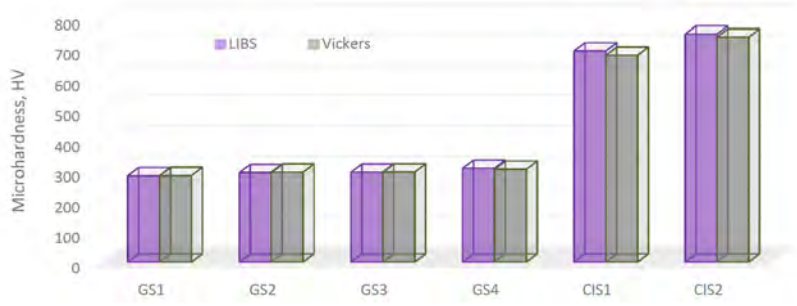

Fig. 1: Comparison of LIBS and Vickers method. Determination of microhardness of glass (GS1, GS2, GS, GS4) and cast iron (CIS1, CIS2) samples using LIBS and standard Vickers method.

Proflometric measurements were used to confirm that the LIBS method does minimal damage to the target and is almost nondestructive for the investigated materials. The results obtained in two different studies [1,2] have successfully demonstrated applications of the TEA CO_2 laser based LIBS setup for testing the hardness of materials (Figure 1.).

Acknowledgements
The research was funded by the Ministry of Education, Science and Technological Development of the Republic of Serbia (451-03-9/2021-14/200017).

References
[1] M. Momcilovic, S. Zivkovic, J. Petrovic, I. Cvijovic-Alagic, J. Ciganovic, An original LIBS system based on TEA CO 2 laser as a tool for determination of glass surface hardness. Applied Physics B, **125**(11), 2019, pp.1-7.
[2] M. Momcilovic, J. Petrovic, J. Ciganovic, I. Cvijovic-Alagic, F. Koldzic, S. Zivkovic, Laser-Induced Plasma as a Method for the Metallic Materials Hardness Estimation: An Alternative Approach. Plasma Chemistry and Plasma Processing, **40**(2), 2020, pp.499-510.

[*]Corresponding author: jpetrovic@vinca.rs
[†]Corresponding author: milos@vinca.rs

A Constrained Fermionic Dynamics study of near Ground state properties and Isospin Symmetry of the Nuclear Systems

T. Depastas[*1], **G.A. Souliotis**[†1], **K. Palli**[1], **M. Veselsky**[2], **H. Zheng**[3,4], **A. Bonasera**[3,4]

1. Institute of Physics, Bijenička c. 46, 10000 Zagreb, Croatia

2. Institute of Experimental and Applied Physics, Czech Technical University, Prague, Czech Republic

3. Cyclotron Institute, Texas A&M University, College Station, Texas, USA

4. Laboratori Nazionali del Sud, INFN, Catania, Italy

The nuclear interaction is one of the most fascinating and complicated forces in nature, as it results from the yet not completely studied strong nuclear correlations of quarks and gluons. The nuclear N-body problem has been studied at various levels of theory ranging from microscopic effective QCD Lagrangians to hydrodynamical models [1]. In the present work, we employed the CoMD (Constrained Molecular Dynamics) model that provides an approximate solution to the nuclear dynamics problem through the Time Dependent Variational Principle leading to Hamiltonian equations of motion [2]. The total nuclear wavefunction is taken as a direct product of one-body nucleonic wavefunctions, parametrised as Gaussian wavepackets. The fermionic character of the nucleons is taken into account with a constraint of the available phase-space.

For the solution of the equations of motion, the initial configuration of nucleons is required. The configuration space is obtained via a Simulated-Annealing algorithm and its characteristics depend heavily on the parameters of the effective interaction. We studied the effects of these parameters and developed a process for global optimisation of a configuration based upon its binding energy, rms radius, average density and average phase space occupation fraction.

In parallel, we studied the Giant Dipole Resonance (GDR) which is one of the most interesting phenomena of low energy nuclear dynamics. This resonance mode consists of an off-phase oscillation of neutrons against the protons. In our study, we developed a theoretical treatment of GDR based on the CoMD formalism. The effect of the parameters of the effective interaction to the GDR characteristics were studied. Additionally, we calculated the GDR spectra for the optimised configurations of several nuclei. We plan to systematically study the characteristic energy and the width of the GDR peak across the nuclear chart with the goal of obtaining stringent constraints of the nuclear equation of state [2],[3].

Finally we have studied the possible isospin symmetry breaking (ISB)[4] of the near ground state properties of several isobaric and isotopic chains. Following the theory of s=1/2 spin, the eigenvalues of Isospin operators characterise the type of the nucleon. A neutron has +1/2 third projection eigenvalue, while a proton has a -1/2. Specifically, we calculated variation of the GDR spectrum's characteristics, binding energies and neutron skins as a function of the isospin. The calculations were accompanied by an extension of the theoretical GDR description. We conclude that the approximate isospin symmetry is broken both explicitly and spontaneously near the drip lines.

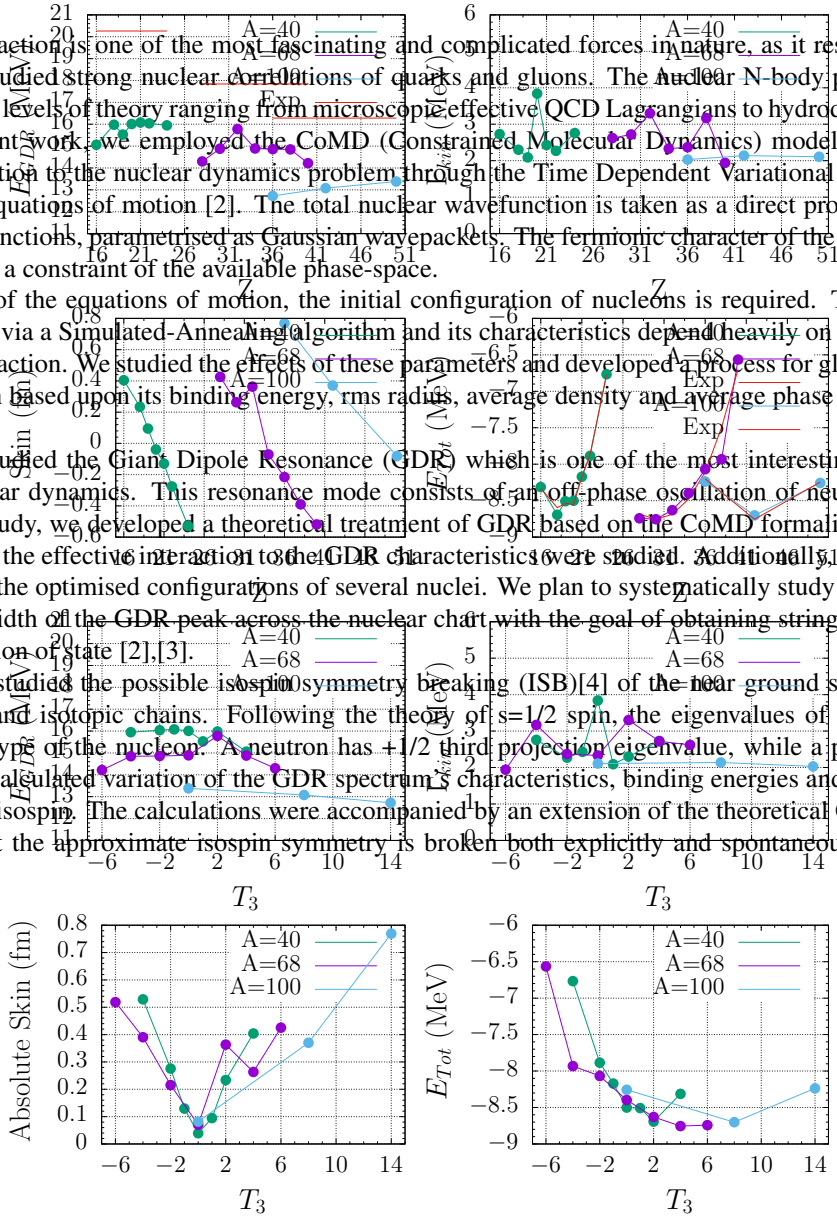

Fig. 1: Near ground state properties as a function of Isospin 3^{rd} projection quantum number (τ_3). The left pannel presents the variation of the absolute value of neuron skin and the right panel of the total (binding) energy. The green curve correspsonds to the $A = 40$, the purple to the $A = 68$ and the cyan for the $A = 100$ isobar.

References

[1] R. Wang, Z. Zhang, L.W. Chen, C.M. Ko, Y.G. Ma Phys. Let. B **807**, 135532 (2020).
[2] M. Papa, T. Maruyama, A. Bonasera Phys. Rev. C **64**, 024612 (2001).
[3] G. Giuliani, H. Zheng, A. Bonasera Prog in Part and Nuc Phys **76**, 116-164 (2014).
[4] D.E. Hoff *et al.* Nature **850**, 52 (2020).

[*]Corresponding author: tdepastas@chem.uoa.gr
[†]Corresponding author: soulioti@chem.oua.gr

A new end-station for synchrotron spectroscopy of helium droplets reveals interatomic Coulombic decay on a Fano resonance

B. Bastian[*1], **J. D. Asmussen**[1], **L. B. Ltaief**[1], **M. Mudrich**[†1]
1. Department of Physics and Astronomy, Aarhus University, Ny Munkegade 120, 8000 Aarhus C, Denmark

Helium nanodroplets (HND) offer a unique environment for fundamental studies of superfluid helium and quantum liquids [1] and as a cold matrix for studies on chemical reactions or high resolution spectroscopy of embedded atoms and clusters [2]. The energy dependent absorption coefficient gives basic insight into the nature of He droplets [3]. Photoelectron-photoion coincidence measurements in the 60 eV photon energy range have revealed Fano resonances that are broadened and shifted with respect to the atomic lines [4]. Measuring electron spectra of He nanodroplets furthermore permits to disentangle different nonlocal electronic decay processes. One example is the interatomic Coulombic decay (ICD) process

$$2\,\mathrm{He} + h\nu \longrightarrow \mathrm{He} + \mathrm{He}^{+*} + \mathrm{e}^-_{\mathrm{sat}} \longrightarrow \mathrm{He}^+ + \mathrm{He}^+ + \mathrm{e}^-_{\mathrm{sat}} + \mathrm{e}^-_{\mathrm{ICD}}$$

that has been observed after ionizing and exciting a He atom in a droplet [5]. Here, we present a new end-station for the AMOLine of the ASTRID2 synchrotron in Aarhus. It combines a HND source with different doping options and a combined velocity map imaging (VMI) and time-of-flight spectrometer for coincidence electron spectroscopy. First experiments have evidenced a recently predicted ICD process [6] at the Fano resonance at 60.3 eV photon energy.

The combination of a helium droplet source with two chambers for gas doping or oven cells allows to pick up a range of different dopants. More flexibility can be obtained with the future options of a water cluster source or a seeded supersonic expansion. The setup is installed as a new end-station for the undulator of the AMOLine that gives access to photon energies from 5 eV to 150 eV [7]. The spectrometer with a delay line detector allows to record coincidence and multi-coincidence spectra of electron (in coincidence with ions) or ion kinetic energies. Electrons up to 90 eV kinetic energy are detected with an optimal energy resolution reaching $\Delta E/E = 1\,\%$.

First results for electron spectra at the 60.3 eV Fano resonance are presented in Fig. 1. Integrated peak intensities are shown on the right hand side. At the resonance, the 36 eV photoline from direct $\mathrm{He} + h\nu \longrightarrow \mathrm{He}^+$ ionization is suppressed and the appearance of a low energy peak near 15 eV is indicative for the ICD process

$$2\,\mathrm{He} + h\nu \longrightarrow \mathrm{He} + \mathrm{He}^{**}(2s2p+) \longrightarrow \mathrm{He}^+ + \mathrm{He}^* + \mathrm{e}^-_{\mathrm{ICD}}.$$

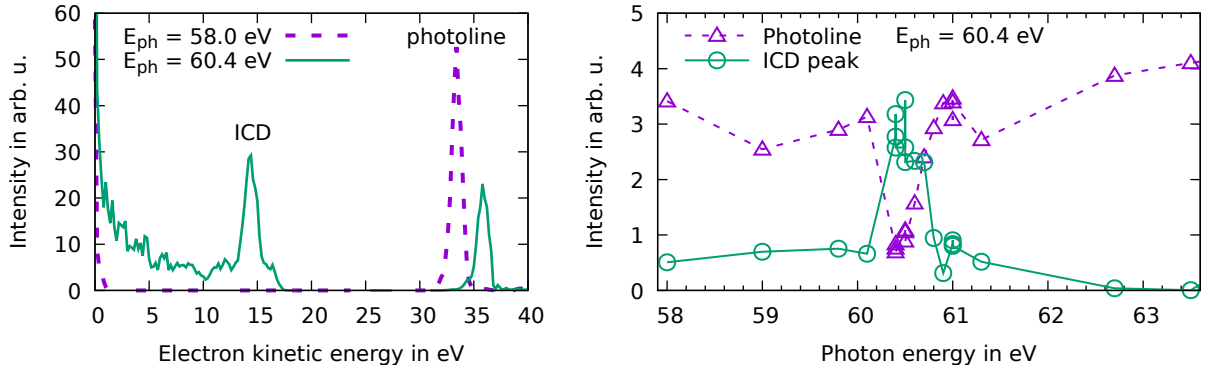

Fig. 1: Electron kinetic energy spectra in coincidence with He^+ and integrated intensities as a function of photon energy. Helium droplets were formed with a stagnation pressure of 30 bar and nozzle temperatures of 14 K (left) and 12 K (right).

References

[1] M. P. Ziemkiewicz, D. M. Neumark, O. Gessner, Int. Rev. Phys. Chem., **34:2**, 239 (2015).
[2] J. P. Toennies, A. F. Vilesov, Angewandte Chemie International Edition, **43.20**, 2622 (2004).
[3] M. Joppien, R. Karnbach, T. Möller, Phys. Rev. Lett., **71**, 2654 (1993)
[4] A. C. LaForge *et al.*, Phys. Rev. A, **93**, 050502 (2016)
[5] M. Shcherbinin *et al.*, Phys. Rev. A, **96**, 013407 (2017)
[6] Jabbari, G., Gokhberg, K., Cederbaum, L. S., Chem. Phys. Lett., **754**, 137571 (2020)
[7] `https://www.carlsbergfondet.dk/da/Forskningsaktiviteter/Forskningsprojekter/Andre-forskningsprojekter/Lars-Henrik-Andersen_Ions-Under-Fire`

[*]Corresponding author: bbastian@phys.au.dk
[†]Corresponding author: mudrich@phys.au.dk

Rotational energy relaxation of diatomic molecules in superfluid helium nanodroplets. The case of the HCl, DCl and TCl molecules.

E. Sanchez[*1], **M. Blancafort**[1], **M. González**[†1]
1. Departament de Ciència dels Materials i Química Física and IQTC, University of Barcelona, Martí Franquès 1, 08028 Barcelona, Spain

Superfluid helium nanodroplets (HeNDs; T=0.37 K) can be doped with a wide variety of impurities. The quantum nature of this solvent presents remarkable behaviours, making HeNDs very interesting from both the physical and chemical perspectives [1][2].

HeNDs can be used, for instance, as low-temperature spectroscopic matrices. The low interaction between the solvent and the impurities (atoms or molecules) in combination with their superfluid behaviour render HeNDs very adequate to study the structure of ultra-cold reaction products [3] among other applications.

Hence, it is important to understand how HeNDs affect the relaxation processes of excited molecular or atomic species embedded in them. As in the case of the vibrational relaxation [4], there is only a single theoretical study on the dynamics of rotational relaxation inside HeNDs (H_2 and isotopic variants) [5].

The aim of this work is to **study the effects of HeNDs on the rotational energy relaxation process of the HCl molecule, taking also into account the DCl and TCl isotopic variants**. A hybrid theoretical model is used [6], where the helium is described using time-dependent density functional theory (TDDFT) and the molecule is described using standard quantum mechanics (wave function). The comparison of our results with previous findings of our laboratory regarding the H_2 system [5], which is a faster rotor, has allowed us to investigate the effect of the helium-molecule interaction, rotational energy gap and asymmetry of the molecule on the dynamics. The DCl and TCl isotopic variants have also been included in order to obtain additional insight into the mechanism of the rotational relaxation inside HeNDs.

The relaxation times of HCl, DCl and TCl are much smaller than those of H_2, D_2 and T_2, in accordance with the lower rotational energy gap and stronger interaction with the solvent of the former. Besides, the systems studied here are slower rotors than H_2 and isotopes, thus allowing helium to adapt better to their motion. Moreover, a remarkable **non-monotonic behaviour has been found in the rotational relaxation of the selected molecules** after excitation to the $|j = 1, m_j = 0\rangle$ rotational state.

This work has been supported by the Spanish Ministry of Science, Innovation and Universities (project ref. MDM-2017-0767) and the Autonomous Government of Catalonia (project ref. 2017SGR 348).

References

[1] Toennies J. P., Vilesov A. F., "Superfluid Helium Droplets: A Uniquely Cold Nanomatrix for Molecules and Molecular Complexes", *Angew. Chem. Int. Ed.*, **43**, 2622-2648 (2004).
[2] Yang S., Ellis A. M., "Helium Dorplets: A Chemistry Perspective", *Chem. Soc. Rev.*, **42**, 472-484, (2013).
[3] Franke P. R., Brice J. T., Moradi C. P., Schaefer H. F., Douberly G. E., "Ethyl + O_2 in Helium Nanodroplets: Infrared Spectroscopy of the Ethylperoxy Radical", *J. Phys. Chem. A*, **123**, 3558–3568 (2019).
[4] Vilà A., Paniagua M., González M., "Vibrational Energy Relaxation Dynamics of Diatomic Molecules inside Superfluid Helium Nanodroplets. The Case of the I_2 Molecule", *Phys. Chem. Chem. Phys.*, **20**, 118–130 (2017).
[5] Blancafort-Jorquera M., Vilà A., González M., "Rotational Energy Relaxation Quantum Dynamics of a Diatomic Molecule in a Superfluid Helium Nanodroplet and Study of the Hydrogen Isotopes Case". *Phys. Chem. Chem. Phys.*, **21**, 21007–21021 (2019).
[6] Vilà A., González M., Mayol R., "Photodissociation Dynamics of Homonuclear Diatomic Molecules in Helium Nanodroplets. The Case of $Cl_2@(^4He)_N$". *J. Chem. Theory Comput.*, **11**, 899-906 (2015).

[*]Corresponding author: esancham21@alumnes.ub.edu
[†]Corresponding author: miguel.gonzalez@ub.edu

Photodissociation of Br2 in Superfluid Helium Nanodroplets. Importance of the Recombination Process

A. Vilà[1] **M. González**[*1],
1. Departament de Ciència dels Materials i Química Física and IQTC, University of Barcelona, Spain

The superfluid ^{4}He nanodroplets (HeNDs; T=0.37 K) have opened a very interesting research area from a chemical perspective: chemical reactivity at very low temperature, synthesis of non-stable (in ordinary conditions) molecules and nanoclusters, etc [1,2]. However, although there has been some progress, still little is known on the reaction dynamics of processes involving HeNDs (finite quantum solvent).

Here, we have studied the interesting chemical bond breaking process resulting from the photodissociation of a bromine molecule placed inside a HeND when it is excited from the ground to the B electronic excited state: $Br_2(X) + h\nu \rightarrow Br_2(B) \rightarrow Br + Br^*$. This corresponds to the second photodissociation process in HeNDs that has been investigated theoretically. We have employed a hybrid theoretical method which was previously applied by us to the photodissociation of the related Cl_2 system [3-5]. Thus, a phenomenological time dependent density functional theory (TDDFT) approach has been used to describe the HeND at zero temperature [6], while the diatomic molecule has been treated using standard quantum dynamics (wave packet).

The main dynamic properties have been examined. Thus, we have analyzed the microscopic mechanism, photodissociation probability, velocity distribution of the dissociated atoms (when they are far enough from the HeND), the influence of the nanodroplet size (N=100-1000 helium atoms), etc. These properties have been compared with those of gas phase in order to determine the influence of this finite quantum solvent. Moreover, the results have also been compared with those obtained for the related Cl_2(B) photodissociation in HeND [3,4]. Differing from Cl_2(B), which fully dissociates for the nanodroplet sizes indicated above, the dissociation probability of Br_2(B) is in the range 0.83-0.00 for N=100-1000. This important difference comes from the fact that the Br_2(B) excess of energy with respect to the atomic dissociation is smaller than that for Cl_2(B).

Finally, it should be noticed that the velocity distribution of the dissociated atoms has a strong oscillating character for all the HeNDs examined, as it happens for the Cl_2(B) case. This phenomenon arises from confinement quantum interferences that are generated at the early times of the photodissociation process, which were reported for the first time in HeNDs in references [3,4].

References

[1] Toennies J. P., Vilesov, A., "Superfluid Helium Droplets: A Uniquely Cold Nanomatrix for Molecules and Molecular Complexes", Angew. Chem. Int. Ed., **43**, 2622 (2004).
[2] Yang, S., Ellis, A. M., "Helium Droplets: A Chemical Perspective", Chem. Soc. Rev., **42**, 472 (2013).
[3] Vilà, A., González, M., Mayol, R., "Photodissociation Dynamics of Homonuclear Diatomic Molecules in Helium Nanodroplets. The Case of $Cl_2@(^4He)_N$", J. Chem. Theory Comput., **11**, 899 (2015).
[4] Vilà, A., González, M., Mayol, R., "Quantum Interferences in the Photodissociation of Cl_2(B) in Superfluid Helium Nanodroplets $(^4He)_N$", Phys. Chem. Chem. Phys. **17**, 32241 (2015).
[5] Vilà, A., González, M., "Mass Effects in the Photodissociation of Homonuclear Diatomic Molecules in Helium Nanodroplets. The Inelastic Collision and Viscous Flow Energy Exchange Regimes", Phys. Chem. Chem. Phys., **18**, 27630 (2016).
[6] Dalfovo, F., Lastri, A., Pricaupenko, L., Stringari, S., Treiner, J., "Structural and Dynamical Properties of Superfluid Helium: A Density-Functional Approach", Phys. Rev. B, **52**, 1193 (1995).

*Corresponding author: miguel.gonzalez@ub.edu

Characterization of tin plasma driven by high-energy, 2-µm-wavelength light

L. Behnke[1,2], **R. Schupp**[1] **Z. Bouza**[1,2], **Y. Mostafa**[1,2], **A. Lassise**[1], **L. Poirier**[1,2], **J. Sheil**[1], **Z. Mazzotta**[1], **M. Bayraktar**[3], **W. Ubachs**[1,2], **R. Hoekstra**[1,4], **O. Versolato**[*1,2]

1. Advanced Research Center for Nanolithography, Science Park 106, 1098 XG Amsterdam, The Netherlands

2. Department of Physics and Astronomy, and LaserLaB, Vrije Universiteit, De Boelelaan 1081, 1081 HV Amsterdam, The Netherlands

3. Industrial Focus Group XUV Optics, MESA+ Institute for Nanotechnology, University of Twente, Drienerlolaan 5, 7522 NB Enschede, The Netherlands

4. Zernike Institute for Advanced Materials, University of Groningen, Nijenborgh 4, 9747 AG Groningen, The Netherlands

Tin laser-produced plasmas are used as sources of extreme ultraviolet (EUV) light at 13.5 nm wavelength in nanolithography [1]. Tin plasmas driven by lasers operating at wavelengths of 1 and 10 µm are widely studied with respect to their emission characteristics in the EUV regime. We present experimental data from tin plasmas driven by a 2-µm-wavelength laser operating in the yet-unexplored range between the 1 and 10 µm cases. Plasmas driven by a 2-µm laser provide intermediate plasma densities that help to understand the role of fundamental atomic properties in the generation of usable EUV light.

Comparative studies of tin plasmas driven by lasers of either 1- or 2-µm wavelength are conducted. In these experiments, small droplets of molten Sn are dispensed from a droplet generator inside a vacuum vessel and are irradiated by one of the two drive-lasers. Relevant plasma characteristics such as emission spectra and the emitted in-band energy around 13.5 nm are observed for different target dimensions and laser parameters. The experiments show a significant reduction of spectral line broadening at 13.5 nm in going from 1- to 2-µm drive laser wavelength (λ) under otherwise similar conditions. The change in line broadening is attributed to a near-linear scaling of the relevant plasma mass density with λ^{-1} and thus a corresponding scaling of optical depth at 13.5 nm. The 2-µm-driven plasma with reduced relevant density paired with controllable drive-laser-pulse duration and plasma dimension allows for further detailed studies of the opacity-related broadening that may limit future solid-state-laser driven sources of EUV light. The experiments provide insight into the fundamental atomic opacity limits of converting drive laser light to useful EUV photons.

References

[1] O. O. Versolato, Plasma Sources Sci. Technol. (Topical Review) 28 (2019) 083001

[*]Corresponding author: o.versolato@arcnl.nl

Photocatalytic properties of zinc oxide prepared by thermal degradation of the cellulose template

R.Radičić[*1], **G.Ambrožić**[†2,3]
1. Institute of Physics, Bijenička c. 46, 10000 Zagreb, Croatia
2. University of Rijeka, Department of Physics, Radmile Matejčić 2, 51000 Rijeka, Croatia
3. Center for Micro- and Nano Sciences and Technologies, University of Rijeka, Radmile Matejčić 2, 51000 Rijeka, Croatia

Wastewater pollution with organic dyes has become one of the leading environmental problems. A non-toxic and environmentally friendly method of wastewater treatment is based on the photocatalytic ability of semiconductors such as zinc oxide (ZnO) [1]. ZnO is an II-IV semiconductor that is characterized by excellent optical, electrical, optoelectric, and photochemical properties and has a wide application in photocatalysis, sensors, solar cells, antimicrobial materials, and more [2].

This work aims to prepare, characterize and investigate the photocatalytic properties of hybrid materials based on: 1) cellulose and zinc oxide (ZnO), and 2) ZnO structures obtained by a polymer templated thermal decomposition of the previously prepared ZnO/cellulose hybrids.

We synthesized ZnO on two different cellulose substrates, Sodra Green T and UPM Conifer, using the thermal atomic layer deposition (t-ALD) method. In doing so, we applied standard process conditions for the growth of a 50 nm ZnO film on a silicon substrate. After that, the hybrid materials were calcinated in the programmable furnace to obtain pure ZnO. The samples were characterized using a field emission scanning electron microscope (FE-SEM) and X-ray photoelectron spectroscopy (XPS). In the study of photocatalytic activity of the samples, we used methyl orange (MO) as a model organic pollutant. Changes in the absorbance of the MO solution was monitored using a UV / Vis spectrophotometer.

Our results showed that calcinated samples have a larger active surface area as a result of the formation of solid porous tubular structures. Furthermore, ZnO who was synthesized on Sodra Green T cellulose showed a larger amount of reactive surface OH groups, indicating better photocatalytic activities. After calcination of the hybrid materials, the resulting ZnO showed strong photocatalytic activity. Within 80 min there is complete mineralization and decolorization of MO, while before calcination of samples within 240 min there was no discoloration or mineralization of MO. Also, ZnO deposited on Sodra Green T cellulose proved to be a better photocatalyst than ZnO deposited on UPM Conifer cellulose.

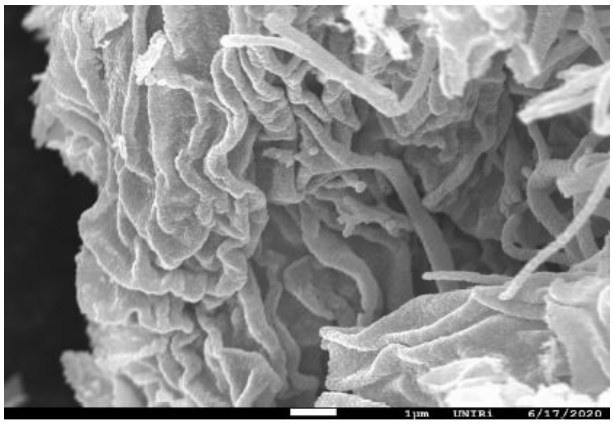

Fig. 1: FE-SEM image of ZnO tubular structures obtained after calcination of ZnO/cellulose hybrid.

References

[1] C. Nie, J. Dong, P. Sun, C. Yan, H. Wu, and B. Wang, RSC Adv., **7**, 36246 (2017).
[2] C. Jagadish and S.J. Pearton, *Zinc Oxide Bulk, Thin Films and Nanostructures: Processing, Properties, and Applications* (Elsevier Science, 2006).

[*]Corresponding author: rradicic@ifs.hr
[†]Corresponding author: gabriela.ambrozic@phy.uniri.hr

TiO_2 nanoparticles synthesized by pulsed laser ablation in water as catalyst in photodegradation of organic pollutants under UV and visible light irradiation

Damjan Blažeka[*1] **Julio Car**[1], **Vedran Kojić**[2], **Andreja Gajović**[2], **Ivana Grčić**[3], **Nikša Krstulović**[1]

1. Institute of Physics, Bijenička cesta 36, 10000 Zagreb, Croatia
2. Rudjer Bošković Institute, Bijenička cesta 54, 10000 Zagreb, Croatia
3. Geotehnički fakultet, Hallerova aleja 7, 42000 Varaždin, Croatia

The pulsed laser ablation in liquid is simple and green method for synthesis of high purity nanoparticles [1]. The Nd:YAG laser at wavelength 1064 nm is used for hitting and ablating the Ti target immersed in water. Interaction between laser pulse (duration 5 ns) and target induces the formation of hot plasma plume above the ablated target, that contains the atoms and ions both from target and surrounding water. The nanoparticles are formed during cooling down of hot plasma plume in the processes of nucleation and condensation. Ablation of Ti target in water leads to formation of colloidal dispersion of TiO_2 nanoparticles. SEM revealed that TiO_2 nanoparticles are spherical and have Log-Normal size-distribution with maximal diameter at 5 nm and XRD has shown that they are amorphous. After heating treatment of the colloidal dispersion, the TiO_2 nanoparticles have crystallized. The photocatalytic tests [2] of non-heated, heated and reference Aeroxide P25 nanoparticles are performed both for UV and visible light. The photodegradation of the Methylene Blue and Diazepam dilluted in the colloidal TiO_2 dispersions is monitored. The crystallized TiO_2 nanoparticles have shown significantly larger photocatalytic efficiency for visible light when compared to amorphous and P25 nanoparticles, while their photocatalytic efficiency for UV light is slightly better than P25 in the photodegradation of Methylene Blue. XPS revealed the significant presence of Ti^{3+} atoms in heated TiO_2 which have positive impact on photocatalytic efficiency.

References

[1] N. Krstulović, K. Salomon, I. Capan and O. Budimlija, Appl. Surf. Sci. 440, 916-925 (2018).
[2] D. Blažeka, J. Car, N. Klobučar, A. Jurov, J. Zavašnik, A. Jagodar, E. Kovačević and N. Krstulović, Materials. 13, 4357 (2020).

Acknowledgments
This research was supported by the Croatian Science Foundation under the project HrZZ - PZS-2019-02-5276

[*]Corresponding author: dblazeka@ifs.hr

Sulphur concentration influence on morphology and optical properties of MoS_2 monolayers

A. Senkić[*1,2,3], **A. Supina**[1,2,3], **J. Bajo**[4], **V. Jadriško**[1,3], **B. Radatović**[1,3], **N. Vujičić**[1,3]
1. Institute of Physics, Bijenička c. 46, 10000 Zagreb, Croatia
2. Department of Physics, University of Rijeka, Ulica Radmile Matejčić 2, 51 000 Rijeka, Croatia
3. Center of Excellence for Advanced Materials and Sensing Devices, Institute of Physics, Bijenička cesta 46, HR-10000 Zagreb, Croatia
4. Department of Applied Physics, KTH Royal Institute of Technology, SE-100 44 Stockholm, Sweden

MoS_2 in its two-dimensional (2D) form is one of the most studied materials in the last decade due to its promising applications in semiconducting industry (photosensors [1], optoelectronics [1], photovoltaics [1] etc.). One of the main approaches in synthesis of semiconducting 2D materials is chemical vapour deposition (CVD) technique, schematically shown in Fig. 1. In this work we have systematically investigated how synthesis parameters (growth temperature T_G, sulphur temperaure T_S and carrier gas flow) influence sample quality. As a result, correlation between synthesis parameters and sample's morphology and optical response were obtained.

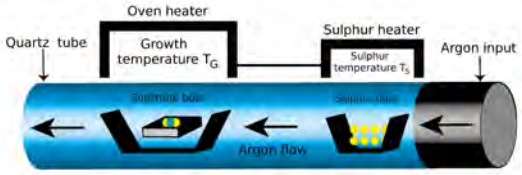

Fig. 1: Schematic illustration for the CVD setup.

By changing mentioned synthesis parameters the Mo:S ratio was consistently tuned which, in turn, modified both morphology and optical response of the sample (Fig. 2). As the ratio is approaching to the ideal value of 1 : 2, the morphology of samples becomes more symmetric, triangular with even edges while the PL and Raman spectra intensities for given sample increase. If the sulphur concentration is increased compared to the ideal stoichiometric ratio, the samples become dendritic with uneven edges and optical response is poor. On the other hand, if the molybdenum concentration is increased by increasing T_G, vertical growth is preferred rather than lateral, and bilayers or multiple-layered islands are formed.

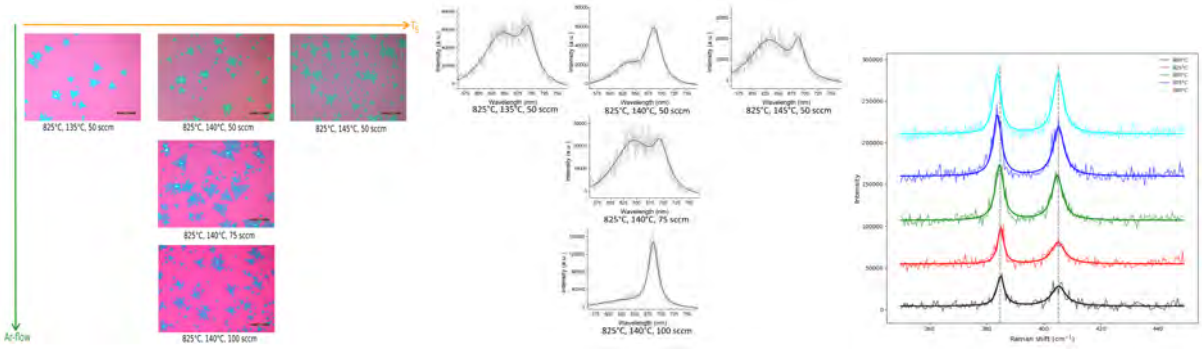

Fig. 2: Left: Morphological evolution of CVD grown MoS_2 islands. Given synthesis parameters are in following order: growth temperature, sulphur temperature, argon flow. Scale bar is 100 μm. Middle: Evolution of photoluminescence spectra of MoS_2 islands. Solid black lines represent non-linear fit using two Lorentzian functions. Right: Raman spectra of samples made at different growth temperatures. Sulphur temperature is 140°C and argon flow 75 sccm. Solid lines represent non-linear fit using two Lorentzian functions. Vertical grey lines are only eye-guides.

Raman spectra of samples grown at different T_G ($800-900$°C) are shown on the right side of Fig. 2. The difference between centres of these two Raman modes increases with the growth temperature increase [2]. One possible explanation for this behaviour is increased induced tensile strain resulting from the high-temperature growth process. Complementary structural characterization by atomic force microscope (AFM) and scanning electron microscope (SEM) were used to determine existence of grain boundaries and cracks in crystal basal plane, showing that optimisation of synthesis parameters leads to high-quality crystal morphology. Our further work will focus on exploring the optical properties of crystals in low-temperature limit.

References

[1] Q.H. Wang, K. Kalantar-Zadeh, A. Kis et al. Nature Nanotech **7**, 699-712 (2012).
[2] Zusong Zhu et al. Mater. Res. Express **6** 095011 (2019).

*Corresponding author: asenkic@ifs.hr

New stringent test of bound-state QED: high-resolution measurement of an intra-shell transition in He-like uranium

R. Loetzsch*[1], H. Beyer[2], U. Spillmann[2], D. Banas[4], P. Dergham[3], L. Duval[5], J. Glorius[2], R. Grisenti[2], A. Gumberidze[2], P.-M. Hillenbrand[2], P. Indelicato[5], Y. Litvinov[2], P. Jagodzinski[4], E. Lamour[3], N. Paul[5], G. Paulus[1,6], N. Petridis[2], M. Scheidel[2], R.S. Sidhu[2], S. Steydli[3], K. Szary[4], S. Trotsenko[2], I. Uschmann[1,6], G. Weber[6], Th. Stöhlker[1,2,6], M. Trassinelli†[3],

1. Institut für Optik und Quantenelektronik, Friedrich-Schiller-Universität Jena, 07743 Jena, Germany
2. GSI Helmholtzzentrum für Schwerionenforschung, 64291 Darmstadt, Germany
3. Institut des NanoSciences de Paris, CNRS, Sorbonne Universités, Paris, France
4. Institute of Physics, Jan Kochanowski University, Kielce, Poland
5. Laboratoire Kastler Brossel, Sorbonne Université, CNRS, ENS-PSL Research Univ., Collége de France, Paris, France
6. Helmholtz-Institut Jena, Jena,Germany

He-like ions, being the simplest multi-body atomic systems, offer the unique possibility to test QED correlation and electron-electron interaction effects. For such a simple system, theory can provide high-accuracy prediction. However, the presence of extremely high electric fields, as for high-Z ions, provides still a significant challenge and different approaches leads to different results. A first attempt to test such contributions has been made in an experiment in 2007 [1]. There, the energy difference between the two $2p_{3/2} \rightarrow 2s_{1/2}$ intra-shell transitions in He-like and Li-like uranium ions was measured. The final accuracy of 1 eV (for 4.5 keV photon energy) was not sufficient to effectively test the theoretical predictions but provided proof that the $[1s_{1/2}, 2p_{3/2}]\ ^3P_2$ state can be populated efficiently in ion-atom collisions.

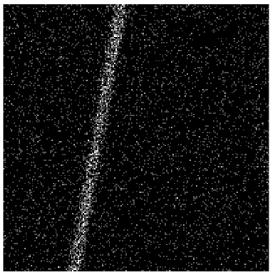

Fig. 1: Position-sensitive detector image of the $2p_{3/2} \rightarrow 2s_{1/2}$ transition in He-like uranium. Dispersion is in the horizontal direction. The slant of the line is caused to the Doppler shift due to the ion kinetic energy of 41 MeV/u.

We present here a new relative measurement of the intra-shell transitions in He- and Li-like uranium with an accuracy gain with respect to the past experiment by more than one order of magnitude. The experiment was conducted at the internal gas jet target of the ESR at GSI. We employed twin spectrometers with two bent Ge(220) crystals, both under 90°observation angle to the ion beam and equipped with X-ray CCDs. By appropriately choosing the ion velocities, the energies of the two transitions ($\sim$ 4509 eV for He-like U and 4459.37 eV for Li-like U) correspond to basically the same X-ray photon energy in the laboratory frame (4319 eV) with a drastic reduction of many systematic effects. A FWHM resolution of $\sim$ 2.7 eV has been obtained, mainly due to the Doppler broadening caused by the finite size of the gas jet. After several days of data acquisition, we collected more than 1000 photons per transition, allowing for a statistical accuracy of about 0.03 eV. To additionally control the systematics in the experiment, we also measured reference lines from a stationary Zn fluorescence target as well as the intra-shell transition from Be-like uranium ions. Preliminary results of the experiment will be given. We aim for an accuracy of $\sim$ 0.2 eV on the absolute energy of the intra-shell transition in He-like uranium, mainly dictated by the accuracy of the Li-like uranium reference line, and of $\sim$ 0.06 eV for the relative measurement between those lines. This will allow for an unmatched test of electron correlation effects and two-loop QED contributions in few electron systems in strong electric fields, which are in the order of 0.8 eV.

This research has been conducted in the frame-work of the SPARC collaboration, experiment E125 of FAIR Phase-0 supported by GSI. It is further supported by the Extreme Matter Institute EMMI and by the European Research Council (ERC) under the European Union's Horizon 2020 research as well as by the innovation pro-gramme (Grant No 682841 "ASTRUm") and the grant agreement n° 6544002, ENSAR2. We acknowledge substantial support by ErUM-FSP APPA (BMBF n° 05P19SJFAA) too.

References

[1] M . Trassinelli, A. Kumar, H.F. Beyer, *et al.*, Eur. Phys. Lett. **87**, 63001 (2009).

*Corresponding author: robert.loetzsch@uni-jena.de
†Corresponding author: martino.trassinelli@insp.jussieu.fr

Kr 3d shake-up photoelectron spectra and angular distributions

M. D. Kiselev[*1,2,3], **A. N. Grum-Grzhimailo**[3]
1. Faculty of Physics, Lomonosov Moscow State University, Moscow 119991, Russia
2. Pacific National University, Khabarovsk 680035, Russia
3. Skobeltsyn Institute of Nuclear Physics, Lomonosov Moscow State University, Moscow 119991, Russia

The advent of X-ray free electron lasers and fourth generation synchrotron radiation sources has given a new impetus to the development of atomic inner shell photoelectron spectroscopy. The complex electron spectra contain many lines due to the shake-up satellites. The shake-up mechanism can be described quantitively only in advanced theoretical models. Bearing in mind future experiments with new brilliant sources of the XUV radiation, we consider 3d-photoionization of Kr, centering on the photon energies from 80 eV to 200 eV and binding energies from 110 eV to 135 eV. The satellite photoelectron spectrum in this region was studied [1], but no information is available so far about photoelectron angular distribution of the satellite lines.

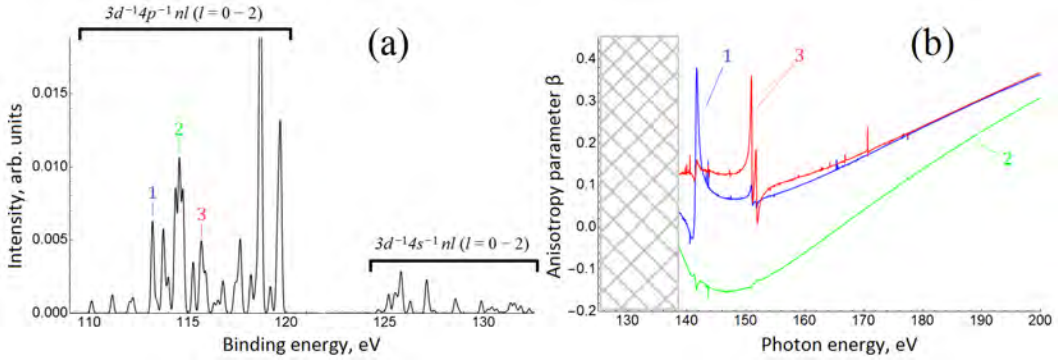

Fig. 1: (a) Photoelectron spectrum calculated for the photon energy of 190 eV. The bandwidth (0.1 eV) of the photon beam and energy resolution of an electron detector (Gaussian with FWHM = 0.15 eV) are taken into account to simulate a potential experiment. The numbers indicate three individual shake-up states with dominant configurations $[Ar]3d^{10}4s^24p^5(^3D)5p\,[^2F_{5/2}]$ (1), $[Ar]3d^{10}4s^24p^5(^1F)5p\,[^2D_{5/2}]$ (2), $[Ar]3d^{10}4s^24p^5(^3D)6p\,[^2D_{5/2}]$ (3). (b) Anisotropy parameters β for the lines 1, 2, and 3 as functions of the photon energy, without the convolution. The shaded area covers the region of autoionizing states with rapid oscillations of β, which are impossible to resolve on the graph.

We consider the reaction (in the dipole approximation)

$$\gamma + Kr([Ar]3d^{10}4s^24p^6) \to Kr^+(\alpha_f J_f) + e(\varepsilon\ell)\,,$$

where ε and ℓ denote photoelectron energy and its orbital momentum, respectively, J_f is the total angular momentum of the residual Kr^+ ion with α_f further identifying its particular state. The photoionization amplitudes were calculated by an R-matrix method with B-splines using the BSR program [2] with partial allowance for the non-orthogonality of electron orbitals and diagonalization of the Breit-Pauli Hamiltonian to take into account relativistic effects. Extensive basis sets included hundreds of configuration state functions leading in total to 627 photoionization channels. The photoelectron angular distributions are of the form

$$W(\theta) = W_0\,[1 + \beta\,P_2(\cos\theta)]\,,$$

where $P_2(x)$ is the Legendre polynomial, θ is the angle determined by the direction of the emitted photoelectron and the polarization vector of the XUV radiation, and β is the anisotropy parameter.

Our typical results are shown in Fig. 1. The photoelectron spectrum is clearly separated into two regions corresponding to $3d^{-1}4p^{-1}nl\,(l=0,1,2)$ and $3d^{-1}4s^{-1}nl\,(l=0,1,2)$ satellites. The lowest states with the binding energies from 110 eV to 113 eV are mostly conjugate shake-up resonances, while the direct (normal) shake-up mechanism dominates the strong lines. The anisotropy parameter for different satellite lines shows in many cases similar behavior as function of the photon energy above 160 eV. More results and their detailed analysis will be presented at the conference.

References

[1] D. J. Bristow, J. S. Tse, and G. M. Bancroft, Phys. Rev. A **25**, 1 (1982).
[2] O. Zatsarinny, Comput. Phys. Commun. **174**, 273 (2006).

*Corresponding author: md.kiselev94@gmail.com

Photoelectron circular dichroism via multiphoton ionization with varying pulse duration

H. Lee[*1], **S. Ranecky**[1], **S. Vasudevan**[1], **N. Ladda**[1], **T. Ring**[1], **T. Rosen**[1], **S. Das**[1], **J. Ghosh**[1], **H. Braun**[1], **D. Reich**[2], **A. Senftleben**[1], **and T. Baumert**[†1]

1. Institute for physics and CINSaT, Universität Kassel, 34132 Kassel, Germany

2. Dahlem Center of Complex Quantum Systems and Department of Physics, Freie Universität Berlin, 14195 Berlin, Germany

Photoelectrons from randomly oriented chiral molecules ionized by circularly polarized light can have an asymmetric momentum distribution with respect to the propagation direction of the laser beam. This effect is called photoelectron circular dichroism (PECD). In this contribution, we studied PECD of a few monoterpenes, such as fenchone, thiofenchone and camphor, by using laser pulses with different time durations from 30 fs to 5 ns. The laser pulses were centered at 380 nm to induce 2+1 resonant-enhanced multiphoton ionization via B- and C-band [1] and photoelectrons from each band were distiguished by different photoelectron energies. As the pulse duration increases, the effect of different relaxation dynamics of B- and C-band were clearly observed as a change of the ratio between photoelectron contributions from B- and C-band. We could model the observed behavior by simplified quantum mechanical model using Lindblad formalism including decoherence and estimate lifetimes of B- and C-band electronic states [2].

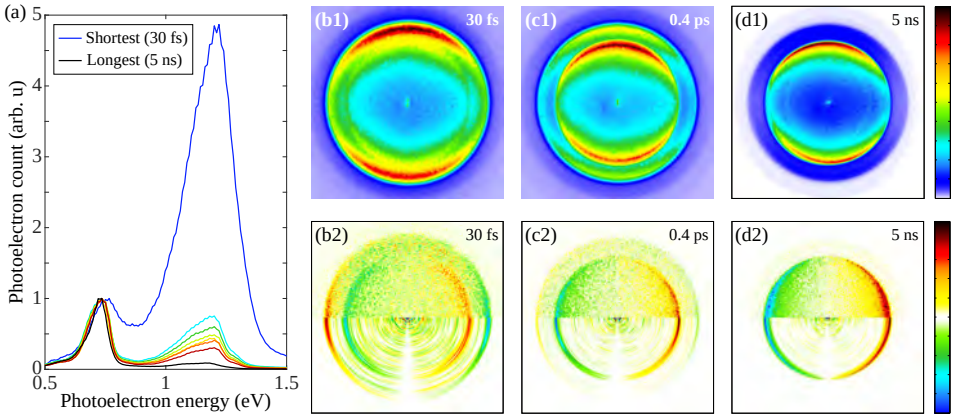

Fig. 1: (a) Photoelectron energy spectrum measured by using pulses with various durations from 30 fs (blue solid line) to 5 ns (black solid line). The peak near 0.75 eV is from the ionization passage through B-band and the other peak near 1.2 eV is from C-band. (b1-d1) Photoelectron angular distributions (PADs) recorded with velocity map imaging (VMI) technique. The propagation direction of the laser pulses is left to right. Each PAD is respectively measured with linearly polarized 30 fs (b1), 0.4 ps (c1) and 5 ns (d1) laser pulses. The inner concentric circle corresponds to the contributions from B-band, and the outer circle corresponds to C-band. The increasing contribution from B-band as well as the decreasing contribution from C-band as functions of the pulse duration are clearly shown. (b2-d2) PECD images from raw data (upper half) and from Abel inverted data (lower half) correspond to pulse durations of 30 fs (b2), 0.4 ps (c2) and 5 ns (d2). First, a PAD measured with left cirularly polarized (LCP) pulse was subtracted from a PAD measured with right circularly polarized (RCP) pulse, to obtain the difference between LCP and RCP PAD. Then anti-symmetrization along the vertical axis was applied to extract and show asymmetric part with respect to the propagation direction of the laser pulses. The asymmetry of C-band contribution fades as the pulse durations becomes longer, while the asymmetry of B-band contribution is always pronounced.

References

[1] A. Kastner et al., J. Chem. Phys. **147**, 013926 (2017)

[2] H. Lee et al., in preparation.

[*]Corresponding author: hgyeol@uni-kassel.de

[†]Corresponding author: tbaumert@uni-kassel.de

From exponentials to power laws and back again

Klavs Hansen[*1]

1. Center for Joint Quantum Studies and Department of Physics, School of Science, Tianjin University, 92 Weijin Road, Tianjin 300072, China

Unimolecular decays provide a very efficient method to determine several parameters of a decaying system when its decay is measured in thermal equilibrium, e.g. the binding energy as extracted from an Arrhenius plot [1] In molecular beams this is approach encounters serious problems caused by the difficulties with control of internal energy distributions. Even energy distributions with a modest width lead to $1/t$ decays, vs. the expected exponential [2],[3]. This in practice prevents determination of the variation of rate constants with the excitation energy and we are seeming at an impasse for clusters and radicals that can not be prepared in a single-species canonical thermal ensemble.

However, it turns out that the non-exponential nature of the power law decay allows the determination of the parameters of rate constants. The method is based on reheating of the system and determining the change in the effective zero time for the reheated component. It therefore makes constructive use of the non-exponential decay rate that caused the problem in the first instance. It is documented is in [4] and will be described in detail in the presentation with thermionic emission from C_{60}^- as a case study, using data from [5]. It will also be demonstrated how the technique allows some spectral information of the radiative cooling to to be extracted from the experimental data in [5].

References

[1] S. Arrhenius, Z. Physik. Chem. **4**, 226 (1889)
[2] K. Hansen, J.U. Andersen, P. Hvelplund, S.P. Møller, U.V. Pedersen, and V.V. Petrunin, Phys. Rev. Lett. **87**, 123401 (2001)
[3] Klavs Hansen, Mass Spectrometry Reviews, 4, (2021) DOI 10.1002/mas.21630
[4] K. Hansen, Phys. Rev. A **102**, 052823 (2020)
[5] A.E.K. Sundén, M. Goto, J. Matsumoto, H. Shiromaru, H. Tanuma, T. Azuma, J.U. Andersen, S.E. Canton, and K.Hansen, Phys. Rev. Lett. **103**, 143001 (2009)

*Corresponding author: klavshansen@tju.edu.cn

Nondipole and channel-interference effects in the case of Kr 4p direct photoionization and 3p/3d Auger decay

L. Ábrók[*1,2], **T. Buhr**[3], **S. Schippers**[3], **Á. Kövér**[1], **A. Müller**[4], **A. Orbán**[1], **S. Ricz**†[1]

1. Institute for Nuclear Research, Hungarian Academy of Sciences (MTA Atomki), H-4001 Debrecen, Hungary
2. Doctoral School of Physics, University of Debrecen, Egyetem sqr. 1, H-4032 Debrecen, Hungary
3. I. Physikalisches Institut, Justus-Liebig-Universität Gießen, 35392 Giessen, Germany
4. Institut für Atom- und Molekülphysik, Justus-Liebig-Universität Gießen, 35392 Giessen, Germany

The description of the photoionization process at low photon energies is mostly limited to the dipole approximation, higher-order terms are usually neglected. However, both theoretical and experimental studies confirmed that first and second-order nondipole terms can affect the angular distributions even at photon energies of a few tens of eV [1]. These effects become important for example in the case of Cooper-minima and autoionization. In the latter case the relaxation process of the excited states, realized through inner electron processes, and the direct photoionization interfere. Thus the different anisotropy parameters can vary strongly within a small photon energy range resulting in notable angular distribution changes.

The angular distributions of Kr 4p photoelectrons were measured in the vicinity of the resonantly excited states of the inner shells 3p and 3d at the synchrotron light source DORIS III in Hamburg, Germany applying linearly polarized light. The ESA-22D electron spectrometer was used to detect the electrons in the polar angular range of 0°-360° [2]. The Kr 3d and 3p shells were excited at around 90 eV [3] and 220 eV [4] photon energy, respectively. The interference of the direct ionization and the participator Auger process was investigated at different photon energies. We have developed a theoretical model and calculated angular differential cross section for the ejected electrons considering higher-order terms (electric dipole, quadrupole and octupole) in the interaction Hamiltonian. In our model we also included the Auger decay based on a simplified two step process. The anisotropy parameters were extracted from the experiments by fitting the theoretical expression including higher-order terms.

Strong photon energy dependence was observed for the anisotropy parameters including forward-backward asymmetry that can only be explained by the presence of the multipole terms (Fig. 1).

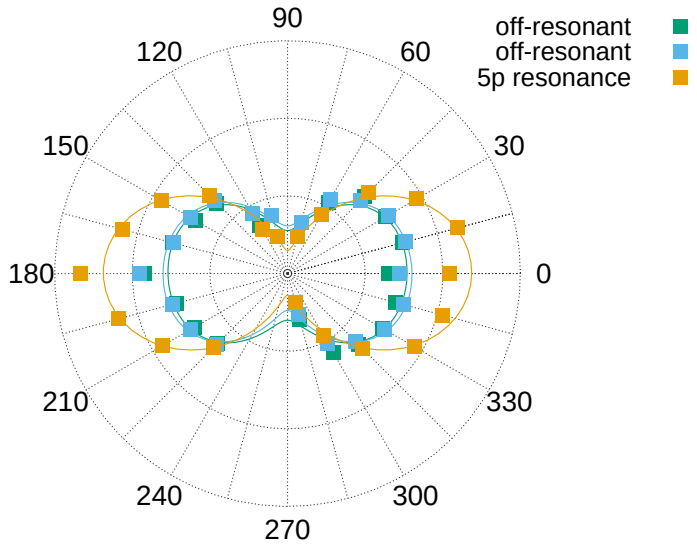

Fig. 1: Normalized angular distributions of the Kr 4p photoelectrons relative to the photon polarization vector measured at different photon energies : at the 3d→5p resonance (91.21 eV) and in its vicinity (90.93 eV, 91.03 eV).

References

[1] B. G. Pradhan *et al* J. Phys. B: At. Mol. Opt. Phys. **44**, 201001 (2011).
[2] S. Ricz *et al* Phys. Rev. A **65** 042707 (2002).
[3] S. Ricz *et al* Phys. Rev. A **81** 043416 (2010).
[4] L. Ábrók *et al*, in preparation.

*Corresponding author: abrok.levente@atomki.hu

Excitation of the $4p^5 5s^2\ ^2P_{1/2,3/2}$ states in strontium by electron impact

V. Borovik[1], **I. Shafranyosh**[1], **O. Borovik**[*2]
1. Faculty of Physics, Uzhgorod National University, Voloshina vul. 54, 88000, Uzhgorod, Ukraine
2. Institute of Electron Physics, Universitetska vul. 21, 88017, Uzhgorod, Ukraine

Direct ionization of the $4p^6$ subshell in Sr leads to the formation of the ionic $4p^5 5s^2\ ^2P_{1/2,3/2}$ doublet states which are represented in the Auger spectra by the most intense and well-resolved lines (Figure 1(a)). The excitation functions of these lines reflect the energy-dependent behavior of the $4p^6$ ionization process and are currently the only source of information on the ionization cross section of the $4p^6$ subshell in Sr atoms.

Here we report our first data on the excitation functions of the $4p^5 5s^2\ ^2P_{1/2,3/2}$ states in an impact-energy range from their excitation thresholds at 28.18 eV ($^2P_{3/2}$) and 29.15 eV ($^2P_{1/2}$)[1] up to 600 eV. The apparatus and measuring procedure were described elsewhere [2]. The data were obtained by determining the normalized intensities of lines in the Auger spectra measured at the observation angle of 54.7° in series, step-by-step for different impact-energy values. Spectra were recorded at the incident- and ejected-electron energy resolution of 0.3 eV and 0.06 eV, respectively. The incident-electron and ejected-electron energy scales were calibrated by using the photoabsorption data [3]. The uncertainties of energy scales were estimated to be ±0.1 eV for incident and ±0.05 eV for ejected electrons. The relative uncertainty of the data, after accounting for fluctuations of the experimental conditions, did not exceed 10%. Exceptions are the near-threshold energy regions where the uncertainty reached 15%.

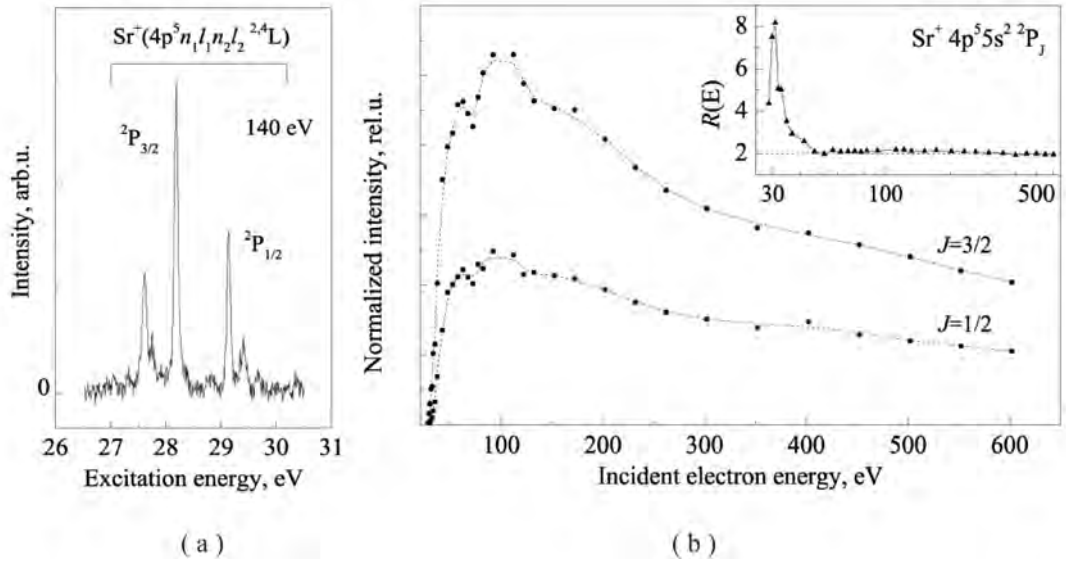

Fig. 1: (a) - the Auger spectrum of Sr atoms at impact-energy value of 140 eV. (b) - the excitation functions of the $4p^5 5s^2\ ^2P_{1/2,3/2}$ states. Inset shows the ratio $R(E)=I_{3/2}(E)/I_{1/2}(E)$.

Figure 1(b) shows the measured excitation functions of the $4p^5 5s^2\ ^2P_{1/2,3/2}$ states. As can be seen, the excitation functions are similar in shape in the entire impact-energy region under study. Similar observation was earlier reported in excitation of the $3p^5 4s^2\ ^2P_{1/2,3/2}$ states in Ca [4]. Two enhancements of the cross section around 60 and 90 eV are observed in both functions but their origin is not clear yet. Our preliminary estimations employing RDW calculations for atomic autoionizing states [5] show that the maximum excitation cross sections for $^2P_{3/2}$ and $^2P_{1/2}$ states should not exceed 1.1 and 0.5×10^{-16}cm^2, respectively.

The inset in Figure 1 (b) shows the ratio $R(E)$ of the normalized intensities of the lines $^2P_{3/2}$ and $^2P_{1/2}$ as a function of the incident electron energy. At near-threshold energies, the ratio reaches about 8, and above 50 eV approaches the statistical value of 2, as one would expect in *LS*-coupling for the states with J = 3/2 and J = 1/2.

References

[1] M.D. White *et al*, J. Phys. B **12**, 315 (1979).
[2] A. Borovik *et al*, J. Phys. B **38**, 1081 (2005).
[3] M.W.D. Mansfield and G.H. Newsom, Proc. R. Soc. A **377** 431 (1981).
[4] B. Feuerstein *et al*, Abstracts of VI ECAMP (Siena), 4-53 (1998).
[5] A. Kupliauskiene *et al*, J. Phys. B **50**, 225201 (2017).

*Corresponding author: baa1948@gmail.com

Magnetic deflection of neutral sodium-doped ammonia clusters

J. V. Barnes[1], **M. Beck** [1], **S. Hartweg** [1], **D. Stolba** [1], **A. Luski** [2], **B. L. Yoder** [1], **J. Narevicius** [2], **E. Narevicius** [2], **R. Signorell**[*1]

1. Department of Chemistry and Applied Biosciences, ETH Zürich, Zürich 8093, Switzerland
2. Department of Chemical Physics, Weizmann Institute of Science, Rehovot 76100, Israel

The discovery of concentration-dependent colours of alkali metal-ammonia solutions in the early 19th century by Sir Humphry Davy and later reported by W. Weyl [1], sparked a large series of experimental and theoretical work on excess electrons in alkali metal ammonia solutions [2] (and references therein). However, the underlying correlation effects of the solvated electrons are still not well understood. While correlation effects have been probed by magnetic measurements on alkali metal solutions, [3], [4] the involved diamagnetic and paramagnetic species have not yet been identified in bulk phase experiments.[2]
We describe the setup and the performance of a new pulsed Stern-Gerlach deflector, and present results for sodium atoms and small sodium-doped ammonia clusters $Na(NH_3)_n$ ($n = 1-4$) in a molecular beam. To test the performance of the deflector we deflect Na atoms, which inherently show the deflection behaviour of an atomic free spin $\frac{1}{2}$ system. The sodium-doped ammonia monomer ($NaNH_3$) exhibits the deflection of an atom-like free spin $\frac{1}{2}$ system, while all lager clusters show much smaller deflections and therefore cannot be described as an atom-like free spin spin $\frac{1}{2}$ system. Experimental deflection ratios are compared with values calculated from molecular dynamics simulations, assuming a free spin $\frac{1}{2}$ system with the corresponding particle momentum. The comparison reveals that intracluster spin relaxation in $NaNH_3$ takes place on a time scale significantly longer than 200 µs. Assuming that intracluster relaxation is the cause of the reduced deflection, relaxation times seem to be on the order of 200 µs for all larger clusters $Na(NH_3)_n$ ($n = 2-4$). We propose an acceleration of intra-cluster spin relaxation in $n > 1$ clusters as a result of Zeeman-like spin rotation coupling. The emergence of very low frequency internal rotation modes for $n > 1$ leads to a drastic increase in the thermally accessible density of rovibrational states to which the spin can couple, which could explain the abrupt decrease of the deflection for clusters with $n > 1$. Our work is a first attempt to understand the magnetic properties of isolated, weakly-bound clusters. Emphasis is placed on how the magnetic properties of an atomic free spin $\frac{1}{2}$ system of Na is perturbed by an increasing number of NH_3 molecules. In more general terms, we focus on how the magnetic properties evolve from atom-like to molecular deflection behavior as a function of cluster size.

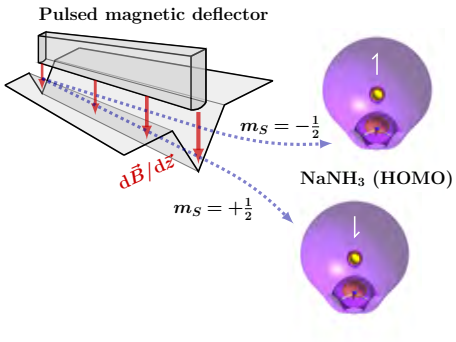

Fig. 1: A new pulsed Stern-Gerlach setup elucidates the spin relaxation dynamics of small weakly-bound $Na(NH_3)_n$ clusters.

References

[1] W. Weyl, Ann. Phys. **199**, 350 (1864).
[2] E. Zurek, P. P. Edwards and R. Hoffmann, Angew. Chem. Int. Edit. **48**, 8198 (2009).
[3] N. W. Taylor and G. N. Lewis, *Proceedings of the National Academy of Sciences of the United States of America*, **11**, 456 (1925).
[4] S. Freed and N. Sugerman, J. Chem. Phys. **11**, 354 (1943).

[*]Corresponding author: ruth.signorell@phys.chem.ethz.ch

Dynamic nuclear spin polarization in Nitrogen–Vacancy centers in diamond

L. Busaite[*1], **R. Lazda**[1], **A. Berzins**[1], **M. Auzinsh**[1], **R. Ferber**[1], **F. Gahbauer**[1]
1. Laser Centre, University of Latvia, Rainis Boulevard 19, LV-1586 Riga, Latvia

Nitrogen–Vacancy (NV) centers are defects in diamond that consist of a nitrogen atom in place of one of the carbon atoms with an adjacent vacancy. NV centers exhibit many characteristics that are suitable for quantum metrology and quantum information applications [1-3].

We measured experimentally and calculated numerically signals that revealed the dynamic nuclear spin polarization of nitrogen in negatively charged nitrogen-vacancy (NV) centers in diamond over a wide range of magnetic field values from 0 to 1100 G covering both the excited-state level anti-crossing (ESLAC) and the ground-state level anti-crossing (GSLAC) magnetic-field regions (Fig. 1). We focused on the less studied ground-state level anti-crossing region. The nuclear spin polarization was determined from the measurements of the optically detected magnetic resonance (ODMR) signals. A very large (up to $96 \pm 2\%$) nuclear spin polarization of nitrogen was achieved according to the measurements. We also measured the influence of angular deviations of the magnetic field from the NV axis on the nuclear spin polarization efficiency. The results show that in the vicinity of the ground-state level anti-crossing, the nuclear spin polarization is more sensitive to this angle than in the vicinity of the excited-state level anti-crossing. The results of the research are published in [4].

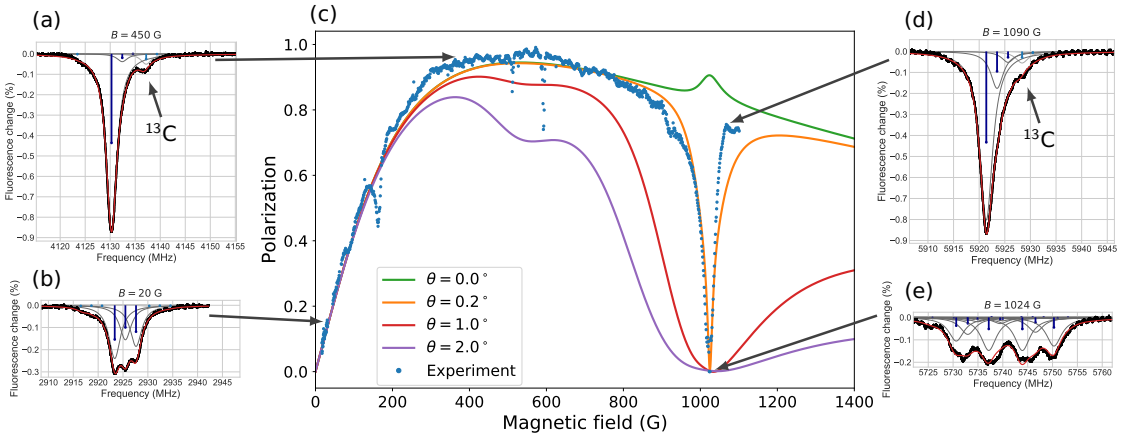

Fig. 1: (a), (b), (d), (e): ODMR signals at individual magnetic field values. (c): Experimental (blue dots, each representing one ODMR measurement) and theoretical (solid curves) nuclear spin polarization as a function of magnetic field. The signal changes more drastically as a result of angular deviations in the GSLAC region compared to the ESLAC region. The pumping rate for theoretical calculations was $\Gamma_p = 5$ MHz. The experimental ODMR curve fit determined that the magnetic field angle $\theta = 0.2°$, which is in good agreement with the calculated curve at magnetic field angle $\theta = 0.2°$.

References

[1] G. Popkin, Science **354**, 1090 (2016).
[2] T. D. Ladd, F. Jelezko, R. Laflamme, Y. Nakamura, C. Monroe, and J. L. O'Brien, Nature **464**, 45 (2010), 1009.2267.
[3] K. Heshami, D. G. England, P. C. Humphreys, P. J. Bus-tard, V. M. Acosta, J. Nunn, and B. J. Sussman, Journal of Modern Optics **63**, 2005 (2016).
[4] L. Busaite, R. Lazda, A. Berzins, M. Auzinsh, R. Ferber, and F. Gahbauer, Physical Review B **102**, 24101 (2020).

*Corresponding author: laima.busaite@lu.lv

Theoretical study of vibrational (de-)excitation of NO_2 and N_2O by low-energy electron impact

Mehdi Ayouz[*1], **Hainan Liu**[2], **Chi Hong Yuen**[3], **Samantha Fonseca dos Santos**[4], **Pietro Cortona**[2], **Viatcheslav Kokoouline**[3]

1. LGPM CentraleSupélec, CNRS-UMR8580, Université Paris-Saclay 91190 Gif-sur-Yvette, France
2. SPMS CentraleSupélec, CNRS-UMR8580, Université Paris-Saclay 91190 Gif-sur-Yvette, France
3. Department of Physics, University of Central Florida, 32816, Florida, USA
4. Department of Physics, Rollins College, 32789, Florida, USA

We present cross sections for vibrational (de-)excitation of NO_2 and N_2O by low-energy electron impact. Calculations are performed using a theoretical approach based on a combination of the normal mode approximation for vibrational states of the target molecule, fixed-nuclei electron-target scattering matrices and the vibrational frame transformation employed to evaluate the scattering matrix for vibrational transitions. Results are presented for excitations between the ground and first two excited vibrational states for NO_2 (see Fig. 1), and between the ground and first excited vibrational state for N_2O (see Fig. 2) in all the vibration modes for both target molecules. Thermally-averaged rate coefficients are derived from the obtained cross sections for temperatures in the 10-10000 K interval. For NO_2, a comprehensive set of calculations are performed for assessing the uncertainty of the present calculations. The uncertainty assessments indicate that the computed observables for vibrational (de-)excitation is reasonable for later use in NO_2−containing plasma kinetics modeling. For N_2O, the NO and NN stretching modes cross-section behavior agrees reasonably well with the available experimental data as displayed in Fig. 2.

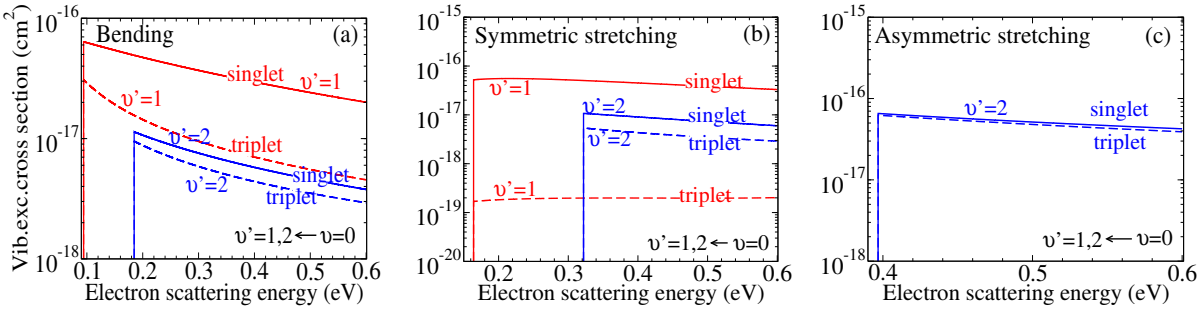

Fig. 1: Calculated cross sections as functions of the electron scattering energy for the vibrational excitation of NO_2 being initially in the lowest vibrational state $v = 0$ for the three normal modes (see the text for detailed discussion): (a) cross sections for $v' = 1,2 \leftarrow v = 0$ transitions for bending mode; (b) for symmetric stretching mode; (c) for asymmetric stretching mode.

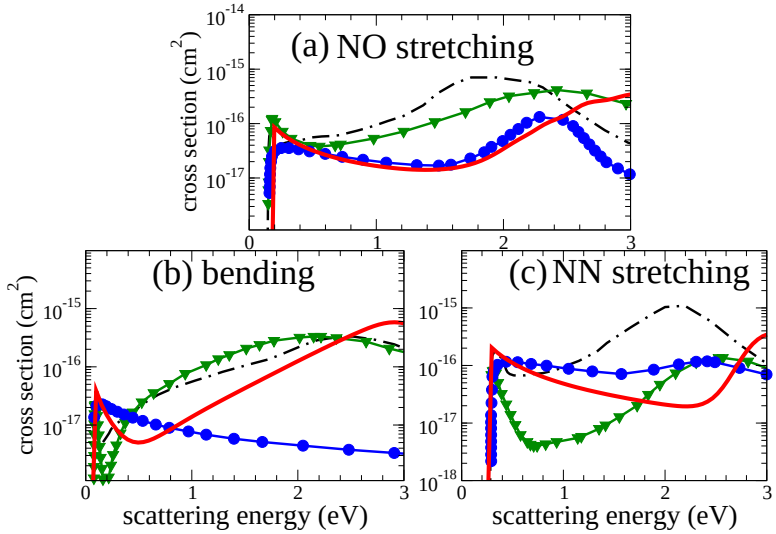

Fig. 2: Comparison of the present N_2O theoretical results with available experimental cross sections for the vibrational $v = 0 \rightarrow v' = 1$ excitation of the (a) NO stretching, (b) bending, and (c) NN stretching modes. The experimental results are taken from Hayashi [M. Hayashi and K. Akashi, Handbook of plasma material science (1992)] (solid line with circles), Allan and Skalický [M. Allan and T. Skalický, J. Phys. B: At., Mol. Opt. Phys. 36, 3397 (2003)] (solid line with triangles), and Nakamura [Y. Nakamura, Proc. of the 28th ICPIG p. 224 (2007)] (dashed-dotted line)

*Corresponding author: mehdi.ayouz@centralesupelec.fr

The VUV absorption spectra arising from collisions of Kr and Xe atoms with H_2 molecules in the short-wave region near the resonance lines $^{1,3}P_1$–$^1S_0$

O.S. Alekseeva[*1], **A.Z. Devdariani** [2], **M.G. Lednev**[3], **A.L. Zagrebin**

1. Saint Petersburg Electrotechnical University "LETI", ul. Professora Popova, 5, 197376, St. Petersburg, Russia

2. Saint Petersburg Herzen State Pedagogical University of Russia, nab. Reki Moiki, 48, 191186, St. Petersburg, Russia

3. Saint Petersburg Mining University, 21st Line V.O., 2, 199106, St. Petersburg, Russia

The calculations of the collision-induced quasimolecular absorption spectra in the short-wave region near the resonance lines of $^{1,3}P_1$ – $^1S_0$ of Kr and Xe atoms in H_2 atmosphere are performed for the first time. As the potential energy surfaces (PES) we use PES for the excited states obtained in the framework of the pseudopotential and the effective Hamiltonian methods [1, 2], *ab initio* quantum-chemical PES for the ground state of Kr+H_2 [3] and the flat PES approach for the ground state. In the region that is essential for the radiative transitions under consideration the dipole moment varies insignificantly. Therefore it can be replaced by the dipole moment of the corresponding atomic transition. The calculations of the spectral distributions of the absorption coefficients are carried out in the well-known quasistatic approach for two extreme cases: fast rotation of the molecule during the collision and slow rotation. It has been established that the results obtained from both approaches almost coincide. Furthermore, the use of the flat PES approach for the ground state leads to the result that is almost twice underestimated in compare with the use of *ab initio* PES. The analogous calculations for the thermal collisions of Kr and Xe atoms with He atoms give the results which are in good agreement with the available experimental data [4, 5]. The calculated spectral distributions of the absorption coefficients for Kr($^1P_1$)+H_2 is presented in Fig. 1 .

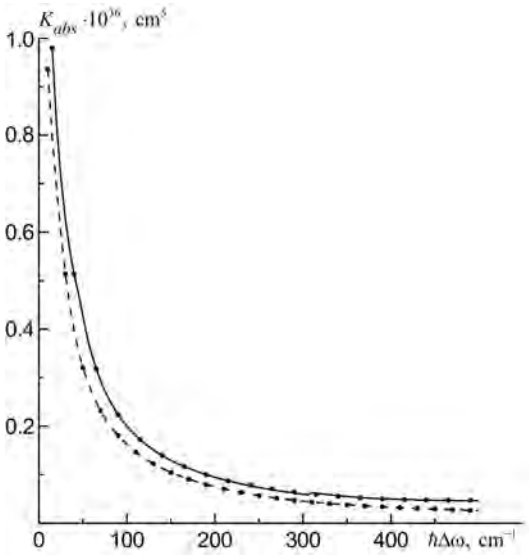

Fig. 1: The spectral distributions of the absorption coefficients for Kr($^1P_1$)+H_2. Solid and dashed lines represent the results obtained with the use of the averaged calculated and the flat PES for the ground state respectively, dots correspond to the absorption coefficients firstly calculated for the different orientations of H_2 molecule and averaged after.

References

[1] A.L. Zagrebin, E.P. Permogorova, Opt. Spectrosc. **71**, 252 (1991).
[2] A.Z. Devdariani, A.L. Zagrebin, and K.B. Blagoev, Annales de Physique **14**, 467 (1989).
[3] Y.Z. Zhou, D.Q.Xie, J. Chem. Phys. **123**, 134323 (2005).
[4] O. Alekseeva, V. Alekseev, A. Devdariani, M. Lednev and A. Zagrebin in *AIP Conference Proceedings*, **1290**, 231, (2010).
[5] A. Devdariani, A.L. Zagrebin, and M. Lednev, Opt. Spectrosc. **128**, 167 (2020).

*Corresponding author: o.alek@rambler.ru

Combined VCI and instanton approach for computation of vibrational spectrum in asymmetric well systems

M. Eraković[1], **M. T. Cvitaš**[*1]
1. Ruđer Bošković Institute, Bijenička cesta. 54, 10000 Zagreb, Croatia

In systems with potential energy surfaces that contain multiple symmetry-related minima, vibrational eigenfunctions are delocalized, which results in the energy splitting of vibrational levels. The splitting is a consequence of tunnelling between different minima. It can be experimentally measured, using, e.g. high-resolution microwave spectroscopy, and it encodes timescales of rearrangements between minima. If potential has minima of slightly different energies or different frequencies, vibrational energies will be a combination of tunnelling contribution and difference in energies of wavepackets localized in the minima. Such asymmetry can be found in molecules which possess different conformers, in molecules embedded in matrices, where environment imposes asymmetry on the potential energy surface, or in molecules which are partially isotopically substituted and isotope moves into inequivalent position upon rearrangement. If asymmetry is sufficiently large, different vibrational states of different minima mix as a consequence of tunnelling.

In this contribution, we develop a Jacobi field instanton method [1] for computing tunnelling interaction matrix elements between vibrational states of different minima. We show that in combination with vibrational configuration interaction (VCI) [2] for computing energies of localized wavefunctions, an accurate vibrational spectrum can be obtained. The two methods complement each other since VCI provides excellent energies of localized wavepackets, but poor description of wavefunctions in the barrier, which is essential to compute tunnelling contribution. On the other hand, instanton method yields tunnelling matrix elements with great accuracy, but works in harmonic approximation around minima, which is too inaccurate to be used for localized energies. We apply this approach to the case of partially deuterated malonaldehyde.

References

[1] M. Eraković, M. T. Cvitaš, J. Chem. Phys. **153**, 134106 (2020).
[2] K. Christoffel, J. Bowman, Chem. Phys. Lett. **85**, 220-224 (1982).

*Corresponding author: mcvitas@irb.hr

Classical degeneracies and unimolecular reaction rates of Lennard-Jones clusters

Chu Hangbing[*1], **Zhang Yibin** [†1], **Klavs Hansen**[1,2]

1. School of Science, Tianjin University,300072 Tianjin, People's Republic of China

2. Center for Joint Quantum Studies and Department of Physics, School of Science, Tianjin University,300072 Tianjin, People's Republic of China

The presence of isomeric states in clusters play a decisive role in the high temperature dynamics, as seen for example in the finite size analogue of freezing/melting. Less well known is the fact that they will also play an important role for unimolecular decays. In the simplest case where isomers appear in the form of a degenerate ground state, this degeneracy will modify the rate constants with a multiplicative factor [1]. Specifically as the ratio of product and reactant degeneracies. Standard methods of calculating rate constants will not be able to capture this effect.

Here we present numerical molecular dynamics simulations of small clusters composed of atoms interacting with the Lennard-Jones two-body potential to quantify the effect. The simulations apply the classical Hamiltonian and are performed at low excitation energies to avoid interference from the emerging melting transition. Rate constants are recorded as averages of reciprocal atomic emission times. The target of the simulations is the effective frequency factor in the expression for the rate constants. Fig.1 shows an example of the fit of the simulated rate constants for one of these clusters. Information about the ground state energies and dissociation energies, E_a, is obtained from [2]. The relation plotted is as follows:

$$k \approx \omega \frac{(E - E_a)^{3N-10}}{E^{3N-7}} \tag{1}$$

where ω is approximately constant.

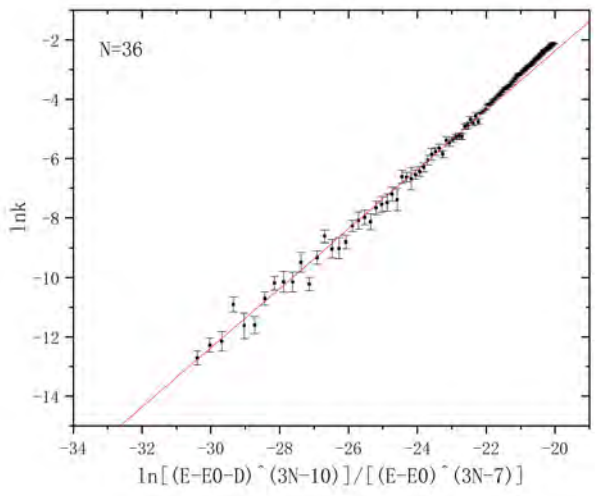

Fig. 1: The left hand side of Eq.1 vs. the energy dependent factor of the right hand side. The logarithmic slope of unity confirms the expression. The value of ω is found as the intercept.

References

[1] Description of unimolecular reaction rates of Lennard-Jones clusters, K. Hansen: J. Phys. B **52**(23) (2019) 235101

[2] Table of Lennard-Jones Cluster Global Minima. [online] Doye.chem.ox.ac.uk. Available at: http://doye.chem.ox.ac.uk/jon/structures/LJ/tables.150.html [Accessed 7 May 2021].

[3] Statistical Physics of Nanoparticles in the Gas Phase, Klavs Hansen, Springer, Dordrecht (2018)

[*]Corresponding author: 3018210166@tju.edu.cn

[†]Corresponding author: 3018210019@tju.edu.cn

Thermally-induced entanglement of atomic oscillators

Pradip Laha[*1], **Lukáš Slodička**[1], **Darren Moore**[1], **Radim Filip**[1]
1. Department of Optics, Palacký University, 17. listopadu 1192/12, 77146 Olomouc, Czech Republic

An array of laser driven ultracold ions confined in a linear Paul trap is an excellent and experimentally viable platform available for the implementation of a wide range of quantum protocols involving quantum simulation [1], for example of Ising spin systems [2], the Bose-Hubbard (BH) model [3] and the Jaynes-Cummings-Hubbard (JCH) model [4]. These systems possess several striking advantages such as the presence of long coherence times, the ability to efficiently manipulate the internal and motional (centre of mass) degrees of freedom, and individual access to each ion allowing implementation of quantum gates between specific ions [5]. Recently, a single ion has been used to investigate quantum phase transitions in mechanical motion [6]. Spontaneous emission of the internal states and damping of the motion of the ions are effectively minimised in state of the art experiments by tuning the appropriate metastable transitions of the ions stored in ultrahigh precision spectroscopy and maintaining low pressures for long times such that collisions with background atoms and other incoherent couplings are negligible [7]. The high level of control afforded by such systems combined with their anticipated scalability in simulating many-body effects provide us with a framework in which the autonomous quantum behaviour that may become a necessity of larger-scale quantum technologies can be investigated.

In particular, a pair of ions interacting in such traps exchange vibrational quanta through the Coulomb interaction. This linear interaction can be anharmonically modulated by coupling to the internal two-level structure of one of the ions. Driven by thermal energy in the passively coupled oscillators, themselves coupled to the internal ground states of ions, the nonlinear interaction autonomously and unconditionally generates entanglement between the mechanical modes of the ions. We examine this counter-intuitive entanglement behaviour for several experimentally feasible model systems and propose parameter regimes where state of the art trapped ion systems can produce such phenomena. For instance, the simplest possible generalisation of the thermally induced entanglement protocols involves a pair of oscillator modes and a single qubit. The two simplest possible arrangements of these three systems involve the qubit coupled to one member of the oscillator pair which is itself coupled via the beamsplitter interaction, or a single qubit acting as mediator between a pair of uncoupled oscillators (Fig. 1). The interaction Hamiltonians of such systems can be expressed in terms of the Jaynes-Cummings (JC) and beamsplitter (BS) interactions as

$$H_I = H_{\mathrm{JC}_1} + H_{\mathrm{BS}_{12}}, \qquad H_{II} = H_{\mathrm{JC}_1} + H_{\mathrm{JC}_2}\,. \tag{1}$$

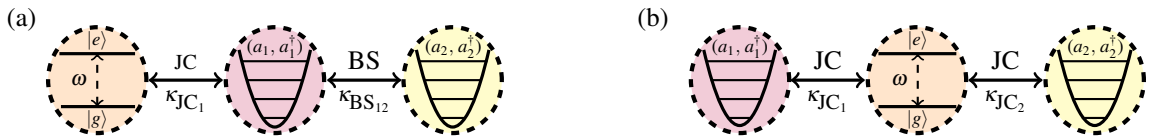

Fig. 1: Schematics of the systems embodied by Hamiltonians H_I (left) and H_{II} (right), respectively.

To study the entanglement dynamics we measure the entanglement between the reduced state of the oscillator pair using the logarithmic negativity (LN). Contrary to intuition, the unitary evolution of these systems produces entanglement between the oscillator pair driven by the temperature difference. For instance, we find that regardless of the coupling strengths, increasing the thermal noise of one of the oscillators (after keeping the other oscillator and the qubit in the ground state, initially) increases the entanglement, up to saturation and up to a critical value of the coupling parameter above which entanglement generation begins to be inhibited again. Also, increasing the mixedness in the remaining components of both the systems decreases the capacity to generate entanglement. In addition, we demonstrate (i) a multiqubit enhancement of such thermally-induced entanglement, (ii) the changes in the system dynamics due to the presence of qubit dephasing and other dissipative agents of open systems, and (iii) entanglement generation when the oscillator pair is prepared initially in a single coherent state and the ground state or phase randomised coherent state and the ground state.

References

[1] R. Blatt and C. F. Roos, Nat. Phys. **8**, 277 (2012).
[2] A. Friedenauer, H. Schmitz, J. T. Glueckert, D. Porras, and T. Schaetz, Nat. Phys. **4**, 757 (2008).
[3] M. Greiner, *et al.*, Nature **415**, 39 (2002).
[4] A. D. Greentree, C. Tahan, J. H. Cole, and L. C. L. Hollenberg, Nat. Phys. **2**, 856 (2006).
[5] J. I. Cirac and P. Zoller, Phys. Rev. Lett. **74**, 4091 (1995).
[6] M.-L. Cai, *et al.*, Nat. Commun. **12**, 1126 (2021).
[7] D. Leibfried, R. Blatt, C. Monroe, and D. Wineland, Rev. Mod. Phys. **75**, 281 (2003).

*Corresponding author: pradip.laha@upol.cz

Many-body theory calculations of positron scattering and annihilation in H_2, N_2, CH_4 and CF_4

C. M. Rawlins[*1], **J. Hofierka** [1], **B. J. Cunningham** [1], **C. H. Patterson** [2] **and D. G. Green**[†1]
1. School of Mathematics and Physics, Queen's University Belfast, Belfast BT7 1NN, United Kingdom
2. School of Physics, Trinity College Dublin, Dublin 2, Ireland

Understanding the fundamental interactions of positrons with matter is important to e.g., develop positron traps, beams and positron emission tomography, and to properly interpret positron-based materials science techniques and understand positron interactions in the Galaxy.

Progress has been made describing positron-atom interactions, e.g., many-body theory calculations have given positron scattering cross sections, annihilation rates [1] and γ spectra [2], and thermalisation rates [3] all in excellent agreement with experiment. For molecules, calculations of positron binding energies have been performed via numerous approaches including quantum Monte Carlo, configuration interaction, NEO (Nuclear Electronic Orbital framework) and APMO (Any-Particle Molecular Orbital theory), finding agreement with experiment to 25% at best for small polar molecules, and failing to predict binding in non-polar molecules (see e.g., [4]).

Calculations of positron scattering or annihilation in molecules are more scarce. Calculations for small molecules have been performed using sophisticated techniques including stochastic variational, *R*-matrix, Kohn-variational, diffusion Monte Carlo and Schwinger-multichannel methods, but only for positron annihilation on the smallest molecule (H_2) does theory agree adequately with experiment (see e.g., [5]).

We have developed a many-body theory description of positron interactions with polyatomic molecules [6]. Here, we use it to calculate *s*-wave positron scattering phase shifts and $Z_{\rm eff}$ *ab initio* for H_2, N_2, CH_4 and CF_4 (which do not bind the positron), delineating the effects of the positron-molecule correlations, and comparing with theory and experiment, where possible, e.g., see Figure 1, which shows the many-body theory calculated phase shifts and $Z_{\rm eff}$ for H_2. We solve the Dyson equation in a Gaussian basis with positron-molecule self energy calculated at the *GW*@(RPA/TDHF/BSE) levels including the virtual-positronium formation (vPs) and positron-hole (p-h) contributions. The Dyson wavefunction normalisation is determined from the energies of discretized positron positive energy pseudostates [7]. The effects of short-range positron-electron correlations on $Z_{\rm eff}$ are included via vertex enhancement factors [2].

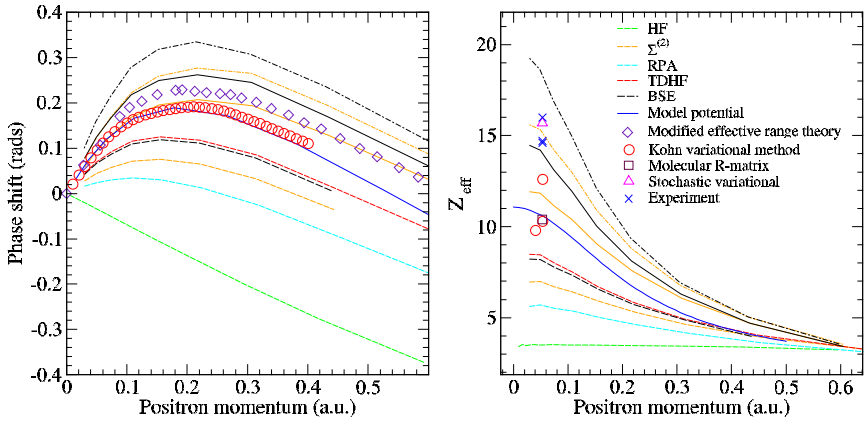

Fig. 1: *s*-wave (a) phase shifts and (b) $Z_{\rm eff}$ for positrons on H_2. Many-body theory calculations in different approximations (see legend), model potential calculation [7] (blue line), Kohn-variational calculations [8] (circles), Modified-effective-range-theory fit of the measured cross section [9] (diamonds) presented for phase shifts. For Many-body theory results, dashed lines are the stated approximations, dot-dashed lines are the stated approximations+vPs and solid lines are the stated approximations+vPs+p-h. Room-temperature values presented for $Z_{\rm eff}$ (see Table 2 in [5]: experiments are blue symbols, the rest from other methods).

References

[1] D. G. Green *et al.*, Phys. Rev. A. **90**, 032712 (2014).
[2] D. G. Green *et al.*, Phys. Rev. Lett. **114**, 093201 (2015).
[3] D. G. Green, Phys. Rev. Lett. **119**, 203403 (2017).
[4] G. F. Gribakin *et al.*, Rev. Mod. Phys. **82**, 2557 (2010).
[5] D. G. Green *et al.*, New J. Phys. **14**, 035021 (2012).
[6] B. J. Cunningham, in preparation.
[7] A. R. Swann and G. F. Gribakin, Phys. Rev. A. **101**, 022702 (2020).
[8] J. N. Cooper *et al.*, J. Phys. B. **41**, 245201 (2008).
[9] K. Fedus *et al.*, Phys. Rev. A **88**, 042715 (2015).

[*]Corresponding author: c.rawlins@qub.ac.uk
[†]Corresponding author: d.green@qub.ac.uk

Centre for Advanced Laser Techniques (CALT)

D. Aumiler[*1]
1. Institute of Physics, Bijenička c. 46, 10000 Zagreb, Croatia

Centre for Advanced Laser Techniques (CALT) is a strategic research infrastructure project of the Republic of Croatia worth close to 16 mil. EUR, funded by the European Regional Development Fund (ERDF). The main goal of the CALT project is to establish a fully equipped, modern scientific research centre specialized in advanced laser and optical techniques. CALT is located at the Institute of Physics (IPZg) in Zagreb, the only research institution in Croatia to have several larger laser/optical systems and relevant expertise, which are the basis for laser-matter interaction studies. CALT will be set as a collection of state-of-the-art laboratories that will be open to users, where both the infrastructure and the expertise will be at service to Croatian, as well as regional RDI community.

CALT's activities; which comprise research, education, and providing access to laser facilities; will address socially important issues through planned research activities in the four domains:

1. Quantum Technology (Quantum simulators and sensors, Quantum atomic clock based on Sr atoms, Frequency comb spectroscopy, National time and frequency laboratory),
2. Plasma Technology (Laser plasmas and applications, High-harmonic generation, Laser micro-structuring, Nonlinear optics),
3. Nano and Bio Systems (Nanospectroscopy and imaging, Optical characterization of materials, Nano-scale topography, Super-resolution microscopy),
4. Ultrafast Dynamics (Ultrafast spectroscopy, THz spectroscopy, Tr-ARPES, Coherent magnetization).

With the end of construction work in June 2021, that included full reconstruction of one of the IPZg buildings, and subsequent equipping the building with laboratory furniture, a total of over 1200 m^2 of fully equipped laboratory space will be available by the end of 2021. Installation and testing of laser systems and equipment will follow throughout 2022, and CALT is expected to become fully functional by the end of 2022.

[*]Corresponding author: aumiler@ifs.hr

Non-equilibrium condensed matter: an open door to new phenomena

D. Mihailovic[*1,2]
1. Jozef Stefan Institute, Ljubljana, Slovenia
2. CENN Nanocenter, Ljubljana, Slovenia

While the focus of ultrafast science in the recent past has been on the study of short timescale phenomena associated with various symmetry breaking transitions, relatively little attention has been paid to the aftermath of the transition. On timescales ranging many decades, system tuning can result in new emergent metastable phases which do not occur naturally. In my presentation I will present three examples of metastable quantum phases in 1T-TaS2, which can be created by tailoring the trajectory of the system in the aftermath of an electronic ordering transition: a quantum jam, a quantum billiard and a state exhibiting quantum melting. Modelling of the electron dynamics using reverse annealing on a D-wave quantum computer shows that quantum materials and quantum simulators show directly analogous emergent phenomena based on only microscopic interactions.

[*]Corresponding author: dragan.mihailovic@ijs.si

Spectroscopy of Laser Produced Plasmas of Highly Charged Ions to Support Short Wavelength Light Source Development

G. O'Sullivan[*1]
1. University College Dublin, Belfield, Dublin 4, Ireland

Laser produced plasmas (LPPs) are versatile sources of extreme ultraviolet (EUV) or soft x-ray (SXR) radiation. Depending on the choice of target they can generate continuum or line radiation and indeed one of the first reported applications was their use as continuum sources for studies of inner shell photoexcitation of atoms and ions [1]. In plasmas of some medium and high Z elements the short wavelength emission spectrum is dominated by intense bands of emission arising from unresolved transition arrays (UTAs) that result from resonance 4d-4f and 4p-4d transitions in a range of ion stages that overlap within a narrow wavelength range and whose intensity and spectral profile is very sensitive to plasma opacity [2]. The critical density of LPPs is approximately $1021(\lambda\mathrm{L}\text{-}2)$ cm^3, where λL is the laser wavelength in μm and plasmas produced by solid state lasers with $\lambda\mathrm{L} \leq 1$ μm, are, in general, optically thick. However, plasma opacity can be reduced by using longer wavelength lasers, reducing the ion concentration using mixed composition or foam targets or using dual pulse irradiation in which a pre-pulse produces a lower density plasma or mist target that is then reheated by the main laser pulse or by using sub nanosecond pulses since opacity also increases with laser pulse duration. These observations have been successfully exploited in EUV lithography sources where power outputs exceeding 200 W in a 2% bandwidth centred on 13.5 nm are generated using tin droplet sources irradiated by a 1.06 μm or 10.6 μm pre-pulse followed by a 10.6 μm main pulse [3]. However, the production of similar power levels at shorter wavelengths remains a major challenge since the conversion efficiency, which depends on the ion stage distribution in the plasma, decreases due to the increased energy needed to produce higher ion stages.

More recently the application of LPPs as sources for biomedical imaging in the water window (2.4 – 4.3 nm) has become a topic of considerable interest following the development of optical components such as multilayer mirrors and zone plates that can be used in this spectral region. Traditionally such work has been performed at synchrotron sources and laboratory based 'table top' alternatives are attractive in order to meet researcher requirements. Microscope systems based on resonance lines of nitrogen and carbon ions have been developed [4] but because of their low brightness, some recent research has focussed on the potential using of UTA emission. This work has being largely based on studies of n = 4 – n = 4 emission in plasmas of very high Z elements and n = 3 – n = 4 transitions in intermediate Z elements. Since imaging requires a small plasma size, lasers with pulse durations of a few hundred picoseconds or less, sufficient to produce the ion stages required but short enough to limit plasma expansion are required. However work needs to be done to establish the optimum laser irradiation conditions for particular promising target materials which in turn depend on the availability of suitable optics. Moreover, such imaging systems are not without competition and alternative strategies based on the use of high harmonics with coherent diffractive imaging are starting to emerge.

References

[1] J. T. Costello, J.-P. Mosnier, E. T. Kennedy, P. K. Carroll and G. O'Sullivan 1991 *Phys. Scr.* **1991** 77.
[2] G. O'Sullivan, B. W. Li, R. D'Arcy, P. Dunne, P. Hayden, D. Kilbane, T. McCormack, H. Ohashi, F. O'Reilly, P. Sheridan, E. Sokell, C. Suzuki and T. Higashiguchi, 2015 *J. Phys. B: Atom. Molec. Opt. Phys.* **48**, 144025.
[3] Oscar O. Versolato 2019 *Plasma Sources Sci. Technol.* **28** 083001.
[4] P. A. C. Takman, H. Stollberg, G. A. Johansson, A. Holmberg, M. Lindblom, and H. M. Hertz, 2007 *J. Microsc.* **226**, 175.

[*]Corresponding author: gerry.osullivan@ucd.ie

Supersolidity in the ultracold: when atoms behave as crystal and superfluid at the same time

F. Ferlaino[*1,2]
1. Institute for Experimental Physics, Universität Innsbruck, Austria
2. Institute for Quantum Optics and Quantum Information (IQOQI), Austrian Academy of Science

Quantum physics often makes possible conceptual paradoxes, which appear ephemeral to our classical intuition. A recent example is the discovery of supersolid states in ultracold dipolar gases. Such states combine properties of superfluidity with those of a crystalline order.

This talk traces the fundamental steps for the observation of supersolidity from the perspective of the Innsbruck experiments. We will discuss how a quantum gas of erbium and dysprosium atoms spontaneously breaks its translational symmetry, creating a periodic modulation of its density, while maintaining a quantum phase coherence. We will show how in our experiments it is possible to drive the system to a supersolid phase transition either by cooling a thermal gas or by modifying the short-range interaction from an unmodulated dipolar condensate. Finally, we will report on the recent observation of extending the supersolid properties to two dimensions, and highlight the open questions which still remain to be understood.

[*]Corresponding author: francesca.ferlaino@uibk.ac.at

Ultracold Fermion Mixtures with Strong Interactions

R. Grimm[*1,2]

1. Institute for Quantum Optics and Quantum Information (IQOQI), Austrian Academy of Sciences, 6020 Innsbruck, Austria
2. Institute of Experimental Physics, University of Innsbruck, 6020 Innsbruck, Austria

Mixtures of ultracold fermionic species with Feshbach resonant interactions offer a rich playground for experiments on strongly interacting states of matter, which are of great fundamental interest and which challenge our understanding. I will report on two different experiments related to the physics of quantum impurities in a Fermi sea [1] and the prospect of creating novel superfluids [2].

Our first experiment [3] is motivated by understanding many-body behavior beyond the widely considered limit of a single impurity in a Fermi sea. How do impurities interact via the medium and what kind of densitydependent effects will arise if the impurity concentration is increased? To tackle these questions experimentally, we study a model system of bosonic ^{41}K impurities immersed in a Fermi sea of ^{6}Li, with control of the interspecies interaction by a Feshbach resonance. We carry out radio-frequency spectroscopy to map out the energy spectrum of the impurities in the strongly interacting regime. We find that for impurity concentrations of up to a few 10% the observed spectrum stays very close to the single-impurity limit; see Fig. 1(a). A striking change, however, occurs if the impurities undergo Bose-Einstein condensation: Fig. 1(b) shows that a new branch emerges in the spectrum with much less energy shift. In the central region of the trap, which is occupied by the BEC, the density of the bosons greatly exceeds the fermion density. Here the interaction physics is governed by the Bose polaron instead of the Fermi polaron.

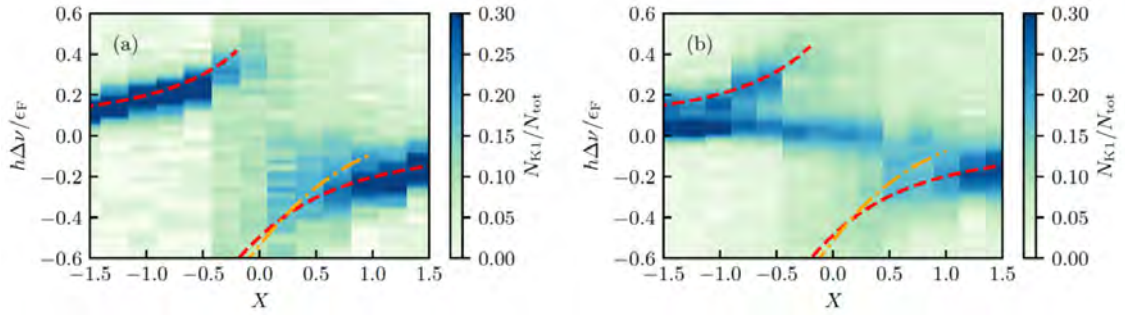

Fig. 1: Spectral response of bosonic ^{41}K atoms immersed in a ^{6}Fermi sea. In (a) the impurity cloud is in the thermal regime, whereas in (b) the impurity cloud is partially Bose condensed (condensate fraction of about 50%). The color scale refers to the fraction of atoms transferred by a radio frequency (detuning $\Delta\nu$ from the bare transition) into the resonantly interacting spin state at an interaction strength $X = -1/(\kappa_F a)$, where κ_F is the Fermi wavenumber and a is the interspecies s-wave scattering length, the latter being controlled by a Feshbach resonance. The comparison of the two spectra reveals the emergence of a new branch related to the condensate fraction. In this situation Fermi and Bose polarons coexist in the trapped impurity cloud.

Our second experiment [4] is driven by the prospect of realizing novel superfluids in mass-imbalanced fermion systems, which favor unconventional pairing mechanisms [2]. We have realized a tunable Fermi-Fermi mixture of ^{161}Dy and ^{40}K atoms and carried out first experiments in the resonant interaction regime near a broad Feshbach resonance. Hydrodynamic expansion profiles reveal a bimodal behavior resulting from mass imbalance. Lifetime studies on resonance show a suppression of inelastic few-body processes by orders of magnitude, which we interpret as a consequence of the fermionic nature of our system. With mass imbalance, tunability, and collisional stability the new mixture offers the key ingredients for reaching exotic superfluid regimes. Comparing experimental results with a beyond-mean-field theory for our system [5] shows that superfluidity is in reach.

We acknowledge support by the Austrian Science Fund FWF within the Doktoratskolleg ALM (W1259-N27) and within Projects No. P32153-N36 and P34104-N.

References

[1] P. Massignan, M. Zaccanti, G. M. Bruun, Rep. Prog. Phys. **77**, 034401 (2014).
[2] K. B. Gubbels and H. T. C. Stoof, Phys. Rep. **525**, 255 (2013).
[3] I. Fritsche, C. Baroni, E. Dobler, E. Kirilov, B. Huang, R. Grimm, G. M. Bruun, P. Massignan, Phys. Rev. A **103**, 053314 (2021).
[4] C. Ravensbergen, E. Soave, V. Corre, M. Kreyer, B. Huang, E. Kirilov, R. Grimm, Phys. Rev. Lett. **124**, 203402 (2020).
[5] M. Pini, P. Pieri, R. Grimm, G. Calvanese Strinati, Phys. Rev. A **103**, 023314 (2021).

*Corresponding author: Rudolf.Grimm@uibk.ac.at

A molecular quantum gas with tunable interactions

J. Ye[*1]
1. JILA, National Institute of Standards and Technology and university of Colorado, Boulder, Colorado, USA

Building on the realization of a degenerate Fermi gas of polar molecules [1], we apply a precisely controlled electric field to molecules confined in different geometries. In two-dimensional optical traps, the E field turns on elastic dipolar interactions by orders of magnitude while suppressing the reactive loss. Efficient dipolar evaporation leads to the onset of quantum degeneracy in 2D [2]. When the electric field is used to tune excited molecular states into degeneracy with the scattering threshold, we observe sharp collision resonances that give rise to three orders-of-magnitude modulation of the chemical reaction rate [3]. This resonant shielding is used to realize a long-lived bulk molecular gas in 3D with tunable, elastic, and anisotropic dipolar interactions [4].

References

[1] L. De Marco, G. Valtolina, K. Matsuda, W. G. Tobias, J. P. Covey, and J. Ye, A degenerate Fermi gas of polar molecules, Science **363**, 853 – 856 (2019).
[2] G. Valtolina, K. Matsuda, W. G. Tobias, J.-R. Li, L. De Marco, and J. Ye, Dipolar evaporation of reactive molecules to below the Fermi temperature, Nature **588**, 239 – 243 (2020).
[3] K. Matsuda, L. De Marco, W. G. Tobias, J.-R. Li, G. Valtolina, G. Quéméner, and J. Ye, Resonant collisional shielding of reactive molecules using electric fields, Science **370**, 1324 – 1327 (2020). .
[4] J.-R. Li, W. G. Tobias, K. Matsuda, C. Miller, G. Valtolina, L. De Marco, R. R. W. Wang, L. Lassablière, G. Quéméner, J. L. Bohn, J. Ye, Controlling anisotropic dipolar interaction with shielding resonance in a three-dimensional molecular quantum gas, arXiv:2103.06246 (2021).

[*]Corresponding author: ye@jila.colorado.edu

A coherent interface between helium Rydberg atoms and chip-based superconducting microwave resonators

D. M. Walker[*1], **L. L. Brown**[1], **S. D. Hogan**[†1]
1. Department of Physics and Astronomy, University College London
Gower Street, London, WC1E 6BT, United Kingdom

Hybrid approaches to quantum information processing involve interfacing quantum systems with complementary characteristics, e.g., superconducting circuits for fast quantum-state manipulation, and gas-phase atoms or molecules for long coherence times [1,2]. In this context, we present a coherent interface between helium Rydberg atoms and a superconducting coplanar waveguide microwave resonator [3]. In these experiments, helium atoms prepared in the $1s55s\,^3S_1$ Rydberg level pass over a superconducting $\lambda/4$ coplanar waveguide microwave resonator. This resonator is operated at 3.8 K and driven at a frequency near its third harmonic, close to resonance with the two-photon $1s55s\,^3S_1 \rightarrow 1s56s\,^3S_1$ (55s $\rightarrow$ 56s) transition in helium at 19.556499 GHz. After interacting with the resonator, the Rydberg atoms are detected by state-selective pulsed electric field ionization. In this setting, Rabi oscillations in the population of the 55s and 56s Rydberg states at frequencies of $\sim$3 MHz have been observed as the time for which the driving field was applied was varied. The coherence time of the atom–resonator-field interaction was greater than 800 ns. By performing Ramsey spectroscopy in the frequency domain, coherence times of the atomic superposition states in excess of 2 μs were measured. Uncancelled DC electric fields close to the superconducting chip surface have been measured to high precision and the spectral characteristics of the resonator mode have also been probed by cavity-enhanced Ramsey spectroscopy [4]. The microwave field distribution close to the resonator has been characterised by measurements of Rabi oscillations in the time domain. These results pave the way for the implementation of long-coherence-time quantum memories [5] and optical-to-microwave photon conversion [6] in this hybrid system.

References

[1] Rabl, De Mille, Doyle, Lukin, Schoelkopf, and Zoller, *Hybrid Quantum Processors: Molecular Ensembles as Quantum Memory for Solid State Circuits*, Phys. Rev. Lett. **97**, 033003 (2006)
[2] Hogan, Agner, Merkt, Thiele, Filipp, and Wallraff, *Driving Rydberg-Rydberg Transitions from a Coplanar Microwave Waveguide*, Phys. Rev. Lett. **108**, 063004 (2012)
[3] Morgan and Hogan, *Coupling Rydberg Atoms to Microwave Fields in a Superconducting Coplanar Waveguide Resonator*, Phys. Rev. Lett. **124**, 193604 (2020)
[4] Walker, Morgan, and Hogan, *Cavity-enhanced Ramsey spectroscopy at a Rydberg-atom–superconducting-circuit interface*, Appl. Phys. Lett. **117**, 204001 (2020)
[5] Petrosyan, Bensky, Kurizki, Mazets, Majer, and Schmiedmayer. *Reversible state transfer between superconducting qubits and atomic ensembles*, Phys. Rev, A **79**, 040304(R) (2009)
[6] Petrosyan, Mølmer, Fortágh, and Saffman, *Microwave to optical conversion with atoms on a superconducting chip*, New J. Phys. **21**, 073033 (2019)

[*]Corresponding author: d.walker.14@ucl.ac.uk
[†]Corresponding author: s.hogan@ucl.ac.uk

Application of Single Photons in Holography

D. Abramović[*1], **N. Demoli**[1,2], **H. Skenderović**[1,2]
1. Institute of Physics, Bijenička c. 46, 10000 Zagreb, Croatia
2. Photonics and Quantum Optics Unit Center of Excellence for Advanced Materials and Sensing Devices, Ruer Bošković Institute, Bijenička c. 54, 10000 Zagreb, Croatia

Holography is usually associated with wave nature of light [1]. However, 1970s Clauser demonstrates that one can distinguish between classical wave and particle model of light [2]. Recent holographic experiments in single photons regime relied on classical light [3] or on photosensitive array [4, 5, 6]. These schemes cannot be considered as true single-photon experiments (ala Feynman double slit Gedankenexperiment), because of the classical light features or a multipixel detector.

Here we present a true single-photon experiment, where hologram is recorded photon by photon. The holograms were recorded by 2D scanning of the single-pixel detector in the image plane of the Twyman-Green interferometer. We used heralded single photons at 810 nm as a source of single-photon illumination, avalanche silicon photodiodes as a single-photon detector and a time-tagging module for the data acquisition.

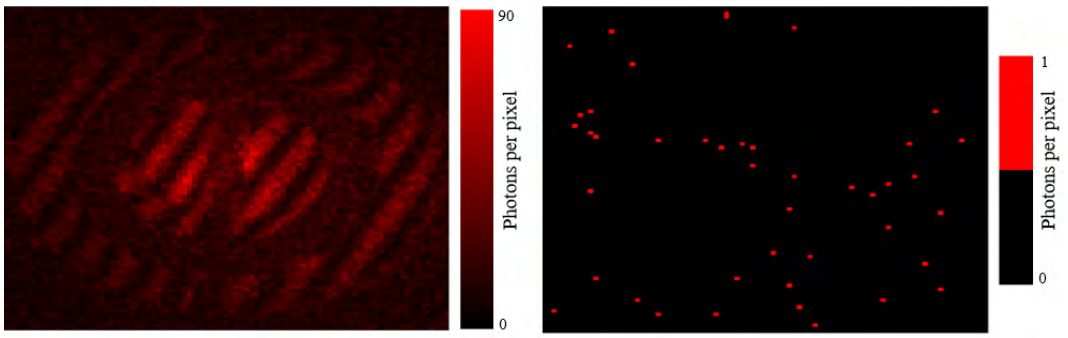

Fig. 1: The hologram (left) and simultaneous events detected by three single photon detectors (where one detector is the heralding detector).

Figure 1 shows a hologram recorded particle by particle and corresponding events that can be described by classical wave model of light. The measured second-order correlation function $g^{(2)}(0) = 0.004(8)$ is among the best recorded compared to the literature [7] and, as such, our source provides excellent basis for true heralded single-photon imaging. The presented approach to quantum holography provides strong and simple evidence that it is feasible to record holograms in conditions of a single-photon interference by heralded single-photon source. From practical point of view, the experiment also demonstrates that the hologram visibility for the heralded technique is much better than for the hologram generated in conditions by non-heralded light source that generates much stronger illumination (more than 70 times stronger).

References

[1] D. Gabor, "Holography, 1948-1971". Nobel Lecture, 1971 (http://www.nobelprize.org).
[2] J. F. Clauser, "Experimental distinction between the quantum and classical field-theoretic predictions for the photoelectric effect", Phys. Rev. D **9**, 853 (1974).
[3] N. Demoli, H. Skenderović, and M. Stipčević, "Digital holography at light levels below noise using a photon-counting approach", Opt. Lett. **39**, 5010 (2014).
[4] H. Defienne, B. Ndagano, A. Lyons, and D. Faccio, "Polarization entanglement-enabled quantum holography", Nat. Phys. **17**, 1 (2021).
[5] F. Devaux, A. Mosset, F. Bassignot, and E. Lantz, "Quantum holography with biphotons of high Schmidt number", Phys. Rev. A **99**, 033854 (2019).
[6] R. Chrapkiewicz, M. Jachura, K. Banaszek, and W. Wasilewski, "Hologram of a single photon", Nat. Photon. **10**, 576 (2016).
[7] M. D. Eisaman, J. Fan, A. Migdall, and S. V. Polyakov, "Invited review article: Single-photon sources and detectors", Rev. Sci. Instrum. **82**, 071101 (2011).

*Corresponding author: dabramovic@ifs.hr

A superconducting radio-frequency quadrupole resonator for metrology experiments with highly charged ions

J. Stark[1] C. Warnecke*[1,2], E. A. Dijck[1], S. Chen[3], M. Wehrheim[1], S. Kühn[1], M. K. Rosner[1], A. Graf[1], J. Nauta[1], J.-H. Oelmann[1], L. Schmöger[1], T. Pfeifer[1], J. R. Crespo López-Urrutia[1]

1. Max-Planck-Institute for Nuclear Physics, Saupfercheckweg 1, 69117 Heidelberg, Germany

2. Heidelberg Graduate School for Physics, Ruprecht-Karls-Universität Heidelberg, Im Neuenheimer Feld 226, 69120 Heidelberg, Germany

3. State Key Laboratory of Magnetic Resonance and Atomic and Molecular Physics, Wuhan Institute of Physics and Mathematics, Innovation Academy for Precision Measurement Science and Technology, Chinese Academy of Sciences, Wuhan 430071, China

Gaining quantum control over the motional modes of cold, highly charged ions (HCI) had been a challenge for the last decades [1] since they lack of fast cycling transitions for laser cooling. Quantum logic spectroscopy (QLS) of the M1 transition in Ar^{+13} which was sympathetically cooled by a single Be^{+} logic ion was just recently accomplished and lowered the relative uncertainty by eight orders of magnitude to about 10^{-15} [2]. Due to their high sensitivity on beyond the Standard Model observables compared to singly charged ions and the possibility to extend current frequency standards to higher frequencies, HCI are of great interest [3]. Some of the possible clock-transitions in the XUV obtain extremely long lifetimes, thus promise the ability of reaching fractional uncertainties below $\Delta\nu/\nu = 10^{-19}$. Additionally they also feature a low susceptibility to external influences [3].
To provide an environment free of noise induced by external alternating electromagnetic fields, we developed a quasi-monolithic, superconducting quadrupole resonator of the Cryogenic Paul Trap Experiment (CryPTEx-SC) at the Max-Planck-Institute for Nuclear Physics in Heidelberg, Germany reaching a very high Q-factor up to $2x10^5$ at the working frequency of about 34 MHz [4]. While the Meisner-Ochsenfeld-effect shields the ions from external magnetic field fluctuations, the motional heating of the radial modes is directly suppressed due to the fidelity of the quadrupole fields. Therefore the cavity provides a promising environment to increase coherence times for QLS experiments, which will lead the way to future measurements of HCI in the Lamb-Dicke regime.

Complementing the trap, we have designed a 50-mm diameter magnifying objective covering a 500 micron field-of-view at a working distance of 57 mm, and optimized for imaging of the trapped Be^{+} ions at 313 nm. For stability and to keep the fields inside the cavity uncompromised from normal conducting surfaces, the 8-lens system directly is mounted on top of the superconducting resonator, and operates at 4 K. We discuss our design and present first commissioning results.

References

[1] L. Schmöger *et al.*, Science **347**, 6227 (2015)
[2] P. Micke, T. Leopold, S. A. King *et al.*, Nature **578**, 7793 (2020)
[3] M. G. Kozlov, M.S. Safronova, J. R. Crespo López-Urrutria, Rev. Mod. Phys. **90**, 045005 (2018)
[4] Stark *et al.*, https://arxiv.org/abs/2102.02793

*Corresponding author: christian.warnecke@mpi-hd.mpg.de

Transverse matter-wave interferometry with Rydberg helium atoms

J.D.R. Tommey[*1] **S.D. Hogan**[1],

1. Department of Physics and Astronomy, University College London, Gower Street, London,WC1E 6BT, United Kingdom

Atoms in highly excited Rydberg states can possess very large induced electric dipole moments, on the order of 10,000 Debye for values of the principal quantum number $n > 55$. These large dipole moments allow forces to be exerted on atoms in these states using inhomogenous electric fields [1]. By employing a combination of microwave pulses, to coherently manipulate the internal states of an atom, and pulsed electric field gradients, to state-selectively manipulate the center-of-mass motion, matter-wave interferometry with Rydberg atoms can be performed [2]. In this talk we will present an implementation of this type of electric Rydberg atom matter-wave interferometry in a transverse geometry with beams of helium atoms [3]. In these experiments the atoms are initially excited to the triplet $|61s\rangle$ Rydberg state inside a wedge shaped pair of electrodes. Superpositions of the $|61s\rangle$ and $|62s\rangle$ states are then prepared by driving a two-photon microwave transition at 14.350 GHz. A sequence of inhomogenous electric field gradient pulses and further microwave pulses complete the implementation of a half-loop Stern-Gerlach type matter-wave interferometer [4]. Phase differences between the arms of the interferometer are measured by state-selective pulsed electric-field ionization. Numerical calculations, accounting for the full phase evolution of the superposition state in the interferometer have been performed to aide in the interpretation of the experimental data. Coherent separations of the atomic momentum states up to 2 nm have been observed, limited by dispersion across the atom beam and residual Stark phase shifts arising because of the geometry of the apparatus. These results open new opportunities for studies of geometric quantum phases for particles with large electric dipole moments [5], with potential applications for gravity measurements with Rydberg positronium atoms [6].

References

[1] S. D. Hogan, "Rydberg-Stark deceleration of atoms and molecules", EPJ Techniques and Instrumentation 3, 1 (2016)
[2] Machluf, S., Yonathan J., and R. Folman. "Coherent Stern–Gerlach momentum splitting on an atom chip." Nature Comms. 4.1 (2013)
[3] Palmer, J. E., and S. D. Hogan. "Electric Rydberg-atom interferometry." Physical Review Letters 122.25 (2019)
[4] Bordé, Ch J. "Atomic interferometry with internal state labelling." Physics Letters A 140.1-2 (1989)
[5] Lepoutre, S, et al. "He-McKellar-Wilkens topological phase in atom interferometry." Physical Review Letters 109.12 (2012)
[6] D. B. Cassidy and S. D. Hogan, "Atom control and gravity measurements using Rydberg positronium", Int. J. Mod. Phys. Conf. Ser. 30, 1460259 (2014)

*Corresponding author: jake.tommey17@ucl.ac.uk

Storage Qubits and Synthetic Dimensions with Ultracold Polar Molecules

L. M. Fernley[1], **P. D. Gregory**[1], **J. A. Blackmore**[1], **S. L. Bromley**[1], **J. M. Hutson**[2] **and S. L. Cornish**[*1].

1. Joint Quantum Centre (JQC) Durham-Newcastle, Department of Physics, Durham University, South Road, Durham, UK, DH1 3LE

2. Joint Quantum Centre (JQC) Durham-Newcastle, Department of Chemistry, Durham University, South Road, Durham, UK, DH1 3LE

The rotational and hyperfine structure of ultracold polar molecules provides a huge Hilbert space in which to encode quantum information. In this work, we create an ultracold gas of optically trapped RbCs molecules in their rovibronic and hyperfine ground state by association from a pre-cooled atomic mixture [1][2]. We demonstrate that we can control the rotational and hyperfine states of the molecules with high fidelity using microwave fields [3]. Using a series of microwave π-pulses, we show that we can access rotational states up to $N = 6$ in the molecule. Furthermore, by applying multiple microwave fields simultaneously, we observe an Autler-Townes doublet in a 3-level ladder of rotational states [4].

Most recently, we have explored the coherence between a pair of hyperfine states in the rotational ground state which together form a storage qubit [5]. We fully characterise the dominant mechanisms for decoherence of the storage qubit using high-resolution Ramsey spectroscopy. Guided by a detailed understanding of the hyperfine structure of the molecule, we tune the magnetic field to where a pair of hyperfine states have the same magnetic moment. These states form a qubit, which is insensitive to variations in magnetic field. Our experiments reveal a subtle differential tensor light shift between the states, caused by weak mixing of rotational states. We demonstrate how this light shift can be eliminated by setting the angle between the linearly polarised trap light and the applied magnetic field to a magic angle of $\arccos(1/\sqrt{3}) \approx 55°$. This leads to a coherence time exceeding 5.6 s at the 95% confidence level.

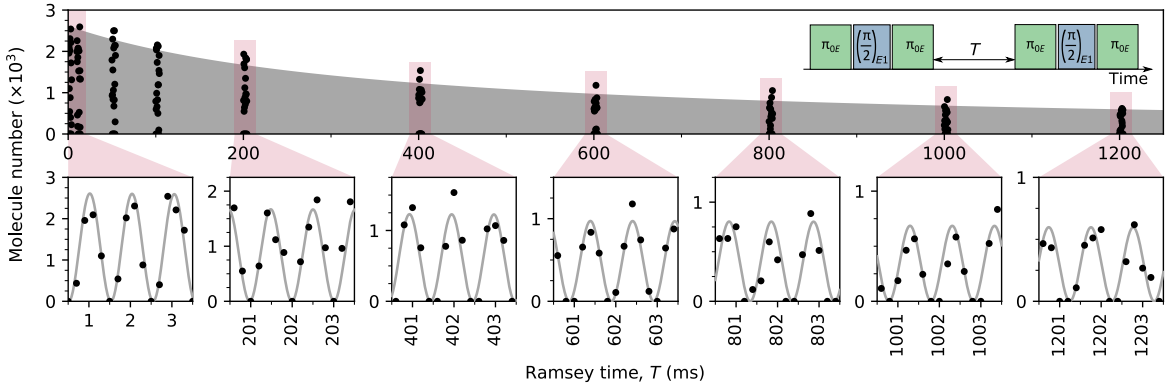

Fig. 1: Long-lived coherence between a pair of hyperfine states in the rotational ground state of optically trapped RbCs molecules. Using our optimal configuration of experimental parameters, we eliminate decoherence from differential Zeeman and tensor light shifts. We measure the coherence using an interrogation time of 1.2 s and find a lower bound on the coherence time of $T_2^* > 5.6$ s at the 95% confidence level.

References

[1] M. P. Köppinger *et al*., Phys. Rev. A. **89**, 033604 (2014).
[2] P. K. Molony *et al*., Phys. Rev. Lett. **113**, 255301 (2014).
[3] P. D. Gregory *et al*., Phys. Rev. A **94**, 041403(R) (2016).
[4] J. A. Blackmore *et al*., Phys. Chem. Chem. Phys. **22**, 27529 (2020).
[5] P. D. Gregory *et al*., arXiv:2103.06310v1 (2021).

*Corresponding author: s.l.cornish@durham.ac.uk

Polarization control of rotationally-resolved third-order molecular response

Grzegorz Kowzan[*1,2], **Myles Silfies**[1], **Neomi Lewis**[1], **Thomas K. Allison**[1]
1. Departments of Physics and Chemistry, Stony Brook University, Stony Brook, NY, USA
2. Institute of Physics, Faculty of Physics, Astronomy and Informatics, Nicolaus Copernicus University, Toruń, Poland

Broadband multidimensional coherent spectroscopy is a powerful tool for studying both molecular structure and dynamics but it is mostly limited to optically thick samples with broad spectral features, due to its low resolution and low sensitivity. It was shown recently that using optical frequency combs and optical enhancement cavities [1], both of these deficiencies can be overcome, paving the way for broadband rotationally-resolved multidimensional spectroscopy.

In broadband 2D IR spectroscopy, it is common to use specific beam polarization angles to suppress parts of the molecular response and simplify structure determination [2]. Similarly in the context of degenerate four-wave mixing and two-color four-wave mixing with narrowband lasers, polarization schemes suppressing particular rotational branches have been used to great effect [3]. Here, we analyze the polarization dependence in the more general case of three-color interaction with time-separated pulses, corresponding to broadband measurements with ultrashort frequency comb pulses. We decompose the total third-order rotationally-resolved response of a single vibrational mode into classes of pathways distinguishable by polarization of incident beams. We present useful sets of experimental polarizations allowing to selectively suppress parts of the response. In particular, we show how to either suppress or maximize amplitudes of the pathways undergoing coherent evolution between the second and third light-matter interaction. We demonstrate these results with simulations of the ν_3 mode (C-Cl stretch) of methyl chloride [4].

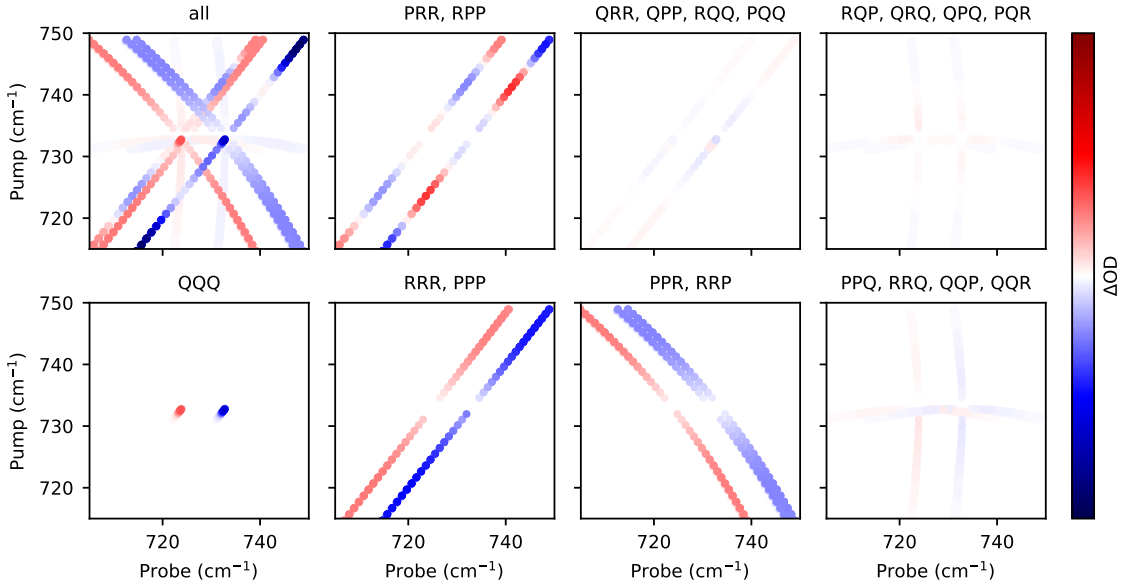

Fig. 1: Non-rephasing third-order rovibrational response of the ν_3 vibrational mode (C-Cl stretch) of $CH_3(^{35}Cl)$ split into classes of pathways with distinct polarization dependence. The upper-row classes are unique to three-color four-wave mixing pathways and undergo coherent evolution between the second and third interaction. The panel titles describe the sequences of rotational branch excitations, e.g. PRR corresponds to P-branch transition followed by two R-branch transitions.

References

[1] B. Lomsadze and S. T. Cundiff, Science **357**, 1389-1391 (2017); T. K. Allison, J. Phys. B **50**, 044004 (2017).
[2] M. T. Zanni, N. Ge, Y. S. Kim, R. M. Hochstrasser. Proc. Nat. Acad. Sci. **98**, 11265 (2001).
[3] A. E. Bracamonte and P. H. Vaccaro, J. Chem. Phys. **119**, 887-901 (2003); D. Murdock, L. A. Burns, P. H. Vaccaro, J. Phys. Chem. A **113**, 13184–13198 (2009).
[4] A. Nikitin, J. P. Champion and H. Bürger, J. Mol. Spectrosc. **230**, 174-184 (2005).

*Corresponding author: grzegorz@kowzan.eu

Nuclear spin squeezing by continuous quantum non-demolition measurement: a theoretical study

A. Serafin[1], **Y. Castin**[*1], **M. Fadel** [2] **P. Treutlein** [2] **A. Sinatra** [1]
1. Laboratoire Kastler Brossel, 24 rue Lhomond, Paris CEDEX 05, France
2. Unibas University of Basel, Petersplatz 1, P. O. Box 4001 Basel, Suisse

Helium-3 in its ground state enjoys the remarkable property of having a purely nuclear spin 1/2, perfectly isolated from the outside world even in an environment as hostile to quantum coherences as a gas of helium in a centimetric cell at room temperature and a pressure of the order of a millibar. By well-mastered nuclear polarization techniques,reaching a polarization of 90%, we can then routinely prepare (for example for lung imaging by nuclear magnetic resonance [1]) a giant collective nuclear spin with an extremely long lifetime. Recently, a coherence time T2 larger than 60 hours was measured in ultra-precise magnetometry devices [2], that seems limited only by the longitudinal decay time T1 due to collisions with the cell walls. These numbers make the macroscopic nuclear spin in a room temperature gas an ideal system for the production, the study and the use of entangled states, and therefore a competitor of cold atomic gases and Bose-Einstein condensates in metrology and quantum information processing [3].

In our work published in Comptes Rendus Physique [4] we propose to take advantage of the weak coupling of ground-state helium-3 nuclear spin to its environment to produce long-lived macroscopic quantum states, nuclear spin squeezed states, in a gas cell at room temperature. To perform a quantum non-demolition measurement of a transverse component of the polarized collective nuclear spin, we maintain a population in helium-3 metastable state with a discharge. The collective spin associated to $F = 1/2$ metastable level hybridizes with the ground state one by metastability exchange collisions. To access nuclear spin fluctuations, one continuously measures the light leaking out of an optical cavity, where it has interacted dispersively with the metastable state collective spin. In a three coupled collective spin model (nuclear, metastable and Stokes), we calculate moments of the nuclear spin squeezed component I_z conditioned on the time averaged optical signal. For a homodyne detection scheme, we solve the stochastic equation for the system state conditioned on the measurement; the conditional expectation value of I_z depends linearly on the signal and the conditional variance of I_z does not depend on it. The conditional variance decreases as $(\Gamma_{sq})^{-1}$, where the squeezing rate Γ_{sq} depends linearly on the light intensity in the cavity at weak atom-field coupling and saturates at strong coupling to the ground state metastability exchange effective rate, proportional to the metastable atom density. Including de-excitation of metastable atoms at the walls, which induces nuclear spin decoherence with an effective rate γ_α we find a limit $\propto (\gamma_\alpha/\Gamma_{sq})^{1/2}$ the conditional variance reached in a time $\propto (\gamma_\alpha \Gamma_{sq})^{-1/2}$.

References

[1] J. MacFall, H. Charles, R. Black, H. Middleton, J. Swartz, B. Saam, B. Driehuys, C. Erickson, W. Happer, G. Cates, G. Johnson, C. Ravin,"Human lung air spaces: potential for MR imaging with hyperpolarized He-3",Radiology **200** (1996), p. 553.
[2] C. Gemmel, W. Heil, S. Karpuk, K. Lenz, C. Ludwig, Y. Sobolev, K. Tullney, M. Burghoff, W. Kilian, S. Knappe-Grüneberg, W. Müller,A. Schnabel, F. Seifert, L. Trahms, S. Baeßler, "Ultra-sensitive magnetometry based on free precession of nuclear spins", Eur. Phys. J. D **57** (2010), p. 303.
[3] T. R. Gentile, P. J. Nacher, B. Saam, T. G. Walker, "Optically polarized3He", Rev. Mod. Phys. **89** (2017), 045004.
[4] Serafin, Alan and Castin, Yvan and Fadel, Matteo and Treutlein, Philipp and Sinatra, Alice. Comptes Rendus Physique **22** (2021). DOI : 10.5802/crphys.71

[*]Corresponding author: yvan.castin@lkb.ens.fr

Complementary atoms and molecules for rigorous bounds on P,T-violation

Konstantin Gaul[*1], **Robert Berger**[1]
1. Fachbereich Chemie, Philipps-Universität Marburg, Hans-Meerwein-Straße 4, 35032 Marburg, Germany

"New physics" beyond the standard model, as for instance described by supersymmetric models, can be probed by studying violations of discrete symmetries, i.e. space parity (P), time-reversal (T) and charge conjugation (C). Many different hypothetical sources of simultaneous violation of P- and T-symmetry can be discussed on the elementary particle level, such as P,T-odd currents between quarks and electrons or permanent electric dipole moments (EDMs) of elementary particles. All these fundamental P,T-odd interactions could induce net P,T-odd moments in bound systems such as atoms and molecules [1]. Thus, a measurement of a P,T-odd EDM of an atom or a molecule is difficult to interpret and predict due to possible interference of the various fundamental sources of P,T-violation. Nonetheless, due to enormous electronic structure enhancements of such P,T-odd effects in polar molecules, low-energy high-precision experiments on these molecules can give access to the TeV energy-regime [2]. With the proposal of laser-cooling of polyatomic molecules and its experimental evidence, new possibilities to improve molecular searches for P,T-violation employing the advantages of polyatomic molecules were demonstrated [3].

In this contribution possible sources of discrete symmetry violation are summarized and their effects on spectra of diatomic and small polyatomic molecules are discussed. Requirements of molecules for high-precision spectroscopy that aims to measure a permanent molecular EDM are elucidated. Trends of P,T-violation within the periodic table of elements determined with quasi-relativistic calculations [4] as well as measurement models for disentanglement of sources of P,T-violation in molecules are discussed [5]. Simple analytical models, which are gauged by *ab initio* calculations, help to identify suitable atoms and molecules for experiments.

References

[1] I. B. Khriplovich and S. K. Lamoreaux, CP Violation without Strangeness (Springer, Berlin, 1997).
[2] D. DeMille, Physics Today 68, 34 (2015); V. Andreev, D. G. Ang, D. DeMille, J. M. Doyle, G. Gabrielse, J. Haefner, N. R. Hutzler, Z. Lasner, C. Meisenhelder, B. R. O'Leary, C. D. Panda, A. D. West, E. P. West, X. Wu, and A. C. M. E. Collabo- ration, Nature 562, 355 (2018).
[3] T. A. Isaev, R. Berger, Phys. Rev. Lett. 116, 063006 (2016); I. Kozyryev et. al., Phys. Rev. Lett. 118, 173201 (2017); I. Kozyryev, N. R. Hutzler, Phys. Rev. Lett. 119, 133002 (2017).
[4] K. Gaul and R. Berger, J. Chem. Phys. 147, 014109 (2017); K. Gaul, R. Berger, J. Chem. Phys. 152, 044101 (2020), arXiv:1907.10432 [physics.chem-ph].
[5] K. Gaul, S. Marquardt, T. A. Isaev, and R. Berger, Phys. Rev. A 99, 032509 (2019), arXiv:1805.05494 [physics.chem-ph]; K. Gaul and R. Berger, Phys. Rev. A 101, 012508, (2020), arXiv:1811.05749 [physics.chem-ph].

*Corresponding author: konstantin.gaul@staff.uni-marburg.de

Amplification of Light Signal on V-type Atomic System

S. Petrosyan[1], **A. Aleksanyan**[*2,3], **E. Gazazyan**[2,4,5]

1. National Polytechnic University of Armenia, 0009, Yerevan, Republic of Armenia
2. Institute for Physical Research, NAS, 0203 Ashtarak, Republic of Armenia
3. Laboratoire Interdisciplinaire Carnot de Bourgogne, UMR CNRS 6303, UBFC, 21000 Dijon, France
4. Yerevan State University, 0025 Yerevan, Republic of Armenia
5. Institute for Informatics and Automation Problems, NAS, 0014, Yerevan, Republic of Armenia

In this work, the population dynamics of the V-type atomic system in the field of Gaussian pulses [Fig. 1 a)], are investigated, using numerical analysis. Our results are significantly different from the results in the framework of the resonance approximation. There are two types of techniques. In the first technique, there is an interaction with two Gaussian-shaped laser pulses, which are not in the two-photon resonance condition during the whole process. The laser pulses duration are fixed and show no difference. In the second technique, there is an interaction with two Gaussian laser pulses, where the transition $|2\rangle \rightarrow |1\rangle$ is symmetrically and linearly scanned close to its resonance frequency [1-3], which is expressed as

$$\Delta_{1,2}(t) = \Delta_{1,2}(0) - 2\Delta_{1,2}(0) \cdot \frac{t}{T_c}$$

with T_c the consideration time, $\Delta_{1,2}(0)$ the detuning value in the beginning of the process and t the time.

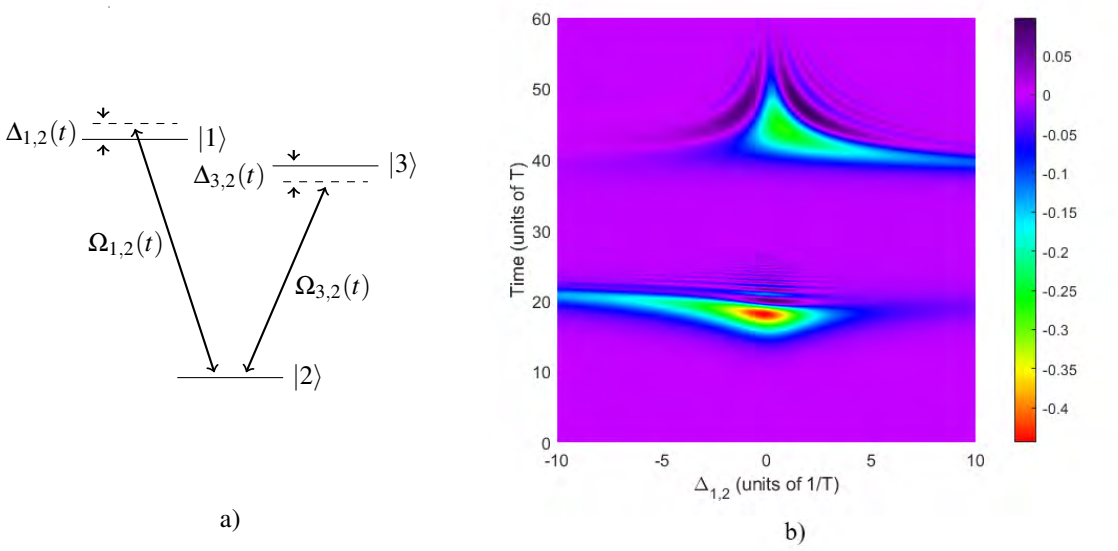

Fig. 1: a) V-type atomic system levels scheme, b) Amplification (Z-axis) dependence on the initial value of the scan (X-axis) and the process consideration time (Y-axis). All parameters are normalized to the average pulse duration T.

Figure 1 b) shows two amplification peaks. The first peak (viewed in red) is much stronger than the second peak. We present that in the three-level V-type system the amplification is more effective when using symmetrical and linear scanning around the resonant frequency.

Detailed analyses of the numerical solutions of the non-stationary equations for the density matrix of the three-level V-type system are carried out.

Funding. A. Aleksanyan acknowledges the funding support CO.17049.PAC.AN from the Graduate School EUR EIPHI.

Acknowledgements. The authors thank Hovhannes Harutyunyan for proofreading.

References

[1] Emil A. Gazazyan, "Interactions of femtosecond pulses with Λ-type atoms", Journal of Contemporary Physics (Armenian Academy of Sciences) volume 51, pages 22–27(2016) [Online]. Available: https://doi.org/10.3103/S1068337216010047

[2] A. Yu. Aleksanyan, "Effective Full Population Transfer in M-System Using Scanning Technique", Journal of Contemporary Physics (Armenian Academy of Sciences), 56, pages6–12(2021) [Online]. Available: https://link.springer.com/article/10.3103/2FS1068337221010035

[3] Emil Gazazyan, Gayane Grigoryan, Aram Papoyan, "Amplification of a Weak Circularly Polarized Light Signal in a Multilevel Atomic Medium", Journal of Contemporary Physics (Armenian Academy of Sciences) 51, pages22–27(2016), [Online]. Available: https://link.springer.com/article/10.3103/2FS1068337211040013

*Corresponding author: arthuraleksan@gmail.com

Latest Results of the High-Precision Penning Trap Mass Spectrometer PENTATRAP

M. Door*[1], J. R. Crespo López-Urrutia[1], P. Filianin[1], W. Huang[1], C. M. König[1], K. Kromer[1], Y. Novikov[2], A. Rischka[1], R. X. Schüssler[1], Ch. Schweiger[1], S. Sturm[1], S. Ulmer[3], S. Eliseev[1], K. Blaum[1],

1. Max-Planck-Institut für Kernphysik, Saupfercheckweg 1, 69117 Heidelberg, Germany
2. Petersburg Nuclear Physics Institute, 188300 Gatchina, Russia
3. RIKEN, Ulmer Initiative Research Unit, Wako, Saitama 351-0198, Japan

This contribution presents the latest high-precision atomic mass measurements using highly charged ions at the Penning-trap mass spectrometer PENTATRAP [1] located at the Max-Planck-Institute for Nuclear Physics in Heidelberg. It recently has proved its capabilities of performing mass-ratio measurements on highly charged ions of stable nuclides with a relative uncertainty of a few ppt, i.e. in the low 10^{-12} range [2,3]. With a broad measurement program PENTATRAP plans to contribute to experiments on tests of special relativity [4], bound-state QED [5], neutrino-physics [6] and 5th force search [7]. The following unique features of PENTATRAP facilitate high-precision mass-ratio measurements: (1) Cryogenic detection systems with single ion sensitivity and phase-sensitive Fourier Transform Ion Cyclotron Resonance (FT-ICR) image-current detection methods; (2) Highly charged ions provided by external ion sources; (3) A stack of five Penning traps used to perform simultaneous measurements and systematic checks; (4) Ultra-stable magnetic field and trapping potentials. Results on recent measurements on the Xe isotopic chain and on Re-Os will be presented.

References

[1] J. Repp *et al.*, Appl. Phys. B **107**, 983 (2012).
[2] R. X. Schüssler, H. Bekker, M. Braß *et al.*, Nature **581**, 42–46 (2020).
[3] P. Filianin, C. Lyu, M. Door, K. Blaum, W. J. Huang *et al.*, Phys. Rev. Lett., submitted (2021).
[4] S. Rainville *et al.*, Nature **438**, 1096 (2005).
[5] F. Köhler-Langes, *et al.*, Nature Comm. **7**, 10246 (2016).
[6] L. Gastaldo *et al.*, Eur. Phys. J. ST **226**, 1623 (2017).
[7] D. A. Nesterenko *et al.*, Int. J. Mass Spectrom. **458**, 116435 (2020).

*Corresponding author: door@mpi-hd.mpg.de

On the limits of the theoretical calculation of inelastic confinement-induced resonances

Tomás Sánchez-Pastor[*1], **Alejandro Saenz** [2], **Fabio Revuelta** [1]

1. Grupo de Sistemas Complejos, Escuela Técnica Superior de Ingeniería Agronómica, Alimentaria y de Biosistemas, Universidad Politécnica de Madrid, Avda. Puerta de Hierro 2-4, 28040 Madrid, Spain.

2. AG Moderne Optik, Institut für Physik, Humboldt-Universität zu Berlin, Newtonstrasse 15, 12489 Berlin, Germany.

Ultracold quantum atoms (UCA's) have become a topic of great interest over the last years since the experimental realization of the first Bose-Einstein Condensate [1]. Nowadays, UCA 's lie among the most promising platforms for quantum information and computation due to the excellent degree of control that we have to manipulate and control them. One way to do so consists in tuning the interparticle interactions with the help of Feshbach resonances by application of external magnetic fields [2].

Moreover, quantum gases are routinatively confined in optical traps of different shape and geometry (optical lattice, tweezers, dipolar traps, etc.). Changing the trapping potential enables an alternative way to manipulate the atomic sample through the so-called *inelastic confinement-induced resonances (ICIR's)*, which were first observed in a ground-breaking experiment in Innsbruck [3]. The origin of the ICIR's lies on the coupling of the center-of-mass (CM) and relative-motion (rm) coordinates due to the nonlinearities in the trapping potential. Consequently, they are absent in perfectly harmonic traps.

In this communication, we examine the limits of the theory of the ICIR's by comparison with full CI *ab initio* simulations. For this purpose, we calculate the energy spectrum of a system formed by two Lithium atoms by solving the corresponding six-dimensional Schrödinger equation. ICIR's manifest as avoided crossings in the spectrum, due to the interaction between the least-bound (molecular) state and the first-trap state. Our results show that the theory is accurate for quasi-one-dimensional traps [3], [5], but has severe limitations in the case of three-dimensional settings. Further details will be reported elsewhere [4].

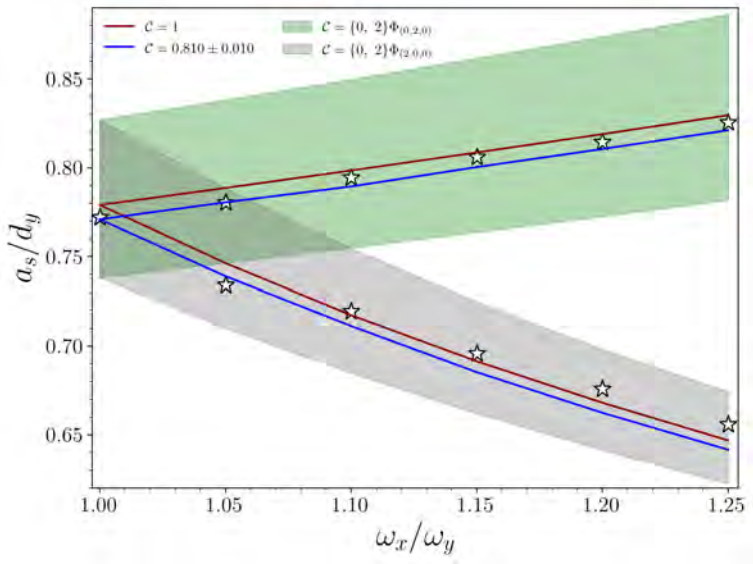

Fig. 1: Position of the inelastic confinement-induced resonances in terms of the ratio between the scattering length and the characteristic transversal size, a_s/d_y, as a function of the ratio between the transversal frequencies, ω_x/ω_y, for two Lithium atoms in a quasi-one dimensional trap $\omega_x, \omega_y >> \omega_z$. Anisotropy is responsible of the splitting of the resonance in two branches, being the top (bottom) one associated with two center-of-mass excitations in the y (x) direction. The *ab initio* simulations (white stars) agree well with our theoretical predictions [4] (blue solid lines), as well as by those given in Ref. [5] (red solid lines), which both lie within the limits of the theory (colored shaded areas).

References

[1] K. B. Davis *et al.*, Phys. Rev. Lett., **75**, 3969 (1995); M. H. Anderson *et al.*, Science **269**, 198 (1995).
[2] C. Chin, R. Grim, P. Julienne, and E. Tiesinga, Rev. Mod. Phys. **82**, 1225 (2010).
[3] E. Haller, *et al.*, Phys. Rev. Lett., **104**, 153203 (2010).
[4] T. Sánchez-Pastor, A. Saenz, and F. Revuelta *On the limits of the theoretical calculation of inelastic confinement-induced resonances, to be published.*
[5] S. Sala, P.-I. Schneider, and A. Saenz, Phys. Rev. Lett., **109**, 073201 (2012); S. Sala, and A. Saenz, Phys. Rev. A **94**, 022713 (2016).

*Corresponding author: t.ssanchez-pastor@upm.es

Spatial Bloch oscillations of a quantum gas in a "beat-note" superlattice

L. Masi[*1], **T. Petrucciani**[†2], **G. Ferioli**[1], **G. Semeghini**[1], **G. Modugno**[1,2,3], **M. Inguscio**[1,2,4], **M. Fattori**[1,2,3]

1. CNR Istituto Nazionale Ottica, 50019 Sesto Fiorentino, Italy

2. European Laboratory for Nonlinear Spectroscopy (LENS), 50019 Sesto Fiorentino, Italy

3. Department of Physics and Astronomy, University of Florence, 50019 Sesto Fiorentino, Italy

4. Department of Engineering, Biomedical Campus University of Rome, 00128 Roma RM, Italy

In this work we report the realization of a novel optical lattice for the manipulation of ultra-cold atoms where arbitrarily large separation between the sites can be achieved without renouncing to the stability of retroflected lattices, usually limited by the available laser sources with narrow linewidth. Superimposing two short-wavelength optical lattices with commensurated wavelengths, we realize an intensity periodic pattern with a beat-note like profile, where the regions with high amplitude modulation provide the potential minima for the atoms, Fig. 1.

The condition we impose on the wavelength is $\lambda_1 n = (n+1)\lambda_2$ with n integer, and working with n=20 and $\lambda_1 \approx 1\mu$m we realize an effective lattice period around 10 μm. To investigate the properties of this beat-note superlattice (BNSL) we prepare a Bose Einstein condensate with the possibility to tune the interatomic interaction by means of a magnetic Feshbach resonance. We employ it to measure the energy gaps between the first three bands and we study in-trap Bloch oscillation with negligible interaction in presence of small external forces.

The long lasting (1 second) oscillations between sites separated by ten microns we report prove the high stability of this potential and it is a valuable tool for the precise manipulation of atoms at large distances in a wide range of applications, for example trapped atom interferometry [1], quantum simulation with optical lattices [2]-[5] and for the development of future quantum technologies.

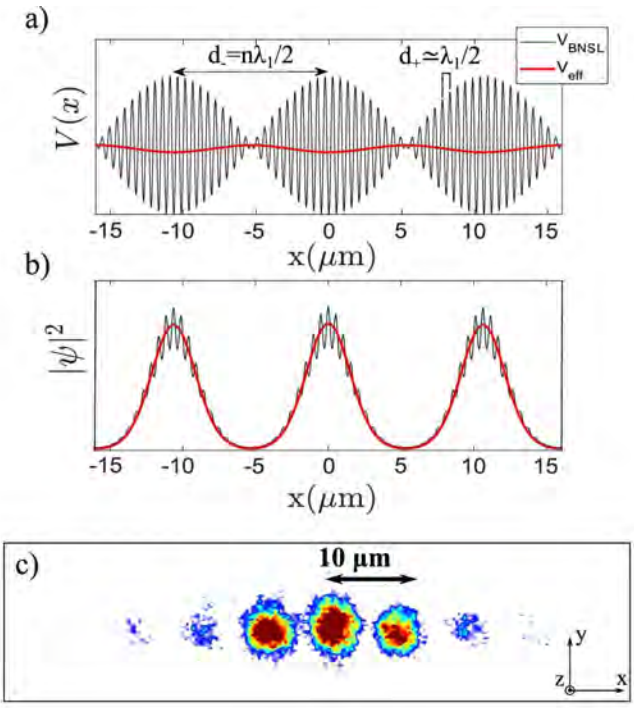

Fig. 1: a) Plot of the beat-note optical lattice (thin line) and the correspondent effective potential Veff (thick line). b) Profile of the ground-state atomic wavefunction in the presence of a BNSL (thin line) and in the presence of a standard large spacing optical lattice with a depth equal to the effective depth of the BNSL (thick line). c) Density distribution of a non interacting condensate in the ground state of the BNSL that shows the spatial modulation with a period of 10 μm.

References

[1] G. Spagnolli, G. Semeghini, L. Masi, G. Ferioli, A. Trenkwalder, S. Coop, M. Landini, L. Pezz'e, G. Modugno, M. Inguscio, A. Smerzi, and M. Fattori, Phys. Rev. Lett. **118**, 230403 (2017).

[2] S. Blatt, A. Mazurenko, M. F. Parsons, C. S. Chiu, F. Hu- ber, and M. Greiner,Phys. Rev. Lett. **A 92**, 021402 (2015).

[3] J. Vijayan, P. Sompet, G. Salomon, J. Koepsell, S. Hirthe, A. Bohrdt, F. Grusdt, I. Bloch, and C. Gross, Science **367**, 186 (2020).

[4] T. A. Hilker, G. Salomon, F. Grusdt, A. Omran, M. Boll, E. Demler, I. Bloch, and C. Gross, Science **357**, 484 (2017).

[5] G. Salomon, J. Koepsell, J. Vijayan, T. Hilker, J. Ne- spolo, L. Pollet, I. Bloch, and C. Gross, Nature (London) **565**, 56 (2019).

[*]Corresponding author: masi@lens.unifi.it

[†]Corresponding author: petrucciani@lens.unifi.it

Angular and Radial Roton Excitations in an Oblate Dipolar Quantum Gas

J.-N. Schmidt[*1], **J. Hertkorn**[1], **M. Guo**[1], **K.S.H. Ng**[1], **S.D. Graham**[1], **P. Uerlings**[1], **T. Langen**[1], **M. Zwierlein**[2], **T. Pfau**[†1]

1. 5. Physikalisches Institut and Center for Integrated Quantum Science and Technology, Universität Stuttgart, Pfaffenwaldring 57, 70569 Stuttgart, Germany

2. MIT-Harvard Center for Ultracold Atoms, Research Laboratory of Electronics, and Department of Physics, Massachusetts Institute of Technology, Cambridge, Massachusetts 02139, USA

Elementary excitations leave a characteristic footprint in the fluctuations of a quantum mechanical system. We report on first signatures of radial and angular roton excitations around a droplet crystallization transition in oblate dipolar Bose-Einstein condensates by direct in situ measurements of the density fluctuations near this transition. This approach allows for a direct extraction of the static structure factor simultaneously at all momenta. We analyse its radial and angular behaviour to identify the particular radial and angular excitations by the characteristic symmetries of their spatial patterns. The fluctuations peak as a function of interaction strength indicating the crystallization transition of the system and their characteristic length scale slightly shifts. By comparing our observations to a theoretically calculated excitation spectrum, we connect the crystallizations mechanism with the softening of the angular roton modes [1]. This understanding is an important step towards the realization of a dipolar supersolid in two-dimensional oblate trapping geometries [2], which is just the starting point to an rich phase diagram of structured patterns [3].

References

[1] J.-N. Schmidt, J. Hertkorn, M. Guo, F. Böttcher, M. Schmidt, K.S.H. Ng, S.D. Graham, T. Langen, M. Zwierlein, T. Pfau, arXiv:2102.01461 (accepted in PRL).

[2] J. Hertkorn, J.-N. Schmidt, M. Guo, F. Böttcher, K.S.H. Ng, S.D. Graham, P. Uerlings, H.P. Büchler, T. Langen, M. Zwierlein, T. Pfau, arXiv:2103.09752.

[3] J. Hertkorn, J.-N. Schmidt, M. Guo, F. Böttcher, K.S.H. Ng, S.D. Graham, P. Uerlings, T. Langen, M. Zwierlein, T. Pfau, arXiv:2103.13930.

[*]Corresponding author: jn.schmidt@physik.uni-stuttgart.de

[†]Corresponding author: t.pfau@physik.uni-stuttgart.de

Quantum Monte Carlo study of strongly interacting bosonic one-dimensional systems in periodic potentials

K. Dželalija[*1], **L. Vranješ Markić** [1]
1. Faculty of Science, University of Split, Ruđera Boškovića 33, HR-21000 Split

We present diffusion Monte Carlo (DMC) and path-integral Monte Carlo (PIMC) calculations of a onedimensional Bose system with realistic interparticle interactions in a periodic external potential. Our main aim is to test the predictions of the Luttinger liquid (LL) theory [1-3], in particular with respect to the superfluid-Mott insulator transition at both zero and finite temperatures, in the predicted robust and fragile superfluid regimes. For that purpose, we present our results of the superfluid fraction ρ_s/ρ_0, the one-body density matrix, the two-body correlation functions, and the static structure factor. The DMC and PIMC results in the limit of very low temperature for ρ_s/ρ_0 agree, but the LL model for scaling ρ_s/ρ_0 does not fit the data well. Algebraic decay of correlation functions is observed in the superfluid regime and exponential decay in the Mott-insulator one, as well as in all regimes at finite temperature for distances larger than a characteristic length.

The system under study is composed of N bosons of mass m with the Hamiltonian

$$\hat{H} = -\frac{\hbar^2}{2m}\sum_{i=1}^{N}\Delta_i + \sum_{i<j}^{N} U(r_{ij}) + \sum_{i=1}^{N} V_{ext}(x_i), \tag{1}$$

where N is the number of ^{4}He atoms of mass m, $r_{ij} = |x_i - x_j|$, $U(r)$ represents the interaction between ^{4}He atoms modeled by the Aziz potential [4] and $V_{ext}(x)$ is the external potential corresponding to the optical lattice.

In this work, we considered periodic external potential of the form

$$V_{ext}(x) = V_0 \sin^2(kx), \tag{2}$$

where $k = \pi/a_0$, with $a_0 = L/N$ the lattice constant, so that there is one atom per lattice site.

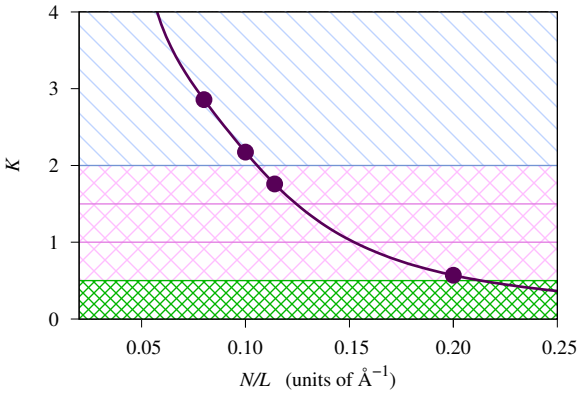

Fig. 1: Luttinger liquid parameter K as a function of the density. The bottom area corresponds to the quasi-solid regime with $K < 0.5$. The superfluid regime which is robust to periodic potential ($K > 2$) is at the top.

The system was studied thoroughly for four densities (Fig. 1), two in expected robust superfluid phase ($K > 2$) and two in fragile superfluid phase ($K < 2$). Despite the difference in microscopic models, when the bare Luttinger liquid parameters are equal, the obtained values of the critical depth for the superfluid insulator transition are close to both experimental and theoretical results in ultracold gases [5-7], demonstrating the LL universality.

References

[1] F. D. M. Haldane, Phys. Rev. Lett. **47**, 1840 (1981).
[2] A. Imambekov, T. L. Schmidt, and L. I. Glazman, Rev. Mod. Phys. **84**, 1253 (2012).
[3] M. A. Cazalilla, R. Citro, T. Giamarchi, E. Orignac, and M. Rigol, Rev. Mod. Phys. 83, 1405 (2011).
[4] R. A. Aziz, F. R. W. McCourt, and C. C. K. Wong, Mol. Phys. **61**, 1487 (1987).
[5] E. Haller *et al.*, Nature (London) **466**, 597 (2010).
[6] G. E. Astrakharchik, K. V. Krutitsky, M. Lewenstein, and F. Mazzanti, Phys. Rev. A **93**, 021605(R) (2016).
[7] G. Boéris *et al.*, Phys. Rev. A **93**, 011601(R) (2016).

*Corresponding author: kresimirdzelalija@pmfst.hr

Large, deep, and homogeneous optical lattices created in monolithic crossed cavities

A. J. Park[1,2], **N. Šantić**[1,2], **J. Trautmann**[1,2], **A. Heinz**[1,2], **V. Klüsener**[1,2], **I. Bloch**[1,2,3], **S. Blatt**[*1]

1. Max Planck Institute of Quantum Optics, Hans-Kopfermann-Straße 1, 85748, Garching, Germany

2. Munich Center for Quantum Science and Technology, 80799 München, Germany

3. Fakultät für Physik, Ludwig-Maximilians-Universität München, 80799 München, Germany

We have developed ultra-high-vacuum compatible cavities to create large-scale, two-dimensional optical lattices for use in experiments with ultracold atoms. The assembly consists of an octagon-shaped spacer made from ultra-low-expansion glass, to which we optically contact cavity mirrors, leading to a high degree of mechanical and thermal stability. The advantages of such cavities include increasing the system sizes in quantum gas microscopes by an order of magnitude compared to the state-of-the-art, improving the lattice homogeneity, and enhancing the lattice depth. We have integrated the cavities into an ultracold Strontium machine and benchmarked the size and homogeneity of the lattice by imaging the intensity profile via atomic clock shifts. Our clock spectroscopy can also locally resolve the vibrational modes, thus allowing us to locally probe temperatures. We do not observe discernible heating while holding the atoms in the lattices up to 15 seconds, and we observe atom lifetime of a minute. Our results present a viable solution to create ultracold atoms experiments where compactness, stability, and large, deep lattices can be achieved simultaneously.

[*]Corresponding author: sebastian.blatt@mpq.mpg.de

Ion loss events in a Rb-Ca^+ cold hybrid trap: photodissociation, black-body radiation and non-radiative charge exchange

Xiaodong Xing[*1], **Humberto da Silva Jr**[2], **Romain Vexiau**[1], **Nadia Bouloufa-Maafa**[1], **Olivier Dulieu**[†1]

1. Laboratoire Aimé Cotton, Université Paris-Saclay/CNRS, 91400, Orsay, France

2. Department of Chemistry and Biochemistry, University of Nevada, 89154, Las Vegas, USA

The 'hybrid' trap merging ultracold atoms and cold ions opens up fascinating avenues to investigate ion-atom interactions and formation of cold molecular ions for various applications [1,2,3]. The advantage of such atom-ion experiments is that we can detect the ion loss event as one of key fingerprints to identify processes and distinguish product branching ratios. Even though ion loss has been commonly present in ion-atom collisions as an universal behavior, to acknowledge the reactive mechanism is always a complex and non-intuitive problem.

In Basel, a hybrid trap for ultracold ^{87}Rb atoms and cold $^{40}Ca^+$ ions has been implemented, and already delivered many results [3-6]. Three competing processes have been identified in the trap dynamics, and investigated both theoretically and experimentally: radiative association of $RbCa^+$ molecular ions, radiative charge transfer and non-radiative charge exchange [7,8]. However, the precise role of the involved lasers has still to be investigated.

We present theoretical calculations related to three processes: photodissociation of the created molecular ions, the influence of black-body radiation (BBR), and non-radiative charge exchange based on novel molecular data compared to Ref. [7]. The Ca^+ cooling laser with 397 nm wavelength is demonstrated to be capable of inducing the dissociation of the cold $RbCa^+$ ions, beyond a given threshold for their internal states. The analysis of BBR effect reveals that the surviving $RbCa^+$ are not destructed by BBR-induced photodissociation. Finally, the non-radiative charge exchange calculations, despite the significant differences in our new set of molecular data compared to those of Ref. [7], yield rates in good agreement with experimental data.

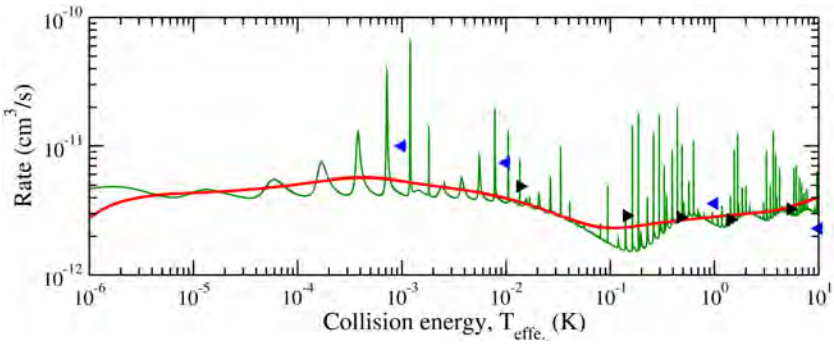

Fig. 1: Calculated non-radiative charge exchange reaction rate as a function of the collision energy. Non-thermalized rate (green), Boltzmann thermalized rate (red), Boltzmann thermalized rate (blue) of Ref. [7], and experimental data (black) of Ref. [4].

Our theoretical calculations are able to characterize the vibrational distribution of the traped $RbCa^+$ at the ground state. The obtained specific range of vibration states $16 \leq v \leq 28$ implys that photodissociation would destroy the molecules with $v \geq 29$, and the deeper bound molecular ions with $v \leq 15$ are unlikely formed within radaitive association process. Besides, we discover that the photodissociation-induced ion loss of ground state molecular ion would be commonly presented in other ultracold Calcium-ion-alkali-metal-atom systems due to the cooling lasers of Ca^+.

References

[1] T. Feldker, H. Fürst, H. Hirzler, H. V. wald, M. Mazzanti, D. Wiater, M. Tomza, Nat. Phys. **16**, 413-416 (2020)
[2] M. Tomza, K. Jachymski, R. Gerritsma, A. Negretti, T. Calarco, Z. Idziaszek, P. S. Julienne, Rev. Mod. Phys. **91**, 035001 (2019)
[3] A. Mohammadi, A. Krükow, A. Mahdian, M. Deiß, J. Pérez-Ríos, H. da Silva Jr., M. Raoult, O. Dulieu, J. H. Denschlag, Phys. Rev. Research **3**, 013196 (2021)
[4] F. J. H. Hall, M. Aymar, N. Bouloufa-Maafa, O. Dulieu, S. Willitsch, Phys. Rev. Lett. **107**, 243202 (2011)
[5] F. J. H. Hall, S. Willitsch, Phys. Rev. Lett. **109**, 233202 (2012)
[6] S. Willitsch, Mol. Phys. **31**, 175 (2012)
[7] F. J. H. Hall, O. Eberle, G. Hegi, M. Raoult, M. Aymar, O. Dulieu, S. Willitsch, Mol. Phys. **111**, 2020-2023 (2013)
[8] A. K. Belyaev, S. A. Yakovleva, M. Tacconi, F. A. Gianturco, Phys. Phys. A **85**, 042716 (2012)
[9] M. Tacconi, F. A. Gianturco, A. K. Belyaev, Phys. Chem. Chem. Phys. **13**, 19156-19164 (2011)

[*]Corresponding author: xiaodong.xing@universite-paris-saclay.fr
[†]Corresponding author: olivier.dulieu@universite-paris-saclay.fr

Mapping of ion motion spectra in a linear Paul trap

K. Pleskacz[*1], **Ł. Kłosowski**[1], **M. Piwiński**[1],
1. Institute of Physics, Faculty of Physics, Astronomy and Informatics,
Nicolaus Copernicus University in Toruń, Grudziądzka 5, 87-100 Toruń, Poland

The basic idea of an ion trap is to confine a charged particle in a free space using electric and / or magnetic fields. In 1953 Paul developed a quadrupole ion trap using an alternating electric field with radio frequency Ω [1]. Oscillating electric field combined with perfect quadrupole geometry and electrostatic potential provides a minimum in the total energy of the ion at the trap center and creates a quadrupole effective trapping potential with eigenfrequency ω. In the ideal linear trap, the motion of ions can be written in the form of Mathieu equations [2]. Stable solution of such equations can be analyzed by means of a stability diagram showing the stability regions of the ion in a and q domain.

However, the quadrupole field in real traps contains higher-order field components, such as octupole [3], [4], which makes the ion motion in the trap more complex. This is the direct cause of the formation of nonlinear resonances in the motion of ions in the potential of the trap. This phenomenon can be observed as the ions' escape from the trapping region, which is caused by a rapid increase in their kinetic energy gained from the electric field of the trap. In the stability diagram resonances form characteristic lines, which were observed experimentally and discussed in our previous work [4].

The numerical simulations for different trapping conditions (a and q) were carried out to observe ion motion in the trap potential. The results obtained for the quadrupole potential mixed with higher order harmonics were analyzed. In addition, the Fourier transform was used to determine the characteristic spectra in the frequency domain. The spectra were compiled and presented as two-dimensional maps (see an example in Fig.1) Calculations were performed for the parameters in the area of stability for which nonlinear resonances can be expected. The discrepancies between adiabatic approximation and numerical simulation data were observed, which requires further research (Fig 1).

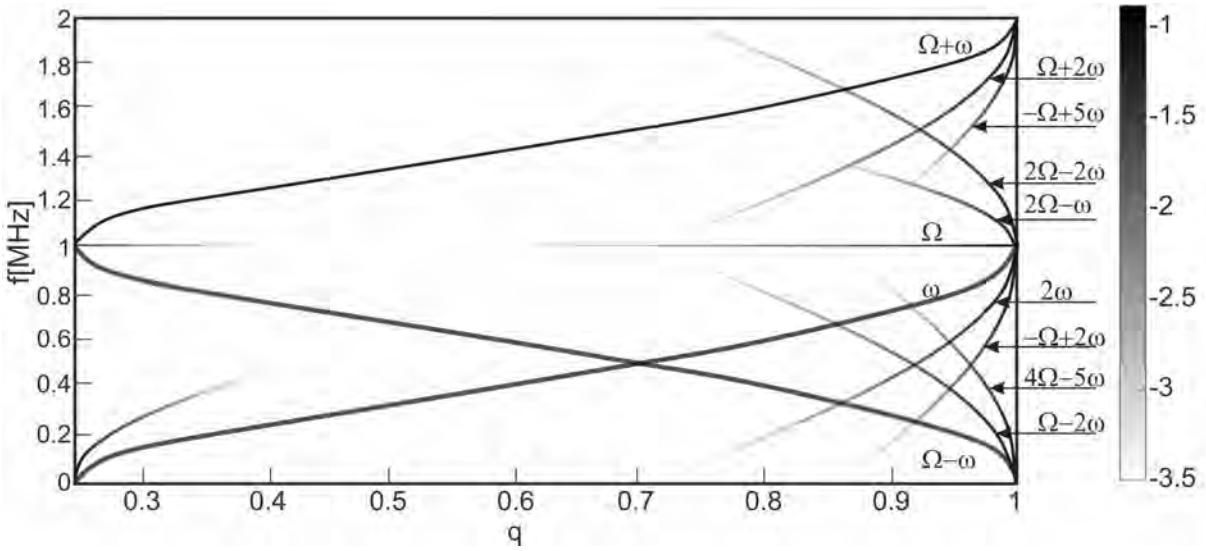

Fig. 1: Map of frequency domain as a function of the parameter q for ion in quadrupole field disturbed with an octupole for a fixed value of a=0.05. Grayscale is mapped on a logarithmic scale and relate to the amplitude.

References

[1] W. Paul, H. Steinwedel, Z. Naturforsch. **8A**, 448 (1953).
[2] F. G. Major, V.N. Gheorghe, G. Werth *Charged Particle Traps* (Springer Berlin Heidelberg New York, 2005).
[3] R. E. March, J. Mass Spectrom. **32**, 351 (1997).
[4] Ł. Kłosowski, M. Piwiński, K. Pleskacz, S. Wójtewicz, D. Lisak, J. Mass Spectrom. **53**, 541 (2018).

*Corresponding author: pleskacz@doktorant.umk.pl

A Cavity-Enhanced Microscope for Cold Atoms

Tigrane Cantat-Moltrecht[*1], **N. Sauerwein**[1], **J.-P. Brantut**[†1]
1. Laboratory for Quantum Gases, Institute of Physics, EPFL, CH-1015 Lausanne, Suisse

We have set up a novel type of atom microscope, consisting of cold Lithium 6 atoms in a high-finesse cavity, combined with high-numerical-aperture optics (0.37). This combined system allows to trap the atoms in a combined dipole trap made up of a micro-tweezer at 780 nm and an intra-cavity dipole-trap at 1342 nm. These beams trap the atoms inside the 671 nm near-concentric cavity mode addressing the D2 transition of ^{6}Li. A fourth beam at 460 nm addressing the $2P \rightarrow 4D$ transition of ^{6}Li, tightly-focused through the high-NA optics, will allow to control the detuning between the D2 transition and the cavity field at 671 nm by light-shifting the energy of the $2P_{3/2}$ state. As atom-cavity coupling depends non-linearly on atom-cavity detuning, this "light-shifting beam" will provide temporal and spatial control over atom-cavity coupling, with a super-resolution effect realizing this novel type of "Cavity Enhamced Microscope" [1]. This will also open up new avenues for fine control over cavity-mediated interactions among an atomic ensemble, leading to interesting regimes for quantum simulation.

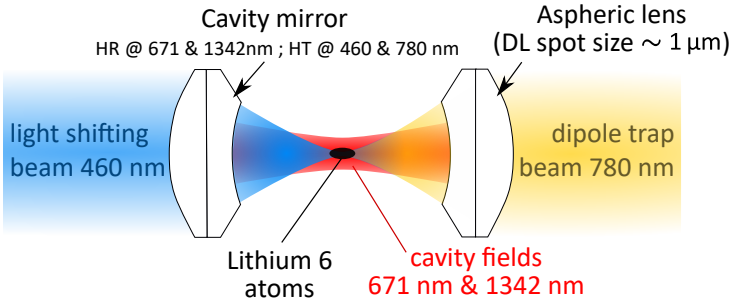

	high finesse	high NA
near-resonant	671 nm (atom-cavity interaction)	460 nm (light-shifting beam)
far off resonance	1342 nm (intracavity dipole trap)	780 nm (micro-tweezer dipole trap)

Fig. 1: Left : Scheme of the cavity system and relevant light fields, whose functions are summarized in the table.

Currently, Li6 atoms can be trapped and imaged inside the intra-cavity dipole trap at 1342nm and dispersive interaction of the atomic cloud with the cavity mode has been verified. Thanks to a simple model for the geometry of atom-cavity coupling, we are developing a method for estimating the temperature of the atoms through dispersive cavity measurements.

The next steps towards a working Cavity-Enhanced Microscope is the preparation of ultra-cold atomic ensembles. We hope to achieve efficient cooling by suing cavity cooling techniques: the atoms scatter photons from a pump beam into the cavity mode and release kinetic energy in the process [2,3]. Our combination of a narrow linewidth cavity (451 kHz) and strongly confining dipole traps (600 kHz to 2 MHz trapping frequencies) is an ideal setup for realizing this type of cavity cooling in a resolved sideband regime, which could lead to near ground state cooling for single atoms.

I will summarize the important ideas and technical developments behind the design, present the current status of our experiment and the next steps towards resolved-sideband cavity cooling.

References

[1] D. Yang et al., Phys. Rev. Lett. **120**, 133601 (2018)
[2] V. Vuletic et al., Phys. Rev. A **64**, 033405 (2001)
[3] M. Hosseini et al., Phys. Rev. Lett. **118**, 183601 (2017)

[*]Corresponding author: tigrane.cantatmoltrecht@epfl.ch
[†]Corresponding author: jean-philippe.brantut@epfl.ch

One dimensional Yb gases with two-body losses: strong quantum correlations in the Zeno regime

L. Rosso[1], D. Rossini[2], A. Biella[1,3] L. Mazza*[1], A. Ghermaoui[4], M. Bosch Aguilera[4], R. Vatré[4], R. Bouganne[4], J. Beugnon[4], F. Gerbier[4]

1. Université Paris-Saclay, CNRS, LPTMS, 91405 Orsay, France

2. Dipartimento di fisica dell'Università di Pisa and INFN, 51627 Pisa, Italy.

3. INO-CNR BEC Center and Dipartimento di Fisica, Università di Trento, 38123 Povo, Italy

4. Laboratoire Kastler Brossel, Collège de France, CNRS,ENS-PSL Research University, Sorbonne Université, 75005 Paris, France

We consider strong two-body losses in quantum gases trapped in one-dimensional optical lattices. We first consider the bosonic case. We exploit the separation of time scales typical of a system in the many-body quantum Zeno regime to establish a connection with the theory of the time-dependent generalized Gibbs ensemble. Our main result is a simple set of rate equations that capture the simultaneous action of coherent evolution and two-body losses. This treatment gives an accurate description of the dynamics of a gas prepared in a Mott insulating state and shows that its long-time behaviour deviates significantly from mean-field analyses (see Fig. 1). The possibility of observing our predictions in an experiment with ^{174}Yb in a metastable state is also discussed [1]. We then move to the fermionic case, where experiments with ^{173}Yb have already been performed: our theoretical approach pinpoints the importance of spin in determining the full dynamics of the system [2].

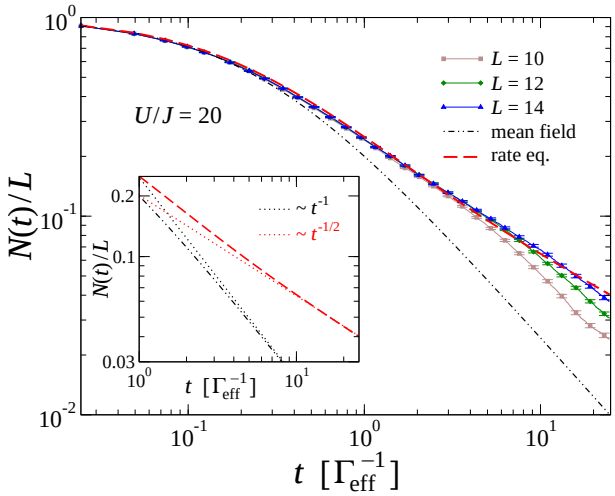

Fig. 1: Time-evolution of the number of atoms for an initial bosonic Mott insulator according to the rate equations (dashed red line). Our result is benchmarked with simulations based on quantum trajectories for $L = 10$, 12 and 14 (each point is averaged over 10^4 trajectories). The dot-dashed black line represents the mean-field solution $N(t)/L$. The inset highlights the different long-time decay as t^{-1} for the mean-field solution and as $t^{-1/2}$ for the rate equation.

References

[1] D. Rossini, A. Ghermaoui, M. Bosch Aguilera, R. Vatré, R. Bouganne, J. Beugnon, F. Gerbier and L. Mazza, *Strong correlations in lossy one-dimensional quantum gases: from the quantum Zeno effect to the generalized Gibbs ensemble*, arXiv:2011.04318 (2020).

[2] L. Rosso, D. Rossini, A. Biella and L. Mazza, *One-dimensional spin-1/2 fermionic gases with two-body losses: weak dissipation and spin conservation*, arXiv:2104.07929 (2021).

*Corresponding author: leonardo.mazza@universite-paris-saclay.fr

Fast in-situ absorption imaging of the local density of ultra-cold atoms in an optical lattice using an imaging lattice

R. Veyron[*1], **J.B. Gerent**[1], **V. Mancois**[1], **G. Baclet**[1], **P. Bouyer**[1], **S. Bernon**[1]

1. Laboratoire Photonique Numerique et Nanosciences (LP2N), Univ. de Bordeaux - CNRS - Institut d'Optique Graduate School, France

Quantum gas microscopes have become a major element for quantum simulations using ultra-cold atoms in optical lattices. Long-range order as antiferromagnetic correlations between lattice sites have been observed in far field optical lattices using density and spin resolved microscopy. Decreasing the lattice period would increase the interaction energies in those systems to enter deeply into quantum regimes.
Our group proposed a theoretical work [1] where the lattice period can be reduced by trapping atoms in close proximity (down to tens of nanometers) with a nano-structured surface generating sub-wavelength lattice potentials. At such a distance from the surface, the attractive Casimir-Polder force between the atoms and the surface needs to be compensated. The surface is engineered by a spatially varying field to doubly dress the ground state which forms a controllable trapping potential with a tunable trapping position.
In such sub-wavelength lattices, one needs to overcome the diffraction limit to image in-situ the lattice sites. In this work, we present the experimental characterisation of a sub-wavelength imaging method applicable to quantum gas microscopes. The setup consists in imaging the sites of an 1D optical lattice initially loaded with a Bose-Einstein Condensate of ^{87}Rb with a period of 532 nm by dressing the excited state with a second optical lattice with a period of 768 nm. Absorption imaging in 20 μs of the density distribution is demontrasted. The limits of the current setup and the limits of the method will be detailed.

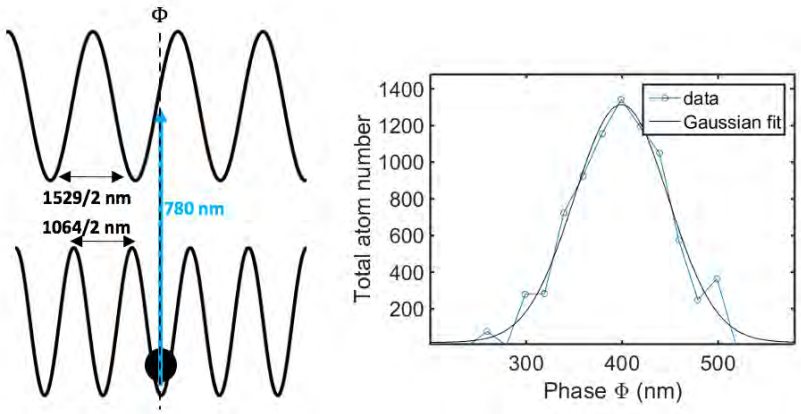

Fig. 1: Ground state lattice generated by an optical lattice at the wavelength of 1064 nm and the excited state lattice generated by an optical lattice at 1529 nm. Both are coupled with a repumper laser at 780 nm. Scanning the phase between the lattice gives access to the density in 1 site. The width of the Gaussian fit reflects the convolution of the density profile with the resolution of the sub-wavelength imaging method.

References

[1] M. Bellouvet et al., Phys. Rev. A 98, 023429 (2018)

*Corresponding author: romain.veyron@institutoptique.fr

Photoassociation of Rb and Hg atoms near the ^{87}Rb D_1 line at 795 nm

R. Muñoz-Rodriguez[*1], **M. Witkowski**[1], **M. Borkowski**[1], **P. S. Żuchowski**[1], **R.Ciuryło**[1], **M. Zawada**[1]
1. Institute of Physics, Nicolaus Copernicus University, Grudziądzka 5, 87-100, Toruń, Poland

Ultracold molecules produced with a mixture of alkali and closed shell alkaline earth like atoms are of special interest since they possess both electric and magnetic dipole moments which could allow their control by means of external fields [1]. Such type of molecules could be used for quantum simulations and for high precision measurements of magnetic fields [2], the electron-proton mass ratio and in the search of the limit of the electronic dipole moment of the electron [3].

The simultaneous laser cooling and trapping of Rb and Hg atoms with the ultimate goal to achieve cold RbHg molecules by photoassociation is motivated by the current research on open-shell polar molecules such as the RbSr [4],[5], RbYb [6], LiYb [7],[8] and CsYb [9],[10].

With the photoassociation of Rb and Hg atoms at 795 nm, we embark into the creation of an interesting but challenging type of molecule with very promising prospects and applications. For example, Meyer and Bohn [11] have proposed dimers containing Hg atoms as good candidates for experimental search for electric-dipole moment of the electron (eEDM). Furthermore, due to its small Van der Waals interaction, dimmers containing Hg atoms are suitable for revealing new types of interaction between barions [12]. For last, due to the plethora of Hg bosonic isotopes, there are 10 possible combinations of RbHg molecules, thus opening up the door to the mass tuning of the scattering length. Fig.1 describes our most recent results regarding to the theory and the experiment.

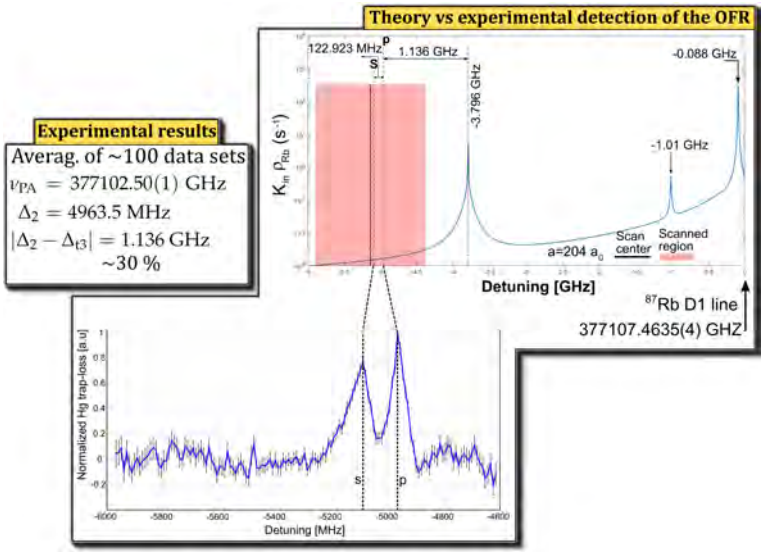

Fig. 1: Comparison between the measured trap-loss spectrum and the calculated photoassociative loss rate for the ^{202}Hg atoms near the ^{87}Rb D_1 line [13]. The two lines in the detected photoassociation spectrum correspond to two partial waves involved in Rb-Hg collisions, *s* and *p*, respectively. The *p*-wave line position was determined using an optical frequency comb, which yielded Γ_{PA} = 377102.5(1) GHz. The covered range is shown in light red color and the dashed lines show the detuning for the *s* and *p*-wave lines at Δ_1 =-5086.4 MHz and Δ_2 = -4963.5 MHz, respectively. The calculated center of the closest PA line in the scanned range and the measured top of the *p*-wave line differ by 1.136 GHz.

References

[1] P. S. Żuchowski, J. Aldegunde, and Jeremy M. Hutson, Phys. Rev. Lett. 105, 153201.
[2] A. Micheli, G. K. Brennen, and P. Zoller, Nature Physics 2.5, 341–347.
[3] E. R. Meyer, J. L. Bohn, and M. P. Deskevich, Phys. Rev. A 73, 062108.
[4] Benjamin Pasquiou et al., Phys. Rev. A 88, 023601.
[5] Vincent Barbé et al., Nature Physics 14.9, 881–884.
[6] F. Baumer et al., Phys. Rev. A 83, 040702
[7] Vladyslav V. Ivanov et al., Phys. Rev. Lett. 106, 153201
[8] Hideaki Hara et al., Phys. Rev. Lett. 106, 205304.
[9] Alexander Guttridge et al., Phys. Rev. A 97, 063414.
[10] Daniel A. Brue and Jeremy M. Hutson, Phys. Rev. A 87, 052709.
[11] E. R. Meyer and J. L. Bohn, Phys. Rev. A 80, 042508.
[12] E. J. Salumbides et al., Phys. Rev. D 87, 112008.
[13] M. Borkowski, R. Munoz-Rodriguez, M. B. Kosicki, R. Ciuryło, P. S. Żuchowski 2017 Phys. Rev. A 96, 063411.

*Corresponding author: rodolfomr@umk.pl

Quantum Monte Carlo Simulation of Polaron Tunneling

A.S. Popova[*1], **V. V. Tiunova**[†1], **A. N. Rubtsov**[1,2]

1. Russian Quantum Center, Bolshoy Bulvar 30, bld. 1, Skolkovo, Moscow 121205, Russia

2. Department of Physics, Lomonosov Moscow State University, Leninskie gory 1, Moscow 119991, Russia

A single mobile impurity, which interacts with a phonon bath, forms a polaron. The polaron model was developed to define the coupling between electrons and lattice phonons in a dielectric crystal [1] in the first half of the twentieth century. Today it also describes a an impurity atom immersed a Bose-Einstein condensate (BEC), where interaction strength goes far beyond the parameter range relevant for solids [2]. Research of impurities into an ultra-cold environment be also useful for a deeper understanding the physics of neutral atoms in optical traps [3] and quantum dots [4].

In this work, we are interested in the study of the incoherent tunneling effect [5] in the BEC-impurity set-up. Generally, a tunneling particle, which interacts with a bath, is hard to study both analytically and numerically. To overcome this issue, we develop a special modification of the QMC method to consider tunneling of a single impurity immersed in BEC (Frolich-Bogolubov model [2]) and trapped in a double-well potential in one dimension. In the main, the proposed Quantum Tunneling Monte Carlo (QTMC) method uses the idea of reducing the initial many-body task to a single particle problem by including correlations of all orders in a numerically exact way. Our algorithm samples the impurity trajectories in imaginary time on a coarse time grid with the step, which enables us to simulate a tunneling effect for the impurity effectively. Our algorithm samples the impurity trajectories in imaginary time on a coarse time grid with the step, which enables us to simulate a tunneling effect for the impurity effectively. We calculate the density of states from the imaginary-time Green's function, using the maximum entropy method (MaxEnt).

We discover the crossover from phonon-assisted tunneling in weak interaction strength to self-trapping for strong coupling in the BEC-impurity system (Fig. 1), using the QTMC method [5]. For the continuous bosonic spectrum, there is a crossover region and these two phenomena coexist in the intermediate strength regime. Moreover, we identify the density of state peaks as quasiparticle peaks and estimate their effective mass. For a phonon-assisted tunneling region, the effective mass of an impurity decreases while a heavy quasiparticle emerges for strong coupling. We believe that these phenomena can be observed in the recent experimental set-ups [6] with an addition of two close harmonic optical dipole traps for an impurity atom.

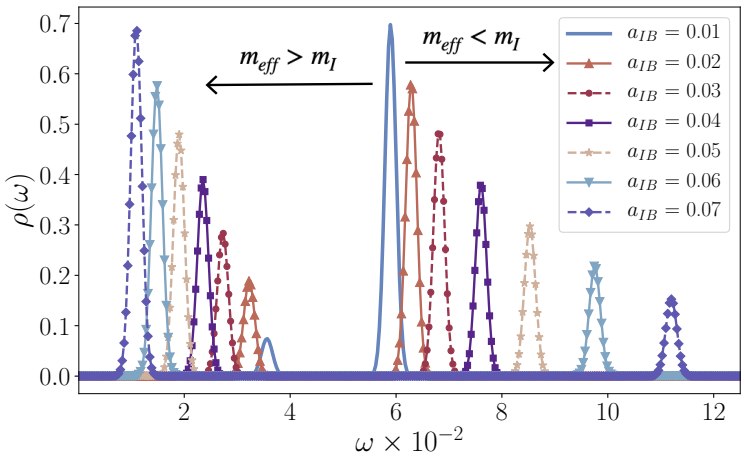

Fig. 1: Spectral densities of states for 39K tunneling impurity, which interacts with the continuous spectrum of Bogoliubov excitations in 87Rb condensate; aIB is the interaction strength

References

[1] L. Landau and S. Pekar, Effective mass of a polaron, Zh. Eksp. Teor. Fiz. **18**, 419 (1948).
[2] J. Tempere, W. Casteels *et al.*, Phys. Rev. B **80**, 184504 (2009).
[3] H. Bernien *et al.*, Nature **551**, 579 (2017).
[4] T. Stauber, R. Zimmermann, and H. Castella, Phys. Rev. B **62**, 7336 (2000).
[5] Popova, A. S., V. V. Tiunova, and A. N. Rubtsov, Phys. Rev. B **103(15)**, 155406 (2021).
[6] N. B. Jørgensen, Nils B.*et al.*, Phys. Rev. Lett. **117**, 055302 (2016).

[*]Corresponding author: a.popova@rqc.ru
[†]Corresponding author: vv.vyborova@physics.msu.ru

High Precision Calibration of Molecular Oxygen Absorption Lines Using Transitions in Highly Charged Ions

R. Steinbrügge*[1], S. Kühn[2], S. Bernitt[3,2], J. R. Crespo-López Urrutia[2], M. Leutenegger[4],

1. Deutsches Elektronensynchrotron DESY, Notkestr. 85, 22607 Hamburg, Germany
2. Max-Planck-Institut für Kernphysik, Saupfercheckweg 1, 69120 Heidelberg, Germany
3. Helmholtz-Institut Jena, Fröbelstieg 3, 07743 Jena, Germany
4. NASA/Goddard Space Flight Center, 8800 Greenbelt Road, Greenbelt, Maryland 20771, USA

The absorption lines of neutral atomic oxygen observed in numerous Chandra and XMM-Newton spectra show a large discrepancy to the rest wavelength measured in the laboratory. If interpreted as an astrophysical Doppler shift, this would indicate implausible gas velocities in the order of 300 km/s. The laboratory measurements have been calibrated using transitions in molecular O_2, whose absolute energy calibration almost all trace back to a single experiment performed in 1974.

In this contribution we present measurements of O_2 transition energies using transitions in highly charged ions as energy reference. The x-ray beam of a synchrotron light source is used to ionize O_2 in a gas cell while counting photoions with channeltron. To calibrate the photon beam energy, the PolarX-EBIT was installed upstream of the gas cell. This electron beam ion trap features an off-axis electron gun, allowing the photon beam to pass through the trap along its main axis [2]. In the trap helium-like nitrogen ions were produced and resonantly excited by the photon beam, using their $1s^2 - 1snp$ transitions as energy references.

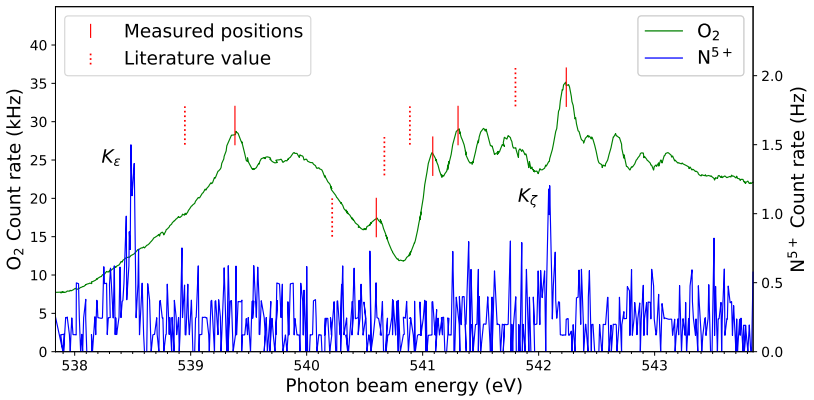

Fig. 1: Spectra of O_2 photoions and the simultaneously measured fluorescence of He-like nitrogen. The K_ε ($1s^2 - 1s6p$) and K_ζ ($1s^2 - 1s7p$) lines were used to calibrate the photon beam energy. Vertical lines mark the position of the measured features (solid) and the corresponding literature value (dashed) [2].

As the transition energies of helium-like systems can be calculated with high precision, we achieved an absolute energy accuracy for the O_2 lines down to 8 meV during our first campaign at BESSY II [3]. We find a difference of about 450 meV in the O_2 transitions compared to the literature values [2]. This shift was confirmed in a second experiment at PETRA III beamline P04, reaching a statistical uncertainty of 2 meV with a systematic error below 15 meV. Applying our values to the atomic oxygen measurements reduces the velocity of the galactic neutral oxygen to be consistent with zero.

Our measurements demonstrate the accuracy and reproducibility of transitions in highly charged ions as an energy calibration reference. We have applied similar techniques with photon energies of up to 15 keV at PETRA III beamline P01. Due to the plethora of ion species, this method is applicable to a large range of photon energies.

References

[1] P. Micke *et. al*, *The Heidelberg compact electron beam ion traps*, Rev. Sci. Instrum. **89**, 063109 (2018).
[2] T. Tanaka *et. al*, *Symmetry-resolved x-ray absorption fine structure and resonant Auger-spectator-electron decay study of O 1s→Rydberg resonances in* O_2, Phys. Rev. A **78**, 022516 (2008)
[3] M. A. Leutenegger *et al.*, High-Precision Determination of Oxygen K_α Transition Energy Excludes Incongruent Motion of Interstellar Oxygen, Phys. Rev. Lett. **125**, 243001 (2020).

*Corresponding author: rene.steinbruegge@desy.de

Characterizing a Nb superconducting radio-frequency resonator for trapping highly charged ions

J. Stark[1,2], C. Warnecke[1,2], E. A. Dijck*[1], S. Chen[1,3], S. Kühn[1,2], M. K. Rosner[1,2], A. Graf[1], J. Nauta[1,2], J.-H. Oelmann[1,2], L. Schmöger[1], M. Wehrheim[1], T. Pfeifer[1], J. R. Crespo López-Urrutia[1]

1. Max Planck Institute for Nuclear Physics, Saupfercheckweg 1, 69117 Heidelberg, Germany

2. Heidelberg Graduate School for Physics, Ruprecht Karl University of Heidelberg, Im Neuenheimer Feld 226, 69120 Heidelberg, Germany

3. State Key Laboratory of Magnetic Resonance and Atomic and Molecular Physics, Wuhan Institute of Physics and Mathematics, Innovation Academy for Precision Measurement Science and Technology, Chinese Academy of Sciences, Wuhan 430071, China

In a novel ion trap concept, the CryPTEx-SC experiment at the Max Planck Institute for Nuclear Physics, Heidelberg, Germany combines a linear Paul trap with a superconducting radio-frequency cavity to form a quadrupole trap with ultralow-noise trapping fields [1]. The niobium cavity operating at 34 MHz at a temperature of 4 K features a high quality factor $Q \approx 10^5$, which filters the RF trap drive and blocks electric field noise at undesired frequencies. This is expected to strongly suppress motional heating rates and associated frequency shifts that would otherwise limit the accuracy achievable in laser spectroscopy measurements. In addition, the nearly full enclosure by superconducting material blocks magnetic field fluctuations from reaching the trapped ions through the Meissner–Ochsenfeld effect.

Goal of the project is to perform precise frequency metrology with highly charged ions in the developed apparatus. Highly charged ions are excellent candidates for the development of next-generation optical atomic clocks and are sensitive probes for changes in fundamental constants [2]. Read-out and sympathetic laser cooling of highly charged ions will be implemented using quantum logic spectroscopy with co-trapped Be^+ ions [3].

We will present the current status of characterizing the operation of the superconducting resonator ion trap. Using an all-optical excitation scheme, the motional modes of trapped Be^+ ions are excited to determine the secular trapping frequencies and characterize the generated electric fields in radial and axial directions. In addition, several potential sources of RF losses are investigated to identify what ultimately limits the resonator quality factor. Thermally induced normal-conducting charge carriers cause losses when increasing the temperature of the superconductor. Nonzero magnetic field magnitude at the onset of superconductivity when cooling down through the critical temperature produces moderate losses, indicating flux trapping within the superconductor. Changes to the magnetic field after reaching the superconducting state do not produce an observable change, which is consistent with the Meissner–Ochsenfeld effect. Observations of nonlinear effects in the resonance spectrum with a strong dependence on the intra-cavity field strength are subject to ongoing investigations.

References

[1] J. Stark et al., arXiv:2102.02793 (2021)
[2] M. G. Kozlov et al., Rev. Mod. Phys. **90**, 045005 (2018)
[3] P. Micke et al., Nature **578**, 60 (2020)

*Corresponding author: elwin.dijck@mpi-hd.mpg.de

Controlling phototionization with attosecond time-slit experiment

Y-C Cheng[1], S Mikaelsson[1], S Nandi[1], L Rämisch[1], C Guo[1], A Harth[1], J Vogelsang[1], M Miranda[1], C L Arnold[1], A L'Huillier[1], M Gisselbrecht[*1]

1. Department of Physics, Lund University, P. O. Box 118, SE-22100 Lund, Sweden

Photoionization is one of the most fundamental and fastest processes in nature, where an electron is emitted from matter after absorption of a high-energy photon. Its dynamic on the attosecond timescale is traditionally studied using an extreme ultraviolet field (XUV). The development of phase-controlled few-cycle infrared (IR) laser pulses opens the door to the production of a few atto-second pulses[1]. We show that in this new regime of light-matter interaction, between the streaking technique with a single attosecond pulse[2] and RABBITT technique with a train of attosecond pulses[3], photoionisation dynamics can be interpreted as a time-slit experiment, allowing unprecedented control of electron emission[4].

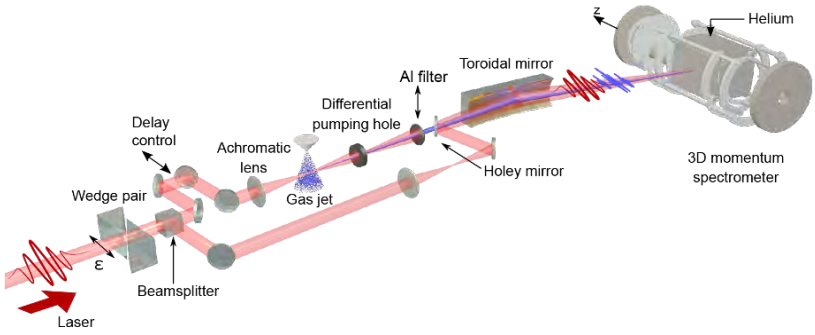

Fig. 1: Experimental setup. A 200 kHz tailored sequence of few XUV attosecond pulses is generated and focused by a gold-coated toroidal mirror into a 3D momentum spectrometer, where it intersects an effusive helium jet. An Al filter can be introduced to eliminate the co-propagating IR field. Before the achromatic lens, a portion of the initial pulse is split off and can be recombined with the generated attosecond pulses via a holey mirror at a chosen time delay.

The experiment, depicted in Fig. 1, was carried out using high order harmonic generated from a 200 kHz optical parametric chirped pulse amplification laser, emitting few-cycle pulses ($\leq$6-fs), CEP stabilized, around 800 nm. The resulting attosecond pulse trains consist of 3-4 pulses with controllable phase difference [1]. When the ultrashort XUV light pulses impinge on atoms together with the generating IR field, multiple coherent ultrabroad-band electron wave packets are created and characterized with a 3D momentum electron-ion spectrometer [5]. By scanning the CEP of the driving laser, the delay between the XUV and the IR fields remains constant while the relative phases between attosecond XUV pulse are changed. As a result, the individual phase of electronic wave packets emitted during an IR optical cycle time can be controlled, allowing thus to manipulate interferences between successive electron wave packets in the presence of the dressing field.

Our measurements reveal a strong CEP- dependent asymmetry of the photoelectron spectra emitted along the polarization axis. Within the framework of the strong field approximation, we show that the amplitude and phase modulation of both IR and XUV fields are at the origin of the symmetry breaking, due to interferences between electronic wavepackets. The control of photoionization, made possible by the extreme temporal confinement of the light-matter interaction, paves the road for the manipulation of ultrafast processes with time slit-experiments.

References

[1] C Guo et al., J. Phys. B. **51**, 034006 (2018).
[2] R Pazourek et al., Rev. Mod. Phys. **87**, 765 (2015).
[3] J M Dahlström et al., Chem. Phys. **414**,53 (2013).
[4] Y-G Chen et al., PNAS **117**, 10727 (2020).
[5] M Gisselbrecht et al., Rev. Sci. Instr. **76**, 013105 (2005).

*Corresponding author: mathieu.gisselbrecht@sljus.lu.se

Hyperfine Structure Analysis of Atomic Holmium in the Visible Range

B. Özdalgiç[*1,2], **Gö. Başar**[3], **S. Kröger**[4], **A. Kruzins**[5], **M. Tamanis**[5], **R. Ferber**[5]

1. Graduate School of Sciences and Engineering, Koc University, TR-34450 Sariyer, Istanbul, Turkey
2. Department of Opticianry, Advanced Vocational School, Dogus University, TR-34775, Istanbul, Turkey
3. Faculty of Science, Department of Physics, Istanbul University, TR-34134 Vezneciler, Istanbul, Turkey
4. University of Applied Science Berlin, Wilhelminenhofstr. 75A, D-12459 Berlin, Germany
5. Laser Centre, The University of Latvia, Jelgavas Street 3, LV-1004 Riga, Latvia

Holmium (Ho) with the atomic number 67 is the eleventh element in the group of so-called lanthanide or rare earth elements in the periodic table. It has only one stable isotope, which has the mass number 165. The nuclear spin of this isotope is $I = 7/2$. Due to its relatively large nuclear magnetic dipole moment of $\mu_I = 4.17\,(3)\ \mu_N$, for most of the lines, the hyperfine structure (hfs) is clearly visible in optical spectra [1].

Emission spectra of Ho were recorded by a high-resolution Bruker IFS 125HR Fourier transform (FT) spectrometer, with a resolution of 0.025 cm^{-1} at the Laser Centre of the University of Latvia. In the experimental setup, optical bandpass interference filters were inserted into the beam path between the hollow cathode discharge and the FT spectrometer to reduce the background caused by the intensity noise. The Ho plasma was generated in a hollow cathode discharge lamp. The cathode was cooled with liquid nitrogen in order to reduce Doppler broadening.

The research of line identification and hyperfine structure analysis of the spectra of Ho measured by several spectroscopic techniques has been the subject of many studies by our group in recent years [2-7]. The measured spectra covers a spectral range from 12 000 to 31 500 cm^{-1} (from UV to NIR).

This study is a continuation of the previous work of our group, in which the FT spectra of Holmium in the visible region was investigated in terms of line identification and hyperfine structure analysis [5-7]. In these spectra 4 193 lines were assigned to atomic and ionic Ho. We were able to classify 1 067 of these lines, in terms of the energy levels between which they occur. The spectra of Ho are very dense and complex due to the unfilled $4f$ electron shell. Even though, we have identified 4 186 of the lines seen in the spectra according to the degree of ionization, we could not classify more than half of them, as the known energy levels of Ho are considerably less than the unknown levels. 987 of the 1 067 lines, classified in total, belong to atomic Ho. After classification, we performed hyperfine structure analysis for more than 170 spectral lines of these 987 atomic Ho lines. When we were selecting these transitions, we particularly considered that the hyperfine structure constants of at least one of the energy levels were not previously determined or determined by large error bars.

In this study, we determined the magnetic dipole hfs constants A of five energy levels with the program FITTER [8]. Four of these, whose magnetic dipole hfs constants A were found in our previous studies, were recalculated by the analysis of different spectral lines. The magnetic dipole hfs constant A of one level is found for the first time in the present study. The hfs constants of this level could not be determined in the previous analysis, due to the saturation effect. The hfs spectra of some transitions were not well reproduced during the fit, because the strong components of the transitions carry more weight than the weaker ones. In these cases, we were unable to determine the magnetic dipole and the electric quadrupole hfs constants together. In this study, we overcame this problem by fixing the electric quadrupole hfs constants B, and we determined the magnetic dipole hfs constants A of five levels by analysis of six spectral lines.

An overview of all these results will be given.

References

[1] N. J. Stone, Atomic Data and Nuclear Data Tables, **90**, 75 (2005)
[2] N. Al-Labady. et al., The Astrophysical Journal Supplement Series, **228**, 16 (2017)
[3] Gö. Başar, et al., The Astrophysical Journal Supplement Series, **228**, 17 (2017)
[4] Gö. Başar, et al., Journal of Quantitative Spectroscopy & Radiative Transfer **243**, 106809 (2020)
[5] B. Özdalgic et al., The Astrophysical Journal Supplement Series, **240**, 27 (2019)
[6] B. Özdalgic et al., The Astrophysical Journal Supplement Series, **240**, 28 (2019)
[7] B. Özdalgic, Gö. Başar and S. Kröger, The Astrophysical Journal Supplement Series, **244**,41 (2019)
[8] A Zeiser et al., to be published.

*Corresponding author: bozdalgic@dogus.edu.tr

Precision spectroscopy with In^+ / Yb^+ Coulomb crystals

J. Keller*[1], T. Nordmann[1], H. N. Hausser[1], H. Liu[1], L. Schomburg[1], N. Bhatt[1], J. Kiethe[1], L. Surzhikova[1], T. E. Mehlstäubler[1],

1. Physikalisch-Technische Bundesanstalt, Bundesallee 100, 38116 Braunschweig, Germany

Precision spectroscopy with trapped ions benefits from their isolation from environmental disturbances and a high level of experimental control. Steady progress in the characterization and control of systematic shifts has enabled trapped-ion optical clocks with fractional frequency uncertainties below 1×10^{-18} [1]. The low signal-to-noise ratio of a single ion, however, requires averaging times of many days to resolve a transition at this level. This limitation can be overcome by the parallel interrogation of multiple ions. We have previously shown that, with the use of precision machined ion traps optimized for this application [2][3], the interrogation of mixed-species chains with multiple clock ions can in principle allow uncertainties in the 10^{-19} range as well [4]. Here, we report on recent progress towards an In^+ / Yb^+ multi-ion clock.

We have implemented the first site-resolved internal state detection of In^+ ions in Coulomb crystals via fluorescence on the $^1S_0 \leftrightarrow {}^3P_1$ transition at 230 nm (see Fig. 1a). Figure 1b shows a scan of the $^1S_0 \leftrightarrow {}^3P_0$ clock transition at 236 nm in a sympathetically cooled single In^+ ion using this scalable approach.

Control of systematic uncertainties in heterogeneous crystals requires experimental management of the ion order within the crystal, which can be disturbed, e.g. by background gas collisions. We present calculations of sympathetic cooling efficiency and its dependence on the crystal configuration. In the experiment, we monitor the order via spatially resolved fluorescence signals during the cooling stage. We have developed sequences of trapping potential changes which restore given crystal configuration within ca. 100 ms to 300 ms (see Fig. 1c) and report on measurements of their reliability. We further report on other automated mitigation strategies for common issues in order to progress towards unattended clock operation.

This project has been supported by the Deutsche Forschungsgemeinschaft (DFG, German Research Foundation) through grant CRC SFB 1227 (DQ-mat, project B03) and through Germany's Excellence Strategy - EXC-2123 QuantumFrontiers - 390837967. This work has been supported by the EMPIR projects 17FUN07 "Coulomb Crystals for Clocks" and 18SIB05 "Robust Optical Clocks for International Timescales". This project has received funding from the EMPIR programme co-financed by the Participating States and from the European Union's Horizon 2020 research and innovation programme.

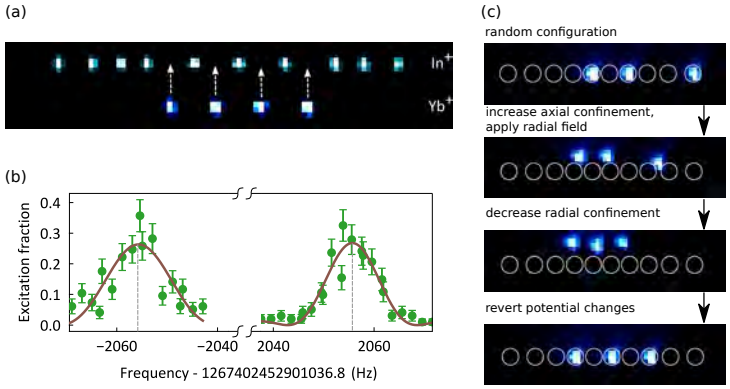

Fig. 1: (a) Simultaneous EMCCD exposure of In^+ (230 nm) and Yb^+ (370 nm) ions in a linear Coulomb crystal. (b) Scan of the $^1S_0 \leftrightarrow {}^3P_0$ clock transition in In^+ at 236 nm with 100 ms pulses. The left (right) signal corresponds to the $m_F = 9/2$, $m_{F'} = 9/2$ ($m_F = -9/2$, $m_{F'} = -9/2$) component. (c) Deterministic Coulomb crystal reordering for reproducible cooling dynamics and systematic shifts. The example shows one of our techniques applied to an In^+ (dark) / Yb^+ (fluorescing) crystal.

References

[1] S. Brewer *et al.*, Phys. Rev. Lett. **123**, 033201 (2019)
[2] J. Keller *et al.*, Phys. Rev. Appl. **11**, 011002 (2019)
[3] T. Nordmann *et al.*, Rev. Sci. Instrum. **99**, 11301 (2020)
[4] J. Keller *et al.*, Phys. Rev. A **99**, 013405 (2019)

*Corresponding author: jonas.keller@ptb.de

Dual-comb spectroscopy based on measurements of cavity resonances

D. Charczun[*1], **A. Nishiyama**[1], **G. Kowzan**[1], **A. Cygan**[1], **T. Voumard**[2], **T. Wildi**[2], **T. Herr**[2], **E. Obrzud**[3], **V. Brasch**[3], **D. Lisak**[1], **P. Masłowski**[†1]

1. Institute of Physics, Faculty of Physics, Astronomy and Informatics, Nicolaus Copernicus University in Toruń, Grudziadzka 5, 87-100 Torun, Poland

2. Center for Free-Electron Laser Science (CFEL), German Electro-Synchrotron (DESY), Notkestr. 85, 22607 Hamburg, Germany

3. 3. CSEM - Swiss Center for Electronics and Microtechnology, 2000 Neuchâtel, Switzerland

Dual comb spectroscopy (DCS) has quickly become one of the most popular implementations of direct frequency comb spectroscopy due to its robustness and relative simplicity [1]. However, cavity-enhanced DCS has not yet been thoroughly explored with only several demonstrations until now [2-5], all of which required knowledge of the reference spectrum and an additional correction due to molecular dispersion affecting comb-cavity matching [6]. As a way to circumvent those limitations of cavity-enhanced DCS, we present a way to measure absorption and dispersion from measured widths and positions of enhancement cavity modes for a methane mixture with nitrogen. This method has been previously demonstrated with continuous wave (CW) lasers [7] and broadband comb-based mechanical Fourier-transform [8], and dispersive [9] spectrometers.

To perform our measurements we used two 25 GHz wide combs with 1 GHz repetition rates, generated from CW laser light with electro-optical modulators and shifted with acousto-optical modulators [10]. The first comb, or the sample comb, is transmitted through the cavity and combined with the second comb light to obtain the dual comb signal. Part of the CW laser light is split before the comb generation to lock the sample comb to the cavity with the Pound-Drever-Hall locking scheme.

The cavity mode measurement is performed by registering a series of dual comb interferograms with varying frequency differences between the sample comb and the cavity. Each interferogram is then Fourier transformed producing a spectrum. Each of the spectra provides a single point for each measured cavity mode. The spectra are interleaved to obtain mode shapes, which are fitted with Lorentzian curves. Fitted mode widths and positions are presented in fig 1. a) and b) and compared with the spectra calculated using the HITRAN database. As HITRAN's accuracy for measured transition intensities is within 10%, the measured data is in a very good agreement with the fitted model.

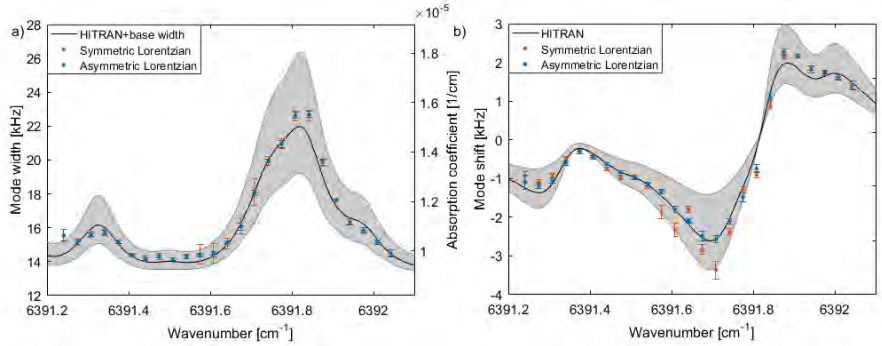

Fig. 1: a) Spectrum of resonance widths of the enhancement cavity filled with methane in nitrogen (20% mixture) that can be recalculated into a loss coefficient. b) Spectrum of cavity mode shifts proportional to resonant molecular dispersion, corrected by a linear term to fit out broadband dispersion of inert gas and cavity mirrors. Orange and blue points are cavity mode widths fitted respectively with symmetric and asymmetric Lorentzian curves. Error ranges are 3 statistical fit uncertainties. Black lines are simulations calculated using the HITRAN model, grey areas are maximum errors calculated with the provided uncertainties of line strengths and line widths.

References [1] I. Coddington, N. Newbury, W. Swann, "Dual Comb Spectroscopy", Optica, 3, 414-426 (2016).
[2] B. Bernhardt et al.., "Cavity-enhanced dual-comb spectroscopy", Nature Photonics 4, 55-57 (2010).
[3] A. J. Fleisher et al., "Coherent cavity-enhanced dual-comb spectroscopy", Opt. Express, 24, 10424 (2016).
[4] N. Hoghooghi et al., "Broadband coherent cavity-enhanced dual-comb spectroscopy" Optica 6, 28 (2019).
[5] W. Zhang, X. Chen, X. Wu, Y. Li, H. Wei, "Adaptive cavity-enhanced dual-comb spectroscopy", Photonics Research 7, 883-889 (2019).
[6] A. J. Fleischer, D. A. Long, J. T. Hodges, "Quantitative modeling of complex molecular response in coherent cavity-enhanced dual-comb spectroscopy" J. Mol. Spec. 352, 26–35 (2018).
[7] A. Cygan et al., "One-dimensional frequency-based spectroscopy", Opt. Express 23, 14472 (2015).
[8] L. Rutkowski, A. C. Johansson, G. Zhao, T. Hausmaninger, A. Khodabakhsh, O. Axner, A. Foltynowicz, "Sensitive and broadband measurement of dispersion in a cavity using a Fourier transform spectrometer with kHz resolution", Opt. Express 25, 21711 (2017).
[9] G. Kowzan, D. Charczun, A. Cygan, R. S. Trawiński, D. Lisak, P. Masłowski, "Broadband Optical Cavity Mode Measurements at Hz-Level Precision With a Comb-Based VIPA Spectrometer", Sci Rep. 9, 8206 (2019).
[10] T. Wildi et al. "Photo-acoustic dual-frequency comb spectroscopy", Nature Comm.11, 4164 (2020).

[*]Corresponding author: charczun@doktorant.umk.pl
[†]Corresponding author: pima@fizyka.umk.pl

Extended Spectroscopic Data and Deperturbative Analysis of $A^1\Sigma_u^+$ and $b^3\Pi_u$ States in K_2

M. Tamanis[*1], **I. Klincare**[1], **I. Brakmane**[1], **A. Lapins**[1], **A. Kruzins**[1], **R. Ferber**[1], **A. Zaitsevskii**[2,3], **E. Pazyuk**[2], **A. Stolyarov**[2],

1. Laser Center, Faculty of Physics, Mathematics and Optometry, University of Latvia, 19 Rainis blvd, Riga LV-1586, Latvia
2. Department of Chemistry, Moscow State University, 119991 Moscow, Leninskie gory 1/3, Russia
3. NRC Kurchatov Institute - PNPI, Orlova Roshcha, Gatchina 188300, Russia

Though the mixed by spin-orbit interaction $A^1\Sigma_u^+$ and $b^3\Pi_u$ states in K_2 have been under intensive spectroscopic research, see [1,2] and references therein, there are energy regions scarcely covered by experimental data; also, these data involve only the $^{39}K^{39}K$ isotopomer. In present study we considerably increased the amount and abundance of accurate term values, which include the data for $^{39}K^{41}K$ and $^{41}K^{41}K$ isotopomersas well. Term values of the $A^1\Sigma_u^+$ and $b^3\Pi_u$ states were obtained from laser-induced fluorescence(LIF) $A^1\Sigma_u^+\ b^3\Pi_u \rightarrow X^1\Sigma_g^+$ Fourier-Transform spectra recorded by Bruker IFS-125HR spectrometer with spectral resolution set to 0.03 cm^{-1}. Ti:Sapphire lasers and various diode lasers with excitation frequencies within 9800 – 13800 cm^{-1} were used to excite the naturally abundant K_2 isotopomers produced in a linear heat-pipe oven. Collision-induced population transfer within rotational levels J' of the excited state provided data systematically spanned over nearby J'-values. The newly obtained $A^1\Sigma_u^+$ and $b^3\Pi_u$ states term values data are presented in Fig. 1. Overall, more than 6000 experimental term values were determined for $^{39}K_2$, 800 term values for $^{39}K^{41}K$, and 17 term values for $^{41}K^{41}K$. The new data cover energy range from 11000 to 16500 cm^{-1} spanning over J'-range from 3 to 160. Their accuracy limited only by the Doppler effect is 0.015 cm^{-1}, or even better.

The present and Ref.[2] $A^1\Sigma_u^+\ b^3\Pi_u$ data sets belonging to $^{39}K_2$ have been simultaneously treated in the framework of the coupled-channel deperturbation analysis yielding empirical interatomic potentials and spin-orbit coupling functions valid until the common $(4P)K + (4S)K$ dissociation limit. The massinvariant properties of the deperturbed molecular parameters are confirmed by a good agreement of the term values predicted for $^{39}K^{41}K$ and $^{41}K_2$ isotopomers with their experimental counterparts. To additionally validate the deperturbation model constructed from energy-based data only, we compared the experimental $A^1\Sigma_u^+\ b^3\Pi_u \rightarrow X^1\Sigma_g^+$ LIF relative intensity distributions with their simulated counterparts. The highly accurate ab initio potential energy curves, spin-orbit coupling functions and relevant transition dipole moments [3] were exploited for the deperturbation analysis.

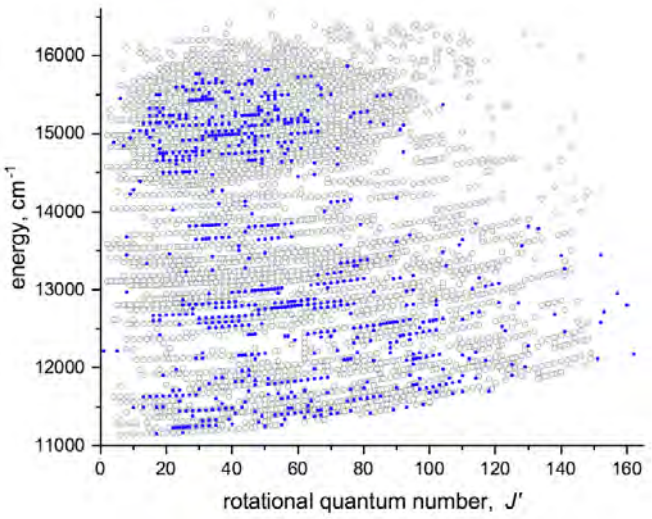

Fig. 1: Newly obtained experimental data field of $A^1\Sigma_u^+\ b^3\Pi_u$ K_2 rovibronic term values; black circles – $^{39}K^{39}K$, blue points – $^{39}K^{41}K$.

References

[1] M. R. Manaa *et al.*, J. Chem. Phys., **117**, 11208 (2002).
[2] St. Falke *et al.*, J. Chem. Phys., **125**, 224303 (2006).
[3] V. Krumins *et al.*, JQSRT **256**, 107291 (2020).

*Corresponding author: maris.tamanis@lu.lv

Mid-Infrared Mode-Resolved Cavity Ring-Down Vernier Spectrometer using an Interband Cascade Laser Based Chip-Scale Optical Frequency Comb

Tzu-Ling Chen[*1], **Lukasz A. Sterczewski, Douglas Ober**[1], **Charles Markus**[1], **Mahmood Bagheri**[2], **Mitchio Okumura**[†1]

1. Division of Chemistry and Chemical Engineering, California Institute of Technology, Pasadena, CA, 91125, USA
2. Jet Propulsion Laboratory, California Institute of Technology, Pasadena, California 91109, USA

As a broadband coherent laser source, optical frequency combs (OFCs) have shown their extraordinary abilities in both temporary resolution and spectral resolution for molecular sensing [1]. To improve the sensitivity and resolution, choosing a laser emitted in molecular fingerprint mid-infrared regime and coupling it into an optical cavity are essential for enhancing the absorption length and weak signal. Recently, chip-scale OFCs emerge as promising alternatives to existing bulky femtosecond laser systems for their more compact sizes and monolithic electronic and feedback integration. An Interband Cascade Laser (ICL) comb is one of chip-scale electrically driven semiconductor laser with advantages over other semiconductor lasers particularly in 3-4 μm [2], which associated with the absorption of C-H bonds.

Here we present a preliminary result on mid-infrared mode-resolved cavity ring-down vernier spectrometer utilizing a 3.3 μm ICL comb systems (optical power $\sim$4 mW) and a high finesse cavity (Finesse$>$6500). The cavity is not only used for cavity ring-down spectrometer but served as a mode filter for performing vernier spectrum while the cavity mode spacing are carefully adjusted to match to the repetition frequency of the ICL comb ($\sim$10 GHz). The cavity ring down time is around 1.3 μs, corresponding to 1.2 kilometers of the effective path length. The preliminary result of the cavity ring-down vernier spectrum is shown in Fig. 1, where there are only 6 comb lines. The signal to noise ratio of the ring down curve and the comb lines expansion will be further improved using RF injection locking.

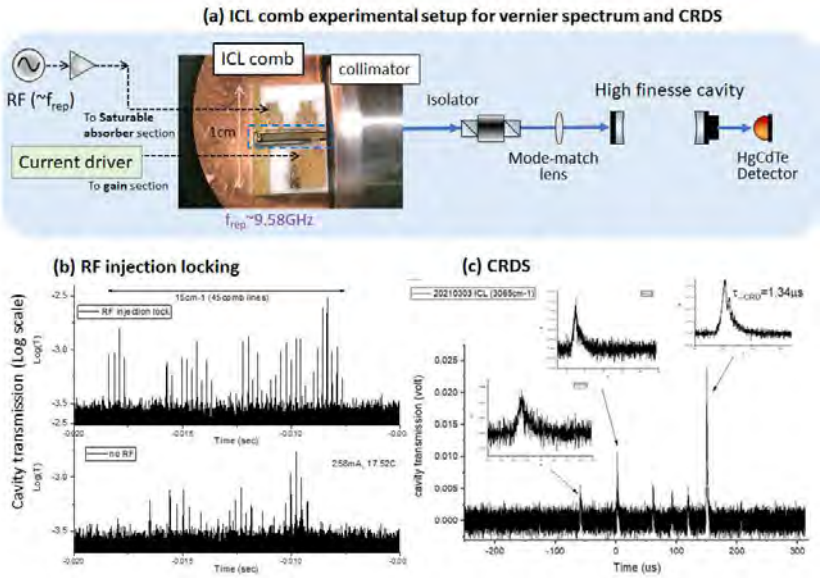

Fig. 1: (a)ICL comb experimental setup for cavity ring-down vernier spectroscopy. (b) The laser-cavity coupling efficiency and comb spectrum spanning can be improved using RF injection locking (3.0μm quantum-well comb). (c) Preliminary result of cavity ring-down vernier spectrum with only 6 comb lines.

References

[1] Bjork, B. J.,*et al.*. Science, **354**(6311), 444 (2016)
[2] Mahmood Bagheri, *et al.*. Scientific Reports, **8**(1), 3322 (2018).

[*]Corresponding author: aquantum@caltech.edu
[†]Corresponding author: mo@caltech.edu

Determination of the hyperfine structure constant and the g-factors of $^3He^+$

S. Dickopf[*1], **M. Müller**[1], **N. S. Oreshkina**[1], **A. Rischka**[1], **A. Schneider**[1], **B. Sikora**[1], **I. Valuev**[1], **S. Ulmer**[2], **J. Walz**[3,4], **Z. Harman**[1], **C. H. Keitel**[1], **A. Mooser**[1], **K. Blaum**[1]

1. Max-Planck-Institute für Kernphysik, Saupfercheckweg 1, 69117 Heidelberg, Germany
2. RIKEN, Ulmer Fundamental Symmetries Laboratory, 2-1 Hirosawa, Wako, Saitama, 351-0198, Japan
3. Institut für Physik, Johannes Gutenberg-Universität Mainz, Staudingerweg 7, 55128 Mainz, Germany
4. Helmholtz-Institut Mainz, Staudingerweg 18, 55128 Mainz, Germany

Quantum-jump spectroscopy in Penning traps, which utilizes the continuous Stern-Gerlach effect, has been used to carry out the most precise g-factor measurements of charged particles, such as free [1] and bound [2] electrons, the positron [3], the proton [4] and the antiproton [5]. By applying similar techniques to hydrogen-like ^{3}He we measured the transition frequencies of four ground-state hyperfine transitions in a 5.7 T magnetic field. From the obtained transition frequencies the electronic and the nuclear g-factor were determined with a precision of a few hundred ppt. Moreover, the value of the hyperfine structure constant of ^{3}He was improved by more than one order of magnitude.

This measurement is the first direct measurement of the nuclear g-factor of ^{3}He, which therefore contributes to establish ^{3}He magnetometers as an independent standard for high-precision magnetometry with unprecedentedly small systematics [6, 7]. Furthermore, the low uncertainty of the hyperfine structure constant makes it sensitive to nuclear structure effects. This allows an independent determination of the Zemach radius.

The current status of the hyperfine structure measurement as well as future plans for an improved nuclear magnetic moment measurement on $^3He_2{}^+$ will be discussed [8].

References

[1] D. Hanneke, S. Fogwell and G. Gabrielse, Phys. Rev. Lett. **100**, 120801 (2008).
[2] S. Sturm *et al.*, Phys. Rev. Lett. **107**, 023002 (2011).
[3] R. S. Van Dyck, P. B. Schwinberg and H. G. Dehmelt, Phys. Rev. Lett. **59**, 26–29 (1987).
[4] G. Schneider *et al.*, Science **358**, 1081–1084 (2017).
[5] C. Smorra *et al.*, Nature **550**, 371–374 (2017).
[6] A. Nikiel, P. Blümler, W. Heil et al., Eur. Phys. J. D **68**(11), 330.(2014).
[7] A. Rudzinski, M. Puchalski and K. Pachucki, J.Chem. Phys. **130**(24), 244102 (2009).
[8] A. Schneider *et al.*, Ann. Phys. (Berlin) **531**, 5 (2019).

*Corresponding author: dickopf@mpi-hd.mpg.de

Terahertz Electrometry using Precision Spectroscopy of the Hydrogen Deuteride Molecular Ions

F. L. Constantin[*1],
1. Laboratoire PhLAM, CNRS UMR 8523, University of Lille, 59655 Villeneuve d'Ascq, France

Rydberg atom spectroscopy was exploited to provide stable, accurate and SI-traceable detection of microwave electric fields with sub-wavelength resolution [1]. Various approaches enabled detection of weak electric fields at the μV/cm level with a sensitivity limited by the photon shot noise. For the hydrogen molecular ions, the simplest molecular systems, the energy levels [2,3] and their shifts in external fields [4,5] are predicted accurately by quantum electrodynamics calculations. Recently, Doppler-free spectroscopy of cold and trapped HD^+ ions allowed significant improvements in resolution and accuracy [6-8]. This contribution proposes a new method to measure a THz electric field in a Cartesian reference frame based on the comparison of the measurements of the lightshifts induced on a two-photon transition of HD^+ with the ab-initio theoretical predictions [9].
The measurements may be performed using experimental setups with HD^+ ions trapped and sympathetically cooled using laser-cooled Be^+ ions [6-8]. The two-photon rovibrational transitions of HD^+ shown in Fig. 1.a may be detected by resonant enhanced multiphoton dissociation with uncertainties estimated by 2 Hz using the quantum projection noise limit for single-ion spectroscopy. A static magnetic field, applied to the ion trap with three coil pairs that are not necessarily orthogonal, is exploited to define the quantization axis and to tune the HD^+ energy levels. The comparison of Zeeman spectroscopy measurements of the $(v,L,F,S,J,J_z) = (0,0,1,2,2,-2) - (2,2,1,2,4,0)$ transition with the predictions of the ab-initio theory allows to characterize the relative orientation of the coils that generate the magnetic field, the coil-to-field parameters, and the residual magnetic field. The orientation and strength of a reference 10^{-4} T magnetic field may be determined with uncertainties estimated at the mrad level and the 10^{-7} T level, respectively. Furthermore, a linearly polarized THz-wave slightly detuned to the $(v,L,F,S,J) = (0,0,1,2,2) - (0,1,1,2,3)$ hyperfine component is characterized using the lightshift induced on the $(v,L,F,S,J,J_z) = (0,0,1,2,2,2) - (2,0,1,2,2,2)$ transition. This approach enables weak THz electric field detection at the μV/m level and calibration with 10 μV/m-level accuracy (Fig. 1.b), by exploiting magnetic field tuning of the HD^+ energy levels. In addition, the amplitudes and the phases of the components of the THz electric field in the Cartesian laboratory frame are characterized from six lightshift measurements for three calibrated values of the magnetic field and two orientations. For a reference THz-wave with an intensity of 1 W/m^2, the amplitudes of the components of the electric field may be characterized with μV/m-level uncertainties or better (Fig. 1.c). The uncertainties of the phases of the electric field components are at the mrad level or better [9].

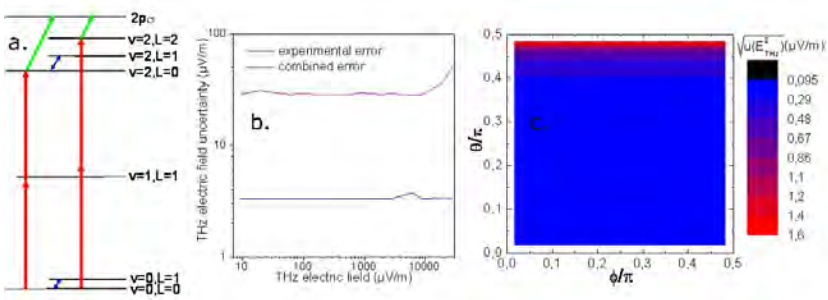

Fig. 1: a. Energy levels of HD^+ addressed for THz-wave sensing. Two-photon transitions (red lines), THz-wave driven electric dipole couplings (blue lines), dissociation (green lines). b. Uncertainty of the THz electric field amplitude in function of the THz electric field amplitude. c. Uncertainty in the characterization of a linearly polarized THz electric field in function of the orientation of the polarization vector defined with spherical angles.

References

[1] C. S. Adams, J. D. Pritchard, and J. P. Shaffer, J. Phys. B **53**, 012002 (2020).
[2] V. I. Korobov, L. Hilico, and J.-Ph. Karr, Phys. Rev. Lett. **118**, 233001 (2017).
[3] V. I. Korobov *et al*, Phys. Rev. A **102**, 022804 (2020).
[4] D. Bakalov, V. I. Korobov, and S. Schiller, J. Phys. B **44**, 025003 (2011).
[5] S. Schiller *et al*, Phys. Rev. A **89**, 052521 (2014).
[6] S. Alighanbari *et al*, Nature **581**, 152 (2020).
[7] S. Patra *et al*, Science **369**, 1238 (2020).
[8] I. Kortunov *et al*, Nat. Phys. (2021). DOI : 10.1038/s41567-020-01150-7.
[9] F. L. Constantin, Atoms **8**, 70 (2020).

*Corresponding author: FL.Constantin@univ-lille1.fr

Excitonic effects in CVD grown mono- and bilayer MoS_2 in the low-temeprature limit

A. Senkić[1,2], J. Bajo[3], A. Supina[1,2], V. Jadriško[1,2], B. Radatović[1,2] and N. Vujičić*[1,2]

1. Institute of Physics, Bijenička c. 46, 10000 Zagreb, Croatia

2. Center of Excellence for Advanced Materials and Sensing Devices, Institute of Physics, Bijenička c. 46, 10000 Zagreb, Croatia

3. Department of Applied Physics, KTH Royal Institute of Technology, SE-100 44 Stockholm, Sweden

Two-dimensional (2D) transition metal dichalcogenide (TMD) semiconductors exhibit strong light-matter coupling and possess direct band gaps in the visible and infrared spectral ranges, making them potentially interesting candidates for various applications in optics and optoelectronics [1]. Weak dielectric screening and in-plane geometrical confinement give rise to an extraordinarily strong Coulomb interaction of electron-hole pairs resulting in interesting many-body phenomena, such as the formation of excitons and, also, higher order excitonic quasiparticles. Excitons are tightly bound in these materials and dominate the optical response even at room-temperature [2], making TMDs and related VdW heterostructures a new platform for exploring fundamental exciton physics.

We investigated optical emission form chemical vapor deposition (CVD) grown MoS_2 mono- and bilayer nanocrystals in broad temperature range (from 4.2 K up to 350 K) in order to completely characterize influence of growth parameters on sample quality and its electronic structure since sample reproducibility and stability as well as their intrinsic high optical quality are crucial for high-quality device applications [3]. Temperature-dependant experiments give information on optical transition linewidths due to interaction with acoustic and optical phonons. Also, different approaches to sample preparation and conservation via hBN encapsulation in order to access additional information on their optical and spin-valley properties will be presented.

References

[1] B. Radisavljevic *et al.*, Nat. Nanotehnol. **6**, 147 (2011); R. S. Sundaram *et al.* Nano Lett. **13**, 1416 (2013); J. Ross *et al.* Nat. Nanotehnol. **9**, 268 (2014).

[2] M. Ugeda *et al.*, Nat. Nanotehnol. **13**, 1091 (2014)

[3] A. Senkić *et al.*, in preparation.

*Corresponding author: natasav@ifs.hr

A new set of oscillator strengths in moderately charged indium ions for the spectral analysis of hot white dwarfs

S. Gamrath[*1] **P. Quinet**[†1,2], **P. Palmeri**[1]
1. Physique Atomique et Astrophysique, Université de Mons, Belgium
2. IPNAS, Université de Liège, Belgium

A few years ago, the discovery of lines of trans-iron elements in the spectrum of the hot white dwarf RE 0503289 [1] encouraged us to begin doing systematic calculations of transition probabilities and oscillator strengths in different heavy elements ($Z > 26$) in their moderately ionization stages, typically from 3+ to 6+ (see e.g. [2]). With the newly calculated data obtained for twelve elements (Zn, Ga, Ge, Se, Kr, Sr, Zr, Mo, Te, I, Xe, Ba and Cu), extreme overabundances, due to radiative levitation, were highlighted in RE 0503-289 [3]. With the high quality spectra recorded by the Space Telescope Imaging Spectrograph (STIS) onboard the Hubble Space Telescope (HST), astrophysicists are able to identify line per line, element per element, and thus to improve calculations and abundance analyses. However, for the reliable spectral analysis of hot, compact stars, non-local thermodynamic equilibrium (NLTE) model-atmospheres are mandatory. In contrast to LTE models, where occupation numbers of atomic levels are determined by Saha and Boltzmann equations, they have to be calculated in detail, i.e. all radiative and collisional transitions between all levels have to be considered. In other words, for bound-bound transitions reliable radiative parameters are required, not only for lines that are identified in the observation but for the complete model atoms that are considered in the model-atmosphere calculations. In order to extend our previous investigations, the present work is focused on indium ions, from In IV to In VII, for which the radiative data are very sparse in literature. More precisely, new radiative decay rates (oscillator strengths and transition probabilities) were computed using the pseudo-relativistic Hartree Fock (HFR) method originally introduced by Cowan [4], and modified for taking core-polarization (CPOL) effects into account, giving rise to the so-called HFR+CPOL approach [5,6]. For each ion, this method was combined with a semi-empirical procedure to optimize some radial integrals by fitting the calculated energy levels with available experimental data. Our results will be presented at the conference.

References

[1] K. Werner et al., Astrophys. J. 753, L7 (2012)
[2] T. Rauch et al., ASP Conf. Ser. 509, 183 (2017)
[3] P. François, M. Spite and F. Spite, Astron. Astrophys. 274 (1993) 821-824
[4] R.D. Cowan, The Theory of Atomic Structure and Spectra, Univ. California Press, Berkeley (1981)
[5] P. Quinet et al., Mon. Not. R. Astr. Soc. 307, 934 (1999)
[6] P. Quinet et al., J. Alloys Comp. 344, 255 (2002)

[*]Corresponding author: sebastien.gamrath@umons.ac.be
[†]Corresponding author: pascal.quinet@umons.ac.be

A model for determination of diameter and concentration of metal nanoparticles synthesized by laser ablation in water

J. Car[*1], **D. Blažeka**[1], **T. Bajan**[1], **L. Krce**[2], **I.Aviani**[2], **N. Krstulović**[1]
1. Institute of Physics, Bijenička c. 46, 10000 Zagreb, Croatia
2. University of Split, Faculty of Science, Department of Physics, Ruđera Boškovića 33, 21000 Split, Croatia

In this work a model is developed for quantitative and calibration-free determination of colloidal metal nanoparticle diameter and concentration synthesized by laser ablation in water [1-4]. Model is valid under assumption that total ablated material is transferred into nanoparticles which is proved by Mie theory under dipole approximation and Beer Lambert law using experimentally determined crater volumes, size distributions and photoabsorbances. The model accounts for determination of nanoparticle diameter and concentration using only crater volume and photoabsorbance as experimental input. The model was developed under theoretically expected equality of nanoparticle concentrations obtained independently by photoabsorbances and volume of the crater and under dipole approximation of Mie theory. It is shown that a priori unspecified diameter of nanoparticles in model derivation turns out to be in 1 sigma range of mode diameter of size distribution of nanoparticles obtained by AFM analysis. Introduction of quadrupole terms in extinction cross section gave the same result for diameter considering size ranges of nanoparticles used in this work. Therefore, for nanoparticle sizes below specific diameter limit which is yet to be determined, dipole approximation is justified for quantitative analysis of nanoparticles properties. The model is verified by comparing the nanoparticle size distributions obtained by AFM and TEM imaging with the mode and mean nanoparticle diameter calculated from the absorbance data. It allows fast and simple colloidal metal nanoparticle quantitative analysis without use of electron microscopy or relevant experimental techniques.

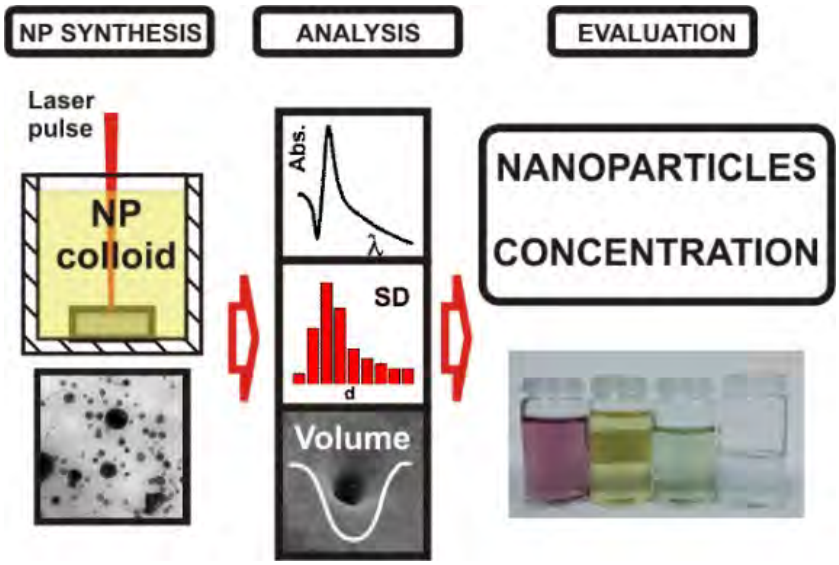

Fig. 1: Graphical abstract consisting of NP synthesis, analysis and evaluation

References

[1] Krstulović, N.; P. Umek, P.; Salamon, K.; Capan, I.: Synthesis of Al-doped ZnO nanoparticles by laser ablation of ZnO:Al2O3 target in water. Mater. Res. Express 2017, 4, 105003.
[2] Krstulovic, N.; Salamon, K.; Budimlija, O.; Kovac, J.; Dasovic, J.; Umek, P.; Capan, I.: Parameters optimization for synthesis of Al-doped ZnO nanoparticles by laser ablation in water. Appl. Surf. Sci. 2018, 15, 916-925.
[3] Krstulovic, N.; Shannon, S.; Stefanuik, R; Fanara, C.: Underwater-laser drilling of aluminium. Int. J. Adv. Manuf. Technol. 2013, 69, 1765-1773.
[4] Krstulovic, N.; Milosevic, S.: Drilling enhancement by nanosecond-nanosecond collinear dual-pulse laser ablation of titanium in vacuum. Appl. Surf. Sci. 2010, 256, 4142-4148.

*Corresponding author: jcar@ifs.hr

Radiative cooling of cationic carbon clusters, C_N^+

Hu Wei[1], **Zhang Rui**[1], **Shimpei Iida**[2], **Hajime Tanuma**[2], **Kei Masuhara**[2], **Haruo Shiromaru**[2], **Toshiyuki Azuma**[3], **Klavs Hansen**[*1,4]

1. School of Science, Tianjin University, Tianjin 300350, China
2. Tokyo Metropolitan University, Tokyo 192-0397, Japan
3. Atomic, Molecular & Optical Physics Laboratory, RIKEN, Saitama 351-0198, Japan
4. Center for Joint Quantum Studies and Department of Physics, School of Science, Tianjin University, Tianjin 300350, China

The radiative cooling of highly excited carbon cluster cations of sizes N = 9, 11-12, 17-27 has been studied in the Tokyo Metropolitan electrostatic storage ring. The clusters were produce by laser ablation and accelerated to 15 keV, which gave circulation times of several tens of microseconds [1]. Neutral decay products were detected at the end of both straight sections of the ring. From the exponential suppression of the 1/t power law decay [2], the radiative cooling constants were extracted, similar to the the procedure used in [3]. The cooling rate constants vary with cluster size from a maximum at N = 9 of 2.4×10^4 s^{-1} and a minimum at N = 17 of 3.6×10^3 s^{-1}. The high rates indicate that photon emission takes place from electronically excited ions, providing a strong stabilizing cooling of the molecules.

References

[1] S. Jinno, T. Takao, K. Hanada, M. Goto, K. Okuno, H. Tanuma, T. Azuma, and H. Shiromaru, Nucl. Instrum. Methods Phys. Res., A **572**, 568 (2007)
[2] K. Hansen, J. U. Andersen, P. Hvelplund, S. P.Møller, U. V. Pedersen, and V. V. Petrunin,Phys. Rev. Lett. **87**, 123401 (2001)
[3] F.-Q. Chen,N. Kono, R. Suzuki, T. Furukawa, H. Tanuma, P. Ferrari, T. Azuma, J. Matsumoto, H. Shiromaru, V. Zhaunerchyk and K. Hansen, Phys.Chem.Chem.Phys., **21**, 1587 (2019)

*Corresponding author: KlavsHansen@tju.edu.cn

Electronic structure and Bonding Properties of Diatomic Molecule FeS

M. A. Mermigki[*1], **D. Tzeli**[1,2]

1. Laboratory of Physical Chemistry, Department of Chemistry, National and Kapodistrian University of Athens, Zografou GR-15784, Greece

2. Theoretical and Physical Chemistry Institute, National Hellenic Research Foundation, 48 Vassileos Constantinou Ave., Athens 116 35, Greece

Iron–sulfur clusters are ubiquitous. [1] They play a major role in industrial catalysis and especially in hydrodesulfurization. [2,3] and they are preferred over oxide catalysis because of their resistance against poisoning. [4] Additionally, they appear in the dust in the interstellar medium and the exact nature of interstellar amorphous silicate grains is still an open question. [5] They are also involved in many biological systems operating as active centers of proteins in processes such as photosynthesis, respiration, and nitrogen fixation. [6] The key for their remarkable reactivity is their low-lying electronic states. It is particularly important to be understood the intrinsic electronic structure of the Fe-S clusters as well as their modifications by their surroundings in order the functionalities of the iron-sulfur proteins to be interpreted.

Here, we present a theoretical study of the diatomic FeS molecule, employing the CAS, MRCI, and CCSD(T) methodologies in conjunction with the aug-cc-pV5Z. There is a debate regarding the identity of the ground state, $^5\Delta$ or $^5\Sigma^+$. Here we show that the $^5\Delta$ is the ground state in agreement with the experimental data [7]. The $^5\Delta$ and $^5\Sigma^+$ states are almost degenerate energetically, while the following excited state is the $^7\Sigma^+$ state. The bond length of $^5\Delta$ is defined at 2.02 Å and its dissociation energies is calculated at 98.4 kcal/mol. Finally, the electronic structure and the bonding properties of the molecule are analyzed. It is of interest that states of high spin multiplicity are low-lying in energy. The electronic energy levels of even the same spin are dense providing a natural explanation for the ubiquity of these clusters in nature and in catalysis.

References

[1] T. G. Spiro, Ed. Iron-Sulfur Proteins, Wiley-Interscience, New York, (1982).
[2] B. Liang, X. Wang, and L. Andrews. J. Phys. Chem. A, **113**, 5375 (2009).
[3] M. S. Nurmaganbetova, M. I. Baikenov, M. G. Meiramov, A. A. Mukhtar, A. T. Ordabaeva, V. A. Khrupov, Pet. Chem. **41**, 26 (2001).
[4] S. Ba1rsch, D. Schro1der, and Helmut Schwarz, and P. B. Armentrout. J. Phys. Chem. A **105**, 2005 (2001).
[5] M. Köhler, A. Jones, and N. Ysard. A&A **565**, L9 (2014).
[6] D. Kessler and J. Papenbrock, Photosynthesis Research **86**, 391 (2005).
[7] D. J. Matthew, E. Tieu, M. D. Morse, J. Chem. Phys. **146**, 144310 (2017).

*Corresponding author: marmermigki@chem.uoa.gr

High-precision laser spectroscopy measurements of the prominent 3C/3D oscillator-strength ratio in Fe XVII

S. Kühn[*1], **S. Bernitt**[1], **M.A. Leutenegger**[2], **C. Shah** [2,1], **R. Steinbrügge** [3], **M. Togawa** [1], **T. Pfeifer** [1], **J. Crespo López-Urrutia** [1]

1. Max-Planck Institut für Kernphysik Heidelberg, Saupfercheckweg 1, 69126 Heidelberg, Germany
2. NASA/Goddard Space Flight Center, 8800 Greenbelt Rd, Greenbelt, Maryland 20771, USA
3. Deutsches Elektronen-Synchrotron DESY, Notkestraße 85, 22607 Hamburg, Germany

For more than 40 years, most astrophysical observations and laboratory studies of two key soft X-ray diagnostic $2p$-$3d$ transitions, 3C and 3D, in Fe XVII ions found oscillator-strength ratios f_{3C}/f_{3D} disagreeing with theory [1]. This discrepancy hampered the proposed plasma diagnostic utility based on the observed intensity ratios ever since [2]. In previous laboratory measurements, the ratio was determined by scrutinizing the photon emission of an electron-impact excited plasma. First X-ray laser spectroscopy experiments at a free-electron laser (FEL) confirmed the discrepancy between experiments and theory independently of electron-excitation cross sections that could have falsified previous laboratory measurements [3]. Recently, the 3C/3D oscillator-strength ratio was measured by resonantly exciting the transitions utilizing highly brilliant and monochromatic X-ray synchrotron light. Thereby, two proposed systematical effects that could have lowered the results of the FEL measurements were excluded. The synchrotron measurement appeared to confirm previous experimental values and thus, exacerbated the long-lasting emission problem of Fe XVII [4].

In newest measurements, a three-fold improvement of the experimental resolution and a significant increase in the signal-to-noise ratio revealed a systematical underestimation of the observed ratio in the first synchrotron measurement, see Figure 1. The result of these measurements $f_{3C}/f_{3D} = 3.51(7)$ is in excellent agreement with the newest state-of-the-art theoretical predictions and finally resolves the long-lasting conundrum. Additionally, for the first time, the individual natural linewidths of lines 3C and 3D, among others, were determined with an uncertainty of $\approx 15\%$. This allows to benchmark theories not only by the oscillator-strength ratio but also by their prediction of the individual transition lifetime. The findings of the measurement now allow the observed intensity ratios of 3C and 3D to enable their usefulness in the diagnostics of astrophysical spectra.

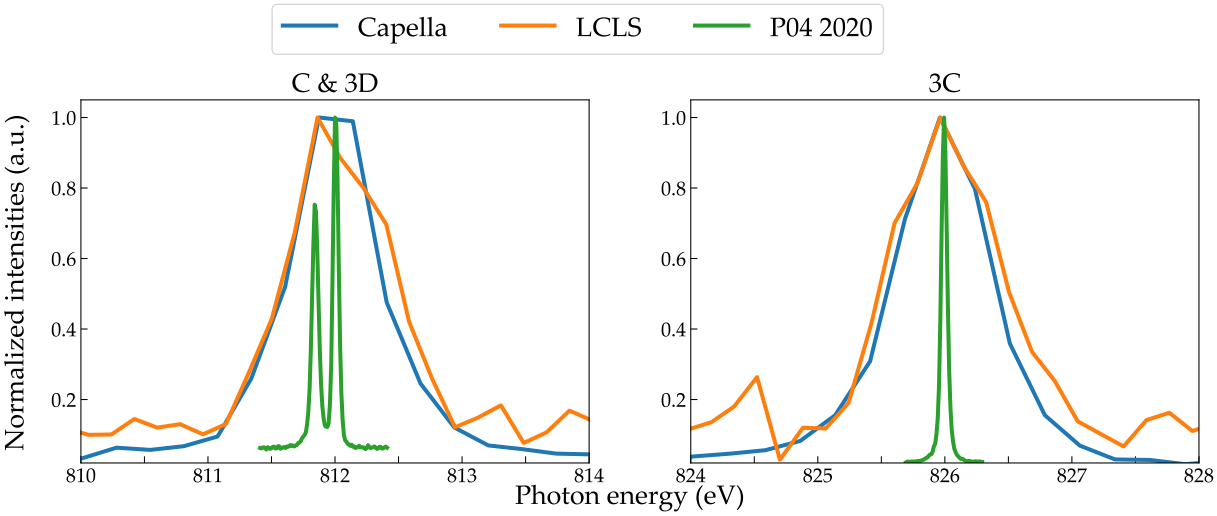

Fig. 1: Comparison of the observed and measured line profiles of lines 3C and 3D of Fe XVII as well as line C of Fe XVI. Blue: Observation of the emission spectrum of Capella using the XMM-Newton observatory. Orange: Laser spectroscopy measurements at LCLS. Green: Newest measurements conducted at beamline P04 of the PETRA III synchrotron.

References

[1] G.V. Brown et al. A brief review of the intensity of lines 3C and 3D in neon-like Fe XVII. Canadian Journal of Physics (2008)
[2] G.V. Brown et al. Diagnostic utility of the relative intensity of 3C to 3D in Fe XVII. PRL (2001)
[3] S. Bernitt et al. An unexpectedly low oscillator strength as the origin of the Fe XVII emission problem. Nature (2012)
[4] S. Kühn et al. High Resolution Photoexcitation Measurements Exacerbate the Long-Standing Fe XVII Oscillator Strength Problem. PRL (2020)

*Corresponding author: steffen.kuehn@mpi-hd.mpg.de

Novel method for preparing nanoscale atomically thin heterostructure devices

V. Jadriško[*1,2,3], **B. Radatović**[†1,2,3], **B. Pielić**[1,2,3], **N. Vujičić**[1,2,3] **and M. Kralj**[1,2,3]
1. Institute of Physics, Bijenička c. 46, 10000 Zagreb, Croatia
2. Center of Excellence for Advanced Materials and Sensing Devices, Institute of Physics, Bijenička cesta 46, HR-10000 Zagreb, Croatia
3. Center for Advanced Laser Techniques, Institute of Physics, Bijenička cesta 46, HR-10000 Zagreb, Croatia

Current state of preparing 2D materials for use in devices was mostly focused on Chemical Vapor Deposition (CVD) methods and exfoliation from the bulk crystals. While CVD offers great scalability potential which is necessary for future device fabrication it also lacks in controllable parameters and properties of synthesised materials. On the other hand, exfoliation from bulk crystals offers great sample quality but no realistic way of scaling to mass producing which is a must for future devices. Another option is to use Molecular Beam Epitaxy (MBE) method

of synthesising in ultra-high vacuum (UHV) conditions which offers unparalleled control of growth parameters. [1] One of the obstacles of current growth procedures is reliance on Ir(111) or Au(111) substrates which promotes growth. Such metallic substrates quench the optical response of grown materials making them inconvenient for use in optoelectronic devices. Here we present MBE growth of nanoscale sized islands of MoS2 synthesized on

uniform sheets of graphene on top of the Ir (111) substrate. [2] Obtained MoS2/Graphene/Ir(111) heterostructure is transfered to a suitable substrate such as SiO2/Si wafers which offers great optoelectronic performance of devices. Initial optical characterisation unveils successful transfer of the samples and room condition stability. [3]

References

[1] Niels Ehlen et al 2019 2D Mater. 6 011006
[2] Joshua Hall et al 2018 2D Mater. 5 025005
[3] V. Jadriško et al, in preparation

[*]Corresponding author: vjadrisko@ifs.hr
[†]Corresponding author: bradatov@ifs.hr

Mass spectrometry and ICCD imaging of atmospheric pressure plasma jet with spiral electrodes

N. Selaković[*1], **D. Maletić**[1,2], **G. Malović**[1], **Z. Lj. Petrović**[3]
1. Institute of Physics Belgrade, Pregrevica 118, 11080 Belgrade, Serbia
2. Institute of Physics, Bijenička 46, 10000 Zagreb, Croatia
3. Serbian Academy of Sciences and Arts, Kneza Mihaila 35, 11000 Belgrade Serbia

Here we use spiral electrodes for generating an atmospheric pressure plasma jet APPJ. Their geometry allows the formation of discharges along relatively large source lengths [1]. We use ICCD fast imaging and mass spectrometry to observe discharge propagation as well to determine the chemical composition [2]. A possible application of this type of non-thermal plasma could be in medicine for sterilization of catheters and infusion hoses [3].

In this study, the source that we used was made of a 30 cm long glass tube around which two copper wires were wrapped into a spiral. These two wires did not touch at any point and were set at approximately equal distances of about 10 mm compared to each other. We used 4 slm of helium as a feeding gas during all experiment. One of the wires was powered with sine wave at 70 kHz excitation frequency and the other one was grounded. The applied voltage was generated using signal generator. The signal was amplified with custom made amplifier and transformer before it was applied to the powered electrode. We have used high voltage probe in order to measure the high voltage. The oscilloscope was used to capture signals of current and voltage in order to calculate power delivered to the discharge [4].

A molecular beam mass spectrometer MBMS (HIDEN HPR60) was used to detect neutrals, positive and negative ions mass spectra derived from APPJ discharge. In Fig. 1 one can notice a rich spectrum of negative ions obtained in APPJ's plume dominated by oxygen species such as O^-, OH^-, O_2^- and O_3^-. Also, water clusters $O^- \cdot (H_2O)n$ and $OH^- \cdot (H_2O)n$ can be observed. ICCD and electrical measurement results showed the appearance of a pulsed streamer at the maximum of the positive half-cycle of the voltage signal. In addition, we could notice the appearance of discharge within the glass tube which was following powered electrode during the negative half-cycle and grounded electrode during the positive half-cycle.

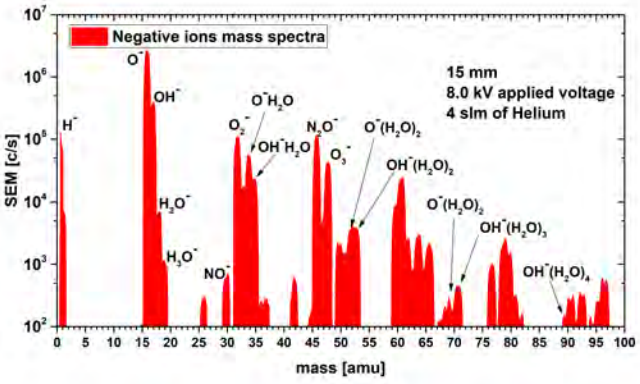

Fig. 1: Negative ions mass spectra 0-100 amu (15 mm distance between APPJ and MBMS, applied voltage 8.0 kV, helium flow rate 4 slm)

Mass spectrometry results showed similar concentrations of positive and negative ions for the same experimental conditions dominated by oxygen and nitrogen species. No water clusters were observed for positive ions. The ICCD acquisition provided insight into the propagation of discharge within the glass tube as well as within the plume which propagates in ambient room.

References

[1] M. Polak, J. Winter, U. Schnabel, J. Ehlbeck and K. D. Weltman, Plasma Processes and Polymers, **9(1)**, 67-76 (2012).
[2] A. Stancampiano., N. Selaković, M. Gherardi, N. Puač, Z. Lj. Petrović and V. Colombo. Journal of Physics D: Applied Physics, **5**1(48), 484004 (2018).
[3] T. Sato, O. Furuya, K. Ikeda and T. Nakatani. Plasma Processes and Polymers, **5**(6), 606-614 (2008).
[4] D. Maletić, N. Puač, G. Malović, A. Djordjević, and Z. LJ. Petrović, Journal of Physics D: Applied Physics, **5**0(14), 145202 (2017).

*Corresponding author: nele@ipb.ac.rs

Photoelectron circular dichroism in racemic mixtures

A. Blech[*1], **L. Greenman**[2], **R. Dörner**[3], **C. P. Koch**[1],
1. Department of Physics, Freie Universit ¨at Berlin, Berlin, Germany
2. Department of Physics, Kansas State University, Manhattan, KS 66506, USA
3. Institut für Kernphysik, Goethe-Universität, Frankfurt am Main, Germany

Photoionisation and measurment of the photoelectron's angular distribution allows to extract valuable information about molecular structure and intramolecular dynamics. In the special case of chiral molecules, which cannot be superimposed with their mirror images, the laboratory-frame photoelectron angular distributions show a distinct forward-backward asymmetry with respect of the light propagation direction, if the ionising light source is circularly polarised. This asymmetry is called photoelectron circular dichroism (PECD) and even survives the average over all possible molecular orientations, as it is the case for an ensemble of randomly oriented molecules[1]. As a pure electric dipole effect, PECD has a high signal strength. Hence, it established itself as a versatile probe of dynamics in chiral molecules. In samples of randomly oriented molecules, the strength of PECD is directly related to the enantiomeric excess and vanishes in the limit of a racemic mixture. However, it has been demonstrated recently that the rotational state of an molecular ensemble can be controlled in an enantioselective manner[2]. Here, we show that this opens the possibility to observe PECD even in racemic mixtures. We aim to propose an efficient scheme for measuring PECD in a racemic molecular ensemble starting from an isotropic initial state and to provide a systematic theoretical analysis of the electric dipole response in racemic mixtures.

References

[1] N. Böwering *et al.*, Phys. Rev. Lett. **86**, 1187 (2001)
[2] I. Tutunnikov *et al.*, J. Phys. Chem. Lett. **9**, 1105–1111 (2018)

*Corresponding author: alexander.blech@fu-berlin.de

Old recipes to the rescue of modern data on the hyperfine structure of Xe I

Christophe Blondel[*1], **Cyril Drag**[1]

1. Laboratoire de Physique des plasmas, UMR 7648, Centre national de la recherche scientifique, École polytechnique, Université Paris-Saclay, Sorbonne Université, Observatoire de Paris, Institut polytechnique de Paris, route de Saclay, F-91128 Palaiseau, France

Investigation of the hyperfine structure of the natural isotopes of xenon, ^{129}Xe and ^{131}Xe, with a nuclear spin $I = 1/2$ and $3/2$ respectively, was recently extended to an unprecedented number of excited levels of Xe I [1-2]. The authors of the survey nevertheless regret that "There does not appear to be any obvious pattern or trend in these values of A^{129}, A^{131} and B^{131} as a function of the angular momentum quantum numbers J, ℓ, and K" [2].

XXth century investigations, however, had shown quantitatively how appropriate it could be to attribute most of the hyperfine structure of Xe I excited states to the interaction of the $6p^5\,{}^2P_j$ core with the nucleus. Based on this, variation of the dipole and quadrupole hyperfine coefficients A and B stems straightforwardly from the different possible coupling schemes of the atomic angular momenta, from one or the other possible fine-structure states j of the core, through a defined value K of the momentum that arises from coupling the core with the orbital momentum ℓ of the outer electron, including the spin $s = 1/2$ of the same electron, to end up with a well-defined value J of the total angular momentum of the electron shell [3-6]. With the use of elementary Racah algebra, the hyperfine dipole parameter A appears proportional to an angular coefficient κ, such as:

$$\kappa(j,\ell,K,J) = \frac{[4J(J+1)+4K(K+1)-3]\,[K(K+1)+j(j+1)-\ell(\ell+1)]}{8J(J+1)K(K+1)j(j+1)} \tag{1}$$

Formula (1) has taken explicit advantage of the fact that the p^5 core has an $\ell_C = 1$ orbital angular momentum and that both this core and the outer ℓ electron have an $s = 1/2$ spin. Figure 1 shows how well experimental A parameters actually appear correlated with κ (with a proportionality coefficient that itself depends on the nuclear magnetic momentum), which may thus serve as the wanted "obvious pattern" [2] for the (j,ℓ,K,J) dependence of the hyperfine dipole coefficient.

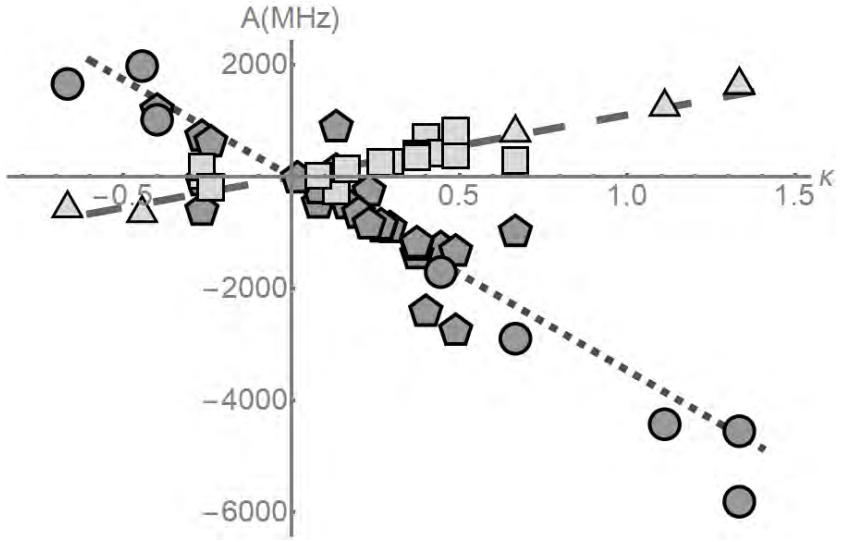

Fig. 1: Dipolar parameters $A\left[(p^5)_j\ell[K]_J\right]$ of ^{129}Xe (pentagons and circles) and ^{131}Xe (squares and triangles), in MHz, shown vs. their expected κ ratio to the monoelectronic dipole-hyperfine parameter of the core. Pentagons and squares (resp. circles and triangles) stand for the $j = 3/2$ "unprimed" (resp. $j = 1/2$ "primed") levels. The dashed and long-dashed lines show the general trend of the ^{129}A and ^{131}A to follow a linear dependence with respect to the κ factor deduced from the hypothesis of a pure core-hfs effect. As expected, the ratio of the slopes corresponds to the ratio of the nuclear gyromagnetic coefficients, $\gamma_{129}/\gamma_{131} \simeq -3.37$.

A similar analysis for the quadrupole coefficient will be shown at the conference.

References

[1] M. Kono, Y. He, K.G.H. Baldwin & B.J. Orr, J. Phys. B: At. Mol. Opt. Phys. **46**, 035401 (2013).
[2] M. Kono, Y. He, K.G.H. Baldwin & B.J. Orr, J. Phys. B: At. Mol. Opt. Phys. **49**, 065002 (2016).
[3] C. Bauche-Arnoult & J. Bauche, Ann. Phys.-Paris **14**, 341 (1968).
[4] S. Liberman, J. Phys. (Paris) **30**, 53 (1969).
[5] S. Liberman, J. Phys. (Paris) **32**, 867 (1971).
[6] Sylvain Liberman, thèse d'État, Faculté des sciences d'Orsay, 1971.

*Corresponding author: christophe.blondel@lpp.polytechnique.fr

Numerical Simulation of Argon Microdischarge for Plasma Deactivation Technology

A. S. Petrovskaya[*1], **A. B. Tsyganov**[1], **S. V. Surov**[2], **A. Yu. Kladkov**[2], **D. A. Blokhin**[2], **P. O. Gredasov**[3],

1. InnoPlasmaTech LLC, Line 17 V.O., 4-6, Liter V, 199034, Saint-Petersburg, Russia

2. Science and Innovation JSC, ROSATOM, Kadashevskaya st., 32/2, 115035, Moscow, Russia

3. Leningrad NPP, Rosenergoaton JSC- Electric power division of ROSATOM, Industrial Zone 188540, Sosnovy Bor, Russia

In this work, we performed the results of the numerical simulation of a microdischarge in argon at atmospheric pressure. The investigated type of microdischarge is used in a new thermo-plasma technology for the selective extraction of the radioactive isotope 14C in the deactivation treatment of the irradiated reactor graphite surface.

At present time, some complicated and economically unprofitable methods for deactivation of the irradiated reactor graphite and other structural elements of the nuclear power plants are under consideration. For example, to solve the recycling reactor graphite problem (the irradiated graphite volume is estimated to be 100 thousand tons in the world).

We offer a new technology for irradiated reactor graphite decontamination with inert gas (argon) plasma sputtering and thermo-treatment. In more detail the description of our technology is presented in [1, 2]. The microdischarge is ignited in argon at the pressure 1 atm. between the treated surface (the cathode) and the collector electrode (the anode). The gap between the electrodes is selected of the order of 1 mm. The operating voltage on the discharge gap is applied by the power supply source in the range of 400-600 V, the discharge current density is regulated in the range (0.01 – 1) A/cm2. After discharge ignition argon ions are accelerated in the cathode sheath, where main part of discharge voltage is dropped and sputter carbon and other atoms from the surface of reactor graphite (the cathode). The sputtered atoms from the cathode are diffusing in the inert gas of the gap and are precipitating on the anode (collector) electrode surface. Inert gas is circulated by a pump with inflow from the perimeter of the anode and outflow to the pumping out tube in the center of the anode.

To assess the operating parameters of the thermo-plasma deactivation technology, the argon microplasma discharge was simulated. The numerical model includes equations for the electronic and non-electronic components of the plasma, Poisson's and Boltsman's equations, boundary conditions and 28 plasma-chemical reactions involving particles of argon plasma. Based on the numerical model, the following parameters of the microdischarge were calculated: the cathode sheath value, the concentration of plasma particles, the current density of argon ions, the sputtering rate of the reactor graphite surface by argon ions.

The magnitude of the cathode sheath is 140 V, the maximum values of the concentration of neutral argon atoms Ar , electrons n_e, atomic argon ions Ar^+, molecular argon ions Ar_2^+ and Ar_3^+, metastable atoms Ar^{met} and molecules Ar_2^{met}: [Ar]=$2.44 \cdot 10^{25}$ m^{-3}, $n_e = 8 \cdot 10^{19}$ m^{-3}, [Ar^+]=$5 \cdot 10^{18}$ m^{-3}, [Ar_2^+]=$7 \cdot 10^{19}$ m^{-3}, [Ar_3^+]=$7 \cdot 10^{18}$ m^{-3}, [Ar^{met}]= $5 \cdot 10^{18} m^{-3}$, [Ar_2^{met}] = $5 \cdot 10^{17}$ m^{-3}. With the obtained parameters, the rate of ion sputtering of GR-280 reactor graphite by argon ions is no less than 75.7 nm/s.

These results obtained for the first time and interested for plasma physics application and nuclear power for solving the problem of irradiated reactor graphite decontamination.

Acknowledgements

This work is supported by The Foundation for Assistance to Small Innovative Enterprises (FASIE) – contract No3832ГС1/63219.

References

[1] A.S.Petrovskaya, A.Yu.Kladkov, S.V.Surov, M.R.Stakhiv, A.B.Tsyganov IOP Conf. Series: Journal of Physics: Conf. Series **1461**, 012132 (2020).

[2] A.S.Petrovskaya, A.B.Tsyganov, M.R.Stakhiv Patent RU No2711292, International patent application PCT/RU2019/000816.

*Corresponding author: anita3425@yandex.ru

Photoelectron circular dichroism of heavier chalcogenofenchones using near ultra-violet femtosecond laser pulses

A. Senftleben*[1], S. Vasudevan[1], M. Kour[2], S. Das[1], J. Ghosh[1], D. Kargin[3], N. Ladda[1], H. Lee[1], S.T. Ranecky[1], I. Vindanović[3], T. Rosen[1], T. Baumert[1], R. Berger[2], H. Braun[1], R. Pietschnig[3], T.F. Giesen[1]

1. Institut für Physik and CINSaT, Universität Kassel, Heinrich-Plett-Str. 40, 34132 Kassel, Germany

2. Fachbereich Chemie, Philipps Universität Marburg, Hans-Meerwein Str. 4, 35032 Marburg, Germany

3. Institut für Chemie und CINSaT, Universität Kassel, Heinrich Plett-Str. 40, 34132 Kassel, Germany

Photoelectron spectra and photoelectron circular dichroism (PECD) measurements after femtosecond laser resonance enhanced multi-photon ionization (2+1 REMPI) are reported for chalcogenofenchones with variation of the chalcogen atom from oxygen to sulfur and selenium. Short pulses allow for excitation and ionization of the intermediate states out of an almost frozen nuclear configuration and reduce the influence of internal conversion processes. Keeping the excitation wavelength fixed, the contributing resonances and ionization energies are tuned in a bathochromic fashion by chemical substitution of heavier atoms. Intermediate electronic states excited during the REMPI process are assigned based on the measured photoelectron spectra and *ab initio* quantum chemical calculations. The bathochromic shifts cause the heavier chalcogenofenchones to have absorption in the visible region, which opens the door for future laser excitation, and control studies on the important fenchone prototype.

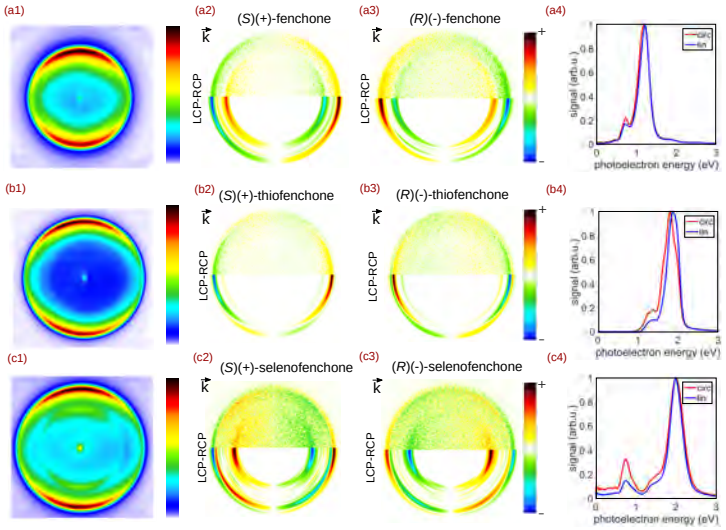

Figure 1: Photoelectron results for (a) fenchone, (b) thiofenchone and (c) selenofenchone after 2+1 resonance-enhanced multiphoton ionization at an incident wavelength of around 376 nm. Column 1 displays the raw images containing the photoelectron angular distributions after ionizing with linealry polarized light. Photoelectron circular dichroism (PECD) images are presented in column 2 and 3 for the *(S)* and *(R)* enantiomers, respectively. Each of the PECD images contains raw data in the upper half and Abel inverted distributions in the lower half. Column 4 contains the photoelectron spectra for circular (red) and linear (blue) polarized light.

*Corresponding author: Dr. Arne Senftleben, email: arne.senftleben@uni-kassel.de

Cold interactions and collisions between helium ions (He^+) and metastable helium atoms (He^*)

Jacek Gębala[*1], **Michał Przybytek**[2], **Marcin Gronowski**[1], **Michał Tomza**[†1]

1. Faculty of Physics, University of Warsaw, Pasteura 5, 02-093 Warsaw, Poland

2. Faculty of Chemistry, University of Warsaw, Pasteura 1, 02-093 Warsaw, Poland

Cold hybrid ion-atom systems recently emerged as a new area for fundamental research in quantum physics and chemistry. In my work, I investigate the dynamics of helium ions immersed in ultracold metastable helium atoms. We calculate accurate potential energy curves for a ground state He+ ion interacting with He atom in the lowest-energy metastable ^3S state. We enploy the full configuration interaction method, equivalent to exact diagonalization, with large single-particle Gaussian basis sets extrapolated to the complete basis set limit. We include the leading adiabatic and relativistic corrections and use the potential energy curves to predict the scattering lengths for atom-ion collisions. We also investigate the spectroscopic properties of the system, namely we calculate the rovibrational levels and spectroscopic constants of the molecular ion in excited states for three stable isotopologues.

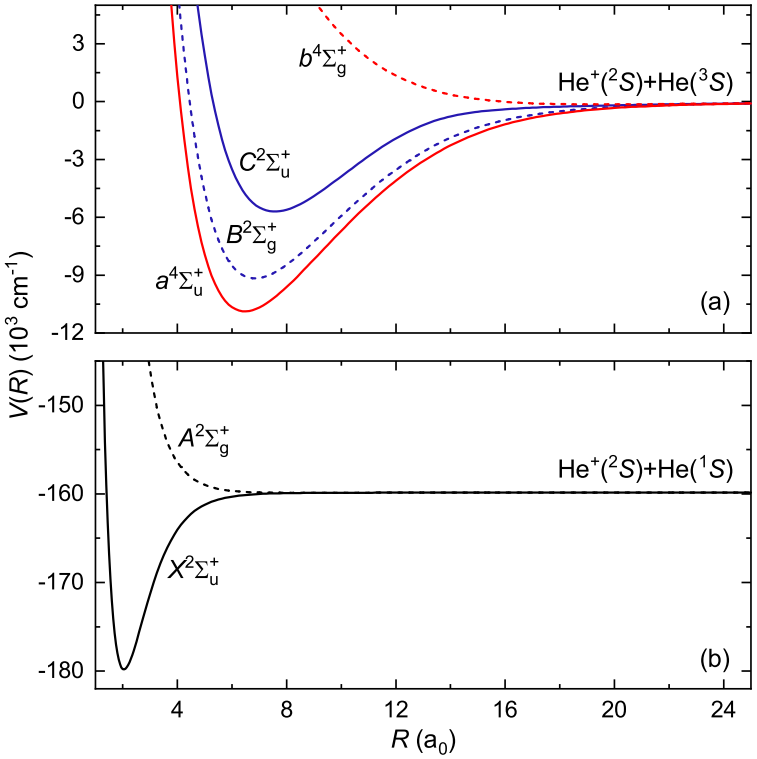

Fig. 1: The non-relativistic potentials energy curves of the He_2^+ molecular ion in the ground and excited electronic states

*Corresponding author: j.gebala@student.uw.edu.pl

†Corresponding author: michal.tomza@fuw.edu.pl

Chirp and intensity dependence of the circular dichroism in ion yield of 3-methylcyclopentanone measured with femtosecond laser pulses

S. Das[*1], **J. Ghosh**[1], **T. Ring, S. Vasudevan**[1], **H. Lee**[1], **N. Ladda**[1], **S. T. Ranecky**[1], **T. Rosen**[1], **A. Senftleben**[1], **T. Baumert**[1], **H. Braun**[†1]

1. Institut für Physik, Universität Kassel, Heinrich-Plett-Strasse 40, 34132 Kassel, Germany

One of the methods to differentiate between the two enantiomers of a chiral molecule is Circular Dichroism (CD). It arises due to the difference in absorption of left and right circularly polarised light by the two enantiomers. The difference in absorption can also be mapped to the difference in ionisation of the enantiomers and is known as CD in ion yield [1,2], cf. Fig. 1(a). This anisotropy for a particular transition can be quantified as follows [3]:

$$g = \frac{4 \cdot |\vec{\mu}| \cdot |\vec{m}| \cdot \cos\theta}{|\vec{\mu}|^2 + |\vec{m}|^2} = 2 \cdot \frac{I_{lcp} - I_{rcp}}{I_{lcp} + I_{rcp}} \tag{1}$$

where $\vec{\mu}$ and $\vec{m}$ are the electric and magnetic dipole moment at an angle θ, and I_{lcp} and I_{rcp} are the ion yields due to left and right circularly polarised light.

As the CD in ion yield arises due to the interplay of the electric and magnetic dipole moments, one may expect that their manipulation or structural changes in the molecule could alter the anisotropy. Our attempt to use shaped femtosecond laser pulses to coherently control the anisotropy of a chiral molecule starts with this study of the effect of linear chirp or group delay dispersion (GDD) on the anisotropy. The candidate molecule for this experiment is 3-methylcyclopentanone (3-MCP). From our previous experiments [4] we found that the 3-MCP molecule has prominent anisotropy around 309 nm and around 324 nm. In the study we present here, we perform all the experiments at 309 nm, where 3-MCP shows higher anisotropy. In this wavelength range a 1+1+1 resonance-enhanced multi-photon ionisation (REMPI) takes place in 3-MCP through the $\pi^* \leftarrow n$ transition.

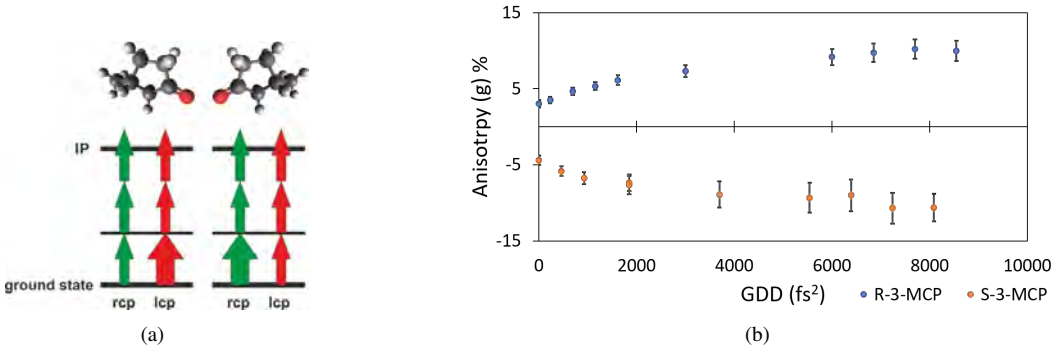

(a) (b)

Figure 1: (a) The difference in absorption of left and right circularly polarised light to the intermediate state is mapped to the ion yield of the enantiomer, when ionised in resonance-enhanced multiphoton ionisation scheme, (b) experimental result of the effect of GDD on the anisotropy

For the current experiments, we use our home built Time of Flight (ToF) mass spectrometer with our recently established twin peak measurement setup [4]. The twin peak method has the capability to measure ion yields for both helicities within the same laser shot, hence reducing the laser fluctuation error and also the error related to the rotation of the quarter wave-plate. To further account for systematic errors in the measurements we use the achiral reference of potassium to correct the anisotropy of the chiral molecules. A pair of prism compressors is used in the beam path to manipulate the chirp in the pulse. We observe similar trend of enhanced anisotropy for higher GDD pulses for the (*R*)- and the (*S*)-3-MCP molecules, cf. Fig. 1(b). To see whether this change in anisotropy occurs purely due to introducing chirp or intensity variation, we have furthermore studied the intensity effect on anisotropy which will be discussed in details in our poster.

References

[1] U. Boesl and A. Bornschlegl, ChemPhysChem, **7**, 2085, 2006
[2] H. G. Breunig et al., ChemPhysChem, **10**, 1199, 2009
[3] U. Boesl et al., Anal. Bioanal. Chem., **405**, 6913, 2013
[4] T. Ring et al., Rev. Sci. Instrum., **92**, 033001, 2021

[*]Corresponding author: Sagnik Das, email: sagnikd@uni-kassel.de
[†]Corresponding author: Dr. Hendrike Braun, email: braun@physik.uni-kassel.de

Radiative recombination of twisted electrons with highly charge ions

A.V. Maiorova[*1], **A. A. Peshkov**[2,3], **A. Surzhykov** [2,3,4]

1. Center for Advanced Studies, Peter the Great St. Petersburg Polytechnic University, 195251 St. Petersburg, Russia
2. Physikalisch–Technische Bundesanstalt, D–38116 Braunschweig, Germany
3. Institut für Mathematische Physik, Technische Universität Braunschweig, D–38106 Braunschweig, Germany
4. Laboratory for Emerging Nanometrology Braunschweig, D-38106 Braunschweig, Germany

The radiative recombination (RR) of electrons with highly–charged heavy ions has been in the focus of experimental and theoretical research over the last three decades [1]. It is one of the dominant processes in relativistic ion–atom (or ion–electron) collisions that allows to explore the details of light–matter coupling in the high–energy and strong–field regime. Moreover, the application of the radiative recombination for the diagnostics of spin–polarized ions beams in storage rings attracts currently considerable attention [2]. This diagnostics method is based on the *rotation* of the linear polarization of emitted recombination photons for the case when electron is captured into a bound state of initially polarized hydrogen–like ion. A special interest to such (initially) hydrogen–like ions arise from the fact that they are essential for investigating spin–flip atomic transitions and parity–violation phenomena in high–Z domain as well as for the search of a permanent electric dipole moment [3].

In the past, the application of the radiative recombination for the diagnostics of spin–polarized ion beams has been discussed exclusively for the "conventional" plane–wave electrons. During the recent years, however, the twisted (or vortex) electron beams have been proposed as a promising new tool for atomic collision studies [4]. Carrying non–zero projection of the orbital angular momentum (OAM) onto their propagation direction and, hence, possessing enlarged magnetic dipole moment, these electron beams can be used to study magnetic phenomena in solid–state physics and light–matter coupling. One can expect, therefore, that OAM–induced effects will play also important role in the radiative recombination of spin–polarized heavy ions and can significantly modify the linear polarization of emitted photons.

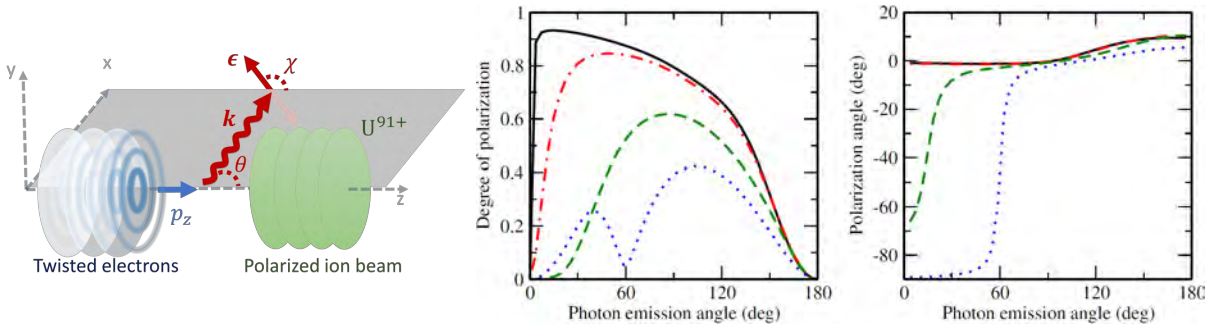

Fig. 1: Left panel: The geometry for the radiative recombination of twisted electrons with longitudinally polarized hydrogen–like uranium U^{91+} (1s) ions. Right panel: The degree and tilt angle of the linear polarization of K–RR photons for the capture of plane–wave (black solid line) as well as Bessel twisted electrons with the energy 100 keV. For the latter case, calculations have been performed for the opening angles θ_p = 10 deg (red dash–dotted line), 30 deg (green dashed line) and 45 deg (blue dotted line).

In this contribution, we present a theoretical study of the radiative recombination of twisted electrons with initially hydrogen–like (finally helium–like) ions. By using solutions of the relativistic Dirac's equation and the density matrix approach, see Refs. [5,6], we explored (i) how the linear polarization of recombination x–rays is affected if incident ions are themselves spin–polarized, and (ii) whether this polarization transfer can be enhanced by the electron "twistedness". Results of our theoretical analysis, supported by detailed calculations (see Fig. 1, for example), suggest that the sensitivity of the "x–ray–polarization rotation" method for the diagnostics of ion beams can indeed be improved if vortex electrons are used in place of plane–wave ones. Moreover, we argue that the use of twisted electrons is indispensable is one needs to investigate the properties of "structured" ion beams, whose (local) intensity and polarization vary within their cross sectional area [7].

References

[1] J. Eichler and Th. Stöhlker, Phys. Rep. **439**, 1 (2007).
[2] A. Surzhykov, S. Fritzsche, Th. Stöhlker, and S. Tashenov, Phys. Rev. Lett. **94**, 203202 (2005).
[3] A. Bondarevskaya *et al.*, Phys. Rep. **507**, 1 (2011).
[4] K. Y. Bliokh *et al.*, Phys. Rep. **690**, 1 (2017).
[5] V. A. Zaytsev, V. G. Serbo, and V. M. Shabaev, Phys. Rev. A **95**, 012702 (2017).
[6] A. V. Maiorova, A. A. Peshkov, and A. Surzhykov, Phys. Rev. A **101**, 062704 (2020).
[7] A. V. Maiorova, A. A. Peshkov, and A. Surzhykov, to be submitted (2021).

*Corresponding author: majorova_av@spbstu.ru

Strong Two-Electron-One-Photon Transitions in Li-like Ions

S. Bernitt[*1,2], **M. Togawa**[2], **S. Kühn**[2], **R. Steinbrügge**[3], **C. Shah**[4,2], **P. Amaro**[5], **J. R. Crespo López-Urrutia**[2],

1. Helmholtz-Institut Jena, Fröbelstieg 3, 07743 Jena, Germany
2. Max-Planck-Institut für Kernphysik, Saupfercheckweg 1. 69117 Heidelberg, Germany
3. Deutsches Elektronen-Synchrotron DESY, Notkestraße 85, 22607 Hamburg, Germany
4. NASA Goddard Space Flight Center, 8800 Greenbelt Road, Greenbelt, Maryland 20771, USA
5. Department of Physics, NOVA School of Science and Technology, NOVA University Lisbon, 2829-516 Caparica, Portugal

In systems with multiple bound electrons, excitations and subsequent decays can often be descibed in terms of one single electron transitioning from one set of quantum numbers to another. However, even in few-electron systems, the inclusion of multi-electron processes can become necessary to accurately predict properties, like photoabsorption cross sections and observable decay channels in fluorescence spectra. In this contribution we present experiments in which we observed two-electron-one-photon (TEOP) transitions in trapped Li-like ions.

In an experiment conducted at beamline P04 of the synchrotron facility PETRA III, a portable electron beam ion trap (EBIT) [1] was used to provide a target of highly charged oxygen ions for the monochromatized synchrotron photon beam. The photon energy was continuously scanned over the range from 570 eV to 740 eV while recording x-ray fluorescence from the ions. Figure 1 shows the result of such a measurement, in which the fluorescence following resonant excitations of electronic transitions in He-like O^{6+} and Li-like O^{5+} is visible. While most of these decays are dominated by fluorescence photons having the same energy as the ones used for excitation, the excited state $[(1s2s)_1 5p_{3/2}]_{3/2;1/2}$ of O^{5+} primarily decays via TEOP, at lower photon energies. We have found that this enhanced TEOP decay originates in a strong correlation with the near-degenerate state $[(1s2p_{3/2})_1 4s]_{3/2;1/2}$ [2].

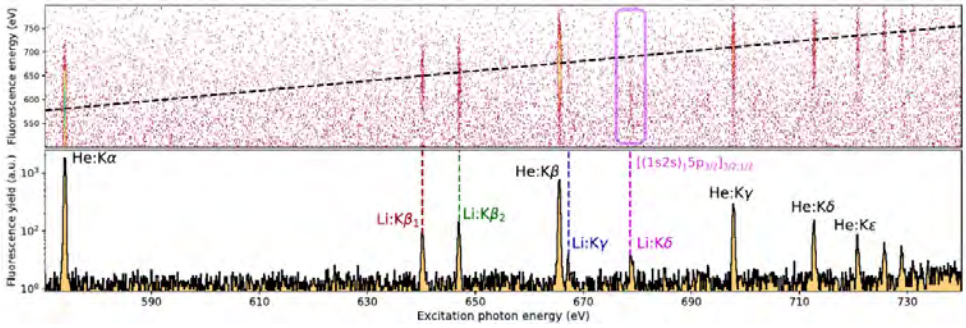

Fig. 1: Histograms of fluorescence events. The top part is showing the excitation photon energy and the detected fluorescence photon energy. Events with both energies being equal are situated on the dashed line. The bottom part shows the total number of events as a function of the excitation energy. Fluorescence following the resonant excitation of transitions in He-like O^{6+} and Li-like O^{5+} is labeled. Labeled in violet in both parts is fluorescence associated with the excited state $[(1s2s)_1 5p_{3/2}]_{3/2;1/2}$, which is dominated by the TEOP process.

The x-ray spectra of few-electron oxygen ions are of great importance for hot gas diagnostics in astrophysics. Our results demonstrate the need to study TEOP transitions and include them in plasma models used for the interpretation of astrophysical x-ray spectra.

In another experiment, at beamline P01 of PETRA III, we resonantly excited transitions from the K to the M shell in Li-like Br^{32+}, around 14 keV. Alongside excitations to $1s2s3p$ states, we also observed TEOP transitions to $1s2p3s$ states, directly excited by the synchrotron photons. The TEOP excitation channels exhibit transition rates comparable to the ones of direct single-photon excitations.

Both measurements show how high-resolution photoexcitation experiments with trapped ions can enable detailed studies of multi-electron processes, that such processes are present even in few-electron systems, and have to be included in accurate plasma models.

References

[1] P. Micke *et al.*, Rev. Sci. Instrum. **89**, 063109 (2018).
[2] M. Togawa *et al.*, Phys. Rev. A **102**, 052831 (2020).

*Corresponding author: bernitt@mpi-hd.mpg.de

Low-Energy Dissociative Recombination of CH^+

J. Forer[*1], **X. Jiang**[2], **C.H. Yuen**[3], **I.F. Schneider** [4], **J. Zs. Mezei** [5], **M. Ayouz**[6], **V. Kokoouline**[1]

1. Department of Physics, University of Central Florida, 32816, Florida, USA

2. Université Paris-Saclay, CentraleSupélec, CNRS, Laboratoire SPMS, 91190, Gif-sur-Yvette, France

3. Department of Physics, Kansas State University, Manhattan, 66506, Kansas, USA

4. LOMC CNRS-UMR6294, Université du Havre, Université Normandie, Le Havre, France; LAC CNRS-UMR9188, ENS Cachan, Université Paris-Saclay, Orsay, France

5. Institute for Nuclear Research, Hungarian Academy of Sciences, Debrecen, Hungary

6. Université Paris-Saclay, CentraleSupélec, Laboratoire LGPM, 91190, Gif-sur-Yvette, France

We present a theoretical approach to studying the dissociative recombination (DR) of CH^+ in an energy range where the direct and indirect DR mechanisms can be important. This method makes use of fixed-nuclei R-matrix scattering calculations, rovibrational frame transformation with a complex absorbing potential, and quantum defect theory to compute the DR cross-sections from the ground $X^1\Sigma^+$ state of CH^+. The neutral $2^2\Pi$ dissociative state, presently accepted as the main dissociation pathway [1], is created by the closed excitation channels of CH^+. It is represented impl ıd $A^1\Pi$.

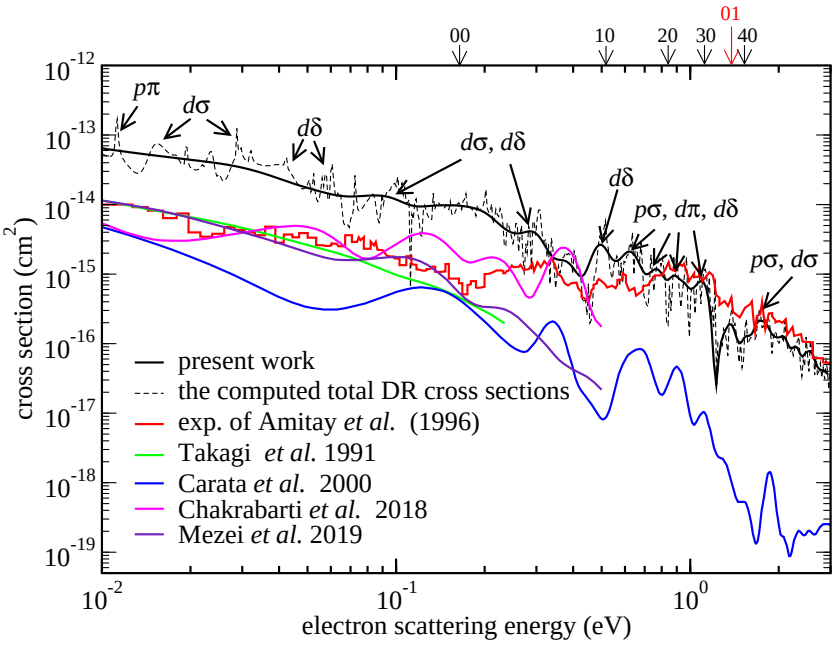

Fig. 1: The total DR cross-sections of CH^+ from its ground vibronic state are compared against experimental results [1] and previous theoretical calculations [2], [3], [4], [5]. Both the convolved (solid black) and unconvolved (dashed black) results are plotted. In-figure arrows identify various resonances, while arrows above the figure indicate vibronic channel thresholds. The left number is the vibrational quantum number, while the right indexes the electronic states of CH^+.

So far, our results for the DR cross-sections, ignoring the rotational structure, are close to experimental results [1] above 0.03 eV, but are larger at low energies. This could be due to the neglected rotational structure, whose implementation we are finalizing. The DR probabilities for different partial waves of the incoming electron were calculated to identify prominent resonances; considerable contributions came from *d*-waves, which were not considered previously.

References

[1] Z. Amitay *et al.*, Phys. Rev. A, **54**, 4032 (1996)
[2] H. Takagi *et al.*, J. Phys. B, **24**, 711 (1991)
[3] L. Carata *et al.*, Phys. Rev. A, **62**, 052711 (2000)
[4] K. Chakrabarti *et al.*, J. Phys. B, **51**, 104002 (2018)
[5] Z.J. Mezei *et al.*, Atoms, **7**, 82 (2019)

*Corresponding author: j.forer@knights.ucf.edu

Spontaneous Electron Emission Versus Dissociation in Internally Hot Silver Dimer Anions

P. Jasik[*1,2], **J. Franz**[1,3], **D. Kędziera**[4], **T. Kilich**[1,3], **J. Kozicki**[1,3], **J.E Sienkiewicz**[1,3]

1. Faculty of Applied Physics and Mathematics, Gdańsk University of Technology, G. Narutowicza 11/12, 80-233 Gdańsk, Poland

2. BioTechMed Center, Gdańsk University of Technology, G. Narutowicza 11/12, 80-233 Gdańsk, Poland

3. Advanced Materials Center, Gdańsk University of Technology, G. Narutowicza 11/12, 80-233 Gdańsk, Poland

4. Faculty of Chemistry, Nicolaus Copernicus University, Gagarina 7, 87-100 Toruń, Poland

Referring to a recent experiment reported by Anderson *et al.* [1], we theoretically study the process of a two-channel decay of the diatomic silver anion (Ag_2^-), namely the spontaneous electron ejection giving Ag_2 + e^- and the dissociation leading to Ag^- + Ag [2]. The ground state potential energy curves (Fig. 1: left panel) of the silver molecules of diatomic neutral and negative ion were calculated using proper pseudo-potentials and atomic basis sets. We also estimated the non-adiabatic electronic coupling between the ground state of Ag_2^- and the ground state of Ag_2 + e^-, which in turn allowed us to estimate the minimal and mean values of the electron autodetachment lifetimes. The relative energies of the rovibrational levels allow the description of the spontaneous electron emission process, while the description of the rotational dissociation is treated with the quantum dynamics method [2] [3] as well as time-independent methods [4]. The results of our calculations (Fig. 1: right panel) are verified by comparison with experimental data. We also formulate some prospects to control such a process using strong couplings to decrease significantly its timescale.

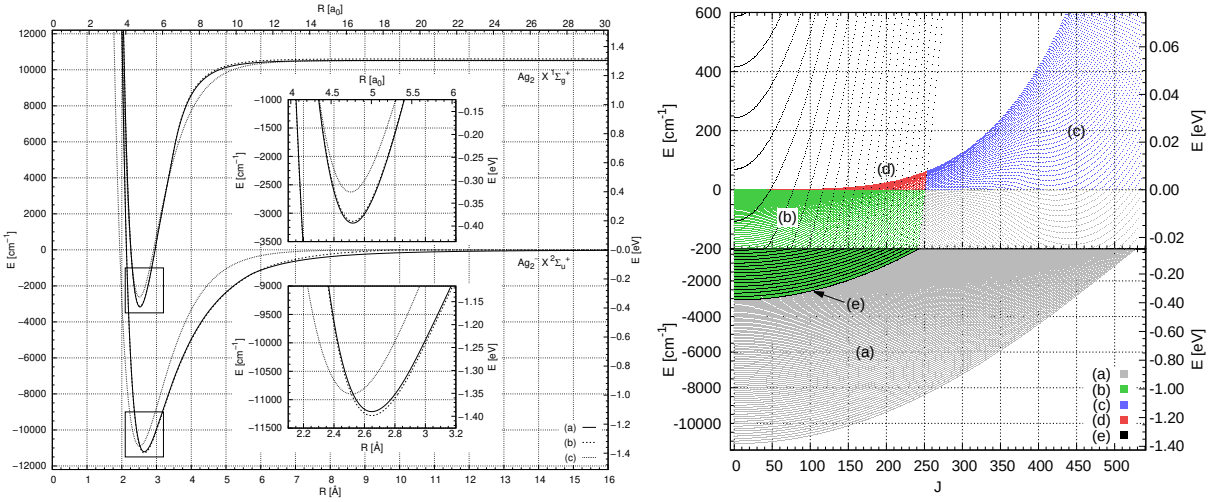

Fig. 1: (left panel) Potential energy curves for the Ag_2^- and Ag_2 ground states: (a) current work; (b) current work with original basis set of Peterson and Puzzarini [5]; (c) Morse potentials generated by experimental and theoretical parameters [1]. (right panel) A map of rovibrational levels of Ag_2^- and Ag_2: (a) no decay possible; (b) spontaneous electron emission only; (c) fragmentation only; (d) both decay modes possible; (e) rovibrational levels of Ag_2.

The calculated mean value of the vibrational non-adiabatic couplings between all considered rovibrational levels is very small, of the order of 10^{-9} a.u. This means that the spontaneous electron emission process can be long and has a mean lifetime estimated by our approach of a few seconds, although the shortest lifetimes are on a millisecond scale (i.e. $\sim$250 ms).

In turn, the mean lifetime of the predissociation reaction calculated for the considered quasibond states is smaller compared to the electron autodetachment reaction and equals around 250 ms. It means that the fragmentation reaction is generally faster than the spontaneous electron emission reaction occurring even on pico- and nanosecond scale, but some overlap in time (starting with milliseconds) of both channels can be observed, leading to vie of these two decay pathways of the Ag_2^- molecule. All the above confirms the experimental results on the timescale of reactions given by Anderson *et al.*[1].

References

[1] E.K. Anderson, A.F. Schmidt-May, P.K. Najeeb, G. Eklund, K.C. Chartkunchand, S. Rosén, Å. Larson, K. Hansen, H. Cederquist, H. Zettergren, and H.T. Schmidt, Phys. Rev. Lett. 124, 173001 (2020).

[2] P. Jasik, J. Franz, D. Kędziera, T. Kilich, J. Kozicki, and J.E. Sienkiewicz, J. Chem. Phys. 154, 164301 (2021).

[3] P. Jasik, J. Kozicki, T. Kilich, J.E. Sienkiewicz, and N.E. Henriksen, Phys. Chem. Chem. Phys. 20, 18663 (2018).

[4] P. Jasik, "sPYtroscopy - the computer program, written in Python, for computing rovibrational spectra of diatomic molecules including an arbitrary number and types of couplings between electronic states", unpublished, (2020).

[5] K.A. Peterson and C. Puzzarini, Theor. Chem. Acc. 114, 283 (2005).

*Corresponding author: patryk.jasik@pg.edu.pl

Penning ionization of Camphor molecules in He nanodroplets by EUV photoexcitation: electron-ion coincidence spectroscopy

S. De[1], **S. Mandal**[2], **S. Sen**[3], **L. B. Ltaief**[1,4], **R. Richter**[5], **M. Mudrich**[1,4], **V. Sharma**[*3], **S. Krishnan**[†1]

1. Department of Physics and QuCenDiEM group, Indian Institute of Technology Madras, Chennai 600036, India.
2. Department of Physics, Indian Institute of Science Education and Research, Pune 411008, India.
3. Department of Physics, Indian Institute of Technology Hyderabad, Kandi, Telangana 502285, India.
4. Department of Physics and Astronomy, Aarhus University, 8000 Aarhus C, Denmark.
5. Elettra Sincrotrone, Basovizza, 34149 Trieste, Italy.

Superfluid He is a remarkable nanoscale quantum system which can be employed as a cold spectroscopic matrix. This offers the opportunity to explore the dynamics of photoionization of atoms or molecules embedded at sub-kelvin temperatures, 370 mK [1],[2],[3],[4]. Camphor ($C_{10}H_{16}O$) is a volatile monoterpene ketone with importance in medicine and other applications [5],[6]. This system has long served as a benchmark chiral molecule, for asymmetries in angle-resolved photoelectron spectra [7],[8],[9],[10]. Therefore, it is important to investigate this molecule and its oligomers embedded in a low temperature environment, here, He droplets.

We performed photoelectron spectroscopy on Camphor doped with He nanodroplets using EUV synchrotron radiation at the circular polarization (CiPo) beamline of Elettra Synchrotron Trieste, Italy. Using a velocity map imaging (VMI) spectrometer we recorded photoelectron spectra in coincidence with photoions detected by time-of-flight (ToF) spectrometry for the photon energies in the range 19...26 eV. Photoelectron spectra correlated to Camphor photoions recorded for excitation by 21.43 eV photons reveals significant Penning ionization. We uncover consequent photofragmentation processes leading to ions from the dopant molecules in their ground and excited states. We report typical photoelectron spectra measured in coincidence with these ions in the environment of the He nanodroplet, such as the one depicted in figure 1 below: the photoelectron kinetic energy spectrum measured in coincidence with monomer Camphor ion for effusive molecules which are not hosted in droplet is show in green, for photoexcitation at $h\nu$ = 21.43 eV. The overlayed red curve is the corresponding spectrum from doped molecules embedded in He nanodroplets. These photoelectron spectra are similar to what was reported for the case of acene molecules [11] such as Coronene [12] doped in droplets. Evidently, there is significant scattering of Penning electrons with the surrounding He atoms. We present and discuss these in this article.

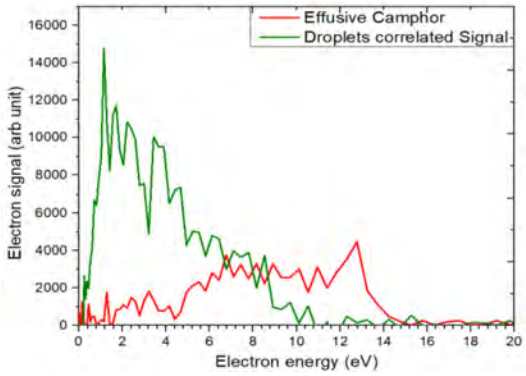

Fig. 1: Photoelectron energy spectra measured in coincidence with camphor monomer ($[C_{10}H_{16}O]^+$) ion at photon energy $h\nu$ = 21.43 eV. Here red line corresponds for effusive camphor and green line corresponds for Penning ionization electron spectrum (background subtracted droplet correlated signal). The He expansion conditions are stagnation pressure P_0 = 40 bar and nozzle temperature T_0 = 14K.

References

[1] D. Buchta, S. R. Krishnan *et al.*, 2013 J. Phys. Chem. A, **117**, 4394.
[2] D. Buchta, S. R. Krishnan *et al.*, 2013 J. Chem. Phys., **139**, 084301.
[3] Peterka, D. S *et al.*, 2007 J. Phys. Chem. A, **111**, 7449.
[4] Peterka, D. S *et al.*, 2006 J. Phys. Chem. B, **110**, 19945-19955.
[5] Zuccarini Paolo. 2009 J. Appl. Sci. Environ. Manage. **13**(2):6974
[6] Sherkheli Muhammad Azhar *et al.*, 2009 J. Pharm. Pharmaceut. Sci. **12**.1:11628
[7] Nahon, L. *et al.*, 2006 The Journal of chemical physics, **125**(11), 114309
[8] Nahon, L. *et al.*, 2010 Physical Review A, **82**(3), 032514
[9] Lux, C. *et al.*, 2012 Angewandte Chemie International Edition, **51**(20), 5001-5005
[10] Lux, C. *et al.*, 2015 Journal of Physics B: Atomic, Molecular and Optical Physics, **49**(2), 02LT01
[11] M. Shcherbinin *et al.*, 2018 J. Phys. Chem. A, **122**, 1855-1860.
[12] Ltaief, L.B *et al.*, 2021 J Low Temp Phys **202**, 444–455.

[*]Corresponding author: vsharma@iith.ac.in
[†]Corresponding author: srkrishnan@iitm.ac.in,

Many-body theory of positron binding in polyatomic molecules

J. Hofierka*[1], B. J. Cunningham[1], C. M. Rawlins[1], C. H. Patterson[2], D. G. Green†[1]
1. School of Mathematics and Physics, Queen's University Belfast, Belfast BT7 1NN, United Kingdom
2. School of Physics, Trinity College Dublin, Dublin 2, Ireland

Positrons bind to molecules leading to vibrational excitation and spectacularly enhanced annihilation (see [1] for a review). Whilst positron binding energies have been measured via resonant annihilation spectra for around 75 molecules in the past two decades [1], an accurate *ab initio* theoretical description has remained elusive. Of the molecules studied experimentally, calculations exist for only 6, and for these, standard quantum chemistry approaches have proved severely deficient, agreeing with experiment to at best 25% accuracy for polar molecules, and failing to predict binding in non-polar molecules. The theoretical difficulty lies in the need to accurately account for strong positron-molecule correlations including polarisation of the electron cloud, screening of the positron-molecule Coulomb interaction by molecular electrons, and the unique process of virtual-positronium formation (where a molecular electron temporarily tunnels to the positron). Their roles in positron-molecule binding have yet to be elucidated.

We have developed a diagrammatic many-body description of positron-molecule binding in polyatomic molecules that takes *ab initio* account of the correlations [2]. We solve the Dyson equation for the positron quasiparticle wavefunction in a Gaussian basis, constructing the positron-molecule self-energy including the *GW* contribution that describes polarisation, screening and electron-hole interaction interactions (at RPA/TDHF/BSE levels), the ladder series of positron-electron interactions that describes virtual positronium formation, and the ladder series of positron-hole interactions.

We have used it to calculate binding energies for a range of polar and non-polar molecules, focussing chiefly on the molecules for which both theory and experiment exist [2]. Delineating the effects of the correlations, we show, in particular, that virtual-positronium formation significantly enhances binding in organic polar molecules, and moreover, that it is essential to support binding in non-polar molecules including CS_2, CSe_2 and benzene. Overall, we find the best agreement with experiment to date (to within a few percent in some cases). The method also enables the calculation of the positron bound wavefunction (see Fig. 1), and of the positron-electron contact density (annihilation rate in the bound state).

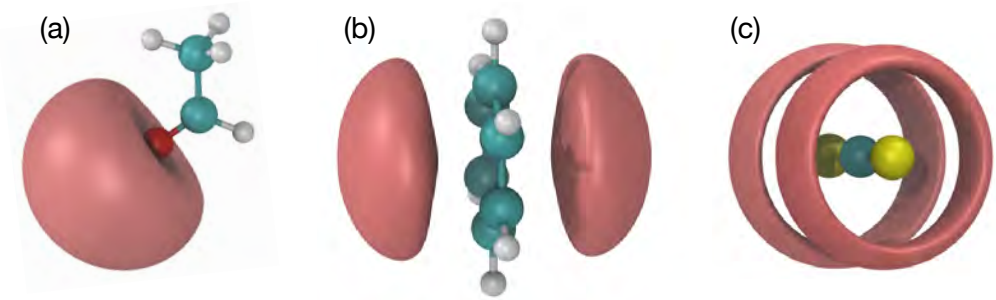

Fig. 1: Present many-body theory calculated bound-state positron density for (a) acetaldehyde (polar, isovalue at 0.62 of maximum density), (b) benzene (non-polar, isovalue at 0.83 of maximum density), and (c) CS_2 (non-polar, isovalue at 0.99 of maximum density)

References

[1] G. F. Gribakin, J. A. Young, and C. M. Surko, Rev. Mod. Phys. **82** 2557 (2010)
[2] B. J. Cunningham, J. Hofierka, C. M. Rawlins, C. H. Patterson and D. G. Green, *In preparation*

*Corresponding author: jhofierka01@qub.ac.uk
†Corresponding author: d.green@qub.ac.uk

Probing Casimir-Polder interactions of Rydberg atoms in vapour cells

B. Dutta[1], **J. C. de Aquino Carvalho**[1], **H. Failache**[2], **I.Maurin**[1], **D. Bloch**[1], **A. Laliotis**[*1]

1. Laboratoire de Physique des Lasers, UMR7538 CNRS, Université Sorbonne Paris Nord, 93430, Villetaneuse, France

2. Instituto de Fisica, Facultad de Ingeneria, Universidad de la Republica, J. Herrera y Reissig 565, 11300, Montevideo, Uruguay

Highly excited alkali atoms (Rydbergs) have gained attention as candidates for quantum technology applications. This is because Rydbergs interact strongly with their neighbors thus favoring the observation of collective phenomena. Thin vapor cells [1] and fiber-based devices have been proposed as solid-state platforms for probing Rydberg excitations. These systems interface atoms with dielectric surfaces at the micro or nanometric scale, highlighting the need for experimental and theoretical investigations of Casimir-Polder, Rydberg-surface interactions.

Rydberg-surface interactions are also of fundamental interest when the atomic size, scaling as $n^{\star 2}$ ($n^{\star}$ is the principle quantum number corrected by the quantum defect), is no longer negligible compared to the atom-surface separation, z. In this case, the dipole approximation, giving an interaction energy proportional to z^{-3}, is not valid and higher-order terms need to be taken into account. Quadrupole interaction terms in the atom-surface interaction manifest themselves with a novel distance dependence of z^{-5} [2] that has not been experimentally investigated yet.

The Rydberg-surface interaction was first measured with low-lying nS Rydberg states ($n = 10-13$) of sodium atoms, demonstrating the $-C_3/z^3$ interaction law (where C_3 is the van der Waals coefficient) [3]. Nevertheless, more recent experiments with high-lying rubidium Rydbergs ($n = 32-43$) confined in thin vapor cells [1] were difficult to interpret, sparking closer theoretical investigations of the Rydberg-surface interactions.

Here we use the well-developed technique of selective reflection spectroscopy to measure the Casimir-Polder interaction between $Cs(15D_{3/2})$ atoms and a sapphire surface. The experiments are performed in a sapphire cell with an set-up similar to the one reported in [4]. The cesium atoms are excited by a strong pump laser to the first cesium resonance ($6P_{1/2}$) and subsequently selective reflection is performed on the $6P_{1/2} \rightarrow 15D_{3/2}$ transition at $\lambda = 512$nm (see Fig.1a). Selective reflection probes excited atoms at a distance of approximately $\lambda/2\pi$ (see [4] and references therein). Our measurements rely on the interpretation of our experimental spectra using a simple theoretical model [5] that neglects the effects of atomic motion.

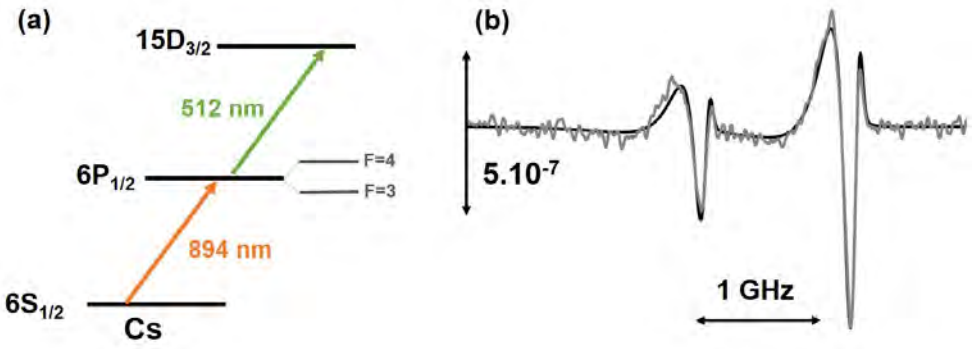

Fig. 1: (a) Relevant cesium energy levels. (b) Selective reflection spectrum normalized by the off-resonant reflection (gray line) along with the theoretical fit (black line). The cesium pressure is 25mTorr. The two peaks correspond to the $6P_{1/2}$ hyperfine manifold (both levels are populated due to collisions [4]), separated by 1.17 GHz.

In Fig.1b we show a selective reflection spectrum, along with the best theoretical fit assuming an interaction energy of $-C_3/z^3$. Our theoretical model describes well the experimental spectra. The best fits are obtained for a van der Waals coefficient of $C_3 \approx 10\text{MHz}\,\mu\text{m}^3$ assuming a collisional broadening of $\Gamma \approx 160$MHz. The measured C_3 coefficient is larger than the theoretically predicted value of $\approx 4\text{MHz}\,\mu\text{m}^3$. The assumption of motionless atoms is justified in this experiment because Casimir-Polder shifts at typical probing distances are larger than Doppler shifts. We are currently working on improving our theoretical models to include the effects of atomic motion. This could lead to better quality fits of our experimental spectra and more accurate measurements of the C_3 coefficient. We envisage probing higher-lying Rydberg states in order to test the limits of the dipole approximation and probe quadrupole interactions [4]. The experiment is funded by the ANR project SQUAT (ANR-20- CE92-0006-0.1).

References

[1] H. Kübler, J. P. Shaffer, T. Baluktsian, R. Löw1 and T. Pfau, Nat. Photonics. **4**, 112-116 (2010).
[2] J. A. Crosse, S.A. Ellingsen, K. Clements,S. Y. Buhmann and Stefan Scheel, Phys. Rev. A. **82**, 010901(R) (2010).
[3] V. Sandoghdar, C. I. Sukenik, E. A. Hinds and S. Harroche, Phys. Rev. Lett. **68**, 3432-3435 (1992).
[4] A. Laliotis, T. Passerat de Silans, I. Maurin, M. Ducloy and Daniel Bloch, Nat. Commun. **5**, 4364 (2014).
[5] M. Ducloy and M. Fichet, J. Phys. II France **1**, 1429-1446 (1991).

*Corresponding author: laliotis@univ-paris13.fr

Positron cooling in N_2 and CF_4 gases

A. R. Swann*, **D. G. Green**†

School of Mathematics and Physics, Queen's University Belfast, Belfast BT7 1NN, United Kingdom

Developments in positron trapping, accumulation, and delivery of positrons in beams over the last few decades [1] have enabled the study of low-energy antimatter interactions with atoms and molecules [2][3], and formation, exploitation, and interrogation of positronium and antihydrogen [4]. In a typical setup, ∼500 keV positrons from a ^{22}Na source are slowed to eV energies by a solid-neon moderator and guided into a Surko trap [5], where thermalization to room temperature is achieved via collisions with N_2 and/or CF_4 gases. Regarding theory, recently, a Monte Carlo approach [6] using accurate many-body-theory cross sections [7] gave a complete description of thermalization in noble gases, obtaining excellent agreement with experiment [8][9]. But cooling in molecular gases is not well understood theoretically, even for N_2 and CF_4, despite their important use. Recent experiments for CF_4 indicated that the positron momentum distribution remains Maxwellian throughout the cooling, suggesting a mechanism beyond simple excitation of the dominant ν_3 and ν_4 vibrational modes (which alone would be expected to lead to 'pile-ups' of the distribution below the vibrational thresholds; see Fig. 1).

Here, we calculate the evolution of the momentum distribution $f(k)$ and positron temperature T during cooling in N_2 (via rotational excitation) and CF_4 (via vibrational excitation) using a Monte Carlo approach, simulating the experiments of Natisin *et al* [10]. We use the Born-dipole and Born-quadrupole cross sections, respectively. Figure 1 shows the evolution of $f(k)$ (left panel) and T (right panel), respectively, for CF_4, calculated with the inclusion of the dominant ν_3 and ν_4 modes, and the ν_1 mode. The predicted evolution of T is in excellent agreement with experiment, and although we observe 'pile-ups' at the vibrational thresholds, the inclusion of ν_1 enables combination cooling below the lowest threshold (ν_4). We are now investigating the effect of positron-positron collisions, determining whether the experimental positron-to-gas-density ratio is sufficient to effect rapid Maxwellianization.

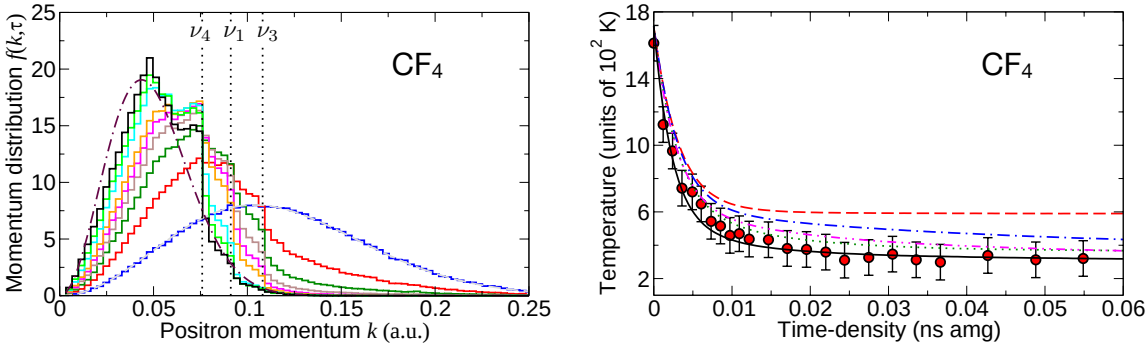

Fig. 1: Left panel: $f(k)$ for cooling in CF_4. Values of time-density (the product of the time in ns and the CF_4 number density in amg): 0 (blue), 0.002 (red), 0.004 (dark green), 0.006 (brown), 0.008 (magenta), 0.01 (orange), 0.02 (cyan), 0.03 (light green), 0.06 (black). Dashed line: initial Maxwell-Boltzmann distribution for $T = 1700$ K. Dot-dashed line: Maxwell-Boltzmann distribution for 300 K. Dotted lines: vibrational thresholds.

Right panel: T for cooling in CF_4. ν_3 only (red), $\nu_3 + \nu_4$ (blue), $\nu_3 + \nu_4$ with scaling (green), $\nu_3 + \nu_4 + \nu_1$ (magenta), $\nu_3 + \nu_4 + \nu_1$ with scaling (black), experiment [10] (red circles).

References

[1] J. R. Danielson *et al.*, Rev. Mod. Phys. **87**, 247 (2015).
[2] C. M. Surko, G. F. Gribakin, and S. J. Buckman, J. Phys. B **38**, R57 (2005).
[3] G. F. Gribakin, J. A. Young, and C. M. Surko, Rev. Mod. Phys. **82**, 2557 (2010).
[4] The ALPHA Collaboration, Nat. Phys. **7**, 558 (2011).
[5] C. M. Surko, M. Leventhal, and A. Passner, Phys. Rev. Lett. **62**, 901 (1989).
[6] D. G. Green, Comp. Phys. Comm. **224**, 362 (2018).
[7] D. G. Green, J. A. Ludlow, and G. F. Gribakin, Phys. Rev. A **90**, 032712 (2014).
[8] D. G. Green, Phys. Rev. Lett. **119**, 203403 (2017).
[9] D. G. Green, Phys. Rev. Lett. **119**, 203404 (2017).
[10] M. R. Natisin, J. R. Danielson, and C. M. Surko, J. Phys. B **47**, 225209 (2014).

*Corresponding author: a.swann@qub.ac.uk
†Corresponding author: d.green@qub.ac.uk

Four-body universality which extends from classical to quantum systems

Petar Stipanović[*1], **Leandra Vranješ Markić**[1], **Andrii Gudyma**[2], **Jordi Boronat**[3]

1. University of Split, Faculty of Science, R. Boškovića 33, 21000 Split, Croatia
2. Max Planck Institute for Microstructure Physics, Weinberg 2, 06120 Halle, Germany
3. Department of Physics, Universitat Politècnica de Catalunya, Campus Nord B4-B5, E-08034, Barcelona, Spain

Universal relationship of scaled size and scaled energy, which was previously established for two- and three-body systems in their ground halo state [1], is examined for four-body systems [2].

Four-body exact ground-state estimate of self-binding is obtained by the diffusion Monte Carlo method, while structural properties are extracted by pure estimators [3]. Previously in the case of helium trimers, a similar approach enabled comparison of theoretically predicted structural properties [4] with the most recent experimental results [5] and [6], which were obtained by Coulomb explosion imaging of diffracted helium clusters.

A detailed study was performed in the halo region, where systems are extremely weakly bound and prefer more to be in classically forbidden regions. Strengthening the inter-particle interaction we extend the exploration all the way to classical systems. Different scaling length were tested and universal size-energy law has been found for homogeneous tetramers in the case of interaction potentials decaying predominantly as r^{-6}. The universal size-energy line is also applicable to mixed four-body systems, if their structure is homogeneous-like.

References

[1] P. Stipanović, L. Vranješ Markić, I. Bešlić and J. Boronat, Phys. Rev. Lett. **113**, 253401 (2014). DOI: 10.1103/PhysRevLett.113.253401
[2] P. Stipanović, L. Vranješ Markić, A. Gudyma and J. Boronat, Scientific Reports **9**, 6289 (2019). DOI: 10.1038/s41598-019-42312-9
[3] J. Casulleras and J. Boronat, Phys. Rev. B **52**, 3654 (1995). DOI: 10.1103/PhysRevB.52.3654
[4] P. Stipanović, L. Vranješ Markić and J. Boronat, J. Phys. B: At. Mol. Opt. Phys. **49**, 185101 (2016). DOI: 10.1088/0953-4075/49/18/185101
[5] J. Voigtsberger et al., Nature Communications **5**, 5765 (2014). DOI: 10.1038/ncomms6765
[6] M. Kunitski et al., Science **348**, 551 (2015). DOI: 10.1126/science.aaa5601

*Corresponding author: pero@pmfst.hr

Gouy phase-matched angular and radial mode conversion in four-wave mixing

Andrew Daffurn[*1], **Rachel F. Offer**[2], **Erling Riis**[1], **Paul F. Griffin**[1], **Sonja Franke-Arnold**[3], **Aidan S. Arnold**[1]

1. Department of Physics, SUPA, University of Strathclyde, Glasgow G4 0NG, UK
2. Department of Physics, The University of Adelaide, SA 5005, Australia
3. School of Physics and Astronomy, SUPA, University of Glasgow, Glasgow G12 8QQ, UK

We couple the orthogonal azimuthal and radial mode numbers of structured light, in the form of Laguerre-Gaussian beams, via four-wave mixing (FWM) in a heated rubidium vapour [1]. The selection rules for the angular mode number are governed by angular momentum conservation ([2] , [3], [4]), while the role of the radial mode number is more obscure([5] , [6]). One would not normally expect these orthogonal components to interact but we demonstrate experimentally that a clean Laguerre-Gauss mode $\mathrm{LG}_p^\ell = \mathrm{LG}_1^0$ can be generated via FWM using LG_0^1 and LG_0^{-1} near-infrared pump beams – but only if the length of the atomic medium is greater than the Rayleigh range of the interacting light fields. This leads to strikingly different conversion behaviour in thick- and thin-medium regimes; with the Gouy phase, and it's relative importance in each regime, the crucial component in understanding this conversion. Our experimental investigation of the transition between these two regimes bridges the gap between previous experiments in atomic thick media and work in nonlinear crystals. This sets the basis to explore efficient radial-to-azimuthal and radial-to-radial mode conversion in the thick-medium regime.

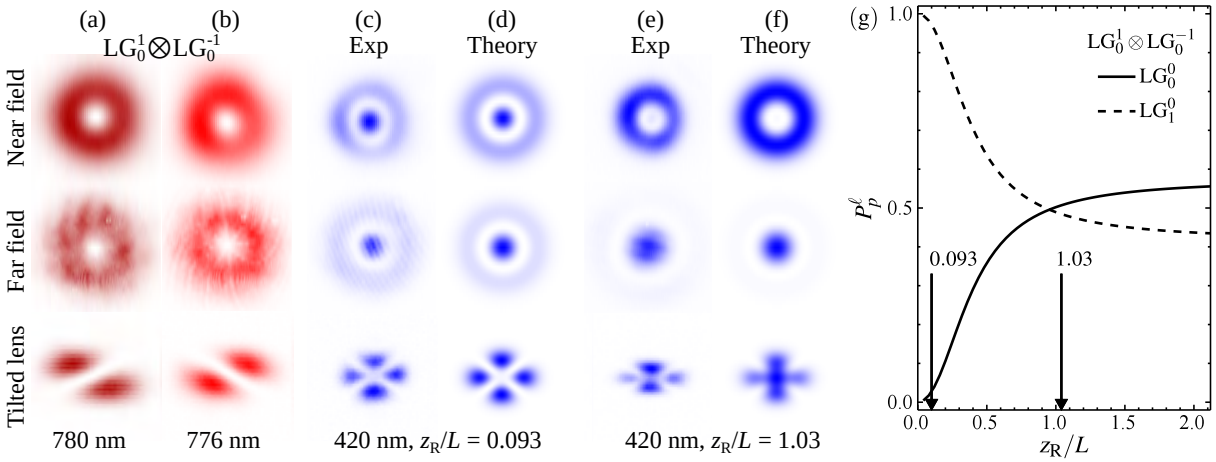

Figure 1: FWM for pump modes with opposite ℓ: LG_0^1 at 780 nm (a) and LG_0^{-1} at 776 nm (b). For a thick medium, we observe 420 nm light in an almost pure LG_1^0 mode (c), in agreement with our model (d). For a thin medium the experimental (e) and predicted (f) light is a coherent superposition of LG_0^0 and LG_1^0. Each image triplet in (a)-(f) corresponds to the near-field (top) far-field (middle) and tilted lens (bottom) beam intensity. In (g) we simulate the impact of the medium thickness on the mode purity of the generated light, with $\mathrm{LG}_0^1 \otimes \mathrm{LG}_1^{-1}$ input.

References

[1] R. F. Offer, A. Daffurn, E. Riis, P. F. Griffin, A. S. Arnold, and S. Franke-Arnold, Phys. Rev. A. **103**, L021502 (2021).
[2] A. M. Akulshin, I. Novikova, E. E. Mikhailov, S. A. Suslov, and R. J. McLean, Opt. Lett. **41**, 1146 (2016).
[3] A. Chopinaud, M. Jacquey, B. Viaris de Lesegno, and L. Pruvost, Phys. Rev. A. **97**, 063806 (2018).
[4] R. F. Offer, D. Stulga, E. Riis, S. Franke-Arnold, and A. S. Arnold, Commun. Phys. **1**, 84 (2018).
[5] H.-J. Wu, L.-W. Mao, Y.-J. Yang, C. Rosales-Guzmán, W. Gao, B.-S.Shi, and Z.-H. Zhu, Phys. Rev. A. **101**, 063805 (2020).
[6] W. T. Buono, A. Santos, M. R. Maia, L. J. Pereira, D. S. Tasca, K. De-choum, T. Ruchon, and A. Z. Khoury, Phys. Rev. A. **101**, 043821 (2020).

*Corresponding author: andrew.daffurn@strath.ac.uk

The most complete and advanced laser portfolio - Femtosecond & Nanosecond

Ti:Sa solutions: from TW to multi-PW

Arco: #Ti: Sapphire #Amplifiers #Ultra intense femtosecond lasers
Up to 40 W, single shot to multi-kHz, CEP
Pulsar: #Ultra intense #Ultrafast laser #Reliability #state of the art
Up to multi-PW, single shot to 10 Hz, sub 20 fs
Laser 4.0 HE – embedded intelligence for ultrafast photonics

Applications:
> Attophysics > Spectroscopy > Filamentation
> Plasma & particle acceleration > THz
> X-Ray Imaging > Proton therapy

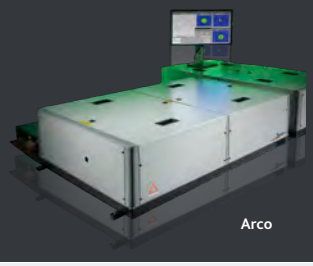
Arco

Amplitude

Nanosecond Lasers

NEW Elite: #Innovation #Performance #Best value
100 J @ 1053 nm & 75 J @ 527 nm Single beam

Applications:
> Pumping of PW-class laser systems > Laser driven shock applications
> Compression > LIDT metrology > High energy frontier physics


Elite

High rep rate Ytterbium solutions, industrial grade

Tangor & Tangerine: #high power, #high flux, #FemtoBurst™ #FemtoTrig™
Up to 300 W, Down to 15 fs, CEP

Applications:
> Ultrafast Spectroscopy > HHG > Attoscience

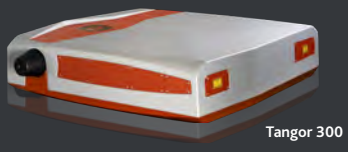
Tangor 300

High energy Ytterbium solutions, industrial grade

Magma: #High energy #Ultrafast laser #Laser 4.0 HE
Up to 500 mJ, Down to 500 fs, multi-kHz, diode-pumped

Applications: > THz > ICS > Filamentation > Photocathode


Magma

Amplitude
www.amplitude-laser.com

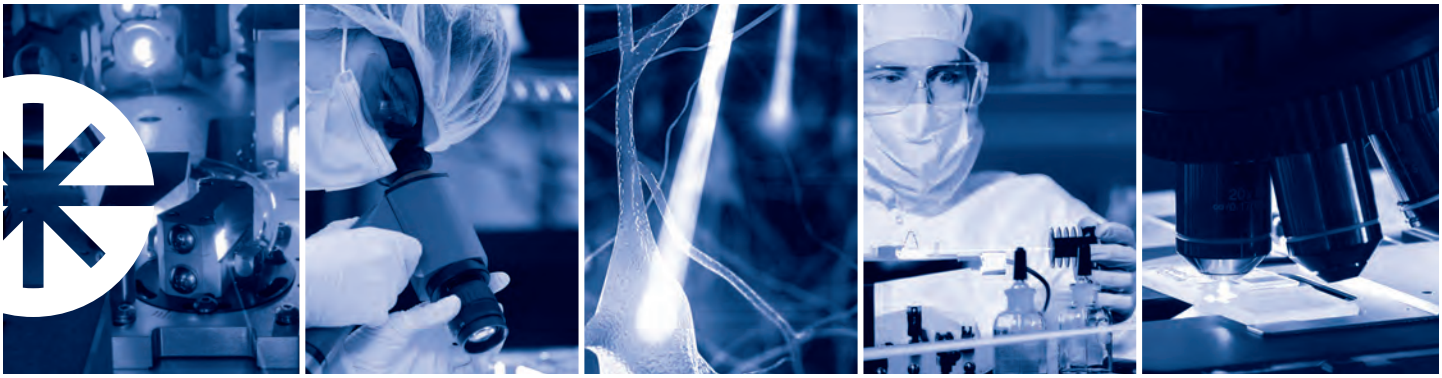

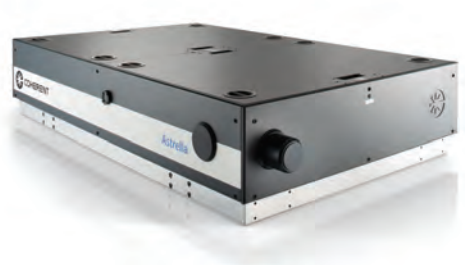

INDUSTRIAL-GRADE ULTRAFAST LASERS TO ADVANCE YOUR RESEARCH

Whether you are working at 1 kHz or 1 MHz, Coherent femtosecond amplifiers operate at extraordinary levels of quality, accuracy, and repeatability. Our HALT designed, HASS verified scientific lasers deliver industrial-grade reliability.

Join the Industrial Revolution in Ultrafast Science
coherent.com/industrial-revolution

COHERENT®
Superior Reliability & Performance

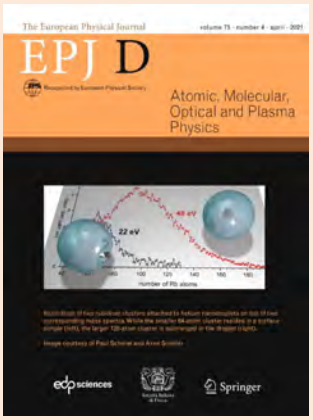

Visit the portal www.epj.org to:
read the journal
submit your manuscript
sign up for ToC Alerts

Why publish in EPJ D?

- Global readership
- Press releases for selected papers
- Fast online publication
- Expert & fast editorial handling
- Open Access / Read & Publish

Accessible in over 9000 institutions worldwide

EPJ D - Atomic, Molecular, Optical and Plasma Physics

Editors-in-Chief:
Almut Beige, University of Leeds, UK
Joachim Burgdörfer, Vienna University of Technology, Austria
Sylwia Ptasinska, University of Notre Dame, IN, USA

EPJ D brings you top-quality research in atomic, molecular, optical and plasma physics, as well as cluster physics, cold molecules, quantum gases, lasers, photonics, quantum optics, and quantum information.

Recent Topical Issues:

- Quantum Aspects of Attoscience
  Guest Eds: Carla Figueira de Morisson Faria, Andrew Brown and David B. Cassidy
- Low Temperature Plasmas: Processes and Diagnostics for Future Applications
  Guest Eds: Steven Shannon, Jeon Geon Han and Eva Kovacevic
- Spectroscopy of biomolecular ions in vacuo
  Guest Eds: Thomas Schlathölter, Gustavo Ariel Pino and Steen Bronsted Nielsen
- Atoms and Molecules in a Confined Environment
  Guest Eds: C.N. Ramachandran, Vincenzo Aquilanti, Henry Ed Montgomery and N. Sathyamurthy
- Topological Ultracold Atoms and Photonic Systems
  Guest Eds: G. Juzeliūnas, R. Ma, Y.-J. Lin and T. Calarco
- Quantum Technologies for Gravitational Physics
  Guest Eds: Tanja Mehlstäubler, Yanbei Chen, Guglielmo M. Tino and Hsien-Chi Yeh

Open Calls for Papers: https://epjd.epj.org/epjd-open-calls-for-papers

***few-cycle* Inc**. is a young Canadian company founded in 2014 as a spin-off of the laser research center ALLS at INRS Montreal and dedicated to the development of cutting-edge femtosecond technology. The mission of the company is to redefine optical parametric amplification through the proprietary FOPA technology as well as to enable laser upgrades based on adaptable stretched hollow-core fiber systems for pulse compression.

***few-cycle* Inc.** has demonstrated the effectiveness of the free-standing, stretched fiber compressor setup for various high-power laser systems with extreme performance, including:

1) Highest pulse energies ever achieved via self-phase modulation in HCF compression: up to 13mJ output in 2 cycle duration at 3.7 um wavelength (T. Balciunas et al., Lasers ASSL 2016) and 40mJ compressed output from an Yb amplifier (G. Fan et al.,Opt. Lett. 46:896, 2021).

2) Very long fibers up to 6m (Y. G. Jeong et al., Scientific Reports 8:11794, 2018).

3) Very high transmission: 80% achieved with ~3m long fibers [16, 17] and 97% (corresponding to the theoretically predicted limit) with a 1-m long, large diameter fiber (Jeong et al., CLEO 2021).

4) Compression ratios of >30 (Scientific Reports 8:11794, 2018).

5) Efficient compression of pulses at average powers of up to 250W (D. Wilson et al., EOSAM 2021, submitted)

TLD Photonics designs and manufactures high-end lasers and optical systems for industry and research. Our strong ties to leading Swiss universities allow us to develop groundbreaking products and through the extensive industrial experience of our team, we ensure that the real-world applications remain at the core of our developments. TLD Photonics core competencies lie in the design and manufacturing of femtosecond lasers on Titanium Sapphire & Ytterbium basis, high performance Optical Coherence Tomography and industrial optical systems. The main applications of TLD Photonics products are laser micromachining, nonlinear microscopy, and spectroscopy, to name a few.

Explore Quantum Research with MKS Products

- CW Tunable Lasers
- Double Density Tables & Breadboards
- High-Performance Opto-Mechanics

mks | Newport™ | Spectra-Physics®

moglabs

Injection Locked Amplifiers

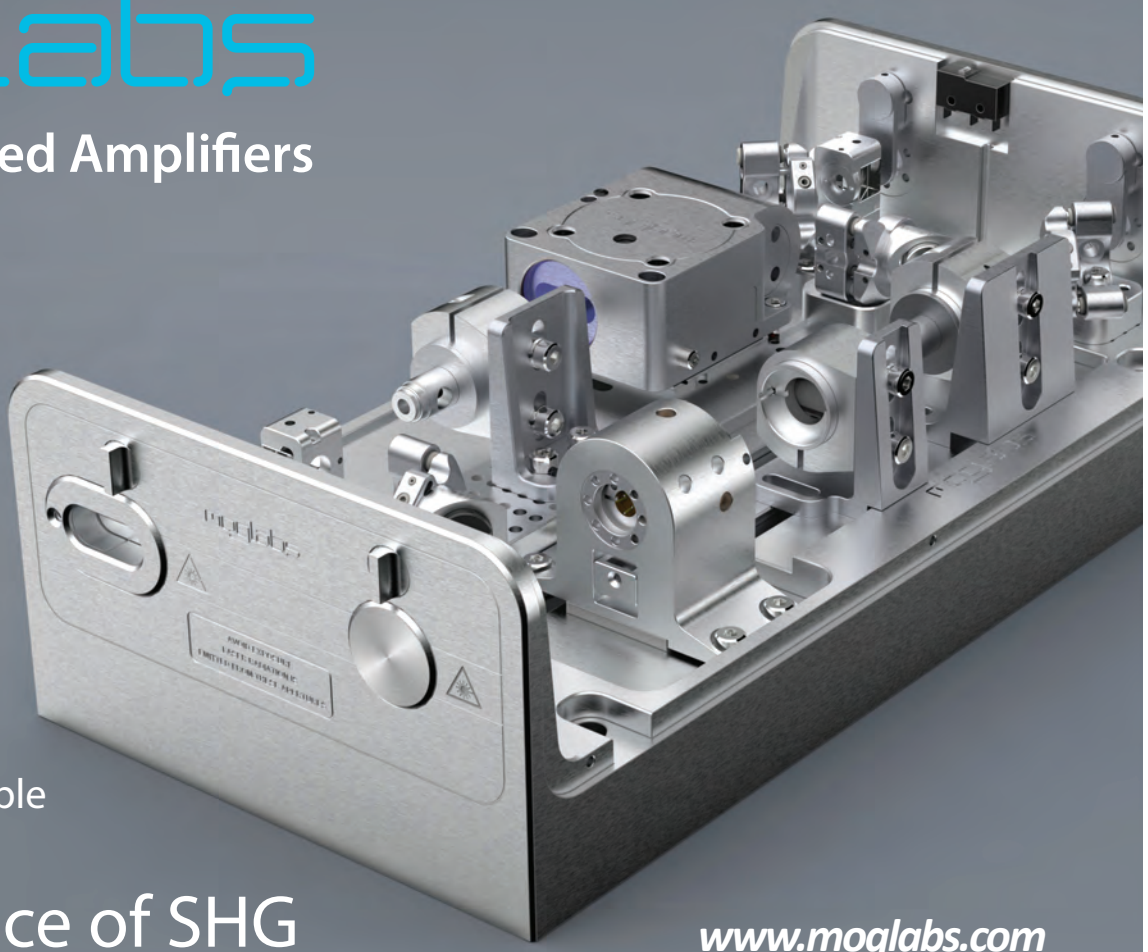

370nm 100mW
399nm 300mW
461nm 1000mW
Many others available

Half the price of SHG

www.moglabs.com